



University
of Glasgow

Jones, Sarah Elizabeth (2010) *The effect of cAMP elevation on intracellular signalling pathways in prostate epithelial cells*. PhD thesis.

<http://theses.gla.ac.uk/1668/>

Copyright and moral rights for this thesis are retained by the author

A copy can be downloaded for personal non-commercial research or study, without prior permission or charge

This thesis cannot be reproduced or quoted extensively from without first obtaining permission in writing from the Author

The content must not be changed in any way or sold commercially in any format or medium without the formal permission of the Author

When referring to this work, full bibliographic details including the author, title, awarding institution and date of the thesis must be given

The effect of cAMP elevation on intracellular signalling pathways in prostate epithelial cells

Sarah Elizabeth Jones

BSc. (Hons) Microbiology with Biotechnology
MRes. Molecular functions in disease

Submitted in fulfilment of the requirements for the Degree of Doctor of
Philosophy

Division of Molecular and Cellular Biology

Faculty of Biomedical and Life Sciences

University of Glasgow

October 2009

Supervisor: Dr. T. M. Palmer

Abstract

Chronic IL-6 signalling contributes to the pathophysiology of many diseases including prostate cancer. Relevant to prostate cancer is the ability of the pro-inflammatory cytokine IL-6 to activate the oncogenic signalling protein STAT3, thus inhibition of STAT3 activation is a popular avenue of research to augment prostate cancer therapies. In this study, the endogenous anti-inflammatory molecule cAMP was investigated as a mechanism by which to inhibit IL-6-induced STAT3 activation in the DU145, LNCaP and PZ-HPV-7 prostate epithelial cells.

Elevation of cAMP attenuated IL-6-mediated activation of STAT3 which was mimicked *via* selective activation of the exchange protein activated by cAMP. Inhibition of protein kinase A (PKA) alone also attenuated IL-6-induced STAT3 activation, suggesting a role for PKA activity in sustained IL-6 signalling in these cells. In DU145 and PZ-HPV-7 cells, the inhibitory effect of cAMP elevation was correlated with an increase in protein levels of suppressor of cytokine signalling 3. However, this was not the case in LNCaP cells in which cAMP elevation was instead associated with morphological changes consistent with neuroendocrine-like differentiation associated with terminal disease.

PKA activation was required for cAMP-mediated changes in LNCaP cell morphology and could be recapitulated by reagents which inhibited RhoA/ROCK signalling, suggesting that cAMP elevation is able to inhibit RhoA activation *via* a PKA-dependent pathway. Additionally, cAMP elevation activated ERK1/2 and selective blockade of ERK signalling attenuated the effects of cAMP elevation on cell morphology. Selective activation of ERK1/2 did not induce the early changes in cell morphology associated with increased intracellular cAMP concentrations, suggesting that another, related pathway was responsible for this phenomenon. Genetic or pharmacological inhibition of the MEK5/ERK5 signalling pathway significantly attenuated the rapid cAMP-mediated changes in LNCaP cell morphology, suggesting this pathway may be a possible target by which to inhibit the onset of neuroendocrine differentiation.

To summarise, this study demonstrates that whilst the ability of intracellular cAMP elevation to inhibit STAT3 activation is common to the prostate epithelial cell lines used, the downstream effects of cAMP elevation can vary dramatically. Thus, whilst modulation of cAMP signalling may represent a suitable therapeutic strategy when considering some aspects of prostate cancer, the impact on other signalling events must be considered.

Contents

1	Acknowledgements.....	1
	Author's Declaration	2
2	Abbreviations	3
3	Introduction.....	11
3.1	Cancer	11
3.1.1	Features of cancerous cells.....	12
3.1.2	Development of cancer	13
3.2	Inflammation.....	14
3.3	Chronic Inflammation and Cancer.....	15
3.3.1	Chronic inflammation promoting carcinogenesis can arise due to a multitude of factors	15
3.3.2	Chronic inflammation contributes to carcinogenesis via numerous mechanisms.....	16
3.3.3	The NFκB pathway links inflammation to cancer	19
3.4	Interleukin-6 Family Cytokines	22
3.4.1	Interleukin –6 cytokine family.....	22
3.4.2	The IL-6 family cytokine receptors.....	23
3.4.3	IL-6 trans-signalling.....	28
3.4.4	IL-6 and disease states	28
3.5	The JAK-STAT pathway	29
3.5.1	Janus Kinases	30
3.5.2	Signal transducers and activators of transcription	31
3.5.3	Activation of the JAK-STAT pathway	33
3.5.4	The role of JAK-STAT in disease.....	36
3.5.5	Negative Regulation of JAK-STAT.....	38
3.5.5.1	<i>Dephosphorylation</i>	38
3.5.5.2	<i>Polyubiquitylation</i>	39
3.5.5.3	<i>SOCS proteins</i>	39
3.5.5.4	<i>PIAS proteins</i>	40
3.5.5.5	<i>Methylation</i>	42
3.6	The MAP kinases	42
3.6.1	ERK1/2.....	43
3.6.2	ERK5.....	44
3.6.3	ERKs and cancer.....	47
3.7	cAMP signalling	50

3.7.1	cAMP generation	50
3.7.2	Protein Kinase A	52
3.7.3	EPAC	54
3.7.4	Other cAMP sensors	57
3.8	Actin polymerisation and cell motility.....	59
3.8.1	The WASP-WAVE protein network.....	59
3.8.2	The Arp2/3 complex	61
3.8.3	RhoGTPases and actin dynamics.....	63
3.8.4	RhoGTPases and cancer.....	64
	Fig. 3.12: Regulation of signalling pathways by Rho.....	65
3.9	Project Rationale	66
4	Materials.....	68
5	Methods.....	71
5.1	Cell culture	71
5.1.1	Culture of DU145 cells	71
5.1.2	Culture of LNCaP cells	71
5.1.3	Culture of PZ-HPV-7 cells.....	72
5.1.4	Culture of HEK293 cells.....	72
5.1.5	Culture of HUVECs	72
5.2	Transfections	73
5.2.1	Cell transfection with cDNA plasmids	73
5.2.2	Transfection of cells with siRNA.....	73
5.3	Molecular biology	74
5.3.1	Plasmid DNA constructs	74
5.3.2	Bacterial Strains and Media	74
5.3.3	Preparation of competent <i>E. coli</i>	74
5.3.4	Transformation of competent <i>E. coli</i>	75
5.3.5	Preparation of glycerol stocks.....	75
5.3.6	Preparation of plasmid DNA.....	75
5.3.6.1	Plasmid DNA preparation using QIAprep Spin Miniprep.....	75
5.3.6.2	Plasmid DNA preparation using Qiagen Maxi Plasmid kit	76
5.3.7	Determination of DNA purity and concentration	76
5.4	Generation and maintenance of recombinant adenovirus	77
5.4.1	Generation of myc-tagged human A _{2A} AR-expressing adenovirus	77
5.4.2	Large-scale preparation of recombinant adenoviruses.....	77
5.4.3	Titration of adenoviruses.....	78

5.4.4	Infection of LNCaP cells with recombinant adenovirus	79
5.4.5	Radioligand binding assay	79
5.5	Stimulation of prostate epithelial cells with exogenous cytokine	80
5.5.1	Membrane translocation of RhoA	80
5.6	Analysis of proteins by western blotting	81
5.6.1	Whole cell lysate preparation	81
5.6.2	Determination of protein content	81
5.6.3	Immunoblotting	82
5.7	Fsk-induced dendrite outgrowth	83
5.7.1	Fsk-induced NE differentiation in LNCaP cells	83
5.7.2	Effect of inhibitors on Fsk-induced NE differentiation	83
5.7.3	³ H-Leucine incorporation assay	83
5.8	Microscopy techniques	84
5.8.1	Determination of dendrite outgrowth	84
5.8.2	Immunofluorescence	84
5.9	Densitometric and statistical analysis	86
6	Characterisation of prostate epithelial cell responses to exogenous cytokines....	87
6.1	Introduction	87
6.1.1	STAT3 activation in prostate cancer	88
6.2	Cell systems	90
6.3	Results	91
6.3.1	Treatment of prostate epithelial cells with rhuIL-6 results in tyrosine phosphorylation of STAT3	92
6.3.2	Basal activation of STAT3 in prostate epithelial cell lines	93
6.3.3	The ability of rhuIL-6 to induce STAT3 activation is concentration dependent	97
6.3.4	Prostate epithelial cell lines display different responses to STAT-activating cytokines	101
6.3.5	Ectopic expression of JAK1 restores the ability of LNCaP cells to activate STAT1 in response to rhuIL-6	109
6.4	Discussion	110
7	Elevation of cAMP attenuates STAT3 phosphorylation in prostate epithelial cells	117
7.1	Introduction	117
7.2	Results	120
7.2.1	Effect of Fsk on IL-6-mediated activation of STAT3	120

7.2.2	The role of <i>de novo</i> protein synthesis in Fsk-mediated attenuation of STAT3 activation.....	124
7.2.4	Contribution of PKA and EPAC to Fsk-mediated attenuation of STAT3 activation.....	133
7.2.5	Fsk-mediated decreases in IL-6-induced STAT3 activation correlate with increases in SOCS3.....	137
7.3	Discussion.....	144
8	Elevation of cAMP induces LNCaP differentiation.....	150
8.1	Introduction.....	150
8.1.1	NE cells in the prostate.....	150
8.1.2	LNCaP differentiation to a NE-like phenotype.....	151
8.2	Results.....	153
8.2.1	Phase contrast microscopy analysis of changes in LNCaP cell morphology.....	153
8.2.2	Treatment with Fsk rapidly induces changes in LNCaP morphology.....	153
8.2.3	Early changes in LNCaP cells morphology do not require <i>de novo</i> protein synthesis.....	154
8.2.4	Fsk-induced changes in LNCaP cell morphology depends on an intact microtubule network.....	159
8.2.5	The ability of Fsk to induce increases in mean dendrite length requires adenylyl cyclase activity.....	163
8.2.6	Treatment with H89 mimics the effects of Fsk on LNCaP morphology.....	166
8.2.7	Treatment with myr.PKI ₁₄₋₂₂ inhibits the effect of Fsk on LNCaP morphological changes.....	169
8.2.8	Inhibitors affecting cAMP signalling are efficacious in the experimental system used.....	174
8.2.9	Inhibition of Rho-ROCK signalling mimics the effect of Fsk treatment.....	176
8.2.10	Inhibition of RhoA activity mimics the effects of Fsk on LNCaP morphology.....	178
8.2.11	Expression of constitutively active RhoA blocks Fsk-induced increases in mean dendrite length.....	186
	Fig 8.10: Identification of residues within the N-terminus of human Rho family members which are important for interaction with C3T.....	188
8.2.12	Actin depolymerisation mimics the effects of Fsk on LNCaP cell morphology.....	189

8.2.13	Selective activation of PKA recapitulates the effect of Fsk on LNCaP cell morphology	195
8.2.14	Establishment of a role for EPAC in Fsk-mediated changes in LNCaP cell morphology	201
8.3	Discussion	205
8.3.1	The roles of PKA and EPAC in LNCaP differentiation	205
8.3.2	Inhibition of RhoA mediates Fsk-induced changes in LNCaP cell morphology	208
9	The role of ERK activation in Fsk-induced changes in LNCaP morphology....	212
9.1	Introduction	212
9.1.1	NGF-induced neurite extension	212
9.1.2	The role of cAMP elevation in neurite outgrowth	214
9.1.3	The roles of cAMP in ERK1/2 activation	215
9.2	Results	217
9.2.1	Fsk induces Thr ²⁰² and Tyr ²⁰⁴ phosphorylation of ERK1/2 in LNCaP cells	217
9.2.2	Selective inhibition of the ERK1/2 pathway impairs Fsk-induced changes in LNCaP morphology	219
9.2.3	Selective activation of ERK1/2 does not mimic the effect of Fsk treatment in LNCaP cells	220
9.2.4	Expression of a dominant negative ERK5 inhibits Fsk-induced increases in mean dendrite length	230
9.2.5	Selective inhibition of MEK5 blocks Fsk-mediated changes in mean dendrite length in LNCaP cells	234
9.3	Discussion	237
10	Expression of the adenosine A_{2A} receptor alters LNCaP morphology.....	250
10.1	Introduction	250
10.2	The A _{2A} adenosine receptor	251
10.2.1	A _{2A} AR structure	251
10.3	Results	254
10.3.1	Titration of AdV.A _{2A} AR in LNCaP cells	254
10.3.2	Ligand binding assay.....	256
10.3.3	A _{2A} AR expression induces changes in LNCaP morphology	256
10.3.4	Expression of the A _{2A} AR is associated with NE-like morphological changes in LNCaP cells	258

10.3.5	The A _{2A} AR-selective inverse agonist ZM241385 blocks AdV.A _{2A} AR-mediated changes in LNCaP cell morphology.....	263
10.4	Discussion	267
11	Final discussion	272
12	Future directions	276
12.1	Investigation of gp130-STAT1 interaction in response to IL-6 stimulation.....	276
12.2	The role of SOCS proteins in cAMP-mediated attenuation of STAT3 activation 277	
12.3	The role of cAMP compartmentalisation in NE differentiation.....	280
12.4	The interplay of the PKA/actin/ERK5 signalling pathways	281
13	References	284

List of tables

		Page
Chapter 5		
Table 5.1	Antibodies used in immunoblotting	85
Chapter 9		
Table 9.1	Prediction of kinase phosphorylation sites within members of the ERK5 signalling cascade	246
Chapter 10		
Table 10.1	Association between eGFP fluorescence and NE-like morphology in LNCaP cells	261

List of figures

		Page
Chapter 3		
Fig. 3.1	Mechanisms by which chronic inflammation can contribute to carcinogenesis	17
Fig. 3.2	Activation of NF κ B signalling via the classical IKK-I κ B pathway	20
Fig. 3.3	Ribbon structures of IL-6 and OSM	25
Fig. 3.4	The IL-6 family cytokine receptors	27
Fig. 3.5	JAK domain organisation	32
Fig. 3.6	Domain organisation of STAT proteins	35
Fig. 3.7	Activation of the Ras-Raf-MEK1/2-ERK1/2 signalling pathway downstream of growth factor and cytokine receptors	46
Fig. 3.8	Schematic representation of human ERK1/2 and ERK5	48
Fig. 3.9	Activation of the PKA holoenzyme by cAMP	53
Fig. 3.10	Domain organisation of the human EPAC proteins	56
Fig. 3.11	Mechanism for actin-mediated protrusion of the leading edge downstream of extracellular stimuli	60
Fig. 3.12	Regulation of signalling pathways by	65
Chapter 6		
Fig. 6.1	Treatment of DU145 prostate epithelial cells with 10 ng/ml rhuIL-6 induces tyrosine phosphorylation of STAT3 but not STAT1	94
Fig. 6.2	Treatment of LNCaP prostate epithelial cells with 10 ng/ml rhuIL-6 induces tyrosine phosphorylation of STAT3 but not STAT1	95

		Page
Fig. 6.3	Treatment of PZ-HPV-7 prostate epithelial cells with 10 ng/ml rhuIL-6 induces tyrosine phosphorylation of STAT3 and STAT1	96
Fig. 6.4	Effect of conditioned and fresh medium on rhuIL-6-induced pTyr ⁷⁰⁵ STAT3 in DU145 prostate epithelial cells	98
Fig. 6.5	Effect of conditioned and fresh medium on rhuIL-6-induced pTyr ⁷⁰⁵ STAT3 in LNCaP prostate epithelial cells	99
Fig. 6.6	Effect of conditioned and fresh medium on rhuIL-6-induced pTyr ⁷⁰⁵ STAT3 in LNCaP prostate epithelial cells	100
Fig. 6.7	Effect of IL-6 concentration on STAT3 activation in DU145 cells	102
Fig. 6.8	Effect of IL-6 concentration on STAT3 activation in LNCaP cells	103
Fig. 6.9	Effect of IL-6 concentration on STAT3 activation in PZ-HPV-7 cells	104
Fig. 6.10	Effect of STAT activating cytokines on STAT1 and STAT3 activation in DU145 cells	106
Fig. 6.11	Effect of STAT activating cytokines on STAT1 and STAT3 activation in LNCaP cells	107
Fig. 6.12	Effect of STAT activating cytokines on STAT1 and STAT3 activation in PZ-HPV-7 cells	108
Fig. 6.13	Expression of JAK1 in LNCaP cells restores STAT1 phosphorylation in response to rhuIL-6	111

Chapter 7		Page
Fig. 7.1	Inhibition of IL-6-induced STAT3 activation in DU145 prostate epithelial cells	121
Fig. 7.2	Inhibition of IL-6-induced STAT3 activation in LNCaP prostate epithelial cells	122
Fig. 7.3	Inhibition of IL-6-induced STAT3 activation in PZ-HPV-7 prostate epithelial cells	123
Fig. 7.4	Effect of emetine on Fsk-induced attenuation of STAT3 activation in DU145 cells	126
Fig. 7.5	Effect of emetine on Fsk-induced attenuation of STAT3 activation in LNCaP cells	128
Fig. 7.6	Effect of emetine on Fsk-induced attenuation of STAT3 activation in PZ-HPV-7 cells	130
Fig. 7.7	Efficacy of emetine in LNCaP cells	132
Fig. 7.8	The contribution of PKA and EPAC to Fsk-mediated attenuation of STAT3 activation in DU145 cells	134
Fig. 7.9	The contribution of PKA and EPAC to Fsk-mediated attenuation of STAT3 activation in LNCaP cells	135
Fig. 7.10	The contribution of PKA and EPAC to Fsk-mediated attenuation of STAT3 activation in PZ-HPV-7 cells	136
Fig. 7.11	Fsk-mediated attenuation of STAT3 activation in DU145 cells is correlated with an accumulation of SOCS3 protein	139
Fig. 7.12	Fsk-mediated attenuation of STAT3 activation in LNCaP cells is not correlated with an accumulation of SOCS3 protein	141

		Page
Fig. 7.13	Fsk-mediated attenuation of STAT3 activation in PZ-HPV-7 cells is correlated with an accumulation of SOCS3 protein	142
 Chapter 8		
Fig. 8.1	cAMP elevation induces morphological changes in LNCaP cells but not in DU145 or PZ-HPV-7 cells	155
Fig. 8.2	The ability of Fsk to induce prolonged but not initial changes in LNCaP morphology requires de novo protein synthesis	160
Fig. 8.3	Fsk-induced changes in LNCaP morphology require an intact microtubule network	164
Fig. 8.4	Treatment with the AC-selective inhibitor t-Bu-SATE inhibits the effect of Fsk on LNCaP morphology	167
Fig. 8.5	Treatment with the PKA-selective inhibitor H89 mimics the effect of Fsk on LNCaP morphology	170
Fig. 8.6	Treatment with the PKA-selective inhibitor myrPKI ₁₄₋₂₂ mimics the effect of Fsk on LNCaP morphology	172
Fig. 8.7	Efficacy of inhibitors of cAMP signalling	175
Fig. 8.8	Inhibition of ROCK signalling by Y27632 recapitulates the effect of Fsk on LNCaP morphology	179
Fig. 8.9	Inhibition of RhoA causes changes in LNCaP morphology consistent with NE-like differentiation	183
Fig. 8.10	Identification of residues within the N-terminus of human Rho family members which are important for interaction with C3T	187

		Page
Fig. 8.11	Expression of a dominant negative RhoA blocks Fsk-induced changes in LNCaP cell morphology	190
Fig. 8.12	Disruption of the actin cytoskeleton recapitulates the effects of Fsk treatment on LNCaP cell morphology	196
Fig. 8.13	Selective activation of PKA mimics the effect of Fsk on LNCaP cell morphology	199
Fig. 8.14	Effect of EPAC1 siRNA on Fsk-induced changes in LNCaP cell morphology	202
 Chapter 9		
Fig. 9.1	Treatment with Fsk activates ERK1/2 in LNCaP cells	218
Fig. 9.2	The ability of Fsk to induce changes in LNCaP morphology requires MEK1/2 activity	221
Fig. 9.3	Expression of Myc.Raf1:ΔER allows selective activation of ERK1/2	223
Fig. 9.4	Selective activation of ERK1/2 results in changes in LNCaP morphology but at later time points than seen following Fsk treatment	225
Fig. 9.5	Ectopic of dominant ERK5 impairs the ability of Fsk to induce morphological changes in LNCaP cells	232
Fig. 9.6	The ability of Fsk to induce changes in LNCaP morphology requires MEK5 activity	235
Fig. 9.7	Sequence alignment of ERK1, ERK2 and ERK5 indicating proline-rich regions	243

Chapter 10		Page
Fig. 10.1	Titration of the AdV.A _{2A} AR in LNCaP cells	255
Fig. 10.2	Binding curve of ³ H-ZM241385 in LNCaP cells infected with AdV.GFP or AdV. A _{2A} AR	257
Fig. 10.3	Expression of the A _{2A} AR in LNCaP cells mimics Fsk-induced morphological changes	259
Fig. 10.4	Infection percentages for AdV.GFP and AdV.A _{2A} AR in LNCaP cells	262
Fig. 10.5	Treatment with the A _{2A} AR-selective inverse agonist ZM241385 inhibits AdV.A _{2A} AR-mediated changes in LNCaP morphology	264

1 Acknowledgements

There are so many people that I would like to thank for their help and support throughout my PhD. There is no particular order to my thanks as everyone as has been supportive at different times and in different ways and no-one has played a greater or lesser role in helping through the “PhD stress”.

Firstly, I would like to thank the Wellcome Trust PhD programme at Glasgow, Prof. Bill Cushley, Dr. Darren Monkton and Dr. Olwyn Byron for the opportunity to come to Glasgow and for allowing me to develop professionally out with my research due to the excellent programme which they oversee. I am extremely grateful to Dr. Tim Palmer, my supervisor, for all of his help, support and guidance throughout my PhD and without whom none of this would have been possible. I also would like to thank Billy (especially for Thursday climbing), Claire (for being generally fabulous and being a great shoulder to cry on), Gillian (for happy star jump time), Hayley, Jamie, Kirsty, Shona and Vicky for all their support throughout every aspect of my PhD and for making the lab such an enjoyable place to work, especially for the wine!

Throughout my research, I have had a huge amount of support from my friends and I would like to thank all of them for listening to me and for understanding when I’m late or cancel plans because the dark room has eaten me. Special thanks go to Andrea, Anette, Ash, Beka, Kirsty and Louise for lunch/tea/cake/venison; GUMC, particularly Team Pie, Steak Club, Georgie, Judith, Cathy and Cathy for the hills, food and parties; the Vixens for their general fabulousness/tea/soup; Ewan for putting up with me; Helen and Audrey for wine/dinner/climbing; Amy and Emily for being at the end of the phone and Craig and Katrina for reminding me that I am not alone!

By no means least, I would like to thank my family for their unwavering support and belief in me, despite referring to my beautiful, beautiful graphs as “pictures”! Thank you so much; there is no way I could have done this without your love and help. And I guess finally, I wish to dedicate this thesis to the memory of my late granddad, Dr. Frank Jones, without whom my interest in science would never have been kindled and I would have far fewer grey hairs!

Author's Declaration

I hereby declare that the thesis which follows is my own, original composition and that all work has been performed by me unless otherwise acknowledged. Furthermore, none of this work has been previously presented as part of an application for a Higher Degree.

Sarah Elizabeth Jones

March 2010

2 Abbreviations

4OHT	4-Hydroxytamoxifen
6-Benz-cAMP	N ⁶ -Benzoyl-3', 5'- cyclic monophosphate
8-pCPT-cAMP	8- (4-Chlorophenylthio)- 2'- O- methyladenosine- 3', 5'- cyclic monophosphate
A	Acidic domain
A_{2A}AR	A _{2A} adenosine receptor
AC	Adenylyl cyclase
AdV	Adenovirus
AKAP	A kinase anchoring protein
AndR	Androgen receptor
ANOVA	Analysis of variance
Arp	Actin-related protein
ATF	Activating transcription factor
BCA	Bicinchoninic acid
BMI	Body mass index
BSA	Bovine serum albumin
C	Catalytic subunit of PKA
C_{1/2}	Cytosolic domain 1/2 of AC
C3T	C3 Transferase
CAC	Colitis-associated carcinoma
cAMP	3',5'-cyclic adenosine monophosphate
cAMP-A	High affinity cAMP binding site
cAMP-B	Low affinity cAMP binding site
CBP	CREB-binding protein
CEBP	CCAAT-enhancer binding proteins
cGMP	cyclic guanosine monophosphate
CHAPS	3-[(3-Cholamidopropyl) dimethylammonio]-1-propanesulfonate hydrate

CHD	Cytokine homology domain
CLC	Cardiotrophin-like cytokine
CNG	Cyclic nucleotide-gated ion channel
CNrasGEF	Cyclic nucleotide Ras GEF
CNS	Central nervous system
CNTF	Ciliary neurotrophic factor
Co	Cofilin homology
CRE	cAMP response element
CREB	CRE-binding protein
CREM	CRE modulator
CST	Cell Signalling Technology
DBD	DNA binding domain
DAB	Diaminobenzadine
DEPC	Diethyl pyrocarbonate
DMEM	Dulbecco's minimal essential medium
DMSO	Dimethylsulphoxide
DOK-1	Downstream of kinase 1
DPBS	Dulbecco's phosphate buffered saline
ECL	Enhanced chemiluminescence
Eg	Erythropoietin receptor/gp130 chimera
EGF	Epidermal growth factor
eGFP	Enhanced green fluorescent protein
EGM-2	Endothelial growth medium 2
Em	Emetine
EtOH	Ethanol
EPAC	Exchange protein activated by cAMP
ER	Oestrogen receptor
ERK	Extracellular signal-regulated kinase

F-actin	Filamentous actin
FBS	Foetal bovine serum
FERM	Protein 4.1, ezrin, radixin, moesin
FGF	Fibroblast growth factor
fMLP	formyl-Met-Leu-Pro
Fsk	Forskolin
G-actin	Globular actin
GAP	GTPase activating protein
GAPDH	Glyceraldehyde-3-phosphate dehydrogenase
G-CSF	Granulocyte colony stimulating factor
GDI	GDP-dissociation inhibitor
GEF	Guanine nucleotide exchange factor
GFAP	Glial fibrillary acidic protein
GFP	Green fluorescent protein
GPCR	G-protein coupled receptor
gp130	Glycoprotein 130 kDa
H89	N-[2-(<i>p</i> -bromocinnamyl) amino) ethyl]-5-isoquinoline-sulfonamide dihydrochloride
HB-EGF	Heparin-binding EGF-like factor
HCC	Hepatocellular carcinoma
HCN	Hyperpolarisation-activated, cyclic nucleotide-gated ion channel
HDAC	Histone deacetylase
HEK	Human embryonic kidney
hGH	Human growth hormone
hGHR	Human growth hormone receptor
HIF	Hypoxia-induced factor
HPV	Human papillomavirus
HRP	Horse radish peroxidase

HUVEC	Human umbilical vein endothelial
IBD	Inflammatory bowel disease
IBMX	Isobutylmethylxanthine
ICER	Inducible cAMP early repressor
Ig	Immunoglobulin
IFN	Interferon
ifu	Infectious unit
IHC	Immunohistochemical
IκB	Inhibitory κB
IKK	IκB kinase
IL	Interleukin
JAK	Janus kinase
JH	JAK homology
JNK	c-Jun NH ₂ -terminal kinase
KIR	Kinase inhibitory region
KSFM	Keratinocyte serum free medium
LB	Luria-Bertani
LB^{Amp}	LB supplemented with ampicillin
LB^{Kan}	LB supplemented with kanamycin
LB^{Tet}	LB supplemented with tetracycline
LIF	Leukaemia inhibitor factor
LIFR	LIF receptor
LIMK	LIM kinase
LPS	Lipopolysaccharide
mAb	Monoclonal antibody
MAP	Microtubule-associated protein
MAPK	Mitogen activated protein kinase
MAPKK	Mitogen activated protein kinase kinase

MAPKKK	Mitogen activated protein kinase kinase kinase
MEF	Murine embryonic fibroblasts
MEM	Minimal essential medium (Eagle's)
memIL-6R	Membrane-associated IL-6 receptor
MeOH	Methanol
MG132	Carbobenzoxy-L-leucyl-L-leucyl-L-leucinal
MMP	Matrix metalloproteases
MOI	Multiplicity of infection
MT	Microtubule
mycRaf1:ΔER	myc-tagged Raf1:oestrogen receptor chimera
myrPKI₁₄₋₂₂	Myrsitoylated PKA inhibitor 14-22 amide
NE	Neuroendocrine
NEM	N-ethyl maleimide
NFκB	Nuclear factor kappa B
NGF	Nerve growth factor
NK	Natural killer
NLS	Nuclear localisation signal
NPF	nucleation-promoting factors
NPN	Neuropontin
NSAID	Non-steroidal anti-inflammatory drug
NSE	Neuron-specific enolase
ORF	Open reading frame
OSM	Oncostatin M
OSMR	OSM receptor
pAb	Polyclonal Ab
PACAP	Pituitary adenylyl cyclase activating protein
PAGE	Polyacrylamide gel electrophoresis
PBS	Phosphate buffered saline

PBST	PBS containing 0.1 % (v/v) Tween 20
PCa	Prostate cancer
PDE	Phosphodiesterase
PE	Phycoerythrin
PIAS	Protein inhibitors of activated STATs
PKA	Protein kinase A
PKA-C	Constitutively active PKA
PKC	Protein kinase C
PKN	Protein kinase novel
PLC	Phospholipase C
PLD	Phospholipase D
PMSF	Phenylmethanesulphonyl fluoride
pRb	Retinoblastoma protein
PSA	Prostate-specific antigen
pSer	Phospho-serine
pThr	Phospho-threonine
pTyr	Phospho-tyrosine
qRT-PCR	Quantitative real time polymerase chain reaction
R	Regulatory subunit of PKA
RA	Ras-associating
RArt	Rheumatoid arthritis
Rec	Receptor
Rec*	Activated receptor
REM	Ras-exchange motif
RGS	Regulators of G-protein signalling
rhu	Recombinant human
RIPA	Radio-immunoprecipitation assay
RNS	Reactive nitrogen species

ROCK	Rho-associated protein kinase
ROS	Reactive oxygen species
RPMI	RPMI 1640 medium
SDS	Sodium dodecyl sulphate
SFK	Src family kinases
SH	Src homology
SHP	SH2-containing phosphatase
sIL-6R	Soluble IL-6R
SOCS	Suppressor of cytokine signalling
SRE	STAT-responsive element
STAT	Signal transducer and activator of transcription
STAT3-C	Constitutively active STAT3
SUMO	Small ubiquitin-like modifier
TAD	Transactivator domain
t-Bu-SATE	2',5'-dideoxy-3'-AMP-bis(t-Bu-SATE)
TBS	Tris buffered saline
TBST	Tris buffered saline containing 0.1 % (v/v) Tween 20
TBST-M	TBST containing 5 % (w/v) non-fat milk powder
TCA	Trichloroacetic acid
TcR	T-cell receptor
TE	Tris-EDTA buffer
TGF	Transforming growth factor
TLR	Toll-like receptor
TNF	Tumour necrosis factor
TORC	Transducer of regulated CREB
Trk	Tropomyosin-receptor-kinase
U0126	1,4-Diamino-2,3-dicyano-1,4- <i>bis</i> (2-aminophenylthio)butadiene
Ub	Ubiquitin

UC	Ulcerative colitis
V	Verprolin homology
VEGF	Vascular endothelial growth factor
VIP	Vasoactive intestinal peptide
WAS	Wiskott-Aldrich syndrome
WASP	WAS protein
WAVE	WASP-family verprolin-homologous domain
WHO	World Health Organisation
Y27532	(1)-(R)- <i>trans</i> -4-(1-aminoethyl)-N-(4-pyridyl) cyclohexanecarboxamide dihydrochloride

3 Introduction

3.1 Cancer

Cancer is an ancient disease, detected in human remains from *circa* 2000 BC (Greaves, 2000) and currently describes a group of approximately one hundred potentially fatal conditions accounting for 13% of all global annual deaths (WHO, 2006). The term “cancer” is generically ascribed to the growth of malignant tumours which develop in tissues following abnormal cellular growth and subsequent neoplasm development. The terms neoplasm and tumour are used interchangeably to describe multicellular masses which develop in tissues as a result of abnormal cell growth and can subsequently progress to malignancy dependent on the tumour environment (Pierce & Damjanov, 2006).

Neoplasms are cellular masses composed of parenchymal cells and stroma which grow at an elevated rate with respect to the surrounding normal tissues, regardless of an inciting stimulus. Tumour parenchymal tissue may resemble either normal tissue or be poorly differentiated and undergo rapid proliferation. Contrary to popular belief, the majority of neoplastic cells do not undergo more rapid cell cycle progression in comparison to normal cells but rather neoplasm growth occurs so rapidly due to the larger number of neoplastic cells which are proliferating (Pierce & Damjanov, 2006).

Neoplasm development occurs via a number of stages and requires an initiating stimulus. Stimuli may be mechanical, such as tissue injury, or be chemical in nature, including tobacco smoke and chemical irritants (Coussens & Werb, 2002;Pierce & Damjanov, 2006) and result in a reversible change in cellular phenotype, a process known as metaplasia (Pierce & Damjanov, 2006). Continued stimulation results in changes in cellular organisation and subsequent abnormal growth produces dysplastic tissue which may progress to malignant growth following continued stimulation (Clevers, 2004;Pierce & Damjanov, 2006).

Following development of a solid mass, tumours may be categorised as either benign or malignant neoplasms. Benign tumours are typically composed of well differentiated cells which divide slowly (Pierce & Damjanov, 2006). Morphologically and functionally, benign tumours resemble normal tissue and only rarely cause damage as a result of tumour expansion and compression of normal tissues. In contrast, malignant tumours are

composed of pleomorphic cells of variable shape and size and display an ability to grow uncontrollably, culminating in invasion of adjacent tissue (Pierce & Damjanov, 2006). Growth of malignant cells along tissue spaces, especially nerves, allows invasion of vascular and lymphatic vessels whereupon single or clumps of malignant cells may become detached from the tumour and disseminate to distal tissues via a process known as metastasis. Metastatic cells can then give rise to secondary tumours at sites distinct from the primary tumour (Pierce & Damjanov, 2006). Metastases are associated with over 90% of all cancer-related deaths (WHO, 2006) and thus represent a poor prognosis for the patient.

Cancer arises due to a collection of stochastic events which result in genomic alterations in a cell (van Kempen et al., 2006). Typically, these mutations act to promote cellular proliferation via either gain-of-function mutations in genes which promote progression through the cell cycle (oncogenes) or loss of functions in genes which impede cell cycle progression (tumour suppressor genes) (Hanahan & Weinberg, 2000; Moeller & Sheaff, 2006). As a result of these accumulated genomic changes, cancerous cells are exempt from normal cell cycle control and are able to proliferate indefinitely, a process known as transformation (Hanahan & Weinberg, 2000; Pierce & Damjanov, 2006).

3.1.1 Features of cancerous cells

Despite the vast repertoire of human cancers and the variety of organs which are affected by malignancies, it has been proposed that all cancerous cells share six common characteristics (Hanahan & Weinberg, 2000). The first of these is the ability to grow independently of exogenous growth factors. In culture, growth of normal cells is reliant on the addition of exogenous, soluble growth factors from either medium supplements or from other cell types. The process by which soluble growth factors released from neighbouring cells are able to stimulate the growth of normal cells is known as heterotypic signalling (Hanahan & Weinberg, 2000). Reciprocal heterotypic signalling between cell types allows growth of a diverse cell community. However, growth of cancerous cells frequently occurs independently of heterotypic signalling, thus promoting tumour cell growth over that of normal tissue cells. There are three broad mechanisms by which independence from heterotypic signalling can be achieved. Firstly, cancer cells can themselves produce growth factors which they require for growth and thus stimulate their own proliferation via autocrine signalling (Hanahan & Weinberg, 2000; Okamoto *et al.*, 1997). Secondly, responses to growth factors typically occur downstream of recognition by cell surface receptors. Alteration of either the growth factor receptor intracellular or extracellular

domains, particularly those domains associated with regulating tyrosine kinase activity, can result in growth factor receptors which are constitutively active (Hanahan & Weinberg, 2000). Consequently, intracellular signalling pathways are activated in a growth factor-independent manner, therefore receptor modifications can represent a second mechanism by which cancer cells can be freed from exogenous growth factor requirements. Alteration of integrin expression on cancer cells can also promote proliferation in the absence of growth factors required by normal cells (Hanahan & Weinberg, 2000).

In addition to their ability to proliferate in the absence of heterotypic signalling, cancer cells are also able to proliferate more readily than normal cells due to their insensitivity to normal antigrowth signals. In normal cells, proteins such as the retinoblastoma protein (pRb) and transforming growth factor β (TGF β) inhibit G1 to S phase transition in the cell cycle and thus impede proliferation (Moeller & Sheaff, 2006). Cancer cells frequently lose responsiveness to TGF β and contain mutations in the gene encoding pRb which act to enhance cancer cell growth and proliferation (Hanahan & Weinberg, 2000). Other common features displayed by the majority of cancer cells are an ability to evade apoptosis, an unlimited capacity for replication and the metastatic potential of cancer cells to disseminate to distal tissues and organs (Hanahan & Weinberg, 2000; Pierce & Damjanov, 2006). In order to sustain solid tumour growth, tumour cells also promote sustained angiogenesis within developing tumours *via* elevated levels of the transcription factor, hypoxia-induced factor- (HIF-) 1 α and the pro-angiogenic signalling molecule vascular endothelial growth factor (VEGF) expression (Semenza, 2000).

3.1.2 Development of cancer

Cancer cells have distinctly different growth profiles compared to normal cells due to the progressive accumulation of mutations within the genome of malignant cells (Hanahan & Weinberg, 2000). However, mutations need to accumulate in a number of specific genes in order to produce a malignant phenotype. Considering that maintenance of genomic integrity is a highly efficient process, accumulation of the required array of mutations by a single cell would be expected to occur rarely (Hanahan & Weinberg, 2000). The rate of cancer in the global population is greater than would be expected if cancer arose solely by random mutation, thus factors other than mutation must predispose cells to malignancy. It has been proposed that precancerous cells have an inherently unstable genome due to mutation of the p53 tumour suppressor protein (Hanahan & Weinberg, 2000). In normal cells, p53 acts to impede cell cycle progression in the presence of DNA damage until such

a time that the damage has been repaired (Hussain & Harris, 2006). In circumstances where the DNA damage is so extensive as to be irreparable, p53 initiates apoptosis of the damaged cell and so prevents inheritance of genomic alterations (Moeller & Sheaff, 2006). Mutations in p53 are amongst the most common associated with carcinogenesis (Hussain & Harris, 2006) and may thus represent a mechanism by which premalignant cells become transformed and subsequently expand into a solid tumour. Of relevance to this project, mutations in the gene encoding p53 have been correlated with exposure to conditions associated with chronic inflammation (Hussain & Harris, 2006).

3.2 Inflammation

The inflammatory response is a critical response to infection and is characterised by the four cardinal symptoms of pain, heat, redness and swelling of the affected tissue (Sullivan & Linden, 1998). This pro-inflammatory phenotype arises in tissues due to localised vasodilation and disruption of the vascular endothelium, resulting in tissue oedema and sequestration of circulating leukocytes. Activation of tissue-localised leukocytes further propagates the inflammatory response via the release of mediators including cytokines, chemokines and lipid mediators, and subsequently results in the clearance of infection (Sullivan & Linden, 1998).

There are numerous factors which can induce inflammation in response to pathogen invasion. These include the Toll-like receptors (TLRs) expressed on a variety of leukocytes including lymphocytes, natural killer (NK) cells, peripheral blood mononuclear cells and antigen presenting cells (Muzio & Mantovani, 2001). Members of this receptor family recognise specific pathogen virulence motifs and include TLR2 and TLR4 which are involved in the recognition of bacterial surface antigens (Muzio & Mantovani, 2001). Additionally, pathogens can activate the complement cascade, either via antibody recognition or directly binding via lipopolysaccharide (LPS) or surface sugar residues (Mollnes et al., 2002), resulting in an inflammatory response (Gerard & Gerard, 2002). Some pathogens, such as *Aspergillus fumigatus*, contain proteases which are able to directly cleave some complement components, namely the C3 and C5 components (Nagata & Glovsky, 1987). Cleavage of C3 and C5 results in the release of the C3a and C5a anaphylatoxins (Nagata & Glovsky, 1987; Wetsel et al., 2000) which are potent inflammatory mediators and act at their respective G-protein coupled receptors (GPCRs) to mediate pro-inflammatory events. Anaphylatoxins can promote inflammation via directly promoting chemotaxis and activation of leukocytes or indirectly via the induction of cytokine release (Gerard & Gerard, 2002; Mollnes et al., 2002; Wetsel et al., 2000).

Irrespective of the mechanism by which the inflammatory response is activated, the ultimate goal is to clear infection. However, a prolonged, systemic inflammatory response can be fatal as evidenced by the 53-63% mortality associated with individuals suffering from septic shock (Balk, 2000). Chronic inflammation is implicated in the pathophysiology of numerous diseases including rheumatoid arthritis, sepsis and atherosclerosis (Gomez & Sitkovsky, 2003; Sands & Palmer, 2005; Shouda *et al.*, 2001; Sitkovsky, 2003). Tissue remodelling and changes in cellular responses are frequently associated with persistent inflammation. Similar alterations are seen during malignancy development and thus chronic inflammatory responses are frequently associated with carcinogenesis.

3.3 Chronic Inflammation and Cancer

Inflammation has been proposed to play a key role in carcinogenesis since the 19th century when Virchow described inflammatory cell infiltrates in solid tumours (Moss & Blaser, 2005). Several links between cancer and inflammation have been described since this hypothesis was originally suggested. Chronic inflammation contributes to both initial tumourigenesis and subsequent promotion of tumour growth via multiple mechanisms (Fig. 1).

3.3.1 Chronic inflammation promoting carcinogenesis can arise due to a multitude of factors

Gastric cancer is the second most common fatal human malignancy and is responsible for 12% of all cancer deaths (Schottenfeld & Beebe-Dimmer, 2006). Initiation of gastric cancer is one of the first to be directly attributed to a chronic inflammatory response perpetuated in response to chronic infection with the Gram negative bacterium *Helicobacter pylori* (Moss & Blaser, 2005; Schottenfeld & Beebe-Dimmer, 2006). Infection can promote carcinogenesis via multiple mechanisms, including ligand-independent activation of intracellular signalling cascades, release of pro-inflammatory cytokines and secretion of anti-pathogen antibodies (Moss & Blaser, 2005). Chronic antibody secretion has been associated with an antibody-dependent initiation of tumourigenesis in *de novo* skin carcinogenesis arising from chronic inflammation in mice expressing the E7 protein of human papillomavirus (HPV) (de Visser *et al.*, 2005).

In addition to *H. pylori*, other infectious agents promote a chronic inflammatory response and potentiate carcinogenesis. Incidence of hepatocellular carcinoma (HCC) is strongly

associated with chronic hepatitis arising due to persistent Hepatitis C or Hepatitis B virus infection (Schottenfeld & Beebe-Dimmer, 2006). Other infectious agents associated with a chronic inflammatory response and subsequent tumourigenesis include *Schistosoma haematobium* which is associated with bladder cancer, HPV types 16 and 18 which are involved in cervical cancer (Schottenfeld & Beebe-Dimmer, 2006) and the LMP1 protein of Epstein Barr virus which is associated with nasopharyngeal carcinoma (Tsao et al., 2002).

Chronic inflammation also contributes to the development of cancer independently of infection. Several chronic inflammatory diseases are associated with an increased risk of cancer. One such disease is ulcerative colitis (UC), a form of inflammatory bowel disease (IBD) associated with inflammation of the intestinal epithelium and an increased risk of developing colorectal carcinoma (Greten et al., 2004). Inflammation-induced activation of the NF κ B signalling pathway has been shown to potentiate tumour development in a murine model of non-virally-induced HCC (Pikarsky et al., 2004). Numerous other inflammatory diseases are associated with carcinogenesis including oesophageal cancer and gastroesophageal reflux, gall bladder cancer and choleostatis-induced inflammation and prostate cancer (PCa) and inflammatory atrophy (Schottenfeld & Beebe-Dimmer, 2006).

3.3.2 Chronic inflammation contributes to carcinogenesis via numerous mechanisms

As described above, chronic inflammation can contribute directly to carcinogenesis arising due to infections and chronic inflammatory diseases such as IBD and inflammatory atrophy. Following the establishment of chronic inflammatory responses, there are several mechanisms by which carcinogenesis can be promoted (Fig. 3.1).

Activation of phagocytic cells such as macrophages or neutrophils can induce respiratory burst which results in the generation of reactive oxygen (ROS) and reactive nitrogen species (RNS). ROS and RNS are free radicals and the high levels of these compounds present during a chronic inflammatory response can be sufficient to overwhelm endogenous antioxidants, resulting in damage to cellular proteins and DNA (Finkel & Holbrook, 2000; Jackson *et al.*, 2002; Jezek & Hlavata, 2005). Consequently, signalling through pathways may be altered and genetic mutations may arise, contributing to cancer development. ROS generation has been associated with skin carcinogenesis

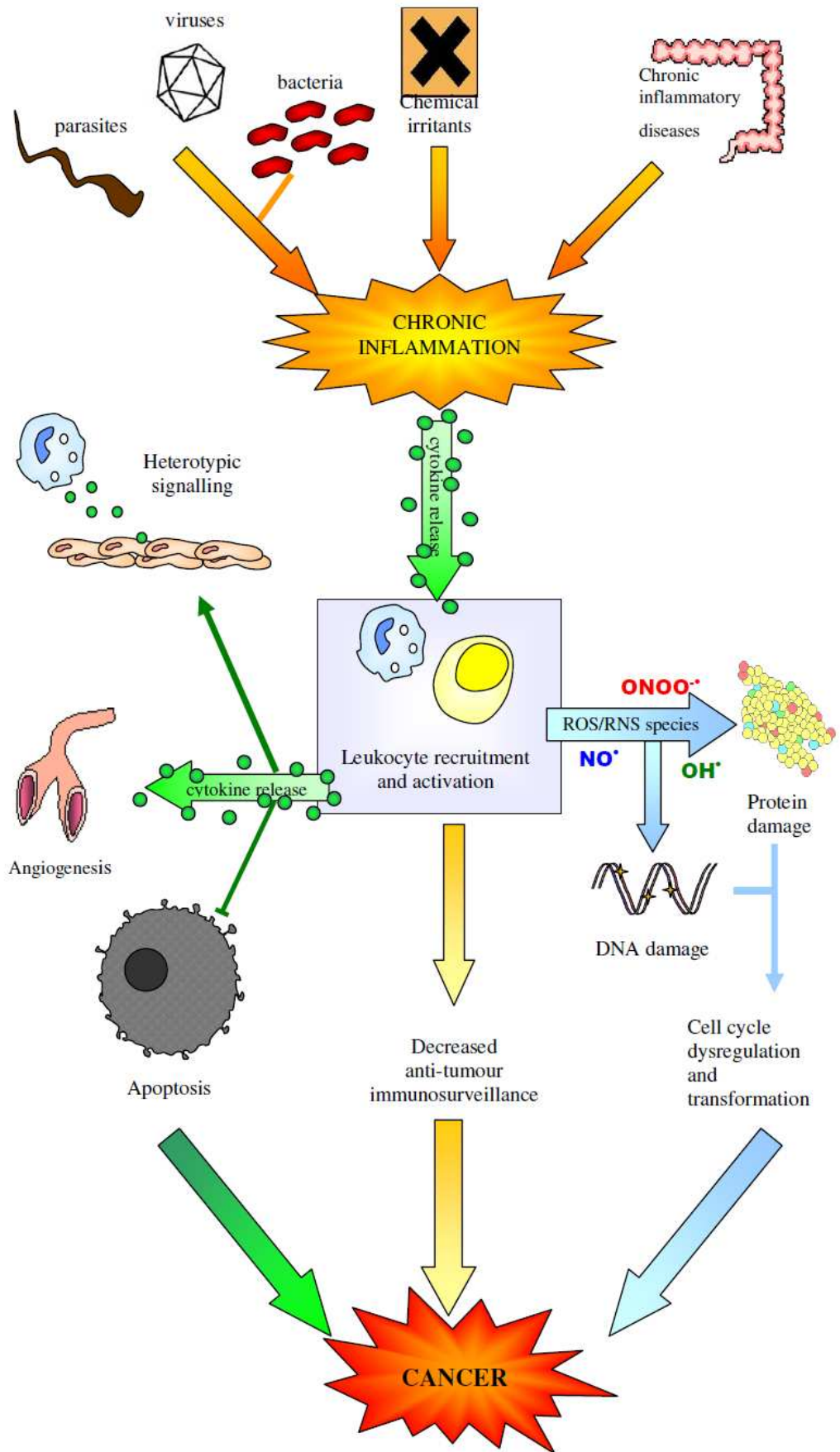


Figure 3.1: Mechanisms by which chronic inflammation can contribute to carcinogenesis

(Dhar *et al.*, 2002). In addition, generation of NO can regulate tumourigenesis and is hypothesised to promote mutations in p53, resulting in cell cycle dysregulation and subsequent risk of cancer development (Hussain & Harris, 2006).

A further mechanism by which inflammation can contribute indirectly to cancer development is to facilitate the recruitment and activation of leukocytes which promote tumour growth via heterotypic signalling. In the inflammation-induced model of CAC described above, deletion of IKK β in myeloid cells resulted in both a 50% decrease in tumour incidence and also a decrease in overall tumour size (Greten *et al.*, 2004). This result suggests that a pro-inflammatory microenvironment is important for initial tumourigenesis and that activation of NF κ B in myeloid cells promotes subsequent tumour growth (Greten *et al.*, 2004). Similarly, in breast carcinomas, elevation of the chemokine CCL2 is associated with accumulation of tumour-associated macrophages and is believed to promote release of macrophage-derived growth and angiogenic factors such as VEGF and Interleukin- (IL-) 8 (CXCL8) to promote tumour growth. It has been suggested that CCL2 also promotes initial tumourigenesis *in vivo* in breast carcinoma models (Rollins, 2006). The pro-inflammatory chemokines CXCL12 and CCL25 have also been similarly implicated in cancer progression (Rollins, 2006).

In addition to the role in which chronic inflammation can play in promoting tumour progression, the inflammatory tumour microenvironment can also act to prevent surveillance and subsequent removal of cancerous cells by the immune system. T-lymphocytes and natural killer (NK) cells play important roles in the immunosurveillance of tumours. However, within a chronic pro-inflammatory environment, T-lymphocyte and NK cell immunosurveillance can be dysfunctional due to multiple reasons including decreased T-cell receptor (TcR) activation (Baniyash, 2006), decreased natural killer (NK) cell activation (Oppenheim *et al.*, 2005) emergence of anti-inflammatory regulatory T-cells and release of IL-10 and tumour growth factor β (TGF β) which promote immune tolerance (Basoni *et al.*, 2005; Bergmann *et al.*, 2007; Laouar *et al.*, 2005; Li *et al.*, 2006a; Steinbrink *et al.*, 1997). Treatment with TGF β inhibitors is being developed as an anti-cancer therapy to alleviate tumour-induced immunosuppression and so accelerate the removal of cancerous cells (Wojtowicz-Praga, 2003).

Activated leukocytes have also been associated with tumour metastases via the release of matrix metalloproteases (MMPs) and subsequent degradation of the extracellular matrix, enabling tumour expansion into interstitial spaces (van Kempen et al., 2006). MMP expression is correlated with the expression of specific chemokine receptors in multiple malignancies (van Kempen et al., 2006). Whilst this is somewhat expected in haematopoietic malignancies, the expression of chemokine receptors in epithelial malignancies implies a role for chemotaxis during cancer progression and is hypothesised to play a role in directing metastasis (Rollins, 2006).

3.3.3 The NFκB pathway links inflammation to cancer

Another method by which inflammation can promote tumour progression is via activation of the nuclear factor kappa B pathway (NFκB), one of the key intracellular pathways activated in response to inflammatory stimuli including LPS, viruses and cytokines such as IL-1β and tumour necrosis factor (TNF) α (Karin, 2006; Osborn *et al.*, 1989). Activation of NFκB and subsequent altered gene expression has been shown to form a mechanistic link between inflammatory signalling and cancer (Karin, 2006).

There are five members of the NFκB transcription family, RelA, RelB, c-Rel, p50/NFκB1 and p52/NFκB2 which all contain a Rel homology domain (RHD). The RHD facilitates multiple functions including DNA binding whilst the transactivation domain found in RelA (p65), RelB and c-Rel enables them to initiate transcription of NFκB-regulated genes. In contrast, NFκB1 and NFκB2 lack transactivator activity and require dimerisation with one of the other family members in order to initiate gene transcription (Bhoj & Chen, 2009). In the absence of stimulation, NFκB family members remain dormant in the cytoplasm of cells due to association with inhibitor of NFκB (IκB) proteins (Fig. 3.2). Several members of the IκB family exist, with IκBα, β and ε being of most importance in mammalian systems due to the presence of N-terminal regions required for signal induced degradation (Karin & Ben Neriah, 2000). Cellular interaction with an inciting stimulus, increases activity of the IκB kinase (IKK) complex as a result of hierarchal protein activation and degradation incorporating signalling molecules such as the IRAK1/TRAF6 complex and the TAB1/TAB2/3/TAK1 complex (Bhoj & Chen, 2009). The IKK complex consists of the IKKα and IKKβ catalytic subunits and is regulated by the IKKγ subunit. IKKγ interacts with IKKβ and is required for full activation of the IKK complex although the mechanism by which IKKγ regulates IKK activation is unknown (Hacker & Karin, 2006; Rothwarf *et al.*, 1998). Phosphorylation of IκB occurs primarily due to IKKβ kinase activity and creates a binding site for the SCF^{βTrCP} ubiquitin ligase, resulting in polyubiquitination and

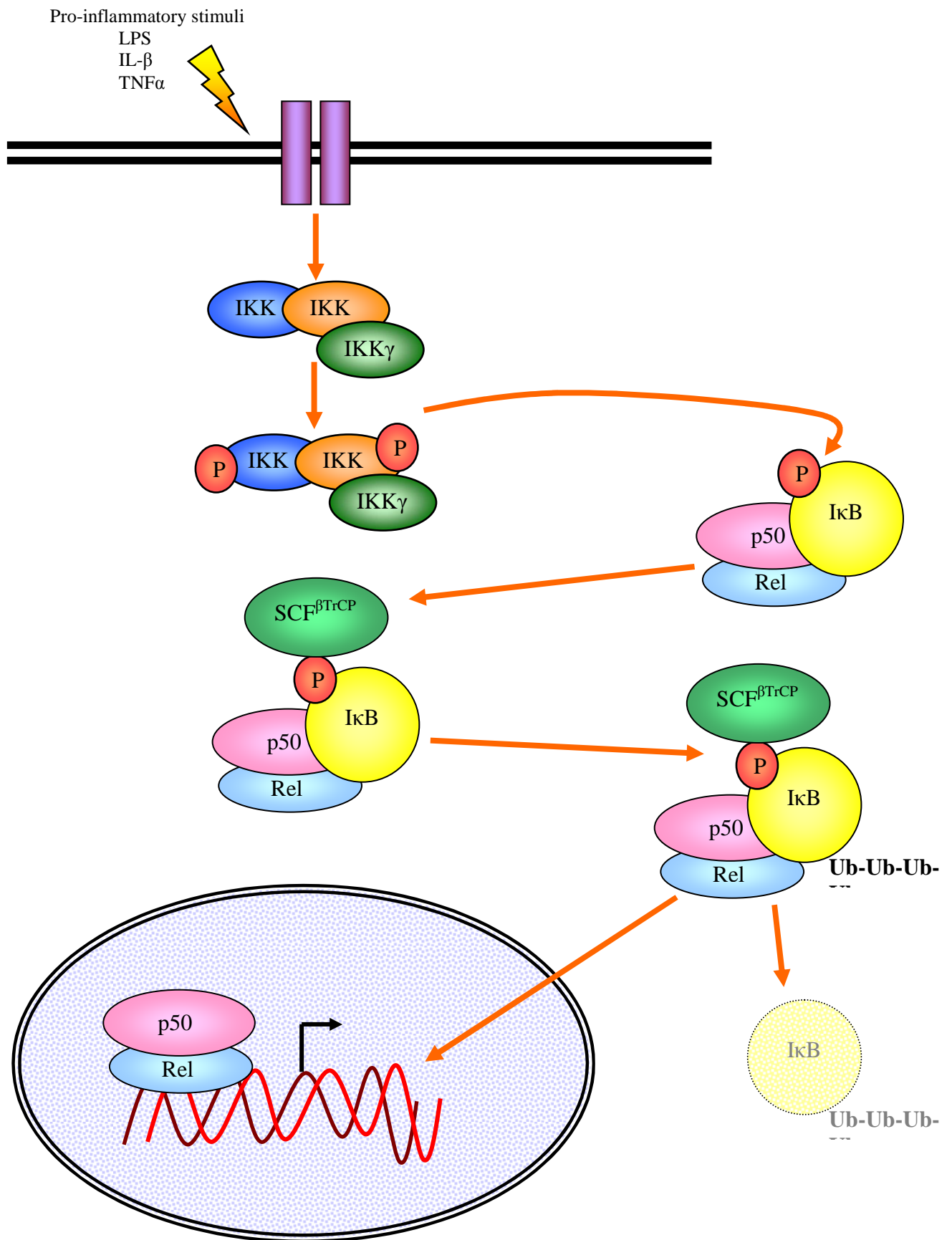


Figure 3.2: Activation of NFκB signalling via the classical IKK-IκB pathway

Pro-inflammatory stimuli result in activation of the IKK complex, resulting in IκB phosphorylation and subsequent polyubiquitination and degradation. The released NFκB transcription factors translocate to the nucleus and activate transcription

proteasomal degradation of the I κ B (Hatakeyama *et al.*, 1999;Karin, 2006). The released NF κ B dimers are then able to translocate to the nucleus and activate transcription of NF κ B-regulated genes including the pro-proliferative cytokine IL-6 and anti-apoptotic proteins such as Bcl-X_L and the caspase 8 inhibitor c-FLIP (Karin, 2006).

IKK γ -mediated activation of IKK β is frequently referred to as the classical pathway of NF κ B activation and results in activation of I κ B α -bound dimers within minutes of pro-inflammatory stimulation (Hacker & Karin, 2006). A non-classical pathway of NF κ B activation involving NF κ B-inducing kinase (NIK), IKK α and NF κ B2 activation has been described, although this pathway is found mainly in B-cells and is reviewed in Bhoj and Chen (Bhoj & Chen, 2009;Hacker & Karin, 2006;Ling *et al.*, 1998).

In murine models of UC, it has been suggested that initial development of colitis-associated carcinoma (CAC) is due to activation of the NF κ B signalling pathway, a key pathway activated during signal transduction downstream of pro-inflammatory stimuli. In this study, Greten *et al* (Greten *et al.*, 2004) demonstrated that deletion of IKK β in intestinal epithelial cells resulted in a 75% decrease in tumour incidence in response to chronic inflammatory stimuli in comparison to control animals in which IKK β function was maintained (Greten *et al.*, 2004). IKK β is a component of the NF κ B pathway which is essential for NF κ B activation downstream of pro-inflammatory cytokine stimulation, thus activation of NF κ B in response to chronic inflammation can drive tumourigenesis in CAC (Greten *et al.*, 2004). The pro-oncogenic role of NF κ B activation in CAC was hypothesised to be due to the anti-apoptotic activities of NF κ B. Deletion of IKK β in the intestinal epithelium resulted in greater areas of apoptosis in response to inflammatory stimulus in comparison to littermate control animals. This increase in apoptosis was shown to be independent of p53 or sustained JNK activity, but was hypothesised to involve alterations in the activation of the anti-apoptotic factor Bcl-X_L. IKK β deletion animals showed decreased induction of Bcl-X_L compared to control specimens (Greten *et al.*, 2004). However, there was no observed difference in the size of tumours between the two animals groups, suggesting that NF κ B signalling in intestinal epithelial cells does not play a vital role in maintaining tumour growth but is more important in initial tumorigenesis (Greten *et al.*, 2004). Inflammation-induced activation of the NF κ B signalling pathway in a murine model of non-viral-induced HCC promoted tumour growth via protecting cancerous cells from apoptosis (Pikarsky *et al.*, 2004).

To summarise, although the inflammatory response is vital for the clearance of infection, unsuccessful resolution of acute inflammation can result in chronic inflammation which can be detrimental. Whether arising from persistent infection or from inflammatory diseases, chronic inflammation can act to promote carcinogenesis, tumour progression and metastasis via a number of distinct mechanisms. There are numerous well-established links between inflammation and the progression of various cancers and treatments involving antioxidants and non-steroidal anti-inflammatory drugs (NSAIDs) have been effective complements to traditional chemotherapy (Thun et al., 2002). Thus, further understanding and manipulation of the inflammatory response may be of future benefit when treating human cancers.

3.4 Interleukin-6 Family Cytokines

3.4.1 Interleukin –6 cytokine family

The term cytokine describes a group of extracellular proteins of approximately 200 amino acids which mediate intercellular signalling and regulate a vast array of physiological phenomena ranging from immune functions to cellular survival (Chow et al., 2002). The IL-6 family of cytokines play an important role in governing haematopoiesis (Heinrich *et al.*, 2003) and regulate a number of cellular functions including differentiation, proliferation and apoptosis (Heinrich *et al.*, 2003; Mitsuyama *et al.*, 2006). Members of the IL-6 cytokine family traditionally include IL-6, IL-11, leukaemia inhibitory factor (LIF), oncostatin M (OSM), cardiotrophin-1 (CT-1), cardiotrophin-like cytokine (CLC), neuropoietin (NPN) and ciliary neurotrophic factor (CNTF) with IL-27 and IL-31 recently entering this family (Heinrich *et al.*, 2003; Mitsuyama *et al.*, 2006).

All IL-6 family member cytokines require the gp130 signal transduction molecule for efficient intracellular signal transduction following interaction of the cytokines with their cognate receptors (Chow et al., 2002). The receptors function typically as tetramers, consisting of two molecules of a non-signalling receptor which recognises the cognate cytokine and two monomers of signal transducing receptors. In case of the IL-6 receptor, IL-6R α forms the non-signalling receptor and the fully activated signalling complex is formed from two monomers each of IL-6, IL-6R α and gp130, although other members of the family form different higher order signalling complexes (Bravo & Heath, 2000). The formation of these high affinity receptor signalling complexes is dominated by the interaction between the cytokine and its non-signalling receptor (Bravo & Heath, 2000). Each member of the IL-6 cytokine family displays the characteristic up-up-down-down

four helix cytokine topology, comprising two pairs of antiparallel helices joined by polypeptide loops (Heinrich *et al.*, 2003). All four helices are straight within IL-6 and IL-11, whilst OSM, LIF and CNTF have a kink in helix A (starred in Fig. 3.3) which may account for differences in receptor complex recruitment and quaternary structure (Heinrich *et al.*, 2003;Skiniotis *et al.*, 2008).

The interaction between human growth hormone (hGH) and its receptor (hGHR) has long been the paradigm for receptor-cytokine interaction, in which hGH interacts with hGHR via two distinct sites (Bravo & Heath, 2000). However, the IL-6 family cytokines are thought to diverge from this model due to three points of interaction between the cytokine and its receptor (Fig. 3.3). The three sites involved in the recognition of the receptor signalling complex by IL-6 are termed Site I, Site II and Site III. Members of the IL-6 cytokine family engage their signalling receptors *via* interaction with Sites II and III whilst Site I is involved in a relatively high affinity interaction with the non-signalling receptor (Bravo & Heath, 2000). The use of Site I to recognise the non-signalling receptor may represent a mechanism by which IL-6 cytokine family members overcome low affinity interactions at Site II with the signalling receptors such as gp130 (Bravo & Heath, 2000).

As indicated in Fig. 3.3, the different receptor interaction sites of IL-6 occupy distinct regions with Site I being located on helix D, Site II comprising a cluster of residues in helices A and C and Site III being formed by F156 and K159 and is involved with interaction of the Ig-like domain of gp130 (Bravo & Heath, 2000;Chow *et al.*, 2001b). Site I in IL-6 and IL-11 is dominated by an arginine residue towards the C-terminus of helix D which is thought, based on similarities to the IL-4/IL-4R α interaction, to form a salt bridge with an aspartate residue on IL-6R α (Bravo & Heath, 2000). A conserved glycine residue is central to Site II and, due to a lack of side chain, forms a hydrophobic pocket within the site to interact with the cytokine receptor homology domain of gp130 (Bravo & Heath, 2000). Successful cytokine-receptor interaction initiates the formation of the higher order signalling complexes required for intracellular signal transduction (Chow *et al.*, 2001a).

3.4.2 The IL-6 family cytokine receptors

The IL-6 family cytokine receptor family can be divided into two groups, dependent on their role in signal transduction. The non-signalling α -receptors IL-6R α , IL-11R α and CNTFR α are responsible for binding their respective ligands and are required for effective signal transduction (Bravo & Heath, 2000;Heinrich *et al.*, 2003). In contrast, LIFR and

OSM do not require non-signalling receptors for effective ligand-receptor interaction and can interact directly with the signalling receptors (Heinrich *et al.*, 2003). LIFR, OSMR and gp130 comprise the signalling receptors of the IL-6 cytokine family and are responsible for activation of intracellular signal transduction (Heinrich *et al.*, 2003). All IL-6 family cytokines require at least one molecule of gp130 for efficient commencement of cellular responses. IL-6 and IL-11 signal via gp130 homodimers whilst the remaining IL-6 family cytokines signal via gp130/LIFR heterodimers (Fig. 3.4). OSM is unique amongst this family due to its ability to recruit a gp130/OSMR heterodimer for signal transduction (Heinrich *et al.*, 2003). It has recently been suggested that IL-27 signals via a unique gp130/WSX-1 heterodimer (Pflanz *et al.*, 2004). The signalling receptors lack intrinsic kinase activity and so are reliant on constitutively associated Janus kinases (JAKs) for effective signal transduction. JAK1, JAK2 and Tyk2 have all been shown to activate intracellular signalling downstream of IL-6 family cytokines (Heinrich *et al.*, 2003).

Interaction between cytokine receptors and their cognate ligand and subsequent receptor activation is mediated by a number of extracellular motifs. All family members contain a cytokine receptor homology domain (CHD) consisting of a seven-stranded β -sandwich which contains a signature WSXWS sequence in the second, C-terminal motif (Bravo & Heath, 2000) and mediates protein-protein interactions (Bischoff *et al.*, 1992). OSMR and LIFR contain two CHD motifs whilst gp130 and all three non-signalling receptors possess only a single CHD (Bravo & Heath, 2000). Interaction between a non-polar CHD residue and the hydrophobic cleft of site II is proposed to be important in receptor recognition of cytokines. The presence of an Ig-like domain at the C-terminus of the membrane proximal CHD has been detected in all IL-6 family cytokine receptors and mediates interaction with site III on the cytokine (Bravo & Heath, 2000). In the case of IL-6 signalling, the presence of the Ig-like domain is required for formation of the hexameric signalling complex (Chow *et al.*, 2001b)

The third and final motif conserved across all IL-6 family cytokine receptors consists of arrays of fibronectin type III domains which play an undefined role in mediating IL-6 family cytokine receptor signalling. Truncation of these domains attenuates cytokine-mediated signalling and it is hypothesised that the domains position gp130 transmembrane domains in proximity (Skiniotis *et al.*, 2005). Indeed, the fibronectin domains of gp130 have been shown to bend towards each other when complexed with IL-6 and IL-6R α and thus enable initiation of intracellular signalling (Skiniotis *et al.*, 2005). Association of

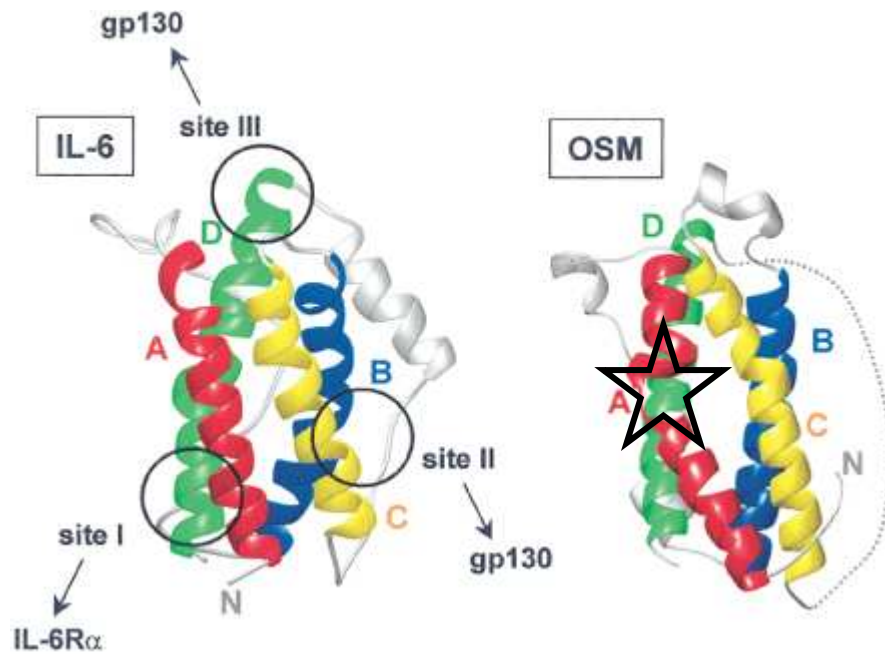


Fig. 3.3: Ribbon structures of IL-6 and OSM

The ribbon structures of IL-6 (left) and OSM (right) indicating the position of the four helices. The sites of interaction with IL-6R α and gp130 are circled on the structure of IL-6. The kink in helix A of OSM is indicated with a star.

Taken from Heinrich, P.C. *et al.* (2003)

gp130 transmembrane domains is critical in facilitating signal transduction and forced dimerisation of these domains can activate intracellular signalling and act to inhibit embryonic stem cell differentiation in the absence of cytokine (Stuhlmann-Laeisz et al., 2006).

Following successful cytokine-receptor interaction, IL-6 family cytokines activate intracellular signalling via the JAK-STAT pathway (see section 3.3). IL-6 signals primarily through activation of STAT3 but can also activate STAT1 following IL-6-IL-6R interaction. In addition to coupling to the JAK-STAT pathway, IL-6 family receptors can also activate mitogen activated protein kinase (MAPK) signalling. LIFR can activate the Ras/Raf/extracellular signal-regulated kinase 1/2 (ERK1/2) pathway in a manner independent of the classical LIFR/JAK/STAT pathway and subsequently acts to arrest growth of medullary thyroid cancer cells (Park et al., 2003). OSM can activate the p38 MAPK, ERK1/2 and c- Jun N-terminal kinase (JNK) following successful activation of OSMR. Tyr 861 of OSMR is required for activation of each of these different signalling molecules and JAK1 is essential for initiation of p38 activity (Boing et al., 2006). The Src-homology 2- (SH2-) containing phosphatase SHP2 has been shown to act as an adapter linking the IL-6R to ERK activation (Terstegen et al., 2000). SHP2 interacts with pTyr759 of gp130 and acts to recruit Gab1 which, in turn, is involved in the activation of ERK1/2 (Takahashi-Tezuka *et al.*, 1998). Gab1 also acts with SHP2 to recruit components of the ERK5 signalling cascade to gp130 (Nakaoka et al., 2003), a pathway required for cardiomyocyte hypertrophy induced by CT-1 (Takahashi-Tezuka *et al.*, 1998). Interestingly, activation of ERKs via protein kinase C (PKC) has been shown to decrease IL-6-induced STAT1 and STAT3 phosphorylation in manner dependent on Tyr759 of gp130. This residue is the site of suppressor of cytokine signalling (SOCS) 1 and SOCS3 recruitment to gp130 and it is proposed that ERK activation can induce SOCS3 expression and so act to attenuate JAK-STAT signalling (Terstegen et al., 2000) (see section 3.5)

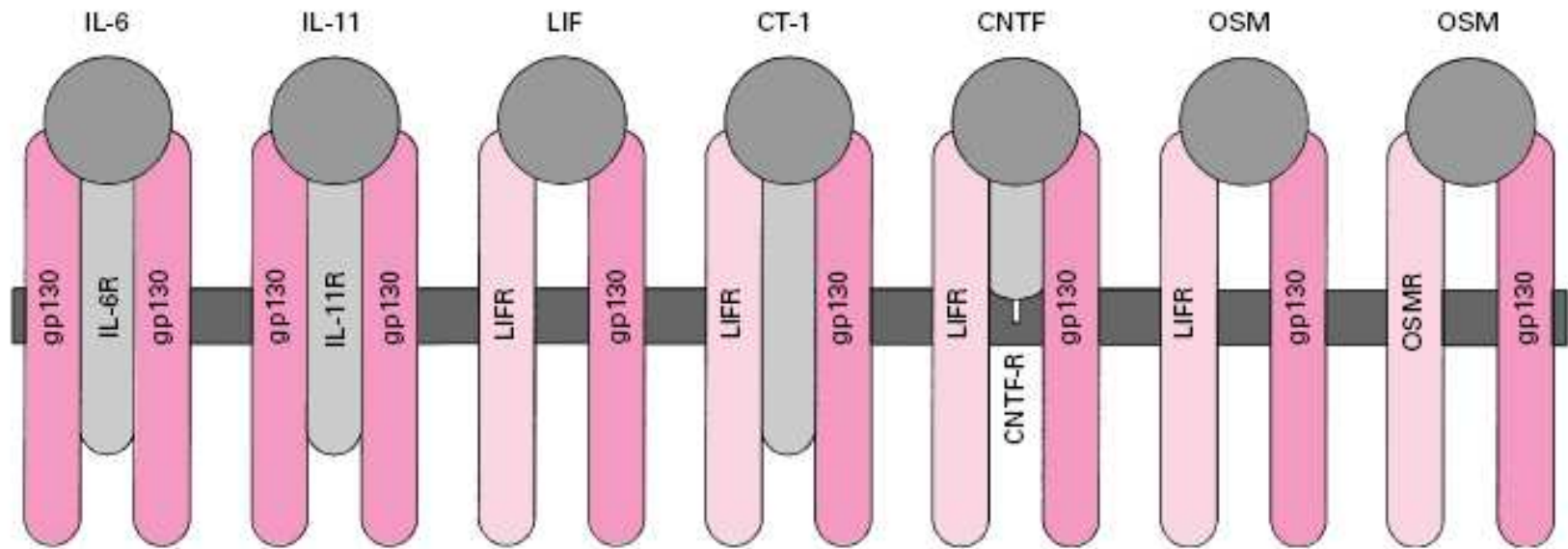


Fig. 3.4: The IL-6 family cytokine receptors.

Cytokines are represented as grey circles whilst the α -receptors are shown in light grey. Signal transducing receptors are shown in light pink (LIFR and OSMR) or dark pink (gp130). IL-6 and IL-11 signal *via* gp130 homodimers whilst other members of the IL-6 cytokine family utilise heterodimers containing gp130 and either LIFR or OSMR.

Taken from Heinrich, P.C. *et al.* (2003)

3.4.3 IL-6 trans-signalling

The IL-6 family cytokines play a crucial role in regulating key physiological responses and thus can activate a variety of cell types. The presence of non-signalling receptors acts to increase the pool of target cells due to a phenomenon known as trans-signalling, which has been best described for IL-6 (Kallen, 2002). The IL-6R α /gp130 complex is expressed by some cells as a membrane bound form (memIL-6R) and mediates intracellular signalling following binding of IL-6 (Kallen, 2002). However, the expression of memIL-6R is relatively restricted whilst expression of gp130 is ubiquitous. A soluble form of IL-6R containing the non-signalling IL-6R α (sIL-6R α) can be released and acts to increase the pool of IL-6 responsive cells (Scheller *et al.*, 2006). Release of sIL-6R α can arise from either shedding of memIL-6R by a cell surface-localised sheddase or as a result of protein expression arising from alternative splicing of memIL-6R mRNA (Kallen, 2002). Circulating IL-6 interacts with sIL-6R α and becomes recruited to gp130 homodimers expressed on cells, resulting in activation of intracellular signalling and perpetuation of the inflammatory response.

Interestingly, it is possible that sIL-6R α can also play an anti-inflammatory role by “mopping up” excess circulating IL-6 (Mitsuyama *et al.*, 2006). Shedding of sIL-6R α is enhanced in inflammatory conditions and thus promotes formation of IL-6/sIL-6R α complexes which can interact with gp130 on cell surfaces. However, a soluble form of gp130 has also been described. Interaction of IL-6/sIL-6R α complexes with this soluble form of gp130 would remove the complexes from the circulation and prevent them from interacting with cellular gp130 to promote cell signalling. In this context it appears that sIL-6R α is acting to “mop up” excess IL-6 and so attenuate activation of IL-6 signalling pathways (Kallen, 2002).

3.4.4 IL-6 and disease states

Given the ability of IL-6 to activate signalling through the JAK-STAT pathway, it is hardly surprising that elevation of IL-6 is correlated with numerous inflammatory conditions. Increased IL-6 concentrations have been associated with an increased frequency of atherosclerotic plaque rupture and subsequent risk of ischaemic stroke (Yamagami *et al.*, 2004). Elevation of both circulating and intestinal IL-6 concentrations has been detected in patients with IBD. Increased mucosal and serum IL-6 levels correlate with active IBD and treatment with anti-IL-6R monoclonal antibodies ameliorates symptoms in a model of ulcerative colitis (Mitsuyama *et al.*, 2006). Due to the elevation of IL-6 levels in active

IBD it may be possible to use IL-6 concentrations as a marker for disease severity in a manner similar to that proposed for ankylosing spondylitis (Bal et al., 2007). Furthermore IL-6 has been shown to be important in other inflammatory diseases including rheumatoid arthritis, diabetes mellitus, multiple sclerosis, Alzheimer's disease and heart disease (Deepa *et al.*, 2006;Kallen, 2002;Koenig *et al.*, 2006;Shouda *et al.*, 2001).

In addition to the role of IL-6 in inflammatory diseases, the cytokine has also been associated with various malignancies. Increased IL-6 concentrations have been detected in colorectal carcinomas and levels are associated with disease severity and tumour progression (Esfandi *et al.*, 2006). The growth of cholangiocarcinomas is also potentiated by IL-6 due to aberrant promoter methylation (Wehbe et al., 2006). IL-6 has long been thought to act as a potent growth factor in multiple myeloma (Hodge *et al.*, 2005) but use of IL-6 as a marker for disease progression may not be reliable (Greco et al., 1994). Increased serum IL-6 in metastatic breast carcinoma is correlated with the degree of metastasis and worse survival (Salgado et al., 2003). Similarly, in prostate carcinoma, IL-6 is associated with cachexia and an increased risk of fatality arising from malignancy development without treatment (Kuroda *et al.*, 2007). Furthermore, increased IL-6 levels can indicate a poor prognosis (Nakashima *et al.*, 2000) and are frequently observed in hormone refractory prostate carcinoma which represents an advanced stage of prostate carcinoma associated with metastasis to the bone and other organs (Crawford et al., 1999).

Given the association of elevated IL-6 levels with numerous inflammatory conditions and malignancies, it is unsurprising that the signalling pathways downstream of the IL-6R have been the focus of much research. As mentioned above, activation of the IL-6R complex primarily promotes activation of the JAK-STAT and ERK1/2 signalling cascades.

3.5 The JAK-STAT pathway

Inflammatory responses are perpetuated by the actions of specific cytokines at their cognate receptors. In section 3.1, the role of the NF κ B was discussed as a signalling pathway downstream of receptors for inflammatory stimuli such as LPS and IL-1. However, whilst activation of the NF κ B pathway may occur early in the inflammatory response, it is by now means the only signalling pathway the inflammatory response.

In addition to NFκB, one of the principal pathways involved in signal transduction downstream of cytokine receptors is the JAK-STAT pathway, which is comprised of the Janus kinases (JAKs) and the signal transducers and activators of transcription proteins (STATs) (Aaronson & Horvath, 2002). Cytokines binding to the class I or II cytokine receptors typically mediate their effects via activation of the JAK-STAT intracellular signalling cascade (Kotenko & Pestka, 2000). Class I and II cytokine receptors are categories within a group of receptors which lack kinase domains in their intracellular domain and require an associated kinase for signal transduction. There is little difference in the tertiary structures between class I and II cytokine receptors, rather the receptors are classified dependent on the cellular responses they elicit (Krause & Pestka, 2005). Class I cytokine receptors are typically involved in regulating the differentiation or expansion of tissues and include the IL-6 family cytokines whereas class II receptors are involved in limiting damage following a tissue insult and include the IFN receptors (Kotenko & Pestka, 2000; Krause & Pestka, 2005). In the case of the IL-6 receptor family, gp130 is associated with both JAK1 and JAK2 in the absence of IL-6 stimulation, indicating a constitutive association between JAKs and the gp130 signalling molecule (Lutticken *et al.*, 1994; Stahl *et al.*, 1994). Tyk2 is also activated by IL-6 as indicated by an increase in phosphorylated Tyk2 following IL-6 stimulation (Stahl *et al.*, 1994).

3.5.1 Janus Kinases

To date, four JAK family members have been described in mammals, birds and fish, comprising JAK1, JAK2, JAK3 and Tyk2 (Kotenko & Pestka, 2000; Leonard & O'Shea, 1998). Encoded by genes comprising approximately 20 exons, JAKs are relatively large proteins with a molecular mass ranging between 120–140 kDa, rendering study of their 3D structure somewhat challenging (Yamaoka *et al.*, 2004). However, primary structure analysis indicates that JAKs contain seven conserved domains known as the JAK homology (JH) domains 1-7 (JH1-7) (Fig. 3.5). Numbered from the carboxyl-terminus, JH1 displays significant homology to typical eukaryotic tyrosine kinase domains, the sequence of which is mostly associated with tyrosine kinases belonging to the Src/epidermal growth factor (EGF) receptor family (Yamaoka *et al.*, 2004). The JH1 domain contains the activation loop which impedes substrate access in the absence of tyrosine phosphorylation (Leonard & O'Shea, 1998). In the case of JAK3, autophosphorylation of Tyr⁹⁸⁰ within the activation loop is associated with an increase in kinase activity. However, autophosphorylation of tyrosine residues within the activation loops of JAKs is not necessarily associated with activation of JAK kinase activity as

autophosphorylation of Tyr⁸⁹¹ of JAK3 negatively regulates kinase activity (Zhou *et al.*, 1997).

The JH2 domain is believed to encode a pseudokinase domain which, despite lacking kinase activity, is hypothesised, to regulate function of the JH1 domain. In a mechanism analogous to other protein tyrosine kinases, an intramolecular interaction between JH1 and JH2 within JAK2 is proposed to inhibit JH1 activity in the absence of stimulus (Saharinen *et al.*, 2003). Successful cytokine receptor interaction results in a conformational alteration that relieves JH1 inhibition, rendering the JAK catalytically active and competent for signal transduction. Interestingly, deletion of JH2 elevates basal JH1 activity but also liberates JAK activation from the constraints of ligand-dependent activation (Saharinen *et al.*, 2003). The JH3 and JH4 domains together comprise an SH2-like domain which, in other proteins, acts as a docking site for tyrosine phosphorylated proteins. At the amino-terminus, JH6-7 form a 300 amino acid Protein 4.1, ezrin, radixin, moesin (FERM) domain which has been implicated in interactions with transmembrane proteins, including cytokine receptors (Yamaoka *et al.*, 2004).

3.5.2 Signal transducers and activators of transcription

There are seven described mammalian members of the STAT protein family; STAT1, STAT2, STAT3, STAT4, STAT5a, STAT5b, and STAT6, all of which are involved in mediating signal transduction downstream of cytokine receptors. STAT1, STAT3, STAT4, STAT5a, and STAT5b range in size from 750-795 amino acid whilst STAT2 and STAT6 are approximately 850 amino acids in length due to the presence of an extended C-terminal region (Darnell, 1997). Despite the difference in C-terminal length, all STAT proteins display conservation of domain organisation with each family member containing a dimerisation domain, a STAT family DNA binding domain (DBD), an SH2 domain and a transactivation domain (Fig. 3.6) (Becker *et al.*, 1998;Hoey & Schindler, 1998).

Following receptor-ligand interaction and subsequent JAK activation, STATs become activated via JAK-mediated phosphorylation on a conserved Tyr located at approximately residue 700 such as Tyr⁷⁰¹ and Tyr⁷⁰⁵ of STAT1 and STAT3 respectively (Darnell, 1997;Hoey & Schindler, 1998). In the case of STAT3 activation arising from IL-6-IL-6R interaction, a conserved pTyr-X-X-Gln motif on gp130 acts as the STAT3 binding site (Lim & Cao, 2006). Activated STATs form V-shaped homo- or heterodimers mediated by

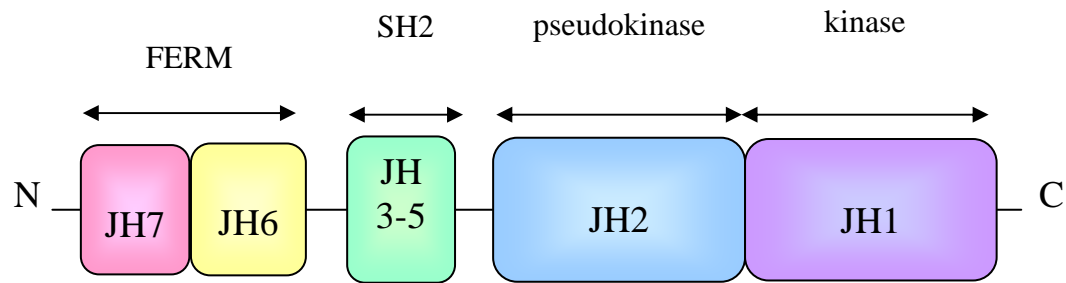


Fig 3.5: JAK domain organisation

Schematic representation (not to scale) of the structure of JAKs indicating the organisation of the kinase, pseudokinase, SH2 and FERM domains.

the N-terminal region of the STAT proteins with the dimerisation interface located at the apex of the V (Hoey & Schindler, 1998). Reciprocal interaction between the pTyr of one STAT monomer and the central SH2 domain of the other facilitates STAT dimerisation, which is required for nuclear import. Several STAT structural features including the DBD, N-terminus and coiled-coil domains have been implicated in regulating nuclear import of STAT dimers (Lim & Cao, 2006; Liu *et al.*, 2005; Ma & Cao, 2006). Nuclear-localised STAT dimers are able to directly induce expression of STAT-responsive genes such as VEGF due to the presence of the C-terminal DBD. The DBD contains a stretch of acidic amino acids and structurally resembles p53 and NFκB due to the presence of an Ig-fold (Hoey & Schindler, 1998). The transactivation domain of many of the STAT proteins contains a conserved Ser residue, corresponding to Ser⁷²⁷ in STAT1 and STAT3. Along with protein kinase Cδ, the p38, ERK1/2 and JNK MAP kinases are all able to phosphorylate this residue. Serine phosphorylation is required for full activation of STAT-mediated transcription but does not enhance STAT DNA binding activity (Lim & Cao, 2006). In contrast, p300/CBP-mediated acetylation of Lys685 of STAT3 enhances nuclear import, DNA binding and transactivation of STAT3 responsive genes (Wang *et al.*, 2005).

3.5.3 Activation of the JAK-STAT pathway

The mammalian STAT proteins are activated following receptor-ligand interaction between class I or II cytokine receptors and their cognate ligand (Kotenko & Pestka, 2000). Such cytokine receptors typically exist as pre-formed dimeric pairs that lack intrinsic kinase activity. Thus, although the receptor is able to bind cytokine, successful signal transduction is reliant on the presence of constitutively associated JAKs (Heinrich *et al.*, 2003; Krebs & Hilton, 2001; van de Geijn *et al.*, 2004). Ligand binding is thought to induce receptor clustering and thus brings JAKs associated with neighbouring receptors into close proximity. JAK activation is achieved following auto- and *trans*-tyrosine phosphorylation events on juxtaposed JAKs, rendering them competent for initiating signal transduction (Aaronson & Horvath, 2002; Kimura *et al.*, 2004; Krebs & Hilton, 2001). In the case of JAK3, autophosphorylation of Tyr⁹⁸⁰ is associated with an increase in kinase activity (Zhou *et al.*, 1997). Analogous tyrosine residues are located at positions 1054 and 1055 in Tyk2, indicating a common form of regulation (Gauzzi *et al.*, 1996). Such a hypothesis is confirmed by evidence that mutation of Tyr¹⁰³³ but not Tyr¹⁰³⁴ of JAK1 results in decreased ligand-independent phosphorylation of STAT5a in COS7 cells (Liu *et al.*, 1997). JAK3-mediated phosphorylation of a peptide corresponding to the activation loop of JAK1 demonstrated that alanine substitution of Tyr¹⁰³³ is poorly phosphorylated by JAK3 (Wang *et al.*, 2003). These results suggest that JAKs are able to phosphorylate other family

members and that the first Tyr residue in the YY doublet is important in JAK activation. Interestingly the FERM domain of JAKs has also been implicated in regulation of JAK kinase activity. In the case of JAK1, mutation of Tyr²⁸¹ and Tyr¹¹² within the FERM domain is associated with enhanced basal and IFN γ -induced phosphorylation of the kinase (Haan *et al.*, 2008). Activated JAKs phosphorylate the intracellular domains of the cytokine receptor on conserved tyrosine residues. These phosphotyrosine (pTyr) residues can then act as docking sites for the intracellular signalling molecules involved in the signal transduction cascade. In the case of gp130, JAK1-mediated phosphorylation of Tyr⁷⁵⁹ is associated with recruitment and subsequent activation of the SH2-containing phosphatase (SHP) -2 (Schaper *et al.*, 1998).

STAT proteins associate with receptor pTyr residues via an interaction between the pTyr and the central SH2 domain found in all STAT proteins (Calo *et al.*, 2003; Shuai *et al.*, 1994). The specificity of the receptor-STAT interaction is thought to arise from sequence variation within the STAT SH2 domain, which enables the STATs to recognise different phosphorylated motifs (Leonard & O'Shea, 1998). For instance, STAT1 is activated downstream of the activated IFN γ receptor via interaction with a pTyr-Asp-Lys-Pro-His motif between residues 440 and 444 but can also be activated downstream of IL-6R (Greenlund *et al.*, 1995; Hemmann *et al.*, 1996). It has been demonstrated that two pTyr-X-Pro-Gln motifs at Tyr⁹⁰⁵ and Tyr⁹¹⁵ of a chimeric erythropoietin/gp130 receptor (Eg) act as sites for STAT1 recruitment via its SH2 domain. STAT3 was also recruited to Eg following receptor activation but bound to motifs associated with Tyr⁷⁶⁷ and Tyr⁸¹⁴ in addition to the Tyr⁹⁰⁵ and Tyr⁹¹⁵ motifs described for STAT1. Mutation of a conserved arginine in the STAT SH2 domain abolished STAT-Eg interaction, indicating that this domain is essential for interaction of STATs with activated receptors (Hemmann *et al.*, 1996). The differential ability of these STAT recruitment sites to bind STAT1 or STAT3 is due to structural differences in the SH2 domain of the STAT proteins. Unlike STAT3, binding of STAT1 to receptor phosphotyrosines requires the presence of the downstream Pro-Gln sequence in order to correctly position the glutamate residue. The binding pocket of the STAT3 SH2 domain is larger than that of STAT1 and so can accommodate the large glutamate side chain without the requirement for proline-mediated positioning (Hemmann *et al.*, 1996). Receptor-associated STATs then undergo phosphorylation by activated JAKs on conserved tyrosine residues in the transactivation domains, corresponding to Tyr⁷⁰¹ in STAT1 (Shuai *et al.*, 1993) and Tyr⁷⁰⁵ in STAT3 (Calo *et al.*, 2003; Kaptein *et al.*, 1996).

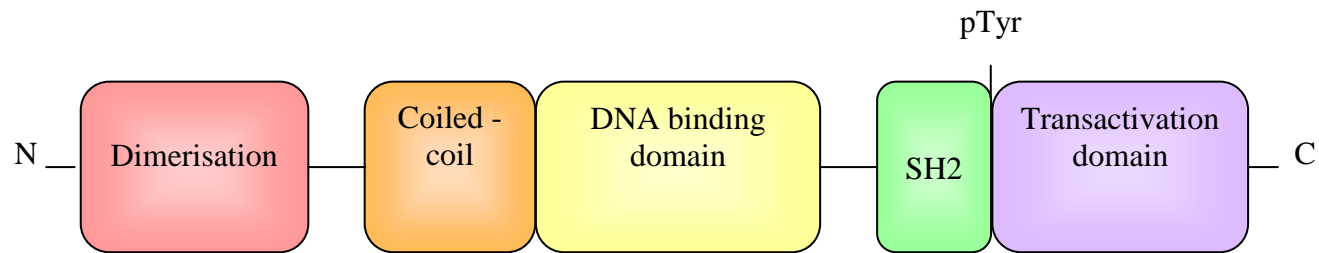


Fig. 3.6: Domain organisation of STAT proteins

Schematic representation (not to scale) of STAT protein domain organisation indicating the relative positions of the dimerisation, coiled-coil, DNA binding, SH2, conserved Tyr and transactivation domains.

Tyrosine phosphorylated STATs then dissociate from the receptor and dimerise via reciprocal interaction between the pTyr of one STAT monomer and the SH2 domain of the other to form STAT homo- and heterodimers (Lim & Cao, 2006). Although the exact mechanism governing STAT dissociation from the activated receptor is unclear, it has been suggested that the nature of the interaction between two STAT monomers is preferable to that between the individual STAT monomers and their docking site and so formation of the first STAT pTyr – STAT SH2 coupling acts to displace STATs from the receptor. In addition to dimerisation, tyrosine phosphorylation is required for successful nuclear translocation of STATs (Calo *et al.*, 2003). STAT dimers directly activate transcription via binding of a β -sheet rich DNA binding domain STAT binding consensus sequences (Calo *et al.*, 2003). The 9-10 bp motifs bound by STAT dimers are typically semipalindromic sequences known as IFN γ -activated sequence (GAS) motifs or STAT-responsive elements (SREs) and have the consensus sequence TTCN₍₃₋₄₎GAA (Leonard & O'Shea, 1998). The DNA binding activity of STATs can be enhanced via association with the p300/CREB-binding protein complex which is thought to acetylate STAT3 at Lys685 (Wang *et al.*, 2005). Acetylation at this residue also augments nuclear accumulation and transcriptional activation of STAT3 although the mechanism by which this occurs is currently unknown (Wang *et al.*, 2005). Additionally, serine phosphorylation potentiates the activity of the transactivation domain but does not affect binding of the activated STAT to DNA (Lim & Cao, 1999; Lim & Cao, 2006).

In addition to JAK-mediated phosphorylation, STATs can also become activated via SFK-mediated tyrosine phosphorylation (Ingleby & Klinken, 2006). This is particularly important in malignant diseases as STAT3 activation is an important event in Src-mediated transformation (Smith & Crompton, 1998).

3.5.4 The role of JAK-STAT in disease

The JAK-STAT pathway is an important pathway involved in signal transduction of downstream of cytokine receptors (Aaronson & Horvath, 2002; Kotenko & Pestka, 2000; Krause & Pestka, 2005). Thus it is of little surprise that dysregulation of JAK-STAT activity has been associated with diseases associated with chronic inflammatory conditions (Elliott & Johnston, 2004; Pernis & Rothman, 2002; Shouda *et al.*, 2001). For example, targeted JAK-STAT inactivation is being investigated as a potential therapeutic strategy in the treatment of rheumatoid arthritis (RArt) due to the detection of elevated IL-6 levels in the synovial fluid of patients with RArt and the ability of this cytokine to induce synovial cell proliferation, exacerbating the disease (Shouda *et al.*, 2001). JAK-STAT activation has

also been implicated in airway hyper-responsiveness in patients with chronic asthma (Pernis & Rothman, 2002). The JAK3-selective inhibitor, CP-690550 promotes immunosuppression in both non-human primates and murine models of inflammation due to a reduction in circulating NK-1.1⁺ cells (Conklyn *et al.*, 2004; Kudlacz *et al.*, 2004). CP-690550 is currently in clinical trials to assess its efficacy as an immune modulator in stable renal allograft patients (van Gurp *et al.*, 2009).

Given the association of JAK-STAT activation with chronic inflammatory diseases, it is hardly surprising that this pathway has also been implicated in a variety of malignancies. Constitutive activation of STAT5a/b has been associated with many neoplasms, especially haematological malignancies (Calo *et al.*, 2003). STAT1 has been proposed as a tumour suppressor whilst activation of STAT3 has been associated with neoplastic progression and inhibition of apoptosis (Calo *et al.*, 2003). The Hodgkin lymphoma-derived cell lines HDLM-2 and L540 display elevated JAK phosphorylation and increased tyrosine phosphorylated STAT1, STAT3, STAT5 and STAT6. The elevation in tyrosine phosphorylated STATs was correlated with constitutive association of STATs with DNA, suggestive of sustained expression of STAT-responsive genes such as the anti-apoptotic Bcl-X_L. Indeed, inhibition of continuous JAK-STAT activity resulted in elevated apoptosis and decreased levels of the anti-apoptotic proteins Bcl-X_L and Bax (Cochet *et al.*, 2006). SOCS-1 deficient mice also display STAT3 hyperactivity and spontaneously develop colorectal carcinomas in an IFN γ -dependent manner (Hanada *et al.*, 2006). STAT3 hyperactivation is also associated with human gastric carcinoma (To *et al.*, 2004) and abnormal dendritic cell differentiation in cancer (Nefedova *et al.*, 2004). Many STAT3-responsive genes are implicated in apoptosis, cell cycle progression and promotion of tumour growth including Bcl-X_L, cyclin D1 and VEGF (Cochet *et al.*, 2006; Leslie *et al.*, 2006; Xu *et al.*, 2005). In prostate carcinoma, autocrine IL-6 stimulation and elevated STAT3 phosphorylation is associated with resistance to apoptosis, androgen-independent growth and metastasis (Barton *et al.*, 2004; Culig *et al.*, 2005; Michalaki *et al.*, 2004; Shariat *et al.*, 2001). Currently, multiple strategies are being investigated to inhibit STAT activation in cancer including inhibition of JAK activity, anti-sense oligonucleotides to STAT mRNA and inhibition of STAT dimerisation (Jing & Tweardy, 2005). Cucurbitacin B is a plant-derived compound which profoundly inhibits activation of STAT3 and STAT5 in human pancreatic cancer cell lines. Treatment with Cucurbitacin B is also associated with an increase in apoptosis and a decrease in Bcl-X_L expression and synergises with gemcitabine, a chemotherapeutic which acts to both inhibit DNA synthesis and promote apoptosis, to prevent cellular growth (Mini *et al.*, 2006; Thoennissen *et al.*, 2009). More

relevant to a new therapeutic, Cucurbitacin B acts to impede xenograft growth *in vivo* as well as displaying *in vitro* efficacy (Thoennissen *et al.*, 2009). Additionally, the use of decoy oligonucleotides has been investigated as a means to inhibit STAT-responsive gene expression in malignancies. These oligonucleotides resemble the SRE found within the promoter regions of STAT-responsive genes and interact with activated STAT dimers, thus competitively blocking interaction with chromosomal STAT-responsive promoters and so impair STAT-mediated gene transcription. Recently, intramuscular administration of a STAT3 decoy oligonucleotide has been shown to inhibit both phosphorylation of STAT3 and cyclin D1 expression in non-human primates and did not display any systemic or localised signs of toxicity. Combined with observations that STAT3 decoy oligonucleotides can inhibit cancer cell proliferation both *in vitro* (Zhang *et al.*, 2007) and *in vivo* (Xi *et al.*, 2005), this therapeutic strategy is currently very attractive as a new treatment for solid tumours.

3.5.5 Negative Regulation of JAK-STAT

Due to their crucial role in mediating signal transduction downstream of pro-inflammatory cytokine receptors and the damaging effect of chronic inflammatory responses, it is necessary to strictly regulate JAK-STAT activation. Several mechanisms have been described by which attenuation of JAK-STAT activity can be achieved, including post-translational modifications, protein degradation and inhibition of protein binding to both receptors and DNA.

3.5.5.1 Dephosphorylation

Due to the crucial role for tyrosine phosphorylation in promoting STAT dimerisation and subsequent transactivator activity, it is not surprising that this stage of STAT activation represents a locus at which STAT activity can be modulated. The SH2-containing phosphatases SHP-1 and SHP-2 have both been implicated in regulating the direct dephosphorylation of STATs. SHP-1 has been shown to decrease tyrosine phosphorylation of STAT6 in response to IL-4 stimulation by targeting cytoplasmic phospho-STAT6 (pSTAT6) for dephosphorylation (Hanson *et al.*, 2003). Similarly, SHP-2 has been shown to directly dephosphorylate cytoplasmic pSTAT5 (Yu *et al.*, 2000). In addition to its role in direct dephosphorylation of STATs, SHP-1 has also been shown to impede JAK-STAT signal transduction at the level of JAKs. SHP-1 can impede JAK phosphorylation following their recruitment to receptors (Starr & Hilton, 1999) and also targets JAK1 in the HTB26 breast cancer cell line for degradation via a proteasome-dependent pathway (Wu *et al.*, 2003). It is also possible to inhibit tyrosine phosphorylation independently of SHP-1 or SHP-2 activity via activation of the JNK MAPK. JNK activity is induced by cellular

stresses and acts to promote phosphorylation of Ser⁷²⁷ in STAT3 (Lim & Cao, 1999). In the same study however, tyrosine phosphorylation of STAT3 and subsequent DNA binding and transcriptional activation was impeded via a mechanism dependent on JNK activation (Lim & Cao, 1999). Interestingly, stimulation of the Jurkat T-cell line activates the protein tyrosine phosphatase CD45 which is associated with recruitment of the downstream of kinase (DOK) -1 protein. Over-expression of DOK-1 in the K562 leukaemic cells line attenuates IL-3 and IFN α -induced activation of JAK1, JAK2 and STAT5. It is hypothesised that, upon activation, CD45 recruits DOK-1 to the cell surface where DOK-1 acts as an adaptor to recruit SHP-1 and so negatively regulate JAK-STAT signalling *via* promotion of protein phosphorylation (Wu *et al.*, 2009).

3.5.5.2 Polyubiquitylation

The ubiquitin-proteasome system plays a crucial role in regulating levels of cellular proteins via controlled protein degradation. Proteasome-mediated regulation of STAT levels has been described for several members of the family. IFN γ -induced activation of STAT1 promoted poly-ubiquitylation of tyrosine phosphorylated STAT1 (pTyr⁷⁰¹STAT1) and levels of the protein were stabilised in the presence of proteasome inhibitors, indicating a role for proteasomal degradation in regulating STAT proteins (Kim & Maniatis, 1996). Degradation of activated STAT5a in the nucleus of 32D cells occurs due to polyubiquitylation by the E3 ubiquitin ligase Ubc5 and is dependent on proteasomal function (Chen *et al.*, 2006). An amphipathic helix between residues 751 and 762 acts as a transcriptional activation domain and is necessary for Ubc5-mediated polyubiquitylation of STAT5a (Chen *et al.*, 2006). The recently identified protein SLIM is a nuclear protein which acts to regulate levels of STAT1 and STAT4 via its E3 ubiquitin ligase activity (Tanaka *et al.*, 2005). Over-expression of SLIM results in impaired STAT1 and STAT4 signalling due to a decrease in STAT protein levels. Conversely, deficiency in SLIM levels results in elevation of STAT proteins levels and enhanced transcriptional responses (Tanaka *et al.*, 2005). Furthermore, treatment with osteopontin leads to SLIM-mediated STAT1 degradation and a decrease in STAT1-responsive genes in RAW264.7 macrophages, indicating a role for STAT polyubiquitylation in the regulation of immune function (Gao *et al.*, 2007). Stable expression of the deubiquitinating enzyme DUB-2 also results in prolonged STAT5 phosphorylation and impedes apoptosis following withdrawal of IL-2 (Migone *et al.*, 2001).

3.5.5.3 SOCS proteins

The suppressor of cytokine signalling (SOCS) proteins comprise eight mammalian proteins designated CIS and SOCS1-7 that are directly induced by activated STATs and so act to

attenuate cytokine-induced JAK-STAT signalling via functioning as part of a classical negative feedback loop (Crocker *et al.*, 2003;Fischer *et al.*, 2004;Kile & Alexander, 2001;Kimura *et al.*, 2004;Naka *et al.*, 1997;Starr *et al.*, 1997). The SOCS proteins are characterised by a C-terminal 40 amino acid “SOCS box” and a central SH2 domain, whilst the N-termini show greater diversity in both length and primary sequence between individual family members (Kile & Alexander, 2001). Of all eight members, the mechanisms by which SOCS1 and SOCS3 inhibit JAK-STAT signalling have been most intensely studied. SOCS1 associates with the activation loop of phosphorylated JAKs via the central SH2 domain of SOCS1 (Endo *et al.*, 1997). SOCS1 and SOCS3 both contain a 12 residue kinase inhibitory region (KIR) which is required for inhibition of JAK activity (Yasukawa *et al.*, 1999). The KIR of both proteins resembles the activation loop of JAKs and is proposed to act as a pseudosubstrate, occluding the active site of JAKs and thereby preventing phosphorylation of JAK substrates to attenuate JAK-STAT signalling (Endo *et al.*, 1997;Kile & Alexander, 2001;Yasukawa *et al.*, 1999). Although SOCS1 is reported to associate with cytokine receptors via interaction with JAKs, SOCS3 recruitment requires tyrosine phosphorylation of receptor cytoplasmic chains in order to inhibit JAK activity (Ilangumaran *et al.*, 2004). The recruitment of SOCS3 to receptor pTyr residues represents a second mechanism by which SOCS proteins attenuate JAK-STAT signalling (Kile & Alexander, 2001). Both CIS1 and SOCS3 have been proposed to sterically hinder recruitment of signalling molecules, including STATs, to activated receptors via binding to membrane proximal receptor pTyr residues (Ilangumaran *et al.*, 2004). Finally, the SOCS proteins form ubiquitin E3 ligases due to the ability of the SOCS box to interact with elongins B and C, cullins 2 and 5, Roc1/Rbx1 and an E2 ubiquitin conjugating enzyme (Johnston, 2004;Kamura *et al.*, 1998). The SOCS E3 ligase can subsequently target proteins with which it interacts for polyubiquitin-mediated proteasomal degradation and so act to attenuate signal transduction at the level of protein stability. For example, JAK2 can be targeted for degradation by SOCS-mediated polyubiquitylation (Johnston, 2004;Kile & Alexander, 2001).

3.5.5.4 PIAS proteins

The protein inhibitors of activated STATs (PIAS) proteins comprise a family of five proteins, PIAS1, PIAS3, PIAS α , PIAS β and PIAS γ (Liao *et al.*, 2000;Rogers *et al.*, 2003). PIAS1 and PIAS3 inhibit signalling following STAT1 and STAT3 activation and act to attenuate responses to IFNs and IL-6 respectively (Liao *et al.*, 2000). The PIAS1-STAT1 association is dependent on STAT1 phosphorylation and dimerisation and involves a direct interaction between residues 392-541 of PIAS1 and residues 1-191 of STAT1

(Liao *et al.*, 2000). The N-terminal region of PIAS1 is implicated in regulating this interaction despite not interacting directly with STAT1 (Liao *et al.*, 2000). The N-terminal region of PIAS proteins contains a LXXLL motif, corresponding to L²⁰-Q²¹-M²²-L²³-L²⁴ of PIASy (Liu *et al.*, 2001). In the case of PIASy, this motif is required for inhibition of STAT1 transactivator activity but not for interaction with STAT1 (Shuai & Liu, 2005). PIAS proteins are able to both positively and negatively regulate cellular signalling pathways, principally via altering transcriptional activation. PIAS1 can inhibit STAT1 binding to DNA and thus impede transcription of STAT-1-responsive genes whilst PIASx inhibits IL-12-induced activation of STAT4-responsive genes via recruitment of histone deacetylases (HDACs) and subsequent chromatin remodelling (Shuai & Liu, 2005). PIAS proteins are also able to act as small ubiquitin-like modifier (SUMO) E3 ligases and SUMOylation of STAT proteins has been implicated in regulating their transactivator activity. In the case of PIAS1-mediated SUMOylation of STAT1, SUMOylation at Lys⁷⁰³ is associated with a decrease in transcription from STAT1 promoter genes (Ungureanu *et al.*, 2005). In addition, PIAS proteins can recruit the CBP/p300 complex to target proteins such as Smad3 which can potentiate Smad3 transcriptional activation in response to TGFβ (Long *et al.*, 2004).

With respect to STAT proteins, PIAS interaction has, thus far, been shown to attenuate JAK-STAT signalling with interactions described between STAT1, STAT3 and STAT4 and PIAS1, PIAS3 and PIASx respectively (Shuai & Liu, 2005). Additionally, an interaction between PIASy and STAT1 has been described (Liu *et al.*, 2001; Shuai & Liu, 2005; Starr & Hilton, 1999). PIAS1 and PIAS3 block the DNA binding activity of STAT1 and STAT 3 whilst PIASy and PIASx are believed to act primarily by recruiting co-repressor molecules such as HDACs in order to repress STAT1 and STAT4 signalling (Liu *et al.*, 2001; Shuai & Liu, 2005). The SUMO E3 ligase activity of PIAS proteins has also been implicated in the negative regulation of cellular signalling. For example, PIASx-β-mediated SUMOylation of p53 acts to impede the activity of p53 (Shuai & Liu, 2005). PIAS1 has been demonstrated to SUMO modify STAT1 on Lys703 but *in vitro* and *in vivo* studies indicate that SUMOylation of STAT1 does not alter transcriptional activation (Rogers *et al.*, 2003). Mutation of Lys703 does not alter the ability of either STAT1 to induce expression of STAT1-responsive genes or the capacity of PIAS1 to act as an inhibitor of STAT signalling (Rogers *et al.*, 2003; Song *et al.*, 2006). Thus it is currently unclear what role PIAS-mediated SUMOylation plays in the regulation of JAK-STAT signalling.

3.5.5.5 Methylation

Arginine methylation of various STAT proteins has been implicated in the regulation of JAK-STAT signalling. Methylation of STAT6 at Arg27 augments IL-4-mediated STAT6 phosphorylation, nuclear transport and transcriptional activity (Chen *et al.*, 2004). Similarly, STAT1 activation induced by IFN α/β is enhanced by arginine methylation at Arg31 (Mowen *et al.*, 2001). However, this data is somewhat controversial and thus it is currently unclear whether arginine methylation genuinely acts to modulate STAT activation.

Activation of the JAK-STAT pathway is regulated *via* a number of distinct mechanisms which may not be surprising given the crucial nature of this signalling pathway in inflammation and cellular survival. Aberrant or sustained activation of STAT signalling contributes to the pathology of multiple disease and thus inhibition of these signalling molecules represents an attractive therapeutic strategy. With regards to malignant disease, inhibition of STAT3 signalling in particular has been investigated as a treatment strategy and pharmaceuticals targeting this pathway may well prove a vital addition to complement the current arsenal of chemotherapeutics.

3.6 The MAP kinases

The mitogen-activated protein kinases (MAPKs) form a group of evolutionary conserved, proline-targeted serine/threonine kinases that have been identified in prokaryotic and eukaryotic organisms (Fox & Smulian, 1999; Turjanski *et al.*, 2007; Wang & Tournier, 2006). Due to their activation by growth factors and cellular stress, MAPK signalling cascades play essential roles in regulating vital cellular functions including proliferation, migration, differentiation and apoptosis (Turjanski *et al.*, 2007). To date, eleven members of the MAPK family have been described in humans which can be further sub-divided into 6 groups based on their sequence homology (Turjanski *et al.*, 2007). Full activation of MAPKs is achieved via phosphorylation on the conserved TXY activation motif arising from sequential activation of MAPK-kinase-kinases (MAPKKKs) and MAPK-kinases (MAPKKs). The currently described MAPKKs include MKK3 and MKK6 for p38 MAPKs, MKK4 and MKK7 for JNKs, MAPK/ERK kinase (MEK) 1 and MEK2 for ERK1/2 and MEK5 for ERK5 (Wang & Tournier, 2006). MAPKKs are activated following serine and threonine phosphorylation by the appropriate upstream MAPKKK.

Generally, MAPKs consist of two domains joined by a flexible linker, the orientation of which plays an important role in regulating catalytic activity (Turjanski *et al.*, 2007). In contrast to the mostly α -helical C-terminal domain, the N-terminal domain contains an extensive amount of β -sheet along with the α C and α L16 helices (Turjanski *et al.*, 2007). The catalytic site is found at the junction of the two domains, containing the ATP-binding site and two binding sites for Mg^{2+} . MAPKs are discriminated from other members of the kinase superfamily by the presence of a 50 residue MAPK insertion in the C-terminus (Turjanski *et al.*, 2007). Dual phosphorylation of the conserved Thr-X-Tyr (where X is a defining feature of different MAPKs) motif located in the MAPK activation loop is required for full enzymatic activity of MAPKs (Turjanski *et al.*, 2007). Traditionally, MAPKs have been grouped based on the amino acid located at the centre of the phosphorylation motif, which in part determines the substrate specificity of the upstream MAPKK (Turjanski *et al.*, 2007). In the case of ERK1/2 and ERK5, the activation motif consists of a TEY motif corresponding to residues 202-204 and 218-220 for human ERK1 and ERK5 respectively (Cook *et al.*, 1997; Payne *et al.*, 1991; Zhou *et al.*, 1995). Of the MAPK family members, this study is most concerned with ERK1/2 and ERK5 due to their association with IL-6 signalling and cancer.

3.6.1 ERK1/2

ERK1/2 are described as the “classical” MAPKs with ERK1 being identified as a kinase activated in response to insulin (Boulton *et al.*, 1990; Rossomando *et al.*, 1989) and ERK2 first described *via* low-stringency screening of a rat brain cDNA library (Boulton *et al.*, 1991). Whilst sharing common mechanisms of activation, ERK1 and ERK2 do not mediate identical intracellular effects following their activation as each MAPK can activate a distinct pool of transcription factors. Of the two MAPKs, ERK2 is most characterised and can be activated by multiple growth factors. Activation of growth factor receptors induces phosphorylation of conserved residues within the receptor that act as recruitment sites for signalling proteins such as SHP2 which can recruit Grb2 and the related protein Gab1 in order to activate the ERK1/2 signalling cascade (Fig. 3.7). In the case of gp130, SHP2 is recruited to pTyr⁷⁵⁹ (Takahashi-Tezuka *et al.*, 1998) can subsequently recruit Gab1 (Takahashi-Tezuka *et al.*, 1998) or Grb2 (Fukada *et al.*, 1996). In the case of Grb2-mediated ERK1/2 activation, the Son of Sevenless (SOS) protein is constitutively associated with Grb and mediates Ras activation by potentiating the exchange of GDP for GTP. Activated Ras then activates members of the Raf family, with Raf-1 being the most commonly activated. Raf-1 in turn activates MEK1/2 which subsequently activates ERK1/2 (Turjanski *et al.*, 2007). Dual phosphorylation of the activation motif is associated

with a 600,000-fold increase in overall ERK2 catalytic activity arising mainly from an increase in the rate of phosphoryl group transfer (Prowse & Lew, 2001). In addition to Ras, Raf-1 can also interact with Rap1 although formation of the Rap1/Raf-1 complex does not result in activation of Raf-1, suggesting that Rap1 may act as a natural inhibitor of Raf-1-mediated ERK1/2 signalling. However, interaction of B-Raf with Rap1 can result in activation of B-Raf and subsequent activation of MEK1/2 and ERK1/2 (Peyssonnaud & Eychene, 2001). Activated ERK1/2 proteins can exert both cytosolic and nuclear effects *via* phosphorylation of their downstream effectors. ERK1/2 can phosphorylate numerous transcription factors including Ets-1, Sap-1, c-Jun, c-Myc and members of the CCAAT enhancer binding protein (C/EBP) family to promote transcription of ERK1/2-responsive genes (Chang *et al.*, 2003; Park *et al.*, 2004) whilst phosphorylation of substrates such as p90^{RSK} promotes activation of transcription factors such as CREB which are not directly phosphorylated by ERK1/2. In addition, ERK1/2 can phosphorylate kinases involved in cell cycle regulation such as Cdk2 and can promote cellular survival *via* indirectly activating the NFκB signalling pathway as a result of IKK phosphorylation (Chang *et al.*, 2003).

Activation of ERK1/2 plays an important role in governing key cellular processes including cellular proliferation and cell growth. Sustained activation of ERK1/2 until late G1-phase is required for successful entry into, but not completion of, the S-phase of the cell cycle (Meloche & Pouyssegur, 2007). However, hyperactivation of ERK1/2 signalling can induce cell cycle arrest due to p21 induction and Cdk2 inhibition (Meloche & Pouyssegur, 2007). Due to their activation by both external stimuli and small G-proteins which play important roles in governing cellular proliferation, it is hardly surprising that aberrant regulation of ERK1/2 signalling is a frequent event in cancers.

3.6.2 ERK5

ERK5 was simultaneously identified in 1995 as a MEK-5 interacting protein in a yeast hybrid screen (Zhou *et al.*, 1995) and *via* screening of a placental cDNA library for MAPK-related sequences (Lee *et al.*, 1995). ERK5 is also known as big MAPK 1 due to a 396 amino acid C-terminal insertion containing the nuclear export and nuclear localisation signals (NES and NLS respectively) required for nuclear shuttling of ERK5 (Fig. 3.8). In addition, the C-terminus of ERK5 undergoes auto-phosphorylation following MEK5-mediated dual phosphorylation and has two proline rich regions (PR1 and PR2) that are thought to facilitate interaction of ERK5 with proteins containing SH3 domains and may be involved in cytoskeletal targeting of ERK5 (Zhou *et al.*, 1995). The N-terminus

performs vital roles in the ability of ERK5 to undergo association with MEK5, oligomerisation and cytoplasmic targeting and displays approximately 50% homology to ERK1/2 (Wang & Tournier, 2006). Similar to ERK1/2, the activation motif of ERK5 consists of Thr²¹⁸-Glu²¹⁹-Tyr²²⁰, which may partially explain the ability of drugs previously thought to be MEK1/2-selective, such as U0126, to also attenuate ERK5 activation (Mody *et al.*, 2001; Wang & Tournier, 2006). ERK5 is preferentially phosphorylated by MEK5 on Thr²¹⁸, a process which has been suggested to induce a conformational change that enables ERK5 to auto-phosphorylate Tyr²²⁰ (Mody *et al.*, 2003). Dual phosphorylation of the TEY motif is associated with an 80% increase in kinase activity of ERK5 towards MBP (Mody *et al.*, 2003). In addition to auto-phosphorylation of Tyr²²⁰, ERK5 also undergoes auto-phosphorylation within the C-terminus which is important in enhancing ERK5-mediated transcription factor activation following dual phosphorylation of TEY²¹⁸⁻²²⁰ by MEK5 (Morimoto *et al.*, 2007). It is possible that MEK5-mediated phosphorylation may stabilise C-terminally phosphorylated ERK5 in an active conformation (Wang & Tournier, 2006) and thus enhance its ability to activate transcription factors. Furthermore, it has been demonstrated that the C-terminal region of ERK5 has potent transactivator activity which is required for induction of myocyte-specific enhancer factor (MEF) 2 activity and can directly activate transcription from the Nur77 promoter in T-cells (Kasler *et al.*, 2000).

Many factors including hyperosmolarity, growth factors and oxidative stress promote MEK-5 mediated dual phosphorylation of ERK5. These phosphorylation events are thought to promote stabilisation of ERK5 in an active conformation. Activation of MEK5 occurs downstream of MEKK2 and MEKK3 dependent on cell type and stimulus with WNK1 being identified as an upstream kinase for MEKK2/3 (Wang & Tournier, 2006).

Activated ERK5 is able induce activation of transcription factors such as MEF2 and Sap-1 (Raman *et al.*, 2007). The similarities between the transcription factors activated by ERK5 and ERK1/2 may help to explain their similar roles in promoting cellular survival. The presence of ERK5 is required for normal cardiac development with *erk5*^{-/-} embryos displaying cardiac defects (Wang & Tournier, 2006). In *Xenopus*, the MEK5/ERK5 pathway is essential for neuronal differentiation. Antisense morpholino-mediated knockdown of either protein reduces neuronal differentiation, indicating the essential nature of the pathway in this process (Nishimoto *et al.*, 2005).

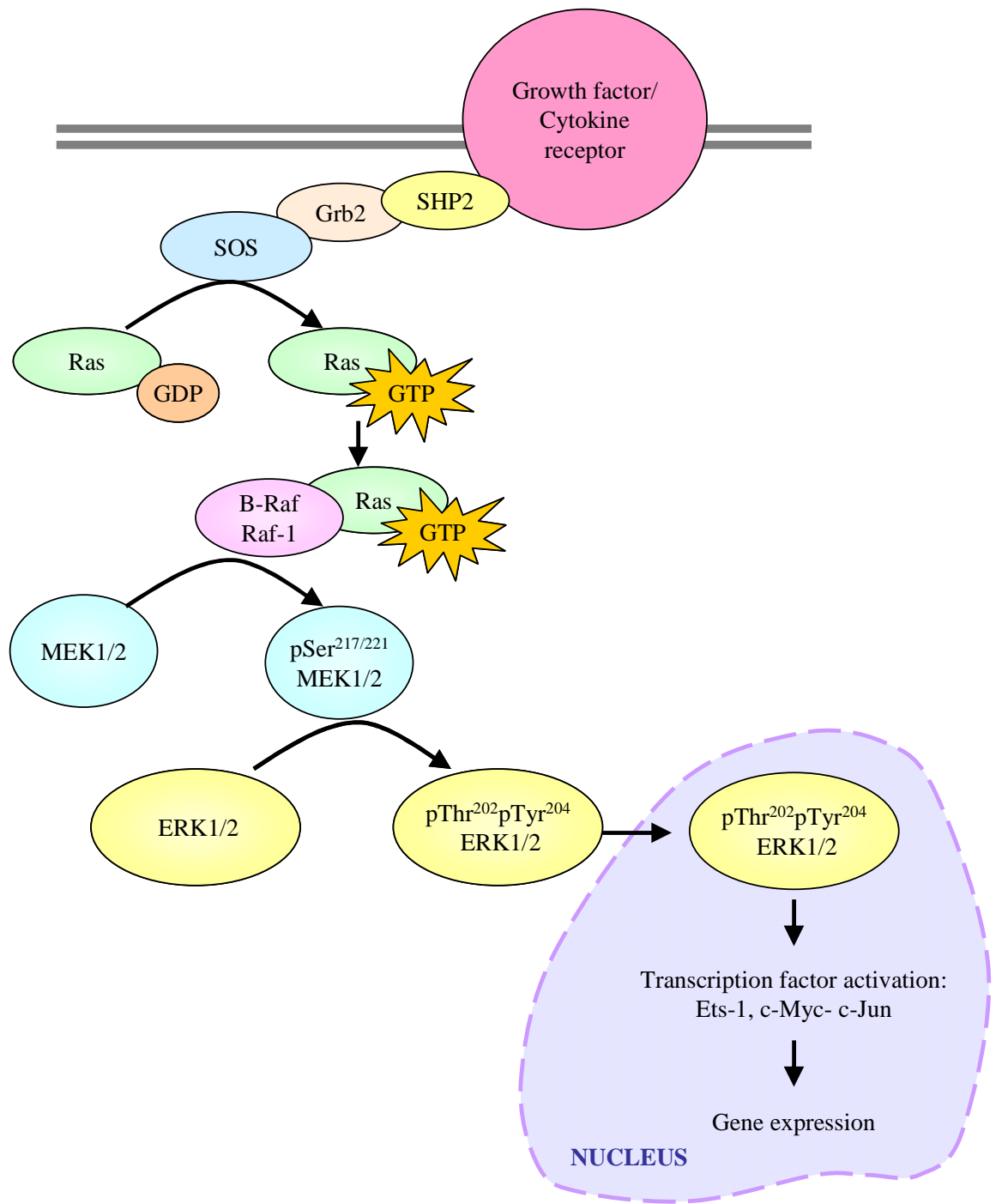


Fig. 3.7: Activation of the Ras-Raf-MEK1/2-ERK1/2 signalling pathway downstream of growth factor and cytokine receptors

The Ras-Raf-MEK1/2-ERK1/2 signalling cascade, numbering of phosphorylated residues refers to positions in MEK1 and ERK1

ERK5 has been implicated in cellular proliferation by regulating entry into mitosis (Zen *et al.*, 2009) and indeed, like ERK1/2 can be activated by mitogenic stimuli including serum (Kato *et al.*, 1997).

3.6.3 ERKs and cancer

Given the regulation of both ERK1/2 and ERK5 by mitogenic stimuli and activation of ERK1/2 by the small G-proteins Ras and Raf, it is unsurprising that both MAPKs have been investigated as therapeutic strategies. Mutations of Ras resulting in activation of the protein have been described in numerous malignancies including pancreatic, colon cancer and papillary thyroid cancer (Roberts & Der, 2007). Similarly, mutational activation of B-Raf has been described in a similar spectrum of malignancies, particularly melanoma, indicating a role for downstream signalling cascades in malignancy progression (Dankort *et al.*, 2009; Roberts & Der, 2007). In HEK293 cells, Raf-1 function is required to activate ERK1/2 downstream of mitogenic stimuli such as serum and phorbol-12-myristate-13-acetate (PMA) and also to activate ERK1/2 following stimulation with oncogenic stimuli such as *v*-Src. In NIH3T3 cells, activation of ERK1/2 synergised with the ability of *v*-*raf* to induce cellular transformation. Together, these results suggest a central role for Raf1-mediated ERK1/2 activation in cellular transformation (Troppmair *et al.*, 1994). Mutations in the *ras* gene resulting in constitutive activation of the protein result in tumorigenesis both *in vitro* and *in vivo* and can be mimicked by over-expression of MEK1 in cell culture models of transformation. It is possible that Raf-1-dependent activation of ERK1/2 is not required for tumour development as Ras mutants which are unable to interact with Raf-1 are able to induce comparable tumorigenesis as Ras mutants which are fully capable of interaction with Raf-1 (Webb *et al.*, 1998). However, Raf-1-interacting Ras induces tumorigenesis more rapidly in murine models and is associated with increased metastasis, indicating a crucial role of Raf-1 in metastasis (Webb *et al.*, 1998). Furthermore, loss of constitutive ERK1/2 signalling in these models inhibits metastasis but not tumour development, suggesting that Raf-1-mediated activation of the MEK1/2-ERK1/2 signalling cascade is required for tumour metastasis (Webb *et al.*, 1998). Activating mutations in Ras are a frequent occurrence in colorectal carcinoma yet effective therapeutic strategies to target Ras activation remain to be discovered. Attention has therefore been focussed on signalling pathways activated downstream of Ras, including activation of ERK1/2. Treatment of colorectal carcinoma cell lines with U0126 and the more recent MEK1/2-selective inhibitor CI-1040 inhibited anchorage-independent growth of cells, indicative of a loss of tumorigenic capacity (Yeh *et al.*, 2009).

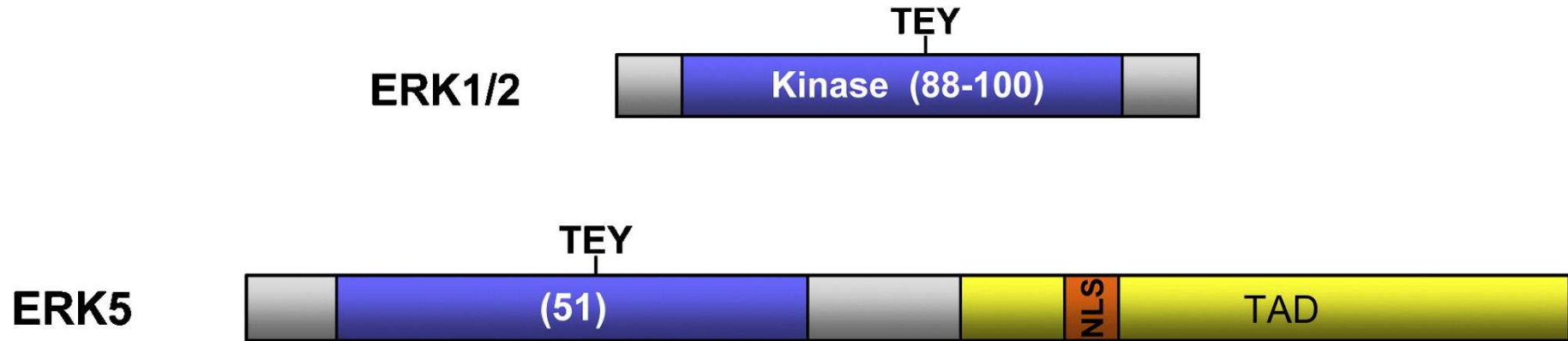


Fig. 3.8: Schematic representation of human ERK1/2 and ERK5

The N-terminal kinase domain is shown in blue and is flanked by N- and C-terminus extensions of varying lengths (grey). The percentage identity of the kinase domain with ERK1 is indicated. The activation loop phosphorylation motif is indicated, the transactivation domain and nuclear localization sequence within ERK5 are indicated by TAD and NLS respectively.

Taken from Coulombe and Meloche (2007)

The MEK1/2-selective inhibitor CI-1040 has been shown to have anti-tumour effects *in vitro* and *in vivo* and, in a phase I clinical trial, was able to reduce ERK1/2 phosphorylation by 46 – 100 % in tumours from patients with a variety of malignancies including lymphoma, melanoma, sarcoma (LoRusso *et al.*, 2005). However, further clinical studies of this inhibitor demonstrated poor antitumour activity in patients. Other MEK1/2-selective inhibitors such as PD035901 which demonstrate improved bioavailability, potency and efficacy compared to CI-1040 are currently under assessment as anti-cancer therapeutics (LoRusso *et al.*, 2005). Interestingly, Yeh *et al.* (2009) demonstrated that ERK1/2 phosphorylation may be higher in normal vs. neoplastic tissue, suggesting that inhibition of ERK1/2 activation may not be a suitable therapeutic strategy due to concerns regarding cytotoxicity in normal cells. Similarly, metastatic PCa lesions display decreased ERK1/2 phosphorylation in comparison to localised lesions (Grubb *et al.*, 2009), suggesting that use of ERK1/2 phosphorylation as an indicator of therapy efficacy may not be suitable at all stages of a malignancy.

In addition to the role that ERK1/2 plays in regulating tumour development and metastasis, the signalling cascade is also important in preventing apoptosis of cancerous cells, an effect previously thought to be mediated predominantly by activation of the PI3K pathway. Activated ERK1/2 is able to phosphorylate both the FOXO3a transcription factor and one of its regulated proteins, the pro-apoptotic BIM protein (Balmanno & Cook, 2009). Phosphorylation of FOXO3a promotes its polyubiquitination and proteasomal degradation, thus impeding transcription of *BIM* mRNA, whilst ERK1/2-mediated phosphorylation of BIM itself promotes proteasomal degradation of the protein and so regulates BIM apoptotic activity at a post-translational level (Balmanno & Cook, 2009). Conversely, activation of ERK1/2 is associated with an increase in expression of the anti-apoptotic Bcl-2, BCL_{XL} and Mcl-1 proteins possibly *via* an ERK1/2 → RSK or MSK → CREB signalling cascade (Balmanno & Cook, 2009). Inhibition of MEK decreases Bcl-2, Bcl-X_L and Mcl-1 in pancreatic cancer cells and is associated with an increase in apoptotic cell number (Boucher *et al.*, 2000).

Similar to ERK1/2, ERK5 has also been implicated in cancer progression. In the MCF7 and BT549 breast cancer cell lines, anti-ERK5 siRNA inhibited anchorage-dependent cell growth (Sirvent *et al.*, 2007). In hepatocellular carcinoma, knockdown of ERK5 inhibits cell growth and ERK5 becomes phosphorylated during the G2/M phases of the cell cycle to regulate mitotic entry (Zen *et al.*, 2009). However, activation of ERK5 is not solely associated with enhanced cellular proliferation. High expression of ERK5 in oral squamous

cell carcinoma is associated with lymph node metastasis, indicating that ERK5 may play a role in tumour metastasis (Sticht *et al.*, 2008). The presence of the C-terminal NLS promotes nuclear localisation of ERK5 in the absence of phosphorylation. In the BT474 and SKBR3 breast cancer cell lines, ERK5 is predominantly localised to the nucleus, a process which may be enhanced by phosphorylation of Thr²¹⁸ and Tyr²²⁰, and nuclear localisation of ERK5 is associated with resistance to apoptotic signalling *via* TRAIL (Borges *et al.*, 2007).

Due to the central roles that ERK1/2 and ERK5 play in regulating cellular proliferation and resistance, it is unsurprising that these signalling cascades are being investigated as potential targets for cancer therapies. However, due to the abilities of these proteins to activate multiple transcription factors important in cellular survival, the use of ERK signalling inhibitors as cancer chemotherapeutics may be associated with significant cytotoxic effects in non-malignant cells. Furthermore, due to the apparent differences in the correlation of ERK phosphorylation between both different malignancies and different disease stages of the same cancer, use of ERK pathway signalling inhibitors in cancer therapies must be carefully assessed.

3.7 cAMP signalling

3.7.1 cAMP generation

The ubiquitous second messenger, 3',5' cyclic adenosine monophosphate (cAMP) is generated from intracellular adenosine triphosphate (ATP) by adenylyl cyclases (ACs) (Serezani *et al.*, 2008). Nine membrane-associated and one soluble form of mammalian AC have been described with AC-encoding genes being distributed across multiple chromosomes rather than clustering to a specific region of the genome (Sunahara & Taussig, 2002). Of the 10 AC isoforms, most are expressed highly in the brain with AC6 and AC7 showing ubiquitous tissue expression (Sunahara & Taussig, 2002). AC activation in response to growth factors or hormones is primarily mediated by the stimulatory G α_s (G α_s) protein which forms part of a hetero-trimeric G-protein signalling complex downstream of G-protein coupled receptors (GPCRs, see Chapter 10 for further detail) (Sunahara & Taussig, 2002). In addition to G α_s , other G-proteins can modulate AC activity with inhibition *via* interaction with the inhibitory G α_i protein (G α_i) and the G β /G γ -protein complex. The PKC signalling pathway can also modulate AC activity (Daniel *et al.*, 1998). In contrast to the membrane-bound forms of AC, soluble AC is expressed mainly in the testes and is regulated by bicarbonate ions rather than G α_s . Two splice variants of the

soluble AC have been identified in human and rat testicular tissue and both are thought to contribute to sperm motility (Jaiswal & Conti, 2001).

Membrane-bound ACs show similar domain organisation with a short, cytosolic amino terminus (C₁), followed by two repeats of a six transmembrane domain (TMD) and a C-terminal cytosolic domain (C₂). of approximately 40 kDa (Tesmer *et al.*, 1997). Both of the cytosolic domains are important in catalysis and are also associated with regulation of AC activity. Basal interaction between the cytosolic domains of AC and Gα_s is weak with activation and subsequent GTP-loading of Gα_s required for high affinity interaction between the two proteins. *In vitro*, the C₁ domain of AC5 and the C₂ domain of AC2 can form functional heterodimers which resemble the structure of the AC5 C₁ homodimer (Tesmer *et al.*, 1997). A long, shallow trough which bisects one face of the AC5 C₁/AC2 C₂ heterodimer acts as a binding pocket for AC-activating substrates such as the diterpene forskolin (Fsk). A wide cleft at the interface between the two cytosolic domains functions as the binding site for Gα_s and interacts with the switch II helix on the G-protein (Tesmer *et al.*, 1997).

Following activation of AC and conversion of ATP to cAMP, there are numerous effectors by which elevation of intracellular cAMP concentrations can modulate cellular functions. Whilst cAMP levels within cells may be globally upregulated following AC activation, intracellular compartmentalisation of proteins involved in cAMP signalling are thought to “fine tune” cAMP concentrations into microdomains of high and low cAMP concentration. This compartmentalisation is mainly achieved *via* interaction of signalling proteins with A kinase anchoring proteins (AKAPs) (Baillie *et al.*, 2005). These proteins act as a scaffold for signalling proteins and can recruit the cAMP effector molecules such as protein kinase A (PKA) and exchange proteins activated by cAMP (EPACs) (Baillie *et al.*, 2005). In the case of PKA, an amphipathic helix on the AKAP interacts with the regulatory subunit of the inactive holoenzyme (Carr *et al.*, 1992). However, the AKAP signalling complex is not just associated with positive regulation of cAMP signalling as phosphodiesterases (PDEs) can also interact with AKAPs. To prevent sustained elevation of cAMP, the cyclic nucleotide is degraded *via* the actions of PDEs. Of particular interest are the PDE4 family members which are cAMP-specific PDEs and are the target of a number of therapeutic strategies for diseases such as chronic pulmonary obstructive disease (COPD) and pulmonary hypertension (Baillie *et al.*, 2005; Brown, 2007; Dony *et al.*, 2008; Giembycz, 2006). Thus, dependent on the complement of signalling proteins associated with specific

AKAPs, efficient compartmentalisation of intracellular cAMP concentrations can be achieved.

3.7.2 Protein Kinase A

Protein kinase A (PKA) is thought of as the “classical” cAMP effector molecule and is found *in vivo* as a holoenzyme, consisting of two regulatory (R) and two catalytic (C) subunits (Fig. 3.9) (Daniel *et al.*, 1998). Each R subunit of PKA contains two cAMP binding sites, termed site A and site B which undergo a conformational change upon binding of cAMP (Murray, 2008). The two binding sites are non-identical, but show similar structural organisation, and thus display different affinities for cAMP with site A exchanging cAMP more rapidly than site B. Studies using site A and site B-selective cAMP analogues demonstrate that binding of cAMP to both sites synergistically enhances kinase activity (Robinsonsteiner & Corbin, 1983).

It is thought that cAMP binding to R subunits of PKA acts to stabilise the protein *via* interaction with Arg²⁰⁹ found in the Site A cAMP binding pocket (Dostmann, 1995). As a result of cAMP binding, the C subunits of PKA are released and are able to phosphorylate Ser/Thr residues within the canonical PKA phosphorylation motif on target proteins. The cAMP analogue, Rp-cAMPS inhibits holoenzyme dissociation *via* breaking the interaction between Arg²⁰⁹, which interacts with the phosphate group, and Asp¹⁷⁰ and locks PKA as a holoenzyme (Dostmann, 1995).

Following dissociation of the C subunits from the R subunits, PKA is able to exert its intracellular effect *via* Ser phosphorylation of target proteins which contain the XRRXRSX motif (Kemp & Pearson, 1990). Activated PKA regulates a number of cellular processes including enzymes, ion channels, cytoskeletal apparatus and transcription factors (Daniel *et al.*, 1998). One of the principal downstream targets of PKA is the cAMP responsive element (CRE) binding protein (CREB) which binds the CRE consensus sequence TGACGTCA (Sassone-Corsi, 1998). PKA-mediated phosphorylation of CREB on Ser¹³³ within the RRPSY motif is an important step in CREB activation (Alberts *et al.*, 1994) and is associated with recruitment of the p300/CREB binding protein (CBP) coactivator to the promoter of CREB-responsive genes, ultimately resulting in initiation of gene transcription (Mayr & Montminy, 2001). However multiple kinases can phosphorylate CREB on Ser¹³³ including the MEK/ERK1/2 pathway, glycogen synthase kinase (GSK) 3, p38 MAPK and calmodulin kinase (Johannessen *et al.*, 2004) thus other factors are required to regulate

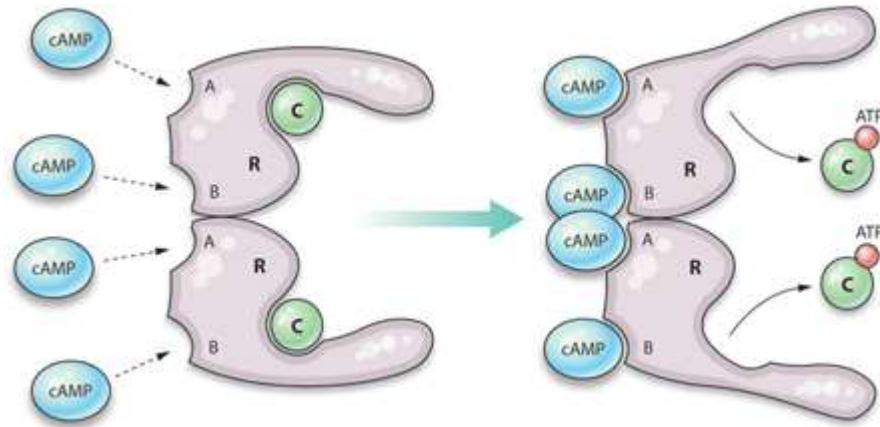


Fig. 3.9: Activation of the PKA holoenzyme by cAMP

The regulatory subunits of PKA (denoted as R) contain the A and B cAMP binding sites and, in the absence of cAMP, are associated with the catalytic subunits (denoted as C). Binding of cAMP results in a conformational change and releases the catalytic subunits which phosphorylate their downstream targets *via* transfer of phosphate from the associated ATP.

Taken from Murray (2008)

CREB-responsive genes in response to cAMP elevation. The transducers of regulated CREB (TORC) proteins potentiate the ability of CREB to initiate gene transcription in response to increases in intracellular cAMP, an event which occurs independently of Ser¹³³ phosphorylation (Conkright *et al.*, 2003). TORC proteins associate with the promoter region of CREB-responsive genes with a requirement for a proximal TATA box element (Conkright *et al.*, 2003). Thus, in order to promote CREB-mediated transcription, the TORC proteins must be localised to the nucleus. Nuclear translocation of TORCs is promoted by cAMP elevation and TORC function is required for CREB-responsive gene expression following cAMP elevation (Bittinger *et al.*, 2004). Thus combined activation by PKA and subsequent interaction with nuclear-localised TORCs promotes the transcription of CREB-regulated genes in response to cAMP elevation.

In order to prevent constitutive activation of CREB, the protein is desphosphorylated by the Ser/Thr phosphatases PP-1 and PP-2A which return the protein to its basal state (Alberts *et al.*, 1994; Mayr & Montminy, 2001). In addition to CREB, PKA can also activate the CRE modulator (CREM) and activating transcription factor (ATF) -1 transcription factors which belong to the same protein family as CREB. However, whilst cAMP elevation induces PKA activation, this event does not always promote gene transcription. In addition to CREB, PKA also activates the inducible cAMP early repressor (ICER) which potently represses gene expression in response to elevated cAMP (Sassone-Corsi, 1998). The ICER open reading frame (ORF) correlates to the C-terminal, DNA-binding domain of CREM and thus lacks the transactivator activity of the full length protein (Stehle *et al.*, 1993). Expression of ICER is driven by a second, intronic promoter within the CREM gene and is strongly induced by cAMP elevation (Sassone-Corsi, 1998). Therefore, cAMP-driven expression of ICER acts to impede transcription of cAMP-responsive genes by binding to CRE elements and thus blocking binding of full-length CREM or CREB. ICER is also able to bind its own promoter, thus inhibiting its own expression and so acting to “reset” gene transcription in response to cAMP elevation (Molina *et al.*, 1993).

3.7.3 EPAC

For many years, PKA was thought to be the sole effector activated by increases in intracellular cAMP concentrations. However, in 1998, the ability of cAMP to activate the Rap-1 signalling protein was found to occur independently of PKA, indicating the presence of another cAMP effector (de Rooij *et al.*, 1998). In the same paper, de Rooij *et al.* (1998) identified a putative cAMP-responsive GEF by searching for sequences with homology to

both cAMP binding domains and to GEFs specific for Ras and Rap. Subsequently, this group identified and cloned a guanine nucleotide exchange factor (GEF) which contains an N-terminal cAMP binding domain and activates Rap-1 in response to cAMP elevation (de Rooij *et al.*, 1998). This protein was termed exchange protein activated by cAMP (EPAC) and the mRNA of EPAC was found to have ubiquitous tissue expression, although higher expression levels were detected in kidney and brain tissue (de Rooij *et al.*, 1998). In addition to the originally described EPAC protein, hereafter referred to as EPAC1, a second, related cAMP-GEF was identified which is expressed predominantly in the brain and adrenal gland (Kawasaki *et al.*, 1998). This protein was termed EPAC2 and displays structural and sequence homology to EPAC1 (Kawasaki *et al.*, 1998).

The EPAC proteins are multi-domain proteins in which the C-terminal catalytic activity is regulated by the N-terminus (Fig. 3.10). The Dishevelled, Egl-10, Pleckstrin (DEP) domain of the N-terminus is involved in the association of the EPACs with cellular membranes and is proximal to cAMP binding domains. EPAC1 contains a single, high affinity binding site for cAMP (cAMP-B) whilst EPAC2 contains two cAMP binding sites which flank the DEP domain (Roscioni *et al.*, 2008). The extreme N-terminal cAMP binding site of EPAC2 displays a lower affinity for cAMP (cAMP-A) than the cAMP-B site and, as yet, the biological function of this site is unknown. A Ras-exchange motif (REM) is situated between the regulatory domains and the catalytic domains and is proximal to a Ras-associating (RA) domain. Activated Ras has been shown to interact with EPAC2 but not EPAC1 *in vitro* (Li *et al.*, 2006b). The interaction between EPAC2 and activated Ras results in cytosol to membrane translocation of activated Ras and is associated with increase membrane activation of Rap1. Combined stimulation with EGF and cAMP elevation promoted membrane translocation of EPAC2. It is thought that the membrane translocation of EPAC2 requires EGF-mediated activation of Ras whilst conformational changes of EPAC2 associated with cAMP are required for the association of the GEF with activated Ras (Li *et al.*, 2006b). Thus activation of EPAC2 and its association with Ras alter the intracellular location of EPAC2 and can modulate the effector pool activated in response to cAMP elevation (Li *et al.*, 2006b). The ability of EPACs to act as GEFs for their downstream proteins is conferred by a C-terminal domain which shows homology to Cdc25 (Roscioni *et al.*, 2008).

Following activation by cAMP binding, EPACs are able to modulate their downstream effectors by promoting the exchange of GDP for GTP. EPACs are able to activate members of the Rap families and to regulate modulators of exocytosis and microtubule

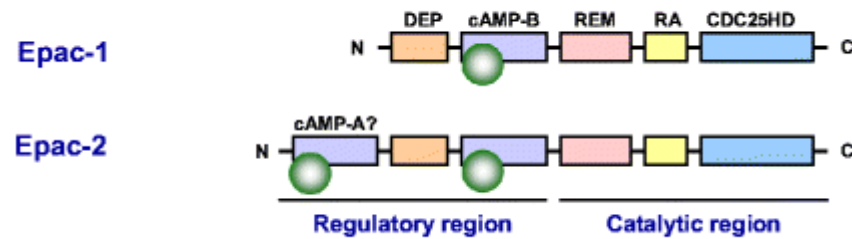


Fig. 3.10: Domain organisation of the human EPAC proteins

Schematic indicating the domain organisation of the EPAC1 and EPAC2 proteins. cAMP-A = low affinity cAMP binding domain, cAMP-B = high affinity cAMP binding domain; DEP = Dishevelled, Egl-10, Pleckstrin domain; REM = Ras exchange motif; RA = Ras-associating domain; CDC25HD = Cdc25 homology domain

Taken from Roscioni *et al* (2008).

dynamics (Roscioni *et al.*, 2008). Thus it is hardly surprising that EPAC activation has been associated with a number of cellular processes. EPAC activation has been implicated in modulation of inflammatory processes *via* inducing expression of the anti-inflammatory SOCS3 protein in HUVECs (Sands *et al.*, 2006) (see Chapter 7) and by activation of PKC ϵ which mediates inflammatory pain perception (Hucho *et al.*, 2005). These two processes may not be unrelated as indicated by the observation that EPAC1-mediated induction of SOCS3 expression requires PKC activation (Borland *et al.*, 2009). EPAC activation is also an important regulator of endothelial barrier function with knockdown of EPAC1 associated with an increase in permeability in HUVECs (Sehrawat *et al.*, 2008). Associated with this phenomenon is the ability of EPAC1 to dynamically and positively regulate MT growth (Sehrawat *et al.*, 2008) which may be mediated *via* interaction of EPAC1 with the light chain 2 of microtubule associated protein (MAP) 1A (Magiera *et al.*, 2004). This interaction is associated with an increased ability of EPAC1 to activate Rap1 through increased sensitivity to cAMP and an increase in cellular adhesion (Gupta & Yarwood, 2005). Given their ability to regulate a number of key cellular signalling pathways, it is unsurprising that research into the EPACs is an expanding field.

3.7.4 Other cAMP sensors

Although PKA and EPACs comprise the most studied cAMP effectors, they are by no means the only cAMP sensors. In addition to EPACs, which function as GEFs for Rap and Ras family members, the cyclic nucleotide Ras GEF (CNrasGEF) has also been shown to activate Ras in response to cGMP and cAMP (Pham *et al.*, 2000). Like EPAC, CNrasGEF has a Cdc25 homology domain associated with GEF activity and an RA domain. Immobilisation of cAMP on agarose beads is able to precipitate GST-bound CNrasGEF *in vitro*. Mutation of a cyclic nucleotide binding domain at the N-terminus of CNrasGEF reduces the ability of cAMP-agarose to precipitate over-expressed CNrasGEF from HEK293 cells, demonstrating that this domain is involved in cAMP binding (Pham *et al.*, 2000). Unlike EPACs, CNrasGEF is activated by both cAMP and cGMP (Pham *et al.*, 2000), suggesting the protein may be able to regulate an even wider range of cellular processes than the EPACs. Association of CNrasGEF with the β 1-adrenoceptor results in Ras activation and is reliant on G α_s -generated cAMP (Pak *et al.*, 2002). It is thought that the frequent association of cAMP-activated Ras with melanomas is due to Ras-mediated activation of ERK1/2 downstream of CNrasGEF. Indeed, CNrasGEF is highly expressed in B16 melanoma cells and knockdown of CNrasGEF is associated with a decrease in Fsk-induced ERK1/2 phosphorylation, suggestive of a role for this protein in melanogenesis (Amsen *et al.*, 2006). Of concern are the observations that CNrasGEF is unable to bind

physiologically relevant concentrations of cAMP *in vitro* and constitutively activates Ras when expressed in Rat1 cells. Such results raise the question of whether CNrasGEF is truly cAMP responsive (Kuiperij *et al.*, 2003).

In addition to direct activation of intracellular signalling proteins, cAMP elevation can also activate transmembrane ion channels. Two classes of cyclic nucleotide-responsive ion channels have been described, the cyclic nucleotide-gated (CNGs) and the hyperpolarisation-activated, cyclic nucleotide-gated (HCNs) ion channels. CNGs are activated directly by binding of cyclic guanosine monophosphate (cGMP) or cAMP whilst HCNs are voltage regulated (Biel, 2009). Whilst widely expressed in peripheral and central neurones, CNGs and HCNs also play distinct roles in signal transduction systems. CNGs are important in signal transduction from olfactory and visual stimuli whilst HCNs play crucial roles in maintaining cardiac function (Biel, 2009). Both types of ion channel display cytosolic localisation of their N and C termini and contain a transmembrane channel comprised of 6 α -helices with the ion-conducting core located between loops 5 and 6 (Biel, 2009). CNGs act as conduit for K^+ and Na^+ and display no preference for either cation whilst HCNs show greater transport of K^+ compared to Na^+ . In addition to monovalent cations, CNGs also provide a channel for transportation of Ca^{2+} across the cell membrane, enabling influx of Ca^{2+} and activation of calcium-sensitive signalling pathways (Biel, 2009). Recently, a more minor role of HCN2 as an ion channel for Ca^{2+} in the presence of both K^+ and Na^+ has been described (Michels *et al.*, 2008). HCNs preferentially bind cAMP whilst cGMP is a more potent activator of CNGs (Biel, 2009). Activation of HCNs has been implicated in a diverse physiological processes including vision (Barrow & Wu, 2009) and regulation of cardiac function (Schulze-Bahr *et al.*, 2003).

Given the important role of cAMP elevation in a number of cellular systems, it is unsurprising that study of this pathway is of interest to a number of research groups. Of particular relevance to this study is the observation that cAMP elevation can inhibit IL-6-induced pTyr⁷⁰⁵STAT3 *via* induction of the SOCS3 protein (Sands *et al.*, 2006). It is possible that modulation of cAMP levels may be of benefit in malignancies such as PCa which are associated with hyperactivation of STAT3 and elevated IL-6 levels (see sections 3.1 and 3.2). However, in addition to pathways associated with transformation, the ability of malignant cells to metastasise is a key event in tumour development.

3.8 Actin polymerisation and cell motility

Changes in actin polymerisation play a crucial role in the ability of cells to adhere to the substratum, form membrane protrusions and migrate. The Rho family GTPases comprise the Rac, Cdc42 and Rho sub-families, with all three controlling different aspects of actin polymerisation. Rac1 is involved in the formation of lamellipodia, Cdc42 in filopodia extension and Rho in the formation of stress fibre formation and focal adhesions. Due to the differing roles that these related proteins play in governing actin dynamics, each of them regulate actin polymerisation via different signalling pathways. For example, Rac1 regulates WAVE-dependent activation of Arp2/3 via binding to IRSp53 whilst Cdc42-induced Arp2/3 activation is facilitated by interaction with WASP (Pullikuth & Catling, 2007; Takenawa & Suetsugu, 2007). In contrast to Rac1 and Cdc42, Rho activation limits the formation of membrane protrusions due to the ability of its effectors, such as mDia and ROCK, to stimulate actin bundling into stress fibres (Pullikuth & Catling, 2007).

The Rho GTPases are key regulators of cellular motility due to their ability to regulate the actin cytoskeleton. Migrating cells have a distinct morphology with a ruffled leading edge followed by a flat, broad lamella and a tail retracting at the rear of the cell. Within the cell itself, there is little similarity between cell types in the nature of actin organisation although protrusion at the leading edge appears to be a common factor driving the migratory process (Wittmann & Waterman-Storer, 2001). Leading edge protrusions arise due to the formation of new actin filaments with new subunits being incorporated at the barbed ends of the existing actin filament (Fig. 3.11) (Pollard & Borisy, 2003). However the barbed ends themselves remain stationary with reference to the substratum and it is *de novo* polymerisation which drives extension of the leading edge (Verkhovskiy *et al.*, 1999). In contrast to the leading edge, actin filaments at the rear of the cell are highly associated with an accumulation of myosin II (Verkhovskiy *et al.*, 1999). Myosin II is important, but not essential, for the retraction of the posterior edge *via* mediating movement of actin filaments past each other (Jay *et al.*, 1995).

3.8.1 The WASP-WAVE protein network

The Wiskott-Aldrich syndrome (WAS) protein (WASP) was originally identified as the causative gene of WAS, an X-linked recessive disease resulting in eczema, thrombocytopenia and immunodeficiency. Expression of WASP is restricted to haematopoietic cells although later description of the related, so-called neural-WASP (N-WASP) proteins was described in neural and other tissues (Takenawa & Suetsugu, 2007).

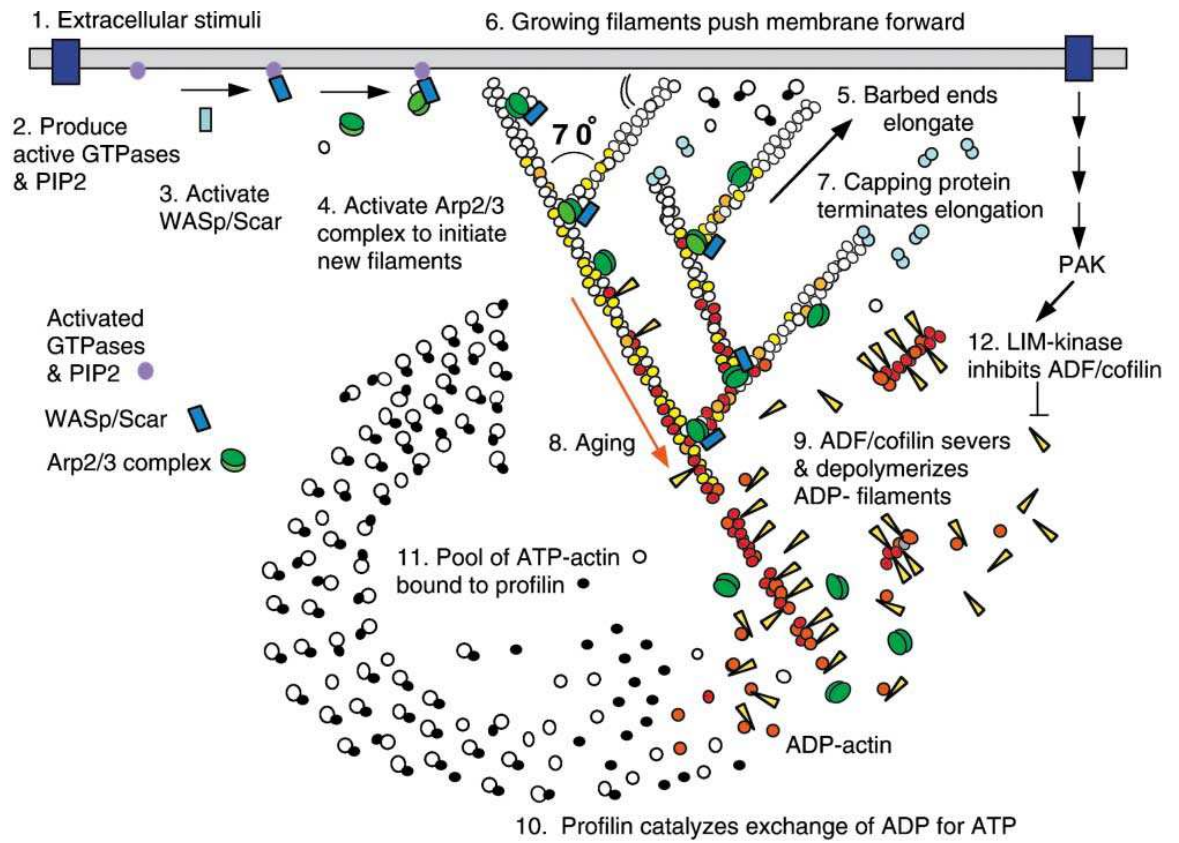


Fig 3.11: Mechanism for actin-mediated protrusion of the leading edge downstream of extracellular stimuli

Taken from Pollard and Borisy (2003).

The proteins share three conserved domains, comprising the C-terminal verprolin-homology domain (V), a central cofilin-homology domain (Co) and an acidic domain (A). Collectively, these three domains enable WASP proteins to interact with monomeric actin and the actin-related protein 2/3 (Arp2/3) complex (Takenawa & Suetsugu, 2007). Screening for proteins containing a similar VCoA arrangement resulted in identification of WASP-family verprolin-homologous protein (WAVE) family that include mammalian WAVE-1, WAVE-2 and WAVE-3 (Suetsugu et al., 1999). In humans, WAVE-2 is expressed ubiquitously, except in skeletal muscle, whilst WAVE-1 and WAVE-3 show particular enrichment in the brain compared to other body tissues (Takenawa & Suetsugu, 2007). Both WASP and WAVE proteins are able to induce generation of new actin filaments via activation of Arp2/3 and subsequent *de novo* nucleation of actin monomers. This process is dependent on a conserved amphipathic helix located in the C region of the proteins (Panchal *et al.*, 2003; Takenawa & Suetsugu, 2007). There appears to be negligible difference in the ability of WAVE and WASP proteins to induce actin filament formation *in vitro* (Suetsugu et al., 1999), indicating that their activation is of equal importance in regulating actin polymerisation. In addition to roles in actin polymerisation, WAVE-1 is able to recruit signalling proteins such as PKA and Abl to the actin cytoskeleton. In the case of PKA, this interaction requires Ile⁵⁰⁵ and Ile⁵⁰⁹ which interact with the regulatory subunit of PKA, resulting in anchorage of PKA to the actin cytoskeleton (Westphal *et al.*, 2000). Thus WAVE-1 may form a link between cAMP signalling and modulation of actin polymerisation.

3.8.2 The Arp2/3 complex

The Arp2/3 complex contains seven polypeptides in total and was first isolated from *Acanthamoeba castellanii* due to its affinity for profilin. Alone, the Arp2/3 complex exhibits little biochemical activity and requires interaction with nucleation-promoting factors in order to become activated and instigate formation of new actin filaments (Goley & Welch, 2006). There are several mechanisms by which formation of actin filaments may be initiated. Whilst it is possible for actin to spontaneously dimerise, this intermediate is highly unstable and thus actin nucleation does not proceed to the trimeric actin nucleus required for subsequent polymerisation. However, association of actin with nucleation-promoting factor proteins (NPFs) such as the Arp2/3 complex, spire proteins and the formins promote actin polymerisation without the need for spontaneous nucleation (Goley & Welch, 2006). In the case of Arp2/3, the active complex is thought to contain Arp2 and Arp3 in close proximity to each other which, due to their sequence homology to actin itself, causes the Arp2/3 complex to act as an actin-like heterodimer and bind monomeric

actin to facilitate formation of a trimeric actin-like nucleus and subsequent polymerisation (Goley & Welch, 2006).

Actin, Arp2 and Arp3 are all capable of binding ATP which promotes actin polymerisation. ATP-bound actin filaments undergo more rapid polymerisation and slower dissociation than ADP-bound filaments (Zheng *et al.*, 2007). Loss of Arp2/3 ATP binding attenuates polymerisation activity, possibly due to the 25-fold more rapid dissociation of Arp2/3 from ADP-bound actin (Zheng *et al.*, 2007). Conversely, proteins such as cofilin, which promote depolymerisation of actin, associate more readily with ADP-bound actin. In addition to ATP hydrolysis, actin polymerisation can also be regulated by interaction with NPFs as described above. NPFs can be subdivided into class I and class II NPFs dependent on both the mechanism by which actin polymerisation is induced and the effect on actin branching.

The class I NPFs include the WASP and WAVE proteins, which are activated by the Rho GTPases Rac1 and Cdc42 whilst the class II NPFs include actin-binding protein-1 of *Saccharomyces cerevisiae*. Class I NPFs bind Arp2/3 through an acidic domain and globular actin (G-actin) through their conserved WASP-homology-2 (WH2) domain to produce a trimeric Arp2/Arp3/G-actin nucleus for subsequent elongation (Goley & Welch, 2006). Class II NPFs which activate Arp2/3 contain an acidic domain, enabling their interaction with Arp2/3 but lack a WH2 domain required for binding of G-actin. Consequentially, the mechanism by which class II NPFs activate actin polymerisation is currently unknown. It is possible that class II NPFs may act to stabilise filamentous actin (F-actin) branches in the developing microfilament as members of this subgroup remain associated with F-actin following formation of a new branch whilst class I NPFs dissociate following branching (Goley & Welch, 2006).

Arp2/3-mediated nucleation can also be activated *via* preformed actin filaments in a process which is thought to be auto-catalytic as the rate of polymerisation increases with the length of actin filament. Formation of new actin branches is thought to be derived from the sides of existing filaments rather than from the fast-growing barbed ends of filaments which are the site of *de novo* actin polymerisation in the extending filament. In keeping with the hypothesis that actin polymerisation occurs more rapidly in the presence of ATP-bound actin, side branching is restricted to areas of the barbed ends of actin filaments containing ATP-bound actin (Goley & Welch, 2006). Formation of branched actin plays

important roles in regulating cytoskeletal dynamics and has been implicated in dendrite spine and synapse formation (Wegner et al., 2008).

3.8.3 RhoGTPases and actin dynamics

The Rho family of GTPases exert their effects on cytoskeletal dynamics *via* activation of downstream targets. Within the Rho GTPase superfamily, the sub-family designated as Rho comprise the RhoA, RhoB and RhoC. Although other proteins have been designated as Rho proteins, e.g. RhoG, this naming refers more to their inclusion in the Rho GTPase superfamily than to similarities to RhoA, B or C (Schmandke *et al.*, 2007). Of most interest to this study is the role of RhoA in regulating actin polymerisation. In the case of RhoA, activation of the downstream kinase ROCK promotes activation of LIM kinase (LIMK) which in turn phosphorylates cofilin. LIMK-mediated phosphorylation of cofilin on Ser³ inhibits the depolymerising activity of cofilin and thus leads to actin filament stability (Fig. 3.12) (Maekawa *et al.*, 1999). In addition, ROCK can phosphorylate and inhibit myosin light chain phosphatase to promote actomyosin contractility and the formation of stress fibres downstream of myosin light chain kinase activity (Maekawa *et al.*, 1999; Papakonstanti & Stournaras, 2008). Finally, RhoA can activate mDia which also binds profilin and so promotes F-actin polymerisation downstream of RhoA activation (Watanabe *et al.*, 1997). Similar to RhoA, Rac1 can also promote activation of LIMK through activation of PAKs and subsequently stabilise F-actin filaments *via* LIMK-mediated inhibition of cofilin. However, Rac1 and RhoA play very different roles in modulating cellular morphology which may arise from differential targeting to cell membranes as a result of post-translational modification (Ridley, 2006).

Whilst RhoGTPases are able to directly induce actin polymerisation, they also regulate, and are regulated by, microtubule (MT) function. MT dissociation is associated with increased Rho activity due to an increase in GTP-Rho, resulting in bundling of actin into stress fibres and subsequent cellular contraction (Pullikuth & Catling, 2007). In the case of RhoA, the GTPase itself does not directly bind MTs but is thought to become activated following association of RhoA GEFs such as p190RhoGEF with the MT network. Consistent with the opposing roles of Rho and Rac on membrane protrusion formation, MT assembly promotes Rac activity and subsequent lamellipodia formation which may be mediated by activation of TrioGEF which activates RhoG, an upstream activator of Rac and Cdc42. Although neither TrioGEF nor RhoG directly bind MTs, their subsequent activity is dependent on an intact MT network. Activation of Rho family proteins can also promote MT stability through Rho-mediated mDia activation and activation of PAK1 by

Cdc42 and Rac. PAK1 serves to stabilise MT by both activating tubulin cofactor B to promote tubulin heterodimerisation and inhibiting the MT destabilising protein stathmin (Pullikuth & Catling, 2007). Furthermore, in *Xenopus* oocytes, physical interactions between the MT network and F-actin have been demonstrated to dynamically modulate F-actin characteristics in a process which requires cytosolic factors (Waterman-Storer *et al.*, 2000). It is thus possible that RhoGTPases and MT may act co-ordinately to regulate actin cytoskeletal dynamics via MT promotion of RhoGTPase activity which in turn acts to stabilise the MT network.

3.8.4 RhoGTPases and cancer

An important event in late-stage malignancies is the emergence of metastatic tumours which are correlated with increases in cellular motility. Given the important role of actin polymerisation in regulating cellular motility, it is unsurprising that Rho GTPases have been implicated in tumour metastasis. Over-expression of Rac1 has been demonstrated in leukaemias and siRNA against Rac1 in cell line models of leukemia which also over-expression Rac1 promoted a decrease in colony formation and proliferation. The Rac1 inhibitor NCS23766 mimicked the effects of Rac1 knock-down and also impaired cellular migration (Wang *et al.*, 2009). Such decreases in cellular migration and tumour invasion are also seen in colorectal carcinoma cells in which Rac1 knock-down has been achieved (Zhao *et al.*, 2009a), indicating an important role for this protein in regulating tumour metastasis. In addition to roles in metastasis, RhoA has also been implicated in cellular transformation with TGF β -mediated activation of RhoA required for efficient transformation by constitutively active Ras and B-Raf (Fleming *et al.*, 2008).

Of particular relevance to this study is the observation that stimulation of the AGS gastric carcinoma cell line with IL-6 promotes cell invasion through Src-mediated activation of RhoA and is correlated with increased tumour cell aggression. Furthermore, increased staining of RhoA was found in later stage tumour tissue compared to normal colonic epithelium in gastric cancer patients (Lin *et al.*, 2007). Ectopic expression of both constitutively active and wild-type RhoA in human primary mammary epithelial cells promoted cellular transformation. Interestingly, a mutant of RhoA which was unable to interact with ROCK or mDia was also able to induce cellular transformation (Zhao *et al.*, 2009b). Interestingly, over-expression of constitutively active or wild-type RhoA also promotes transcription of STAT3-responsive reporter genes *via* a mechanism dependent on a functional STAT3, indicating that the RhoA signalling cascade can also play a role in STAT3 activation. This hypothesis was confirmed by evidence that expression of

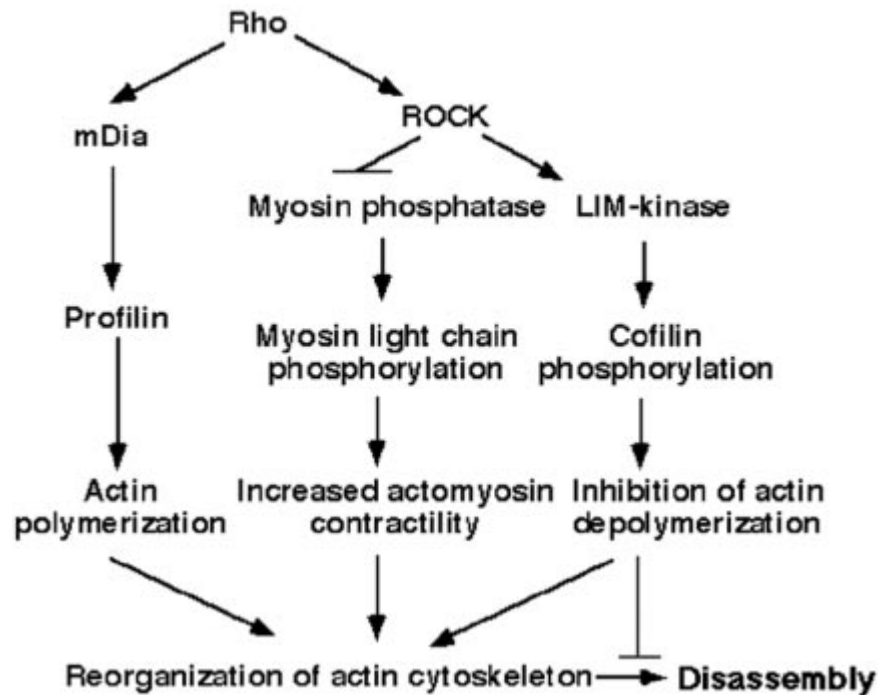


Fig. 3.12: Regulation of signalling pathways by Rho

RhoA is able to phosphorylate mDia to promote activation of profilin and subsequently promote actin polymerisation. Additionally, RhoA phosphorylates ROCK to promote LIMK phosphorylation which inhibits cofilin activity *via* phosphorylation on Ser³. ROCK also inhibits myosin phosphatase activity and thus promotes phosphorylation of myosin light chain and increased actomyosin contraction.

Taken from Maekawa *et al* (1999)

constitutively active RhoA promoted an increase in pTyr⁷⁰⁵STAT3, indication that activation of RhoA does indeed promote activation of STAT3 (Aznar *et al.*, 2001). This observation could, in part, explain the role of RhoA in cellular transformation as activation of STAT3 has been shown to be directly oncogenic (Azare *et al.*, 2007; Bromberg *et al.*, 1999). Inhibition of ROCK impairs nuclear import of STAT3 whilst expression of active ROCK potentiates nuclear accumulation of STAT3. Furthermore, STAT3 is required for stress fibre formation, a RhoA-mediated event, and for RhoA-dependent cellular transformation, indicating a possibly positive feedback loop between STAT3 and RhoA activation (Debidda *et al.*, 2005).

Whilst the relevance of the described interactions between the RhoA and STAT3 signalling networks has yet to be determined *in vivo*, they may provide a new route by which to modulate intracellular signalling in malignant cells. Importantly, in addition to possible roles in cellular transformation, reciprocal activation of the RhoA and STAT3 signalling pathways may contribute to the cellular metastasis and resistance to chemotherapeutics characteristic of latter stages of cancer.

3.9 Project Rationale

Given the association between various malignancies and aberrant IL-6 or STAT3 signalling, it is possible that attenuation of STAT3 activation may be of therapeutic benefit. Of particular interest to this study is PCa as elevation of IL-6 levels is associated with every stage of the disease and is correlated to poor patient prognosis, patient cachexia and death (Kuroda *et al.*, 2007). Previously, elevation of cAMP was found to inhibit IL-6-induced activation of STAT3 through EPAC-mediated induction of SOCS3 expression (Sands *et al.*, 2006). Thus, elevation of intracellular cAMP levels in cell line models of PCa may also attenuate IL-6-induced activation of STAT3. Both anti-apoptotic proteins, such as Bcl-X_L, and proteins associated with cell cycle progression, e.g. cyclin D1, are STAT3-responsive genes, thus blockade of STAT3 activation should promote apoptosis and a decrease in proliferation of PCa cell lines (Cochet *et al.*, 2006; Leslie *et al.*, 2006; Xu *et al.*, 2005). Indeed, selective blockade of STAT3 has been demonstrated to increase apoptosis in cellular models of PCa (Barton *et al.*, 2004). However, the approach used in the Barton *et al.* (2004) study utilised a dominant negative and anti-sense oligonucleotides to inhibit STAT3 signalling. Given that cAMP elevation appears to be an endogenous inhibitor of inflammatory responses, it is possible that manipulation of physiological anti-inflammatory pathways may prove a more suitable therapeutic strategy to inhibit STAT3 activation by IL-6.

To this end, the responses to exogenous cytokines were characterised in three prostate epithelial cell lines representing normal, early-stage and late-stage PCa. Having established suitable conditions in which to investigate IL-6-induced activation of STAT3 in these cell lines, the ability of cAMP to inhibit IL-6-induced increases in pTyr⁷⁰⁵STAT3 was investigated in each cell line. As a result of these experiments, the ability of cAMP elevation to modulate the differentiation and morphology of prostate epithelial cells formed the focus of the latter part of this study.

4 Materials

Abcam, Cambridge, UK

Mouse monoclonal antibody to glyceraldehyde-3-phosphate dehydrogenase (GAPDH, Cat. # ab8245), goat polyclonal antibody to mouse IgG phycoerythrin- (PE-) conjugated (Cat. # ab7002), rabbit polyclonal antibody to pSer¹³³CREB (Cat. # ab30651), rabbit polyclonal antibody to SOCS3 (Cat. # ab16030),

Addgene, Cambridge, MA, USA

pRK5.MycRhoA.N17 (plasmid 15901)

American Type Culture Collection, Teddington, UK

DU145 prostate epithelial cells, LNCaP prostate epithelial cells, PZ-HPV-7 prostate epithelial cells

American Radiolabelled Chemicals, St. Louis, MO, USA

³H-ZM241385

Beckman Coulter, High Wycombe, UK

Ultra-Clear ultracentrifuge tubes

Biolog, Bremen, Germany

8- (4-Chlorophenylthio)- 2'- O- methyladenosine- 3', 5'- cyclic monophosphate (8Me-pCPT-cAMP)

Biorad Laboratories Ltd, Hemel Hempstead, Hertfordshire, UK

Precision plus protein markers, Mini-protean III mini-gel kit

Boehringer Ingelheim, Bracknell, UK

BIX02188

Brandel Inc, Gaithersberg, MD, USA

GF/CGlass fibre filters

Cell Signalling Technology,

Mouse monoclonal antibody to pThr²⁰²pTyr²⁰⁴ERK1/2 (Cat. # 9106), rabbit polyclonal antibody to pThr²¹⁸pTyr²²⁰ERK5 (Cat. # 3371) mouse monoclonal antibody to pTyr⁷⁰¹STAT1 (Cat. # 9171), mouse monoclonal antibody to pTyr⁷⁰⁵STAT3 (Cat. # 9138), rabbit polyclonal antibody to STAT1 (Cat. # 9172), rabbit polyclonal antibody to STAT3 (Cat. # 9132), rabbit polyclonal antibody to JAK1 (Cat. # 3332), rabbit polyclonal antibody to JAK2 (Cat. # 3772), rabbit monoclonal antibody to RhoA (Cat. # 2117), rabbit polyclonal antibody to phospho-PKA substrate (Cat. # 9621)

Clontech, Sainte-Germaine-en-Laye, France

pEGFP-N1

Inverclyde Biologicals, Bellshill, Lanarkshire, UK

Whatman Protran nitrocellulose membrane

Invitrogen, Paisley, UK

Dulbecco's PBS, Keratinocyte serum free medium kit containing bovine pituitary extract and recombinant epidermal growth factor (Cat. # 37010-022), rhodamine-conjugate phalloidin, Lipofectamine 2000 transfection reagent, Optimem, RPMI 1640 medium

Lonza Group Ltd, Basel, Switzerland

Human umbilical vein endothelial cells, Endothelial growth medium 2

Merck Chemicals Ltd, Nottingham, UK

Forskolin (7 β -Acetoxy-8,13-epoxy-1 α ,6 β ,9 α -trihydroxy-labd-14-en-11-one), H89 (*N*-[2-(*p*-bromocinnamyl)amino]ethyl]-5-isoquinoline-sulfonamide dihydrochloride), MG132 (Carbobenzoxy-L-leucyl-L-leucyl-L-leucinal), myristoylated PKA inhibitor 14-22 amide (myrPKI₁₄₋₂₂), N⁶-Benzoyl-cAMP (6-Bnz-cAMP) rabbit polyclonal antibody to pSer¹⁸⁸RhoA, U0126 (1,4-Diamino-2,3-dicyano-1,4-*bis*(2-aminophenylthio)butadiene), Y27632 ((1)-(*R*)-*trans*-4-(1-aminoethyl)-*N*-(4-pyridyl) cyclohexanecarboxamide dihydrochloride)

Perkin-Elmer Life Sciences, Waltham, MA, USA

³H-Leucine, Western Lightning Plus Enhanced chemiluminescence substrate (Cat. # NEL103001EA)

Qiagen, Crawley, West Sussex, UK

HiPerFect siRNA reagent, Qiagen Maxi Plasmid kit, QIAprep Spin Miniprep kit,

R&D Systems

Recombinant human IL-6

Santa Cruz Biotechnology Inc, Santa Cruz, CA, USA

Rabbit polyclonal antibody to ERK5 (Cat. # sc-5626), rabbit polyclonal antibody to EPAC2 (Cat. # 9383), Horseradish peroxidase (HRP)- conjugated swine anti-mouse Immunoglobulin (Ig) G (sc-2463)

Sigma-Aldrich, Poole, Dorset, UK

30% Acrylamide/bisacrylamide solution, 3-[(3-Cholamidopropyl)dimethylammonio]-1-propanesulfonate hydrate (CHAPS), Dulbecco's minimal essential medium, Eagle's Minimal Essential Medium, Emetine dihydrochloride, Endothelial cell trypsin, Foetal bovine serum, HRP- conjugated goat anti-mouse Immunoglobulin (Ig) G , HRP-conjugated goat anti-rabbit IgG, Nocodazole, Penicillin/streptomycin solution, Poly-D-Lysine Hydrobromide, 4-Hydroxytamoxifen, Trypsin-EDTA solution,

Tocris, Avonmouth, Bristol, UK

ZM241385

Universal Biologicals Ltd, Cambridge, UK

Cell-permeable C3 transferase from *Clostridium botulinum* (C3T, Cat. # CT04)

5 Methods

5.1 Cell culture

All cells were cultured at 37°C, 5% (v/v) CO₂ in a humidified atmosphere.

5.1.1 Culture of DU145 cells

DU145 cells were maintained in Eagle's minimal essential medium (MEM) supplemented with 10% (v/v) foetal bovine serum (FBS), 1 mM L-glutamine, 100 U/ml penicillin, 100 µM streptomycin and 1 mM sodium pyruvate. Cell populations were maintained in tissue culture sterile 150 cm² flasks and sub-cultured at approximately 80% confluency.

During cell passage, tissue culture medium was removed and retained in sterile 50 ml centrifuge tubes. DU145 cells were washed with 5 ml Dulbecco's phosphate buffered saline (DPBS) lacking both Ca²⁺ and Mg²⁺. DPBS was discarded and 2 ml of 1x trypsin-EDTA added to the cells. DU145 cells were incubated for 5 – 10 min to allow detachment of the cell monolayer which was aided via gentle tapping. The proteolytic actions of trypsin were neutralised *via* addition of 5 ml of the retained tissue culture medium and cells pelleted via centrifugation at 200 x g for 5 min at room temperature. Cells were then resuspended in a suitable volume of fresh, supplemented MEM and seeded as required.

To store the DU145 cell line, cell pellets were prepared as described during cell passage and the pellets resuspended in supplemented MEM containing 5% (v/v) dimethylsulphoxide (DMSO). Cells were immediately frozen at –80°C overnight prior to transfer to liquid nitrogen for long term storage. To resurrect frozen cells, cell stocks were rapidly defrosted at 37°C and centrifuged at 200 x g for 5 min at 4°C to remove traces of DMSO. The resultant cell pellet was resuspended in 10 ml of fresh medium and the cells maintained as described above.

5.1.2 Culture of LNCaP cells

LNCaP cells were maintained in RPMI 1640 medium supplemented with 10% (v/v) FBS, 1 mM L-glutamine, 100 U/ml penicillin, 100 µM streptomycin and 1 mM sodium pyruvate. Cell populations were maintained in tissue culture sterile 150 cm² flasks and passaged at approx. 80% confluency. To aid adhesion of LNCaP cells, all tissue culture plastic was coated with 0.1 mg/ml poly-D-lysine hydrobromide prior to use.

LNCaP cells were passaged and cryopreserved in supplemented RPMI 1640 medium via an identical process to that described for DU145 cells above.

5.1.3 Culture of PZ-HPV-7 cells

PZ-HPV-7 cells were maintained in keratinocyte serum free medium (KSFM) supplemented with 5 ng/ml recombinant epithelial growth factor, 0.05 mg/ml bovine pituitary extract, 100 U/ml penicillin and 100 µM streptomycin. Cell populations were maintained in tissue culture sterile 150 cm² flasks and passaged at approximately 80% confluency.

PZ-HPV-7 cells were passaged and cryopreserved in supplemented KSFM via a process similar to that described for DU145 cells above. Due to the sensitivity of this cell line to trypsin, cells were passaged with 0.5x trypsin-EDTA which was washed briefly over the monolayer surface and removed prior to incubation at 37°C, 5% (v/v) CO₂ to detach the cell monolayer. In order to cryopreserve PZ-HPV-7 cells, KSFM was supplemented with 10% (v/v) FBS and 5% (v/v) DMSO prior to freezing.

5.1.4 Culture of HEK293 cells

Human embryonic kidney (HEK) 293 cells were maintained in Dulbecco's minimal essential medium (DMEM) supplemented with 10% (v/v) FBS, 1 mM L-glutamine, 100 U/ml penicillin and 100 µM streptomycin. Cell populations were maintained in tissue culture sterile 150 cm² flasks and passaged at approximately 80% confluency.

HEK293 cells were passaged and cryopreserved in supplemented DMEM via an identical process to that described for DU145 cells above except that cell lines were frozen in DMEM supplemented with 10% (v/v) DMSO.

5.1.5 Culture of HUVECs

HUVECs were obtained from commercial sources and maintained in endothelial cell growth medium-2 (EGM-2) supplemented with 2% (w/v) foetal bovine serum, hydrocortisone, ascorbate and recombinant growth factors as recommended by the supplier in tissue culture sterile 150cm² flasks and passaged at 80% confluency. Passage of HUVECs was as described for PZ-HPV-7 cells except that 1 x endothelial cell trypsin was used to detach HUVECs from the tissue culture flasks. In order to prevent passage-related changes in endothelial cell characteristics, HUVEC cells were not used beyond passage five.

5.2 Transfections

5.2.1 Cell transfection with cDNA plasmids

Cells were plated at the density required for each experimental procedure and allowed to adhere overnight at 37°C, 5% (v/v) CO₂. The following day, plasmid DNA was introduced to cells using the Lipofectamine 2000 transfection reagent. Briefly, for one well of a 6 well plate, 100 µl Optimem was mixed with 4 µl Lipofectamine 2000 in a sterile microfuge tube prior to incubation at room temperature for 5 min. In a separate, sterile microfuge tube, a total of 1 µg DNA was added to 100 µl Optimem and mixed by gentle tapping. Following incubation, the entirety of the Lipofectamine 2000/Optimem mixture was added to the microfuge tube containing DNA. The contents were mixed by gentle tapping and incubated at room temperature for 20 min. Cell culture medium on cells was discarded and replaced with 2 ml/well of antibiotic-free, supplemented growth medium. 200 µl of transfection mixture was added per well and cells incubated overnight at 37°C, 5% (v/v) CO₂. At 24 h post-transfection, growth medium was discarded and replaced with 1.5 ml of supplemented growth medium containing antibiotics. Cells were maintained for a further 24 h at 37°C, 5% (v/v) CO₂ prior to use in experiments.

5.2.2 Transfection of cells with siRNA

Cells were plated in 6-well tissue culture plates and grown to 50 – 60 % confluence in the appropriate growth medium. On the day of siRNA transfection, transfections were performed as per manufacturer's recommendations with minor alterations appropriate to the cells types used. All volumes stated are for appropriate for siRNA transfection of one well of a 6-well plate. Briefly, cell culture medium was replaced with 2.3 ml/well of supplemented cell culture medium lacking antibiotics. To prepare the transfection mixtures, 100 pmol/well of the appropriate siRNA was diluted in 100 µl of Optimem I and mixed by vortexing. Subsequently, 12 µl of HiPerFect transfection reagent was added to the diluted siRNA and the transfection mixture vortexed to ensure uniform mixing of the reagents. The transfection mixtures were then incubated for 10 min at room temperature to allow formation of transfection complexes and the transfection mixture added to the cell monolayer in a drop-wise fashion. Cells were incubated overnight at 37°C, 5 % (v/v) CO₂ and culture medium replaced the following day. Cells were then incubated for a further 24 h at 37°C, 5 % (v/v) CO₂ and used in experiments at 48 h post-transfection.

5.3 Molecular biology

5.3.1 Plasmid DNA constructs

pRK5 plasmids encoding Myc-tagged wild-type RhoA and constitutively active RhoA (mycRhoAWT and mycRhoAQ63L respectively) were a kind gift from Professor Alan Hall (University College London, London, UK). A plasmid expressing a Myc-tagged dominant-negative RhoA mutant (mycRhoAT19N) was obtained from Addgene.

Plasmids encoding a Myc-tagged Raf1:Oestrogen receptor chimera (mycRaf1:ΔER), a wild-type ERK5 and dominant negative ERK5-AEF were a generous gift from Dr. Simon Cook (Babraham Institute, Cambridge, UK).

A plasmid encoding an enhanced green fluorescent protein (pEGFP-N1) was obtained from Clontech.

5.3.2 Bacterial Strains and Media

Escherichia coli XL1 Blue bacteria were used for the propagation of plasmid vectors. *E. coli* were grown in sterile Luria-Bertani (LB) media (1% (v/v) bacto-tryptone, 0.5% (v/v) yeast extract, 1% (v/v) NaCl, pH 7) supplemented with either 50 µg/ml ampicillin (LB^{Amp}), 50 µg/ml tetracycline (LB^{Tet}) or 50 µg/ml Kanamycin (LB^{Kan}) as appropriate for selection. Agar plates were prepared by inclusion of 1.5% (w/v) agar in the appropriate LB media. Plates were stored at 4°C prior to use.

5.3.3 Preparation of competent *E. coli*

Overnight cultures of *E. coli* XL1 Blue were prepared in 3 ml LB^{Tet} and used to inoculate 250 ml LB^{Tet} the following day. Cultures were grown at 37°C with agitation until OD₆₀₀=0.35. *E. coli* were transferred to sterile, pre-chilled 250 ml centrifuge tubes and incubated on ice for 60 min. Bacteria were harvested via centrifugation at 6000 x g, 20 min, 4°C and the supernatant discarded. Pellets were washed in 60 ml ice-cold, sterile 0.1 M MgCl₂ prior to centrifugation at 6000 x g, 20 min, 4°C. Pellets were resuspended in ice-cold, sterile 0.1 M CaCl₂ and incubated on ice for 20 min. Competent *E. coli* were then harvested via further centrifugation 6000 x g, 20 min, 4°C and resuspended in ice-cold 15% (v/v) glycerol in 0.1 M CaCl₂. The bacterial suspension was divided into 250 µl aliquots which were rapidly frozen using dry ice/methanol prior to storage at -80°C.

5.3.4 Transformation of competent *E. coli*

Aliquots of competent *E. coli* XL1 Blue were thawed on ice for up to 30 min and 40 µl per transformation transferred immediately to chilled sterile microfuge tubes containing 10 – 50 ng DNA. Cells were incubated on ice for 15 min prior to heat shock at 42°C for 45 sec. The tubes were returned to ice immediately for 2 min prior to addition of 1 ml per transformation of LB media. *E. coli* were incubated at 37°C, 200 rpm for 1 h prior to plating of 100 µl and 800 µl of transformed bacteria onto selective LB agar plates. Plates were allowed to dry under sterile conditions and incubated in a static incubator overnight at 37°C to enable bacterial growth.

5.3.5 Preparation of glycerol stocks

Single colonies were picked from selective LB agar plates and grown to mid-log phase ($OD_{600} = 0.3$) in LB^{Amp} or LB^{Kan} as appropriate. For each glycerol stock, 0.7 ml of bacterial culture was mixed with 0.3 ml sterile 50% (v/v) glycerol in a sterile cryovial. Vials were mixed thoroughly, prior to rapid freezing on dry ice and storage at –80°C.

5.3.6 Preparation of plasmid DNA

Plasmid DNA was purified from overnight cultures using either a QIAprep Spin Miniprep kit or a Qiagen Maxi Plasmid kit following manufacturer's instructions.

5.3.6.1 Plasmid DNA preparation using QIAprep Spin Miniprep

Single colony glycerol stocks were used to inoculate 5 ml of selective LB and cultures were grown overnight at 37°C, 200 rpm. Bacteria were harvested via centrifugation at 13, 200 x *g* for 10 min, 4°C and the resultant pellet resuspended in 250 µl buffer P1 (50 mM Tris.Cl, pH 8.0, 10 mM EDTA, 100 µg/ml RNase A) supplemented with LyseBlue reagent at a ratio of 1:1000. Bacterial lysis was achieved via addition of 250 µl buffer P2 (200 mM NaOH, 1 % (w/v) SDS) and incubation at room temperature for a maximum of 5 min. Lysates were mixed by inversion until a homogenous blue colour was achieved. To neutralise lysis, 350 µl of buffer P3 (3 M potassium acetate, pH 5.5) was added and lysates mixed immediately by inversion. Lysates were then centrifuged at 13, 200 x *g* for 10 min, room temperature to pellet precipitated potassium dodecyl sulphate, SDS-denatured proteins, genomic DNA and cellular debris. Lysates were then applied directly to a QIAprep spin column and centrifuged at 13, 200 x *g* for 10 min. Supernatants were discarded and the column was then washed once with 750 µl buffer PE. Following centrifugation at 13, 200 x *g* for 1 min, supernatant was discarded and residual buffer PE removed via further centrifugation at 13, 200 x *g* for 1 min. DNA was eluted via addition

of 50 μ l sterile DEPC H₂O and centrifugation of QIAprep spin columns at 13, 200 x g for 1 min. DNA preparations were stored at -20°C until use.

5.3.6.2 Plasmid DNA preparation using Qiagen Maxi Plasmid kit

Single colony glycerol stocks were used to inoculate 5 ml of selective LB and cultures were grown for 8 h at 37°C, 200 rpm. This starter culture was then used to inoculate 400 ml of selective LB and the culture grown overnight at 37°C, 200 rpm. Following incubation, bacteria were harvested via centrifugation at 6, 000 x g, 15 min, 4°C and pellets resuspended in 10 ml of buffer P1 supplemented with LyseBlue reagent as described above. Cells were lysed via addition of 10 ml buffer P2 for up to 5 min as described in section 5.3.6.1. To neutralise lysis, buffer P3 (see section 5.3.6.1) was added, lysates mixed immediately by inversion and the lysates incubated on ice. Lysates were then cleared via two centrifugation steps at 20, 000 x g, 10 min, 4°C and the resultant supernatant applied to a Qiagen-tip 500 which had been pre-equilibrated with 10 ml buffer QBT (750 mM NaCl, 50 mM MOPS, pH 7.0, 15 % (v/v) isopropanol, 0.15 % (v/v) Triton X-100). The supernatant was allowed to enter the resin via gravity flow and the tip was then washed twice with 30 ml buffer QC (1 M NaCl, 50 mM MOPS, pH 7.0, 15 % (v/v) isopropanol). DNA was eluted via the addition of 15 ml buffer QF (1.25 M NaCl, 50 mM Tris, pH 8.5, 15 % (v/v) isopropanol) and precipitated via the addition of 10.5 ml of isopropanol at room temperature. Following incubation for 30 min, DNA was pelleted via centrifugation at 15, 000 x g, 15 min, 4°C. The DNA pellet was then washed with 5 ml of 70% ethanol at room temperature and harvested via centrifugation at 15, 000 x g, 15 min, 4°C. The resultant pellet was then allowed to air-dry for 10 min and resuspended in 400 μ l sterile TE buffer (10mM Tris-Cl, pH 7.5, 1 mM EDTA). DNA preparations were stored at -20°C until use.

5.3.7 Determination of DNA purity and concentration

DNA preparations were thawed on ice and diluted in sterile, DEPC-treated water. DNA concentration was determined by measuring the absorbance at 260 nm (A_{260}) and calculated based on the assumption that, with a path length value of 1, a 50 μ g/ml solution of DNA has an A_{260} value of 1. DNA purity was assessed by measuring the absorbance at 280 nm (A_{280}) based on the assumption that, for a pure DNA solution, $A_{260}/A_{280} = 1.8$.

5.4 Generation and maintenance of recombinant adenovirus

5.4.1 Generation of myc-tagged human A_{2A}AR-expressing adenovirus

Recombinant adenovirus encoding the myc-tagged human A_{2A}AR (myc.A_{2A}AR) was generated by Dr William Sands and Dr. Elaine Strong (University of Glasgow, Glasgow, UK) using the “AdEasy” system (He *et al.*, 1997) and has been described previously (Sands *et al.*, 2004).

The pAdEasy1 plasmid contains an open reading frame encoding GFP which is maintained in the recombinant adenovirus and so viral infection of HEK 293 cells can be monitored by fluorescence microscopy. Three - six days post-infection, HEK 293 cells were harvested and disrupted by freeze-thawing to release adenovirus particles. Cleared lysate was used to infect two 150 cm² tissue culture flasks of 70 % confluent HEK 293 cells. Following successful infection, cells were harvested and viral particles collected as before in order to infect twenty 150 cm² flasks for a large scale preparation.

Recombinant adenovirus encoding GFP alone was kindly donated by Professor Robert White (Beatson Institute for Cancer Research, Glasgow, UK).

5.4.2 Large-scale preparation of recombinant adenoviruses

Pure high titre stocks of recombinant adenovirus were obtained by amplification and purification with reference to the method described by Nicklin and Baker (1999). Confluent 150 cm² flasks of low-passage HEK 293 cells were infected with either crude viral extract from previously infected HEK 293 cells or with plaque-purified recombinant adenovirus at an MOI of 0.1-10 per flask and incubated for 2-6 days at 37 °C, 5 % (v/v) CO₂. Once the cytopathic effect of the virus had caused the cells to detach from the flasks, cells were harvested and pelleted by centrifugation (250 g, 10 min, RT). Pellets were stored at - 80° C, ready for viral harvesting and purification.

Cell pellets from twenty 150 cm² flasks were defrosted at room temperature and pooled by resuspension in a total volume of 10 ml room temperature PBS followed by centrifugation (250 x g, 10 min, RT). The resultant single pellet was resuspended in 5 ml PBS and cells were lysed by 5 cycles of freeze/thawing in a dry ice/methanol bath followed by incubation with agitation in a 37 °C water bath. The cell suspension was vortexed vigorously for 30

seconds between cycles to encourage cell breakage. The lysate was cleared by centrifugation (7000 x g, 10 mins, 4 °C) and the supernatant containing the adenovirus was collected for further purification.

Adenovirus obtained by the freeze/thawing method is contaminated with cellular protein and viral debris which may be cytotoxic when used *in vitro*. To obtain a pure preparation, the supernatant from the previous step was separated on a discontinuous CsCl density gradient. The CsCl gradient was created by underlying 3 ml of 1.2 g/ml CsCl solution with 1.5 ml of 1.4 g/ml CsCl solution in a 14 × 95 mm Ultra-Clear centrifuge tube (Beckman). The crude adenovirus extract was applied to the top of the gradient and centrifuged (90 000 x g, 1.5 h, 8 °C) with zero deceleration to produce a translucent white band between the two layers of CsCl, representing pure adenovirus. Zero deceleration was selected during the centrifugation step to prevent disruption of the delicate band by turbulence during braking. The adenovirus band was extracted using a syringe and a 21-gauge needle to puncture the side of the centrifuge tube and then transferred to a 3 ml Slide-A-Lyser dialysis cassette. The extract was dialysed overnight at 4 °C in 600 ml TE buffer (10 mM Tris, pH 7.4, 1 mM EDTA, pH 8.0) with three changes. The following day, the purified adenovirus was diluted in an equal volume of sterile storage buffer (10 mM Tris, pH 8.0, 100 mM NaCl, 0.1 % (w/v) BSA, 50 % (v/v) glycerol) and stored at – 80 °C in 10 µl aliquots.

5.4.3 Titration of adenoviruses

Purified adenovirus was titred using a Cell Biolabs Inc QuickTitre Adenovirus Immunoassay Kit according to the manufacturer's instructions. HEK 293 cells were seeded in poly-D-lysine-coated 24-well tissue culture plates and incubated for 1 hour at 37 °C, 5 % (v/v) CO₂. A series of 10-fold dilutions of the CsCl-purified adenovirus preparation was prepared and used to infect the HEK 293 cells in duplicate. Forty-eight hours later, cells were fixed using ice-cold methanol and then immunostained using a primary antibody directed against the adenoviral capsid protein, hexon (supplied) and a secondary horseradish peroxidase (HRP)-conjugated antibody which recognises the anti-hexon antibody (supplied). Binding of the HRP-conjugated antibody was detected by incubation with a solution of the HRP substrate, diaminobenzidine (DAB; supplied). DAB undergoes oxidative polymerisation in the presence of HRP to produce a dark brown precipitate. Adenovirus-infected cells stained rapidly and were clearly visible under light microscopy as discrete brown patches in the cell monolayer. Positively stained cells were counted in

ten fields at a virus dilution that gave 5-50 positive cells/field when viewed using a 10 × objective. The mean result was determined and used to calculate the number of infected cells per ml of the original adenovirus preparation to give a titre value in infectious units/ml (ifu/ml).

5.4.4 Infection of LNCaP cells with recombinant adenovirus

LNCaP cells were seeded at a density of 2×10^5 cells per well into 6 cm tissue culture plates coated with 0.1 mg/ml poly-D-lysine hydrobromide. To allow adherence, cells were maintained at 37°C, 5% (v/v) CO₂ in RPMI 1640 medium supplemented as described in section 5.1.2 for 24 h. Following adherence, cell culture medium was replaced with fresh RPMI 1640 supplemented as described in section 4.1.2. LNCaP cells were infected with recombinant adenovirus (AdV) containing a construct expressing either GFP (AdV.GFP) or a Myc-tagged A_{2A}AR (AdV.A_{2A}AR) at the appropriate MOI. Cells were subsequently incubated for 24 h at 37°C, 5% (v/v) CO₂ to allow recombinant protein expression. At 24 h post-infection, culture medium was discarded and replaced with fresh, supplemented RPMI 1640 medium. Cells were imaged as described in section 5.7.4 and incubated for a further 24 h at 37°C, 5% (v/v) CO₂ prior to use as described in individual experiments.

5.4.5 Radioligand binding assay

LNCaP cells were seeded into 75 cm² tissue culture flasks coated with 0.1 mg/ml poly-D-lysine HBr at a density of 8.3×10^5 cells per flask and allowed to adhere overnight. The following day, cells were infected with AdV.GFP or AdV.A_{2A}AR at an MOI = 6 ifu/cell and incubated for 24 h at 37°C, 5% (v/v) CO₂. In order to maintain cell viability, cell culture medium was replaced at 24 h post-infection and the cells incubated for a further 24 h at 37°C, 5% (v/v) CO₂. The following day, cell culture medium was removed and the monolayer washed 3 times with 7 ml ice-cold PBS. Cell membranes were prepared on ice by addition of 7 ml of ice-cold lysis buffer containing 10 mM HEPES and 5mM EDTA, pH 7.5. Cells were transferred to a 7 ml glass Douce homogeniser which had been pre-chilled on ice and homogenised by 20 up-and-down strokes. The membrane fraction was extracted following transfer to a pre-chilled centrifuge tube and centrifugation at 13500 x g at 4°C for 30 min and the subsequent pellet resuspended in 400 µl of 50/10 ligand binding buffer containing 50 mM HEPES and 10 mM MgCl₂, pH 6.8. 50 µl of this suspension was retained for subsequent determination of protein concentration. The volume of the remaining membrane suspension was then adjusted to 4 ml with 50/10 ligand binding buffer which was supplemented with 1 U/ml adenosine deaminase. Membranes were transferred to a pre-chilled glass Douce homogeniser and resuspended by 20 up-and-down

strokes. Membranes were then used immediately in the ligand binding assay described below.

In order to accurately assess radioligand binding, a six point ligand binding curve was performed with each point performed in duplicate in a total volume of 250 μ l comprising 50 μ l of the radio-labelled ligand, 150 μ l of the membrane suspension and 50 μ l of either competing ligand or H₂O. Concentrations of ³H-ZM241385, an A_{2A}AR-selective inverse agonist, were prepared in 50/10 binding buffer and used in the assay at final concentrations ranging from 0.25 – 8 nM. In order to assess non-specific binding, membranes were incubated with 50 μ M of the competing ligand NECA, a non-selective adenosine receptor whilst incubation with 50 μ l H₂O in order to assess total binding of ³H-ZM241385. Incubations were performed at 37°C for 60 min and samples harvested *via* vacuum filtration using a Brandel harvester and glass fibre filters pre-soaked in 0.3 % (v/v) polyethylimine. Filters were washed three times in 50/10/1 wash buffer containing 50 mM HEPES, 10 mM MgCl₂ and 1 mM EDTA supplemented with 0.03 % (w/v) CHAPS. Filters were then resuspended in 5 ml scintillation fluid and stored at 4°C overnight to both maximise radioligand extraction and to decrease background chemiluminescence. Binding of ³H-ZM241385 was determined by liquid scintillation counting.

5.5 Stimulation of prostate epithelial cells with exogenous cytokine

Cells were seeded and grown to appropriate confluency as described in section 5.1.1-3. In order to ensure that resultant protein activation arose due to the actions of exogenous agents rather than from growth factors, etc. secreted into the medium during cell growth, culture medium was removed prior to experiments and replaced with an appropriate volume of fresh, supplemented growth medium. To prevent temperature-dependent alterations in cell responses, medium was pre-warmed to 37°C prior to use. Cells were then stimulated as described for individual experiments and harvested for analysis by western blotting as described below.

5.5.1 Membrane translocation of RhoA

LNCaP cells were seeded into 10 cm tissue-culture dishes and grown to 60 -70 % confluence. Upon the day of experiment, culture medium was replaced with 5 ml/dish of fresh, supplemented RPMI 1640 medium and stimulated as described for individual experiments. Following simulations, cells were washed 3 times in 5ml/dish ice-cold PBS and harvested into 300 μ l of ice-cold PBS. Cells were pelleted *via* centrifugation at 300 x g

for 5 min at 4°C and subsequently resuspended in 500 µl of ice-cold KCl relaxation buffer containing 100 mM KCl, 50 mM HEPES pH 7.2, 5 mM NaCl, 1 mM MgCl₂, 0.5 mM EGTA, 100 µM PMSF, 2 µg/ml benzamidine, 2 µg/ml soyabean trypsin inhibitor and a complete protease inhibitor. Lysates were sonicated for 2 x 20 seconds on ice prior to the removal of unbroken cells and nuclei *via* centrifugation at 700 x *g* for 7 min at 4°C. The resultant supernatant was transferred to a 13 x 51 mm Ultra-Clear™ centrifuge tube and volumes were adjusted to 5 ml in KCl relaxation buffer. Cell membranes were harvested by subsequent ultracentrifugation at 50, 000 x *g* for 45 min at 4°C. The supernatant was discarded and the resultant pellet washed in 5 ml of KCl relaxation buffer as described. The washed cell pellet was resuspended in 100 µl of RhoA translocation buffer containing 0.25 M Na₂HPO₄, 0.3 M NaCl, 2.5 % (w/v) SDS, 100 µM PMSF, 2 µg/ml benzamidine, 2 µg/ml soyabean trypsin inhibitor and a complete protease inhibitor. To ensure sufficient solubilisation of the cellular membranes, the lysates were incubated on a rotating wheel at room temperature prior to determination of protein content and SDS-PAGE-fractionation.

5.6 Analysis of proteins by western blotting

5.6.1 Whole cell lysate preparation

Following incubation with appropriate stimuli, stimulation was quenched via discarding the supernatant and washing cells 3 times in ice-cold PBS. Cells were lysed in 100 µl RIPA⁺ (50 mM HEPES pH 7.5, 150 mM sodium chloride, 1% (v/v) Triton X-100, 0.5% (w/v) sodium deoxycholate, 0.1% (w/v) SDS, 5 mM EDTA pH 8, 10 mM sodium fluoride, 10 mM sodium phosphate, 2 µg/ml benzamidine, 2 µg/ml soyabean trypsin inhibitor, 100 µM phenylmethanesulphonyl fluoride (PMSF), 100 µM sodium orthovanadate, and a complete protease inhibitor cocktail) and left to solubilise on ice for 30 min. Lysates were transferred to 1.5 ml microfuge tubes and stored at -80°C prior to analysis by SDS-PAGE fractionation and western blotting.

5.6.2 Determination of protein content

Whole cell lysates were thawed on ice and centrifuged at 9500 x *g* for 15 min at 4°C to remove insoluble cellular debris. The protein concentration of each sample was then estimated using the bicinchoninic acid (BCA) assay performed in a 96-well plate. Briefly, 2 µl of each sample was added to 8 µl of RIPA⁺ buffer in the absence of protease inhibitors. Standard protein concentrations (0-2 mg/ml) were prepared by performing serial dilutions of a stock 2 mg/ml bovine serum albumin (BSA) in the RIPA⁺ buffer described above. All samples were assayed in duplicate.

BCA reagent (1% (w/v) 4,4-dicarboxy-2,2-biquinoline disodium salt, 2% (w/v) anhydrous sodium carbonate, 0.16% (w/v) sodium potassium tartrate, 0.4% (w/v) sodium hydroxide and 0.95% (w/v) anhydrous sodium bicarbonate) was mixed with 4% (w/v) copper (II) sulphate solution in a ratio of 49 parts BCA reagent to 1 part 4% (w/v) copper (II) sulphate. 70µl of this solution was added to each well and the plate incubated for 15 min at room temperature. Following incubation, the protein content was quantified by determining the absorbance at 490nm and extrapolation of protein concentration from the BSA standard curve.

5.6.3 Immunoblotting

Following the BCA assay, samples were equalised for protein content (typically 10 – 50 µg) and volume. Samples were then denatured via addition of an equal volume of SDS loading buffer containing 50 mM Tris pH 6.8, 10% (v/v) glycerol, 12% (w/v) SDS, 0.1 M dithiothreitol and the tracking dye bromophenol blue prior to fractionation via sodium dodecylsulphate-polyacrylamide gel electrophoresis (SDS-PAGE). In order for efficient separation of proteins, resolving acrylamide gels were prepared ranging from 8 – 15 % (w/v) acrylamide. Proteins were separated by 1D electrophoresis in a Tris-Glycine buffer containing 24.7 mM Tris, 0.19 M Glycine and 0.1% (v/v) SDS at 130 V.

Subsequently, fractionated proteins were transferred via electrophoresis to a 0.2 µm diameter Protran nitrocellulose membrane for 45 mins, 400 mA in transfer buffer comprising 24.7 mM Tris, 0.19 M glycine and 20% (v/v) methanol.

To prevent non-specific antibody binding, membranes were incubated for 1 h with Tris-buffered saline (TBS) pH 7.6 containing 0.1% (v/v) Tween 20 (TBST) and 5% (w/v) non-fat milk powder (TBST-M). Membranes were then washed twice for 5 min in TBST prior to addition of the primary antibody as described in Table 4.1. Following incubation with the appropriate primary antibody, membranes were washed five times for 5 min in TBST prior to addition of the appropriate secondary horse radish peroxidase- (HRP-) conjugated antibody. HRP-conjugates were diluted 1 in 1000 in TBST-M from the stock antibody solution. Membranes were incubated on a rotator for 1 h at room temperature with the secondary antibody conjugates prior to washing three times for 5 min in TBST and visualisation of antibody staining using enhanced chemiluminescence (ECL) and X-ray film (Kodak, UK) are per manufacturer's instruction.

5.7 Fsk-induced dendrite outgrowth

5.7.1 Fsk-induced NE differentiation in LNCaP cells

LNCaP cells were seeded at a density of $2-3 \times 10^5$ cells per well into 6 cm tissue culture plates coated with 0.1 mg/ml poly-D-lysine hydrobromide. To allow adherence, cells were maintained at 37°C, 5% (v/v) CO₂ in RPMI 1640 medium supplemented as described in section 5.1.2 for 2 days. Prior to stimulation, tissue culture medium was discarded and replaced with 3 ml per dish of fresh, supplemented RPMI 1640 containing either vehicle (0.1% EtOH) or 10 μM Fsk. LNCaP cells were incubated in a humidified atmosphere at 37°C, 5% (v/v) CO₂ for 5 h prior to imaging using phase contrast light microscopy (see section 5.7.4). Cells were incubated for a further 19 h and imaged again at 24 h post-stimulation prior to harvesting for immunoblotting as described previously.

5.7.2 Effect of inhibitors on Fsk-induced NE differentiation

BIX02188 was a generous gift from Boehringer Ingelheim. LNCaP cells were seeded at a density of $2-3 \times 10^5$ cells per well into 6 well tissue culture plates. To allow adherence, cells were maintained at 37°C, 5% (v/v) CO₂ in supplemented RPMI 1640 for 48 h. Prior to stimulation, medium was removed and replaced with 1 ml per well of fresh, supplemented RPMI 1640 containing vehicle (0.1% DMSO, 0.1% EtOH) or the appropriate inhibitor. To enable effective inhibition, cells were incubated for 1 h at 37°C, 5% (v/v) CO₂ prior to imaging using phase contrast light microscopy (see section 5.7.4). LNCaP cells were then stimulated with vehicle or 10 μM Fsk and incubated for a further 1 h at 37°C, 5% (v/v) CO₂ prior to imaging using phase contrast light microscopy (see section 5.7.4). In order to assess inhibitor efficacy, control wells were stimulated with the appropriate agonist in the presence and absence of inhibitor as indicated in results. LNCaP cells were then harvested for immunoblotting as described in section 5.6. NE differentiation was assessed by determining the changes in Fsk-induced dendrite outgrowth as described in section 5.7.4.

5.7.3 ³H-Leucine incorporation assay

LNCaP cells were seeded into 24-well plates coated at a density of 4×10^4 cells/well and allowed to adhere for 48 h. Prior to assay, culture medium was discarded and replaced with 500 μl/well of fresh, supplemented RPMI 1640 medium containing emetine at concentrations ranging from 0 – 1000 μM with all samples performed in triplicate. Cells were incubated for 2 h at 37°C, 5% (v/v) CO₂ prior to labelling with 7.4 KBq/well of ³H-Leu for 3 h at 37°C, 5% (v/v) CO₂. Following labelling, stimulation was quenched *via*

washing of cells 2 times in 250 µl/well ice-cold 5 % (w/v) trichloroacetic acid (TCA). Cells were then washed 3 times in 250 µl/well ice-cold dH₂O. Finally, cells were lysed into 200 µl/well 1 M ice-cold NaOH and transferred to 5 ml scintillation fluid. Incorporation of ³H-Leu was determined *via* liquid scintillation counting.

5.8 Microscopy techniques

5.8.1 Determination of dendrite outgrowth

Phase contrast light microscopy images were captured at 40x magnification using a Zeiss AxioCam MRc 5 camera attached to a Zeiss Axiovert 40 CFL microscope. Five random fields per treatment were captured and analysed using Image J software (<http://rsbweb.nih.gov/ij/>). Dendrite outgrowth was determined by measuring the greatest distance between the cell body and the tip of the extended dendrite. Thirty cells per field were analysed at random and each experiment was repeated three times to ensure accuracy and reliability of data.

5.8.2 Immunofluorescence

LNCaP cells were seeded into 6 well plates (approx. 3×10^5 cells/well) and grown on sterile coverslips coated with 0.1 mg/ml poly-D-lysine hydrobromide for 48 h. Culture medium was discarded and cells treated with agonist as described for individual experiments. Cell stimulation was halted by washing coverslips three times in 2 ml ice-cold PBS

Cell stimulation was halted by washing coverslips three times in 2 ml/well ice cold PBS. In order to fix the cell monolayer, coverslips were incubated for 15 min at room temperature in 2 ml 4% (w/v) paraformaldehyde in 5% (w/v) sucrose-PBS. Coverslips were washed 3 times in 2 ml PBS prior to solubilisation with 2 ml 0.1% (v/v) Triton X100 in PBS for 2 min at room temperature. Following 3 washes with 2 ml PBS, coverslips were blocked for 30 min at room temperature in the presence of 2 ml PBS containing 5% (w/v) BSA (5% (w/v) BSA-PBS) to prevent non-specific antibody staining. Specific antibodies were diluted as appropriate in 5% (w/v) BSA-PBS and coverslips stained with 100 µl of this preparation overnight at 4°C whilst protected from light.

To remove unbound antibody, coverslips were washed three times in PBS and, where primary antibodies were not directly conjugated to the appropriate fluorophore, incubated with the appropriate secondary antibody at a 1:200 dilution in 5% (w/v) BSA-PBS for 1 h

Table 5.1 Antibodies used in immunoblotting

Antibody	Species	Company	Catalogue number	Diluent	Dilution
pSer ¹³³ CREB	Rabbit pAb	Abcam	30651	5% (w/v) BSA- TBST	1:500
EPAC1	Mouse mAb	Johannes Bos	In-house	TBST-M	1:500
EPAC2	Goat pAb	Santa Cruz	sc-9383	TBST-M	1:1000
pThr ²⁰² pTyr ²⁰⁴ ERK1/2	Mouse mAb	CST	9106	5% (w/v) BSA- TBST	1:1000
ERK1/2	Rabbit pAb	CST	9102	TBST-M	1:1000
pThr ²¹⁸ pTyr ²²⁰ ERK5	Rabbit pAb	CST	3371	5% (w/v) BSA- TBST	1:500
ERK5	Rabbit pAb	Santa Cruz	Sc-1284-R	TBST-M	1:500
GAPDH	Mouse mAb	Abcam	8245	TBST-M	1:20 000
JAK1	Rabbit pAb	CST	3332	TBST-M	1:1000
JAK2	Rabbit pAb	CST	3773	TBST-M	1:1000
Myc (9E10)	Mouse ascites	In-house		TBST-M	1:1000
Phospho-PKA substrate	Rabbit pAb	CST	9621	5% (w/v) BSA- TBST	1:1000
RhoA	Rabbit mAb	CST	2117	TBST-M	1:1000
pTyr ⁷⁰⁵ STAT3	Mouse mAb	CST	9138	5% (w/v) BSA- TBST	1:1000
STAT3	Rabbit pAb	CST	9132	TBST-M	1:1000
pTyr ⁷⁰¹ STAT1	Rabbit pAb	CST	9171	5% (w/v) BSA- TBST	1:1000
STAT1	Rabbit pAb	CST	9172	TBST-M	1:1000

at room temperature. Due to the sensitivity of fluorophores to incident light, subsequent washing and incubation steps were performed in the dark. Coverslips were washed three times in 2 ml PBS and subjected to nuclear staining using Hoescht stain diluted 1:1000 in 5% (w/v) BSA-PBS for 5 min. Coverslips were washed a further three times in 2 ml PBS prior to mounting on glass slides using 40% (v/v) glycerol-PBS. Fluorescent proteins were visualised on a Zeiss fluorescent microscope using 40x objective and images captured as described previously.

5.9 Densitometric and statistical analysis

In order to perform densitometric analysis, scanned images of a minimum of three separate immunoblots were analysed. To ensure that images used represented results acquired in which the response of film was in a linear relationship with the signal intensity, multiple exposures of each immunoblot were collected. Images were analysed using the 1D gel analysis option in TotalLab software and results normalised to vehicle stimulated responses which were given an arbitrary value of 100. To analyse increases in protein phosphorylation, the ratio of phosphorylated protein to either total protein or to a loading control was calculated for each sample and then converted to a percentage of the maximal response detected.

Statistical analysis was performed using the GraphPad Prism4 software package. Where appropriate, normality was assessed using the Kolmogorov-Smirnov test and data subsequently assessed for statistically significant changes using one way analysis of variance (ANOVA) with appropriate post-tests. In cases where data failed the Kolmogorov-Smirnov test, one way ANOVAs were performed with the Dunn's correction for non-parametric distributions and significance compared using the appropriate post-test.

6 Characterisation of prostate epithelial cell responses to exogenous cytokines

6.1 Introduction

Whilst the inflammatory response is a crucial innate immune response to infection, chronic inflammation contributes to the pathophysiology of numerous disease states including atherosclerosis, diabetes, rheumatoid arthritis and cancer (Deepa *et al.*, 2006;Hodge *et al.*, 2005;Kallen, 2002;Koenig *et al.*, 2006;Shouda *et al.*, 2001). Key amongst the pro-inflammatory signal transduction pathways is the JAK-STAT pathway which becomes activated in response to pro-inflammatory cytokine release and is responsible for signal transduction downstream of many class II cytokine receptors including members of the IL-6 cytokine family (Heinrich *et al.*, 2003).

The IL-6 cytokines comprise a group of cytokines which signal *via* the gp130 signal transduction molecule (Heinrich *et al.*, 2003). The IL-6 receptor complex of this family exists as a tetramer of two monomers of the IL-6-recognising receptor (IL-6R) and two monomers of gp130 which is required for signal transduction (Bravo & Heath, 2000;Chow *et al.*, 2001a). Expression of membrane-associated IL-6R/gp130 tetramers (memIL-6R) is relatively restricted although many cells have the potential to respond to free IL-6 due to the fairly ubiquitous expression of gp130 (Scheller *et al.*, 2006). In addition to the memIL-6R complex, activated cells can release a soluble form of IL-6R (sIL-6R) which is able to bind free IL-6 and recruit it to cell-associated gp130, thus increasing the number of IL-6 responsive cells, a phenomenon known as *trans*-signalling (discussed in detail in section 3.2) (Scheller *et al.*, 2006). Pro-inflammatory stimuli can also promote the release of sIL-6R via ADAM10 and ADAM17 sheddase-mediated cleavage of memIL-6R (Mezyk-Kopec *et al.*, 2009;Scheller *et al.*, 2006). Following successful interaction of IL-6 with the IL-6R/gp130 complex, activation of intracellular signalling is mediated by the action of JAKs which are constitutively associated with gp130 (Scheller *et al.*, 2006). The gp130 molecule itself lacks intrinsic kinase activity and thus is reliant on kinase recruitment to promote intracellular signalling. In reference to IL-6 signalling, JAK1, JAK2 and Tyk2 are all implicated in the activation of STAT1 and STAT3 downstream of IL-6R/gp130 with STAT3 being the predominant STAT family member activated in response to IL-6, although STAT1 is also activated (Heinrich *et al.*, 2003).

STAT proteins become activated following JAK-mediated phosphorylation of conserved C-terminal tyrosine residues corresponding to Tyr⁷⁰¹ and Tyr⁷⁰⁵ in STAT1 and STAT3 respectively. The tyrosine phosphorylated STAT monomers then dimerise *via* reciprocal interactions between the central SH2 domain of one monomer and the pTyr residue of the other. Dimerised STAT proteins then translocate to the nucleus where they bind to the promoters of STAT responsive gene and promote transcription *via* their C-terminal transactivation domain (Heinrich *et al.*, 2003).

6.1.1 STAT3 activation in prostate cancer

PCa is one of the most prevalent male-specific malignancies in the Western world. In the UK alone, over 34,000 new cases of PCa are diagnosed every year, corresponding to diagnosis rate of 1 case every 15 minutes (Cancer Research UK, 2005).

Common to many malignancies, development of PCa is correlated with a chronic inflammatory response. In reference to the IL-6 signalling pathway, elevation of IL-6 levels has been correlated with every stage of PCa from early hyperplasia through to patient cachexia and death. As a pre-diagnostic tool, the clinical value of circulating IL-6 levels is somewhat controversial as the results from large cohort studies are influenced by multiple factors such as grouping classifications. In a study of 22,071 male physicians, there was no correlation in prediagnostic plasma IL-6 levels between patients which later developed PCa and healthy individuals. However, when patients were grouped based on their BMI, there was a significant correlation between plasma IL-6 concentrations and onset of PCa development in healthy weight participants (Stark *et al.*, 2009). In patients suffering from early stage PCa, levels of serum IL-6 in excess of 7 pg/ml are associated with poor patient prognosis (Nakashima *et al.*, 2000) whilst levels of IL-6 and IL-6R are increased in non-metastatic tumours (Giri *et al.*, 2001). In later stages of PCa, levels of IL-6 are correlated with terminal disease progression, patient cachexia and death (Kuroda *et al.*, 2007).

As might be anticipated from the importance of IL-6 in PCa, malignant tissue also displays hyperactivation of STAT3 which has been demonstrated to contribute to Src-mediated transformation possibly due to the ability of Src to phosphorylate Tyr⁷⁰⁵ of STAT3 (Smith & Crompton, 1998). Sustained STAT3 activation contributes to carcinogenesis in multiple malignancies including colorectal carcinoma, hepatocellular carcinoma and PCa (Hodge *et al.*, 2005). The pro-oncogenic effects of STAT3 hyperactivation are principally believed to arise from the ability of STAT3 to induce expression of both anti-apoptotic proteins and

those involved in cell cycle regulation (Hodge *et al.*, 2005). Amongst the anti-apoptotic proteins, STAT3 is thought to contribute to the high levels of Bcl-X_L observed in head and neck cell squamous carcinomas (Grandis *et al.*, 2000). Due to its anti-apoptotic and pro-proliferative roles, hyperactivation of this signalling pathway is of particular concern in PCa due to the ability of STAT3 to interact with the N-terminal domain of the androgen receptor (AndR), enhance AndR transactivation and to promote AndR activation in the absence of androgen (Culig *et al.*, 2005; De Miguel *et al.*, 2003; Ueda *et al.*, 2002). Such androgen independence is associated with the emergence of the androgen refractory stage of PCa, subsequent failure of conventional therapeutic strategies and progression to terminal disease.

There have been many studies linking the importance of STAT3 activation to PCa *in vitro*. In the DU145 prostate epithelial cell line, inhibition of STAT3 activation using the JAK inhibitor AG490 promoted apoptosis, demonstrating the anti-apoptotic role of STAT3 in these cells (Barton *et al.*, 2004). A constitutively active mutant of STAT3 (STAT3-C) has been generated due to cysteine substitution of A661 and N663, resulting in STAT3 dimerisation and constitutive transactivator activity in the absence of tyrosine phosphorylation (Bromberg *et al.*, 1999). Injection of nude mice with cells expressing STAT3-C resulted in tumour formation indicating that STAT3-C is directly oncogenic and that STAT3 activation therefore contributes to carcinogenesis (Bromberg *et al.*, 1999). Similarly, expression of STAT3-C in the RWPE-1 prostate epithelial cell line promotes cellular transformation and anchorage-independent growth *in vitro*. Furthermore, STAT3-C expression in these cells enhances cell migration, indicative of an increased metastatic capacity. However, immunohistochemical (IHC) analysis of primary prostate tumours failed to demonstrate a correlation between increased pTyr⁷⁰⁵STAT3 and tumour stage, Gleason score or PSA levels (Azare *et al.*, 2007). Nevertheless, other studies have demonstrated clear links between STAT3 activation and PCa progression *in vivo*. In prostatic tissues from PCa patients, elevation of pTyr⁷⁰⁵STAT3 was demonstrated in comparison to patients without PCa. Within tissues from PCa patients, it was found that pTyr⁷⁰⁵STAT3 levels were greater in cancerous *vs.* normal tissues (Barton *et al.*, 2004). In a separate study, tissue samples derived from PCa patients displayed greater STAT3 DNA binding activity in comparison to patients with no evidence of prostate pathology. However, within the tissue derived from PCa patients, there was no significant difference in STAT3 DNA binding activity between normal and malignant tissue (Dhir *et al.*, 2002).

6.2 Cell systems

In order to study the effects of cAMP elevation on IL-6-induced STAT3 activation, an *in vitro* cell culture system was used. Although it could be argued that such a system is not physiologically relevant, it provides an ideal model for studying intracellular responses directly attributable to rhuIL-6 stimulation due to the lack of other cell or tissue types which may alter IL-6-mediated signalling *via* heterotypic signalling.

The cell lines used throughout this study were chosen due to their rudimentary representation of different stages of PCa. The PZ-HPV-7 cell line has been used as a representation of normal prostate epithelial cell responses to exogenous stimulation and was produced by transformation of normal prostate epithelial tissue with DNA encoding the E6 protein of HPV18 (Weijerman et al., 1994). The LNCaP cell line was derived from a PCa metastasis to the left supraclavicular lymph node of 50 year old Caucasian man and represents an androgen-sensitive cell line indicative of early PCa (Horoszewicz et al., 1983). In contrast, the DU145 cell line, derived from a metastatic lesion to the brain of a 69 year old Caucasian man, represents an androgen-insensitive cell line which is indicative of late stage PCa (Stone et al., 1978). Regarding basal STAT3 activation, STAT3 activation by exogenous IL-6 is thought to be entirely inducible in PZ-HPV-7 cells, somewhat controversial in LNCaP cells, whilst DU145 cells are thought to display basal STAT3 activation in the absence of exogenous stimulation due to autocrine production of IL-6 (Okamoto et al., 1997). In order to perform subsequent analysis of any inhibitory effects of cAMP elevation on STAT activation, the responses of these cells to exogenous cytokines were initially investigated.

DU145, LNCaP and PZ-HPV-7 cells were seeded as described for individual experiments, grown to 80% confluence in the case of DU145 and PZ-HPV-7 cells, and 60-70% confluence for LNCaP cells. DU145 and PZ-HPV-7 cells were grown to 80% confluence to ensure a high protein yield from cell lysates but were not grown to 100% confluency to prevent cells from becoming quiescent which might alter cellular responses to exogenous IL-6. This is particularly important when considering DU145 cells as these cells are reported to be androgen-insensitive and perpetuate their growth in the absence of androgens *via* autocrine release of IL-6 (Okamoto et al., 1997). Thus, highly confluent DU145 cells may have sufficiently high endogenous IL-6 and subsequent activation of the JAK-STAT pathway such that stimulation with exogenous cytokine would fail to result in further activation of the pathway. LNCaP cells were grown to a lower confluency as these cells have a tendency to grow on solid substrata in loosely adherent clumps. Growing of

LNCaP cells to a high percentage confluency results in a greater degree of cell clumps which may affect responses to exogenous cytokine due to a decrease in the relative number of cells which are located on the media-exposed surface of the cell clump. To aid adherence of LNCaP cells to tissue culture plasticware, plates were coated with 0.5 mg/ml poly-D-lysine hydrobromide. Poly-D-lysine is a positively charged amino acid polymer which aids cellular adherence by electrostatic interaction with negatively charged cell surface molecules such as phospholipids (Jacobson & Branton, 1977).

Given the differences between the cell types used in this study in both the stage of PCa which they represent and their culture conditions, it was necessary to characterise the responses of DU145, LNCaP and PZ-HPV-7 cells to exogenous cytokine stimulation. The results presented in this chapter demonstrate differences in IL-6-induced STAT signalling between the cell lines used with the tumour-derived cell lines demonstrating preferential activation of the oncogenic STAT3 signalling pathway rather than the tumour suppressive STAT1 pathway in comparison to control cells.

6.3 Results

Prior to stimulation, the culture medium was replaced with fresh medium to ensure that any observed activation of STAT proteins was due to addition of exogenous cytokine rather than basal STAT activation. In all three cell types tested, treatment with 10 ng/ml recombinant human IL-6 (rhIL-6) resulted in increased detection of STAT3 protein phosphorylated on Tyr⁷⁰⁵ (pTyr⁷⁰⁵STAT3). This residue is critical for STAT3 activation, dimerisation and subsequent transcriptional activation (Calo *et al.*, 2003; Kaptein *et al.*, 1996), thus elevation of pTyr⁷⁰⁵STAT3 following rhIL-6 treatment indicates activation of STAT3. To ensure that changes in pTyr⁷⁰⁵STAT3 were a result of protein activation rather than due to changes in the total amount of STAT3 or protein loading, cell lysates were immunoblotted for total STAT3 protein and the loading control glyceraldehyde-3-phosphate dehydrogenase (GAPDH). The increases in pTyr⁷⁰⁵STAT3 could not be explained by changes in either STAT3 levels or protein loading across the gel, indicating that the results seen are a genuine reflection of STAT3 activation in prostate epithelial cells lines. Similar results were seen for STAT1 activation, with activation of STAT1 being inferred by an increase in detected STAT1 phosphorylated at Tyr⁷⁰¹ (pTyr⁷⁰¹STAT1). Following normalisation for protein loading, the ratio of tyrosine phosphorylated STAT protein to total STAT protein was calculated and expressed as a percentage of the maximal value obtained.

6.3.1 Treatment of prostate epithelial cells with rhuIL-6 results in tyrosine phosphorylation of STAT3

In order to perform subsequent studies investigating attenuation of JAK-STAT signalling downstream of the IL-6R, it was first necessary to determine a suitable time point at which to detect tyrosine phosphorylation of STAT1 and STAT3. Previous work in our laboratory has indicated that STAT protein activation can be detected downstream of the IL-6/sIL-6R α *trans*-signalling complex at 15 – 30 min post-stimulation. In keeping with this, DU145, LNCaP and PZ-HPV-7 cells were stimulated with rhuIL-6 for 0 – 60 min. Given expression of both gp130 and the IL-6-binding receptor in DU145, LNCaP and PZ-HPV-7 cells (Palmer et al., 2004), it was not necessary to stimulate the cells with the *trans*-signalling complex and instead only rhuIL-6 was used to stimulate these cells.

Treatment of DU145 cells with 10 ng/ml rhuIL-6 resulted in an increase in pTyr⁷⁰⁵ STAT3 at 15, 30 and 60 min post-stimulation (Fig. 6.1). Basal activation of STAT3 was detected in these cells, consistent with the autocrine release of IL-6, but was sub-maximal as treatment with 10 ng/ml rhuIL-6 resulted in an increase in pTyr⁷⁰⁵STAT3 at 15 min post-stimulation ($p < 0.05$ vs. 0 h) and showed a decline in pTyr⁷⁰⁵STAT3 back to basal levels by 60 min post-stimulation (Fig. 6.1). Similar results were observed in LNCaP cells, where treatment with rhuIL-6 resulted in an increase in pTyr⁷⁰⁵ at 15 min post-stimulation (Fig. 6.2). However, unlike DU145 cells where detected pTyr⁷⁰⁵STAT3 levels returned to basal at 30 and 60 min post-stimulation, treatment of LNCaP cells with exogenous IL-6 resulted in sustained elevation of pTyr⁷⁰⁵STAT3 at 30 and 60 min ($p < 0.01$ vs. 0 h) (Fig. 6.2). In PZ-HPV-7 cells, treatment with 10 ng/ml rhuIL-6 resulted in elevation of pTyr⁷⁰⁵STAT3 at 15 min and 30 min post-stimulation (Fig. 6.3, $p < 0.01$ vs. 0 h) which declined to basal levels at 60. Taken together, these results indicate that 15 min post-stimulation with rhuIL-6 is a suitable time point at which to observe activation of STAT3 as evidenced by an increase in pTyr⁷⁰⁵STAT3 in each cell type.

In contrast to the similarities in STAT3 activation between the different cell types when treated with rhuIL-6, there were marked differences in STAT1 phosphorylation between the tumour-derived DU145 and LNCaP cell lines when compared with PZ-HPV-7 cells which were derived from transformation of normal prostate epithelium. Whilst treatment with rhuIL-6 resulted in an increase in pTyr⁷⁰¹STAT1 at 15 min post-stimulation in PZ-HPV-7 cells (Fig. 6.3, $p < 0.01$ vs. 0 h), parallel treatment of DU145 and LNCaP cells failed to induce a significant increase in pTyr⁷⁰¹STAT1 (Fig. 6.1 and Fig. 6.3). PZ-HPV-7 cells treated with 10 ng/ml rhuIL-6 for 15 min were included as a positive control for

antibody reactivity, indicating that the lack of detected pTyr⁷⁰¹STAT1 does not arise due a failure of the antibody. In DU145 cells, no detectable increase in pTyr⁷⁰¹STAT1 was detected across all repeats of the experiment (Fig. 6.1), indicating a deficiency of DU145 cells to activate STAT1 in response to rhuIL-6 stimulation. In LNCaP cells a variable and weak increase in pTyr⁷⁰¹STAT1 in response to rhuIL-6 stimulation was seen (Fig. 6.2) which was considerably less robust than that detected in PZ-HPV-7 cells and varied from weakly detectable to completely absent across experiments. These results suggest that there is some defect in the ability of LNCaP cells to activate STAT1 downstream of IL-6R/gp130 signalling. Samples were equalised for protein content both across the different cell types and across gels, thus the difference in STAT1 tyrosine phosphorylation is unlikely to arise from differences in protein loading or STAT1 expression as all cell types tested expressed STAT1 protein with no apparent differences in levels of STAT1 protein. Furthermore, no difference in the apparent molecular weight of STAT1 was observed between the cell types, suggesting that the differences in STAT1 activation following IL-6 treatment do not arise from expression of a truncated STAT1 mutant which lacks the C-terminal region containing Tyr⁷⁰¹. Cleavage by caspase-3 can truncate STAT1 in at Asp⁶⁹⁴ and is thus unable to become activated due to the lack of Tyr⁷⁰¹. However, due to the limitations of resolving proteins *via* 1D gel electrophoresis, it is not possible to exclude the possibility that DU145 and LNCaP cells express a variant of STAT1 which is resistant to tyrosine phosphorylation.

6.3.2 Basal activation of STAT3 in prostate epithelial cell lines

Having determined a suitable time point at which to investigate rhuIL-6-mediated activation of STAT3, the basal activation status of STAT3 in the prostate epithelial cell lines was examined. This is particularly important as DU145 cells are reported to display constitutive activation of STAT3 due to autocrine IL-6 production whilst data surrounding the basal STAT3 activation status in LNCaP cells is more controversial.

DU145, LNCaP and PZ-HPV-7 cells were seeded into 6-well plates and grown to appropriate confluency with cell culture medium being changed every 48 h in order to maintain cell growth. Spent culture medium was collected and retained as conditioned medium. Prior to stimulation, cell culture medium on cells was replaced with either conditioned medium or fresh growth medium. Cells were then stimulated with 10 ng/ml rhuIL-6 for 15 min prior to cell harvesting, SDS-PAGE fractionation and subsequent analysis of pTyr⁷⁰⁵STAT3 levels by immunoblotting.

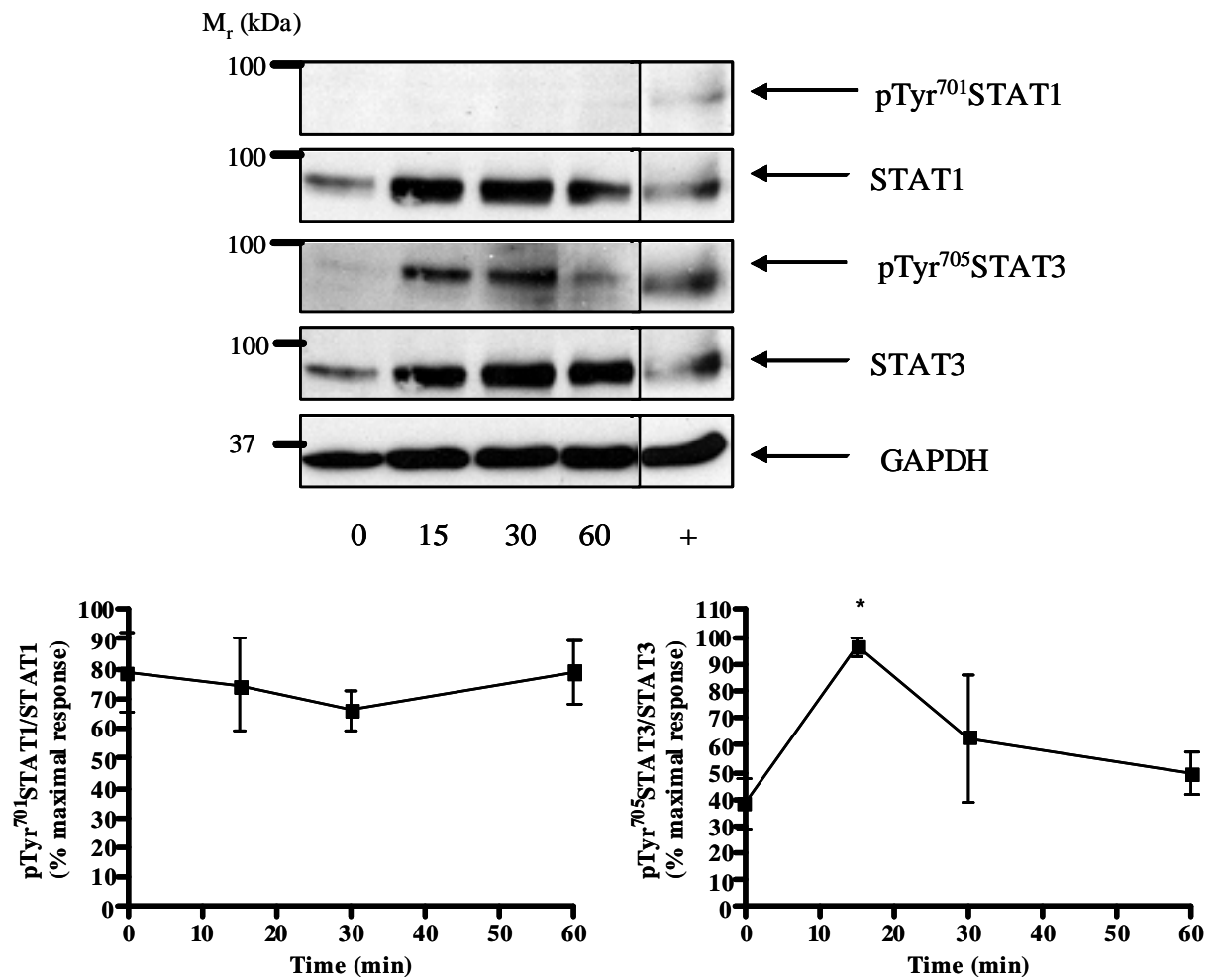


Figure 6.1: Treatment of DU145 prostate epithelial cells with 10 ng/ml rhIL-6 induces tyrosine phosphorylation of STAT3 but not STAT1

DU145 cells were seeded into 6-well plates and treated with 10 ng/ml rhIL-6 for 0 – 60 min prior to fractionation by SDS-PAGE and subsequent immunoblotting. Phospho-specific antibodies were used to detect pTyr⁷⁰¹STAT1 and pTyr⁷⁰⁵STAT3 as indicators of STAT protein activation whilst total levels of STAT1 and STAT3 were used to demonstrate that changes in detected tyrosine phosphorylation of STAT proteins reflected changes in protein phosphorylation and not protein levels. Blots are representative of $n = 3$ individual experiments and densitometry results represent mean values \pm SEM. PZ-HPV-7 cells treated with 10 ng/ml rhIL-6 for 15 min were included as a positive control for antibody reactivity. * = $p < 0.05$ vs. 0 h

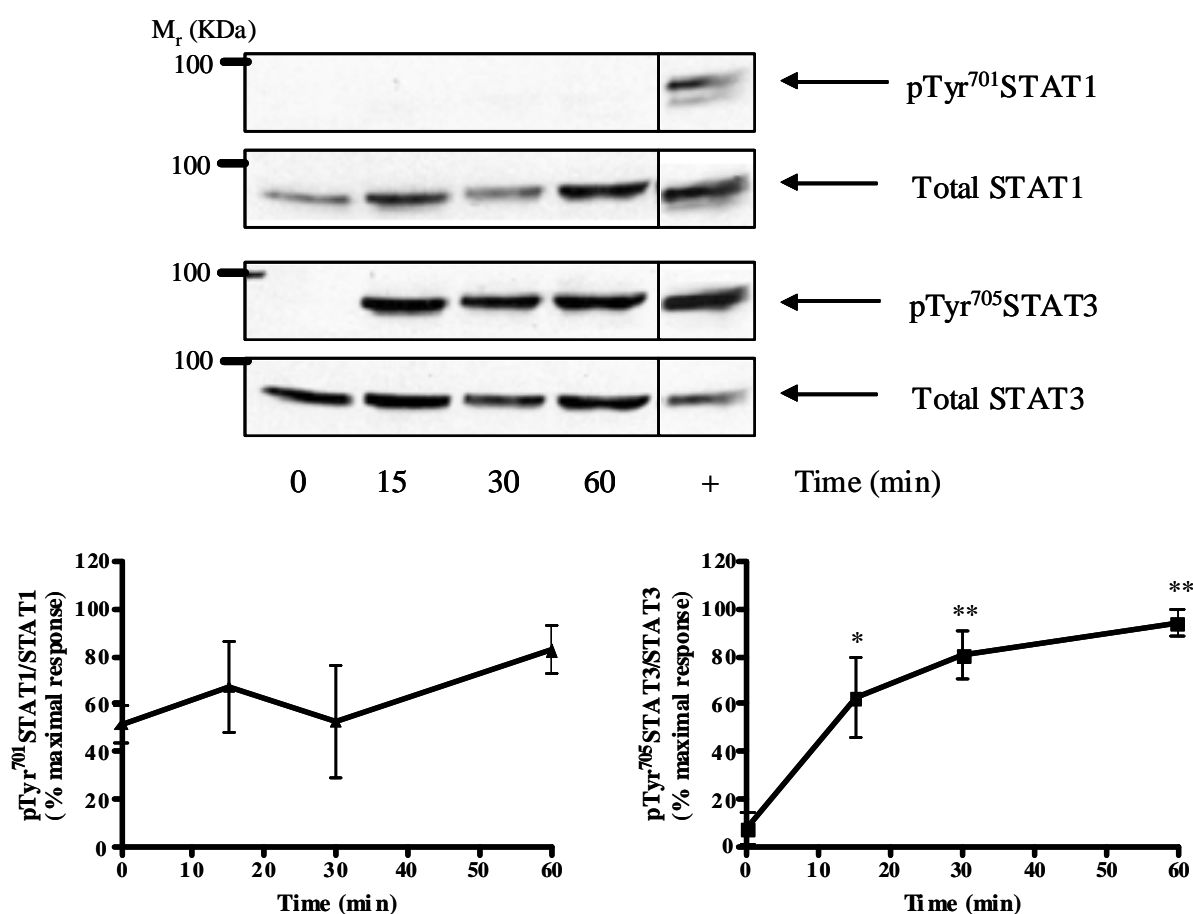


Figure 6.2: Treatment of LNCaP prostate epithelial cells with 10 ng/ml rhIL-6 induces tyrosine phosphorylation of STAT3 but not STAT1

LNCaP cells were seeded into poly-D-lysine coated 6-well plates and treated with 10 ng/ml rhIL-6 for 0 –60 min prior to fractionation by SDS-PAGE and subsequent immunoblotting. Phospho-specific antibodies were used to detect pTyr⁷⁰¹STAT1 and pTyr⁷⁰⁵STAT3 as indicators of STAT protein activation whilst total levels of STAT1 and STAT3 were used to demonstrate that changes in detected tyrosine phosphorylation of STAT proteins reflected changes in protein phosphorylation and not protein levels. Blots are representative of $n = 4$ individual experiments and densitometry results represent mean values \pm SEM. PZ-HPV-7 cells treated with 10 ng/ml rhIL-6 for 15 min were included as a positive control for antibody reactivity ** = $p < 0.01$ vs. 0 h

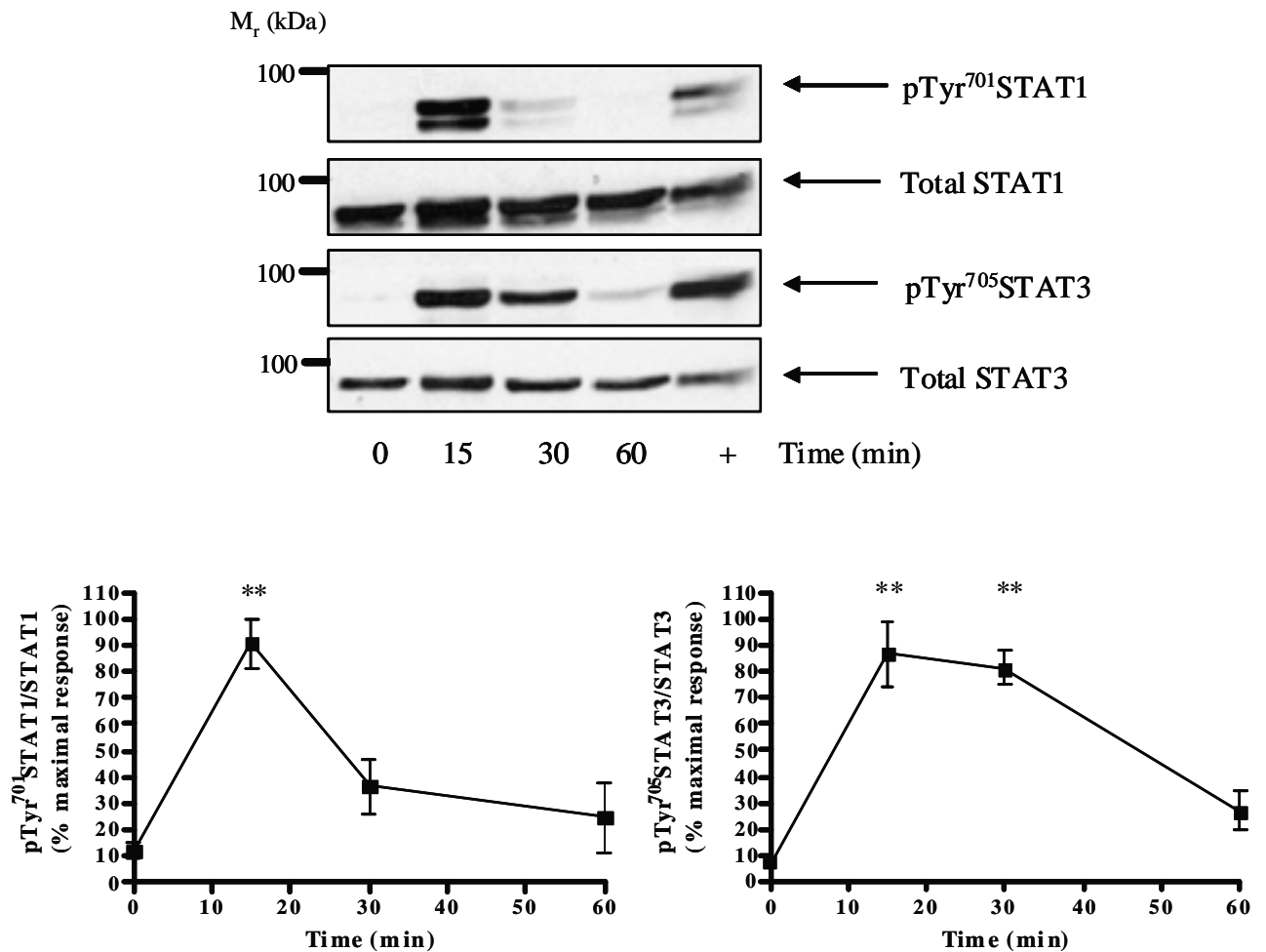


Figure 6.3: Treatment of PZ-HPV-7 prostate epithelial cells with 10 ng/ml rhIL-6 induces tyrosine phosphorylation of STAT3 and STAT1

PZ-HPV-7 cells were seeded into 6-well plates and treated with 10 ng/ml rhIL-6 for 0 – 60 min prior to fractionation by SDS-PAGE and subsequent immunoblotting. Phospho-specific antibodies were used to detect pTyr⁷⁰¹STAT1 and pTyr⁷⁰⁵STAT3 as indicators of STAT protein activation whilst total levels of STAT1 and STAT3 were used to demonstrate that changes in detected tyrosine phosphorylation of STAT proteins reflected changes in protein phosphorylation and not protein levels. Blots are representative of $n = 7$ individual experiments and densitometry results represent mean values \pm SEM. PZ-HPV-7 cells treated with 10 ng/ml rhIL-6 for 15 min were included as a positive control for antibody reactivity ** = $p < 0.01$ vs. 0 h

In all three cell types studied, the ability of rhuIL-6 to induce phosphorylation of Tyr⁷⁰⁵ in STAT3 was not affected by the medium in which the cells were stimulated (Fig. 6.4 – 6.6). Cells grown in conditioned medium did not display increased basal pTyr⁷⁰⁵STAT3, suggesting that, in this experimental system, any basal STAT3 activation is below the detection limit of the immunoblotting procedure. This result was particularly surprising in the case of DU145 cells as these are reported to express autocrine IL-6 (Giri *et al.*, 2001) and thus would be expected to display basal pTyr⁷⁰⁵STAT3. It may be the case that autocrine stimulation with IL-6 activates endogenous negative regulatory pathways in DU145 cells and thus limits basal STAT3 activation. Indeed, it was found that treatment of DU145 cells in conditioned rather than fresh medium had a trend to show a smaller increase in pTyr⁷⁰⁵STAT3 following stimulation with rhuIL-6 (Fig. 6.4). However, this difference was found to be statistically insignificant. In LNCaP and PZ-HPV-7 cells, no discernible difference between IL-6-mediated tyrosine phosphorylation of STAT3 was observed in cells stimulated in conditioned or fresh medium (Fig. 6.5 and Fig. 6.6).

6.3.3 The ability of rhuIL-6 to induce STAT3 activation is concentration dependent

Ultimately, this study aims to investigate mechanisms by which STAT3 activation may be attenuated, thus it was necessary to ensure that a suitable concentration of rhuIL-6 is used throughout the study. Stimulation of the cell lines under investigation with too high a concentration of rhuIL-6 may result in an inability to observe any inhibitory effects of cAMP elevation due to supra-maximal activation of STAT3. DU145, LNCaP and PZ-HPV-7 cells were plated as described above and stimulated with 0 – 100 ng/ml rhuIL-6 for 15 min. In all cell types tested, stimulation with increasing concentrations of rhuIL-6 resulted in an increase in detected pTyr⁷⁰⁵STAT3. In DU145 cells, treatment with rhuIL-6 concentrations of less than 1 ng/ml failed to induce a detectable increase in pTyr⁷⁰⁵STAT3 above basal levels (Figure 6.7). Treatment with 1 – 100 ng/ml rhuIL-6 resulted in a concentration-dependent increase in pTyr⁷⁰⁵STAT3 with maximal STAT3 activation being observed when DU145 cells were treated with 10 ng/ml rhuIL-6 ($p < 0.01$ vs. 0 ng/ml rhuIL-6). A further increase in pTyr⁷⁰⁵STAT3 was not observed in DU145 cells when treated with 100 ng/ml, indicating that 10 ng/ml rhuIL-6 was a suitable concentration of rhuIL-6 to use in future experiments.

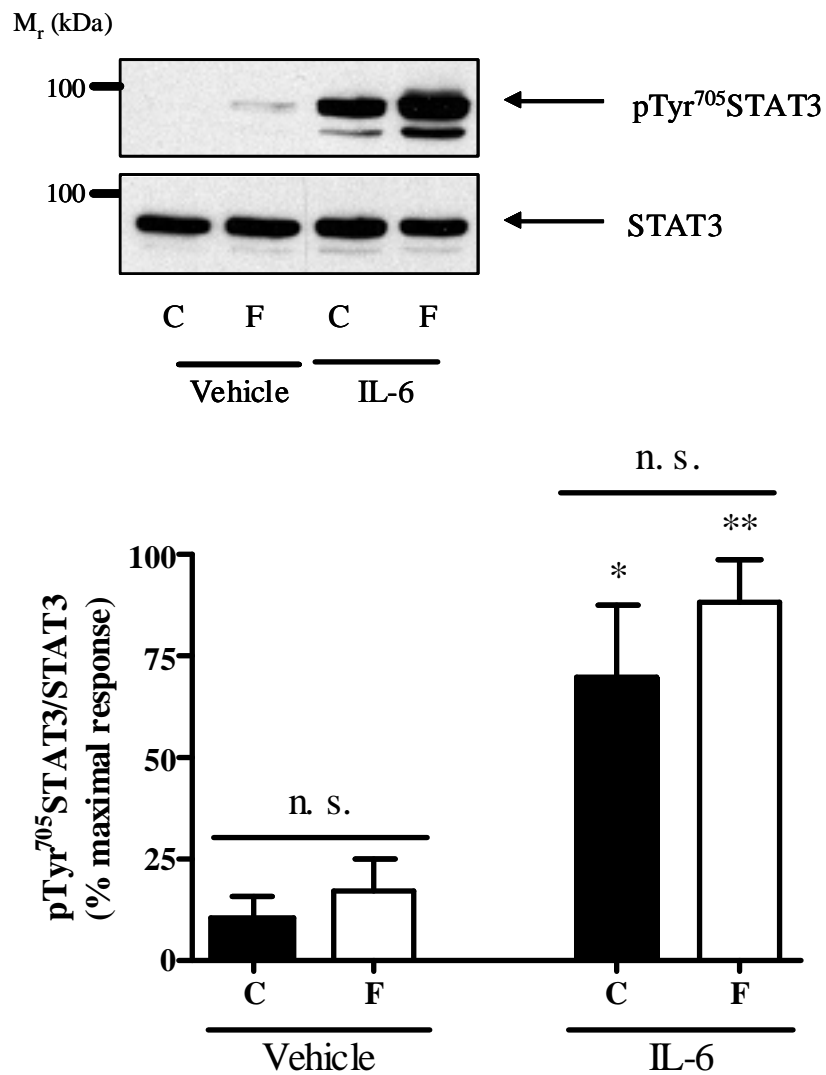


Figure 6.4: Effect of conditioned and fresh medium on rhIL-6-induced pTyr⁷⁰⁵STAT3 in DU145 prostate epithelial cells

In order to assess basal tyrosine phosphorylation of STAT3, DU145 cells were seeded into 6-well plates and grown prior to stimulation with vehicle or 10 ng/ml rhuIL-6 for 15 min in either conditioned medium in which cells had been growing for 48 h (C) or in fresh growth medium (F). Immunoblotting using an antibody specific for pTyr⁷⁰⁵STAT3 was used to determine activation of STAT3 whilst an antibody against total STAT3 was used to demonstrate that changes in detected pTyr⁷⁰⁵STAT3 did not arise due to changes in STAT3 protein levels. Results are displayed as representative blots and mean values \pm SEM for $n = 4$ separate experiments. * = $p < 0.05$ vs. vehicle, ** $p < 0.01$ vs. vehicle, n.s. = $p > 0.05$

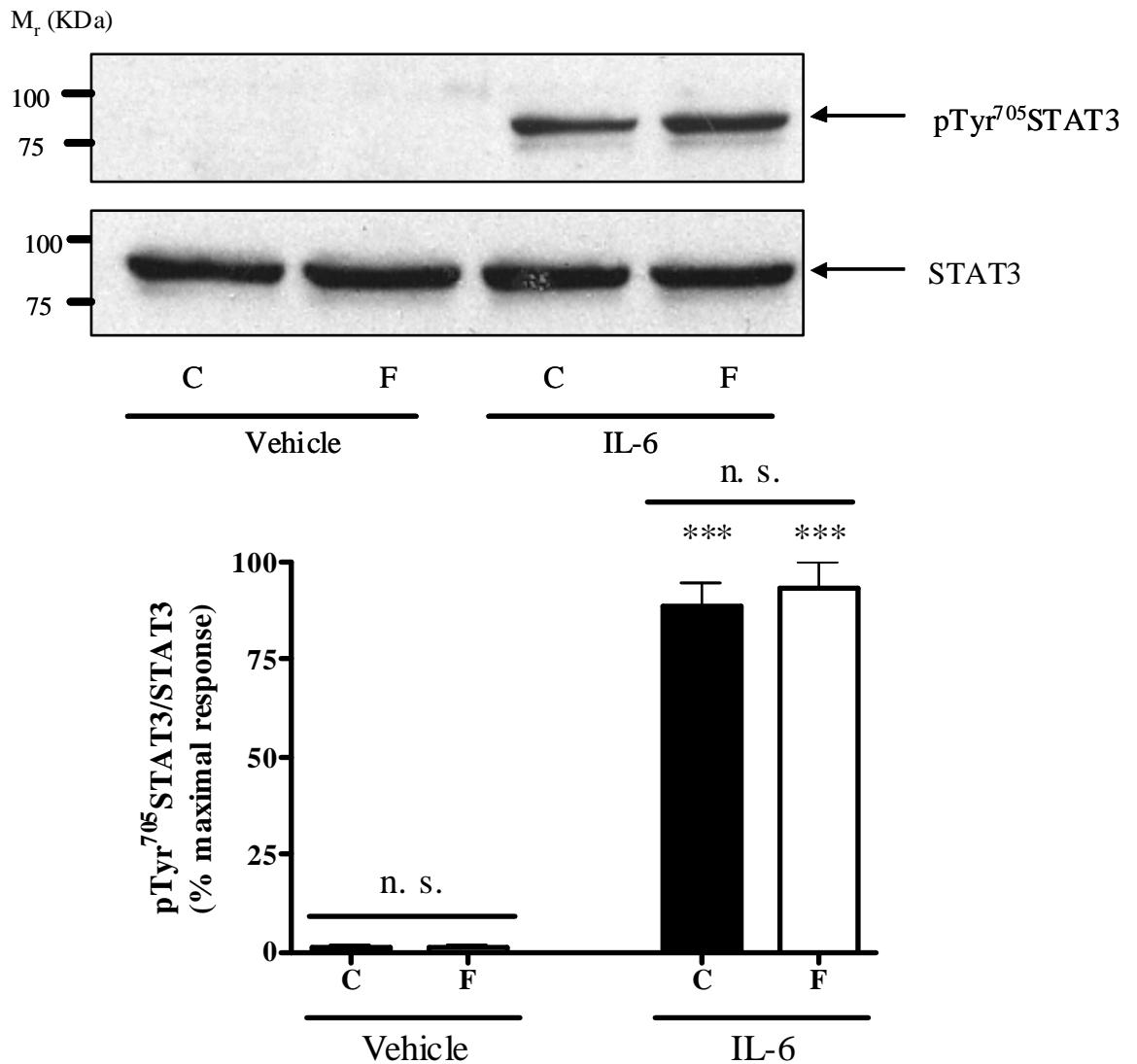


Figure 6.5: Effect of conditioned and fresh medium on rhIL-6-induced pTyr⁷⁰⁵STAT3 in LNCaP prostate epithelial cells

In order to assess basal tyrosine phosphorylation of STAT3, LNCaP cells were seeded into poly-D-lysine HBr coated 6-well plates and grown prior to stimulation with vehicle or 10 ng/ml rhIL-6 for 15 min in either conditioned medium in which cells had been growing for 48 h (C) or in fresh growth medium (F). Immunoblotting using an antibody specific for pTyr⁷⁰⁵STAT3 was used to determine activation of STAT3 whilst an antibody against total STAT3 was used to demonstrate that changes in detected pTyr⁷⁰⁵STAT3 did not arise due to changes in STAT3 protein levels. Results are displayed as representative blots and mean values \pm SEM for $n = 3$ separate experiments.

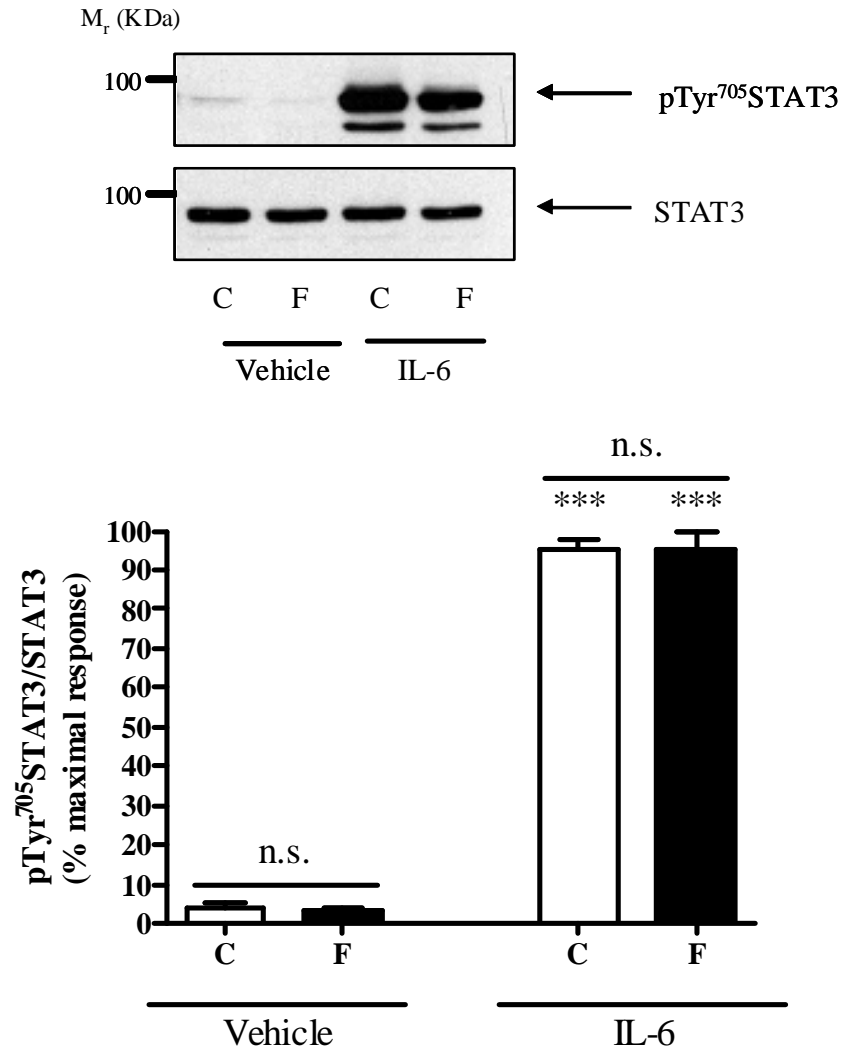


Figure 6.6: Effect of conditioned and fresh medium on rhIL-6-induced pTyr⁷⁰⁵STAT3 in PZ-HPV-7 prostate epithelial cells

In order to assess basal tyrosine phosphorylation of STAT3, PZ-HPV-7 cells were seeded into 6-well plates and grown prior to stimulation with vehicle or 10 ng/ml rhIL-6 for 15 min in either conditioned medium in which cells had been growing for 48 h (C) or in fresh growth medium (F). Immunoblotting using an antibody specific for pTyr⁷⁰⁵STAT3 was used to determine activation of STAT3 whilst an antibody against total STAT3 was used to demonstrate that changes in detected pTyr⁷⁰⁵STAT3 did not arise due to changes in STAT3 protein levels. Results are displayed as representative blots and mean values \pm SEM for $n = 3$ separate experiments. *** = $p < 0.001$ vs. vehicle, n.s. = $p > 0.05$

Similar results were obtained in LNCaP cells which showed an increase in pTyr⁷⁰⁵STAT3 levels following stimulation with 1 ng/ml rhuIL-6 (Fig. 6.8, $p < 0.05$ vs. 0 ng/ml rhuIL-6), 10 ng/ml rhuIL-6 (Fig. 6.8, $p < 0.05$ vs. 0 ng/ml rhuIL-6) and 100 ng/ml rhuIL-6 (Fig. 6.8, $p < 0.001$ vs. 0 ng/ml rhuIL-6). Unlike DU145 cells, stimulation of LNCaP cells with ≥ 10 ng/ml did not result in maximal detection of pTyr⁷⁰⁵STAT3, indicating that concentrations of rhuIL-6 greater than 100 ng/ml are required to maximally activate STAT3 in LNCaP cells. Stimulation of PZ-HPV-7 cells with ≥ 1 ng/ml rhuIL-6 resulted in an increase in pTyr⁷⁰⁵STAT3 which increased further when cells were treated with 10 ng/ml ($p < 0.01$ vs. 0 ng/ml rhuIL-6) and 100 ng/ml ($p < 0.001$ vs. 0 ng/ml rhuIL-6) of exogenous cytokine. The results obtained in PZ-HPV-7 cells regarding the concentration dependency of rhuIL-6-induced STAT3 Tyr⁷⁰⁵ phosphorylation were comparable to those obtained in LNCaP cells in that saturation of STAT3 activation was not observed even when cells were stimulated with 100 ng/ml rhuIL-6.

However, the ability of concentrations of rhuIL-6 greater than 100 ng/ml to induce tyrosine phosphorylation of STAT3 were not investigated as this would cause supra-maximal activation of STAT3 in DU145 cells and may therefore mask any inhibitory actions of cAMP elevation in subsequent studies.

6.3.4 Prostate epithelial cell lines display different responses to STAT-activating cytokines

Previously, treatment with rhuIL-6 induced an increase in pTyr⁷⁰¹STAT1 in PZ-HPV-7 cells but not in either of the tumour-derived LNCaP and DU145 cell lines. STAT1 has been described as a putative tumour suppressor and it is therefore possible that malignant cells have uncoupled STAT1 activation from IL-6-mediated activation of memIL-6R in order to maximise the oncogenic effects of STAT3 activation. However, it is not clear whether DU145 and LNCaP cells have a defect in STAT1 activation in general or whether this phenomenon is solely restricted to the IL-6 signalling pathway.

To address this question, DU145, LNCaP and PZ-HPV-7 cells were treated in parallel with 1000 U/ml recombinant human interferon- (IFN-) α , a STAT1 activator, for 15 or 30 min. Treatment with 10 ng/ml rhuIL-6 was included as a positive control for normal cellular responses to exogenous cytokine as indicated by increases in pTyr⁷⁰⁵STAT3.

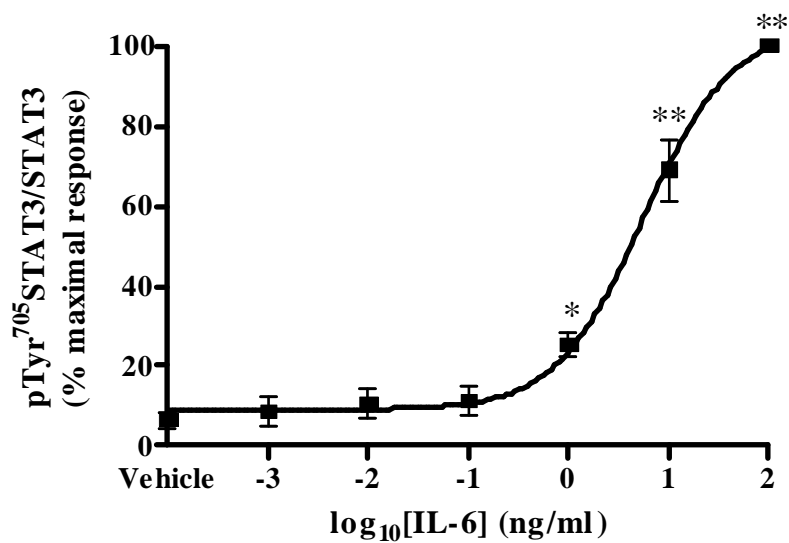
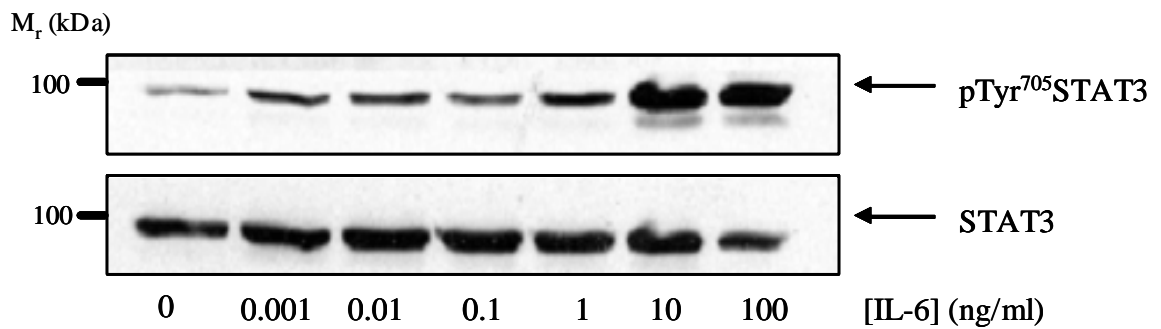


Fig. 6.7: Effect of IL-6 concentration on STAT3 activation in DU145 cells

DU145 cells were seeded into 12-well tissue culture plates and grown to 80 % confluency prior to stimulation for 15 min (37°C, 5 % (v/v) CO₂) with concentrations of rhuIL-6 ranging from 0 (vehicle) – 100 ng/ml. Activation of STAT3 was assessed by immunoblotting for pTyr⁷⁰⁵STAT3 whilst equal protein loading was determined by immunoblotting for STAT3. Blots are representative of $n = 3$ separate experiments and results shown as mean values \pm SEM* = $p < 0.05$ vs. vehicle, ** = $p < 0.01$ vs. vehicle

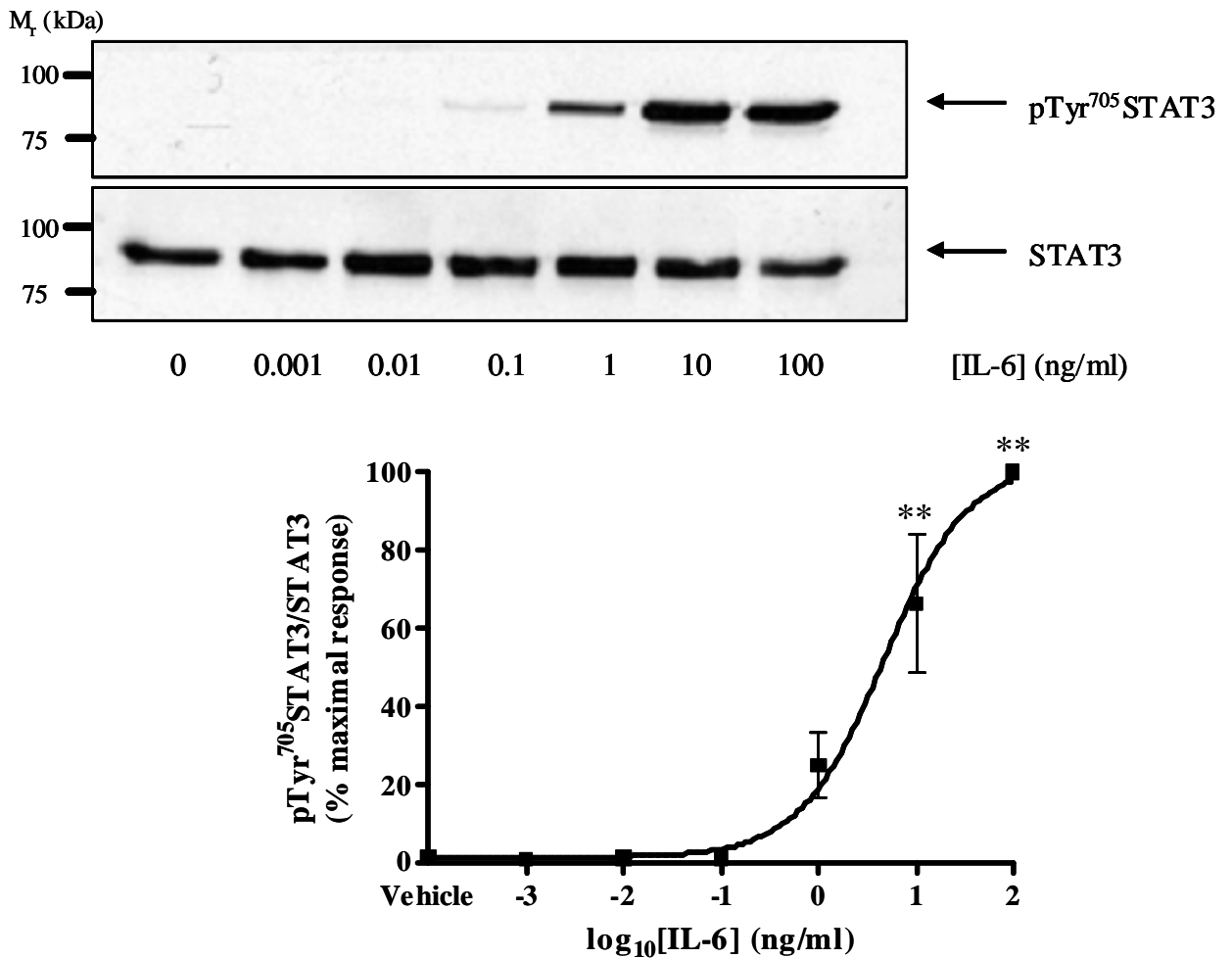


Fig. 6.8: Effect of IL-6 concentration on STAT3 activation in LNCaP cells

LNCaP cells were seeded into 0.1 mg/ml poly-D-lysine HBr coated 12-well tissue culture plates and grown to 70 % confluency prior to stimulation for 15 min (37°C, 5 % (v/v) CO₂) with concentrations of rhuIL-6 ranging from 0 (vehicle) –100 ng/ml. Activation of STAT3 was assessed by immunoblotting for pTyr⁷⁰⁵STAT3 whilst equal protein loading was determined by immunoblotting for STAT3. Blots are representative of *n* = 3 separate experiments and results shown as mean values ± SEM
 ** = *p* < 0.01 vs. vehicle

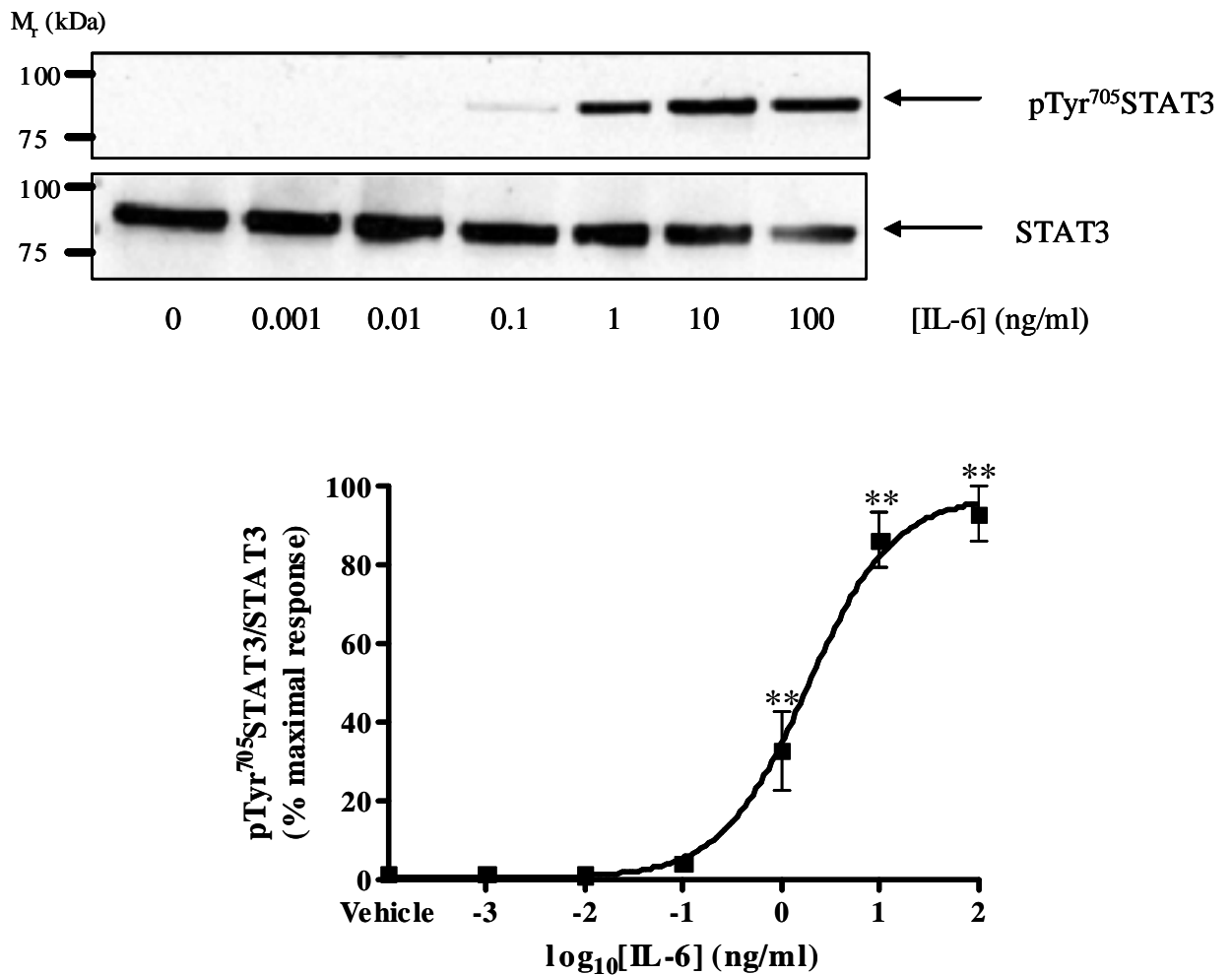


Fig. 6.9: Effect of IL-6 concentration on STAT3 activation in PZ-HPV-7 cells

PZ-HPV-7 cells were seeded into 12-well tissue culture plates and grown to 80 % confluency prior to stimulation for 15 min (37°C, 5 % (v/v) CO₂) with concentrations of rhuIL-6 ranging from 0 (vehicle) – 100 ng/ml. Activation of STAT3 was assessed by immunoblotting for pTyr⁷⁰⁵STAT3 whilst equal protein loading was determined by immunoblotting for STAT3. Blots are representative of $n = 3$ separate experiments and results shown as mean values \pm SEM ** = $p < 0.01$ vs. vehicle

PZ-HPV-7 cells treated with 10 ng/ml rhuIL-6 for 15 min were included as a positive control for elevation of pTyr⁷⁰¹STAT1 and pTyr⁷⁰⁵STAT3. In DU145 cells, treatment with 1000 U/ml IFN α resulted in an increase in detected pTyr⁷⁰¹STAT1 at 30 min post-stimulation ($p < 0.001$ vs. vehicle at 30 min) but not 15 min post-stimulation. In keeping with previous results, treatment with rhuIL-6 resulted in elevation of pTyr⁷⁰⁵STAT3 at 15 and 30 min post-stimulation ($p < 0.05$ vs. vehicle at respective time points), indicating that DU145 cellular responses were comparable to those seen in previous experiments. The results obtained indicate that DU145 cells express STAT1 which is competent for signal transduction due to their ability to tyrosine phosphorylate STAT1 in response to treatment with IFN α . Interestingly, although DU145 cells displayed increased pTyr⁷⁰¹STAT1 following treatment with 1000 U/ml IFN α , no increase in pTyr⁷⁰⁵STAT3 was observed. IFN α has been shown to activate STAT3 in other cell types (Humpalíková β -Ad β m β et al., 2009) and it is possible that the lack pTyr⁷⁰⁵STAT3 in response to IFN α stimulation represents a defect in the IFN α signalling pathway. However, despite IFN α -mediated increases in pTyr⁷⁰¹STAT1, DU145 cells fail to induce STAT1 activation upon stimulation with rhuIL-6. It is possible, given the oncogenic role of STAT3 in prostate cancer and the hypothesised tumour suppressor role of STAT1, that DU145 cells preferentially activate STAT3 in response to IL-6 stimulation rather than STAT1 in order to potentiate cellular proliferation and survival. It is unclear which mechanism is responsible but may include defects in STAT1-gp130 interaction.

Similar to DU145 cells, treatment of LNCaP cells with 10 ng/ml rhuIL-6 resulted in elevation of pTyr⁷⁰⁵STAT3 at 15 and 30 min post-stimulation ($p < 0.01$ vs. vehicle at 15 and 30 min post-stimulation). In contrast to DU145 cells, treatment of LNCaP cells with 1000 U/ml IFN α failed to increase pTyr⁷⁰¹STAT1 at either time point ($p > 0.05$ vs. vehicle at 15 and 30 min). It is therefore possible that LNCaP cells display defects in STAT1 activation in response to cytokine stimulation. This might arise due to a number of reasons including defective JAK activity, STAT1/JAK interaction, STAT1/gp130 interaction or point mutations in STAT1. Unlike DU145 and PZ-HPV-7 cells, LNCaP cells displayed no increases in pTyr⁷⁰¹STAT1 following stimulation with IFN α or rhuIL-6, suggesting that there is a global defect in the ability of these cells to activate STAT1 rather than defects in specific signalling pathways.

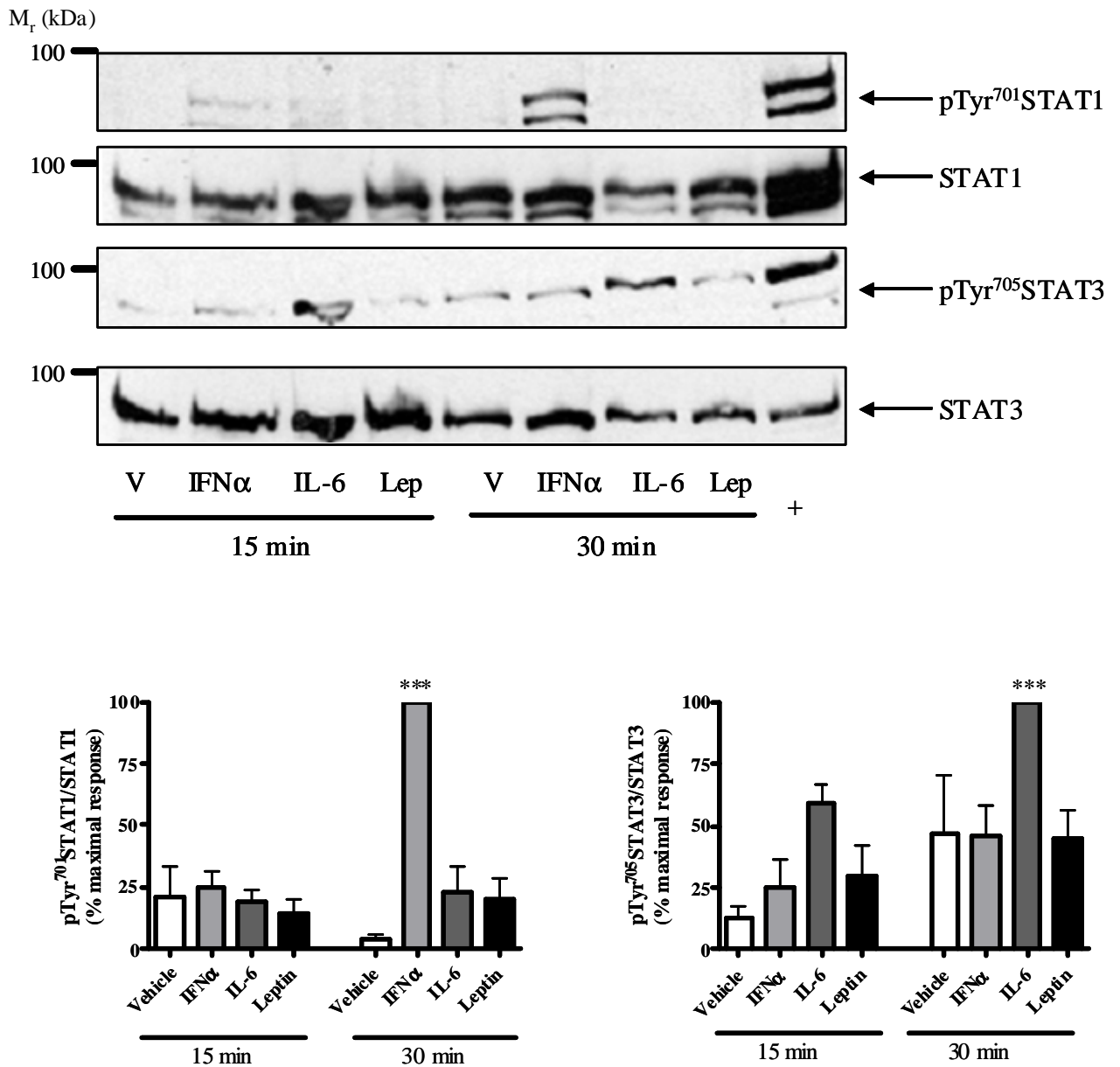


Fig. 6.10: Effect of STAT activating cytokines on STAT1 and STAT3 activation in DU145 cells

DU145 cells were seeded into 6-well tissue culture plates and grown to 80 % confluence prior to stimulation with vehicle (0.1 % (v/v) PBS) or 1000 U/ml rhuIFN α , 10 ng/ml rhuIL-6 or 125 ng/ml leptin for 15 min or 30 min. Cell lysates were fractionated by SDS-PAGE and activation of STAT1 and STAT3 assessed by increases in detected tyrosine phosphorylation of Tyr⁷⁰¹STAT1 and Tyr⁷⁰⁵STAT3. PZ-HPV-7 cells stimulated with 10 ng/ml rhuIL-6 for 15 min were used as a positive control (+) for antibody reactivity. Results are displayed as representative blots and mean values \pm SEM for $n = 3$ separate experiments. *** = $p < 0.001$ vs. vehicle

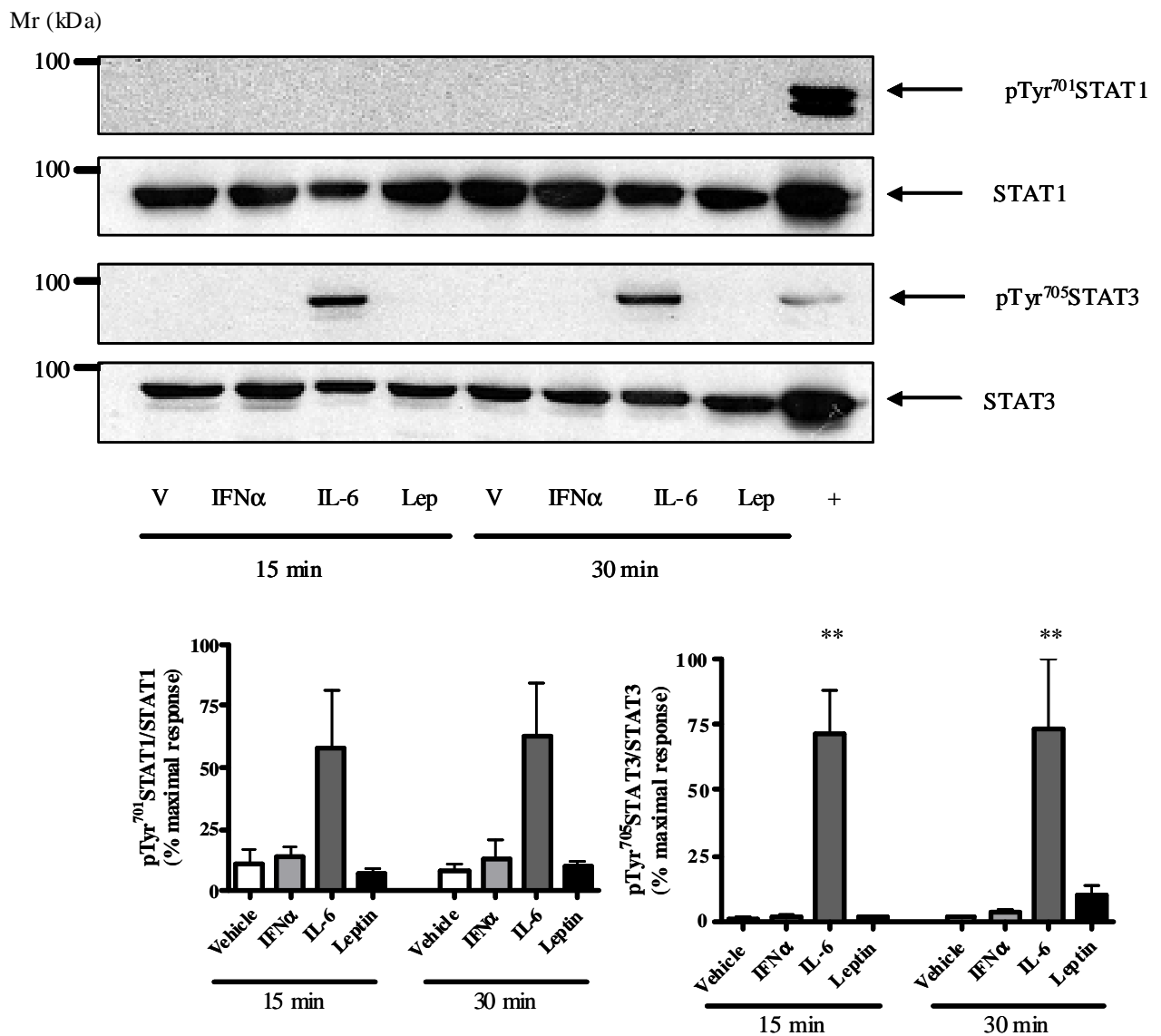


Fig. 6.11: Effect of STAT activating cytokines on STAT1 and STAT3 activation in LNCaP cells

LNCaP cells were seeded into 6-well tissue culture plates and grown to 80 % confluence prior to stimulation with vehicle (0.1 % (v/v) PBS) or 1000 U/ml IFN α , 10 ng/ml rhuIL-6 or 125 ng/ml leptin for 15 min or 30 min. Cell lysates were fractionated by SDS-PAGE and activation of STAT1 and STAT3 assessed by increases in detected tyrosine phosphorylation of Tyr⁷⁰¹STAT1 and Tyr⁷⁰⁵STAT3. PZ-HPV-7 cells stimulated with 10 ng/ml rhuIL-6 for 15 min were used as a positive control (+) for antibody reactivity. Results are displayed as representative blots and mean values \pm SEM for $n = 3$ separate experiments. *** = $p < 0.001$ vs. vehicle

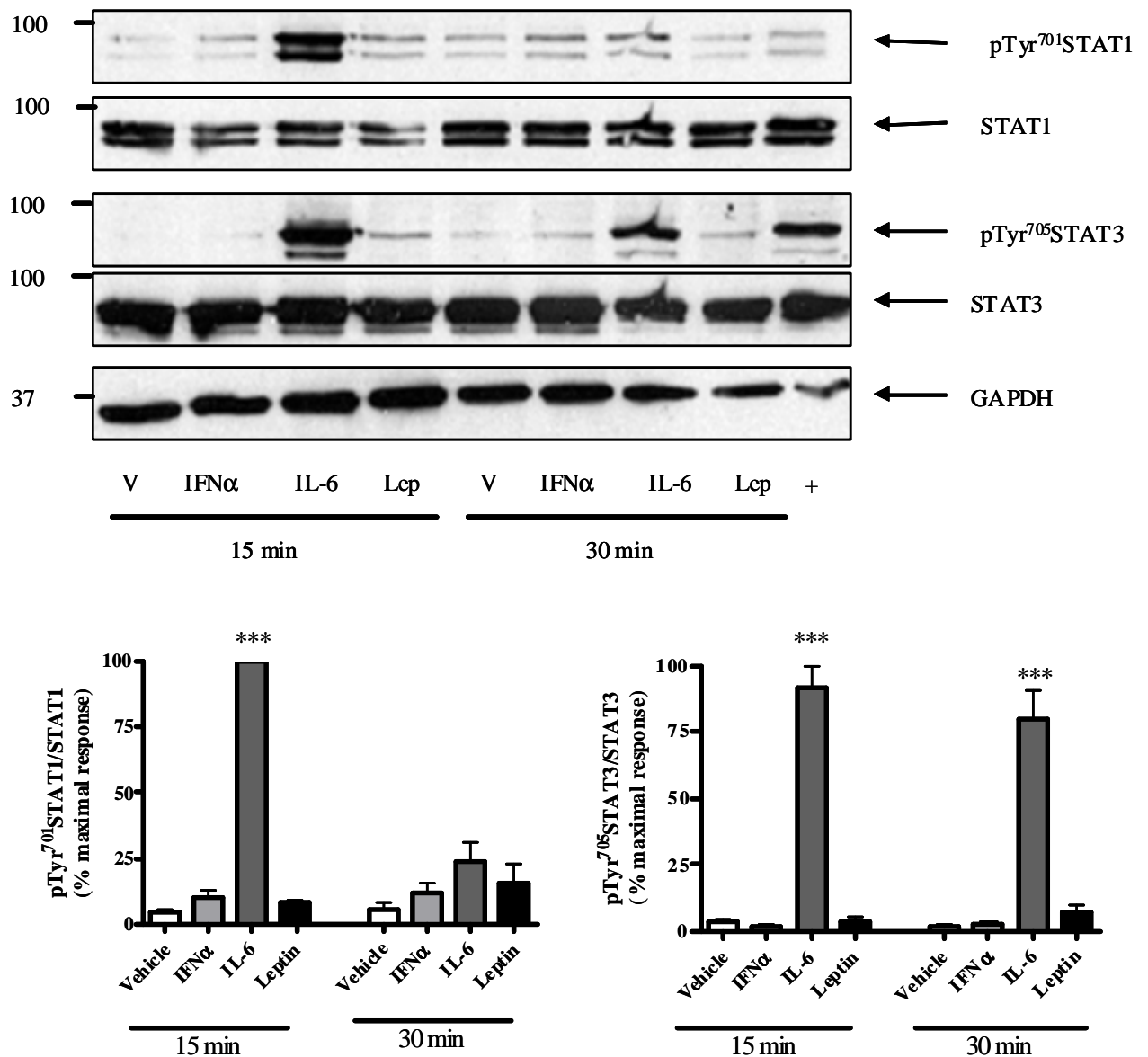


Fig. 6.12: Effect of STAT activating cytokines on STAT1 and STAT3 activation in PZ-HPV-7 cells

PZ-HPV-7 cells were seeded into 6-well tissue culture plates and grown to 80 % confluence prior to stimulation with vehicle (0.1 % (v/v) PBS) or 1000 U/ml IFN α , 10 ng/ml rhuIL-6 or 125 ng/ml leptin for 15 min or 30 min. Cell lysates were fractionated by SDS-PAGE and activation of STAT1 and STAT3 assessed by increases in detected tyrosine phosphorylation of Tyr701STAT1 and Tyr705STAT3. PZ-HPV-7 cells stimulated with 10 ng/ml rhuIL-6 for 15 min were used as a positive control (+) for antibody reactivity. Results are displayed as representative blots and mean values \pm SEM for $n = 3$ separate experiments. *** = $p < 0.001$ vs. vehicle

Whilst the densitometric results indicate that rhuIL-6 was able to induce pTyr⁷⁰¹STAT1 at 15 and 30 min post-stimulation, it is thought that this result might be an experimental artefact as, when bands are present, they appear only as faint bands which may arise from cross-reactivity with pTyr⁷⁰⁵STAT3 in conditions where STAT3 is strongly activated. Such a phenomenon has been observed with this antibody in previous studies (Haan *et al.*, 2005).

Similarly, in PZ-HPV-7 cells, treatment with 1000 U/ml IFN α failed to induce Tyr⁷⁰¹ phosphorylation of STAT1 at 15 or 30 min post-stimulation ($p > 0.05$ vs. vehicle at 15 and 30 min) whilst 10 ng/ml rhuIL-6 resulted in robust elevation of pTyr⁷⁰¹STAT1 at 15 min post-stimulation ($p < 0.001$ vs. vehicle). Similar to previous experiments, treatment with 10 ng/ml rhuIL-6 resulted in an increase in pTyr⁷⁰⁵STAT3 at 15 and 30 min post-stimulation ($p < 0.001$ vs. vehicle at respective time points). PZ-HPV-7 cells represent the normal prostate epithelial responses in this study and display expected STAT1 and STAT3 activation responses to rhuIL-6. It is surprising that these cells do not respond to IFN α with an increase in either pTyr⁷⁰¹STAT1 or pTyr⁷⁰⁵STAT3 as IFN α is involved in the anti-viral response and thus should activate STAT1 and STAT3 in most cell types, even in the absence of STAT tyrosine phosphorylation induced by stimulation with other cytokines such as rhuIL-6. In all three cell lines used, there was no response to leptin at the concentration used despite this concentration previously producing robust STAT3 responses in HUVECs (Woolson *et al.*, 2009), suggesting that the cell lines lack expression of the Ob receptor required for leptin-mediated signalling.

Taken together these results imply that there is defective activation of STAT1 in tumour-derived prostate epithelial cell lines in response to stimulation with rhuIL-6 which is not observed in cells derived from normal prostate epithelium. Such modification of the cellular responses to IL-6 suggests that tumour cells dynamically modify cell signalling pathways in order to maximise tumour development. However, the ability of DU145 but not LNCaP cells to activate STAT1 in response to IFN α suggests that the mechanism by which cells uncouple IL-6R activation from signal transduction to STAT1 is not universal.

6.3.5 Ectopic expression of JAK1 restores the ability of LNCaP cells to activate STAT1 in response to rhuIL-6

It has previously been demonstrated that LNCaP cells are unable to respond to IFN γ stimulation due to a lack of JAK1 expression. As JAK1 has been implicated as a major activator of STAT1 and thus it is possible that the inability of LNCaP cells to activate

STAT1 in response to rhuIL-6 arises due to a lack of JAK1 expression. In order to determine whether this was the case, LNCaP cells were seeded into 6-well plates prior to transfection with either the empty vector pcDNA3 or wild-type JAK1 as described in Chapter 5. Cells were then stimulated with vehicle, 1000 U IFN α or 10 ng/ml rhuIL-6 for 15 and 30 min prior to SDS-PAGE fractionation and subsequent determination of STAT1 and STAT3 activation *via* immunoblotting.

LNCaP cells transfected with pcDNA3 and JAK1 both showed increases in detected pTyr⁷⁰⁵STAT3 at 15 and 30 min post-stimulation with rhuIL-6 (Fig. 6.13), indicating normal cellular responses to exogenous cytokine. No increase in pTyr⁷⁰¹STAT1 was observed following stimulation with rhuIL-6 in LNCaP cells transfected with pcDNA3. Similar to results obtained in non-transfected cells, treatment with 1000 U/ml IFN α or vehicle failed to induce STAT1 or STAT3 activation in LNCaP cells transfected with vector or the JAK1 construct. However, expression of JAK1 in LNCaP cells resulted in an increase in detection of pTyr⁷⁰¹STAT1 following stimulation with 10 ng/ml rhuIL-6 at 15 min post-stimulation. These results indicate that, whilst JAK1 expression is not required for the ability of rhuIL-6 to activate STAT3 in LNCaP cells, it is required for IL-6-mediated activation of STAT1. Interestingly, although expression of JAK1 restored the ability of LNCaP cells to activate STAT1 in response to rhuIL-6, expression of JAK1 did not restore their ability to respond to IFN α , suggesting that defects in STAT1 activation in these cells differ between stimuli.

6.4 Discussion

PCa is the second largest cancer-related killer of men in the Western world, with one new case being diagnosed every 15 minutes in the UK alone (Cancer Research UK, 2005). Many factors contribute to PCa development, including dietary intake of saturated fat (Crowe et al., 2008), body mass index (BMI) (Stark et al., 2009) and chronic inflammatory conditions such as inflammatory atrophy (de Visser et al., 2005). Concomitant with sustained inflammation are the presence of pro-inflammatory cytokines and subsequent activation of associated signalling pathways. Important to this project are the roles which the cytokine IL-6 and subsequent activation of the STAT3 signalling molecule play in PCa progression. To this end, three prostate epithelial cell lines were characterised for their ability to respond to exogenous rhuIL-6.

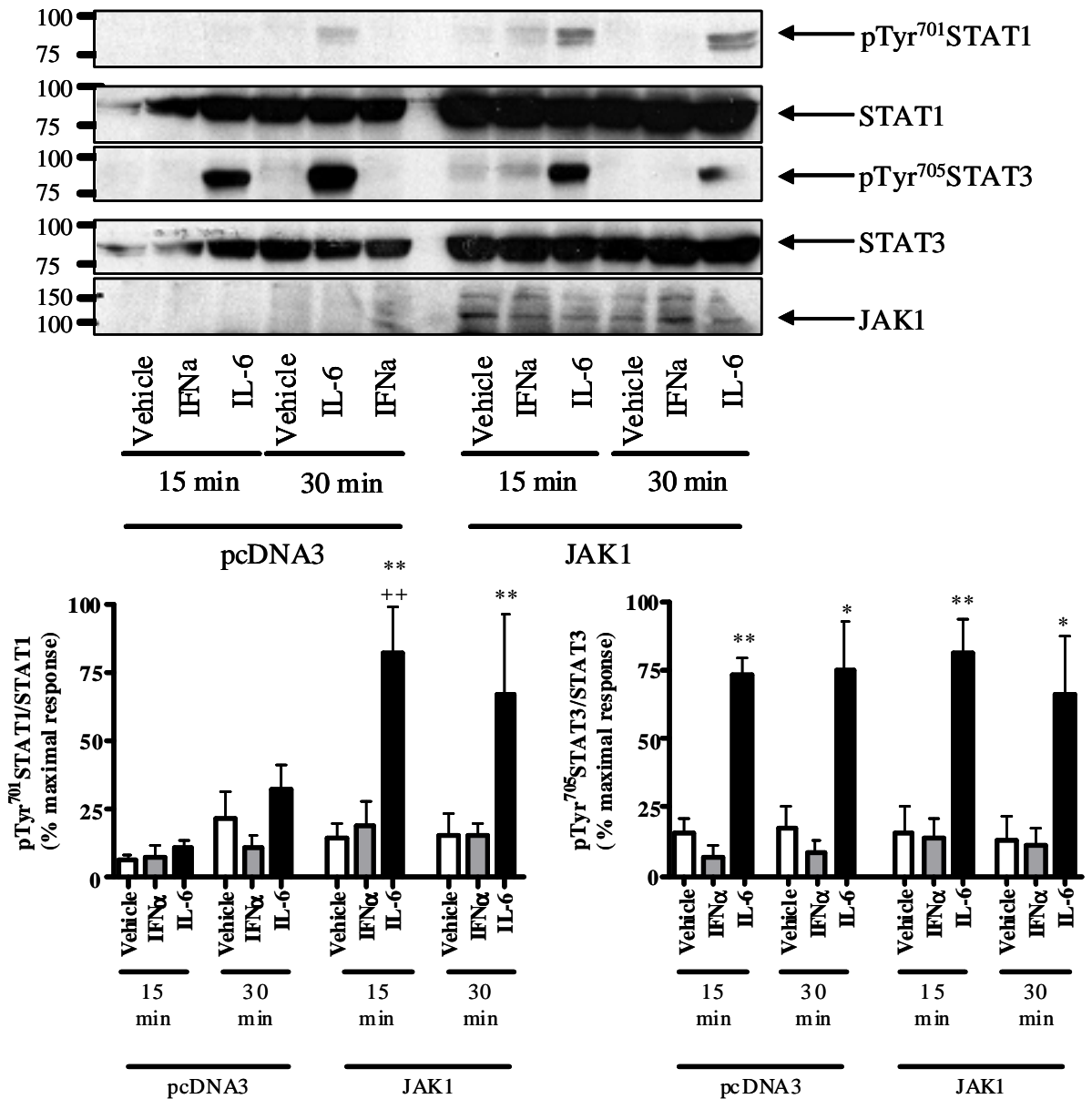


Fig. 6.13: Expression of JAK1 in LNCaP cells restores STAT1 phosphorylation in response to rhIL-6

LNCaP cells were transfected with 1 μ g pcDNA3 or JAK1 cDNA prior to stimulation with vehicle, 1000 U IFN α or 10 ng/ml rhIL-6 for 15 min or 30 min. Cell lysates were fractionated by SDS-PAGE and activation of STAT1 and STAT3 assessed by increases in detected tyrosine phosphorylation of Tyr⁷⁰¹STAT1 and Tyr⁷⁰⁵STAT3. Results are displayed as representative blots and mean values \pm SEM for $n = 3$ separate experiments. * = $p < 0.05$ vs. vehicle, ** = $p < 0.01$ vs. vehicle, ++ = $p < 0.01$ vs. pcDNA3

The DU145 cell line was originally isolated from a CNS lesion in a 69 year-old Caucasian male suffering from widespread, metastatic PCa (Stone et al., 1978). These cells are representative of a highly aggressive, androgen-independent cell line and as such are being used throughout this study as a late stage model of PCa (Okamoto et al., 1997). It has been reported that DU145 cells secrete IL-6 which acts as both an autocrine and paracrine growth factor (Okamoto et al., 1997), thus it might be expected that DU145 cells should display basal activation of STAT3 in the absence of exogenous cytokine. However, when DU145 cells were grown in conditioned medium and analysed for basal tyrosine phosphorylation of STAT3 by immunoblotting, no basal pTyr⁷⁰⁵STAT3 was observed with levels of pTyr⁷⁰⁵STAT being comparable to those observed in cell stimulated in fresh culture medium (Fig. 6.4). Furthermore, treatment of cells grown in conditioned medium with 10 ng/ml resulted in an increase in pTyr⁷⁰⁵STAT3 but to a lesser extent than that observed in cells stimulated in fresh culture medium. Whilst this result was unexpected, it is possible that the perpetual stimulation of IL-6R by secreted IL-6 in DU145 cells results in activation of endogenous inhibitors of the IL-6 signalling pathway and thus impedes further activation of STAT3. Strong candidates for such endogenous inhibitory signalling pathways include induction of the SOCS family proteins which impede JAK-mediated STAT activation (Endo *et al.*, 1997; Ilangumaran *et al.*, 2004; Kile & Alexander, 2001) and activation of the SHP2 tyrosine phosphatase which has been reported to dephosphorylate activated STAT3 in endothelial cells (Ni & Wang, 2003). Both pathways would result in the inhibition of STAT3 tyrosine phosphorylation unlike PIAS3, which specifically interacts with STAT3, and impairs both the DNA-binding and transactivator potential of STAT3 downstream of Tyr⁷⁰⁵ phosphorylation (Chung et al., 1997).

In contrast to the DU145 cell line, the LNCaP, used here as a model of early PCa, and PZ-HPV-7, indicative of normal prostate epithelial response, cell lines showed no difference in the ability of IL-6 to activate STAT3 when cells were stimulated in conditioned *vs.* fresh growth medium. Similarly, no basal pTyr⁷⁰⁵STAT3 was detected in these cells which was anticipated as there are no current reports of IL-6 secretion by either of these cells.

In all three cell lines, the ability of IL-6 to induce STAT3 activation increased with the concentration of rhuIL-6 used above an IL-6 concentration of 0.1 ng/ml (Figs. 2.7-2.9). None of the cell types displayed saturation of STAT3 activation even following treatment with 100 ng/ml rhuIL-6, indicating that the responses observed are not supramaximal and may be inhibited in subsequent studies. Whilst DU145 and PZ-HPV-7 cells demonstrated

transient increases in pTyr⁷⁰⁵STAT3 (Fig. 2.1 and Fig. 2.2 respectively), the duration of rhuIL-6-induced STAT3 activation was more sustained in LNCaP cells (Fig. 2.3), remaining elevated at 60 min post-stimulation. Whilst activation of STAT3 in response to rhuIL-6 at 15-30 min post-stimulation is expected and correlates with published data regarding the activation and nuclear accumulation of STAT3 (Pranada *et al.*, 2004), this response is rarely prolonged in cells due to the induction of endogenous inhibitory mechanisms required to prevent sustained pro-inflammatory signalling and subsequent tissue damage. It is unclear why the response is prolonged in LNCaP cells compared to the other cell types but may be associated with the observation that chronic IL-6 stimulation can induce differentiation of LNCaP cells to a neuroendocrine phenotype *via* activation of gp130 (Palmer *et al.*, 2005).

Of particular interest was the observation that treatment of PZ-HPV-7, but not DU145 and LNCaP cells, with rhuIL-6 resulted in a transient increase in pTyr⁷⁰¹STAT1. Although STAT3 is the major STAT family member activated downstream of IL-6R, STAT1 also becomes activated by IL-6 (Gerhartz *et al.*, 1996). All three cell types express comparable levels of STAT1 protein of the same apparent molecular weight, excluding the possibility that the inability of IL-6 to induce STAT1 activation in DU145 or LNCaP cells arises due to a lack of STAT1 expression. It is possible that these cell lines express a variant of STAT1 that lacks the C-terminal Tyr⁷⁰¹ required for activation downstream of cytokine receptors (Shuai *et al.*, 1992). However, due to the resolution limits of one dimensional SDS-PAGE, only a gross truncation of STAT1 would be detectable, which was not apparent in any of the experiments performed. Further experimental data indicated that the inability of rhuIL-6 to induce robust activation of STAT1 in the tumour-derived cell lines arose due to defects in IL-6 signalling rather than in STAT1 expression. Given the oncogenic properties of chronic STAT3 activation (Azare *et al.*, 2007; Barton *et al.*, 2004; Bromberg *et al.*, 1999), it is possible that DU145 and LNCaP cells, both tumour-derived cell lines, have potentiated activation of STAT3 rather than STAT1 in response to rhuIL-6 in order to promote tumour growth and metastasis. Both cell lines are derived from metastatic lesions, a process which can be enhanced by STAT3-mediated integrin switching (Azare *et al.*, 2007) whilst activation of STAT1 is reported to exert a tumour suppressor effect (Hodge *et al.*, 2005) thus preferential activation of STAT3 compared to STAT1 activation would clearly be beneficial for the maintenance of tumour cell populations. It is also possible that the presence of STAT3 in the DU145 and LNCaP cell lines may prevent activation of STAT1 downstream of the IL-6R as has been shown in

mouse embryonic fibroblasts (MEFs). Wild-type cells do not respond to IL-6 stimulation with a sustained increase in STAT1 activation and thus do not increase expression of STAT1-regulated genes in response to IL-6 stimulation. However, when STAT3 knock-out MEFs are stimulated with IL-6, a sustained increase in pTyr⁷⁰¹STAT1 is observed which is correlated with an increase in STAT1-regulated genes (Costa-Pereira *et al.*, 2002).

To assess whether the inability of rhuIL-6 to induce activation of STAT1 in the tumour-derived DU145 and LNCaP cell lines was due to cellular defects in STAT1 activation, cells were treated in parallel with either 1000 U/ml rhuIFN α or 10 ng/ml rhuIL-6 for 15 or 30 min. The ability of rhuIFN α to increase detected pTyr⁷⁰¹STAT1 in DU145 cells indicates that these cells express a STAT1 protein which is competent for signal transduction downstream of cytokine receptors and that the lack of rhuIL-6-mediated increases in pTyr⁷⁰¹STAT1 arise due to specific aberrations in the IL-6-signalling pathway. Treatment with 1000 U/ml IFN α of either the LNCaP or PZ-HPV-7 cell lines in parallel experiments failed to induce activation of STAT1, which is unexpected given the importance of this cytokine in the innate immune response. PZ-HPV-7 cells retained rhuIL-6-induced Tyr⁷⁰¹ phosphorylation of STAT1, indicating that the cells are still competent to respond to exogenous cytokine and that the lack of STAT1 activation seen with IFN α treatment is specific to the IFN α pathway.

In subsequent experiments (see Chapter 7), it was noted that LNCaP cells, unlike DU145 and PZ-HPV-7 cells, do not express detectable levels of JAK1. It has been suggested that JAK1 is the major JAK family member required for STAT1 activation downstream of the IL-6 receptor (Haan *et al.*, 2005) and LNCaP cells are reported to be insensitive to IFN γ due to a lack of JAK1 expression (Dunn *et al.*, 2005). It was therefore possible that lack of JAK1 expression may account for the inability of both rhuIL-6 and rhuIFN α to induce STAT1 activation in this cell line. To assess this, LNCaP cells were transfected with cDNA encoding either pcDNA3 or wild-type JAK1 and treated with vehicle, rhuIFN α or rhuIL-6 for 15 or 30 min. In cells transfected with JAK1, but not pcDNA3, LNCaP cells displayed increased pTyr⁷⁰¹STAT1 upon treatment with rhuIL-6, indicating that the JAK1 expression restores STAT1 responses to IL-6. However, expression of JAK1 failed to elevate STAT1 tyrosine phosphorylation in response to IFN α treatment, indicating signalling defects downstream of the IFN α receptor.

It is perhaps unsurprising that LNCaP cells display defective activation of STAT1 in response to IFN α stimulation as impaired IFN signalling is a feature of many cancers. A study by Critchley-Thorne *et al* (2009) demonstrated impaired cellular responses to IFN α and IFN γ from breast cancer, melanoma, and gastrointestinal cancer patients although the exact nature of this impairment varied between cancer type. However, it is unusual that PZ-HPV-7 cells do not respond to IFN α treatment with an increase in pTyr⁷⁰¹STAT1 as these are thought to represent normal prostate epithelial responses to cytokines. As these cells respond to rhuIL-6 stimulation with a robust increase in detected pTyr⁷⁰¹STAT1, it would appear that the lack of response to IFN α is a defect specific to the IFN α signalling pathway.

To test whether these cells expressed a functional STAT1 signalling pathway, DU145, LNCaP and PZ-HPV-7 cells were treated with vehicle, 1000 U IFN α or 10 ng/ml rhuIL-6 for 15 and 30 min. All cell types tested responded to exogenous rhuIL-6 with an increase in pTyr⁷⁰⁵STAT3, indicating that cells were undergoing normal responses to exogenous cytokines. At 30 min post-stimulation, DU145 cells showed an increase in pTyr⁷⁰¹STAT1 when treated with IFN α , indicating that these cells do indeed express a functional STAT1 signalling pathway and that there is some defect in STAT1 activation downstream of the IL-6R. Whilst DU145 cells responded to IFN α treatment with an increase in pTyr⁷⁰¹STAT1, neither PZ-HPV-7 cells nor LNCaP cells showed responses to IFN α which is unusual given the essential role of this cytokine in the immune response. Treatment of PZ-HPV-7 cells with rhuIL-6 induced the transient tyrosine phosphorylation of STAT1 as described previously, indicating that the inability of IFN α to activate STAT1 is not due to passage-related changes in signalling pathways. It is possible that PZ-HPV-7 cells lack IFN α receptor expression, thus rendering them insensitive to IFN α stimulation, although this would appear to be a rare event.

Whilst the lack of STAT1 activation in LNCaP cells appears to be due to the lack of JAK1 expression, the mechanism by which IL-6-mediated STAT1 activation in DU145 cells is attenuated appears more complex. The ability of IFN α to induce STAT1 activation in DU145 cells indicates that there are no defects in the ability of JAKs to activate STAT1 in this cell line nor that these cells express STAT1 isoforms which lack Tyr⁷⁰¹. Given the observed activation of STAT1 in response to IFN α it seems reasonable to presume that the inability of IL-6 to induce tyrosine phosphorylation of STAT1 in DU145 cells is a phenomenon specific to the IL-6R/gp130 signalling module. Many cancer cells display

dysregulation of important pathways involved in the ensuring maintenance of genomic integrity whilst the microenvironment surrounding the tumour is often rich in mutation-promoting factors such as ROS (Dhar *et al.*, 2002; Finkel & Holbrook, 2000; Jackson *et al.*, 2002). As the DU145 cell line is derived directly from a malignant lesion, it is therefore possible that these cells may have accumulated mutations in the gp130 molecule which may prevent efficient docking of signalling modules such as JAK1 or STAT1 to phosphotyrosine residues within gp130. Use of a chimeric erythropoietin/gp130 receptor indicates differences in the docking sites used by STAT1 and STAT3. Whilst STAT3 is reported to bind to pTyr⁷⁶⁷ and pTyr⁸¹⁴, STAT1 has been shown to bind to a further two pTyr residues in this model, corresponding to Tyr⁹⁰⁵ and Tyr⁹¹⁵ (Gerhartz *et al.*, 1996). It is possible that DU145 cells have mutations in these STAT1-specific docking sites which may prevent IL-6-mediated STAT1 activation, whilst binding of STAT3 to Tyr⁷⁶⁷ and Tyr⁸¹⁴ may sterically hinder STAT1 recruitment to these sites. Such a hypothesis is supported by the observation that deletion of STAT3 in MEFs promotes sustained activation of STAT1 rather than the transient activation seen in wild-type cells (Costa-Pereira *et al.*, 2002), suggesting that IL-6-mediated STAT3 activation can hinder activation of STAT1.

To summarise, all three cell types phosphorylate STAT3 in response to treatment with exogenous rhuIL-6, indicating that the system is suitable for further use as an *in vitro* model of IL-6-induced cellular signalling in PCa. However, despite similarities in IL-6-mediated STAT3 activation, there were clear differences in the ability of rhuIL-6 to induce STAT1 with the tumour-derived cell lines failing to activate STAT1 in response to exogenous IL-6. It is possible that this phenomenon arises due to the tumour suppressive activities of STAT1 activation. In LNCaP cells, the inability of IL-6 to activate STAT1 is due to a lack of JAK1 expression whilst the mechanism by which this is achieved in DU145 cells is currently unclear.

7 Elevation of cAMP attenuates STAT3 phosphorylation in prostate epithelial cells

7.1 Introduction

Elevation of serum IL-6 levels is associated with a poor patient prognosis at diagnosis and with terminal, androgen refractory disease (Kuroda *et al.*, 2007; Michalaki *et al.*, 2004). Of particular interest is the ability of IL-6 to activate STAT3 *via* phosphorylation of Tyr⁷⁰⁵ and subsequent increases in expression of proteins associated with cell cycle progression and the prevention of apoptosis (Hodge *et al.*, 2005). Constitutively active STAT3 is directly oncogenic *in vivo* (Azare *et al.*, 2007; Bromberg *et al.*, 1999) and is of particular interest in PCa. Both IL-6 and STAT3 can activate the AndR independently of androgen stimulation and thus may provide a mechanism by which activation of STAT3 signalling can promote the androgen-independent growth associated with terminal PCa (Culig *et al.*, 2002; Ueda *et al.*, 2002). Barton *et al.* (2004) demonstrated that inhibition of STAT3 signalling results in apoptosis of PCa cells (Barton *et al.*, 2004) and thus the IL-6/JAK-STAT3 signalling pathway is of particular interest as a therapeutic target for PCa.

Traditionally, inflammatory diseases have been treated with steroidal drugs which can have undesirable side effects such as osteoporosis when used for long periods (Canalis *et al.*, 2007). With reference to STAT3 activation, many strategies currently exist for inhibiting STAT signalling *in vitro* and *in vivo* including inhibition of JAK activity, disruption of STAT dimerisation (Jing & Tweardy, 2005) and the presence of decoy oligonucleotides to impede interaction of STAT3 with its genuine promoters (Sen *et al.*, 2009; Zhang *et al.*, 2007) (see Chapter 3). However, the efficacy of these “next generation” inhibitors has not yet been proven in the clinic although use of decoy oligonucleotides has shown promise in non-human primates (Sen *et al.*, 2009). One strategy which has demonstrated clinical efficacy has been the blockade of IL-6R signalling using the humanised anti-IL-6R antibody Tocilizumab. In April 2008, Tocilizumab was approved for use in juvenile idiopathic arthritis and RA in Japan (Mima & Nishimoto, 2009). Monotherapy with Tocilizumab has proven effective in cases of RA which respond poorly to conventional therapies. However, treatment with Tocilizumab is associated with an increase in serum cholesterol and hyperlipidemia which can be associated cardiovascular disease in some patients (Mima & Nishimoto, 2009). It is possible that a better mechanism by which to attenuate IL-6-induced activation of STAT3 may be to manipulate endogenous anti-inflammatory pathways.

The anti-inflammatory and immunomodulatory roles of cAMP elevation are of particular interest as this second messenger can play an important role in a number of inflammatory diseases. In a murine model of allergic pleurisy, elevation of cAMP due to inhibition of PDE4 activity or treatment with Fsk or cAMP analogues decreased the number of eosinophils in the pleural cavity and was associated with an increase in eosinophil apoptosis due to inhibition of the PI-3-kinase (PI3K) and NF κ B pathways (Sousa *et al.*, 2009). Inhibition of the cAMP-specific PDE, PDE7A, results in a decrease in NK T (NKT) -cell function and cytokine production (Goto *et al.*, 2009). NKT cells are required for the development of airway hyperreactivity in allergic asthma, indicating that these cells play an important role in inflammation-associated diseases (Kim *et al.*, 2009). Deficiency in the A_{2A} adenosine receptor (AR), which elevates intracellular cAMP upon interaction with adenosine (Ado) (see Chapter 10) is associated with increased inflammatory responses *in vivo* and impaired tracheal relaxation in murine models of asthma (Nadeem *et al.*, 2007; Ohta & Sitkovsky, 2001). Inhibition of PDE4 activity has been investigated as a treatment for chronic obstructive pulmonary disorder (COPD) and other PDE inhibitors have already been approved for clinical use. Ibudilast is a non-selective PDE inhibitor which is approved for use in Japan to treat ischaemic stroke and bronchial asthma. Cilomilast is a PDE4-selective inhibitor which has entered phase III clinical trials as a treatment for COPD (Brown, 2007). In animal models of allergic skin disorders, topical application of the PDE4 –selective inhibitor AWD 12-281 reversed ovalbumin-induced allergic skin weals (Hoppmann *et al.*, 2005). It is possible that cAMP elevation in inflammatory skin disorders, such as atopic dermatitis, can attenuate inflammatory cell infiltration *via* a decrease in chemokine secretion downstream of the initial pro-inflammatory stimulus and prevent the establishment of a chronic inflammatory environment. Treatment of the HaCat keratinocyte cell line with Fsk resulted in a decrease in both IFN γ and TNF α -induced chemokine secretion and activation of the NF κ B and p38 MAPK signalling pathways (Qi *et al.*, 2009). Given that the establishment of a chronic inflammatory environment is associated with defective anti-tumour immunosurveillance and subsequent tumour expansion, it is possible that modulation of the inflammatory response downstream of cAMP activation may be of therapeutic benefit.

With particular reference to cancer, elevation of cAMP may be of importance when promoting apoptosis or inhibiting proliferation of malignant cells. Elevation of cAMP inhibits cell cycle progression of myeloid precursor cells following stimulation with granulocyte colony stimulating factor (G-CSF). This effect was mediated by a decrease in

Rb phosphorylation arising from decreased levels of cyclins D2 and D3 and the cyclin dependent kinase 4 (Ward *et al.*, 1996). Phosphorylation of Rb is associated with release of transcription factors such as E2F which are required for cell cycle progression (Ward *et al.*, 1996). Treatment of Ewing's sarcoma CHP-100 cells with the cell-permeable cAMP analogue 8-chloro-cAMP resulted in a decrease in cellular viability which was synergistically enhanced when combined with retinoic acid (Srivastava *et al.*, 1998). Such results suggest that cAMP elevation may prove a suitable therapeutic intervention to complement existing chemotherapeutic options when treating inflammation-associated malignancies.

Of particular relevance to this study is the ability of cAMP elevation to attenuate IL-6/sIL-6R α -induced activation of STAT3 in HUVECs. In these cells, elevation of intracellular cAMP resulted in attenuation of STAT3 activation following stimulation with the IL-6/sIL-6R α *trans*-signalling complex *via* an increase in SOCS3 expression. Activation of EPAC1, but not PKA, was required for this phenomenon as cAMP-mediated induction of SOCS3 was insensitive to PKA inhibition but was recapitulated following selective activation of EPAC1 (Sands *et al.*, 2006). This response has been shown to require both C/EBP β and δ as deletion of either isoform abolishes the ability of cAMP elevation to induce SOCS3 expression in MEFs (Yarwood *et al.*, 2008). Both cAMP elevation and selective activation of EPAC promoted an increase in C/EBP reporter gene expression, indicating that activation of C/EBP β and C/EBP δ are required for this phenomenon (Yarwood *et al.*, 2008). Activation of the ERK1/2 signalling pathway is required for cAMP-induced SOCS3 expression in COS1 cells. EPAC-mediated activation of both PKC α and PKC δ is required for cAMP-induced SOCS3 expression with elevation of intracellular cAMP promoting activation of PKC α simultaneously with activation of ERK1/2 (Borland *et al.*, 2009). It is likely that the effects of PKC activation are mediated downstream activation of phospholipase C (PLC) ϵ as selective ablation of PLC ϵ expression *via* siRNA decreased the ability of cAMP elevation to induce SOCS3 expression (Borland *et al.*, 2009).

Current studies investigating the ability of cAMP to attenuate IL-6-induced STAT3 phosphorylation suggest that it is a common modulator of inflammatory signalling in HUVECs (Sands *et al.*, 2006), MEFs (Sands *et al.*, 2006) and the U937 myeloid precursor cell line (Mullan and Palmer, unpublished observations). It is thus anticipated that elevation of cAMP in the DU145, LNCaP and PZ-HPV-7 cell lines will attenuate IL-6-

induced activation of STAT3 which could be of relevance when considering the key role this signalling pathway plays in PCa development and progression.

In order to investigate the role of cAMP elevation in attenuation of intracellular signalling downstream of the IL-6R, DU145, LNCaP and PZ-HPV-7 cells were treated with the AC-activating compound Fsk for 5 h prior to stimulation with rhuIL-6. In all three cell lines, pre-treatment with Fsk resulted in a decrease in IL-6-induced increases in pTyr⁷⁰⁵STAT3 *via* pathways requiring activation of both PKA and EPAC. In DU145 and PZ-HPV-7 cells, the level of decrease in STAT3 phosphorylation was correlated with increases in detected SOCS3 expression, indicating that SOCS3 is required for this phenomenon. In the case of LNCaP cells, cAMP elevation did not induce changes in SOCS3 expression, suggesting that a different mechanism is responsible for cAMP-mediated attenuation of IL-6 signalling in these cells.

7.2 Results

7.2.1 Effect of Fsk on IL-6-mediated activation of STAT3

Prostate epithelial cells were seeded into 6-well tissue culture dishes as described previously and allowed to grow to appropriate confluence. Cells were then stimulated with either vehicle (0.1 % (v/v) EtOH) or 10 μ M Fsk for 5 h as this has previously been demonstrated to induce optimal expression of SOCS3 in HUVECs. Cells were then stimulated with 10 ng/ml rhuIL-6 for 0 – 240 min in order to induce activation of STAT3. It has previously been demonstrated that expression of the A_{2A} adenosine (Ado) receptor (A_{2A}AR) in HUVECs can induce a decrease in STAT3 activation *via* promoting the polyubiquitination and subsequent proteasomal degradation of activated STAT proteins (Safhi and Palmer, submitted for publication). As the A_{2A}AR is a G α_s -coupled receptor, activation of the receptor will stimulate AC activity and so promote elevation of intracellular cAMP. It is thus possible that treatment with Fsk could mimic these events and so promote degradation of activated STAT3. Sustained stimulation with rhuIL-6 was undertaken in order to exclude the possibility that any effects of cAMP elevation on STAT3 activation did not occur due to degradation of STAT3.

Treatment of DU145, LNCaP and PZ-HPV-7 cells with 10 ng/ml rhuIL-6 resulted in an increase in pTyr⁷⁰⁵STAT3 in both vehicle and Fsk-stimulated cells (Fig. 7.1 – Fig. 7.3). However, pre-treatment with 10 μ M Fsk significantly inhibited IL-6-mediated increases in pTyr⁷⁰⁵STAT3 in all three cell types (Fig. 7.1 – Fig. 7.3, * = $p < 0.05$ vs. vehicle-treated

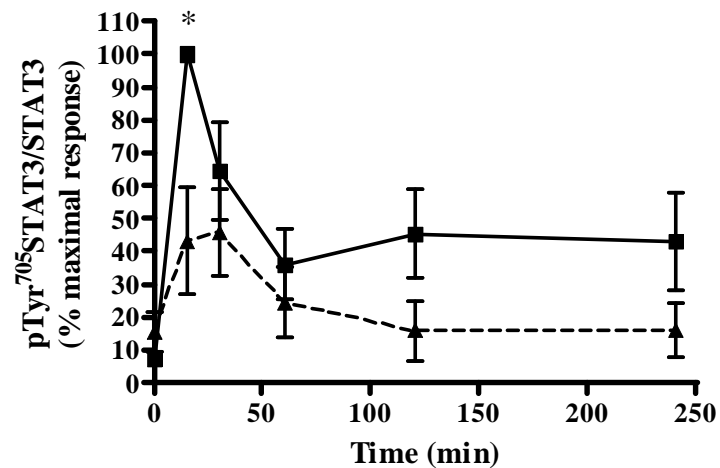
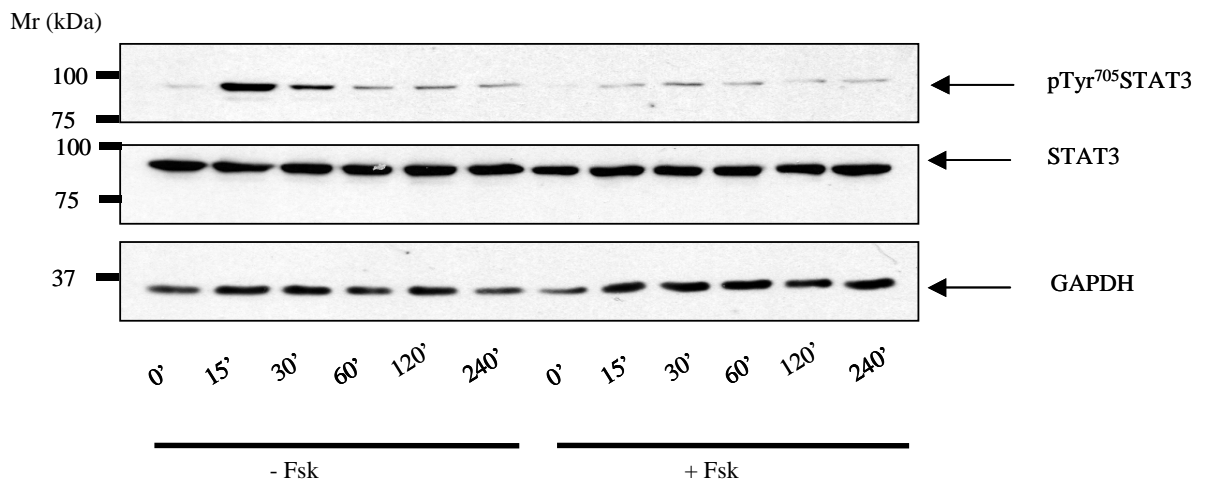


Fig. 7.1: Inhibition of IL-6-induced STAT3 activation in DU145 prostate epithelial cells

DU145 cells were seeded into 6-well plates and stimulated with either vehicle (0.1 % (v/v) EtOH) or 10 μ M Fsk for 5 h prior to stimulation with 10 ng/ml rhuIL-6 for 0 –240 min. Cell lysates were fractionated *via* SDS-PAGE and STAT3 activation assessed *via* immunoblotting for pTyr⁷⁰⁵STAT3. Results are shown as mean values \pm SEM for cells pre-incubated with vehicle (solid line) or 10 μ M Fsk (dashed line) with blots representative for $n = 3$ separate experiments. * = $p < 0.05$ vs. vehicle-treated cells

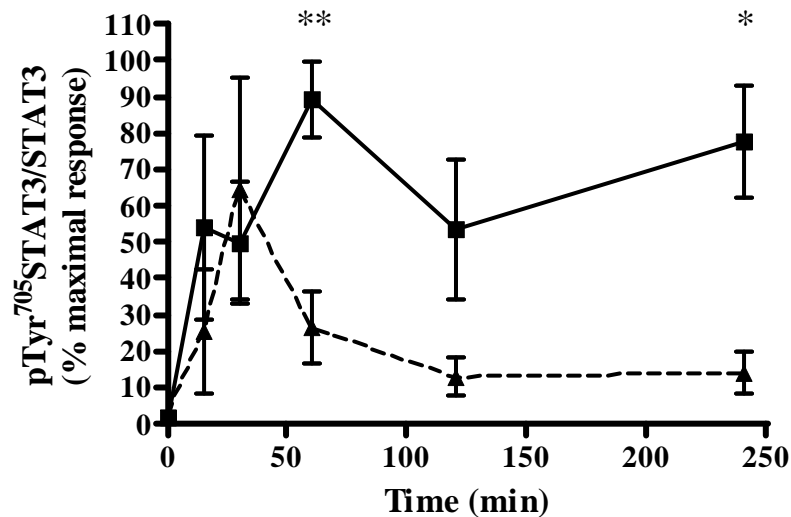
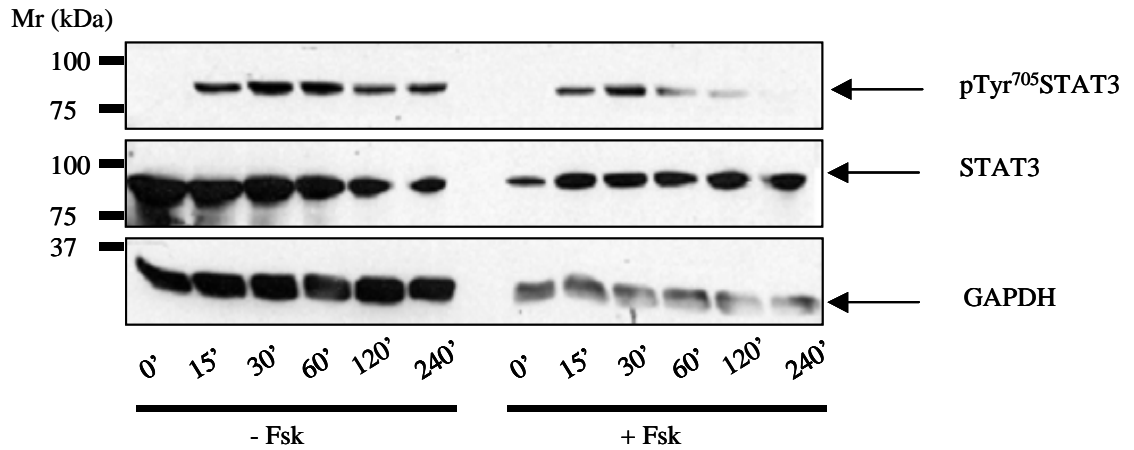


Fig. 7.2: Inhibition of IL-6-induced STAT3 activation in LNCaP prostate epithelial cells

LNCaP cells were seeded into 6-well plates and stimulated with either vehicle (0.1 % (v/v) EtOH) or 10 μ M Fsk for 5 h prior to stimulation with 10 ng/ml rhuIL-6 for 0 –240 min. Cell lysates were fractionated *via* SDS-PAGE and STAT3 activation assessed *via* immunoblotting for pTyr⁷⁰⁵STAT3. Results are shown as mean values \pm SEM for cells pre-incubated with vehicle (solid line) or 10 μ M Fsk (dashed line) with blots representative for $n = 3$ separate experiments. * = $p < 0.05$ vs. vehicle, ** = $p < 0.01$ vs. vehicle

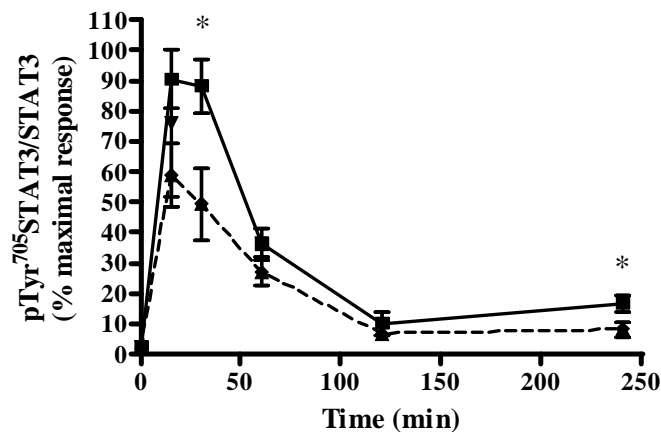
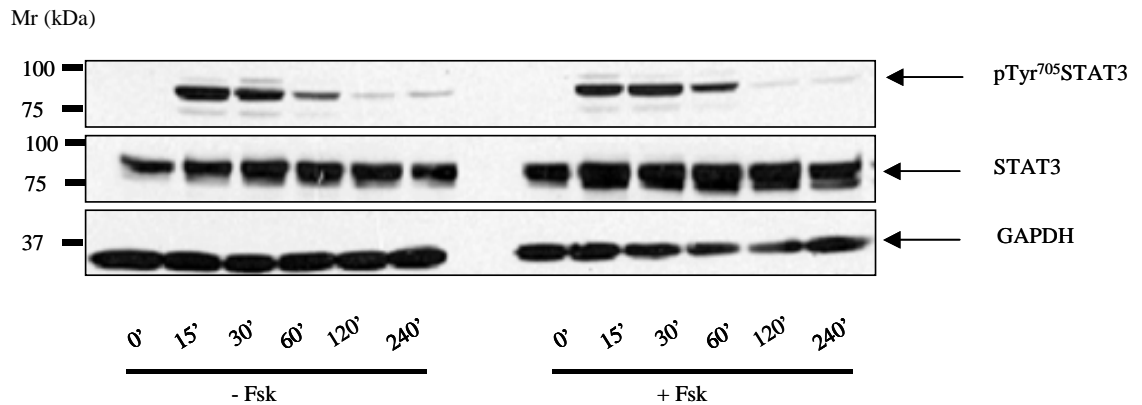


Fig. 7.3: Inhibition of IL-6-induced STAT3 activation in PZ-HPV-7 prostate epithelial cells

PZ-HPV-7 cells were seeded into 6-well plates and stimulated with either vehicle (0.1 % (v/v) EtOH) or 10 μ M Fsk for 5 h prior to stimulation with 10 ng/ml rhuIL-6 for 0–240 min. Cell lysates were fractionated *via* SDS-PAGE and STAT3 activation assessed *via* immunoblotting for pTyr⁷⁰⁵STAT3. Results are shown as mean values \pm SEM for cells pre-incubated with vehicle (solid line) or 10 μ M Fsk (dashed line) with blots representative for $n = 3$ separate experiments. * = $p < 0.05$ vs. vehicle-treated cells, ** = $p < 0.01$ vs. vehicle-treated cells

cells, ** = $p < 0.01$ vs. vehicle-treated cells), indicating that cAMP elevation can inhibit STAT3 activation. The ability of Fsk to inhibit IL-6-induced activation of STAT3 was not correlated with a change in total STAT3 protein levels in any of the cell types tested (Fig. 7.1 – Fig. 7.3), suggesting that degradation of activated STAT3 is not responsible for this phenomenon. The effect of cAMP elevation on IL-6-induced STAT3 phosphorylation was more subtle in PZ-HPV-7 cells in comparison to the tumour-derived cell lines, suggesting a potential mechanism by which to selectively inhibit tumour cell growth. Given previous observations in HUVECs, it is possible that the ability of Fsk to attenuate IL-6-induced activation of STAT3 in prostate epithelial cells is due to induction of SOCS3 expression.

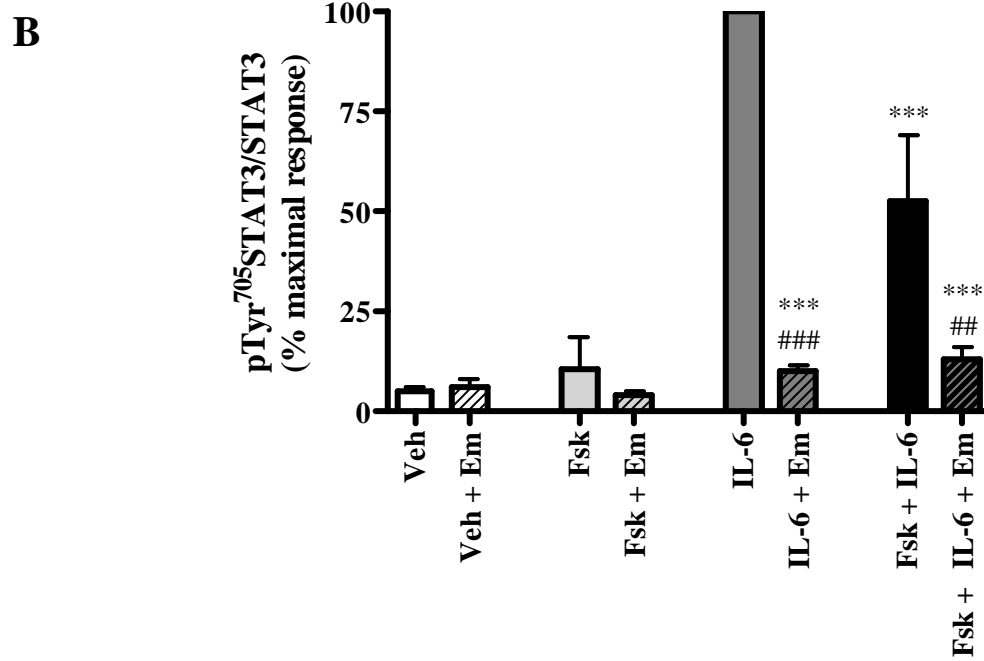
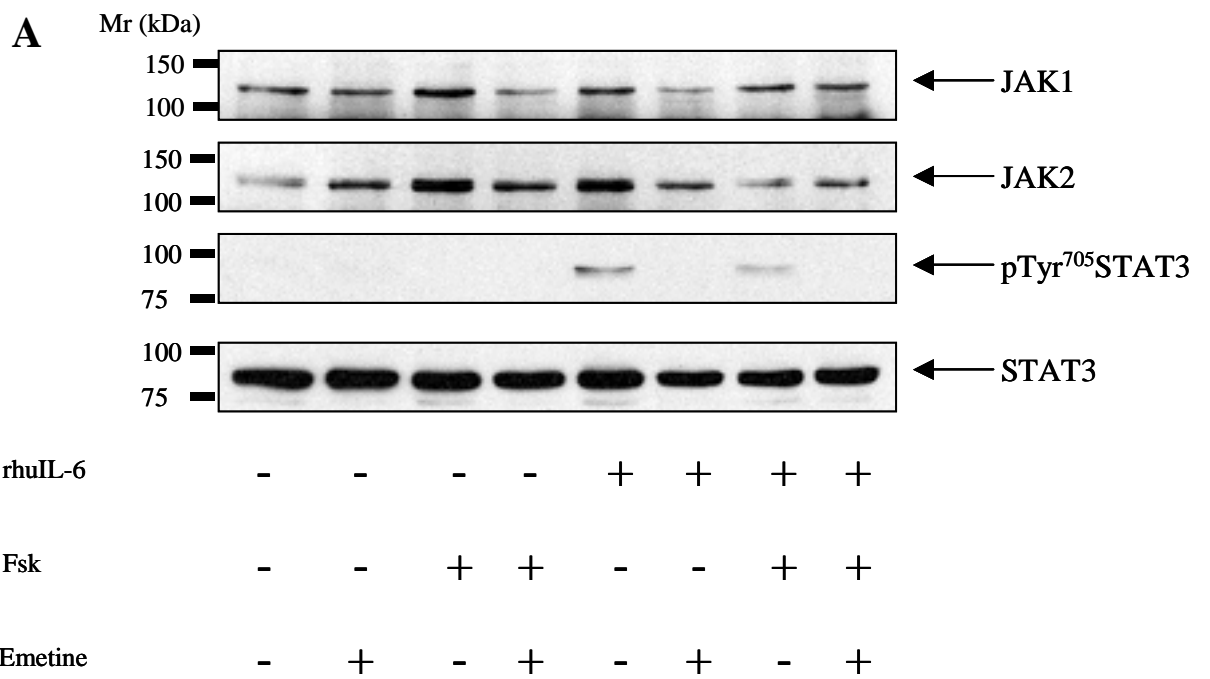
7.2.2 The role of *de novo* protein synthesis in Fsk-mediated attenuation of STAT3 activation

It was previously demonstrated that the ability of cAMP elevation to attenuate IL-6/sIL-6R α -mediated activation of STAT3 in HUVECs was associated with an increase in SOCS3 mRNA (Sands *et al.*, 2006), indicative of a requirement for *de novo* transcription and concomitant protein synthesis. In order to assess whether *de novo* protein synthesis was important in Fsk-mediated attenuation of STAT3 activation in prostate epithelial cells, DU145, LNCaP and PZ-HPV-7 cells were seeded as described previously and incubated with either vehicle (1 % (v/v) DMSO or 100 μ M emetine dihydrochloride, an inhibitor of protein translation (Grollman, 1968), for 2 h prior to incubation with either vehicle (0.1 % (v/v) EtOH) or 10 μ M Fsk for 5 h. Cells were then stimulated with 10 ng/ml rhuIL-6 for 15 min prior to determination of pTyr⁷⁰⁵STAT3 levels *via* immunoblotting.

In all three cell types, treatment with rhuIL-6 resulted in an increase in pTyr⁷⁰⁵STAT3, indicating activation of STAT3. In keeping with previous data, treatment with Fsk attenuated increases in pTyr⁷⁰⁵STAT3, supporting the hypothesis that cAMP elevation can inhibit STAT3 activation (Fig. 7.4 – Fig. 7.6, *** = $p < 0.001$ vs. IL-6, ### = $p < 0.001$ emetine vs. vehicle pre-treatment). Pre-incubation of prostate epithelial cells with 100 μ M emetine had no effect on basal levels of tyrosine phosphorylated STAT3 but inhibited IL-6-induced activation of STAT3 in both the presence and absence of Fsk (Fig. 7.4 – 7.6 *** = $p < 0.001$ vs. IL-6, # = $p < 0.05$ emetine vs. vehicle pre-treatment ## = $p < 0.01$ emetine vs. vehicle pre-treatment, ### = $p < 0.001$ emetine vs. vehicle pre-treatment). It was therefore not possible to assess whether *de novo* protein synthesis was required for the ability of Fsk to attenuate IL-6-induced increases in pTyr⁷⁰⁵STAT3.

To investigate the mechanisms responsible for emetine-mediated attenuation of STAT3 activation, the expression of JAK1 and JAK2 was determined. Of all the receptor-associated signalling components involved in IL-6/gp130 signalling, JAKs undergo the most rapid turnover (Siewert *et al.*, 1999). Thus it is likely that the effect of emetine on IL-6-induced STAT3 phosphorylation arises due to blockade of *de novo* JAK synthesis. As expected, in DU145 and PZ-HPV-7 cells, treatment with emetine resulted in a decrease in JAK1 expression in comparison to cells incubated with vehicle (Fig. 7.4 and Fig. 7.6 # = $p < 0.05$ emetine *vs.* vehicle pre-treatment ## = $p < 0.01$ emetine *vs.* vehicle pre-treatment, ### = $p < 0.001$ emetine *vs.* vehicle pre-treatment). The decrease in JAK1 expression in PZ-HPV-7 cells was statistically significant (Fig. 7.6 # = $p < 0.05$ emetine *vs.* vehicle pre-treatment ## = $p < 0.01$ emetine *vs.* vehicle pre-treatment, ### = $p < 0.001$ emetine *vs.* vehicle pre-treatment), indicating that emetine pre-treatment inhibits IL-6-mediated activation of STAT3 *via* decreasing JAK1 expression. In DU145 cells, a trend towards decreased JAK1 levels following pre-incubation with emetine was displayed but this was not found to be statistically significant. As JAK1 is constitutively associated with gp130, it is possible that, particularly in PZ-HPV-7 cells, JAK1 is the major JAK associated with STAT3 activation following IL-6/memIL-6R interaction. In contrast to DU145 and PZ-HPV-7 cells, LNCaP cells did not express JAK1 and thus expression of JAK2 in these cells was determined. Similar to results obtained in DU145 cells regarding JAK1 expression, treatment with 100 μ M emetine resulted in a trend towards decreased JAK2 expression in LNCaP cell but this was not statistically significant (Fig. 7.5, # = $p < 0.05$ emetine *vs.* vehicle incubation, ## = $p < 0.01$ emetine *vs.* vehicle incubation). Thus these results are only suggestive that decreases in JAK2 expression are responsible for the decrease in IL-6-mediated tyrosine phosphorylation of STAT3 in LNCaP cells.

The decrease in JAK expression in prostate epithelial cells treated with emetine is highly suggestive that emetine is efficacious in this system. However, in order to truly ascertain whether emetine was blocking *de novo* protein synthesis, LNCaP cells were pre-incubated with concentrations of emetine ranging from 0 – 1000 μ M for 2 h at 37°C, 5 % (v/v) CO₂. Cells were then incubated with ³H-Leu for 3 h at 37°C, 5 % (v/v) CO₂ and harvested as described in Chapter 5. Successful radioisotope incorporation was assessed *via* liquid scintillation counting of TCA-precipitated proteins. Treatment of LNCaP cells with emetine concentrations in excess of 1 μ M resulted in a concentration-dependent decrease in ³H-Leu incorporation, indicative of a decrease in *de novo* protein synthesis (Fig. 7.7). These results demonstrate that emetine is efficacious in this system and that 100 μ M is sufficient to block protein synthesis. Therefore, the effect of emetine on STAT3 activation



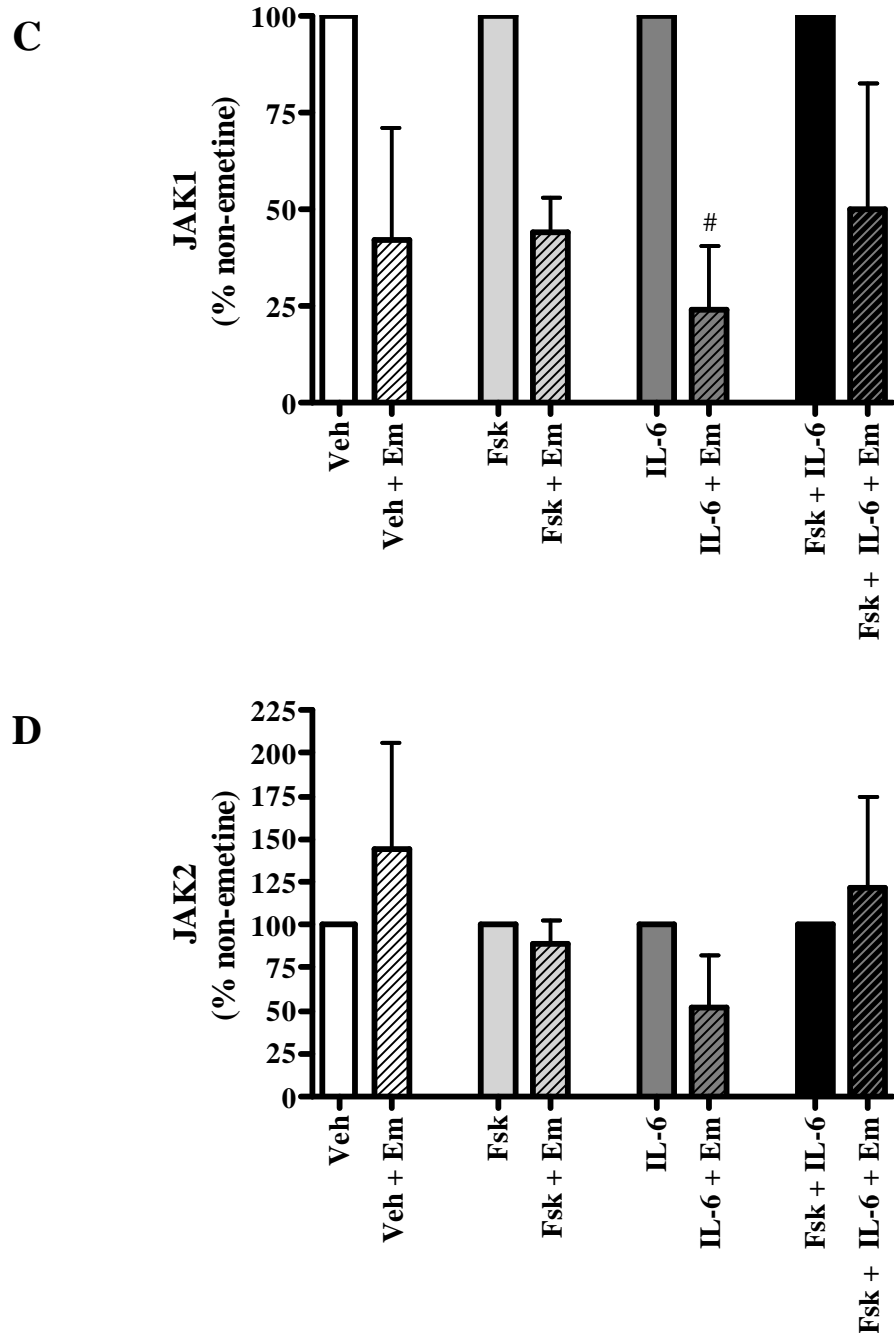
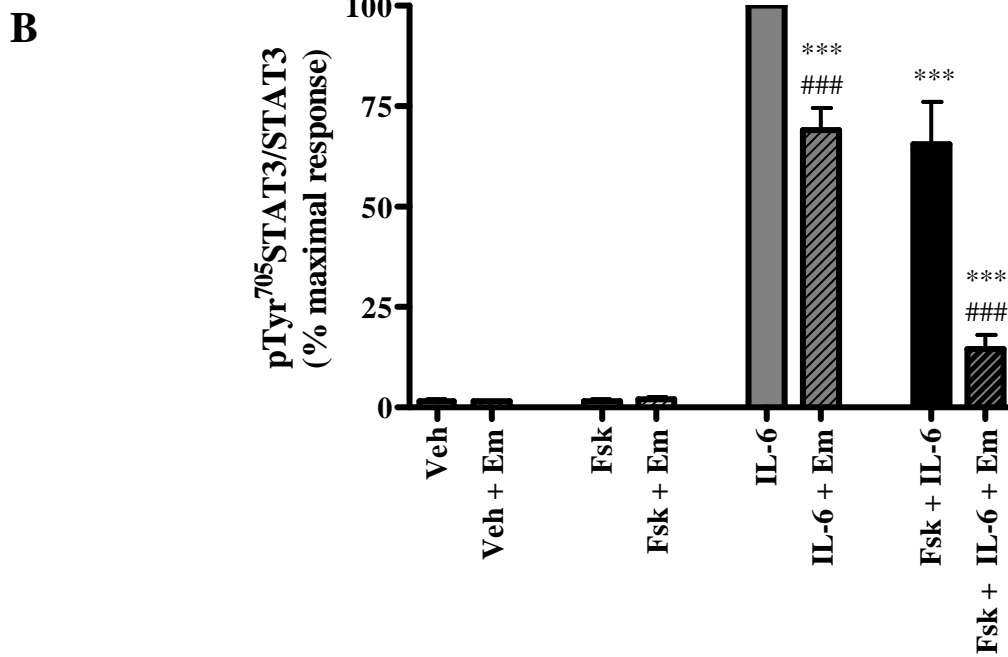
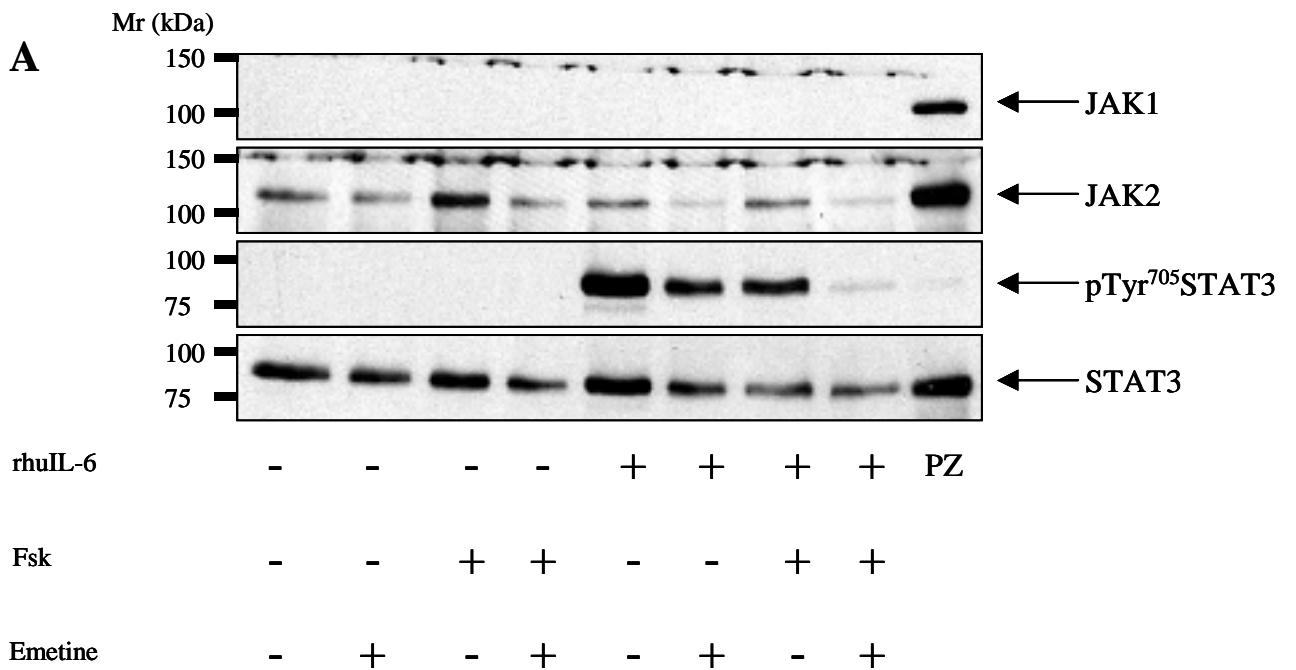


Fig. 7.4: Effect of emetine on Fsk-induced attenuation of STAT3 activation in DU145 cells

DU145 cells were seeded into 6-well tissue culture dishes and grown to 80 % confluence as previously described. Cells were then incubated with either vehicle (1 % (v/v) DMSO) or 100 μ M emetine (Em) for 2 h at 37°C, 5 % (v/v) CO₂ prior to incubation with either vehicle (0.1 % (v/v) EtOH) or 10 μ M Fsk for 5 h. LNCaP cells were then stimulated with 10 ng/ml rhuIL-6 for 15 min and effects on pTyr⁷⁰⁵STAT3 assessed *via* immunoblotting (panels A and B). Effects on JAK1 and JAK2 expression were also investigated (panels A, C and D). Results shown represent mean values \pm SEM for $n = 3$ separate experiments with blots representative of $n = 3$ experiments. *** = $p < 0.001$ vs. IL-6, # = $p < 0.05$ emetine vs. vehicle incubation #### = $p < 0.001$ emetine vs. vehicle incubation



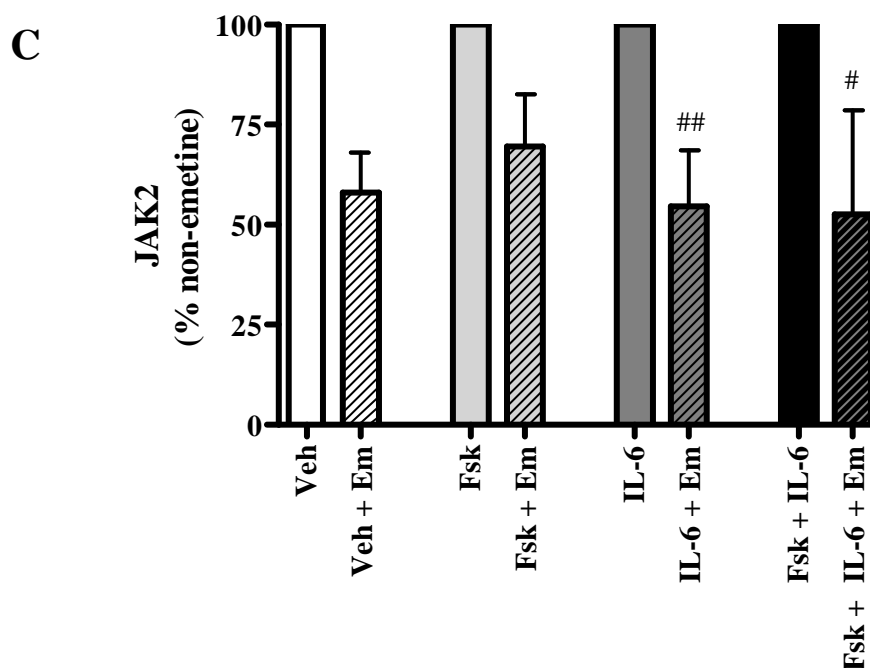
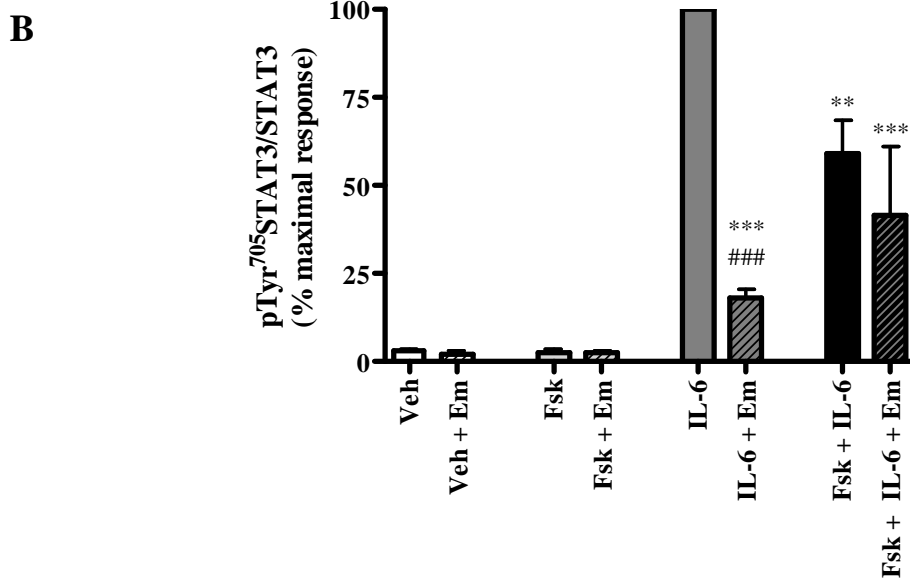
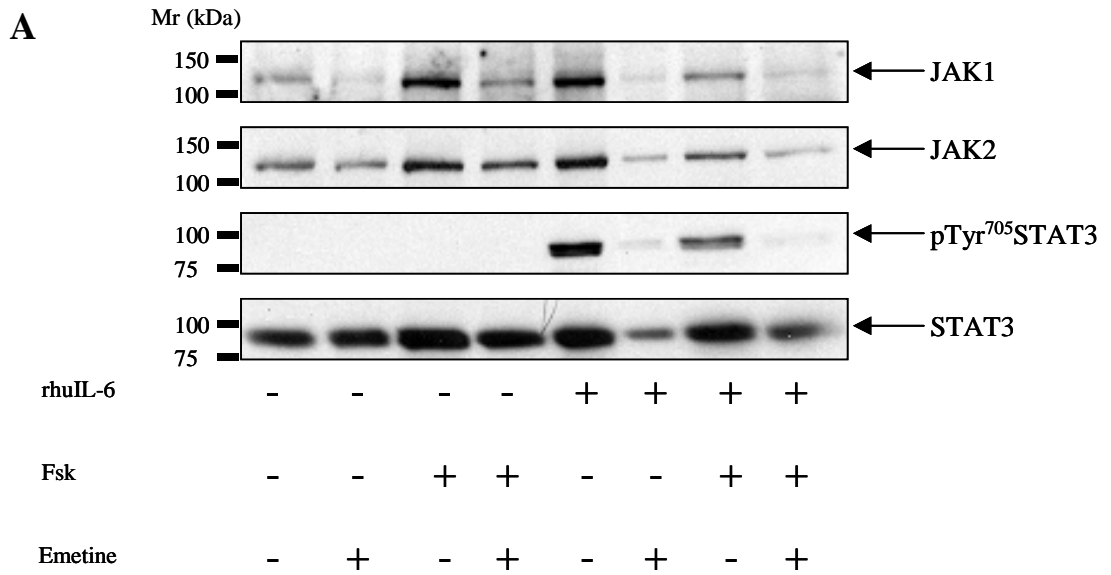


Fig. 7.5: Effect of emetine on Fsk-induced attenuation of STAT3 activation in LNCaP cells

LNCaP cells were seeded into 6-well tissue culture dishes and grown to 60–70% confluence as previously described. Cells were then incubated with either vehicle (1% (v/v) DMSO) or 100 μ M emetine (Em) for 2 h at 37°C, 5% (v/v) CO₂ prior to incubation with either vehicle (0.1% (v/v) EtOH) or 10 μ M Fsk for 5 h. LNCaP cells were then stimulated with 10 ng/ml rhuIL-6 for 15 min and effects on pTyr⁷⁰⁵STAT3 assessed *via* immunoblotting (panels A and B). Effects on JAK1 and JAK2 expression were also investigated (panels A and C) with PZ-HPV-7 cell lysate (PZ) included as a positive control for JAK1 antibody reactivity. Results shown represent mean values \pm SEM for $n = 3$ separate experiments with blots representative of $n = 3$ experiments. *** = $p < 0.001$ vs. IL-6, ### = $p < 0.001$ emetine vs. vehicle incubation



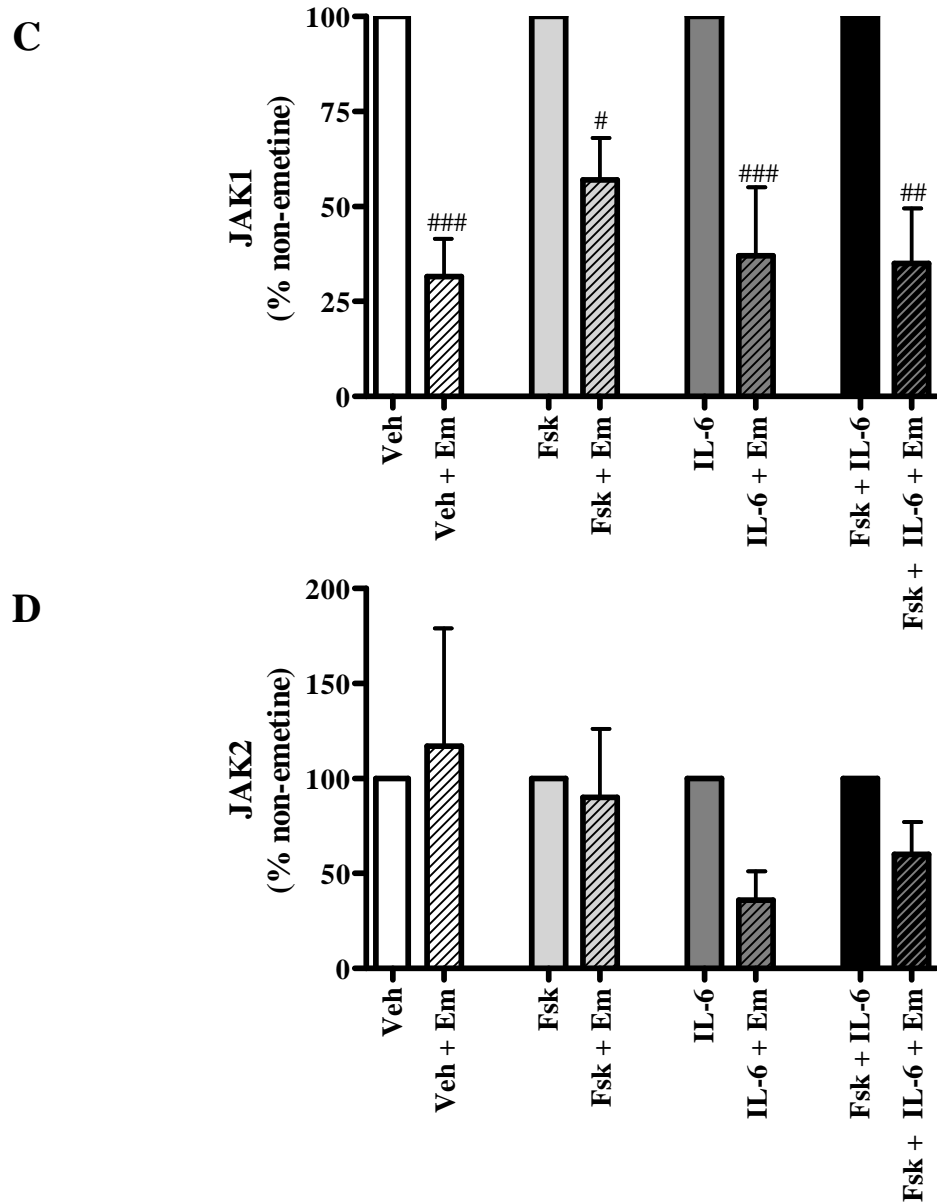


Fig. 7.6: Effect of emetine on Fsk-induced attenuation of STAT3 activation in PZ-HPV-7 cells

PZ-HPV-7 cells were seeded into 6-well tissue culture dishes and grown to 60 – 70 % confluence as previously described. Cells were then incubated with either vehicle (1 % (v/v) DMSO) or 100 μ M emetine (Em) for 2 h at 37°C, 5 % (v/v) CO₂ prior to incubation with either vehicle (0.1 % (v/v) EtOH) or 10 μ M Fsk for 5 h. PZ-HPV-7 cells were then stimulated with 10 ng/ml rhuIL-6 for 15 min and effects on pTyr⁷⁰⁵STAT3 assessed *via* immunoblotting (panels A and B). Effects on JAK1 and JAK2 expression were also investigated (panels A and C). Results shown represent mean values \pm SEM for $n = 3$ separate experiments with blots representative of $n = 3$ experiments. *** = $p < 0.001$ vs. IL-6, # = $p < 0.05$ emetine vs. vehicle incubation, ## = $p < 0.01$ emetine vs. vehicle incubation, ### = $p < 0.001$ emetine vs. vehicle incubation

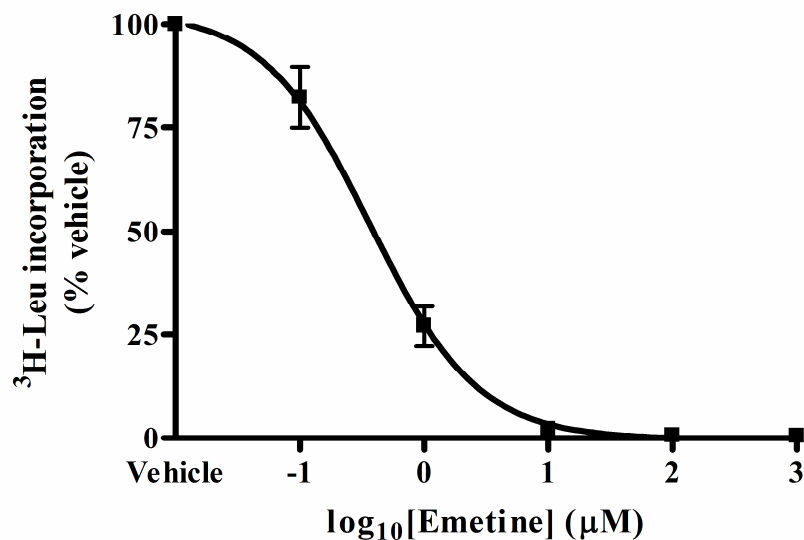


Fig. 7.7: Efficacy of emetine in LNCaP cells

LNCaP cells were seeded as described previously and incubated with 0 – 1000 μM emetine for 2 h at 37°C, 5 % (v/v) CO₂ prior to labelling of *de novo* synthesis peptides with 2 kBq/well ³H-Leu for 3 h at 37°C, 5 % (v/v) CO₂. Cells were harvested by washing in 5 % (w/v) TCA, followed by washing in ice-cold dH₂O. LNCaP cells were lysed into 1 M NaOH and radioisotope incorporation assessed *via* liquid scintillation counting. Results shown are mean values ± SEM for *n* = 2 separate experiments

in prostate epithelial cells is likely due to blockade of translation and, most notably, blockade of JAK synthesis.

7.2.3 Contribution of PKA and EPAC to Fsk-mediated attenuation of STAT3 activation

It has previously been demonstrated that the ability of cAMP elevation to attenuate IL-6/STAT3 signalling in HUVECs is mediated by EPAC-induced expression of SOCS3 (Sands *et al.*, 2006). To assess whether the ability of cAMP to attenuate STAT3 activation in prostate epithelial cells was PKA-dependent, DU145, LNCaP and PZ-HPV-7 cells were incubated with either vehicle (0.1 % (v/v) DMSO) or 10 nM of the PKA-selective inhibitor myrPKI₁₄₋₂₂ for 1 h prior to stimulation with either vehicle (0.1 % (v/v) EtOH) or 10 μ M Fsk for 5 h. In order to assess the role of EPAC in this phenomenon, cells were incubated in parallel with 200 μ M of the EPAC-selective agonist 8Me-pCPT-cAMP for 5 h (Rehmann *et al.*, 2003). Cells were then stimulated with either vehicle (0.1 % (v/v) PBS) or 10 ng/ml rhuIL-6 for 15 min to induce increases in pTyr⁷⁰⁵STAT3. In order to assess efficacy of myrPKI₁₄₋₂₂, cells were incubated in the presence of vehicle or the inhibitor as described above prior to stimulation with 10 μ M Fsk to induce an increase in pSer¹³³CREB as an indicator of PKA activation. The efficacy of 8Me-pCPT-cAMP was determined by incubating HUVECs with 200 μ M 8Me-pCPT-cAMP for 5 h in the presence of 6 μ M MG132 and subsequent immunoblotting for SOCS3 expression (Sands *et al.*, 2006).

In DU145 cells, treatment with rhuIL-6 resulted in increased levels of pTyr⁷⁰⁵STAT3 which was inhibited by pre-incubation with Fsk as determined in previous experiments (Fig. 7.8, ** = $p < 0.01$ vs. IL-6). Interestingly, treatment with myrPKI₁₄₋₂₂ alone also resulted in a significant decrease in IL-6-induced activation of STAT3 (Fig. 7.8, * = $p < 0.05$ vs. IL-6), suggesting that PKA function is required for optimal activation of STAT3 downstream of the IL-6R complex. Combined treatment with myrPKI₁₄₋₂₂ and Fsk resulted in an increase in IL-6-mediated Tyr⁷⁰⁵ phosphorylation of STAT3 but this was not found to be statistically significant. Thus, it is currently unclear whether PKA activation plays a significant role in Fsk-mediated attenuation of STAT3 activation in DU145 cells. In contrast, treatment with 200 μ M 8Me-pCPT-cAMP resulted in attenuation of STAT3 activation (Fig. 7.8, *** = $p < 0.001$ vs. IL-6), suggesting that EPAC activation is important in this phenomenon. The EPAC-selective agonist was shown to be efficacious as expression of SOCS3 in HUVECs, an EPAC-mediated event (Sands *et al.*, 2006), was detected.

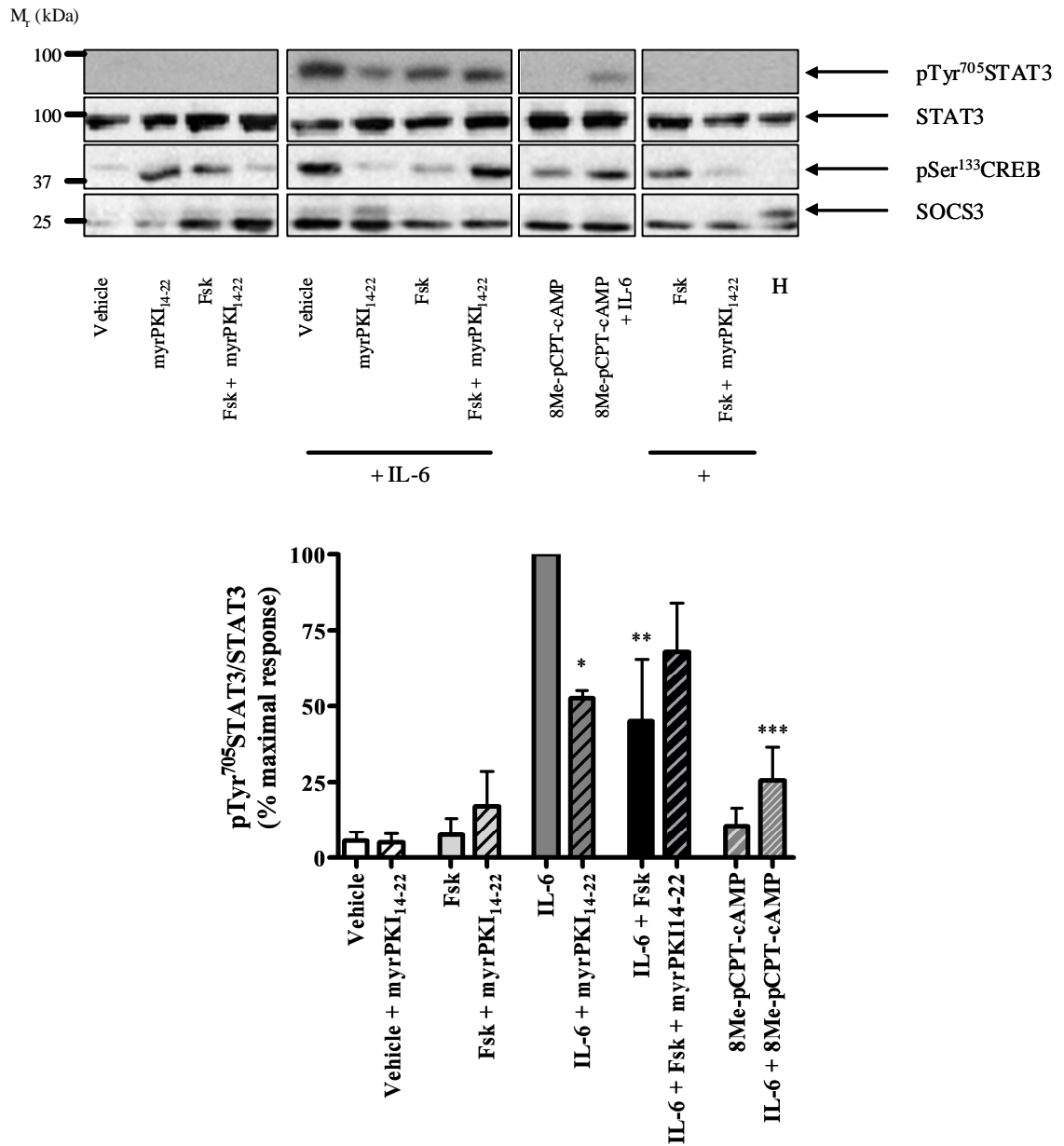


Fig. 7.8: The contribution of PKA and EPAC to Fsk-mediated attenuation of STAT3 activation in DU145 cells

DU145 cells were seeded as previously described and incubated with either vehicle (0.1 % (v/v) DMSO) or 10 nM myrPKI₁₄₋₂₂ for 1 h prior to incubation with vehicle (0.1 % (v/v) EtOH) or 10 μ M Fsk for 5 h. Cells were incubated in the presence of 100 μ M 8Me-pCPT-cAMP for 5 h to induce activation of EPAC. Treatment with 10 ng/ml rhuIL-6 was used to induce increases in pTyr⁷⁰⁵STAT3. Efficacy of myrPKI₁₄₋₂₂ was assessed *via* 15 min incubation with 10 μ M Fsk to induce increases in pSer¹³³CREB (indicated by +) whilst HUVECs incubated for 5 h with 100 μ M 8Me-pCPT-cAMP and 6 μ M MG132 (H) to induce SOCS3 expression served as a positive control for 8Me-pCPT-cAMP efficacy. Results and blots shown are representative of $n = 3$ separate experiments with values displayed as mean \pm SEM. * = $p < 0.05$ vs. IL-6, ** = $p < 0.01$ vs. IL-6, *** = $p < 0.001$ vs. IL-6

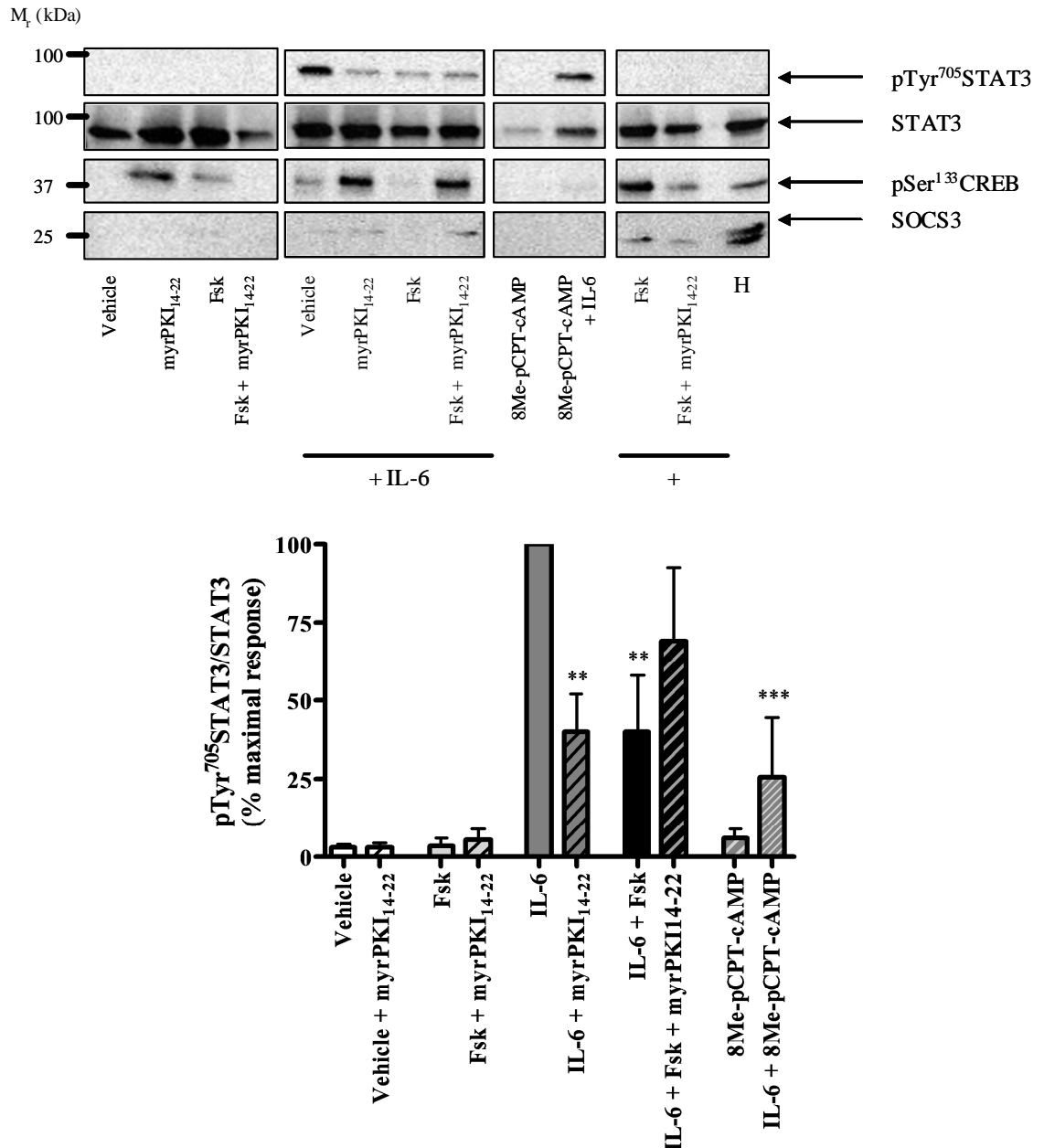


Fig. 7.9: The contribution of PKA and EPAC to Fsk-mediated attenuation of STAT3 activation in LNCaP cells

LNCaP cells were seeded as previously described and incubated with either vehicle (0.1 % (v/v) DMSO) or 10 nM myrPKI₁₄₋₂₂ for 1 h prior to incubation with vehicle (0.1 % (v/v) EtOH) or 10 μ M Fsk for 5 h. Cells were incubated in the presence of 100 μ M 8Me-pCPT-cAMP for 5 h to induce activation of EPAC. Treatment with 10 ng/ml rhuIL-6 was used to induce increases in pTyr⁷⁰⁵STAT3. Efficacy of myrPKI₁₄₋₂₂ was assessed *via* 15 min incubation with 10 μ M Fsk to induce increases in pSer¹³³CREB (indicated by $\bar{\quad}$ +) whilst HUVECs incubated for 5 h with 100 μ M 8Me-pCPT-cAMP and 6 μ M MG132 (H) to induce SOCS3 expression served as a positive control for 8Me-pCPT-cAMP efficacy. Results and blots shown are representative of $n = 3$ separate experiments with values displayed as mean \pm SEM. ** = $p < 0.01$ vs. IL-6, *** = $p < 0.001$ vs. IL-6

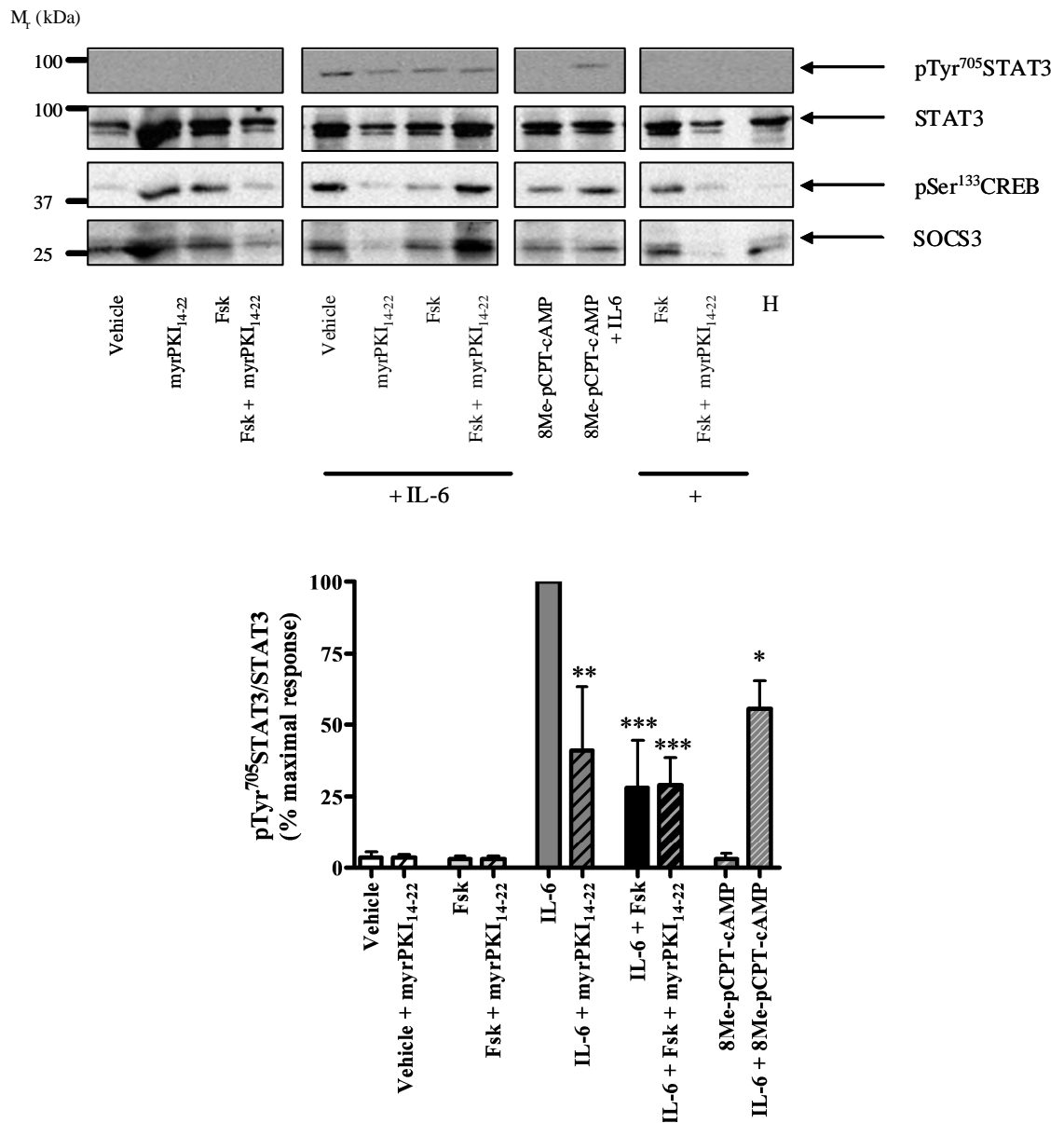


Fig. 7.10: The contribution of PKA and EPAC to Fsk-mediated attenuation of STAT3 activation in PZ-HPV-7 cells

PZ-HPV-7 cells were seeded as previously described and incubated with either vehicle (0.1 % (v/v) DMSO) or 10 nM myrPKI₁₄₋₂₂ for 1 h prior to incubation with vehicle (0.1 % (v/v) EtOH) or 10 μ M Fsk for 5 h. Cells were incubated in the presence of 100 μ M 8Me-pCPT-cAMP for 5 h to induce activation of EPAC. Treatment with 10 ng/ml rhuIL-6 was used to induce increases in pTyr⁷⁰⁵STAT3. Efficacy of myrPKI₁₄₋₂₂ was assessed *via* 15 min incubation with 10 μ M Fsk to induce increases in pSer¹³³CREB (indicated by $\overline{\quad}$ +) whilst HUVECs incubated for 5 h with 100 μ M 8Me-pCPT-cAMP and 6 μ M MG132 (H) to induce SOCS3 expression served as a positive control for 8Me-pCPT-cAMP efficacy. Results shown are representative of $n = 3$ separate experiments with values displayed as mean \pm SEM. * = $p < 0.05$ vs. IL-6, ** = $p < 0.01$ vs. IL-6, *** = $p < 0.001$ vs. IL-6

In LNCaP cells, similar results were obtained where treatment with Fsk resulting in attenuation of IL-6-induced STAT3 activation (Fig. 7.9, $** = p < 0.01$ vs. IL-6). This effect could be mimicked by incubation with myrPKI₁₄₋₂₂, suggesting a role for PKA in STAT3 activation in these cells (Fig. 7.9, $** = p < 0.01$ vs. IL-6). Furthermore, combined treatment with Fsk and myrPKI₁₄₋₂₂ resulted in an increase in IL-6-induced tyrosine phosphorylation of STAT3, although this was not statistically significant, as also observed in DU145 cells. Incubation with 8Me-pCPT-cAMP partially recapitulated the effect of Fsk treatment (Fig. 7.9, $*** = p < 0.001$ vs. IL-6), again suggesting that the ability of cAMP elevation to inhibit IL-6-mediated activation of STAT3 requires EPAC activation. These results were also repeated in PZ-HPV-7 cells (Fig. 7.10, $* = p < 0.05$ vs. IL-6, $** = p < 0.01$ vs. IL-6, $*** = p < 0.001$ vs. IL-6), indicating that there is no difference between the different PCa cell lines regarding the role of PKA and EPAC in cAMP-mediated attenuation of STAT3 activation.

7.2.4 Fsk-mediated decreases in IL-6-induced STAT3 activation correlate with increases in SOCS3

In previous studies, the ability of cAMP elevation to attenuate STAT3 activation has been shown to be mediated by induction of SOCS3 expression (Sands *et al.*, 2006). To assess whether this was the case in prostate epithelial cells, cells were incubated for 5 h at 37°C with either vehicle (0.1 % (v/v) EtOH) or 10 µM Fsk in the presence or absence of 6 µM of the proteasome inhibitor MG132. MG132 was included as SOCS3 can be polyubiquitinated on Lys⁶ and targeted for degradation (Sasaki *et al.*, 2003). Thus blockade of the proteasome should enable accumulation of SOCS3 protein and detection of changes in protein expression *via* immunoblotting. Following incubation with Fsk and/or MG132, prostate epithelial cells were stimulated with 10 ng/ml rhuIL-6 for 15 min prior to assessment of pTyr⁷⁰⁵STAT3 levels *via* immunoblotting.

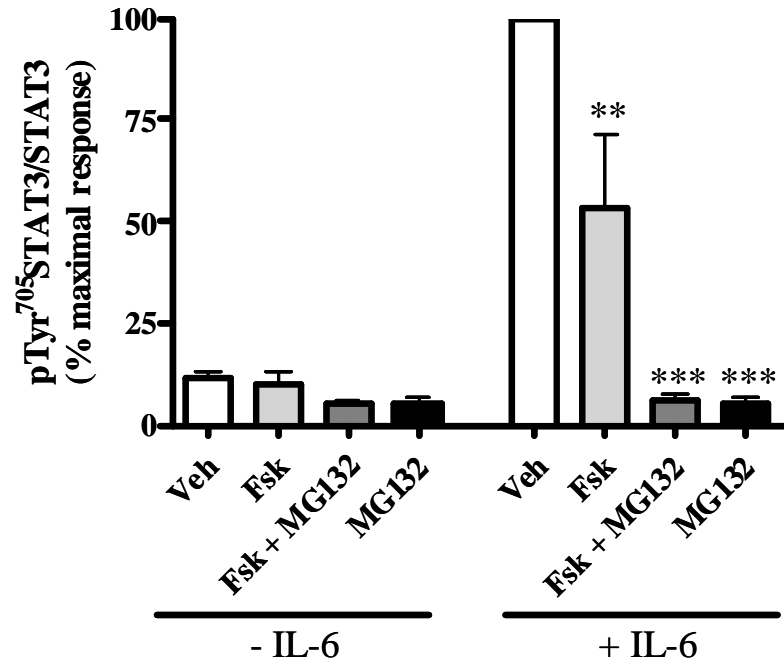
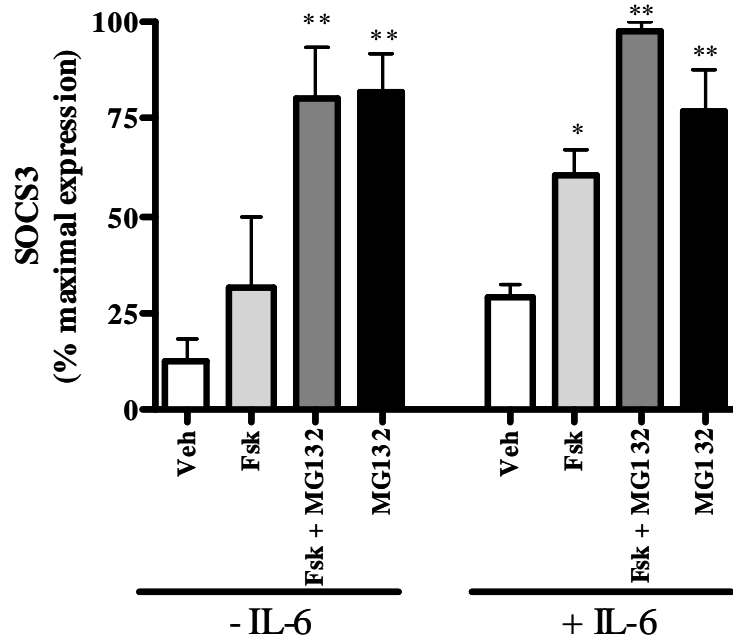
Treatment of prostate epithelial cells with either Fsk, MG132 or a combination Fsk and MG132 did not alter basal levels of pTyr⁷⁰⁵STAT3 in any of the cell lines tested, indicating that any effects on STAT3 activation are due to effects on IL-6 signalling and not non-selective effects.

In DU145 cells, treatment with Fsk alone resulted in a decrease in IL-6-induced increases in pTyr⁷⁰⁵STAT3 (Fig. 7.11, panels A and B, $** = p < 0.01$ vs. IL-6) which was enhanced in the presence of MG132 (Fig. 7.11, panels A and B, $*** = p < 0.001$ vs. IL-6). Interestingly, treatment with MG132 alone also significantly attenuated activation of

STAT3 in response to exogenous rhuIL-6 (Fig. 7.11, panels A and B, *** = $p < 0.001$ vs. IL-6). The degree to which STAT3 activation was inhibited in DU145 cells following treatment with Fsk and/or MG132 was associated with an increase in detected levels of SOCS3 protein. Treatment with Fsk alone resulted in an increase in detected SOCS3 in the presence and absence of rhuIL-6 which was enhanced when cells were co-incubated with MG132 (Fig. 7.11, panels A and C, * = $p < 0.05$ vs. IL-6, *** = $p < 0.001$ vs. vehicle). Interestingly, pre-treatment with MG132 alone resulted in a similar increase in SOCS3 levels as that seen following co-incubation with Fsk and MG132 (Fig. 7.11, panels A and C, * = $p < 0.05$ vs. IL-6, *** = $p < 0.001$ vs. vehicle). These results suggest that the ability of Fsk and MG132 to attenuate STAT3 activation in DU145 cells may be due to a combined stabilisation of endogenous SOCS3 and promotion of *de novo* synthesis arising from cAMP elevation.

Treatment of LNCaP cells with rhuIL-6 induced a robust increase in pTyr⁷⁰⁵STAT3 which was attenuated following MG132 or combined Fsk and MG132 pre-treatment (Fig. 7.12, ** = $p < 0.01$ vs. vehicle). Treatment with Fsk alone showed a tendency to decrease IL-6-induced pTyr⁷⁰⁵STAT3 but this was not found to be statistically significant, suggesting that MG132 is potentiating this effect. Of particular interest is the observation that no SOCS3 expression can be detected in LNCaP cells, even after combined Fsk and MG132 treatment which was able to induce SOCS3 expression in HUVECs (Fig. 7.12). These results suggest that the ability of Fsk and MG132 to attenuate STAT3 activation in LNCaP cells is not mediated *via* induction of SOCS3 and that another pathway is required for this phenomenon.

In PZ-HPV-7 cells, similar results were obtained, whereby treatment with Fsk resulted in a decrease in IL-6-mediated pTyr⁷⁰⁵STAT3 which was enhanced in the presence of MG132 (Fig. 7.13, panels A and B, *** = $p < 0.001$ vs. vehicle). Comparable to results obtained in DU145 cells, treatment of PZ-HPV-7 cells with MG132 alone resulted in a decrease in STAT3 activation (Fig. 7.13, panels A and B, *** = $p < 0.001$ vs. vehicle). Treatment of PZ-HPV-7 cells with Fsk alone did not result in a detectable increase in SOCS3 expression, however combined treatment of PZ-HPV-7 cells with Fsk and MG132 resulted in a significant increase in detected SOCS3 levels (Fig. 7.13, panels A and C, *** = $p < 0.001$ vs. vehicle). Incubation of PZ-HPV-7 cells with MG132 alone did not result in a significant increase in SOCS3 levels, suggesting that Fsk treatment is required for this phenomenon. These results support the hypothesis that cAMP elevation induces SOCS3 expression in PZ-HPV-7 cells.

B**C**

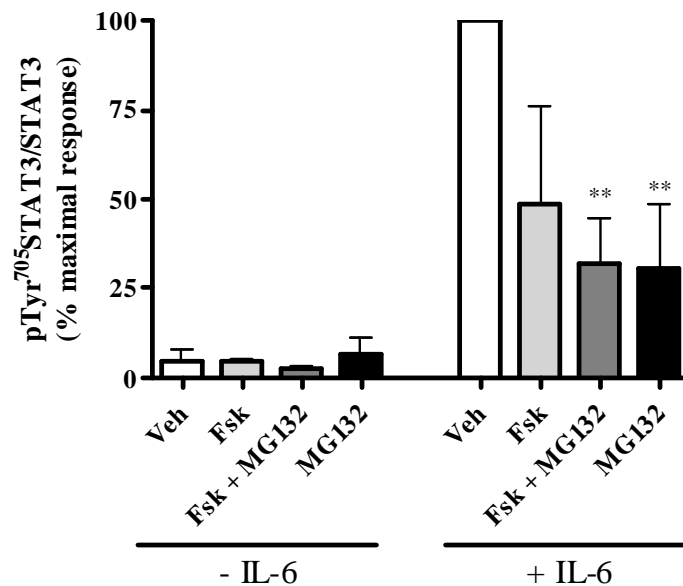
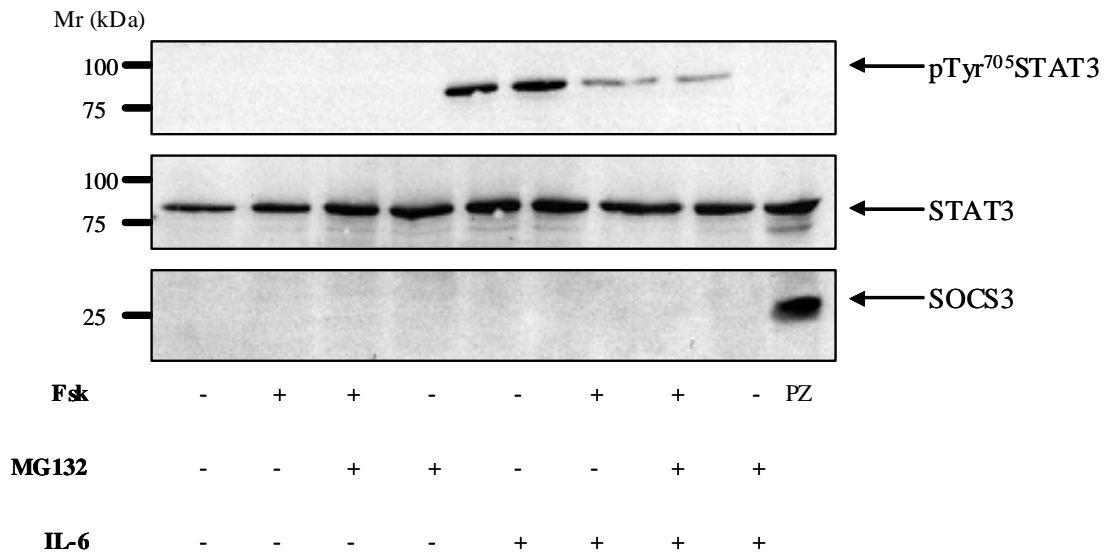


Fig. 7.12: Fsk-mediated attenuation of STAT3 activation in LNCaP cells is not correlated with an accumulation of SOCS3 protein

LNCaP cells were seeded as previously described and incubated with either vehicle (0.1 % (v/v) EtOH) or 10 μ M Fsk for 5 h in the presence or absence of 6 μ M of the proteasomal inhibitor MG132. Cells were stimulated with 10 ng/ml rhuIL-6 for 15 min to induce activation of STAT3. Following SDS-PAGE fractionation, the effect of Fsk and MG132 on detected levels of pTyr⁷⁰⁵STAT3 and SOCS3 was assessed *via* immunoblotting. PZ-HPV-7 cells incubated with 10 μ M Fsk and 6 μ M MG132 (PZ) for 5 h were included as a positive control for SOCS3 antibody reactivity. Results shown are representative of $n = 3$ experiments with values corresponding to mean values \pm SEM. * = $p < 0.05$ vs. IL-6, ** = $p < 0.01$ vs. IL-6 and *** = $p < 0.001$ vs. IL-6

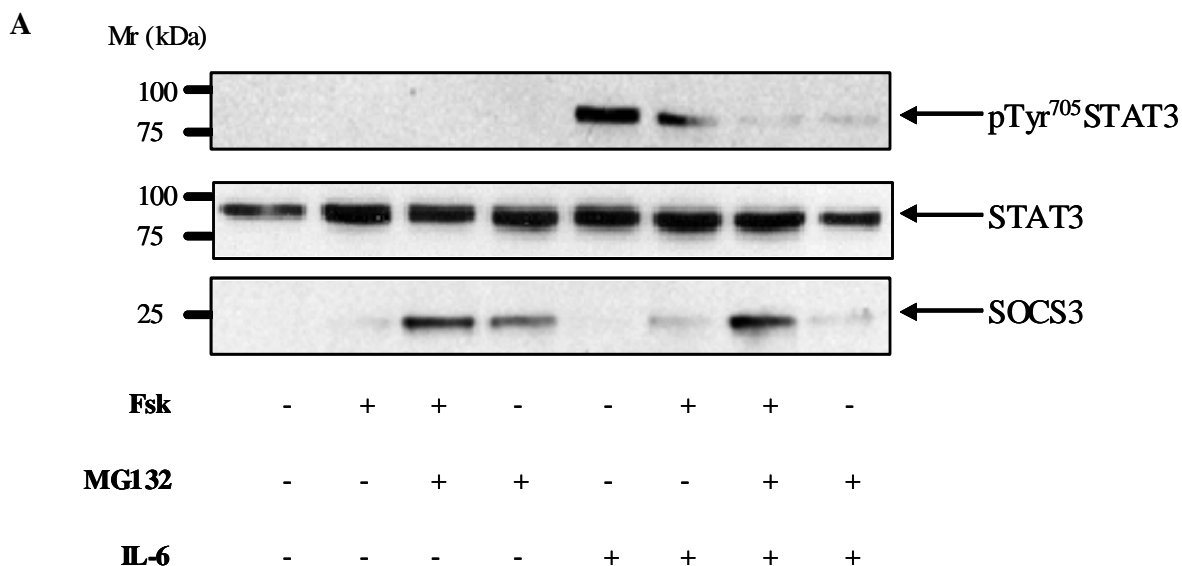
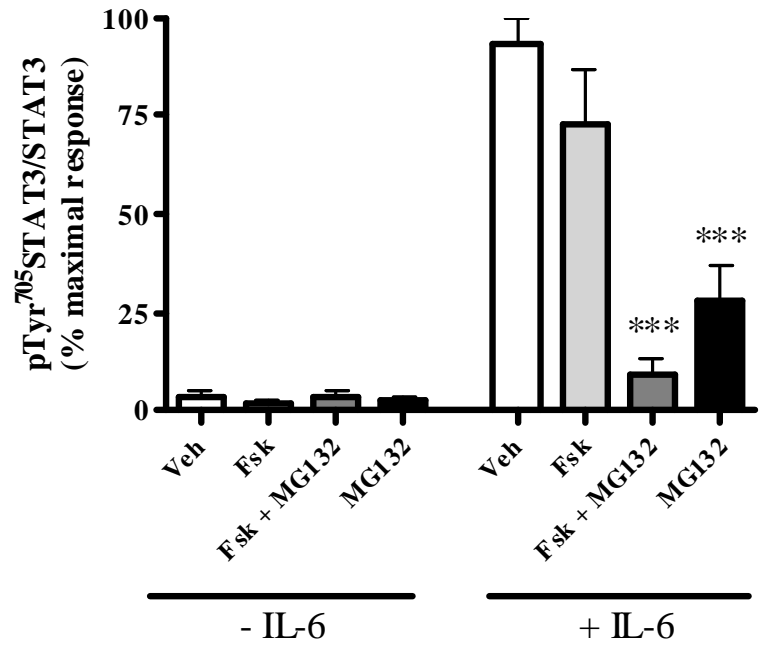
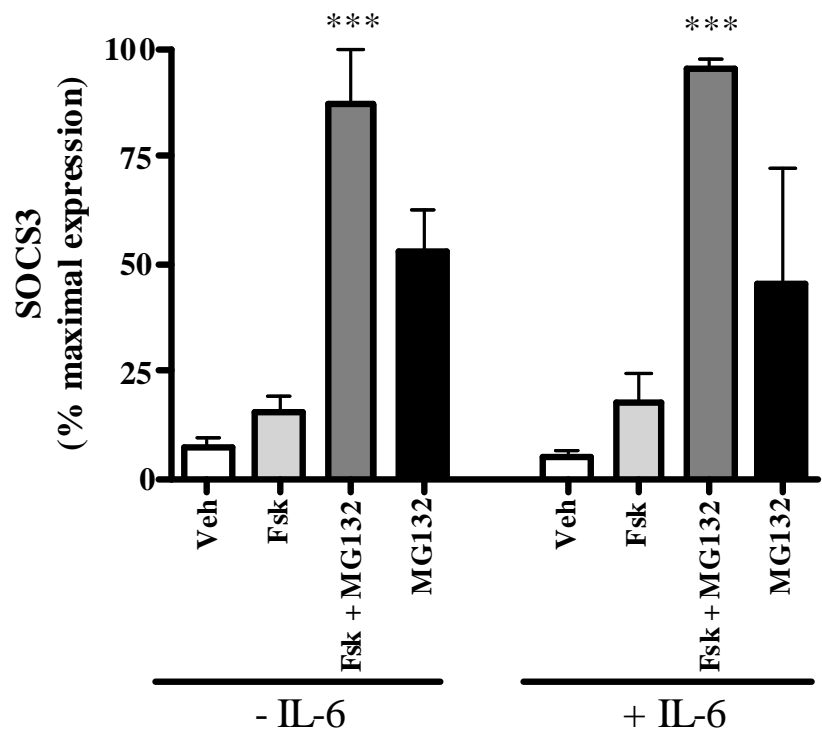


Fig. 7.13: Fsk-mediated attenuation of STAT3 activation in PZ-HPV-7 cells is correlated with an accumulation of SOCS3 protein

PZ-HPV-7 cells were seeded as previously described and incubated with either vehicle (0.1 % (v/v) EtOH) or 10 μ M Fsk for 5 h in the presence or absence of 6 μ M of the proteasomal inhibitor MG132. Cells were stimulated with 10 ng/ml rhuIL-6 for 15 min to induce activation of STAT3. Following SDS-PAGE fractionation, the effect of Fsk and MG132 on detected levels of pTyr⁷⁰⁵STAT3 (panel A and B) and SOCS3 (panel A and C) was assessed *via* immunoblotting. Results shown are representative of $n = 3$ experiments with values corresponding to mean values \pm SEM. *** = $p < 0.001$ vs. IL-6 (panel B) or vehicle (panel C)

B**C**

7.3 Discussion

The ability of cAMP to modulate cytokine signalling has been described in a number of systems. It has previously been demonstrated that cAMP elevation can attenuate inflammatory cytokine signalling in HUVECs, COS1 cells and MEFs *via* induction of SOCS3, an endogenous inhibitor of STAT signalling (Borland *et al.*, 2009; Sands *et al.*, 2006). However, this phenomenon is not restricted to vascular endothelial cells although the mechanism of SOCS3 induction may differ between cell types. The IL-6 family member LIF plays an important role in signalling in the hypothalamo-pituitary-adrenal (HPA) axis with sustained LIF signalling being correlated with excessive glucocorticoid expression and subsequent immunosuppression which can promote tumour progression (Bousquet *et al.*, 2001). Treatment of the AtT20 pituitary adenoma cell line with cAMP-elevating agonists or cAMP analogues additively increased LIF-induced *socs3* mRNA levels. Unlike HUVECs in which SOCS3 expression following elevation of intracellular cAMP requires EPAC (Sands *et al.*, 2006), cAMP-mediated induction of SOCS3 in AtT20 cells occurred *via* a mechanism which required PKA activation (Bousquet *et al.*, 2001). In 3T3-L1 adipocytes, treatment with isoproterenol promoted increases in *socs3* mRNA *via* a pathway dependent on β -adrenergic receptor and subsequent AC activation (Fasshauer *et al.*, 2002). Such studies support the hypothesis that cAMP elevation is an important mechanism by which to induce SOCS3 expression and so inhibit specific cytokine receptor signalling.

In all three cell lines used in this study, it was found that Fsk-mediated elevation of intracellular cAMP resulted in inhibition of IL-6 mediated activation of STAT3. These results are consistent with previous data identifying cAMP-elevating agents or analogues as important regulators of inflammatory signalling. Increases in levels of SOCS3 protein in DU145 and PZ-HPV-7 cells were correlated with a decrease in pTyr⁷⁰⁵STAT3, suggesting that SOCS3 accumulation was responsible for the ability of Fsk and MG132 to attenuate IL-6-mediated activation of STAT3. However, it must be noted, that whilst these results strongly suggest that SOCS3 is responsible for the cAMP-mediated attenuation of STAT3 activation, they do not demonstrate that SOCS3 is responsible for this phenomenon. Selective knockdown of SOCS3 expression *via* selective siRNA or construction of stable shRNA-expressing cell lines would enable the essential role of SOCS3 in this phenomenon to be demonstrated. Preliminary attempts to knockdown SOCS3 expression in the prostate epithelial cell lines have been unsuccessful due to cell death and lack of specific knockdown (data not shown). It is possible that transfection of these cells with a plasmid

encoding a suitable shRNA may be a suitable alternative strategy if future siRNA attempts were ineffective (see section 11.2).

Whilst cAMP-induced attenuation of IL-6-mediated STAT3 activation was correlated with increases in SOCS3 expression in both DU145 and PZ-HPV-7 cells, no detectable levels of SOCS3 expression could be observed in LNCaP cells. Due to the important role of STAT3 activation in various malignancies (Hodge *et al.*, 2005), it might be expected that endogenous inhibitors of STAT3 might be inactivated in tumour-derived cell lines in order to promote tumour growth and disease progression. Indeed, hypermethylation of the SOCS1 promoter has been shown to prevent SOCS1 expression in HCC (Miyoshi *et al.*, 2004). Similarly, hypermethylation of both the SOCS1 and SOCS3 promoters has been described in head and neck carcinoma and introduction of wild-type SOCS3 into cancer cells is correlated with an increase in cellular apoptosis and inhibition of cell growth (Weber *et al.*, 2005). It is possible that the SOCS3 promoter is hypermethylated in LNCaP cells and that treatment with demethylating agents such as 5'-aza-2'-deoxycytidine may restore SOCS3 expression (Wilson & Jones, 1983).

Interestingly, it is apparent that the conditions in which LNCaP cells are cultured may play a role in SOCS3 expression. In LNCaP cells cultured in the absence of IL-6 in the culture medium (LNCaP-IL-6⁻), no basal detection of SOCS3 expression could be detected (Bellezza *et al.*, 2006). However, establishment of the IL-6 refractory cell line, LNCaP-IL-6⁺ resulted in detectable levels of basal SOCS3 mRNA and protein, although the SOCS3/GAPDH ratio varied greatly between individual experiments (Bellezza *et al.*, 2006). The LNCaP-IL-6⁺ cell line is generated *via* culture of LNCaP cells for ≥ 20 passages in the presence of 5 ng/ml rhuIL-6. In LNCaP cells not cultured in the presence of IL-6 the cytokine inhibits cell growth at this concentration (Hobisch *et al.*, 2001). However, LNCaP-IL-6⁺ cells display higher basal proliferation rates than LNCaP-IL-6⁻ cells and decreased binding of IL-6, which may promote resistant to the growth inhibitory effects of IL-6 in LNCaP-IL-6⁻ cells (Hobisch *et al.*, 2001). Of particular note in the study by Bellezza *et al.* (2001) is the observation that treatment with rhuIL-6 did not lead to increases in SOCS3 expression in either LNCaP-IL-6⁻ or LNCaP-IL-6⁺ cells. As IL-6/STAT3-induced SOCS3 expression is well established as a classical negative-feedback loop for STAT3 inactivation (Starr *et al.*, 1997), these results suggest that LNCaP cells may display general defects regarding induction of SOCS3. In LNCaP-IL-6⁺ cells, treatment with rhuIL-6 did not result in an increase in SOCS3 expression above that seen basally whilst in the LNCaP-IL-6⁻ cell line, no basal or IL-6-induced SOCS3 expression was noted

(Bellezza *et al.*, 2006). The inability of a classical inducer of SOCS3 expression to promote an increase in protein expression in the LNCaP-IL-6⁻ cells supports the observation in the current study that cAMP elevation, potentially another common inducer of SOCS3 expression (Barclay *et al.*, 2007; Borland *et al.*, 2009; Bousquet *et al.*, 2001; Fasshauer *et al.*, 2002; Sands *et al.*, 2006; Yarwood *et al.*, 2008), failed to induce SOCS3 and supports the hypothesis that induction of SOCS3 expression is defective in these cells.

It might be argued that, as SOCS3 expression can be induced following long-term treatment with rhuIL-6, the inability of cAMP elevation to induce increases in SOCS3 expression in LNCaP cells is due to defects in cAMP-responsive elements in the SOCS3 promoter of these cells. However, it has been demonstrated that treatment of LNCaP-IL-6⁺ cells with dibutryl-cAMP resulted in a concentration-dependent increase in detected levels of SOCS3 protein (Bellezza *et al.*, 2006), indicative that promoter sequences responsive to cAMP-regulated transcription factors are functional in these cells. However, dibutryl-cAMP-induced increases in SOCS3 expression in LNCaP-IL-6⁺ cells were analysed at 48 h and 72 h post-stimulation with the cAMP analogue (Bellezza *et al.*, 2006) as opposed to the 5 h post-stimulation used in the current study. Whilst expression of SOCS3 could be detected in DU145 and PZ-HPV-7 cells at this time point, signalling differences between the three cell types used might potentially result in temporal variations in cAMP-induced SOCS3 expression. It is to be noted that the ability of dibutryl-cAMP to induce SOCS3 expression was only investigated in LNCaP-IL-6⁺ cells and not in LNCaP-IL-6⁻ or wild-type LNCaP cells (Bellezza *et al.*, 2006). It is possible that prolonged exposure of LNCaP cells to IL-6 might result in alterations of the SOCS3 promoter rendering it more receptive to cAMP-mediated activation. Interestingly, chronic IL-6 signalling has been implicated in systemic lupus erythematosus as a mediator of promoter hypomethylation *via* inhibition of DNA methyltransferase expression (Garaud *et al.*, 2009). It is thus possible that chronic exposure of LNCaP cells to IL-6 during the production of the LNCaP-IL-6⁺ cells may have altered the methylation status of the SOCS3 promoter and subsequently rendered it sensitive to cAMP elevation as observed by Bellezza *et al* (2001).

It is currently unclear as to the mechanism by which cAMP elevation inhibits IL-6-mediated activation of STAT3 in LNCaP cells. Published data predominantly ascribes cAMP-mediated attenuation of cytokine signalling to induction of SOCS3 expression (Borland *et al.*, 2009; Sands *et al.*, 2006; Yarwood *et al.*, 2008). It is possible that another SOCS family member is responsible for this phenomenon in LNCaP cells. SOCS1

expression has been described in a number of PCa cell lines including parental LNCaP cells obtained from the American Type Culture Collection as used in this study. Furthermore, unlike SOCS3 expression, treatment of LNCaP-IL-6⁻ cells with rhuIL-6 results in an increase in detected SOCS1 protein and is associated with growth inhibition of these cells (Neuwirt *et al.*, 2009). Although the authors did not investigate the effect of SOCS1 expression on IL-6-mediated activation of STAT3, it has previously been demonstrated that over-expression of SOCS1 can inhibit STAT3 activation downstream of gp130 (Schmitz *et al.*, 2000). Thus, it is possible that SOCS1 rather than SOCS3 mediates the inhibitory effect of cAMP elevation on IL-6-mediated STAT3 activation in LNCaP cells.

An interesting result from this experiment was the observation that treatment of all three prostate epithelial cell lines with the PKA-selective inhibitor myrPKI₁₄₋₂₂ resulted in a decrease in IL-6-induced activation of STAT3 in the absence of cAMP elevation. This was unexpected as cAMP elevation induces SOCS3 expression *via* activation of EPAC and, previous data in HUVECs has demonstrated that inhibition of PKA had no effect on the ability of IL-6 to induce tyrosine phosphorylation of STAT3 (Sands *et al.*, 2006). However, it is possible that cell type-specific difference in cell signalling pathways may be responsible for the observed differences between HUVECs and the prostate epithelial cell lines used in this study. The results obtained in this study indicate that activation of PKA plays an important role in IL-6-mediated activation of STAT3. Whilst unanticipated, a role for PKA in cytokine-induced STAT activation is not without precedent. In the murine AML-12 hepatocyte cell line, treatment with TGF- β_1 resulted in sustained increase in pTyr⁷⁰⁵STAT3 (Yang *et al.*, 2006). However, either pre-treatment of AML-12 cells with the PKA-selective inhibitor H89 or vector-mediated expression of PKI in these cells resulted in attenuation of TGF- β_1 -induced STAT3 activation (Yang *et al.*, 2006). These results corroborate those from the current study which suggest that PKA activation can potentiate tyrosine phosphorylation of STAT3 although the signalling pathway by which this is achieved is unknown. Results obtained in murine splenocytes demonstrate that PKA activation is required for histamine-induced activation of STAT1 downstream of Ca²⁺-mediated activation of PKC (Sakhalkar *et al.*, 2005). Interestingly, IL-6 was recently demonstrated to induce an increase in cytosolic Ca²⁺ concentration in the rat carotid body glomus (Fan *et al.*, 2009). Similar results were observed in skeletal muscle cells where treatment with 20 ng/ml IL-6 promoted a transient increase in intracellular Ca²⁺ concentration (Weigert *et al.*, 2007). It is possible that IL-6-mediated increases in Ca²⁺ may promote STAT3 activation in a similar manner to that observed following STAT1

activation downstream of histamine stimulation (Sakhalkar *et al.*, 2005). As the latter observation has a requirement for PKA activation, cross-talk between an IL-6/Ca²⁺/PKC signalling pathway and PKA may potentially explain the requirement for this enzyme in sustained IL-6-mediated STAT3 induction.

Whilst the effect of PKA inhibition on IL-6-mediated STAT3 activation in prostate epithelial cells was unexpected, the ability of the EPAC-selective agonist 8Me-pCPT-cAMP to inhibit IL-6-induced STAT3 activation corroborates published data. In HUVECs, the ability of cAMP to inhibit IL-6-mediated STAT3 activation was mediated *via* EPAC activation (Sands *et al.*, 2006). Similar results have been observed in COS1 cells (Borland *et al.*, 2009), indicative that EPAC rather than PKA activation is required for cAMP-induced SOCS3 expression.

The results in this chapter indicate that cAMP elevation in DU145 and PZ-HPV-7 cells are mediated *via* induction of SOCS3 expression. However the pathways involved in this process have not yet been determined. Activation of ERK1/2 and EPAC are required for cAMP-mediated SOCS3 expression (Sands *et al.*, 2006; Woolson *et al.*, 2009) and, given the observation that selective EPAC activation can recapitulate the effect of cAMP in prostate epithelial cells, it is possible that similar pathways are important in SOCS3 expression in prostate epithelial cells. Treatment with selective inhibitors of the ERK1/2 pathway such as U0126 would help to elucidate the molecular pathways involved in SOCS3 induction in prostate epithelial cells. Blockade of protein translation inhibited IL-6-induced STAT3 activation in the absence of cAMP elevation, most likely due to inhibition of JAK synthesis as these components of the IL-6 signalling proteins undergo more rapid turnover than STAT3 or SHP-2 (Siewert *et al.*, 1999). Thus it has not been possible to determine whether *de novo* protein synthesis is required for the ability of cAMP to inhibit STAT3 phosphorylation. In other cell types, it has been demonstrated that cAMP elevation resulted in an increase in *socs3* mRNA (Barclay *et al.*, 2007; Sands *et al.*, 2006). Analysis of *socs3* mRNA expression following cAMP elevation *via* qRT-PCR would indicate whether cAMP elevation promotes an increase of SOCS3 at the transcriptional level.

Whilst cAMP elevation appears to be a common mechanism by which to inhibit IL-6-induced STAT3 activation in prostate epithelial cells, the mechanisms involved vary between cell type. The ability of cAMP to inhibit IL-6-mediated STAT3 activation has been described in a number of cell types, suggesting that it may represent a common mechanism by which to modulate IL-6 signalling. However, whilst cAMP elevation is

associated with protective effects in vascular endothelial cells *via* promotion of barrier function, the use of this intracellular signalling molecule as a modulator of inflammatory signalling must be carefully considered in cancer therapy. Over-expression of PKA has been described in haematological malignancies and is associated with increases in cell growth through PKA-mediated activation of CREB (James *et al.*, 2009; Naviglio *et al.*, 2009; Shankar *et al.*, 2005). Interestingly the PKI family member, PKI β , is over-expressed in castration-resistant PCa with knockdown of PKI β associated with inhibition of PCa cell growth. PKI β was found to associate with the catalytic subunit of PKA and promote nuclear accumulation of PKA, unlike the nuclear export activities of the related protein PKI α (Chung *et al.*, 2009). Expression of PKI β was correlated with activation of Akt and may contribute to malignant progression (Chung *et al.*, 2009). Therefore other factors which promote activation and nuclear accumulation of PKA such as elevation of intracellular cAMP may therefore exacerbate PCa progression. Careful consideration of the use of cAMP elevation as a novel therapeutic strategy in PCa must consequently be undertaken.

8 Elevation of cAMP induces LNCaP differentiation

8.1 Introduction

During experiments to determine the effect of cAMP elevation on rhuIL-6-induced STAT3 activation, it was noted that treatment with Fsk induced morphological changes in LNCaP but not DU145 or PZ-HPV-7 cells. It has been published that elevation of cAMP in LNCaP cells via either β_2 -adrenergic receptor agonists or Fsk treatment induces differentiation of LNCaP cells from prostate epithelial cells to a neuroendocrine (NE) -like phenotype (Deeble et al., 2001).

The human prostate is a complex gland comprising epithelial parenchyma embedded in a matrix of connective tissue. Until puberty, epithelial cells in the prostate exist as multiple layers of immature cells which differentiate into a two-layered epithelium upon reaching puberty containing columnar secretory epithelial cells surrounded by outer cuboidal basal layer comprised principally of basal, secretory luminal and NE cells. The exocrine compartment of the prostate consists of the terminally differentiated secretory luminal cells which secrete prostate-specific antigen (PSA) and are the predominant cell type in normal and hyperplastic prostate epithelium (Lang *et al.*, 2009). Luminal cells express high levels of AR and thus are androgen-dependent for growth. The basal cells lie adjacent to the basement membrane and do not rely on androgens for growth due to low/no AndR expression. NE cells are predominantly found within the basal compartment of the prostate and are non-proliferating, terminally differentiated, androgen-differentiated cells (Lang *et al.*, 2009).

8.1.1 NE cells in the prostate

NE cells represent a group of cells which share structural, metabolic and functional characteristics with neuronal cells and secrete hormones in response to stimulation (Shariff & Ather, 2006). In the immature prostate, NE cells are thought to play an important paracrine role in governing tissue growth and differentiation. Unlike NE cells described in the pituitary and adrenal system, prostatic NE cells are thought to arise from an epithelial stem cell rather than from the neural crest due to the expression of epithelial markers such as PSA and AndR (Cox *et al.*, 1999). Although NE cells can be seen scattered throughout the mature prostate as morphologically heterogeneous cells with irregular dendrite-like extensions, their role in the mature gland is less well understood (Cox *et al.*, 1999). It has been suggested that NE cells may regulate secretory functions in the mature prostate gland (Shariff & Ather, 2006).

Although NE cells comprise a small proportion of the mature prostate gland, expansion of the NE population indicates a poor patient prognosis and has been investigated as a marker for disease progression (Yuan *et al.*, 2007). Due to the reliance of normal prostate epithelial cells on androgens for growth, traditional therapies for PCa typically involve androgen ablation. However, such therapies select for androgen-independent cells, the expansion of which is associated with subsequent disease progression due to the failure of conventional therapeutics. NE cells are such an example of androgen-independent cells within the prostate and are resistant not just to androgen ablation therapy but also to pan-malignancy chemotherapies which are only efficacious against actively dividing cells. Furthermore, whilst NE cells represent a non-proliferating cell population, they are able to promote the growth of neighbouring cells due to the release of mitogenic factors such as bombesin (Noordzij *et al.*, 1996). Tumours comprising solely of NE cells are rare and represent highly aggressive malignancies. More commonly, NE cells are found within tumours as foci of non-dividing cells surrounded by rapidly proliferating epithelial cells (Noordzij *et al.*, 1996).

Recently, much research has been conducted into the value of NE-like cells as a marker for PCa progression. Currently, established methods for monitoring PCa progression include measurement of serum PSA levels and Gleason score. However, these methods of screening are not infallible and therefore other methods of detecting PCa progression have been investigated. The emergence of NE cells as a marker for PCa is somewhat controversial with some studies demonstrating a clear link between NE emergence and PCa stage and others finding no correlation between NE cell populations and disease progression .

8.1.2 LNCaP differentiation to a NE-like phenotype

Due to their importance in PCa progression, much research has been conducted into the mechanisms by which cells undergo differentiation to NE cells. Many stimuli can induce differentiation of normal prostate epithelial cells to a NE-like phenotype including androgen deprivation, cAMP elevation and chronic stimulation with IL-6 (Chen *et al.*, 1992;Deeble *et al.*, 2001).

LNCaP cells have previously been used as a model for NE-like differentiation in response to a multitude of stimuli. Of particular importance for PCa patients undergoing androgen ablation therapy, androgen deprivation can induce differentiation of LNCaP cells to NE-

like cells (Saeed *et al.*, 1997). Additionally, chronic stimulation with IL-6 (Deeble *et al.*, 2001) or over-expression of constitutively active gp130 subunits can induce NE-like differentiation in LNCaP cells, indicating that activation of the gp130 signalling cascade plays an important role in the differentiation process (Palmer *et al.*, 2005). It is thus possible that the ability of IL-6 to induce NE-like differentiation in LNCaP cells arises due to activation of STAT3. Interestingly, treatment with cAMP-elevating agents, which has been demonstrated to inhibit IL-6-induced activation of STAT3 (see chapter 7) also induces NE differentiation of LNCaP cells.

LNCaP cells treated with dibutyl-cAMP and the non-selective PDE inhibitor IBMX undergo differentiation to a neuron-like morphology. This change in cellular morphology is coupled with an increase in neuronal markers such as neuron-specific enolase (NSE) and the presence of dense-core granules which are characteristic of differentiated neurosecretory cells (Bang *et al.*, 1994). Similarly, treatment with Fsk induces NE-like differentiation in LNCaP cells, the effect of which can be recapitulated with β_2 -adrenergic agonists such as isoproterenol and epinephrine (Deeble *et al.*, 2001). These results indicate that cAMP elevation can induce NE-like differentiation in LNCaP cells. Further evidence for the role of cAMP in NE differentiation comes from the observation that over-expression of constitutively active catalytic PKA subunits can induce NE-like differentiation in LNCaP cells (Cox *et al.*, 2000).

Whilst much research has been conducted concerning long-term differentiation of LNCaP cells to a NE-like phenotype, fewer studies have focussed on the signalling pathways regulating the morphological change of LNCaP cells in response to cAMP elevation. Disruption of the early responses involved in NE-like differentiation may prove to be an important complementary therapy to androgen ablation and so prevent NE-like differentiation and expansion of this cell population during chemotherapeutic regimes.

It was found that treatment with Fsk resulted in changes in LNCaP cell morphology consistent with differentiation to a NE-like phenotype, but had no effect on DU145 or PZ-HPV-7 cells. The changes in LNCaP cell morphology predominantly occurred in the first 1 h post-stimulation and, in accordance with published data, were mediated by activation of PKA. Treatment of LNCaP cells with anti-EPAC1 siRNA indicated that there was no role for this pathway on Fsk-induced changes in LNCaP morphology. Unexpectedly, inhibition of the RhoA-Rho-associated protein kinase (ROCK) signalling pathway mimicked the effect of Fsk stimulation, indicating that cAMP in LNCaP cells acts to inhibit RhoA

activation. It is hypothesised that Fsk-induced changes in LNCaP morphology are mediated through PKA-mediated inhibition of RhoA signalling and subsequent effects on the actin cytoskeleton.

8.2 Results

8.2.1 Phase contrast microscopy analysis of changes in LNCaP cell morphology

Many previous studies have focussed on gross changes in LNCaP morphology, which are not quantitative and so may overlook subtle contributions of various signalling pathways to this phenomenon. In order to address this issue, increases in the distance between the cell body and the tip of the longest dendrite-like extension for each cell was used as a quantitative assessment of changes in LNCaP cell morphology consistent with differentiation to a NE-like phenotype (Das *et al.*, 2005). However, although the phrase “mean dendrite length” is used throughout the study to describe this assessment, it should be stressed that the use of the term dendrite or neurite to describe these projections may not be entirely accurate because prostatic NE cells are thought to arise from an epithelial rather than neural progenitor (Shariff & Ather, 2006) and LNCaP cells do not express conventional neuronal markers such as glial fibrillary acidic protein (GFAP) (Bang *et al.*, 1994). However, in the absence of published methods for quantifying LNCaP differentiation *via* histological methods, this is method would appear to be suitable. In order to ensure sufficiently representative sampling of changes in dendrite length, 30 cells per field for 5 random will be analysed per treatment for each time point.

8.2.2 Treatment with Fsk rapidly induces changes in LNCaP morphology

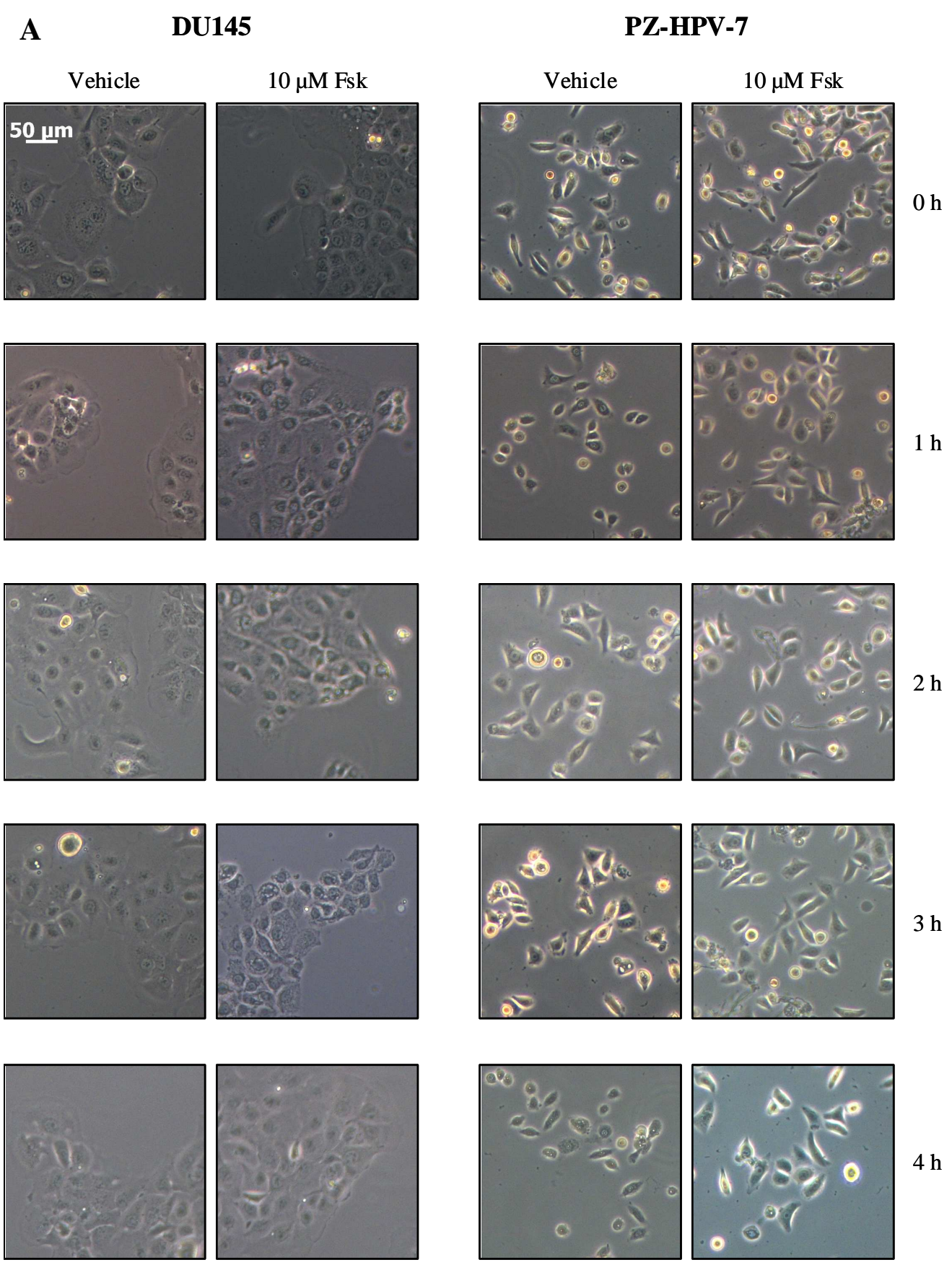
During the experiments investigating the ability of cAMP elevation on rhuIL-6-induced increases in pTyr⁷⁰⁵STAT3, it was noted that LNCaP cells treated for 5 h with 10 μ M Fsk displayed changes in morphology consistent with differentiation to NE-like cells. As the ability of Fsk to inhibit rhuIL-6-mediated tyrosine phosphorylation of STAT3 was universal across the three cell lines tested in this study, cells were stimulated with either vehicle (0.1 % (v/v) EtOH) or 10 μ M Fsk for 0 – 24 h with images captured as described in Chapter 5. DU145 and PZ-HPV-7 cells treated with either vehicle or 10 μ M Fsk displayed no changes in cell morphology at any of the time points observed (Fig 8.1, panel A).

Similarly, LNCaP cells treated with vehicle also displayed no change in cellular morphology at any of the time points investigated (Fig. 8.1, panels B and C), indicating that any subsequent changes in LNCaP morphology in Fsk-treated cells arise due to the actions of Fsk and not due to vehicle effects. In contrast, LNCaP cells treated with 10 μM Fsk displayed a rapid change in cell morphology, which was apparent within 1 h post-stimulation. This morphology is consistent with differentiation to a NE-like phenotype and cells were scored for an increase in mean dendrite length as an assessment of NE-like differentiation. The greatest period of increase in dendrite length was observed within the first hour post-stimulation with mean dendrite length increasing from $18.47 \pm 0.61 \mu\text{m}$ at 0 h post-stimulation to $29.20 \pm 0.97 \mu\text{m}$ at 1 h post-stimulation, rate of increase of approximately $10 \mu\text{m/h}$ (Fig. 8.1, panels B and C, $p < 0.001$ vs. 0 h and vs. vehicle stimulated cells at same time point). Between 1 h and 24 h post-stimulation, a continued increase in mean dendrite length was observed with mean dendrite length increasing to a maximum of $39.43 \pm 1.21 \mu\text{m}$ at 8 h post-stimulation. However, the rate of increase in mean dendrite length over this time period corresponds to only approximately $1.3 \mu\text{m/h}$, indicating that the maximum rate of increase in mean dendrite length occurs in the first 1 h post-stimulation. Whilst the effects of sustained cAMP elevation on LNCaP differentiation to a NE-like phenotype have long been studied, less work has focussed on the pathways mediating the rapid change in morphology arising from Fsk treatment. For this reason, subsequent studies in this project have focussed on the pathways involved in this change in cellular morphology.

8.2.3 Early changes in LNCaP cells morphology do not require *de novo* protein synthesis

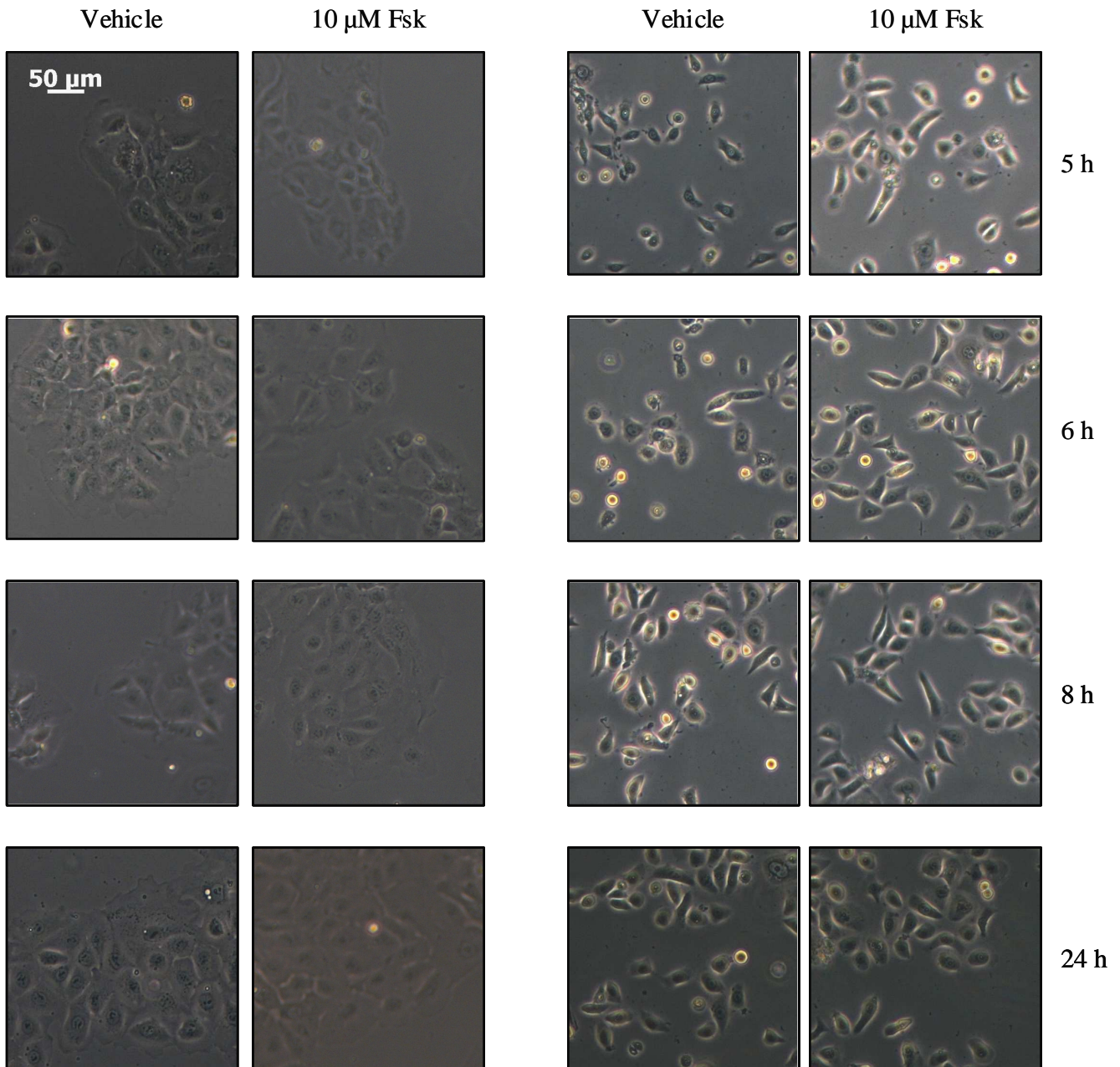
Many differentiation processes require *de novo* protein synthesis arising from altered gene expression profiles. In order to assess whether this was the case in Fsk-induced changes in LNCaP cells, LNCaP cells were seeded as previously described and incubated with 100 μM emetine. Unlike other protein synthesis inhibitors such as cycloheximide, emetine acts to irreversibly block protein translation (Grollman, 1968) by preventing elongation of the nascent protein chain (Tscherne & Pestka, 1975) due to actions on the 40s ribosomal subunit (Jimenez *et al.*, 2002). In order to prevent Fsk-induced changes in protein expression, LNCaP cells were incubated for 2 h prior to stimulation with 10 μM Fsk and subsequent assessment of changes in cell morphology as described previously.

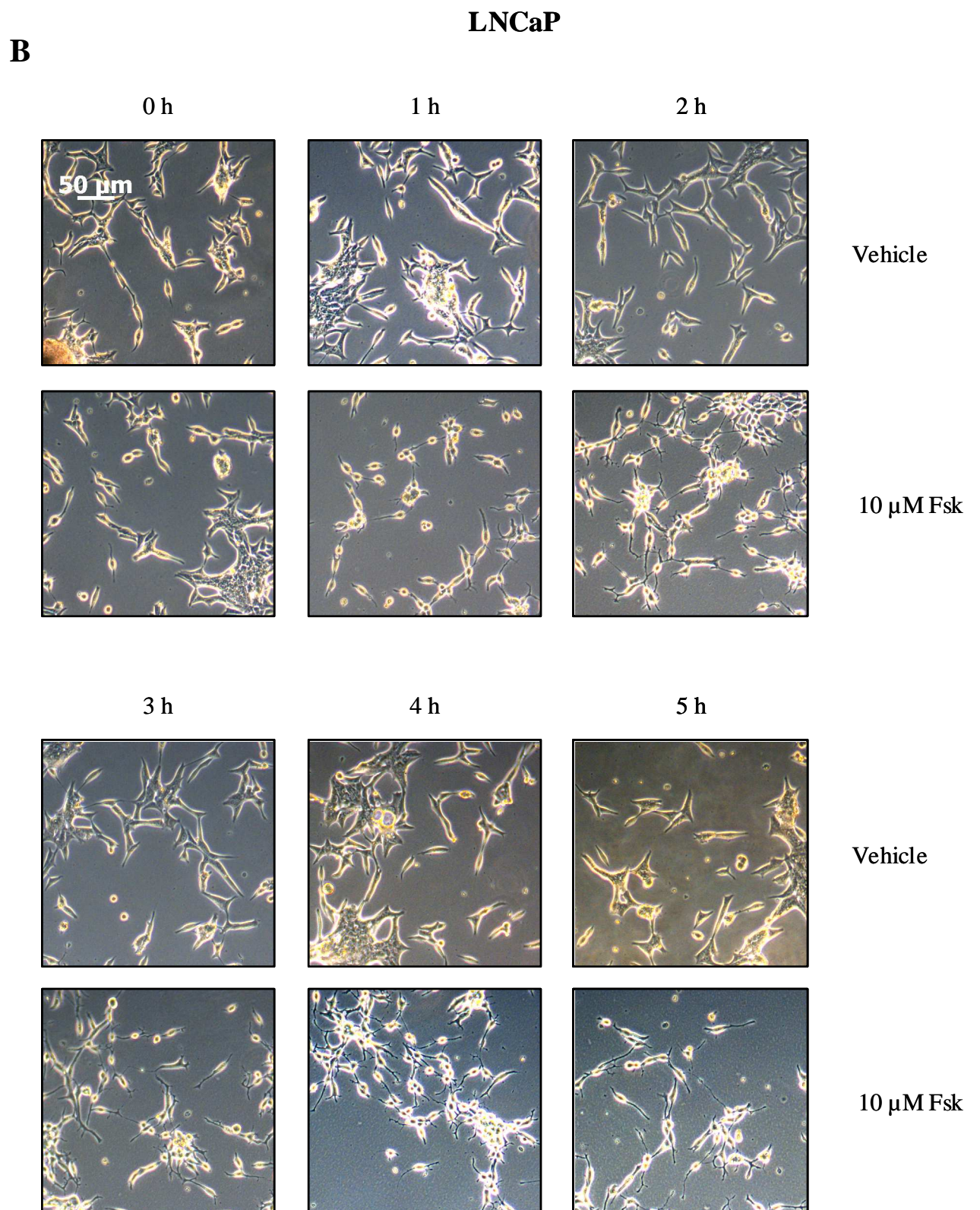
In accordance with previous data, treatment of LNCaP cells with vehicle or emetine in the absence of Fsk failed to induce any changes in cellular morphology (Fig. 8.2, panels A and

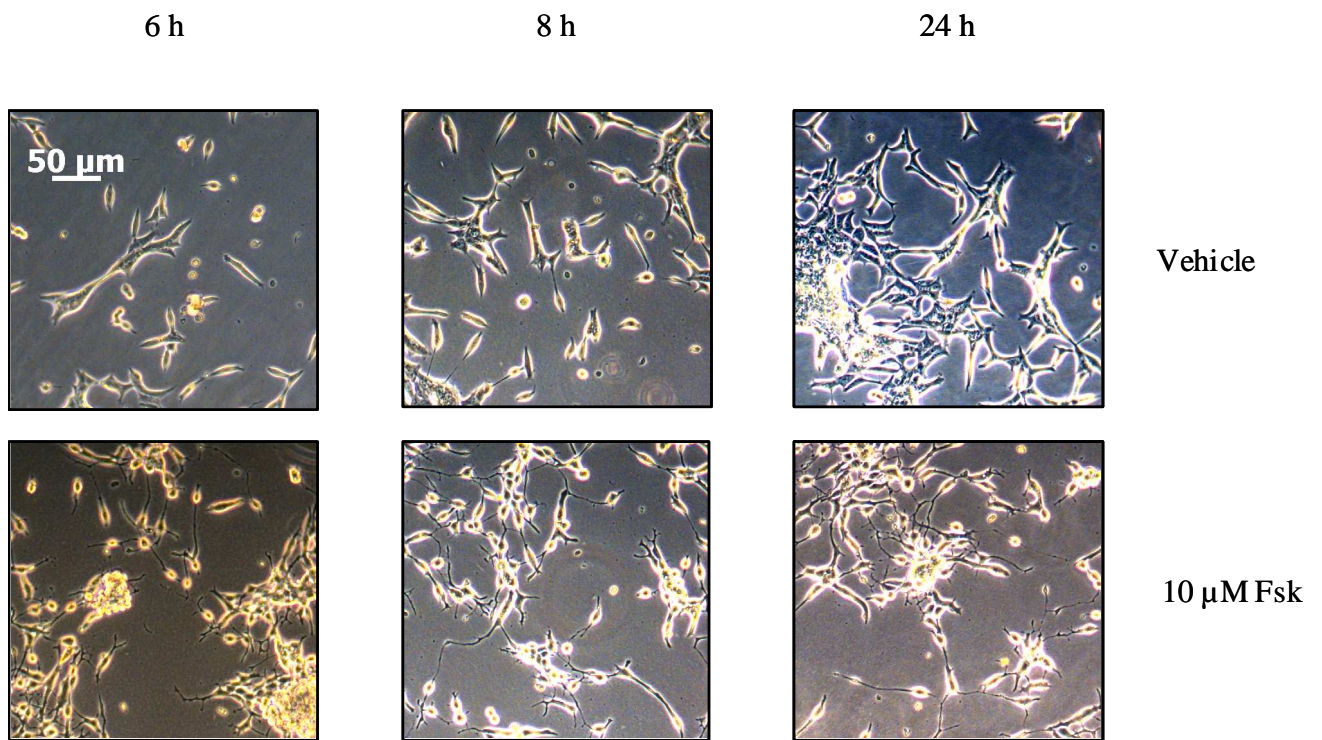


DU145

PZ-HPV-7







C

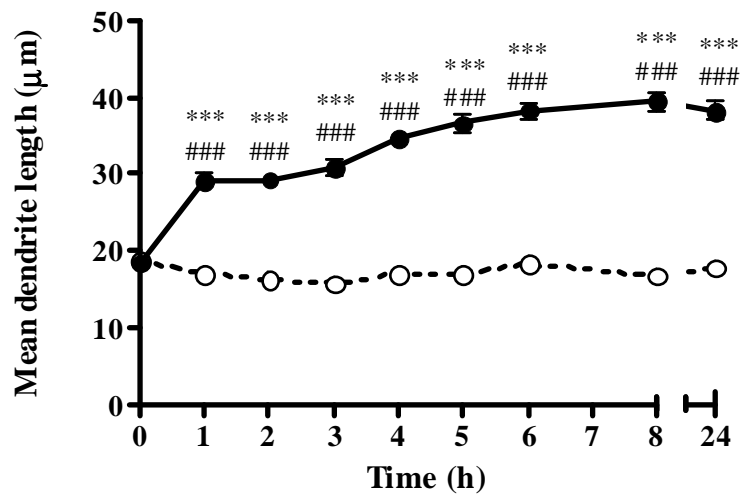


Figure 8.1: cAMP elevation induces morphological changes in LNCaP cells but not in DU145 or PZ-HPV-7 cells

DU145, LNCaP and PZ-HPV-7 cells were seeded into 6 cm dishes and stimulated with vehicle (0.1 % (v/v) EtOH) or 10 μ M Fsk for 0–24 h with images captured at the time points stated (Panel A for DU145 and PZ-HPV-7 cells, panel B for LNCaP cells). LNCaP cell differentiation to a NE-like phenotype was assessed by measuring increases in the maximum distance between the edge of the cell body and dendrite tip per cell (Panel C). Results are shown as mean values \pm SEM for $n = 3$ separate experiments. *** = $p < 0.001$ vs. 0 h, ### = $p < 0.001$ vs. vehicle at same time point.

C, $p > 0.05$), indicating that subsequent increases in mean dendrite length arising from Fsk stimulation occur due to the actions of Fsk and not vehicle effects. Interestingly, treatment with emetine slightly increased the mean dendrite length of LNCaP cells immediately prior to stimulation, but as the increase was of approximately 5 μm , it is not believed to be biologically significant in comparison to the approximately 20 μm increase in mean dendrite length induced by Fsk treatment.

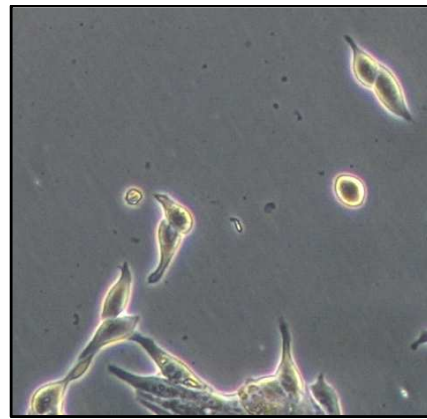
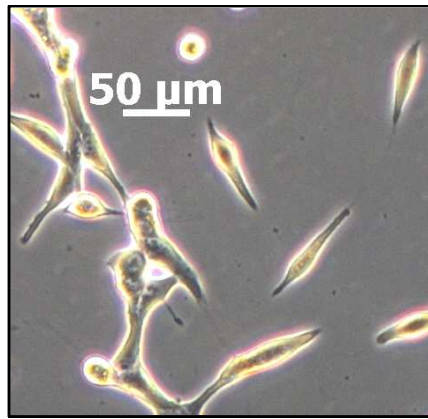
It was found that treatment with emetine had no effect on Fsk-induced increases in mean dendrite length at 1 h post-stimulation (Fig. 8.2, panels B and C, $p > 0.05$ vehicle pre-treatment *vs.* emetine pre-treatment) with cells pre-treated with 100 μM emetine displaying a mean dendrite length of 30.53 ± 0.69 compared to a mean dendrite length equal to 31.09 ± 0.70 μm in LNCaP cells which had not been pre-incubated with emetine (Fig. 8.2 panels B and C, *** = $p < 0.001$ *vs.* 0 h, #### = $p < 0.001$ *vs.* vehicle). However, at 3 h and 5 h post-stimulation with Fsk, LNCaP cells which had been pre-treated with emetine displayed no further increase in mean dendrite length (Fig. 8.2 panels B and C, mean dendrite lengths = 33.81 ± 0.87 μm and 30.74 ± 0.91 μm at 3 h and 5 h post-stimulation respectively, +++ = $p < 0.001$ Fsk + emetine *vs.* Fsk at each time point). In contrast, LNCaP cells which had been stimulated with Fsk in the absence of pre-incubation with emetine displayed a further increase in mean dendrite length at 3 h (mean dendrite length = 43.53 ± 0.91 μm) and 5 h (mean dendrite length = 50.64 ± 1.13 μm , Fig. 8.2 panels B and C, *** = $p < 0.001$ *vs.* 0 h, #### = $p < 0.001$ *vs.* vehicle, \$\$\$ = $p < 0.001$ *vs.* 1 h).

These results suggest that the early response of LNCaP cells to Fsk does not require *de novo* protein synthesis and such an event is important only in later stages of NE-like differentiation.

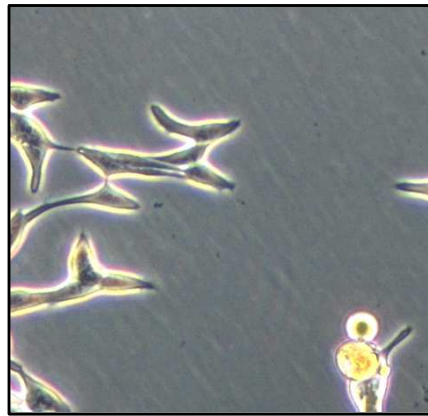
8.2.4 Fsk-induced changes in LNCaP cell morphology depends on an intact microtubule network

Microtubule (MT) transport plays an important role in extension of neurite and dendrite-like extension from the body with transport of membranous vesicles along MTs classically considered the most important role of MTs in neurite extension. The shaft of mature neurite-like structures contain a central MT core which plays an important role in trafficking between the axon head and the cell body, either through the delivery of signalling proteins or adhesion molecules required for neurite initiation or through delivery of membranes to promote the growth of the developing neurite (Dehmelt & Halpain, 2004).

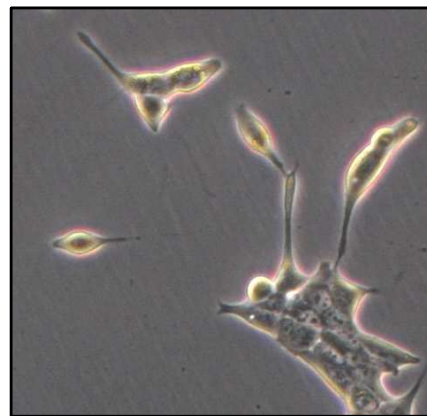
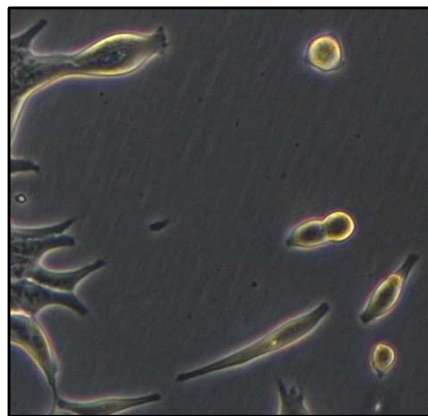
A



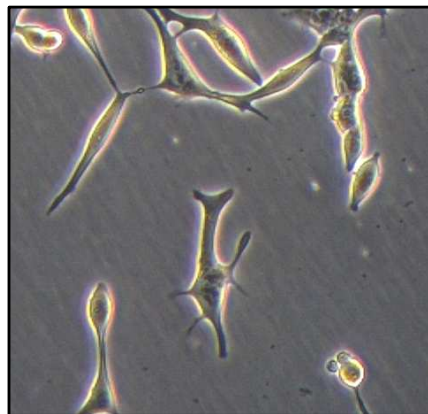
0 h



1 h



3 h

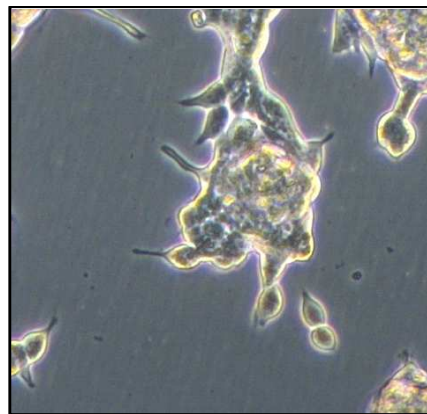


5 h

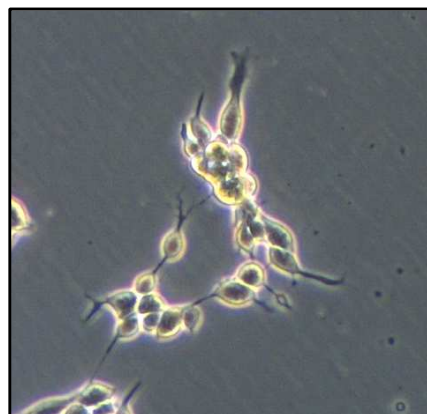
Vehicle

Emetine

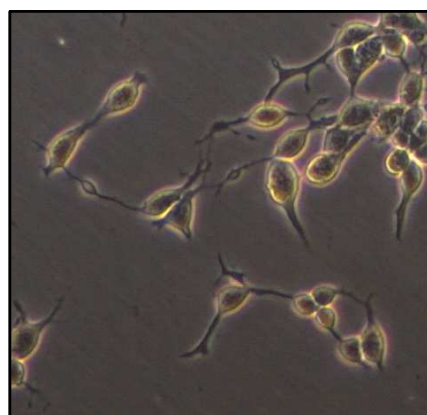
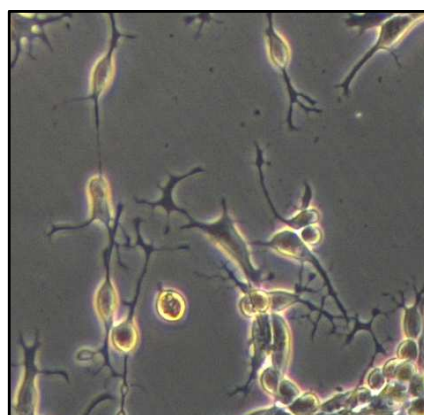
B



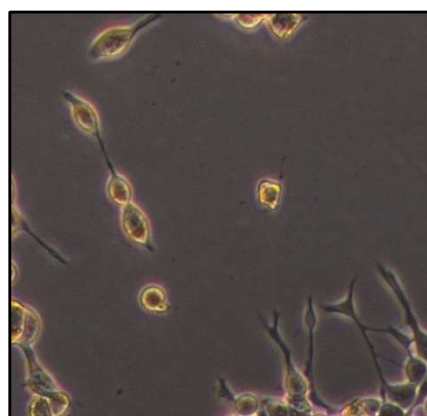
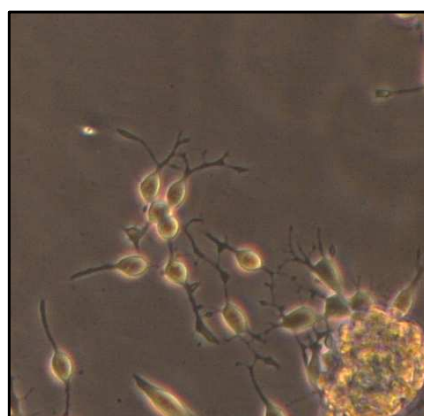
0 h



1 h



3 h



5 h

Fsk

Fsk + Emetine

C

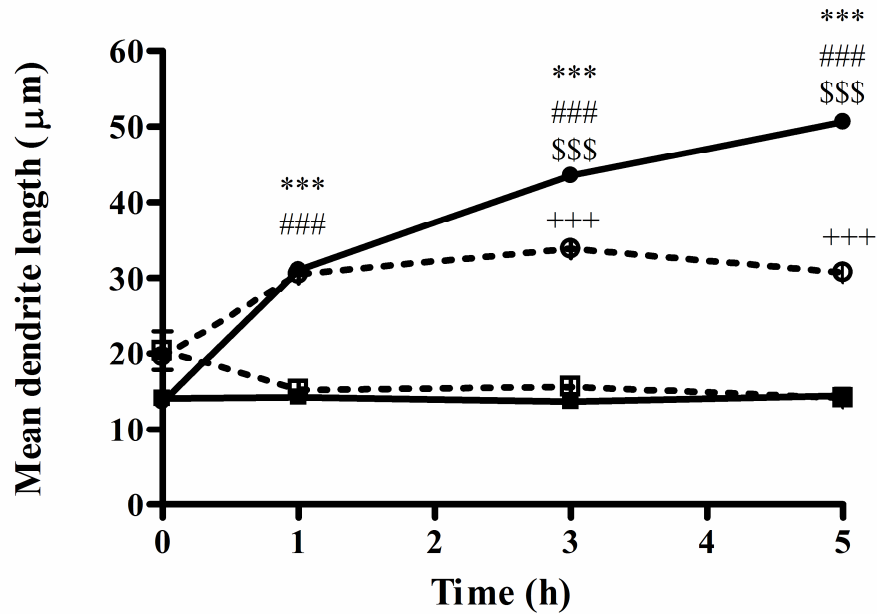


Fig. 8.2: The ability of Fsk to induce prolonged but not initial changes in LNCaP morphology requires *de novo* protein synthesis

LNCaP cells were seeded into 6-well plates and grown to 40 – 50 % confluence. LNCaP cells were incubated with vehicle (0.1 % (v/v) H₂O) or 100 µM emetine for 120 min prior to stimulation with vehicle (0.1 % (v/v) EtOH, panel A and C) or 10 µM Fsk (panels B and C) for 0 – 5 h. Results are presented as mean values ± SEM for $n = 3$ experiments. *** = $p < 0.001$ vs. 0 h, ### = $p < 0.001$ vs. vehicle at same time point, +++ = $p < 0.001$ vs. Fsk treatment., \$\$\$ = $p < 0.001$ vs. 1 h. Results are shown for vehicle treated cells (closed squares), emetine treated cells (open squares), Fsk (closed circles) and Fsk plus emetine (open circles).

Nocodazole depolymerises MT *in vitro* (De Brabander *et al.*, 1976), thus LNCaP cells were treated with either vehicle (0.5 % (v/v) DMSO) or 10 μ M nocodazole for 30 min to depolymerise the MT network prior to stimulation with vehicle (0.1 % (v/v) EtOH) or 10 μ M Fsk for 1 h with phase contrast images captured as described previously immediately prior to nocodazole treatment and immediately post-stimulation. In order to assess nocodazole efficacy, immunofluorescence was performed on LNCaP cells plated in parallel onto poly-D-lysine coated coverslips and stained with anti-tubulin antibody. Successful tubulin staining was visualised using goat AlexaFluor468-conjugated anti-mouse IgG and images subsequently captured using a Zeiss CFL-40 epi-fluorescent microscope as described in Chapter 5, with treatment with nocodazole completely abolishing the MT network (Fig. 8.3, panel B).

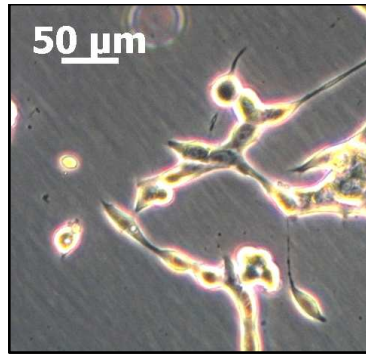
Treatment with vehicle failed to elicit any changes in LNCaP cell morphology whilst treatment with 10 μ M resulted in an increase in mean dendrite length as observed in previous experiments (Fig. 8.3, panel A). Incubation with nocodazole did not inhibit Fsk induced changes in LNCaP morphology but Fsk-induced dendrite-like structures appeared to be morphologically distinct following nocodazole pre-treatment to those dendrites arising in cells which had been pre-incubating Fsk. Evidence of damage to Fsk-induced dendrites following pre-incubation with nocodazole was apparent with dendrites appearing far thinner and, indeed, almost completely disintegrated (Fig. 8.3, panel A, arrows indicate damaged dendrites). These results suggest that an intact MT network is essential for maintenance, but not initiation, of Fsk-induced changes in LNCaP cell morphology.

8.2.5 The ability of Fsk to induce increases in mean dendrite length requires adenylyl cyclase activity

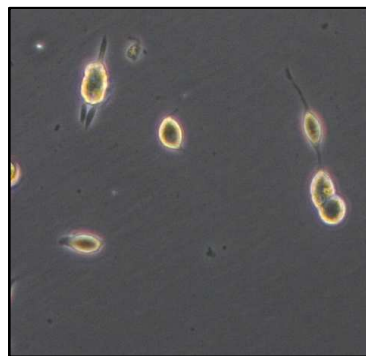
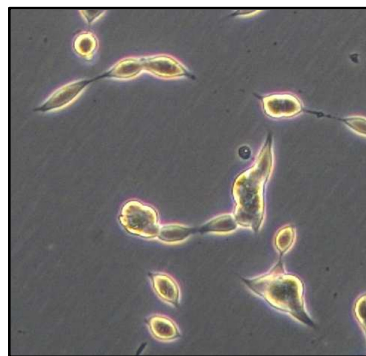
In order to induce intracellular cAMP elevation, Fsk activates membrane ACs to promote the conversion of ATP to cAMP. In order to ensure that the observed effects of Fsk on LNCaP morphology were indeed mediated through activation of AC, LNCaP cells were incubated with either vehicle (0.4 % (v/v) DMSO) or 10 μ M of the AC-selective inhibitor 2',5'-dideoxy-3'-AMP-bis(t-Bu-SATE) (t-Bu-SATE) for 1 h prior to stimulation with vehicle (0.1 % (v/v) EtOH) or 10 μ M Fsk for 1 h with images captured immediately prior to and post-stimulation.

Treatment with vehicle did not result in any discernible changes in LNCaP morphology at 0 h or post-stimulation (Fig. 8.4, panels A and B). Pre-incubation with vehicle followed by

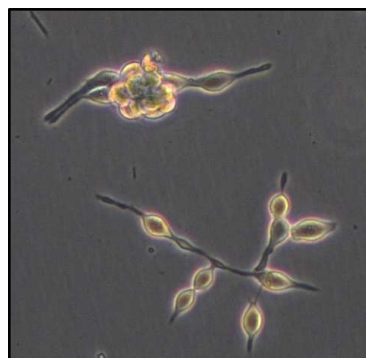
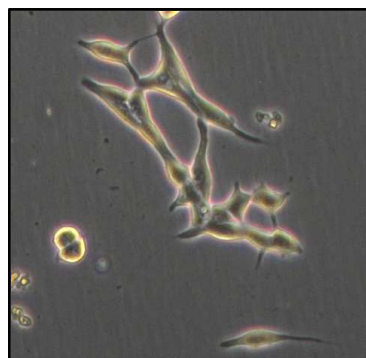
A



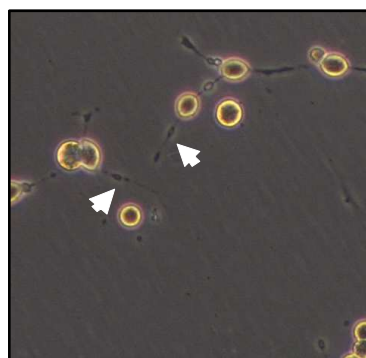
Vehicle



10 μ M Nocodazole



10 μ M Fsk



10 μ M Fsk +
10 μ M Nocodazole

0 h

post-stimulation

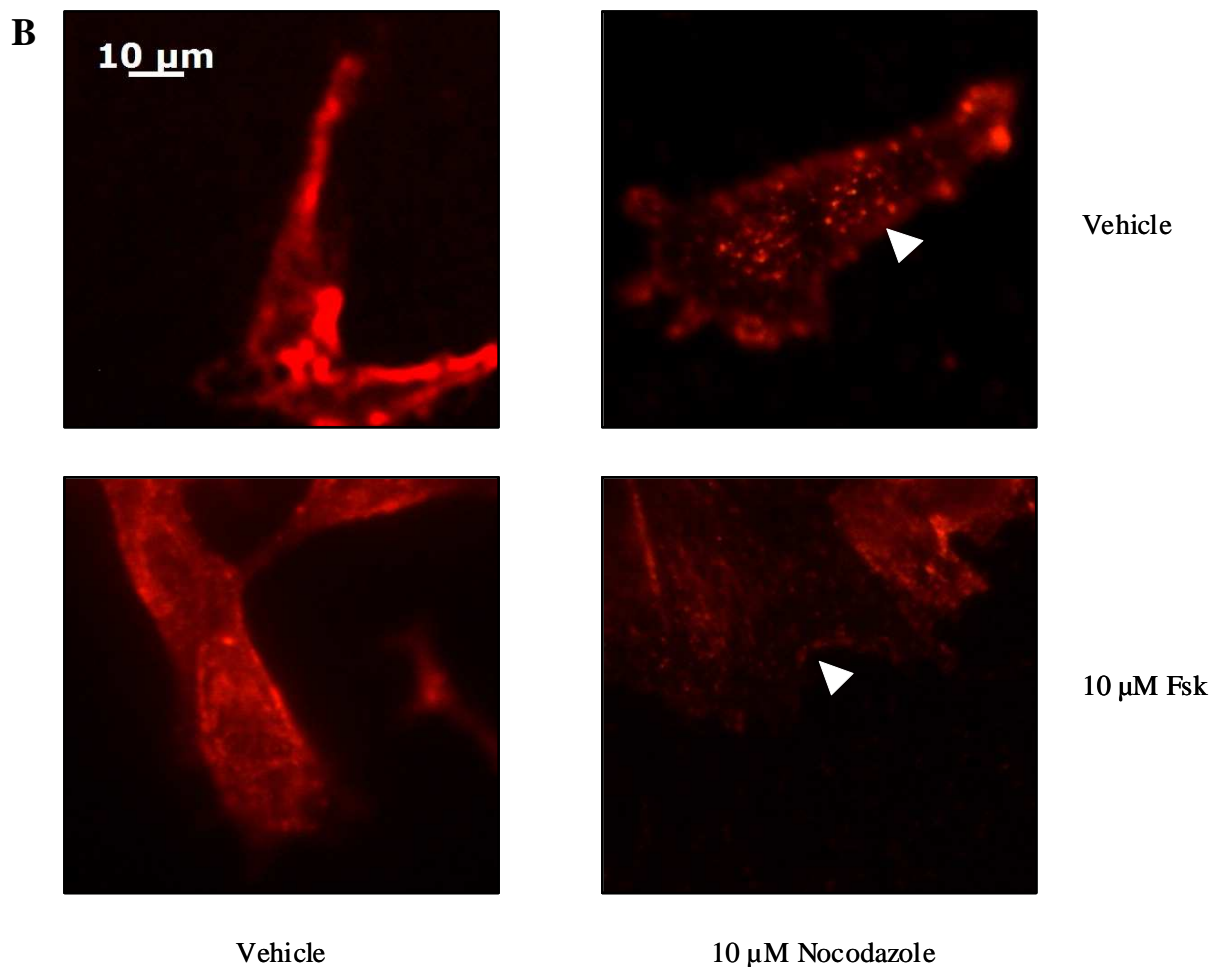


Fig. 8.3: Fsk-induced changes in LNCaP morphology require an intact microtubule network

LNCaP cells were either seeded onto glass coverslips or 6 well tissue culture dishes coated with 0.1 mg/ml poly-D-lysine and grown to 50-60 % confluence. Cells were treated with either vehicle (0.5 % (v/v) DMSO) or 10 μM nocodazole prior to incubation with vehicle (0.1 % (v/v) EtOH) or 10 μM Fsk for 1 h with images captured *via* phase contrast microscopy at 0 h and post-stimulation (panel A). Cells for immunofluorescence were washed 3 x 2 ml/well in cold PBS prior to fixation in 4 % (w/v) paraformaldehyde in 5 % (w/v) sucrose-PBS. Cells were permeabilised at room temperature for 15 min in 0.1 % (v/v) Triton X100-PBS prior to blocking with 5 % (w/v) BSA-PBST and incubation overnight with mouse mAb to tubulin (1:200 in 5 % (w/v) BSA-PBST). Following 3 x 10 min washes in PBST, LNCaP cells were incubated with AlexaFluor468-conjugated anti-mouse IgG (1:250 in 5 % (w/v) BSA-PBST, 1 h, room temperature) followed by a further 3 x 10 min washes in PBST and visualisation of antibody staining using a Zeiss CFL fluorescence microscope at 40 x objective (panel B, arrows indicate disruption of the MT network. Results shown are representative of $n = 3$ separate experiments.

treatment with 10 μM Fsk promoted an increase in mean dendrite length from $25.15 \pm 0.64 \mu\text{m}$ to $32.74 \pm 0.67 \mu\text{m}$ post-stimulation (Fig. 8.4 panels A and B, *** = $p < 0.001$ vs. 0 h, ### = $p < 0.001$ vs. vehicle). Similar to treatment with vehicle, incubation of LNCaP cells with t-Bu-SATE in the absence of Fsk failed to induce an increase in mean dendrite length post-stimulation (Fig. 8.4, panels A and B, $p > 0.05$). However, in LNCaP cells pre-incubated with t-Bu-SATE, the subsequent ability of Fsk to induce an increase in mean dendrite length was significantly decreased with mean dendrite length increasing from $24.59 \pm 0.60 \mu\text{m}$ to $28.93 \pm 0.64 \mu\text{m}$ post-stimulation (Fig. 8.4, panels A and B, ** = $p < 0.01$ vs. 0 h, ### = $p < 0.001$ vs. vehicle, +++ = $p < 0.001$ vs. Fsk).

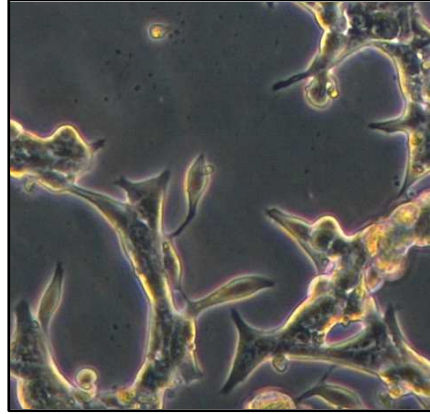
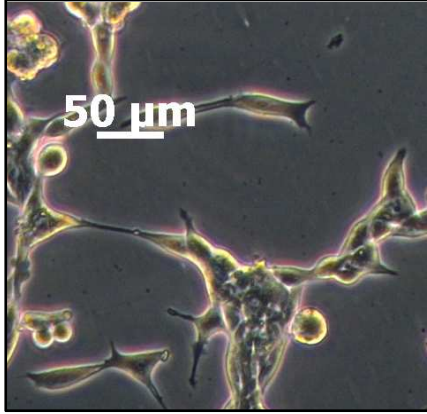
The above results indicate that selective inhibition of AC impedes the ability of Fsk to induce NE-like differentiation of LNCaP cells and that Fsk-mediated differentiation to a NE-like phenotype requires AC activation.

8.2.6 Treatment with H89 mimics the effects of Fsk on LNCaP morphology

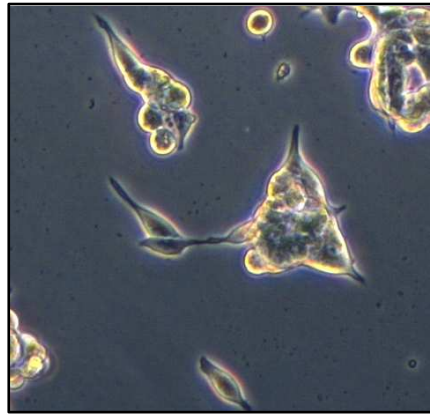
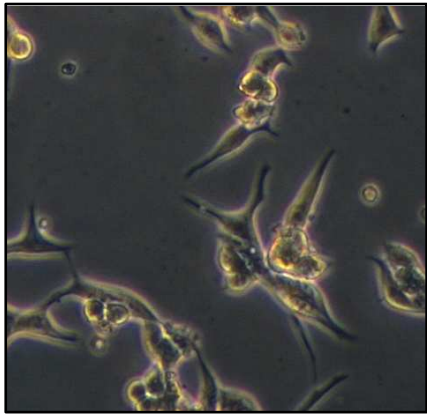
Based on published literature which demonstrates that NE-like differentiation in LNCaP cells is dependent on PKA activation (Cox *et al.*, 2000), it was decided to test whether selective inhibition of PKA inhibited Fsk-induced changes in LNCaP morphology.

LNCaP cells were treated with either vehicle (0.1 (v/v) % DMSO) or 5 μM of the PKA-selective inhibitor H89 for 1 h prior to stimulation with vehicle (0.1 (v/v) EtOH) or 10 μM Fsk. Images of five random fields were captured for each treatment immediately prior to incubation with vehicle or H89 and again following cell stimulation. LNCaP cells treated with vehicle displayed no change in cell morphology or mean dendrite ($18.33 \pm 0.49 \mu\text{m}$ and $18.00 \pm 0.43 \mu\text{m}$ at 0 h and post-stimulation respectively, Fig 8.5, panels A and B). In keeping with previous data, LNCaP cells pre-incubated with vehicle and then treated with 10 μM Fsk for 1 h displayed changes in cell morphology consistent with NE-like differentiation and an increase in mean dendrite from $19.64 \pm 0.48 \mu\text{m}$ at 0 h to $33.09 \pm 0.65 \mu\text{m}$ post-stimulation (Fig. 8.5, panels A and B, *** = $p < 0.001$ vs. 0 h, ### = $p < 0.001$ vs. vehicle post-stimulation). Surprisingly, LNCaP cells treated with 5 μM H89 alone displayed an increase in mean dendrite length at the end of the experiment with mean dendrite length increasing from $19.31 \pm 0.53 \mu\text{m}$ at 0 h to $34.11 \pm 0.73 \mu\text{m}$ post-stimulation (Fig. 8.5, panels A and B, *** = $p < 0.001$ vs. 0 h, ### = $p < 0.001$ vs. vehicle post-

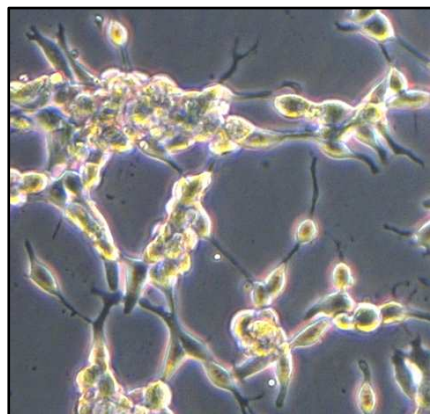
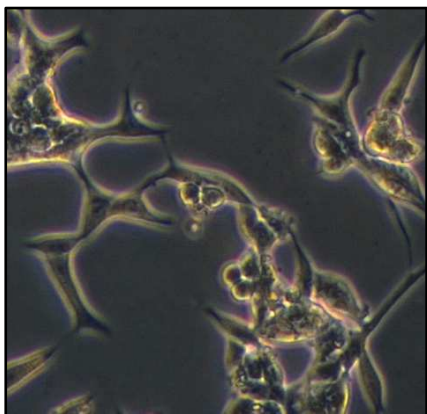
A



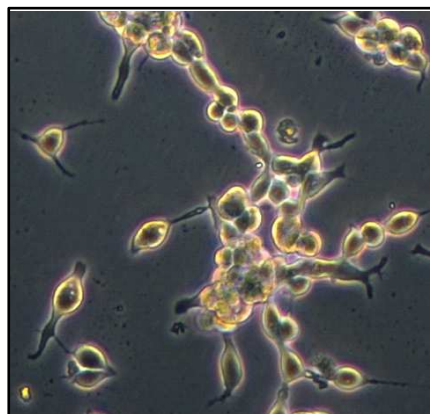
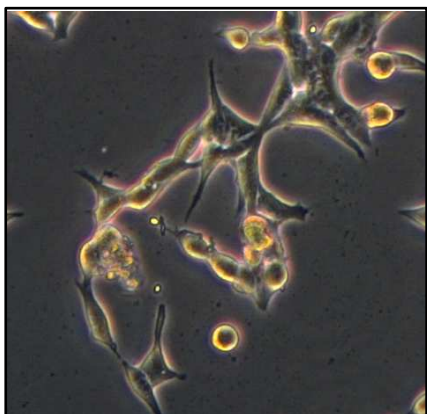
Vehicle



10 μ M t-Bu-SATE



10 μ M Fsk



10 μ M t-Bu-SATE
+ 10 μ M Fsk

0 h

Post-stimulation

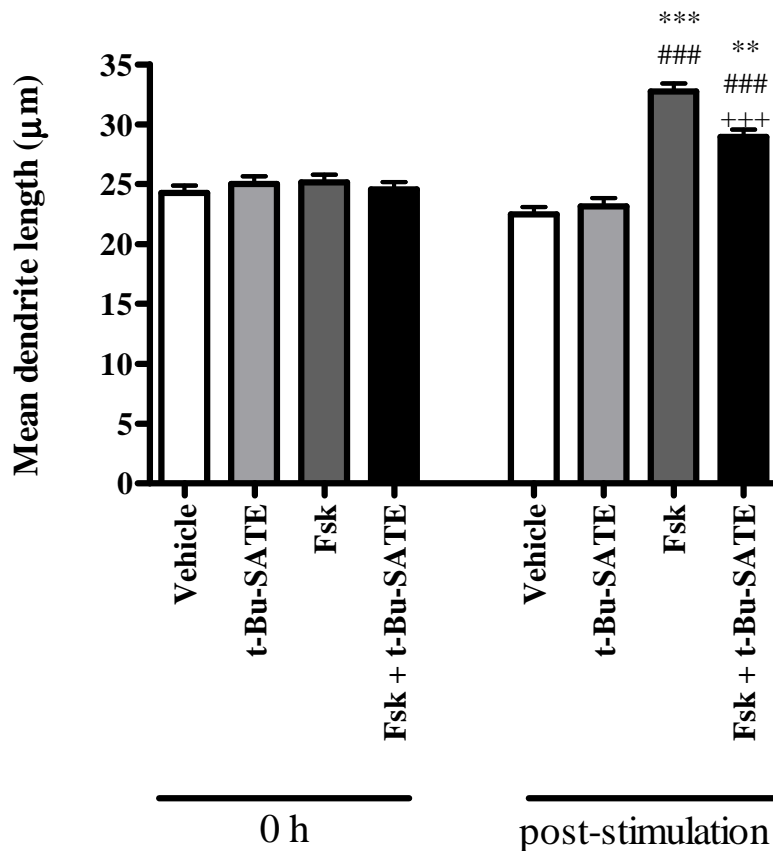


Fig. 8.4: Treatment with the AC-selective inhibitor t-Bu-SATE inhibits the effect of Fsk on LNCaP morphology

LNCaP cells were seeded into 6-well plates and incubated with either vehicle (0.1 % (v/v) DMSO) or 10 µM t-Bu-SATE for 60 min at 37°C, 5 % (v/v) CO₂ prior to stimulation with vehicle (0.1 % (v/v) EtOH) or 10 µM Fsk for a further 60 min at 37°C, 5 % (v/v) CO₂. Images of five random fields per treatment were captured at each time point and changes in LNCaP morphology assessed by measuring mean dendrite length for 30 random cells per field per treatment (panels A and B). Results are presented as mean values ± SEM for *n* = 3 experiments. ** = *p* < 0.01 vs. 0 h, *** = *p* < 0.001 vs. 0 h, ### = *p* < 0.001 vs. vehicle at same time point, +++ = *p* < 0.001 vs. Fsk at 1 h.

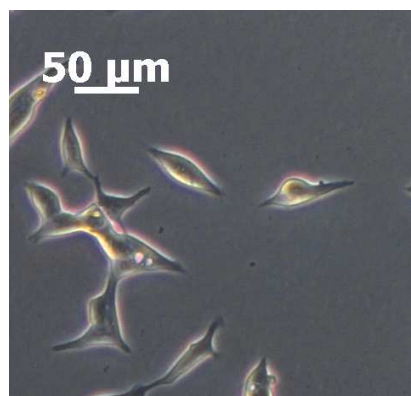
stimulation). Combined pre-incubation with 5 μM H89 and subsequent treatment with 10 μM Fsk induced a similar increase in mean dendrite length from $18.05 \pm 0.41 \mu\text{m}$ at 0 h to $39.10 \pm 0.77 \mu\text{m}$ post-stimulation (Fig. 8.5, panels A and B, *** = $p < 0.001$ vs. 0 h, ### = $p < 0.001$ vs. vehicle post-stimulation). These results suggest that the ability of Fsk to induce changes in LNCaP morphology is mediated by pathways that act independently of PKA activation and that PKA activity may actually act to suppress morphological changes in LNCaP cells consistent with NE-like differentiation. These results are surprising and contravene published data implicating a central role for PKA in Fsk-induced morphological changes. It is possible that the results obtained may arise from non-selective effects of H89 on targets other than PKA.

8.2.7 Treatment with myr.PKI₁₄₋₂₂ inhibits the effect of Fsk on LNCaP morphological changes

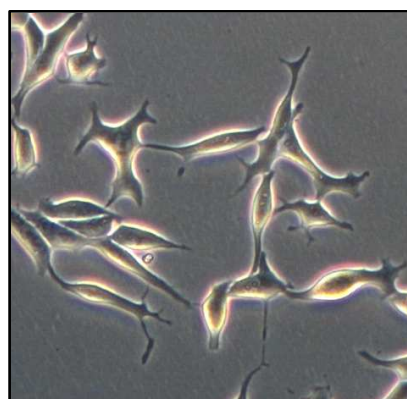
In order to assess whether the effects of H89 on LNCaP morphology arose from inhibition of PKA activity or due to non-selective effects on non-PKA targets, LNCaP cells were incubated with the structurally unrelated PKA-selective inhibitor PKA inhibitor 14-22 amide (PKI₁₄₋₂₂) which had been myristoylated (myrPKI₁₄₋₂₂) to aid cellular permeability. MyrPKI₁₄₋₂₂ is based on an endogenous peptide inhibitor of PKA which is thought to exclusively bind the catalytic subunits of PKA *in vivo* and mimic the inhibitory effect of the regulatory subunit (Murray, 2008). Endogenous PKI is thought to be exclusively specific for PKA and thus myrPKI₁₄₋₂₂ is thought to be a more potent inhibitor than H89 which competitively antagonises ATP binding to PKA (Murray, 2008).

LNCaP cells were seeded into 6-well plates as described earlier and incubated with either vehicle (0.1 % (v/v) DMSO) or 10 nM myrPKI₁₄₋₂₂ for 1 h at 37°C, 5 % (v/v) CO₂ prior to stimulation with either vehicle (0.1 % (v/v) EtOH) or 10 μM Fsk for 1 h. Images of LNCaP cells were captured immediately prior to stimulation and immediately post-stimulation as described in Materials and Methods (Chapter 4). Treatment of cells with vehicle failed to promote an increase in mean dendrite length throughout the experiments (Fig. 8.6, panels A and B, mean dendrite length = $21.86 \pm 0.71 \mu\text{m}$ and $20.45 \pm 0.67 \mu\text{m}$ at 0 h and post-stimulation respectively, $p > 0.05$). Similarly, incubation of LNCaP cells with myr.PKI₁₄₋₂₂ followed by incubation with EtOH did not promote NE-like differentiation in LNCaP cells with mean dendrite lengths of $22.50 \pm 0.76 \mu\text{m}$ at 0 h and $21.03 \pm 0.71 \mu\text{m}$ post-stimulation (Fig. 8.6, panels A and B, $p > 0.05$) Treatment with Fsk in the absence of myrPKI₁₄ promoted an increase in mean dendrite length from $22.41 \pm 0.78 \mu\text{m}$ to $33.28 \pm 0.99 \mu\text{m}$ (Fig. 8.6, panels A and B, *** = $p < 0.001$ vs. 0 h, ### = $p < 0.001$ vs. vehicle). In LNCaP

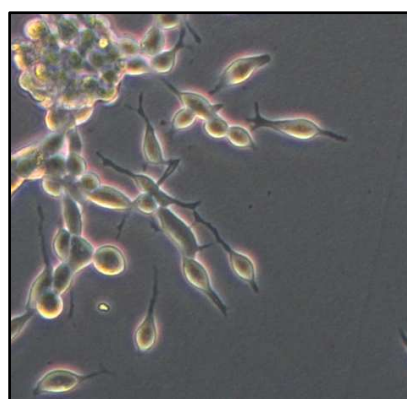
A



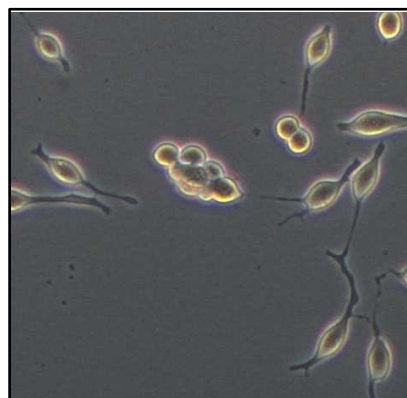
Vehicle



5 μ M H89



10 μ M Fsk



5 μ M H89
+ 10 μ M Fsk

0 h

Post-stimulation

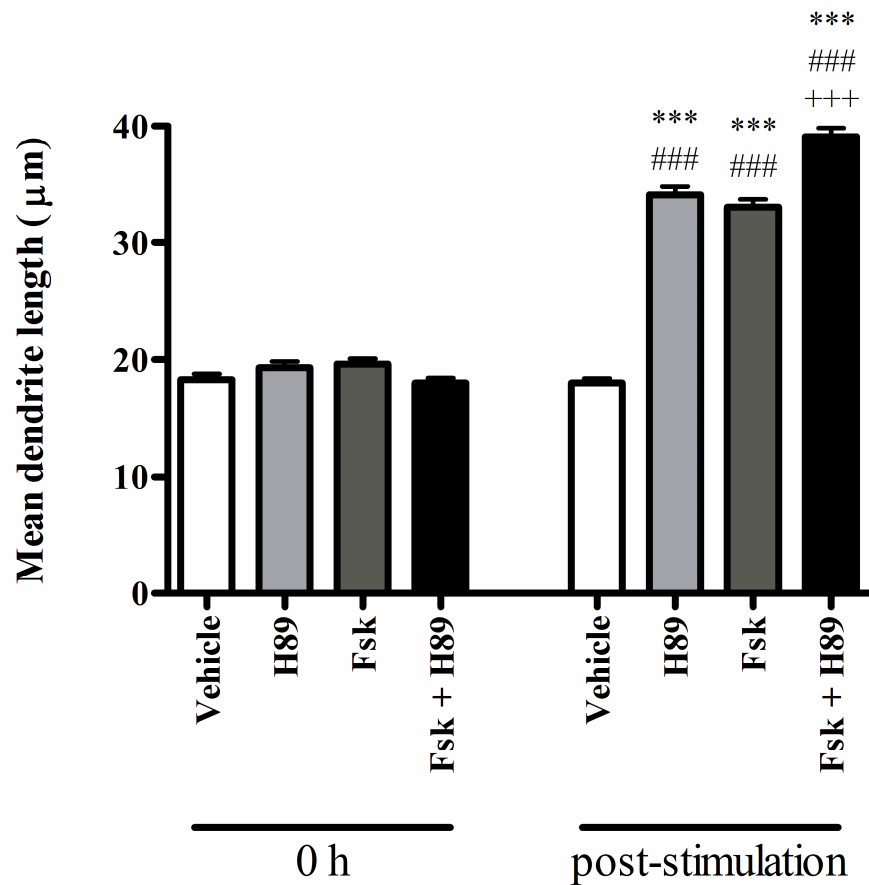
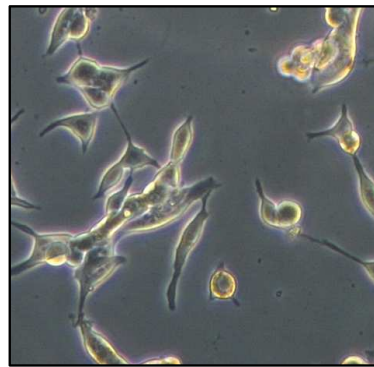
B

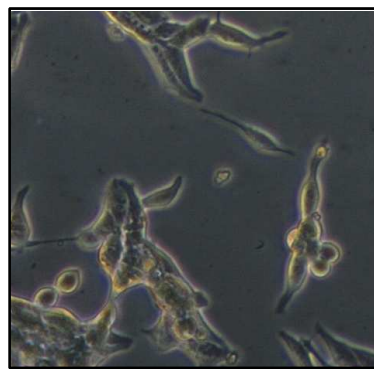
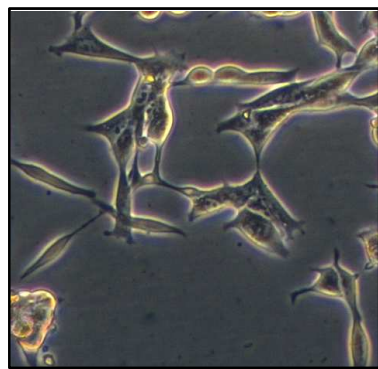
Fig. 8.5: Treatment with the PKA-selective inhibitor H89 mimics the effect of Fsk on LNCaP morphology

LNCaP cells were seeded into 6-well plates and incubated with either vehicle (0.1 % (v/v) DMSO) or 5 µM H89 for 60 min at 37°C, 5 % (v/v) CO₂ prior to stimulation with vehicle (0.1 % (v/v) EtOH) or 10 µM Fsk for a further 60 min at 37°C, 5 % (v/v) CO₂. Images of five random fields per treatment were captured at each time point and changes in LNCaP morphology assessed by measuring mean dendrite length for 30 random cells per field per treatment (panels A and B). Results are presented as mean values ± SEM for *n* = 3 experiments. *** = *p* < 0.001 vs. 0 h, ### = *p* < 0.001 vs. vehicle at same time point, +++ = *p* < 0.001 vs. Fsk at 1 h.

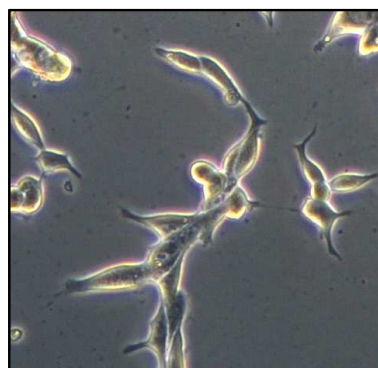
A



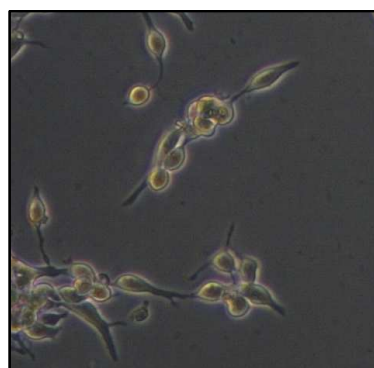
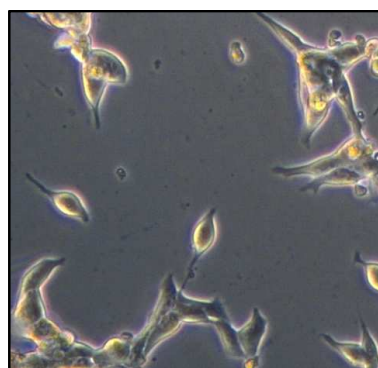
Vehicle



10 nM myr.PKI₁₄₋₂₂



Fsk



10 nM myr.PKI₁₄₋₂₂
+ 10 μ M Fsk

0 h

Post-stimulation

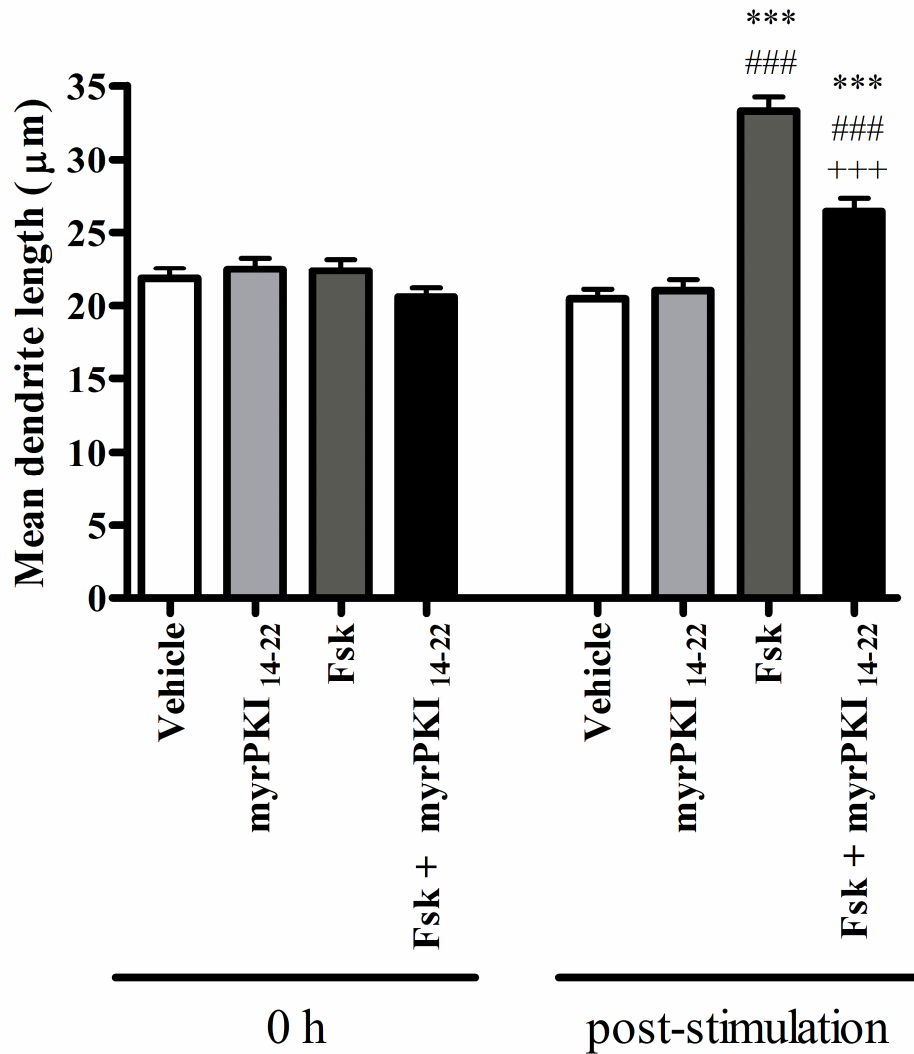


Fig. 8.6: Treatment with the PKA-selective inhibitor myrPKI₁₄₋₂₂ mimics the effect of Fsk on LNCaP morphology

LNCaP cells were seeded into 6-well plates and incubated with either vehicle (0.1 % (v/v) DMSO) or 10 µM myrPKI₁₄₋₂₂ for 60 min at 37°C, 5 % (v/v) CO₂ prior to stimulation with vehicle (0.1 % (v/v) EtOH) or 10 µM Fsk for a further 60 min at 37°C, 5 % (v/v) CO₂. Images of five random fields per treatment were captured at each time point and changes in LNCaP morphology assessed by measuring mean dendrite length for 30 random cells per field per treatment (panles A and B). Results are presented as mean values ± SEM for $n = 3$ experiments. *** = $p < 0.001$ vs. 0 h, ### = $p < 0.001$ vs. vehicle at same time point, +++ = $p < 0.001$ vs. Fsk at 1 h.

cells pre-incubated with myrPKI₁₄₋₂₂, treatment with 10 μ M Fsk was still able to induce an increase in mean dendrite length from $20.57 \pm 0.63 \mu\text{m}$ to $26.44 \pm 0.86 \mu\text{m}$ (Fig. 8.6, panels A and B, *** = $p < 0.001$ vs. 0 h, #### = $p < 0.001$ vs. vehicle). However, the ability of Fsk to induce an increase in mean dendrite length was impaired following incubation with myrPKI₁₄₋₂₂ with mean dendrite length post-stimulation decreasing from $33.28 \pm 0.99 \mu\text{m}$ in the absence of myrPKI₁₄₋₂₂ to $26.44 \pm 0.86 \mu\text{m}$ following pre-incubation with myrPKI₁₄₋₂₂ (Fig. 8.6, panels A and B, +++ = $p < 0.001$ vs. Fsk at 1 h).

The ability of myr.PKI₁₄₋₂₂ to significantly inhibit Fsk-mediated increases in mean dendrite length suggests that the ability of cAMP elevation to promote changes in LNCaP morphology consistent with NE-like differentiation require activation of PKA. Such observations are in keeping with the accepted model of LNCaP differentiation but contradict the previous observation that H89-mediated inhibition of PKA induced increases in mean dendrite length in the absence of cAMP elevation. It is thought that, of the two inhibitors, PKI-based inhibitors represent a more selective inhibitor family than the competitors of ATP binding such as H89 or KT 5720 (Murray, 2008). It is therefore more likely that myr.PKI₁₄₋₂₂-mediated inhibition of Fsk-induced dendrite outgrowth represents the true effect of PKA inhibition on cAMP-induced NE-like differentiation in LNCaP cells and that the ability of H89 to induce morphological changes in these cells arises from non-selective effects.

8.2.8 Inhibitors affecting cAMP signalling are efficacious in the experimental system used

In order to demonstrate that the used, t-Bu-SATE, H89 and myrPKI₁₄₋₂₂, were efficacious in this experimental system, LNCaP cells were seeded into 6-well plates and grown to 70 – 80 % confluence. In order to obtain sufficiently high protein concentrations, it was not possible to perform this analysis on LNCaP cells which had been plated in order to observe dendrite outgrowth as these must be grown to a lower confluence in order to allow dendrites belonging to individual cells to be distinguished. Where possible, analysis of inhibitor efficacy was done in parallel with dendrite outgrowth experiments and always with the same batch of inhibitor used. LNCaP cells were pre-treated with the respective inhibitors for 1 h prior to stimulation with 10 μ M Fsk for 15 min. Inhibitor efficacy was assessed by a decrease in pSer¹³³CREB, a downstream substrate of PKA, and also *via* immunoblotting for a decrease in pThr²⁰²pTyr²⁰⁴ERK1/2 as a secondary indicator because multiple kinases phosphorylate CREB on Ser¹³³. Therefore inhibitor treatment may not

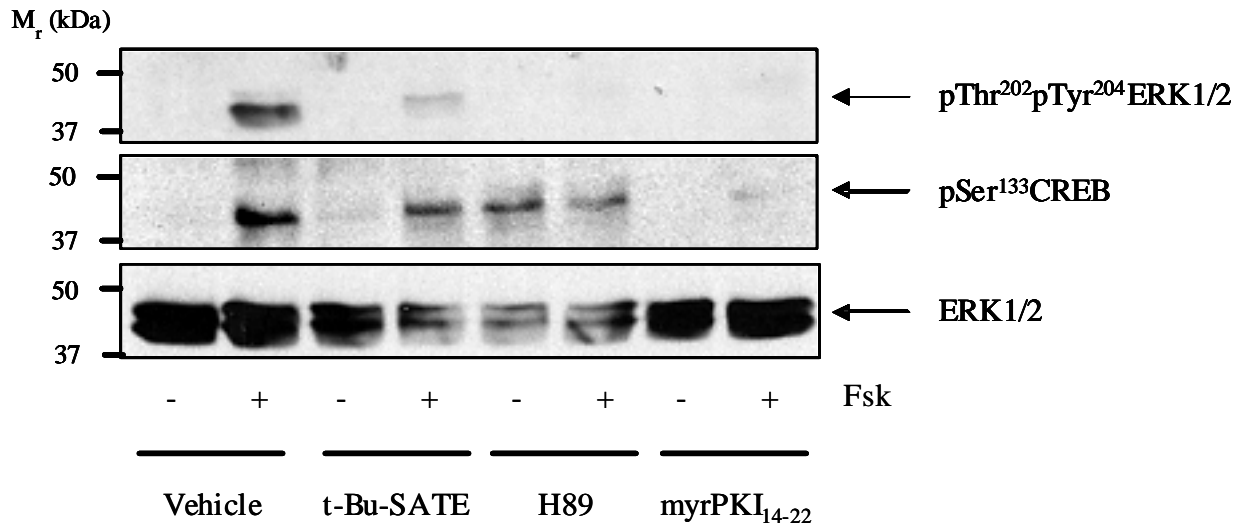


Fig. 8.7: Efficacy of inhibitors of cAMP signalling

LNCaP cells were seeded into 6-well tissue culture plates and grown to 70 % confluence prior to pre-incubation with vehicle (0.4 % (v/v) DMSO), 10 μ M t-Bu-SATE, 5 μ M H89 or 10 nM myrPKI for 1 h. Cells were then stimulated with vehicle (0.1 % (v/v) EtOH) or 10 μ M Fsk for 15 min prior to immunoblotting for pSer¹³³ CREB and pThr²⁰²pTyr²⁰⁴ERK1/2 as indicators of PKA activation. Equal protein loading was determined by immunoblotting for ERK1/2. Blots shown are representative of 3 separate experiments.

completely abolish serine phosphorylation of CREB but may promote inhibition of pThr²⁰²pTyr²⁰⁴ERK1/2, thus demonstrating their efficacy. Treatment with t-Bu-SATE only partially abolished Fsk-induced phosphorylation of CREB and ERK1/2. In preliminary experiments, this is the only concentration of t-Bu-SATE which promoted a decrease in CREB or ERK1/2 phosphorylation (data not shown). As t-Bu-SATE is an AC inhibitor, it is possible that the magnitude of Fsk-induced AC activation in LNCaP cells is supramaximal and thus cannot be completely inhibited by the concentration of t-Bu-SATE used. Pre-treatment with H89 completely abolished Fsk-induced increases in pThr²⁰²pTyr²⁰⁴ERK1/2 but only partially abolished Fsk-induced phosphorylation of CREB. However, myrPKI₁₄₋₂₂ completely abolished Fsk-induced increases in both pThr²⁰²pTyr²⁰⁴ERK1/2 and pSer¹³³CREB. The results shown in Fig. 8.7 suggest that the inhibitors of cAMP-mediated signalling used are indeed efficacious in the experimental system.

8.2.9 Inhibition of Rho-ROCK signalling mimics the effect of Fsk treatment

It was previously found that pre-treatment of LNCaP cells with the PKA-selective inhibitor H89 alone was able to simulate the effects of Fsk on LNCaP morphology and that combined treatment with H89 and Fsk failed to produce a synergistic increase in mean dendrite length, indicating that the two are acting *via* a common pathway. Such data contravenes published data indicating a requirement for PKA activation in cAMP-mediated NE-like differentiation of LNCaP cells (Cox *et al.*, 2000). However, subsequent treatment with the peptide-based myrPKI₁₄₋₂₂ blocked Fsk-induced changes in LNCaP morphology, indicating that this event is PKA-dependent. The mechanisms by which H89 and myrPKI₁₄₋₂₂ act to inhibit PKA are very different and so may explain their different effects on Fsk-induced increases in mean dendrite length in LNCaP cells. Myr.PKI₁₄₋₂₂ is based on an endogenous peptide inhibitor of PKA which mimics the regulatory subunit of PKA and holds the catalytic subunits in an inactive state. Endogenous PKI is highly selective for PKA and the catalytic subunits are thought to be its only *in vivo* substrate (Murray, 2008). In contrast, H89 and the related compound KT 7520, are both competitive antagonists of ATP binding and may therefore show decreased selectivity for PKA in comparison to myr.PKI₁₄₋₂₂ (Murray, 2008). It has been demonstrated that treatment of both the 3T3-L1 adipocyte and the NG 108-15 neuroblastoma-glioma cell lines with H89, at similar concentrations to those used in these experiments, induced cellular differentiation in the absence of other stimuli (Kato *et al.*, 2007; Leemhuis *et al.*, 2002). Of particular note is the observation that in NG 108-15 treatment with H89 can induce neurite outgrowth *via*

inhibition of Rho-activated kinase (ROCK) (Leemhuis *et al.*, 2002). Similarly, H89 was able to induce differentiation in adipocytes *via* a process which could be mimicked by the ROCK-selective inhibitor Y27632, again indicating that H89 is exerting inhibitory effects on ROCKs rather than PKA (Kato *et al.*, 2007). It is possible that actions of H89 on ROCKs in LNCaP cells may explain the opposing effects of myr.PKI₁₄₋₂₂ and H89 on LNCaP morphology.

To test this hypothesis, images of LNCaP cells were captured prior to incubation with either vehicle (0.1 % (v/v) DMSO) or 5 μ M of the ROCK-selective inhibitor Y27632 (Ishizaki *et al.*, 2000) at 37°C, 5 % (v/v) CO₂. LNCaP cells were then incubated for 1 h in the presence of either vehicle (0.1 % (v/v) EtOH) or 10 μ M Fsk and images captured post-stimulation. In keeping with previous experiments, incubation with vehicle did not result in a change in LNCaP morphology (Fig. 8.8, panels A and B, $p > 0.05$ at post-stimulation *vs.* 0 h) and pre-incubation with vehicle did not inhibit Fsk-induced increases in mean dendrite length from $17.86 \pm 0.47 \mu\text{m}$ at 0 h to $32.79 \pm 0.76 \mu\text{m}$ post-stimulation (Fig. 8.8, panels A and B, *** = $p < 0.001$ *vs.* 0 h, #### = $p < 0.001$ *vs.* vehicle at same time point). As anticipated, incubation with Y29632 in the absence of Fsk induced an increase in mean dendrite length from $16.42 \pm 0.43 \mu\text{m}$ to $25.40 \pm 0.57 \mu\text{m}$ although the increase in mean dendrite length was not as great as seen with Fsk treatment alone (Fig. 8.8, panels A and B, *** = $p < 0.001$ *vs.* 0 h, #### = $p < 0.001$ *vs.* vehicle at same time point, +++ = $p < 0.001$ *vs.* Fsk). However, combined treatment of LNCaP cells with 5 μ M Y27632 followed by stimulation with 10 μ M Fsk did not produce a synergistic increase in mean dendrite outgrowth with mean dendrite length increasing from $17.42 \pm 0.46 \mu\text{m}$ to $35.77 \pm 0.77 \mu\text{m}$ throughout the experiment (Fig. 8.8, panels A and B, *** = $p < 0.001$ *vs.* 0 h, #### = $p < 0.001$ *vs.* vehicle at same time point, +++ = $p < 0.001$ *vs.* Fsk). Whilst the increase in Fsk-induced dendrite outgrowth was found to be significantly greater following pre-incubation with Y27632, it is unlikely that an increase in mean dendrite length of 3 μm represents a biologically significant change and is more a result of the large number of cells measured.

In order to assess the efficacy of Y27632 in this experimental system, LNCaP cells were grown on coverslips coated with 0.1 mg/ml poly-D-lysine prior to incubation with Y27632 and Fsk as described above. The actin cytoskeleton was then visualised *via* staining with 10 U/ml rhodamine-conjugated phalloidin as described in Materials and Methods and images subsequently captured using a Zeiss Pascal Exciter laser scanning confocal microscope. Treatment with Y27632 resulted in an increase in punctate regions of actin

staining, indicative of a decrease in actin polymerisation and inhibition of ROCK signalling (Fig. 8.8, panel D, arrows indicate punctate regions)

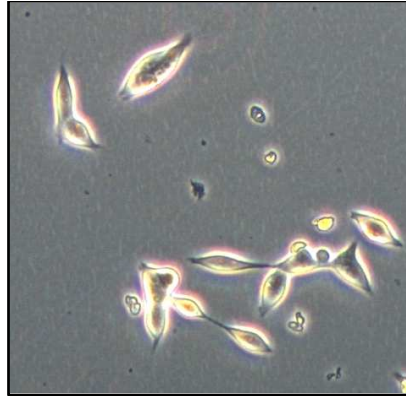
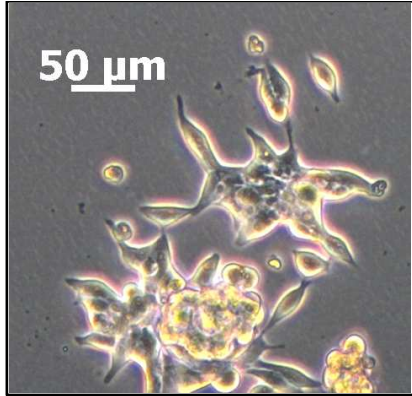
The ability of Y27632 to mimic the effect of Fsk on LNCaP morphology suggests that inhibition of ROCK signalling can promote NE-like differentiation in LNCaP cells. Furthermore, in conjunction with the experiments using myrPKI₁₄₋₂₂, the results support the hypothesis that the effects of H89 on cell morphology arise due to inhibition of ROCK activity rather than PKA-selective effects. The inability of combined Y27632 and Fsk incubation to exert additive effects on increases in mean dendrite length suggest that the two agents act through a common pathway.

8.2.10 Inhibition of RhoA activity mimics the effects of Fsk on LNCaP morphology

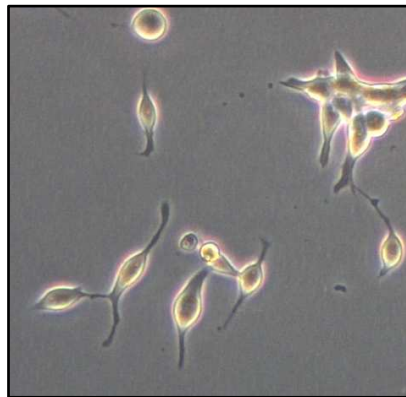
Incubation with the ROCK-selective inhibitor Y27632 induced an increase in mean dendrite length in LNCaP cells and failed to potentiate Fsk-induced increases in mean dendrite length. These results indicate that Fsk may inhibit ROCK activation to promote differentiation to a NE-like morphology. Activation of ROCK occurs downstream of RhoA, therefore it is possible that inhibition of RhoA may also promote the observed changes in LNCaP morphology seen with Y27632. To address this issue, a cell permeable inhibitor of RhoA derived from the C3 transferase (C3T) of *Clostridium botulinum* was used. C3T acts to ADP-ribosylate N41 of RhoA and inhibits activation of RhoA by increasing the steady state GTPase activity of RhoA by 50 – 80 % and thus reducing the time frame in which RhoA is in its GTP-bound, active form (Mohr *et al.*, 1992).

LNCaP cells were seeded into 6-well plates as described previously and grown to approximately 50 % confluency. Prior to each experiment, cell culture medium was replaced with fresh culture medium containing either vehicle (2 % (v/v) PBS) or 4 µg/ml cell permeable C3T. Images were captured at 0 h post-incubation with C3T and again at 6 h post-stimulation at which point robust inhibition of RhoA by C3T should have been achieved. LNCaP cells were then stimulated with vehicle (0.1 % (v/v) EtOH) or 10 µM Fsk for 1 h and images captured post-stimulation as described previously. Treatment with vehicle failed to induce any changes in mean dendrite length at 0 h (20.04 ± 0.57 µm), 6 h (20.63 ± 0.61 µm) and post-stimulation (20.94 ± 0.55 µm, Fig. 8.9, panels A and C), indicating that any changes in mean dendrite length do not arise from vehicle effects. In keeping with previous data, LNCaP cells pre-incubated with vehicle show no change in mean dendrite length at 0 h (23.08 ± 0.66 µm) or 6 h (23.48 ± 0.70 µm) but stimulation

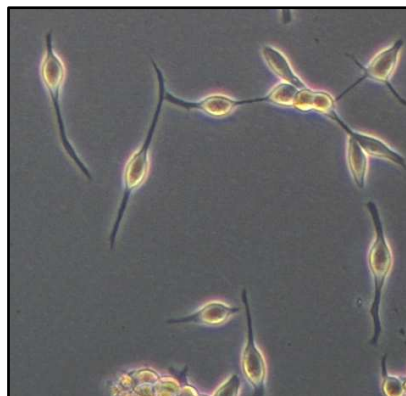
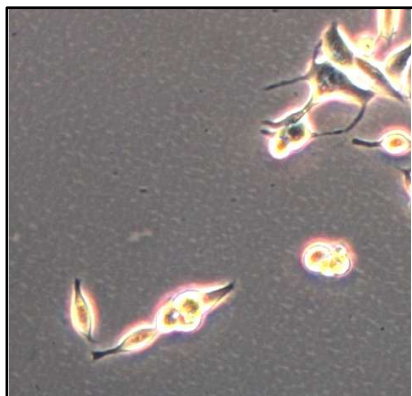
A



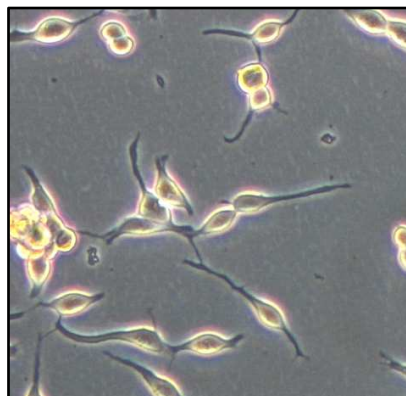
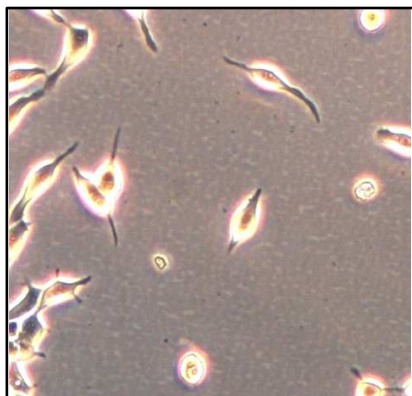
Vehicle



5 μ M Y27632



10 μ M Fsk



5 μ M Y27632
+ 10 μ M Fsk

0 h

Post-stimulation

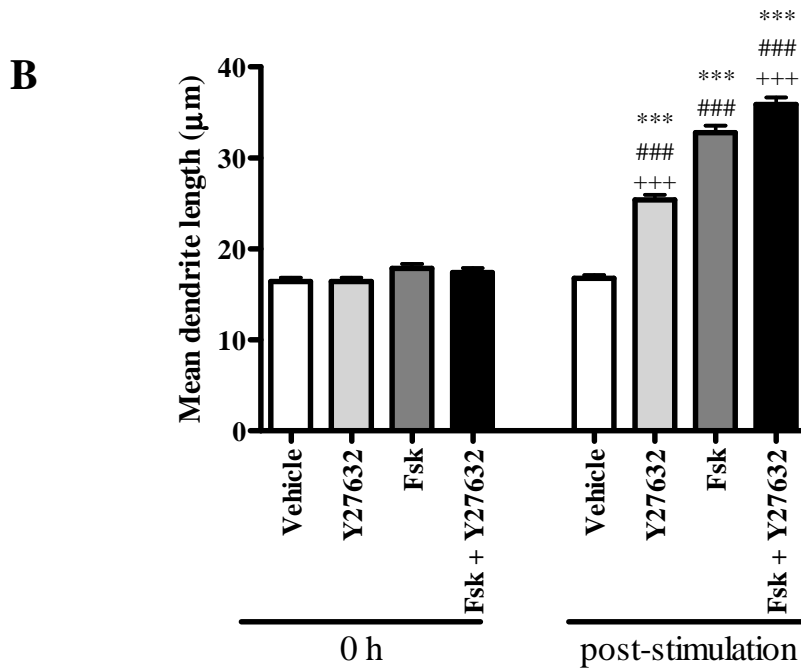
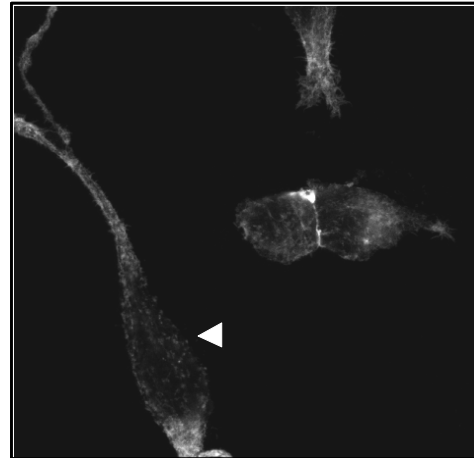
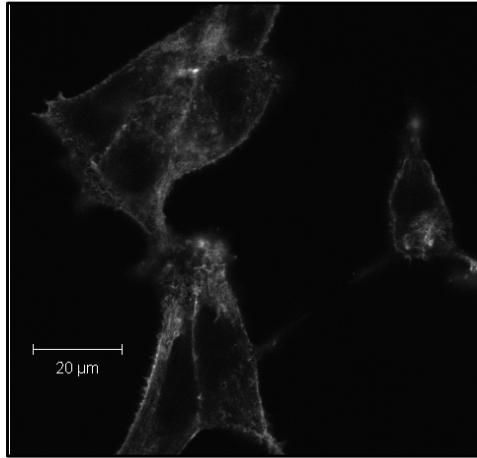


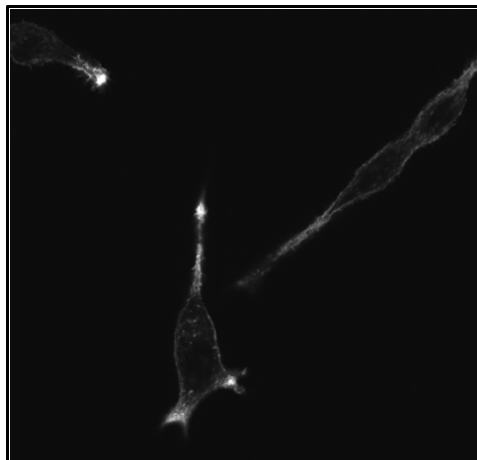
Fig. 8.8: Inhibition of ROCK signalling by Y27632 recapitulates the effect of Fsk on LNCaP morphology

LNCaP cells were seeded into 6-well plates and incubated with either vehicle (0.5% (v/v) DMSO) or 5 μ M Y27632 for 60 min at 37°C, 5 % (v/v) CO₂ prior to stimulation with vehicle (0.1 % (v/v) EtOH) or 10 μ M Fsk for a further 60 min at 37°C, 5 % (v/v) CO₂. Images of five random fields per treatment were captured at each time point (panel A) and changes in LNCaP morphology assessed by measuring mean dendrite length for 30 random cells per field per treatment. Results are presented as mean values \pm SEM for $n = 3$ experiments (panel B). *** = $p < 0.001$ vs. 0 h, ### = $p < 0.001$ vs. vehicle at same time point, +++ = $p < 0.001$ vs. Fsk at 1 h. To assess the efficacy of Y27632, the disruption of stress fibres was visualised by rhodamine-conjugated phalloidin staining of the actin cytoskeleton (panel C). Arrows denote regions of punctate actin cytoskeletal staining, indicative of a decrease in polymerised actin and inhibited ROCK signalling.

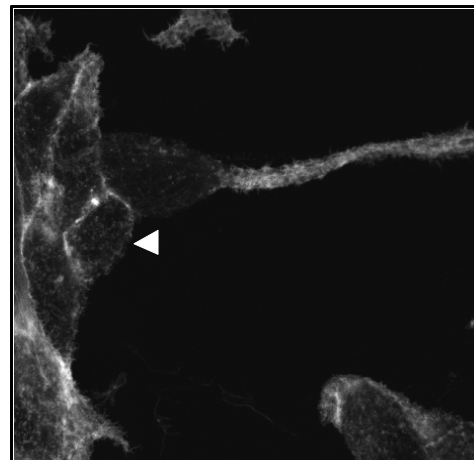
C



Vehicle



Vehicle



5 μM Y27632

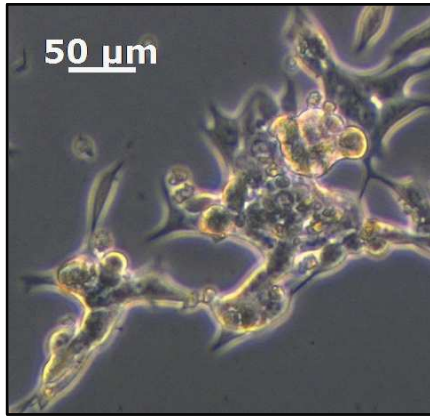
10 μM Fsk

with 10 μM Fsk results in an increase in mean dendrite length to $31.49 \pm 0.74 \mu\text{m}$ (Fig. 8.9, panels A and C, *** = $p < 0.001$ vs. 0 h, #### = $p < 0.001$ vs. vehicle). As expected, treatment with 4 $\mu\text{g/ml}$ C3T resulted in an increase in mean dendrite length from $20.03 \pm 0.63 \mu\text{m}$ at 0 h to $28.45 \pm 0.85 \mu\text{m}$ at 6 h and $31.29 \pm 0.85 \mu\text{m}$ at the end of the experiment (Fig. 8.9, panels B and C, *** = $p < 0.001$ vs. 0 h, #### = $p < 0.001$ vs. vehicle). Similar results were obtained in the LNCaP cells which pre-incubated with C3T for 6 h with mean dendrite length increasing from $21.87 \pm 0.65 \mu\text{m}$ at 0 h to $35.30 \pm 0.88 \mu\text{m}$ at 6 h post-stimulation stimulation (Fig. 8.9, panels B and C, *** = $p < 0.001$ vs. 0 h, #### = $p < 0.001$ vs. vehicle). Stimulation with Fsk failed to induce further increases in mean dendrite length from that seen at 6 h post-incubation with Fsk ($34.63 \pm 0.87 \mu\text{m}$, Fig. 8.9, panels B and C, *** = $p < 0.001$ vs. 0 h, #### = $p < 0.001$ vs. vehicle, $p > 0.05$ vs. 6 h).

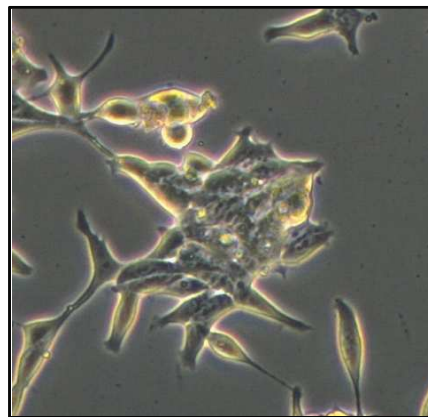
Membrane translocation of RhoA is associated with activation of the protein (Thibault *et al.*, 2000), thus to assess whether Fsk was able to inactivate RhoA, the presence of RhoA in LNCaP membranes was detected. LNCaP cells were treated in serum-free medium for 6 h in the presence of either vehicle (0.1 % (v/v) PBS) or 1 $\mu\text{g/ml}$ C3T prior to stimulation with either vehicle (0.1 % (v/v) EtOH) or 10 μM Fsk for 1 h. Membranes were prepared as described in Chapter 5 and the presence of RhoA in the membrane preparations assessed *via* immunoblotting. As observed in Fig. 8.9 (panel D), treatment with 10 μM Fsk in the presence or absence of C3T resulted in a decrease in detected RhoA in LNCaP cell membrane preparations, suggestive that Fsk is able to inhibit RhoA activation. It must be noted however that equal loading could not be determined due to high background staining of anti- $\text{G}\alpha_i$ antibodies which were used as loading controls for membrane fractions.

The ability of C3T to recapitulate the effects of Fsk on LNCaP morphology suggests that inhibition of RhoA activity is important in the development of this phenotype. Furthermore, the lack of additive increases in mean dendrite length following combined C3T and Fsk treatment imply that the ability of these two compounds to induce NE-like morphological changes in LNCaP cells is mediated by a common signalling pathway. It is possible that treatment with Fsk may act to directly inhibit RhoA. Of particular concern is the observation that TRIO-GEF plays a role in axon guidance and is able to activate RhoG and RhoA/Rac-1 *via* its two distinct GEF domains to promote changes in cell morphology (Bellanger *et al.*, 2000). Due to the lack of published data regarding the specificity of C3T for RhoG in comparison to RhoA, the peptide sequences of all described human Rho family members were aligned using the clustalW algorithm (Thompson *et al.*, 1994) and examined for the presence of key residues implicated in recognition of RhoA by C3T (Fig.

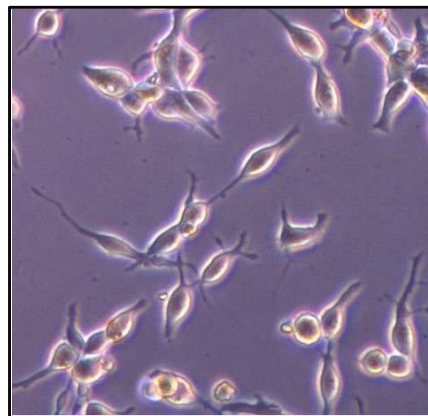
A



0 h



6 h

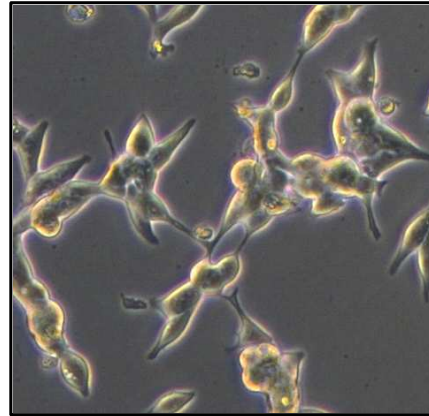


Post-stimulation

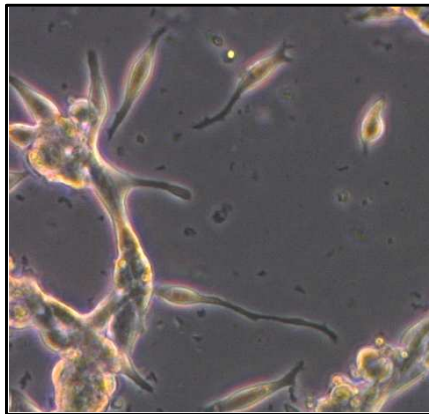
Vehicle

10 μ M Fsk

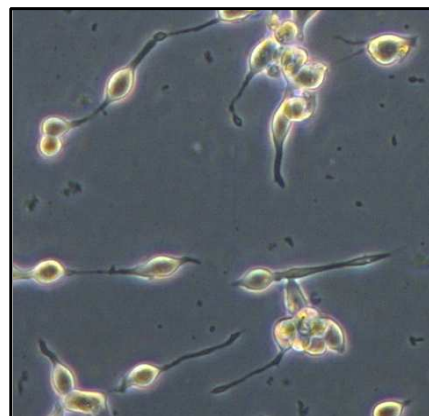
B



0 h



6 h



Post-stimulation

4 $\mu\text{g/ml}$ C3T

4 $\mu\text{g/ml}$ C3T
+ 10 μM Fsk

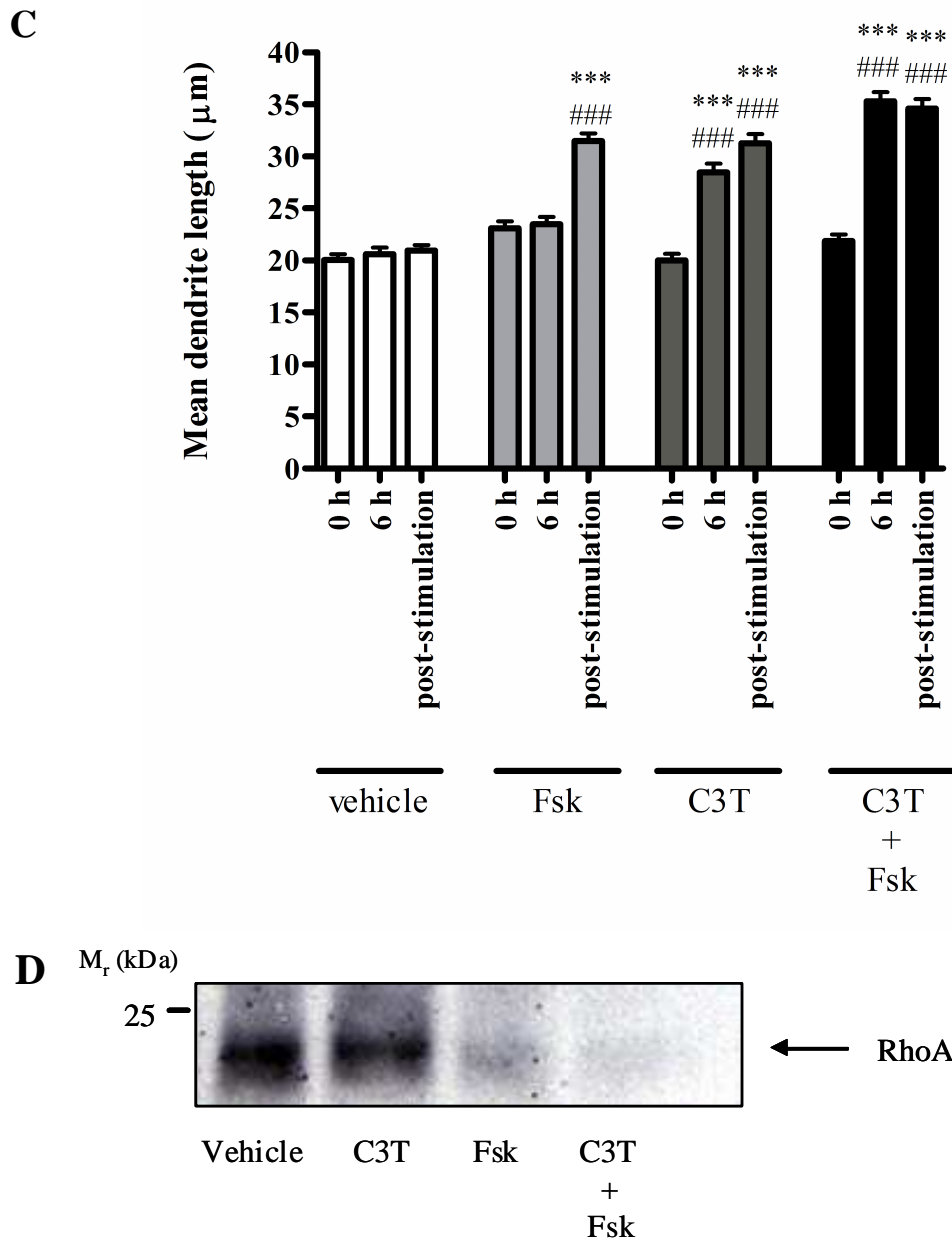


Fig. 8.9: Inhibition of RhoA causes changes in LNCaP morphology consistent with NE-like differentiation

LNCaP cells were plated into 6-well plates and incubated for 6 h with either vehicle (2 % (v/v) PBS) (panel A) or 4 $\mu\text{g/ml}$ C3T (panel B) prior to stimulation with either vehicle (0.1% (v/v) EtOH) or 10 μM Fsk for 1 h. Images were captured as described at 0 h (0 h), 6 h post-stimulation (6 h) and following stimulation with Fsk (post-stimulation). Changes in LNCaP morphology consistent with NE-like differentiation were assessed *via* increases in mean dendrite length (panel C). Activation of RhoA was assessed *via* an increase in membrane localised RhoA (panel D). Results are represented as mean values \pm SEM for $n = 3$ separate experiments. *** = $p < 0.001$ vs. 0 h, ### = $p < 0.001$ vs. vehicle

8.10). The 90 N-terminal residues of RhoA have been demonstrated to provide the minimum sequence required for recognition by C3T with the combined presence of the basic Arg⁵Lys⁶ sequence with the acidic Glu⁴⁷/Glu⁵⁴ motif resulting in an increase in C3T-mediated ADP-ribosylation and promotes binding of RhoA to C3T (Wilde *et al.*, 2000). Mutation of Rac, a non-C3T substrate, to include these motifs promotes interaction with C3T but required the inclusion of mutations either side of the Asp residue (equivalent to S43V and M47E of Rac) to enable full ADP-ribosylation of Rac, indicating that the equivalent residues are important in C3T-mediated ADP ribosylation of RhoA (Wilde *et al.*, 2000). Indeed these residues have been implicated in correct formation of the C3T/NAD⁺/RhoA ternary complex required for ADP-ribosylation (Wilde *et al.*, 2000). Of importance is the observation that only RhoA, RhoB and RhoC have the correct configuration of residues to mediate recognition and ADP-ribosylation by C3T, thus providing evidence that the ability of C3T to induce dendrite outgrowth in LNCaP cells arises due to inhibition of RhoA rather than effects on other Rho family members including RhoG.

8.2.11 Expression of constitutively active RhoA blocks Fsk-induced increases in mean dendrite length

Pharmacological blockade of RhoA/ROCK signalling mimics the effect of cAMP elevation on LNCaP cell morphology. Such results suggest that activation of RhoA would therefore block Fsk-induced changes in LNCaP cell morphology. In order to address this, LNCaP cells were transfected with 1 µg of cDNA encoding either vector (pRK5), wild-type RhoA (myc.RhoAWT), a dominant negative RhoA (myc.RhoAT19N) or a constitutively active RhoA (myc.RhoAQ63L).

LNCaP cells transfected with either vector or myc.RhoAWT displayed no difference in mean dendrite length, indicating that any effects of myc.RhoAT19N or myc.RhoAQ63L expression are not due to the transfection procedure or to over-expression of RhoA. Fsk stimulation of LNCaP cells transfected with myc.RhoAWT resulted in an increase in mean dendrite length comparable with that seen in vector-treated cells, indicating that over-expression of RhoA does not alter cellular responses to Fsk. Expression of the constitutively active myc.RhoAQ63L resulted in a decrease in mean dendrite length in the absence of Fsk stimulation (Fig. 8.11 panels A and B, +++ = $p < 0.001$ vs. other constructs) and prevented Fsk-induced increases in mean dendrite length (Fig. 8.11 panels A and B, +++ = $p < 0.001$ vs. other constructs). These results suggest that activation of RhoA is able to block Fsk-induced changes in LNCaP cell morphology. In contrast, it was expected that

P61586_RhoA -----MAAIRK^{KL}LVIVGDGACGKTCLLIVFSKD 28
P62745_RhoB -----MAAIRK^{KL}LVVVG DGACGKTCLLIVFSKD 28
P08134_RhoC -----MAAIRK^{KL}LVIVGDGACGKTCLLIVFSKD 28
O00212_RhoD -----MTAAQAAGEEAPPG--VRSVKVVLVGDGGCGKTSLLMVFADG 40
P61587_RhoE -----MKERRASQKLSKSI^{MDPNQNVKCK}IVVVGDSQCGKTALLHVFAKD 46
Q9HBH0_RhoF -----MDAPGALAQTAAPGPGRKELK^IVIVGDGGCGKTSLLMVYSQG 42
P84095_RhoG -----MQSIKCVVVG DGAVGKTCLLIC^YTTN 26
Q15669_RhoH -----MLSSIKCVLVGDSAVGKTSLLVRF^TSE 27
O95661_RhoI MGNASFGSKEQKLLKRLRL^LPALLILRAF^KPHRK^{IRDYR}VVVVGTAGV^GKSTLLHKWASG 60
Q9H4E5_RhoJ -----MNCKEGT^DSSCGCRGNDEK^MMLK^{CVV}VGDGAVGKTCLLSYAND 44
P52198_RhoN -----ME-GQSGRCK^IVVVGDAECGKTALLQVFAKD 30
P17081_RhoQ -----MAHGPG-----ALMLK^{CVV}VGDGAVGKTCLLSYAND 32

: *:* . ** : ** :

P61586_RhoA QFPEVYVPTVFE^{NY}VADI^EV^DGKQV^EELALWDTAGQEDYDRLRPLSY^PDTDVILMCF^SSIDS 88
P62745_RhoB QFPEVYVPTVFE^{NY}VADI^EV^DGKQV^EELALWDTAGQEDYDRLRPLSY^PDTDVILMCF^SSVDS 88
P08134_RhoC QFPEVYVPTVFE^{NY}IADI^EV^DGKQV^EELALWDTAGQEDYDRLRPLSY^PDTDVILMCF^SSIDS 88
O00212_RhoD AFPESYTPTVF^ERYM^NLQV^KGK^PVH^LHIWDTAGQDDYDRLRPL^FYPDASV^LLLCFD^VTS 100
P61587_RhoE CFPENYVPTVFE^{NY}TAS^FE^IDTQRI^ELSLWDTSGSPY^DNVRPLSY^PDSDAV^LLICFD^ISR 106
Q9HBH0_RhoF SFPEHYAPSVF^EKYTASV^TVGSKEV^TLNLYDTAGQEDYDRLRPLSY^QNTHLV^LLICYD^VMN 102
P84095_RhoG AFPKEYIPTVFD^{NY}SAQSAVDGR^TVN^LNLWDTAGQEEYDRLR^TLSY^PQTNV^FVIC^FSIAS 86
Q15669_RhoH TFP^EAYKPTVY^ENGVDV^FMDGI^QISLGLWDTAGNDA^FRSIRPLSY^QQADV^VLMCYS^VAN 87
O95661_RhoI NFRHEYLPTIENTY^CQLLGC^SH^GVL^SLHITDSKSGDGN^RALQRH^VIARGHAFV^LVYS^VTK 120
Q9H4E5_RhoJ AFPEEYVPTVFDHYAV^TTV^VGGK^QHLLGLYDTAGQEDYN^QLRPLSY^PNTDV^FLIC^FSV^VN 104
P52198_RhoN AYPGSYVPTVFE^{NY}TAS^FE^IDKRR^EELNMWDTSGSSY^DNVRPLAY^PDSDAV^LLICFD^ISR 90
P17081_RhoQ AFPEEYVPTVFDHYAVS^VTV^VGGK^QYLLGLYDTAGQEDYDRLRPLSY^PM^TDV^FLIC^FSV^VN 92

: * * : : * : * : . : : . : : :

P61586_RhoA PD 90
P62745_RhoB PD 90
P08134_RhoC PD 90
O00212_RhoD PN 102
P61587_RhoE PE 108
Q9HBH0_RhoF PT 104
P84095_RhoG PP 88
Q15669_RhoH HN 89
O95661_RhoI KE 122
Q9H4E5_RhoJ PA 106
P52198_RhoN PE 92
P17081_RhoQ PA 94

Fig 8.10: Identification of residues within the N-terminus of human Rho family members which are important for interaction with C3T

Protein sequences corresponding to the known human Rho family members were retrieved from the UniProt knowledge base and aligned using ClustalW. The N-terminus of RhoA was then compared to other family members in order to assess whether they showed similar motifs to those implicated in the binding of C3T to RhoA and subsequent ADP-ribosylation. **X** = site of ADP-ribosylation, equivalent to N41 **X** = residues involved in C3T recognition, equivalent to R5, K6, E47 and E54 **X** = residues involved in correct ternary complex formation between Rho, C3T and NAD⁺, corresponding to E40 and V43. All amino acid positions refer to the position of these residues in RhoA.

expression of myc.RhoAT19N in LNCaP cells would both mimic the effect of Fsk on LNCaP cell morphology in the absence of other stimuli and potentiate Fsk-induced dendrite outgrowth. However, whilst expression of myc.RhoAT19N resulted in an increase in mean dendrite length in some transfected wells, this effect was minor in comparison to Fsk-induced changes in mean dendrite length and was not uniform for all wells transfected with myc.RhoAT19 (Fig. 8.11 panels A and B, +++ = $p < 0.001$ vs. other constructs).

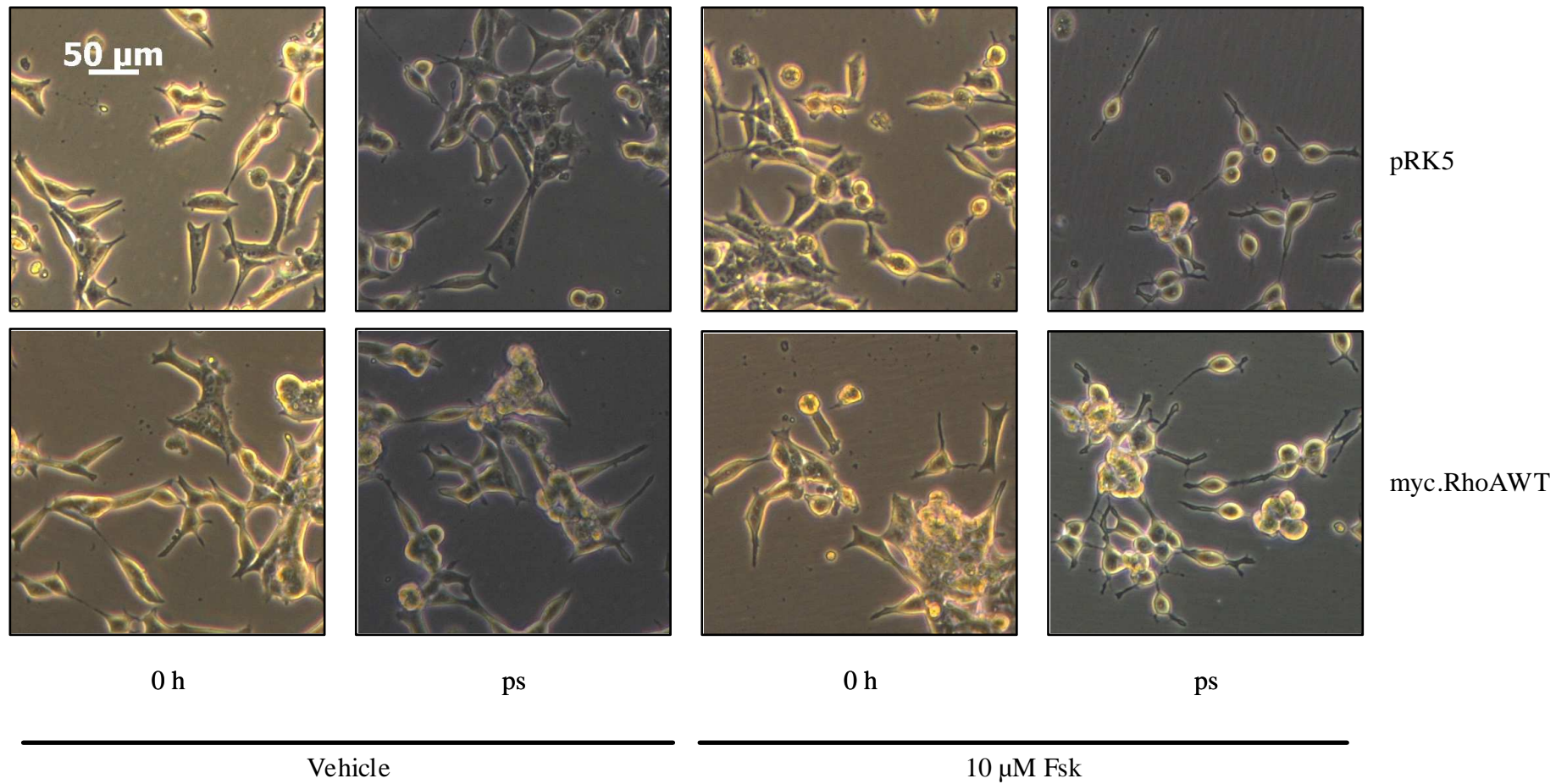
Furthermore, expression of myc.RhoAT19N did not potentiate Fsk-induced changes in LNCaP cell morphology and caused an increase in mean dendrite length comparable with that observed in cells transfected with pRK5 or myc.RhoAWT (Fig. 8.11, panels A and B, *** = $p < 0.001$ vs. 0 h, ### = $p < 0.001$ vs. vehicle). When comparative expression of the different myc.RhoA constructs was determined *via* immunoblotting for the myc epitope, it was found that expression of myc.RhoAT19N was lower than that of the other constructs (Fig. 8.11, panel C).

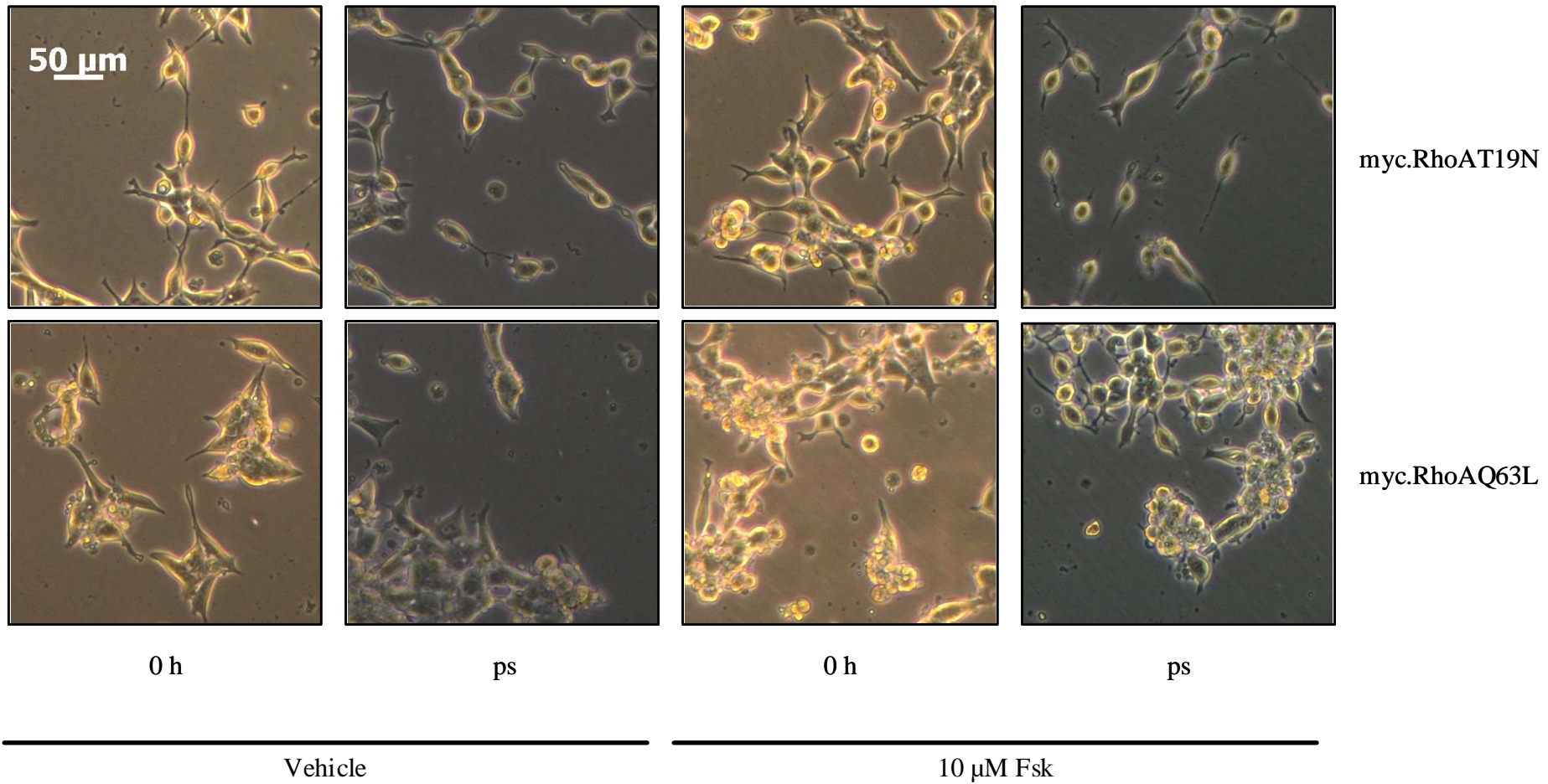
To determine whether the lack of effect of RhoAT19N expression on Fsk-induced dendrite outgrowth was a result of lower expression of myc.RhoAT19N, LNCaP cells were transfected with 1.5 μ g of myc.RhoAT19N. To ensure that any effects of myc.RhoAT19N expression were not a result of increases in the amount of cDNA used, LNCaP cells were transfected in parallel with 1.5 μ g of pRK5. LNCaP cells were also transfected with 1 μ g of either myc.RhoAWT or myc.RhoAQ63L as *per* previous experiments. Whilst LNCaP cells transfected with pRK5, myc.RhoAWT or myc.RhoAQ63L appeared healthy post-transfection, expression of myc.RhoAT19N resulted in cell detachment and death (Fig. 8.11, panel D), indicating that higher expression of dominant negative RhoA in LNCaP cells was not possible.

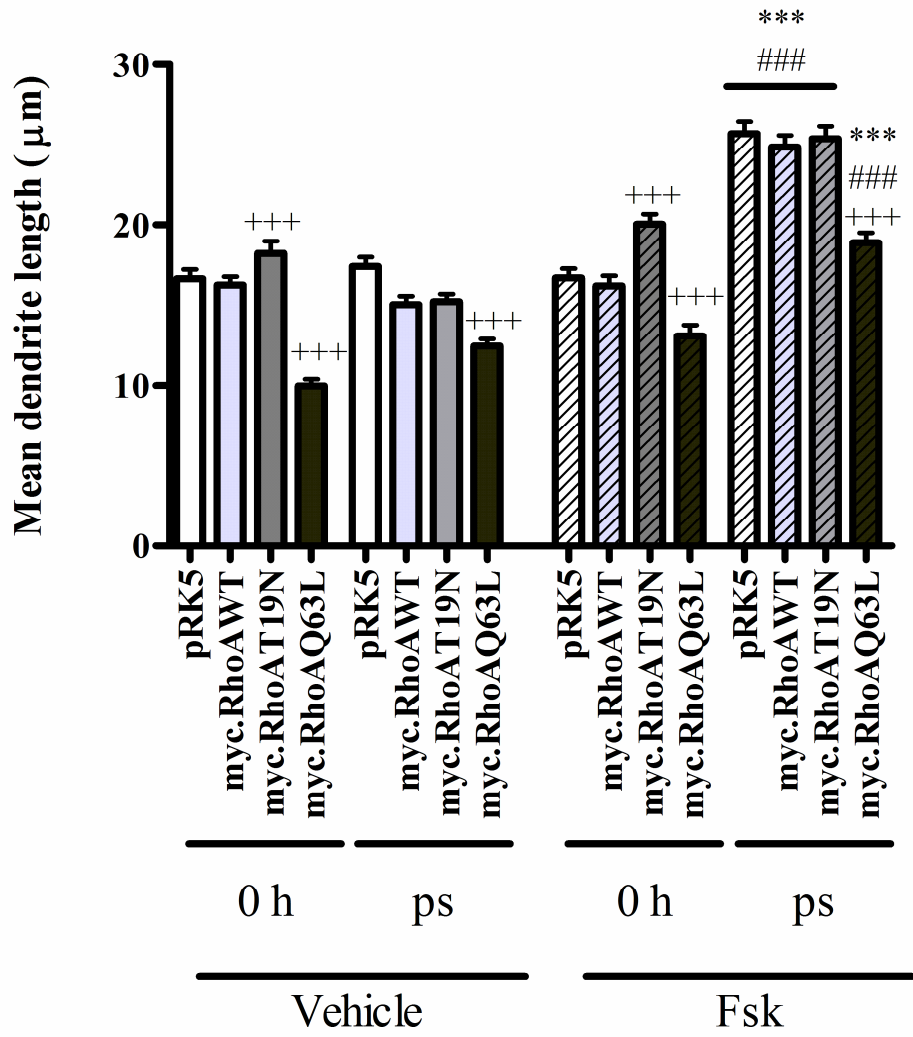
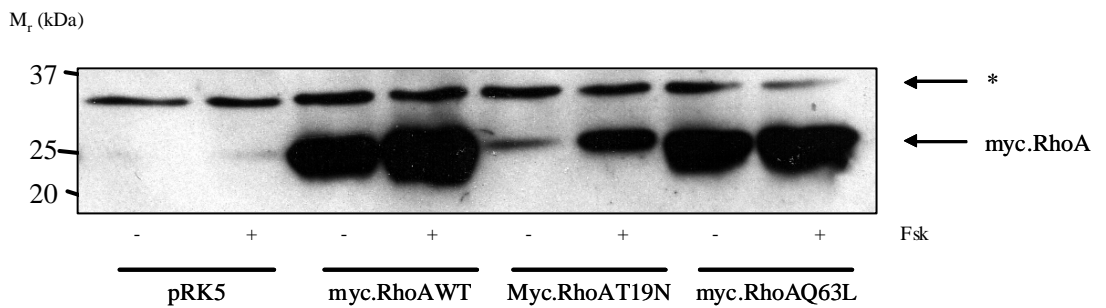
8.2.12 Actin depolymerisation mimics the effects of Fsk on LNCaP cell morphology

Given the importance of the RhoA-ROCK signalling pathway in regulating actin cytoskeletal dynamics, the ability of Fsk to induce dendrite outgrowth in the absence of a functional actin network was assessed. LNCaP cells were seeded onto glass coverslips coated with 0.1 mg/ml poly-D-lysine and grown to 50-60 % confluence. Cells were pre-incubated with either vehicle (1 % (v/v) DMSO) or 100 mg/ml cytochalasin B for 1 h at 37°C, 5 % (v/v) CO₂ in order to disrupt the actin cytoskeleton prior to stimulation with either vehicle (0.1 % (v/v) EtOH) or 10 μ M Fsk for 1 h. Images were captured at 0 h and post-stimulation. In order to determine the efficacy of cytochalasin B, the actin

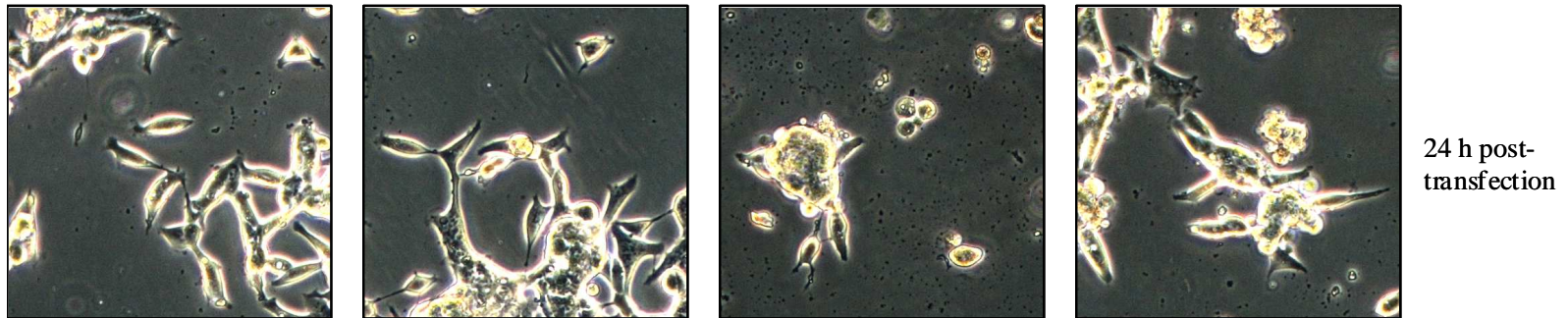
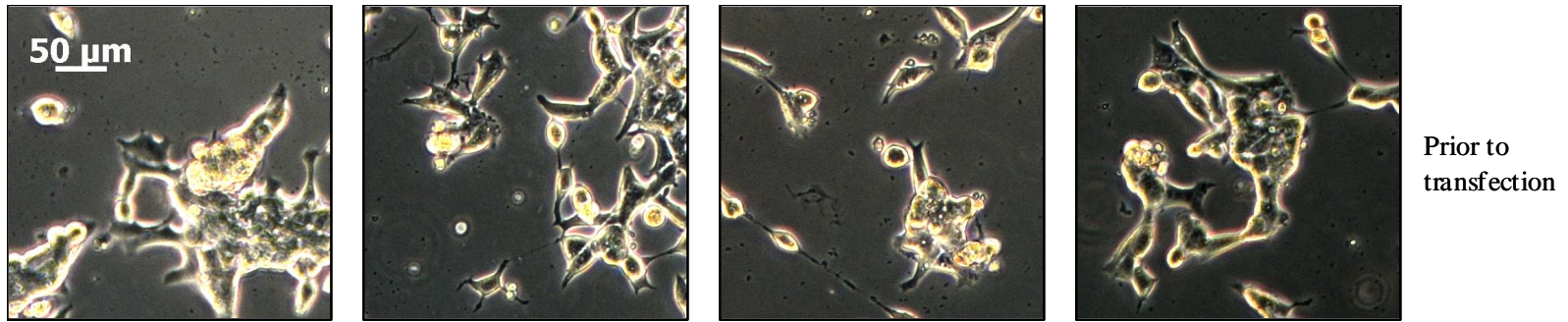
A





B**C**

D



pRK5

myc.RhoAWT

myc.RhoAT19N

myc.RhoAQ63L

Fig. 8.11: Expression of a dominant negative RhoA blocks Fsk-induced changes in LNCaP cell morphology

LNCaP cells were plated into 6-well plates and transfected with 1 μg of either pRK5, myc.RhoAWT, myc.RhoAT19N, myc.RhoAQ63L as described in Chapter 5. Cells were then stimulated with vehicle and 10 μM Fsk and images were captured as described at 0 h (0 h) and 1 h post-stimulation (ps) (panel A). Changes in LNCaP morphology consistent with NE-like differentiation were assessed *via* increases in mean dendrite length (panel B). Expression of RhoA mutants was assessed *via* immunoblotting for the myc epitope (panel C). In order to increase cellular expression of RhoAT19N, LNCaP cells with 1.5 μg of pRK5 and myc.RhoAT19N (panel D). Results are represented as mean values \pm SEM for $n = 3$ separate experiments. *** = $p < 0.001$ vs. 0 h, ### = $p < 0.001$ vs. vehicle, +++ = $p < 0.001$ vs. pRK5

cytoskeleton was visualised using rhodamine-conjugated phalloidin as described in chapter 4 and images captured using a 63 x magnification oil immersion objective on a Zeiss Pascal Exciter 5 laser scanning confocal microscope.

Treatment with cytochalasin B promoted morphological changes consistent with Fsk-induced NE-like differentiation in LNCaP cells in the absence of Fsk stimulation and failed to synergise with Fsk to promote an increase in mean dendrite length (Fig. 8.12, panels A and B). Although treatment with cytochalasin B effectively induced a similar morphology as that seen with Fsk treatment, it must be noted that dendrites occurring following treatment with cytochalasin B appeared less robust than those seen following Fsk treatment as evidenced by gaps in the extensions (Fig. 8.12, panel A, indicated by arrows). As anticipated, treatment with cytochalasin B effectively disrupted the cytoskeleton with a decrease in stress fibres observed between vehicle (Fig. 8.12, panel C, arrow a) and cytochalasin B-treated cells (Fig. 8.12, panel C, arrow B).

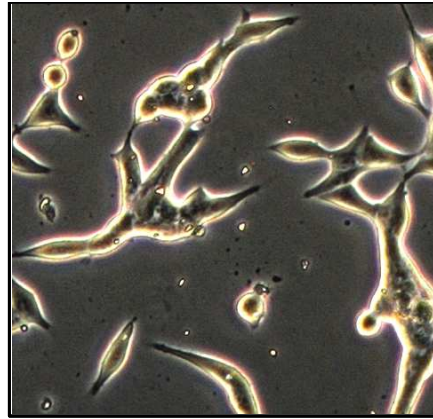
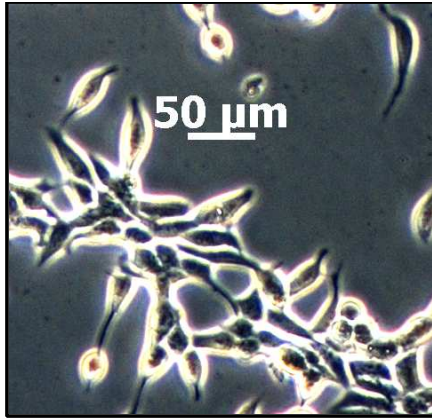
These results suggest that the Fsk is able to modulate actin cytoskeletal dynamics in a similar way to that seen with cytochalasin B treatment and indicate that Fsk is able to inhibit actin polymerisation. Such a result is consistent with the hypothesis that Fsk promotes NE-like differentiation of LNCaP cells through inhibition of RhoA-ROCK signalling.

8.2.13 Selective activation of PKA recapitulates the effect of Fsk on LNCaP cell morphology

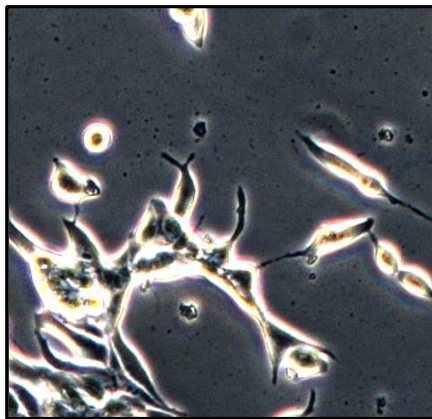
Whilst previous results indicate that the ability of Fsk to induce changes in LNCaP cell morphology is mediated through activation of PKA and simultaneous inhibition of RhoA activity. In order to demonstrate that PKA is indeed the predominant cAMP sensor involved in this phenomenon, LNCaP cells were treated with either vehicle (1 % (v/v) DMSO), 100 μ M of the PKA-selective agonist N⁶-Benzoyl-cAMP (6-Bnz-cAMP), 10 μ M Fsk or a combination of Fsk and 6-Bnz-cAMP for 1 h. Phase contrast images were captured at 0 h and post-stimulation in keeping with previous experiments and LNCaP cells assessed for increases in mean dendrite length.

In keeping with previous data, treatment with vehicle alone failed to induce a change in LNCaP cells morphology, indicating that any effects of Fsk or 6-Bnz-cAMP arose from pharmacological activity of these drugs. Treatment with 10 μ M Fsk resulted in an increase in mean dendrite length from $18.14 \pm 0.45 \mu\text{m}$ at 0 h to $35.11 \pm 0.71 \mu\text{m}$ post-stimulation

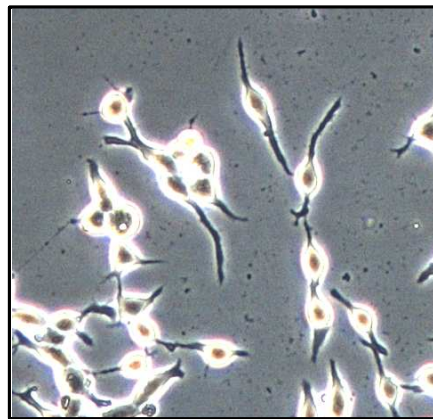
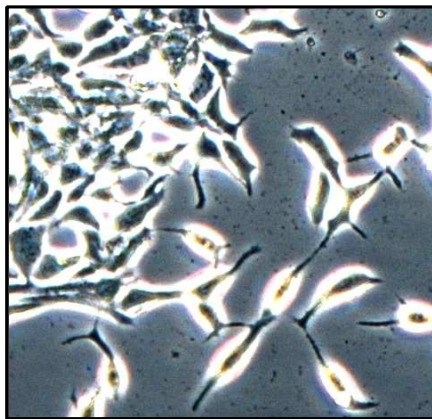
A



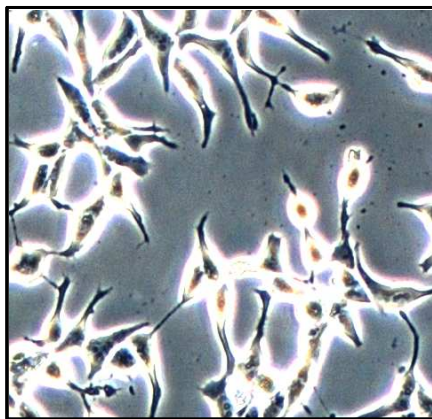
Vehicle



10 mg/ml
Cytochalasin B



10 μ M Fsk



10 mg/ml
Cytochalasin B
+ 10 μ M Fsk

0 h

Post-stimulation

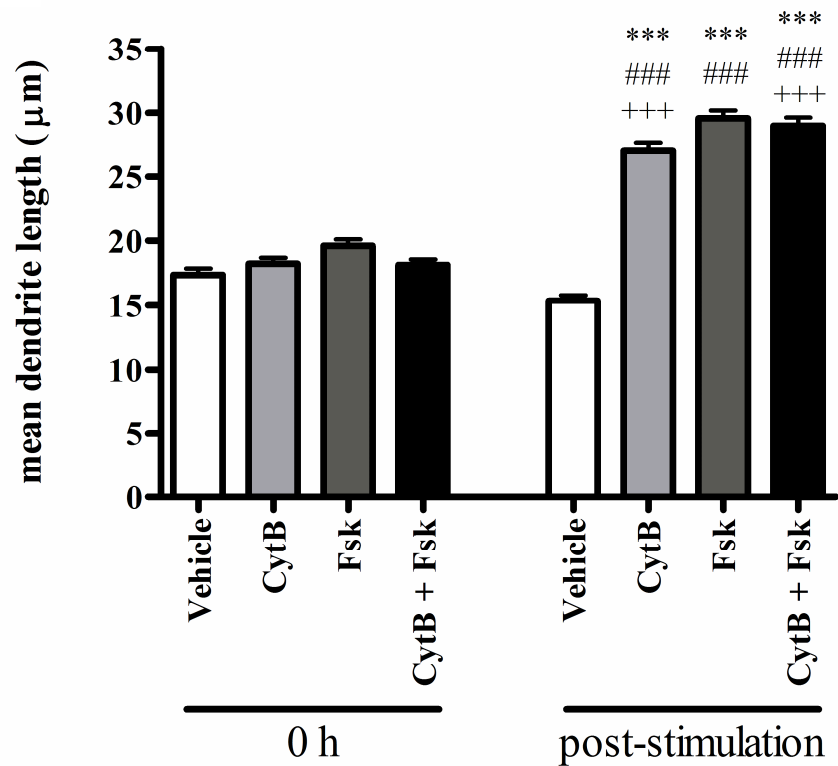
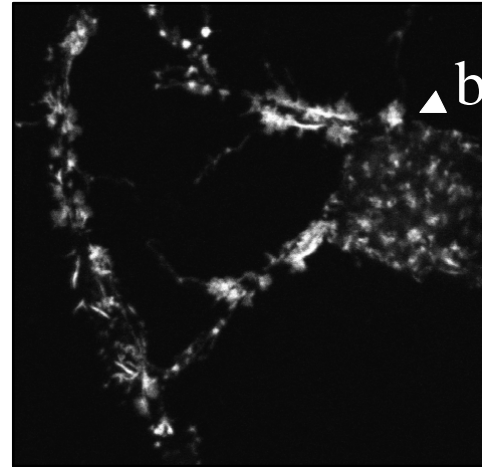
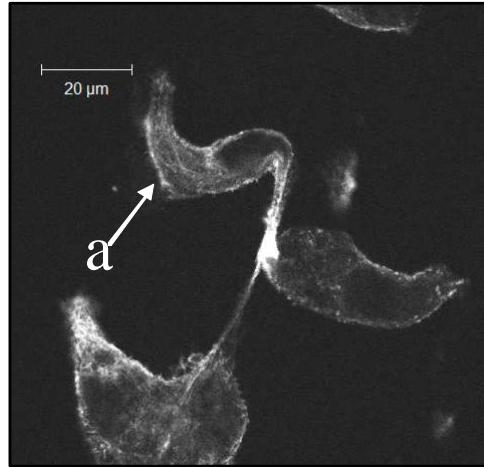
B

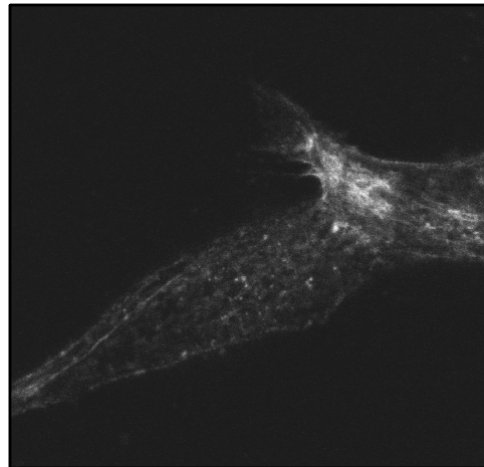
Fig 8.12: Disruption of the actin cytoskeleton recapitulates the effects of Fsk treatment on LNCaP cell morphology

LNCaP cells were plated onto glass coverslips coated with 0.1 mg/ml poly-D-lysine and grown to 60-70 % confluency. Cells were then incubated with either vehicle (1 % (v/v) DMSO) or 100 mg/ml cytochalasin B for 1 h to disrupt the actin cytoskeleton prior to incubation with vehicle (0.1 % (v/v) EtOH) or 10 µM for 1 h. Phase contrast images were captured at 0 h and post-stimulation. Following incubation, LNCaP cells were fixed in 4 % (w/v) paraformaldehyde prior to blocking in 5 % (w/v) BSA-PBST for 30 min and staining with 10 U/ml rhodamine-conjugated phalloidin overnight at 4°C. Successful actin staining was visualised on a Zeiss Pascal Exciter 5 laser scanning confocal microscope using a 63 x magnification, oil immersion objective.

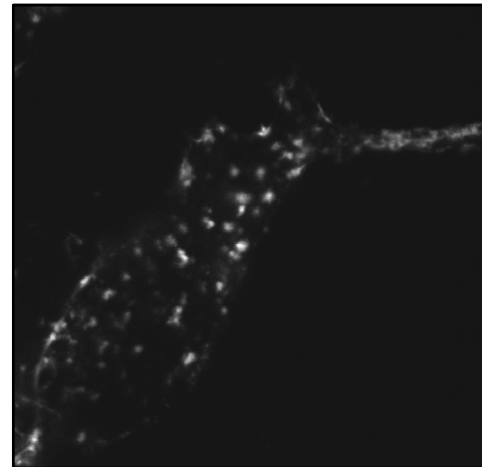
c



Vehicle



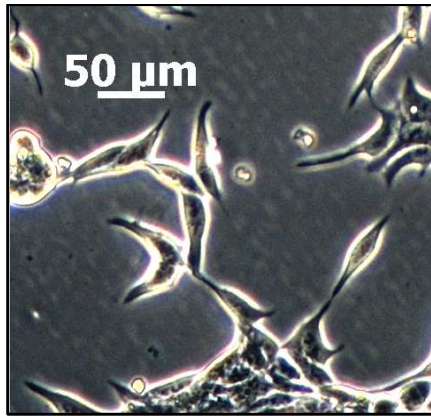
Vehicle



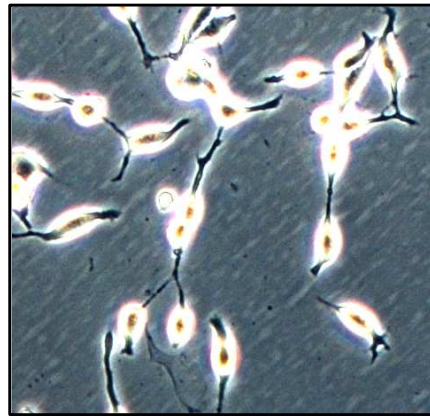
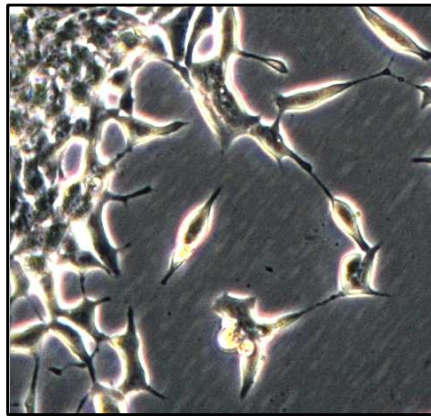
100 mg/ml Cytochalasin B

10 μM Fsk

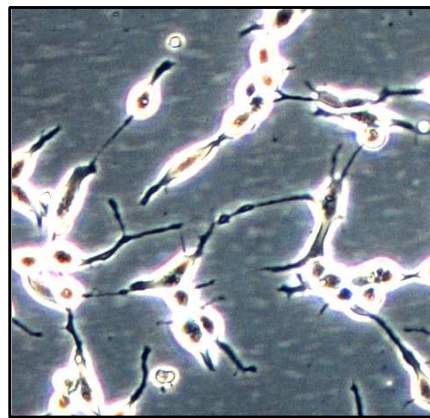
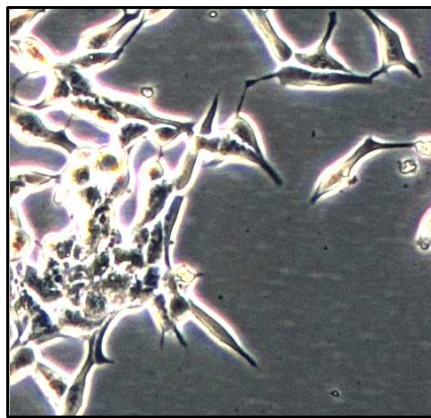
A



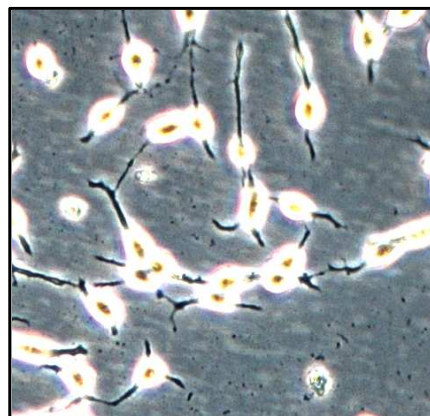
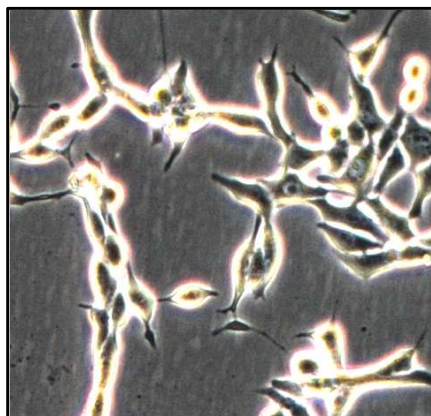
Vehicle



100 μ M 6-Bnz-cAMP



10 μ M Fsk



100 μ M 6-Bnz-cAMP
+ 10 μ M Fsk

0 h

Post-stimulation

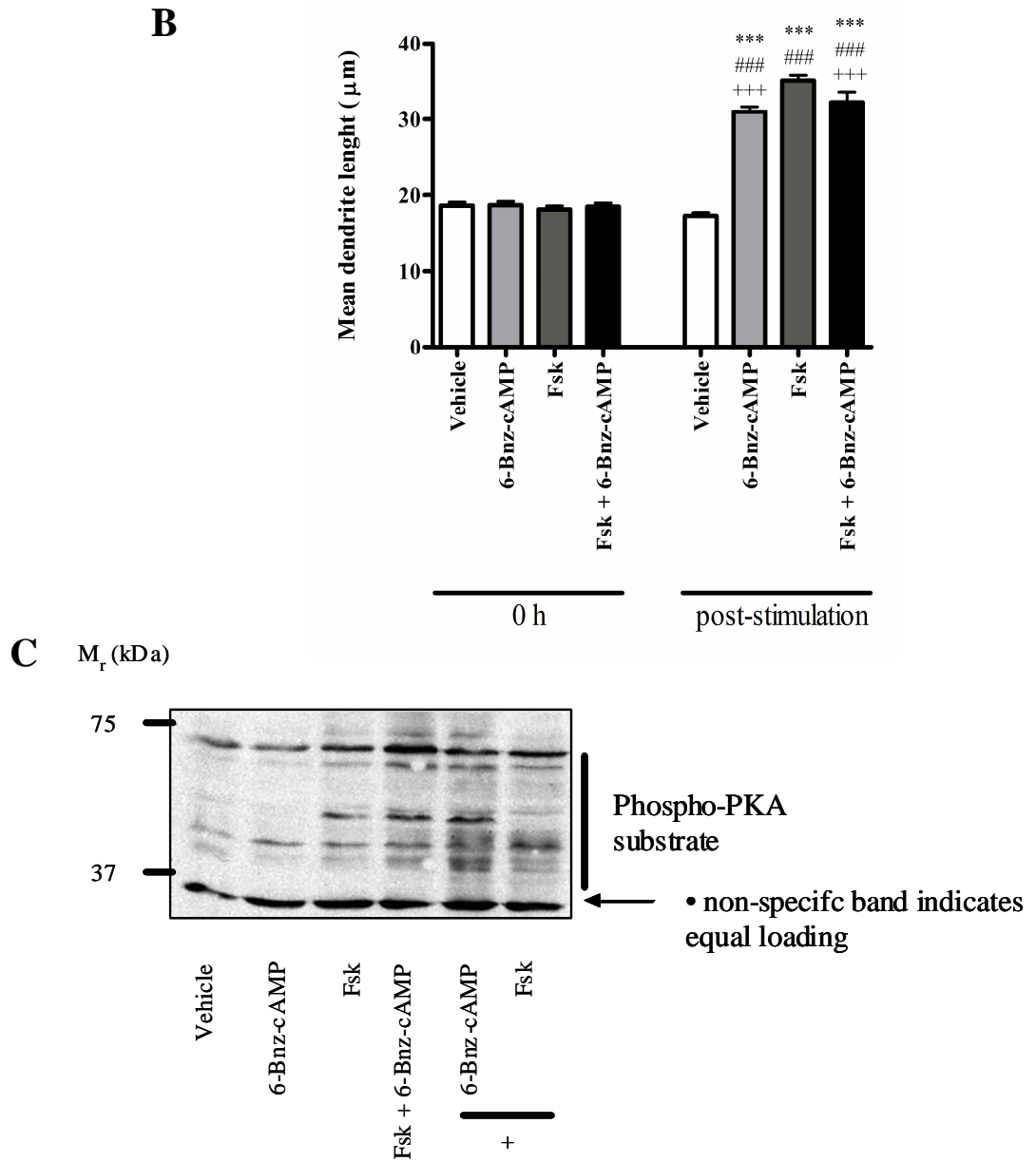


Fig. 8.13: Selective activation of PKA mimics the effect of Fsk on LNCaP cell morphology

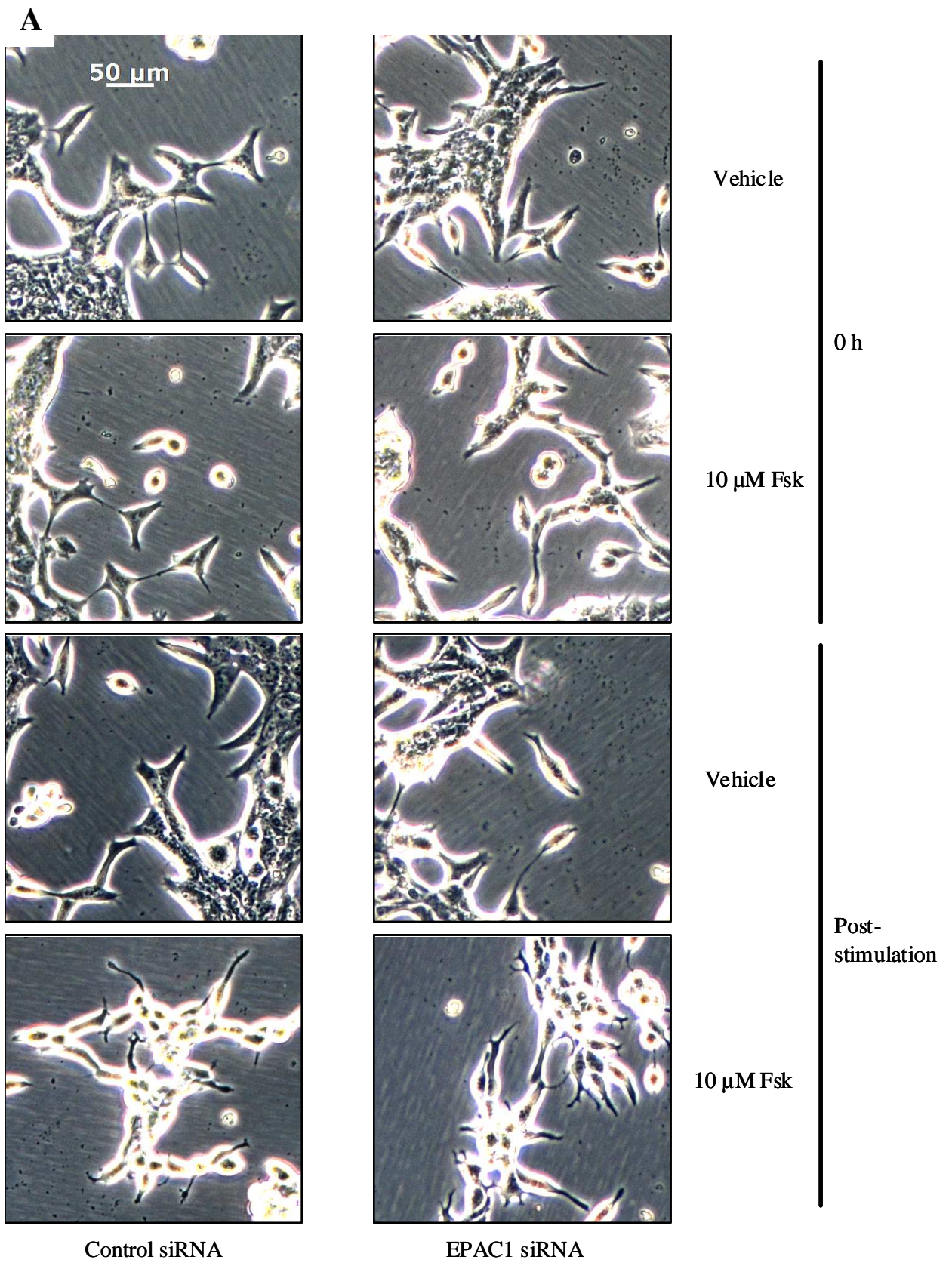
LNCaP cells were plated into 6-well plates and incubated for 1 h with either vehicle (1 % (v/v) DMSO, 0.1 % (v/v) EtOH), 100 µM 6-Bnz-cAMP, 10 µM Fsk or a combination of 10 µM Fsk and 100 µM 6-Bnz-cAMP (panel A). Images were captured as described at the time points indicated and changes in LNCaP morphology consistent with NE-like differentiation were assessed *via* increases in mean dendrite length (panel B). The ability of 6-Bnz-cAMP and Fsk to mediate increases in phospho-PKA substrates was used to indicate efficacy with a 15 min stimulation included as a positive control (panel C) Results are represented as mean values \pm SEM for $n = 3$ separate experiments. *** = $p < 0.001$ vs. 0 h, ### = $p < 0.001$ vs. vehicle, +++ = $p < 0.001$ vs. Fsk

(Fig. 8.13, panels A and B, *** = $p < 0.001$ vs. 0 h, ### = $p < 0.001$ vs. vehicle). Treatment with 100 μ M 6-Bnz-cAMP promoted a similar increase in mean dendrite length from 18.68 ± 0.49 μ m at 0 h to 31.03 ± 0.65 μ m post-stimulation (Fig. 8.13, panels A and B, *** = $p < 0.001$ vs. 0 h, +++ = $p < 0.001$ vs. vehicle, +++ = $p < 0.001$ vs. Fsk). Co-stimulation of LNCaP cells with 10 μ M Fsk and 100 μ M 6-Bnz-cAMP caused an increase in mean dendrite length from 18.49 ± 0.48 μ m at 0 h to 32.28 ± 1.29 μ m post-stimulation (Fig. 8.13, panels A and B, *** = $p < 0.001$ vs. 0 h, +++ = $p < 0.001$ vs. vehicle, +++ = $p < 0.001$ vs. Fsk). Whilst treatment with 6-Bnz-cAMP and co-stimulation with Fsk and 6-Bnz-cAMP resulted in a significant decrease in mean dendrite length compared to Fsk stimulation alone, the difference in mean dendrite lengths is of approximately 4 μ m and thus is unlikely to be biologically significant.

Selective activation of PKA can entirely recapitulate the ability of Fsk to induce changes in LNCaP cell morphology, confirming previous observations that PKA activation was the predominant cAMP effector involved in LNCaP cell differentiation to a NE-like phenotype. This conclusion is further supported by the lack of additive effects following co-stimulation with Fsk and 6-Bnz-cAMP, indicating that activation of other cAMP sensing molecules as a result of Fsk-mediated increases in intracellular cAMP plays an insignificant role in morphological changes in LNCaP cells in comparison to the role of PKA.

8.2.14 Investigation into a role for EPAC in Fsk-mediated changes in LNCaP cell morphology

Whilst it is likely that the changes seen in LNCaP cells during the first hour post-stimulation with Fsk are PKA driven, given the lack of additive effects between 6-Bnz-cAMP and Fsk, a role for EPAC activation must be excluded from this model. In order to establish this, LNCaP cells were treated with 100 pmol of either control or EPAC1 siRNA for 48 h prior to stimulation with either vehicle or 10 μ M Fsk for 1 h. Phase contrast images of LNCaP cells were taken at 0 h and immediately post-stimulation as described in previous experiments. There was no initial difference between mean dendrite length in control and EPAC1 siRNA treated cells, indicating that knockdown of EPAC1 had no effect on cellular morphology. Treatment of either LNCaP cells treated with either control or EPAC1 siRNA with 10 μ M resulted in an increase in mean dendrite length from 12.48 ± 0.79 μ m at 0 h to 26.76 ± 2.75 μ m post-stimulation and from 12.79 ± 0.73 μ m to 26.83 ± 1.23 μ m for control and EPAC1 siRNA treated LNCaP cell respectively (Fig. 8.14, panels A and B, *** = $p < 0.001$ vs. 0 h, ### = $p < 0.001$ vs. vehicle). These results suggest that



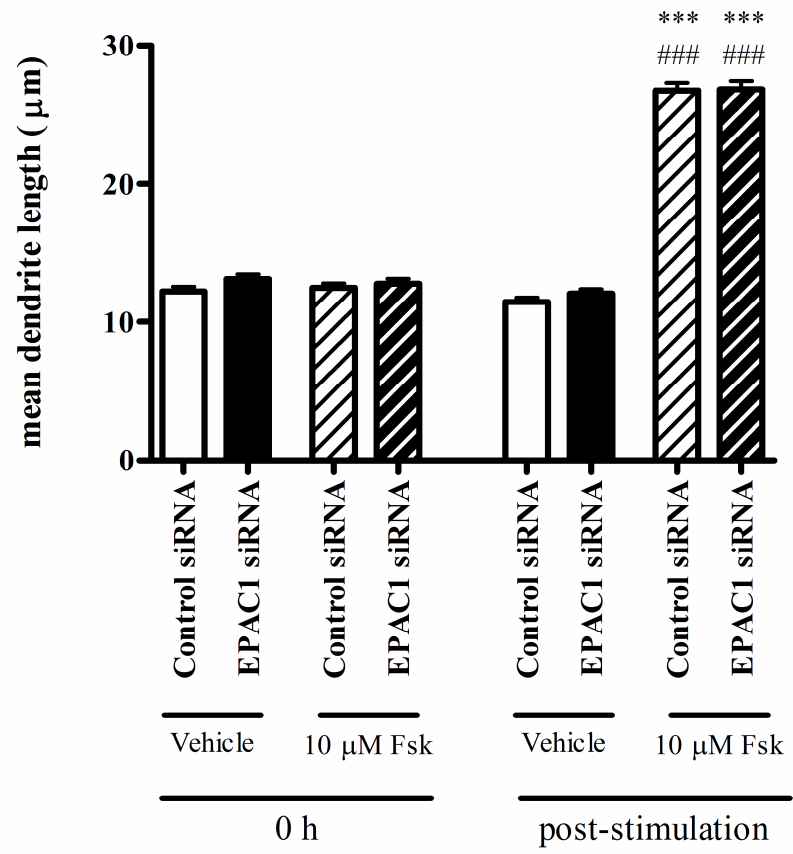
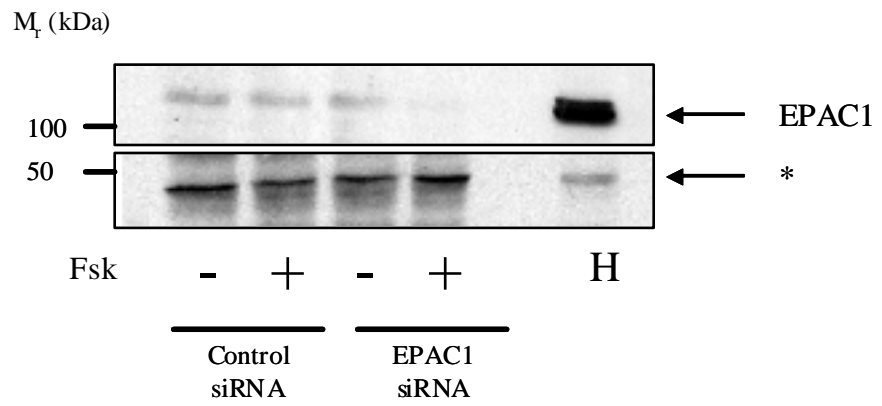
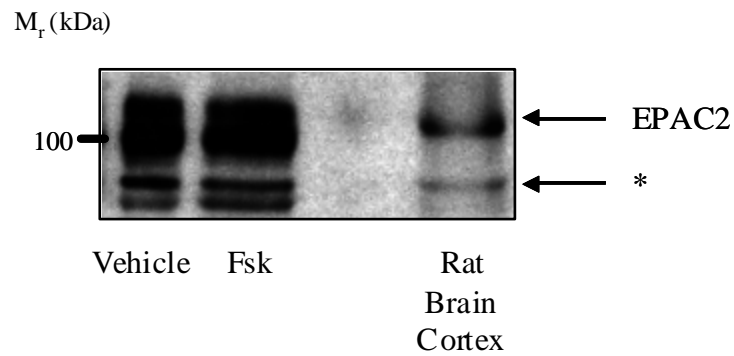
B**C****D**

Fig. 8.14: Effect of EPAC1 siRNA on Fsk-induced changes in LNCaP cell morphology

LNCaP cells were seeded into 6-well tissue culture dishes and transfected with 100 pmol of either control or EPAC1 siRNA as described in Chapter 5. Cells were stimulated at 48 h post-transfection with either vehicle (0.1 % (v/v) EtOH) or 10 μ M Fsk for 1 h and phase contrast images captured at 0 h and 1 h post-stimulation as described previously (panel A). Mean dendrite length was assessed as described in section 8.2.1 and results presented as mean \pm SEM for $n = 3$ separate experiments (panel B). *** = $p < 0.001$ vs. 0 h, ### = $p < 0.001$ vs. vehicle Successful knockdown of EPAC1 was assessed *via* immunoblotting for EPAC1 with HUVEC cell lysates (H) included as a positive control for antibody reactivity (panel C). Expression of EPAC2 was assessed separately in LNCaP cells stimulated with either vehicle (0.1 % (v/v) EtOH) or 10 μ M Fsk for 5 h and lysates of rat brain cortex included as a positive control for antibody reactivity (panel D). Non-specific bands indicate equal protein loading (*)

activation of EPAC1 has no role in Fsk-induced changes in LNCaP cell morphology. However, when cell lysates were immunoblotted for knockdown of EPAC1, detection of the protein in LNCaP cells was not robust, despite loading 100 µg of protein and strong detection of EPAC1 in a HUVEC cell lysate used as a positive control for antibody reactivity (Fig. 8.14, panel C). Therefore, it is not possible to conclude whether EPAC1 was successfully knocked down in LNCaP cells and so a role for the EPAC proteins in this phenomenon cannot be excluded. Importantly, it was demonstrated that LNCaP cells also express EPAC2 (Fig. 8.14, panel D) which may play a more dominant role than EPAC1 in Fsk-induced changes in LNCaP cell morphology and selective knockdown of EPAC2 should be performed to address this. However, it must be stressed that the data obtained in section 8.2.13 indicate no synergistic or additive actions between 6-Bnz-cAMP and Fsk, suggesting that any role for EPAC in this phenomenon may be minor in nature.

8.3 Discussion

During work investigating the ability of Fsk-mediated cAMP elevation to inhibit IL-6-induced STAT3 phosphorylation, it was noted that LNCaP cells displayed an altered morphology when stimulated with 10 µM Fsk in comparison with vehicle-stimulated LNCaP cells. Following a time course of Fsk stimulation, it was apparent that this phenomenon was restricted to LNCaP cells and did not occur in DU145 or PZ-HPV-7 cells (Fig.8.1). In LNCaP cells, Fsk-induced changes in cell morphology were associated with rounding of the cell body, dendrite extension and dendritic branching and are consistent with LNCaP cell differentiation to a NE-like phenotype. Whilst much work has focussed on the ability of Fsk to induce long-term, functional changes in LNCaP cells by promoting NE-like differentiation, less work has examined the mechanisms by which LNCaP cell morphology becomes so dramatically altered. Data obtained in this study indicates that, using an increase in mean dendrite length as an assessment of NE-like differentiation, the majority of morphological changes in LNCaP cells following Fsk treatment occur within the first hour post-stimulation with Fsk (Fig. 8.1). This time point was therefore chosen for subsequent studies of Fsk-induced changes in LNCaP cell morphology.

8.3.1 The roles of PKA and EPAC in LNCaP differentiation

It was found that treatment of LNCaP cells with the PKA-selective inhibitor myr.PKI₁₄₋₂₂ effectively inhibited the ability of Fsk to induce increase in mean dendrite length, indicating that PKA activation is important for this phenomenon. This observation is consistent with previous work by Cox *et al* (2000) who demonstrated that treatment of LNCaP cells with agents, including 5 µM Fsk, which induce NE-like differentiation

promoted a significant increase in PKA activity as measured by increased phosphorylation of the synthetic substrate malantide (Cox *et al.*, 2000). Furthermore, expression of constitutively active PKA catalytic subunit (PKA-C) mutants encoding single codon changes at positions 87 (H→Q) and 196 (W → R) (Orellana & Mcknight, 1992) promoted NE-like differentiation in LNCaP cells in the absence of any other stimulus. The ability of PKA-C to be activated in the absence of stimulation with cAMP-elevating agents appears to be due to loss of regulation by the regulatory subunits of PKA (Orellana & Mcknight, 1992) which would normally bind cAMP in order to release the active catalytic subunits. Combined with data obtained in this study, it would appear that the ability of Fsk to induce NE-like differentiation in LNCaP cells is dependent on PKA activity.

However, whilst PKA activation has been shown to be sufficient to induce NE-like differentiation in LNCaP cells, it was necessary to establish a role for the more recently described EPAC in this phenomenon. In PC12 cells, simultaneous activation of EPAC and PKA is associated with neuronal differentiation whilst exclusive activation of PKA is associated with proliferation of PC12 cells through PKA-mediated phosphorylation of the EGFR and subsequent transient but robust activation of ERK1/2 (Kiermayer *et al.*, 2005). These results suggest that activation of both EPAC and PKA is important for mediating cAMP-induced neuronal differentiation. Indeed it has been shown that treatment of PC12 cells with 8Me-pCPT-cAMP synergistically enhances neurite extension induced by both 6-Bnz-cAMP and NGF, indicating the important role of EPAC in this phenomenon (Christensen *et al.*, 2003). Such interactions between EPAC and PKA may also be applicable in the case of cAMP-induced NE-like differentiation in LNCaP cells, although cell line-specific responses cannot be discounted. In PC12 cells, selective activation of either PKA *via* the PKA-selective cAMP analogue 6-Bnz-cAMP fails to induce neuritogenesis except in the presence of the EPAC-selective cAMP analogue 8Me-pCPT-cAMP. Similarly, treatment with 8Me-pCPT-cAMP alone failed to induce neurite outgrowth but promoted strong increases in the number of cells with neurites when combined with 6-Bnz-cAMP (Christensen *et al.*, 2003). In contrast to PC12 cells, active PKA alone appears necessary to induce NE-like differentiation of LNCaP cells with expression of PKA-C promoting NE-like differentiation in the absence of other stimuli (Cox *et al.*, 2000). However, this study only investigated gross morphological changes, which are not a quantitative measure of differentiation, and did not compare the abilities of Fsk and PKA-C to induce LNCaP cell differentiation. Therefore, subtle differences in the respective abilities of PKA-C and Fsk to induce changes in LNCaP cell morphology arising may have been overlooked. In this study, pre-treatment of LNCaP cells with 10 nM

myrPKI₁₄₋₂₂ significantly but incompletely inhibited Fsk-induced increases in mean dendrite length despite completely blocking Fsk-mediated phosphorylation of Ser¹³³CREB at this concentration. These results suggest that, whilst PKA may play the predominant role in Fsk-induced changes in LNCaP cell morphology, EPAC activation may contribute to this phenomenon.

Indeed, in HUVECs, treatment with 8Me-pCPT-cAMP has been reported to promote actin polymerisation co-ordinately with increased microtubule growth, indicating that EPAC1 is important in mediating cross-talk between the actin cytoskeleton and the MT network (Sehrawat *et al.*, 2008). As depolymerisation of the MT network in LNCaP cells prior to stimulation with Fsk resulted in dendrites which were morphologically distinct from those seen in cells pre-incubated with vehicle (Fig. 8.3), it is possible that EPAC may play a role in governing dendrite integrity. However, incubation of LNCaP cells with 6-Bnz-cAMP totally recapitulated the effects of Fsk treatment on cellular morphology and no additive or synergistic actions were seen between Fsk and 6-Bnz-cAMP (Fig. 8.13). These results support the hypothesis that activation of PKA is the predominant effect in governing changes in LNCaP cell morphology following cAMP elevation and indicate that any role played by EPAC1 is more minor at the early time points studied. However, a role for the EPAC proteins later in LNCaP differentiation cannot be discounted and it must be stressed that only a role for EPAC1 has been investigated. As LNCaP cells also express EPAC2, it is possible that this protein may play a greater role in governing Fsk-induced changes in LNCaP cell morphology (Fig. 8.14).

It is important to note that, at the time points studied, it is unlikely that any contribution of *de novo* protein synthesis to changes in LNCaP cell morphology will be detected. Indeed, pre-treatment with 100 μ M emetine did not inhibit Fsk-induced increases in mean dendrite length at 1 h post-stimulation with effects on Fsk-induced increases in mean dendrite length observed at 3 and 5 h post-stimulation (Fig. 8.2). Given the rapid increase in mean dendrite length observed within the first hour post-stimulation with Fsk (Fig. 8.1), it is more likely that the changes in cellular morphology are due to immediate cytoskeletal alterations rather than as a result of *de novo* synthesis. It is therefore unlikely that any gene products regulated downstream, EPAC proteins will make any significant contribution to the phenotype measured at 1 h post-stimulation with Fsk. Extension of these experiments to look at later time points may well reveal a role for EPAC proteins in this phenomenon.

Such predominance of PKA in this effect may be a reflection of the greater ability of cAMP to activate PKA in comparison to EPAC. Whilst both human EPAC1 and PKA holoenzyme display similar affinities for cAMP (Dao *et al.*, 2006), half-maximal activation (EC_{50}) of EPAC occurs at cAMP concentrations in the micromolar range ($EC_{50} = 45 \mu\text{M}$, (Rehmann *et al.*, 2003). In contrast, the purified PKA holoenzymes of both honeybees and *Candida albicans* show EC_{50} values of approximately 0.1 nM (Leboulle & Muller, 2004; Zelada *et al.*, 1998), indicating that the cAMP is 500 times more potent at activating PKA than it is EPAC1.

Whilst the results obtained strongly support the hypothesis that the ability of Fsk to induce NE-like differentiation in LNCaP cells is largely PKA-dependent, the fact that neither combined inhibition nor activation of EPAC and PKA has been investigated in the current study cannot be ignored. It is possible that combined activation of EPAC and PKA *via* treatment with 8Me-pCPT-cAMP and 6-Bnz-cAMP respectively may act to induce changes in LNCaP cell morphology. Preliminary investigations of the ability of 8Me-pCPT-cAMP alone to induce increases in LNCaP cell morphology failed to indicate a role of EPAC in this phenomenon (data not shown). However, in order to accurately assess changes in mean dendrite length, it is necessary to grow LNCaP cells to sub-confluence which may affect the efficacy of 8Me-pCPT-cAMP as our laboratory has previously noted that the ability of 8Me-pCPT-cAMP to induce SOCS3 expression (Sands *et al.*, 2006) is reduced at lower cell confluences (unpublished observations). Therefore, a better experimental strategy to determine whether the contributions of PKA and EPAC1 to Fsk-induced increases in mean dendrite length are synergistic or additive may well be to determine the effect of combined EPAC1 siRNA with PKA inhibition on Fsk-induced dendrite outgrowth.

8.3.2 Inhibition of RhoA mediates Fsk-induced changes in LNCaP cell morphology

Whilst elucidating the role of PKA in Fsk-mediated changes in LNCaP morphology, it was found that treatment with the PKA-selective inhibitor H89 at a concentration of 5 μM could induce increases in mean dendrite length in the absence of cAMP elevation. The ability of low micromolar concentration of H89 to induce changes in cellular morphology is not unprecedented as treatment of both 3T3-L1 adipocytes and NG 108-15 neuroblastoma cells can induce changes in cellular morphology due to non-selective inhibitory effects of H89 on the ROCK pathway (Kato *et al.*, 2007; Leemhuis *et al.*, 2002). In the case of NG 108-15 cells, treatment with H89 induces neurite outgrowth, a

phenomenon similar to that seen in LNCaP cells, indicating that inhibition of ROCK signalling can induce dendrite outgrowth in LNCaP cells (Leemhuis *et al.*, 2002). This hypothesis was supported by the observation that selective inhibition of ROCK signalling with Y27632 (Ishizaki *et al.*, 2000) could recapitulate the effects of Fsk treatment on LNCaP morphological changes. Furthermore, selective inhibition of RhoA, a major upstream activator of ROCK, could also mimic the effects of Fsk treatment, indicating that Fsk acts to inhibit RhoA. In order to assess this *via* a genetic approach, LNCaP cells were transfected with cDNA encoding either vector, wild-type, a dominant negative or constitutively active RhoA. Expression of vector or wild-type RhoA failed to affect the ability of Fsk to induce increases in neurite outgrowth. Expression of constitutively active myc.RhoAQ63L effectively blocked Fsk-induced increases in mean dendrite outgrowth. However, expression of the dominant negative myc.RhoAT19N failed to recapitulate the effect of Fsk in the absence of stimulation or following treatment with 10 μ M Fsk for 1 h. However, expression of this mutant was lower than that of myc.RhoAWT or myc.RhoAQ63L, which may explain the lack of phenotype associated with myc.RhoAT19N expression. Subsequent attempts to increase myc.RhoA.T19N expression were unsuccessful due to cell death following transfection of the myc.RhoA.T19N cDNA. It is hypothesised such effects arose due to increased expression of a dominant negative RhoA which may act to impede normal cellular adherence and so promote cell death through detachment from the substratum. Cells transfected with equal amounts of vector cDNA did not display such pronounced decreases in cell viability, indicating that the effects seen are specific to the expression of myc.RhoAT19N and not due to effects of increasing the amount of cDNA used in the transfection.

Although expression of myc.RhoAT19N failed to potentiate Fsk-induced increases in mean dendrite length, the ability of constitutively active myc.RhoAQ63L to block the effects of Fsk-induced increases in mean dendrite length in LNCaP cells and the observation that incubation with C3T can mimic Fsk-induced changes in LNCaP morphology strongly suggest that inhibition of RhoA/ROCK signalling is an important requirement for this phenomenon. Furthermore, the inability of Y27632 or C3T to potentiate Fsk-induced increases in mean dendrite length in LNCaP cells suggest that the two mechanisms are acting through a common pathway and that Fsk acts to inhibit RhoA activation.

This hypothesis is further supported by the earlier observations that the ability of Fsk to induce NE-like differentiation in LNCaP cells is PKA-dependent. It has been demonstrated

in multiple cell types that cAMP elevation can inhibit RhoA activation *via* PKA-mediated phosphorylation of Ser¹⁸⁸. Indeed, in the SH-EP neuroblastoma cell line, alanine substitution of Ser¹⁸⁸ is protective against Fsk-induced changes in morphology similar to those seen in LNCaP cells (Dong *et al.*, 1998). In the SGC-7901 gastric carcinoma cell line, treatment with the cell-permeable cAMP analogue CPT-cAMP was associated with a decrease in the ability of lysophosphatidic acid (LPA) to activate RhoA and concomitantly with an increase in pSer¹⁸⁸RhoA (Chen *et al.*, 2005). Of particular reference to this study is the observation that expression of a S188A RhoA mutant in the PC3 prostate cancer cell line prevented CPT-cAMP-mediated antagonism of LPA-induced RhoA activation (Chen *et al.*, 2005). These results suggest that the ability of cAMP to inhibit RhoA activation requires phosphorylation of RhoA on Ser¹⁸⁸. Phosphorylation of this residue is thought to inhibit RhoA activity by promoting interaction of RhoA with the GDP dissociation inhibitor (GDI) (Ellerbroek *et al.*, 2003). GDI binds to the C-terminus of RhoA and can inhibit both GDP dissociation from RhoA and GTP hydrolysis by RhoA (Hakoshima *et al.*, 2003). GDI also plays a crucial role in shuttling RhoA between the cytoplasm and the membrane and interaction with GDI is thought to sequester GDP-bound RhoA in an inactive cytosolic complex (Forget *et al.*, 2002; Qiao *et al.*, 2003). This mechanism of RhoA inhibition may well be conserved in higher eukaryotes as phosphorylation of yeast cellular membranes with the catalytic subunit of PKA promoted extraction of RhoA *via* a GDI-dependent mechanism and is associated with serine phosphorylation of RhoA (Forget *et al.*, 2002).

In addition to direct inhibition of RhoA *via* Ser¹⁸⁸ phosphorylation and subsequent interaction with GDI, serine phosphorylation of RhoA also impedes interaction with ROCK, thus preventing downstream activation of effectors (Dong *et al.*, 1998). In addition to inhibiting activation of ROCK it is also possible that activation of PKA affects other downstream effectors of RhoA. MEFs in which the type 1A regulatory subunit of PKA has been knocked out (*Prkar1a*^{-/-}) show increased motility with treatment of cells with Fsk resulting in an increase in pSer³cofilin, indicative of activation of LIMK (Nadella *et al.*, 2009). As activation of LIMK occurs downstream of ROCK, it may initially appear that this data contravenes previous publications indicating that PKA activation inhibits RhoA-ROCK signalling. However, LIMK has two sites at Ser³²³ and Ser⁵⁹⁶ which are thought to be targets of PKA *in vivo* suggesting that PKA can directly modulate the activity of RhoA effectors (Nadella *et al.*, 2009). It has been proposed that activation of PKA and subsequent phosphorylation of RhoA on Ser¹⁸⁸ may only affect activation of ROCK-dependent pathways as treatment with PKA inhibits association of RhoA with ROCK but

not protein kinase novel (PKN) (Nusser *et al.*, 2006). PKN is a protein kinase showing homology to yeast protein kinase C-related proteins and has been implicated in morphological roles during development (Zhao & Manser, 2005).

In addition to selective inhibition of RhoA effectors, activation of PKA may also affect other small GTPase signalling pathways. In addition to RhoA, PKA is also able to phosphorylate β_1 Pix, a GEF for Cdc42 and Rac1. PKA-mediated phosphorylation of β_1 Pix is associated with interaction with 14-3-3 β , and subsequent inhibition of β_1 Pix GEF activity towards Rac1 and so impaired Rac1-mediated signalling in HEK293 cells (Chahdi & Sorokin, 2007). In contrast, PKA activation had no effect on the GEF activity of β_1 Pix towards Cdc42 (Chahdi & Sorokin, 2007), indicating that cAMP elevation can differentially regulate the Rho family GTPases. Indeed, it has been shown that endothelin-1 can activate Cdc42 *via* a PKA-dependent pathway .

Given the current observations, it is believed that Fsk-mediated elevation of cAMP in LNCaP cells results in activation of PKA which then acts to inhibit RhoA *via* Ser¹⁸⁸ phosphorylation. Subsequent inhibition of ROCK signalling may therefore potentiate the extension of cellular process such as dendrites through Rac1/Cdc42-mediated pathways rather than the adhesive pathways associated with RhoA and result in the NE-like differentiation of LNCaP cells.

9 The role of ERK activation in Fsk-induced changes in LNCaP morphology

9.1 Introduction

In the previous chapter, the pathways by which cAMP elevation induced morphological changes in LNCaP cells were investigated. The results suggest that PKA-mediated inhibition of RhoA activity was a major contributor to cAMP-induced dendrite extension in these cells. However, other signalling pathways can modulate cytoskeletal dynamics and dendrite outgrowth in particular. Key amongst these is activation of the ERK1/2 signalling pathway.

9.1.1 NGF-induced neurite extension

The PC12 pheochromocytoma cell line has long been the model of choice when investigating neuronal differentiation. PC12 cells undergo differentiation to neuronal cells following treatment with a number of stimuli including the neurotrophin nerve growth factor (NGF) (Greene & Tischler, 1976), basic fibroblast growth factor (FGF) (Pollock *et al.*, 1990), cAMP analogues (Schubert & Whitlock, 1977) and pituitary adenylyl cyclase activating peptide (PACAP) -38 (Deutsch & Sun, 1992). NGF-mediated differentiation of PC12 cells is mediated by altered gene transcription downstream of the NGF receptor (TrkA). The NGF receptor belongs to the tropomyosin-receptor-kinase (Trk) family and, following binding of NGF, is activated *via* tyrosine phosphorylation on residues corresponding to Tyr⁶⁷⁹, Tyr⁶⁸³ and Tyr⁶⁸⁴ of the rat NGF receptor (Gryz & Meakin, 2000;Ng *et al.*, 2009). In addition to Tyr⁶⁸³ and Tyr⁶⁸⁴, phosphorylation of Tyr⁷⁹⁴ of the rat TrkA enables recruitment of Grb2 and so act as an adaptor to intracellular signalling pathways (MacDonald *et al.*, 2000).

One of the pathways activated downstream of TrkA is the ERK1/2 signalling pathway. Treatment with NGF results in a sustained activation of both Ras and ERK1/2 which is required for the differentiation of PC12 cells (Qiu & Green, 1992).

Dexamethasone-induced expression of oncogenic N-Ras promotes neuronal differentiation of PC12 cells in the absence of NGF stimulation. Blockade of ERK activity in PC12 cells expressing N-Ras prevents the neurone outgrowth, indicating that Ras-mediated activation of ERK1/2 signalling is required for this phenomenon (Qiu & Green, 1992). Furthermore, it appears that sustained rather than transient activation of ERK1/2 signalling is required

for neuronal differentiation of PC12 cells. EGF fails to differentiate PC12 cells and is associated with transient activation of both MEK1/2 and ERK1/2. In contrast, treatment with NGF resulted in sustained activation of ERK1/2 which was coupled with neurite extension (Traverse *et al.*, 1992). The essential role of ERK activation in PC12 differentiation was demonstrated by Cowley *et al.* (1994). Over-expression of constitutively active MEK1 alone in PC12 cells resulted in changes in morphology consistent with NGF-induced neuronal differentiation. The ability of constitutively active MEK1 to induce neurite outgrowth in PC12 cells requires functional ERK1, which lends further support to the essential role of ERK1/2 signalling in neurite outgrowth (Cowley *et al.*, 1994). Similar results were obtained in PC12 cells in which a constitutively active, nuclear-localised form of ERK2 was expressed (Robinson *et al.*, 1998).

Members of the Ras superfamily are important upstream activators of ERK1/2 (see section 3.4) and much research has been directed towards identifying the signalling pathways required for sustained activation of ERK1/2 during neurite outgrowth. Phosphorylation of Tyr⁴⁹⁰ within TrkA acts as a recruitment site for the adaptor protein Shc. Upon phosphorylation of Shc, this protein can then associate with the Ras/SOS complex and so promote activation of the Ras-Raf-MEK1/2-ERK1/2 signalling cascade (Huang & Reichardt, 2003). A role for Rap1 in NGF-mediated activation of ERK1/2 has been proposed as treatment of PC12 cells with NGF promotes sustained activation of ERK1/2 and also transiently increases GTP-associated Rap1. Although transient, the ability of NGF to induce activation of Rap1 was more sustained than EGF-induced increases in Rap1-GTP, suggesting that activation of Rap1 may contribute to the sustained ERK1/2 response (Obara *et al.*, 2004). Further studies into the respective roles of Ras and Rap1 in promoting sustained activation of ERK1/2 indicate that it is Ras activation which dictates the amplitude of the initial ERK1/2 response and that Rap1 activation is important for the sustained activation of this signalling pathway (Bouschet *et al.*, 2003; York *et al.*, 1998). However the role of Rap1 in neurite outgrowth is unclear as expression of the Rap1 interfering mutant, Rap1N17, blocks sustained ERK1/2 activation in response to NGF, but does not inhibit NGF-induced neurite outgrowth in PC12 cells. These results suggest that neurite outgrowth does not require Rap1 (York *et al.*, 1998). In a recent study, expression of constitutively active mutants of H-Ras and M-Ras but not Rap1 could induce neurite outgrowth in PC12 cells (Sun *et al.*, 2006). Similarly, expression of the two Ras mutants, but not active Rap1, was associated with an increase in phosphorylated ERK1/2. Interestingly, expression of dominant negative mutants of all three GTPases inhibited

NGF-induced neurite outgrowth. Selective inhibition of M-Ras protein expression using siRNA effectively blocked NGF-induced neurite outgrowth, indicating that this protein is required for neurite outgrowth in PC12 cells. NGF promoted sustained activation of only M-Ras but not three other classical Ras isoforms tested, suggesting that this Ras isoform may be important in mediating the sustained activation of ERK1/2 in response to NGF (Sun *et al.*, 2006). M-Ras is highly expressed in the brain and was originally identified as promoting the formation of microspikes *via* reorganisation of the actin cytoskeleton in Swiss 3T3 fibroblasts (Matsumoto *et al.*, 1997). Thus, it is hardly surprising that M-ras has been implicated in neuronal differentiation.

Whilst NGF has been predominantly studied as an inducer of neuronal differentiation, other factors can also promote neurite outgrowth. Treatment with the 38 amino acid peptide, PACAP-38 can induce neuronal differentiation in a number of neuronal cells and is associated with activation of AC (Deutsch & Sun, 1992;Hoshino *et al.*, 1993). PACAP-38 induces neurite outgrowth in SH-SY5Y cells *via* elevation of cAMP and subsequent activation of ERK and p38 MAPK. Furthermore, it was suggested that these events were found to be PKA-independent as selective activation of EPAC in these cells promoted ERK1/2 activation and increased the number of neurite bearing cells (Monaghan *et al.*, 2008).

9.1.2 The role of cAMP elevation in neurite outgrowth

The results obtained by Monaghan *et al* (2008) demonstrate that activation of AC downstream of the PACAP receptor induces increases in intracellular cAMP required for neurite outgrowth in PC12 cells. The ability of cAMP to induce neurite outgrowth has long been described (Schubert & Whitlock, 1977). It has been found that, in the early stages of neuronal differentiation, cAMP analogues synergise with both NGF and FGF to promote neurite outgrowth (Ho & Raw, 1992;Richter-Landsberg & Jastorff, 1986). In the Richter-Landsberg study (1986), cAMP analogues and Fsk did not induce neurite extension in the absence of NGF, however it has been demonstrated by other groups that treatment with cAMP elevating agents such as Fsk can induce neurite outgrowth in the absence of other stimuli (Chijiwa *et al.*, 1990). Similar to NGF, treatment of PC12 cells with Fsk or cAMP analogues can result in ERK1 activation which remains elevated at 2 h post-stimulation (Yao *et al.*, 1998a). However, it must be stressed that, whilst sustained activation of ERK1/2 is important in neurite outgrowth, the ability of cAMP to activate this pathway differs between cell types (Creedon *et al.*, 1996).

9.1.3 The roles of cAMP in ERK1/2 activation

The ability of cAMP to activate ERK1/2 differs between cell types. In the Wistar rat thyroid cells, Fsk-induced cAMP elevation activates Ras by a mechanism which is independent of PKA activation (Tsygankova *et al.*, 2000). In B16 melanoma cells, increases in ERK1/2 phosphorylation and both B-Raf and Ras activity were observed following treatment of cells with a combination of Fsk and isobutylmethylxanthine (IBMX), a PDE inhibitor which non-selectively targets all members. Similar to results obtained by Tsygankova *et al.* (2000), the ability of Fsk and IBMX to induce activation in these cells was found to occur independently of PKA (Busca *et al.*, 2000). However, the signalling pathways responsible for cAMP-induced ERK1/2 activation differ between cell types and stimuli. For example, treatment of PC12 cells with a combination of Fsk and IBMX activates ERK1/2 through Rap1 rather than Ras (Busca *et al.*, 2000). However, when these cells were stimulated with NGF, increases in active Ras were observed (Busca *et al.*, 2000), suggesting that the mechanism of ERK1/2 activation differs between stimuli.

There is disparity within current data as to the relative requirement for PKA and EPAC in the sustained activation of ERK1/2 during neurite outgrowth. The results of Monaghan *et al.* (2008) suggest that PACAP38-mediated neurite outgrowth arises due to activation of EPAC rather than PKA. The EPAC-dependency of this result is corroborated by the observation that activation of EPAC induces a rapid, sustained activation of ERK1/2 in PC12 cells and was associated with increases in neurite outgrowth (Kiermayer *et al.*, 2005). In the study by Kiermayer *et al.* (2005), activation of PKA was associated with a proliferative response rather than the differentiation signal mediated by EPAC activation (Kiermayer *et al.*, 2005). However, the role of EPAC and PKA appears to vary between experimental designs as treatment of PC12 cells with either EPAC or PKA-selective agonists alone fail to induce neurite outgrowth and only do so when cells are treated with both agonists simultaneously (Christensen *et al.*, 2003). However, when considering the requirement for sustained activation of ERK1/2 in neurite outgrowth, it is unsurprising that activation of EPAC following cAMP elevation is linked to neurite outgrowth. EPAC2 is highly expressed in neuronal tissue and, following interaction with cAMP, is able to interact with activated Ras (Li *et al.*, 2006b). The interaction between EPAC2 and Ras recruits EPAC2 to the plasma membrane where it potentiates activation of membrane-bound Rap1 and subsequent activation of ERK1/2 (Li *et al.*, 2006b). Indeed, loss of Ras-binding prevents EPAC2 from activating Rap1 (Liu *et al.*, 2008), which may explain the roles of both of these GTPases in neurite outgrowth.

However, although the above studies suggest a predominant role of EPAC in cAMP-induced neurite outgrowth, a role for PKA cannot be discounted given the observation that activation of both PKA and EPAC is required for neurite outgrowth in response to cAMP elevation (Christensen *et al.*, 2003). Interestingly, a link between NGF and cAMP elevation has been identified whereby NGF can induce activation of a soluble AC *via* a calcium-dependent mechanism (Stessin *et al.*, 2006). Activation of PKA is required for sustained activation of ERK1/2 and gene expression following NGF stimulation (Yao *et al.*, 1998a). However, given the observations by Kiermayer *et al* (2005), the relative contributions of EPAC and PKA to NGF-induced neurite extension in PC12 cells are currently unclear.

Previous work in LNCaP cells demonstrated that the ability of cAMP to induce changes in cellular morphology arose due to PKA-mediated inhibition of RhoA. However, the role of ERK1/2 activation in this response has not been investigated. Activation of ERK1/2 signalling using heparin-binding EGF-like factor (HB-EGF) induces NE differentiation of LNCaP cells in the absence of STAT3 phosphorylation or androgen deprivation (Kim *et al.*, 2002). Similarly, vasoactive intestinal peptide (VIP) induces NE differentiation of LNCaP cells *via* a PKA-dependent pathway. Such results indicate that ERK1/2 activation is an important inducer of NE differentiation in LNCaP cells.

In this study, LNCaP cells were found to rapidly activate ERK1/2 upon stimulation with Fsk and treatment with U0126 blocked the effect of Fsk on cell morphology at 1 h post-stimulation. However, selective activation of ERK1/2 induced an increase in mean dendrite length only at 8 h post-stimulation, suggesting that the rapid effects of Fsk are mediated by another pathway. Along with MEK1/2, treatment with U0126 can also block MEK5 activation and subsequent ERK5 signalling pathways. Expression of a dominant-negative ERK5 construct mimicked the effect of U0126 on Fsk-induced changes in LNCaP cell morphology. A predominant role for ERK5 in early morphological changes in LNCaP cells was further supported by the observation that the MEK5-selective inhibitor BIX02188 blocked Fsk-induced dendrite outgrowth at 1 h post-stimulation. The results suggest that it is cAMP-mediated activation of ERK5 rather than ERK1/2 that is required for the early changes in cell morphology in LNCaP cells upon stimulation with Fsk.

9.2 Results

9.2.1 Fsk induces Thr²⁰² and Tyr²⁰⁴ phosphorylation of ERK1/2 in LNCaP cells

In PC12 cells, stimulation with NGF induces neurite outgrowth associated with sustained ERK1/2 activation and can be reversed following treatment with the MEK1/2-selective inhibitor PD 98059 (Waetzig & Herdegen, 2003). PKA can mediate the sustained activation of ERK1/2 in these cells (Yao *et al.*, 1998a) and it is possible that there are similarities between the cellular pathways employed in PC12 and LNCaP cells. To assess whether a similar pathway holds true in LNCaP cells, the ability of cAMP elevation to activate ERK1/2 was determined. LNCaP cells were seeded into 6-well plates coated with 0.1 mg/ml poly-D-lysine HBr and grown to 70 % confluency. Prior to stimulation with Fsk, LNCaP cells were serum-starved for 2 h to decrease basal activation of ERK1/2. Under normal growth conditions, serum present in cell culture medium can activate ERK1/2 (Scimeca *et al.*, 1991) which can potentially prevent agonist-induced changes in ERK1/2 activation from being observed. Thus, following serum starvation, LNCaP cells were stimulated with 10 μ M Fsk for 0 – 30 min prior to immunoblotting for pThr²⁰²pTyr²⁰⁴ERK1/2. These residues are phosphorylated by the upstream MEK1/2 and are required for the activation of ERK1/2 (Seger *et al.*, 1992). The extent of phosphorylation of ERK1/2 correlates directly with kinase activity as determined by comparing the ability of immunoprecipitated ERK1 to phosphorylate myelin basic protein (Cook *et al.*, 1997). Therefore, assessment of pThr²⁰²pTyr²⁰⁴ERK1/2 levels *via* immunoblotting acts as an indirect readout for ERK1/2 activity. Equal protein loading was assessed by immunoblotting for total ERK1/2 and the ability of Fsk to induce increases in intracellular cAMP was determined by detection of increases in pSer¹³³CREB, a downstream substrate of PKA.

Treatment with 10 μ M Fsk induced an increase in pThr²⁰²pTyr²⁰⁴ERK1/2 in LNCaP cells which was apparent at 5 min post-stimulation and reached maximal levels at 10 min post-stimulation (Fig. 9.1, ** = $p < 0.01$ vs. 0 min). Continued stimulation of LNCaP cells with Fsk for longer than 10 min resulted in no further increase in detected levels of activated ERK1/2 and levels of pThr²⁰²pTyr²⁰⁴ERK1/2 did not decrease throughout the remainder of

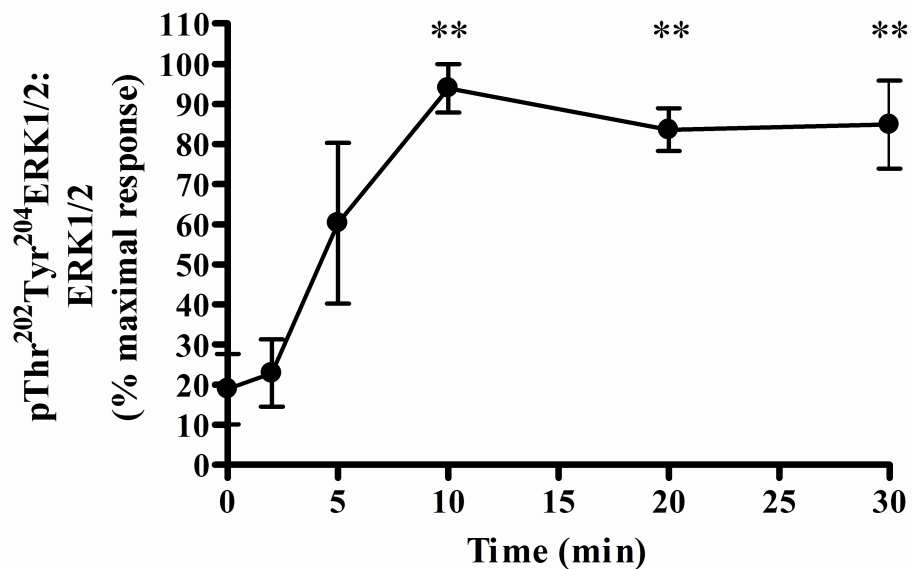
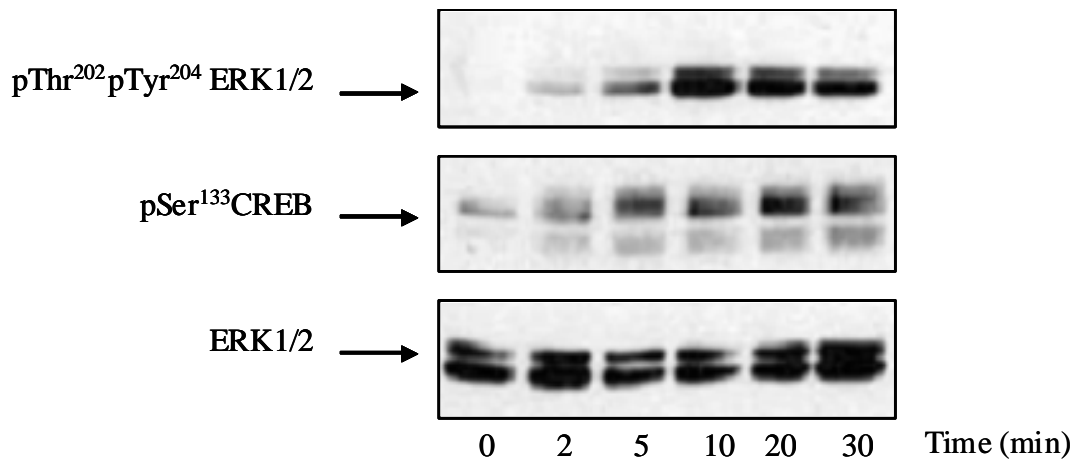


Fig. 9.1: Treatment with Fsk activates ERK1/2 in LNCaP cells

LNCaP cells were plated into 6-well plates coated with 0.1mg/ml poly-D-lysine HBr and grown to 70 % confluency. Cells were serum-starved for 2 h prior to stimulation with 10 μ M Fsk for 0 – 30 min. ERK1/2 activation was assessed *via* immunoblotting for pThr²⁰²pTyr²⁰⁴ ERK1/2 whilst the ability of Fsk to induce increases in intracellular cAMP was determined by immunoblotting for pSer¹³³CREB. Blots shown are representative of $n = 3$ experiments. Results are displayed as mean \pm SEM for $n = 3$ experiments. ** = $p < 0.01$ vs. 0 min time point.

the experiment (Fig. 9.1). The increase in pThr²⁰²pTyr²⁰⁴ERK1/2 was accompanied by parallel increases in pSer¹³³CREB, consistent with the hypothesis that this phenomenon is mediated through elevation of intracellular cAMP (Fig. 9.1).

9.2.2 Selective inhibition of the ERK1/2 pathway impairs Fsk-induced changes in LNCaP morphology

Having demonstrated that treatment with Fsk can induce activation of ERK1/2 in LNCaP cells, the role of this signalling protein in the Fsk-induced changes in LNCaP morphology was then assessed. LNCaP cells were plated into 6 well plates as described and grown to 50 % confluence in order to reliably assess changes in dendrite length. Images of LNCaP cells were captured as described prior to incubation with either vehicle (0.01 % (v/v) DMSO) or 10 μ M of the MEK1/2-selective inhibitor U0126 (Favata *et al.*, 1998) for 1 h at 37°C, 5 % (v/v) CO₂. Cells were then stimulated with either vehicle (0.01 % EtOH) or 10 μ M Fsk for 1 h and further images captured in order to assess changes in mean dendrite length as described previously.

In order to assess the efficacy of U0126, LNCaP cells were plated in parallel and serum-starved for 2 h prior to incubation with U0126 as described above. These cells were then stimulated for 15 min with 10 μ M Fsk as this was previously shown to be a suitable time point at which to determine ERK1/2 activation in LNCaP cells. It is necessary to serum-starve LNCaP cells prior to assessment of ERK1/2 activation due to the ability of serum to activate this signalling cascade. However, serum starvation of LNCaP cells also induces differentiation to a NE-like morphology *via* androgen deprivation (Chen *et al.*, 1992), and thus serum starvation may mask the ability of Fsk to modulate this process. It was therefore necessary to determine U0126 efficacy separately from the effect this inhibitor may have on Fsk-induced dendrite outgrowth. Efficacy of U0126 was assessed by immunoblotting for a decrease in Fsk-induced pThr²⁰²pTyr²⁰⁴ERK1/2 in the presence of U0126. It was found that pre-incubation with U0126 abolished the ability of Fsk to induce an increase in pThr²⁰²pTyr²⁰⁴ERK1/2 in LNCaP cells, indicating efficacy of the inhibitor (Fig. 9.2, panel C).

Treatment of LNCaP cells with either vehicle or 10 μ M U0126 had no apparent effect on LNCaP cell morphology (Fig. 9.2, panels A and B). In keeping with previous data, treatment with 10 μ M Fsk for 1 h induced an increase in mean dendrite length from 16.53 \pm 0.41 μ m to 30.29 \pm 0.67 μ m (Fig. 9.2, panels A and B, *** = p < 0.001 vs. 0 h, ### = p <

0.001 vs. vehicle). LNCaP cells pre-incubated with 10 μ M U0126 displayed an increase in dendrite length when treated with 10 μ M Fsk from $16.20 \pm 0.40 \mu\text{m}$ to $23.90 \pm 0.57 \mu\text{m}$ (Fig. 9.2, panels A and B, *** = $p < 0.001$ vs. 0 h, ### = $p < 0.001$ vs. vehicle). However, the ability of Fsk to induce an increase in mean dendrite length was reduced by approximately 44 % in the presence of U0126 (Fig. 9.2, panels A and B, +++ = $p < 0.001$ vs. Fsk at 1 h), indicating MEK1/2 activity is required, at least in part, for this phenomenon.

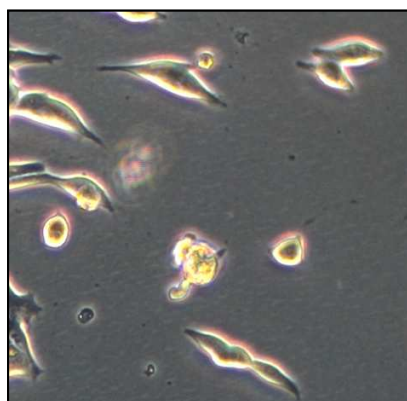
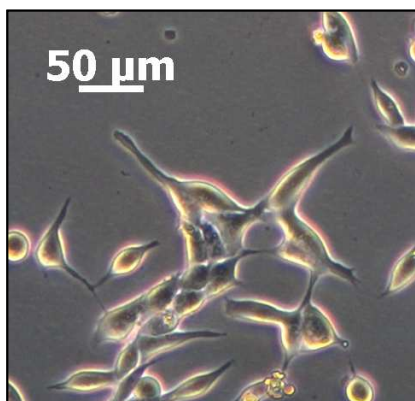
These results suggest that activation of ERK1/2 is required for the ability of Fsk to induce morphological changes in LNCaP cells consistent with differentiation to a NE-like phenotype. However, these experiments do not address whether activation of ERK1/2 alone is sufficient for this phenomenon.

9.2.3 Selective activation of ERK1/2 does not mimic the effect of Fsk treatment in LNCaP cells

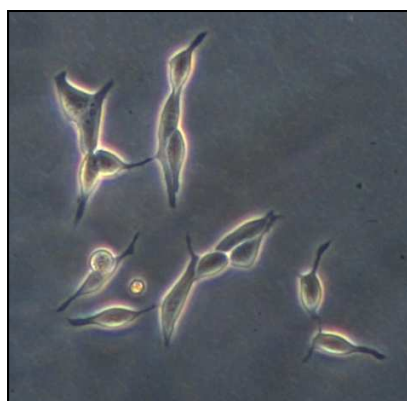
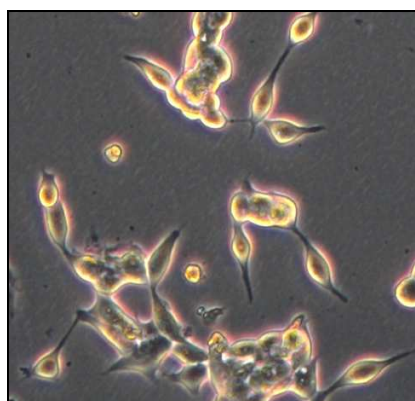
It was been demonstrated that selective inhibition of ERK1/2 activation in LNCaP cells inhibits the ability of Fsk to induce morphological changes in these cells, indicating that activation of ERK1/2 is required for this phenomenon. However, the question of whether activation of ERK1/2 is sufficient to induce these changes in morphology has not been addressed. Due to the essential nature of ERK1/2 in regulating cellular survival, it is not possible to address this problem *via* siRNA approaches, thus selective activation of ERK1/2 *via* a myc-tagged Raf1:oestrogen receptor (ER) chimera (myc.Raf1: Δ ER) was employed. The chimera encodes amino acids 305 – 648 of human Raf1 which encodes the CR3 kinase region fused to the hormone binding domain of the oestrogen receptor (Samuels *et al.*, 1993; Weston *et al.*, 2003). Treatment of cells expressing myc.Raf1: Δ ER with 4-hydroxytamoxifen (4OHT) results in activation of ER and subsequent activation of Raf1 which can then activate the MEK1/2-ERK1/2 signalling pathway.

In order to assess whether treatment of LNCaP cells transfected with myc.Raf1: Δ ER could induce changes in LNCaP morphology through selective activation of ERK1/2, it was first necessary to demonstrate that 4OHT was able to induce pThr²⁰²pTyr²⁰⁴ERK1/2 in these cells. LNCaP cells were transfected with 1 μ g of either vector (pCMV5) or myc.Raf1: Δ ER as described previously and serum-starved for 2 h to decrease basal pThr²⁰²pTyr²⁰⁴ERK1/2 prior to stimulation with 4OHT. LNCaP cells were stimulated with 100 nM 4OHT for 0 – 60 min and the ability of 4OHT to induce activation of ERK1/2 assessed by immunoblotting for pThr²⁰²pTyr²⁰⁴ERK1/2.

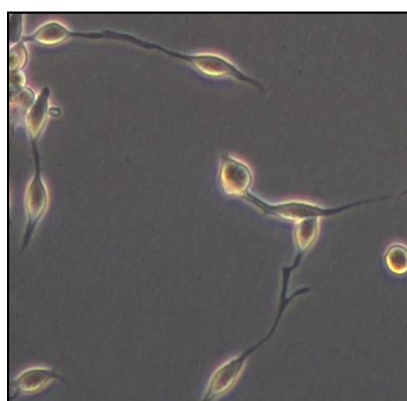
A



Vehicle



10 μ M U0126



10 μ M Fsk



10 μ M Fsk
+
10 μ M U0126

0 h

1 h

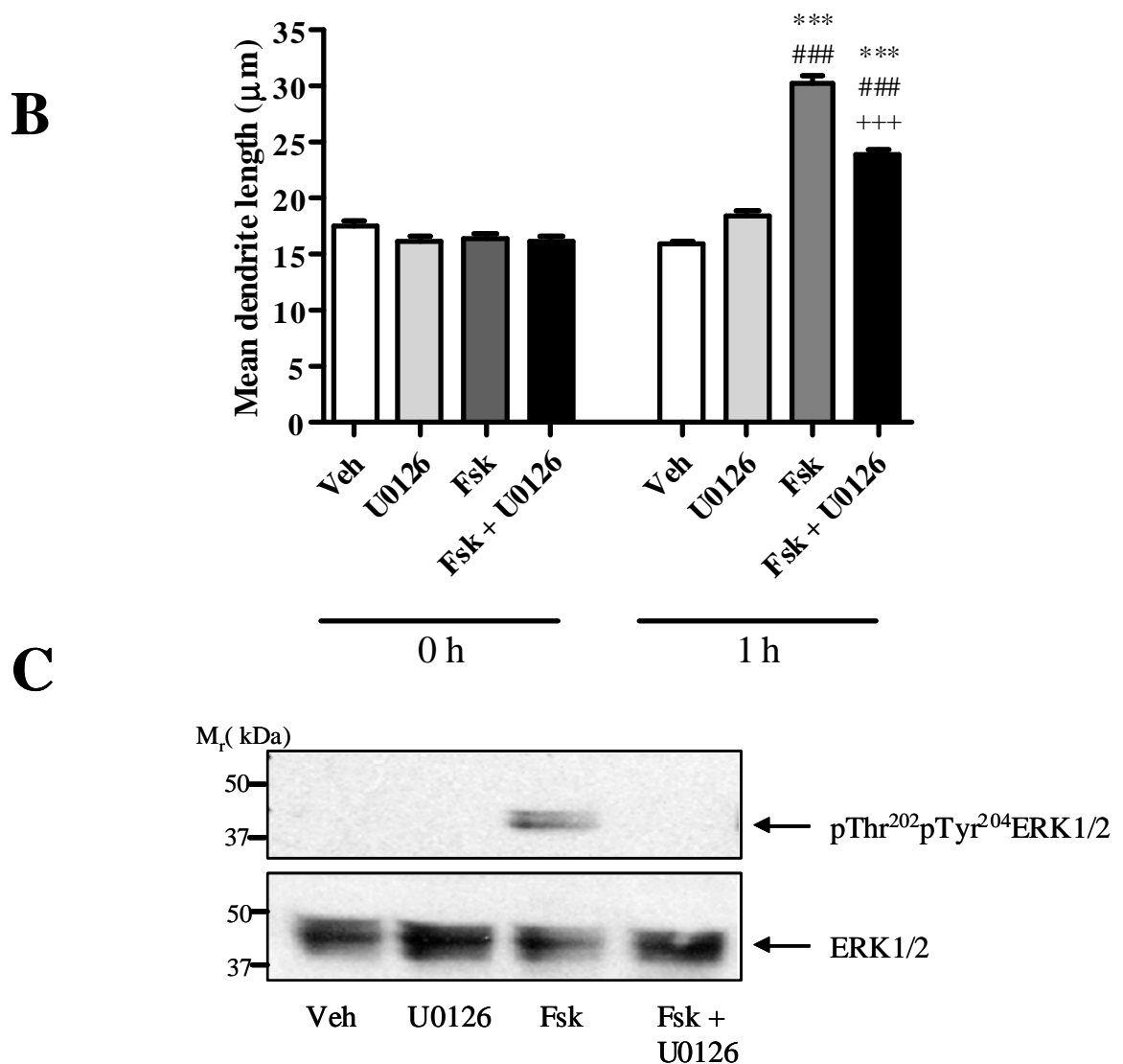


Fig. 9.2: The ability of Fsk to induce changes in LNCaP morphology requires MEK1/2 activity

LNCaP cells were seeded into 6-well plates and grown as described. In order to block activation of ERK1/2, cells were pre-incubated with vehicle (0.1% (v/v) DMSO) or 10 µM of the MEK1/2-selective inhibitor U0126 for 60 min prior to stimulation with vehicle or 10 µM Fsk for 1 h. Cells were assessed for changes in mean dendrite length as an indicator of differentiation to a NE-like morphology (panels A and B). U0126 efficacy was established in parallel experiments in LNCaP cells seeded as described and serum-starved for 2 h prior to incubation with vehicle or 10 µM U0126 for 60 min and subsequent stimulation with vehicle (0.1% EtOH) or 10 µM Fsk for 15 min. the ability of U0126 to inhibit MEK1/2 was assessed by a decrease in pThr²⁰²pTyr²⁰⁴ERK1/2 as detected *via* immunoblotting (panel C) Results are presented as mean values ± SEM for $n = 3$ experiments. *** = $p < 0.001$ vs. 0 h, ### = $p < 0.001$ vs. vehicle at same time point, +++ = $p < 0.001$ vs. Fsk at 1 h.

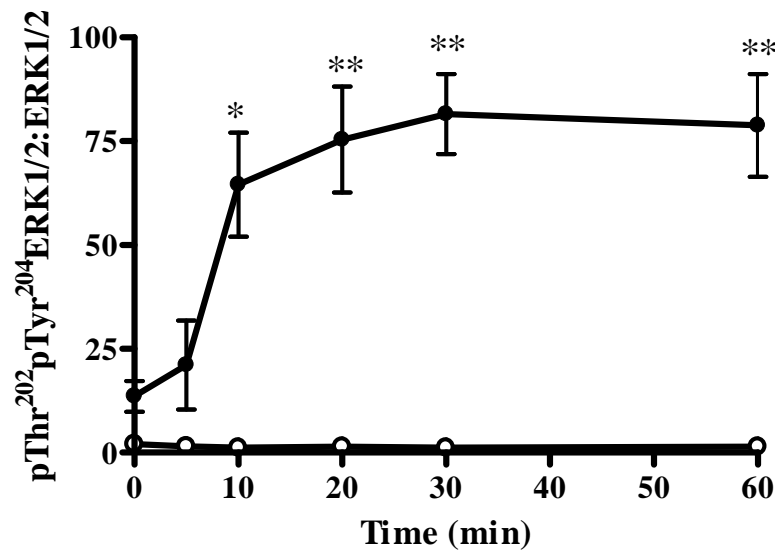
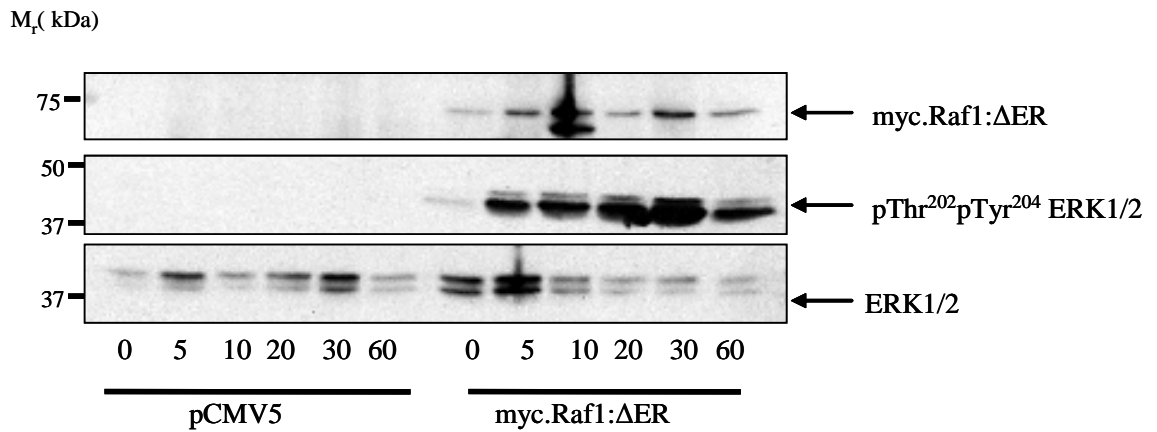


Figure 9.3: Expression of Myc.Raf1:ΔER allows selective activation of ERK1/2

LNCaP cells were transfected with 1 μg of vector (pCMV5) or myc.Raf1:ΔER and serum starved for 2 h prior to stimulation with 100nM 4OHT for 0 – 60 min. The ability of 4OHT to induce activation of ERK1/2 was assessed *via* immunoblotting for pThr²⁰²pTyr²⁰⁴ERK1/2 and successful expression of myc.Raf1:ΔER determined *via* immunoblotting for the myc epitope. Results for LNCaP cells transfected with pCMV5 are represented by open circles whilst results for LNCaP cells transfected with pCMV5.Myc.Raf1:ΔER are represented by closed circles. Blot is representative of *n* = 3 experiments. Results are represented as mean values ± SEM for *n* = 3 experiments. * = *p* < 0.05, ** = *p* < 0.01 vs. 0 h treatment.

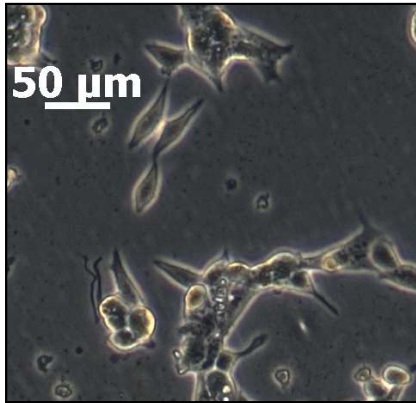
LNCaP cells transfected with pCMV5 displayed no increase in pThr²⁰²pTyr²⁰⁴ERK1/2 following treatment with 100 nM 4OHT (Fig. 9.3), indicating that any changes in ERK1/2 activation result from activation of myc.Raf1:ΔER and not from non-selective effects on endogenous steroid hormone receptors. In contrast to cells transfected with pCMV5, LNCaP cells transfected with myc.Raf1:ΔER displayed a robust increase in pThr²⁰²pTyr²⁰⁴ERK1/2 at 5 min post-stimulation which increased to maximal levels by 20 min post-stimulation (* = $p < 0.05$ vs. 0 h, ** = $p < 0.01$ vs. 0 h). These results indicate that treatment of LNCaP cells expressing myc.Raf1:ΔER is able to selectively activate ERK1/2 in response to 4OHT stimulation.

To assess whether selective activation of ERK1/2 was sufficient to induce changes in LNCaP morphology, LNCaP cells were plated into 6-well plates and transfected with 1 μg CMV5 or myc.Raf1:ΔER as described. On the day of experimentation, cell culture medium was replaced with 1 ml of fresh medium and images of LNCaP cells captured as described. Cells were then stimulated with vehicle (0.1% (v/v) EtOH) or 100 nM freshly prepared 4OHT for 18 h with images captured at the appropriate time points post-stimulation. In order to assess efficacy of 4OHT, LNCaP cells transfected with pCMV5 or myc.Raf1:ΔER were stimulated with 100 nM 4OHT for 15 min immediately prior to the end of the experiment and activation of ERK1/2 assessed by immunoblotting for pThr²⁰²pTyr²⁰⁴ERK1/2. Expression of myc.Raf1:ΔER was confirmed by immunoblotting against the myc epitope.

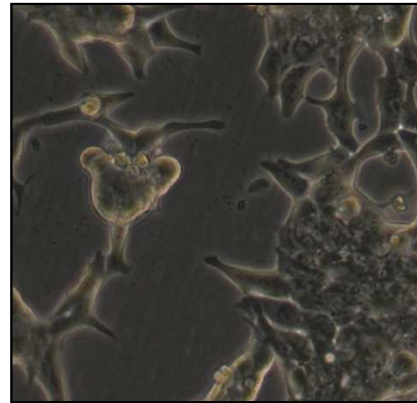
Treatment with vehicle did not alter cellular morphology in LNCaP cells transfected with either pCMV5 or myc.Raf1:ΔER (Fig. 9.4, panels A, B and C, $p > 0.05$). Similarly, LNCaP cells transfected with pCMV5 showed no changes in morphology when stimulated with 100 nM 4OHT for 0 – 18 h (Fig. 9.4, panels B and C, $p > 0.05$). In contrast, LNCaP cells transfected with myc.Raf1:ΔER displayed an increase in mean dendrite length at 8 h post-infection with an increase in dendrite length from 14.93 ± 0.399 μm at 4 h post-stimulation to 22.07 ± 0.586 μm at 8 h post-stimulation (Fig. 9.4, panels B and C, *** = $p < 0.001$ vs. 0 h, ### = $p < 0.001$ vs. pCMV5 at same time point, +++ = $p < 0.001$ vs. vehicle-stimulated myc.Raf1:ΔER). Successful expression of myc.Raf1:ΔER and efficacy of 4OHT was confirmed *via* immunoblotting for the myc epitope and pThr²⁰²pTyr²⁰⁴ERK1/2 respectively (Fig. 9.4, panel D). The results suggest that selective activation of ERK1/2 can induce changes in LNCaP morphology consistent with NE-like differentiation. However, it must be noted that selective activation of ERK1/2 in these cells does not induce a

A

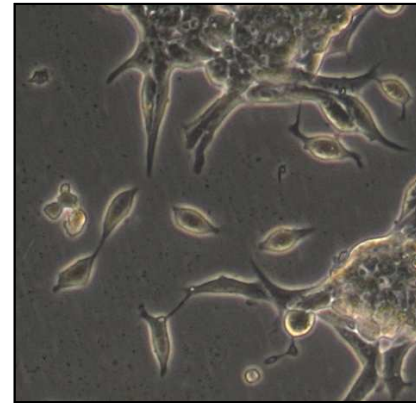
pCMV5: vehicle



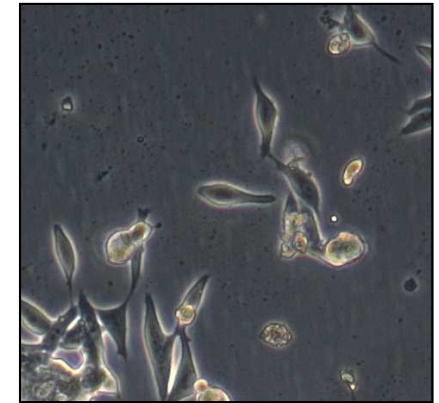
0 h



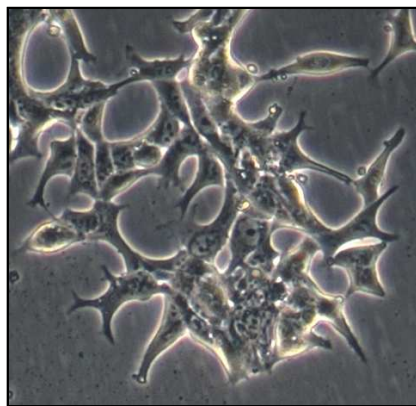
1 h



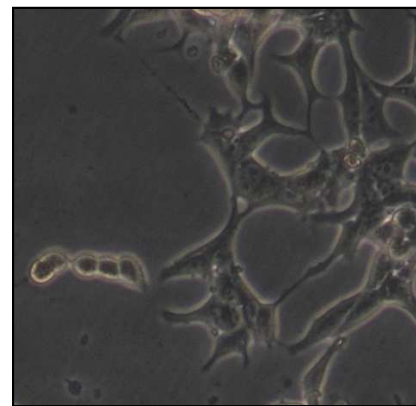
2 h



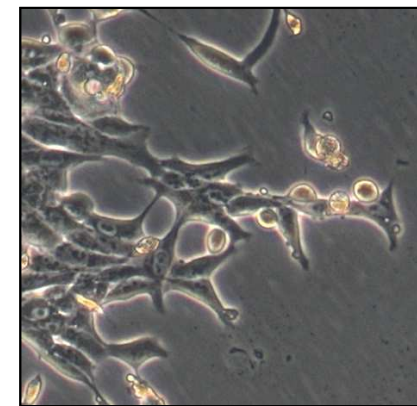
4 h



8 h



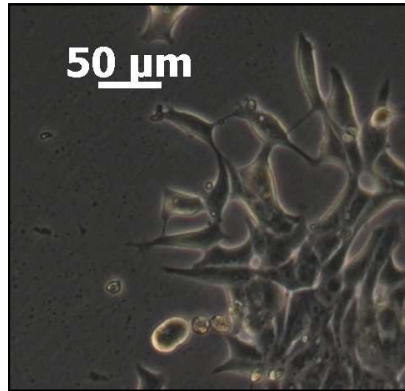
12 h
225



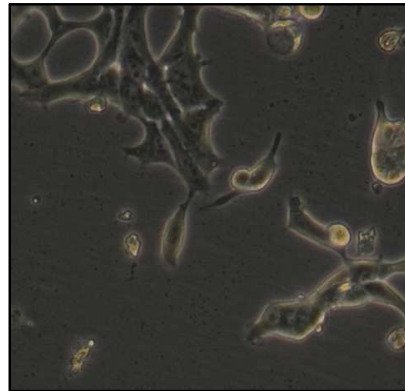
18 h

B

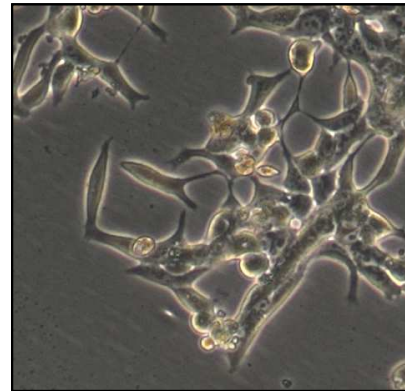
pCMV5: 100nM 4OHT



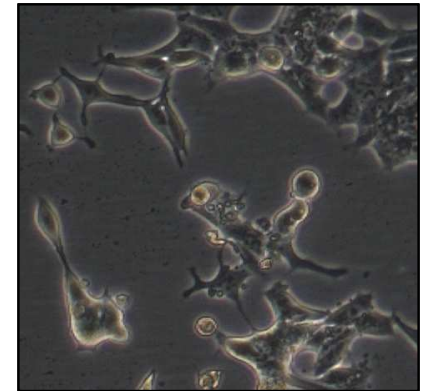
0 h



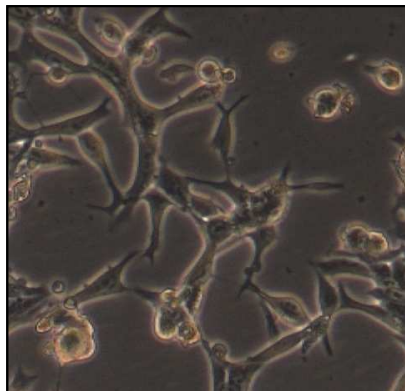
1 h



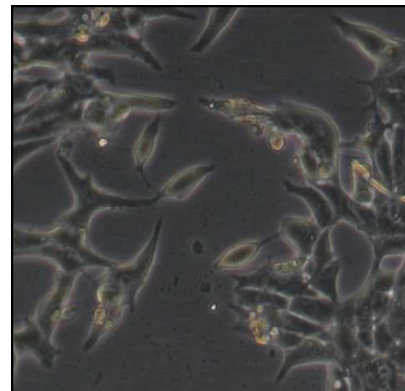
2 h



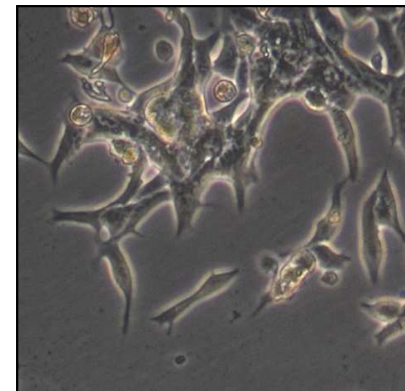
4 h



8 h



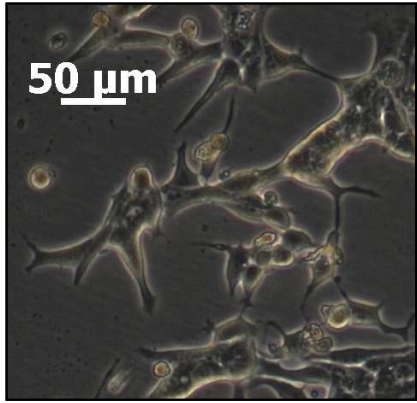
12 h



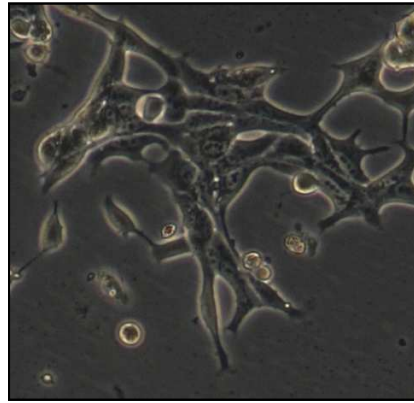
18 h

C

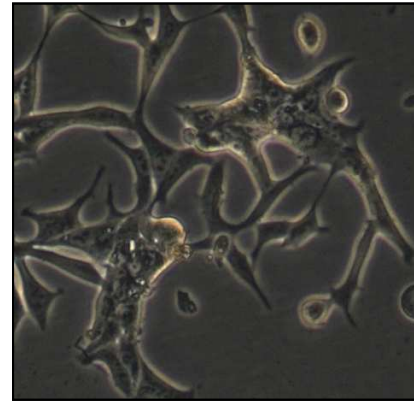
myc.Raf1:ΔER: vehicle



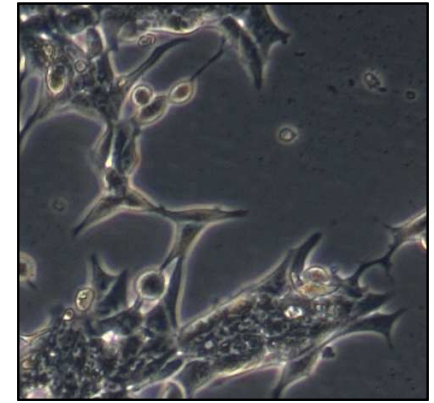
0 h



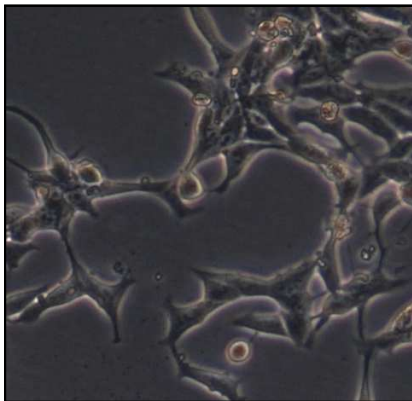
1 h



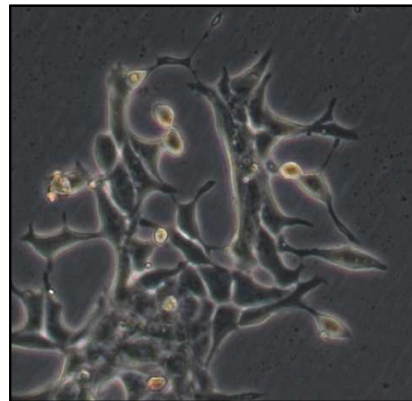
2 h



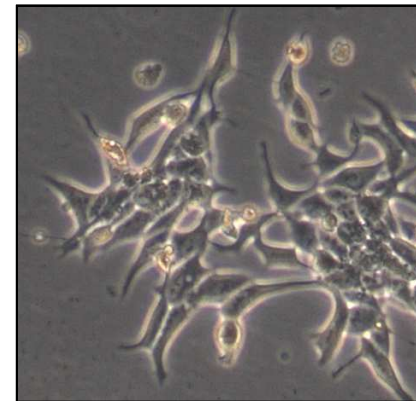
4 h



8 h



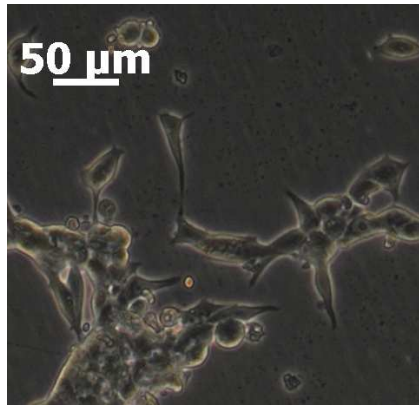
12 h



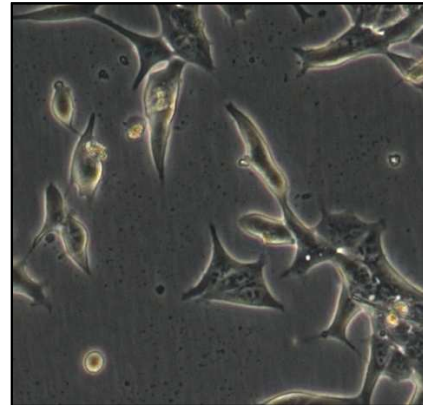
18 h

D

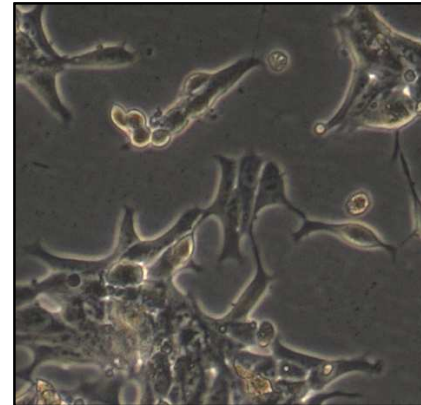
myc.Raf1: Δ ER: 100nM 4OHT



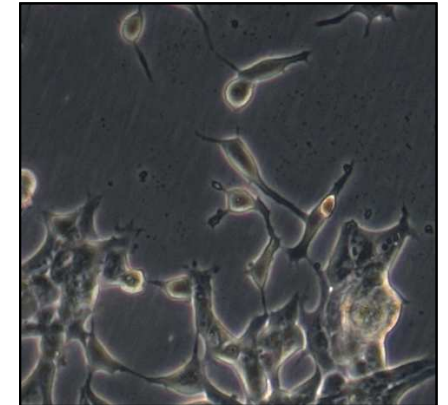
0 h



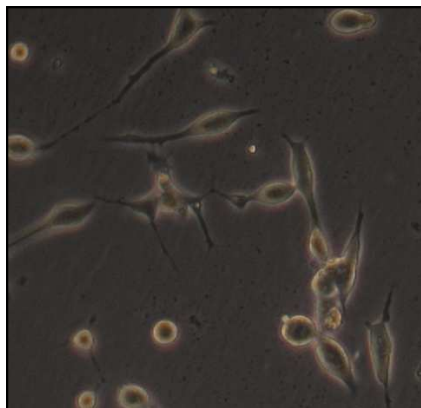
1 h



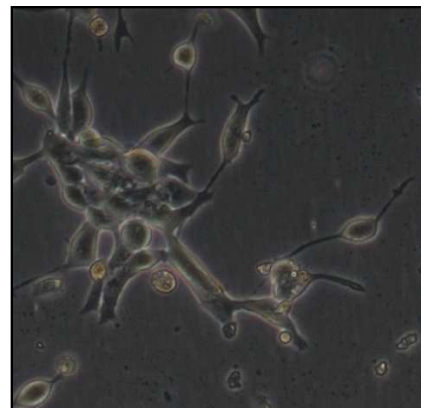
2 h



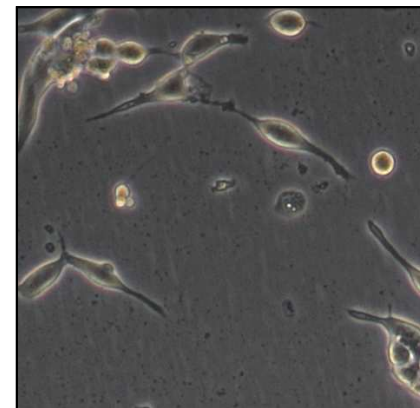
4 h



8 h



12 h



18 h

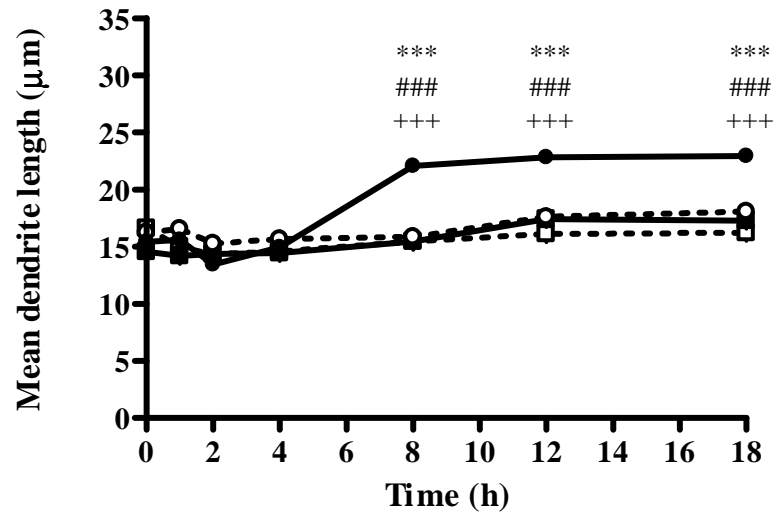
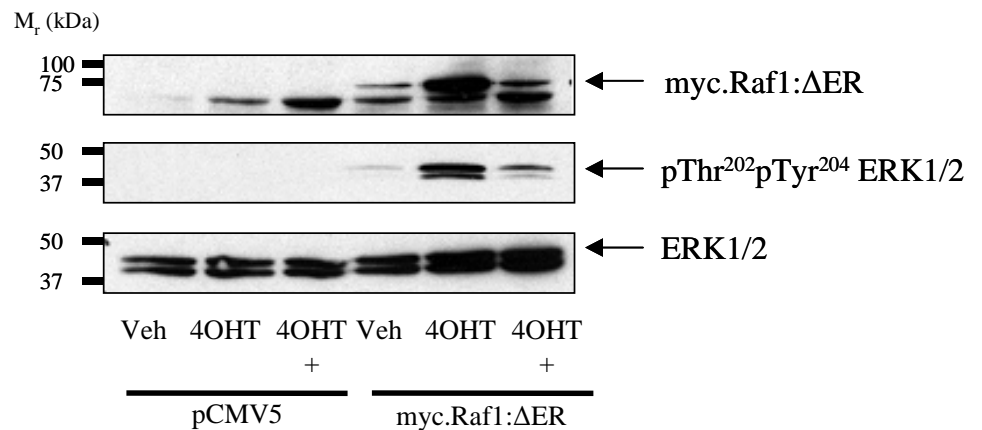
E**F**

Fig. 9.4: Selective activation of ERK1/2 results in changes in LNCaP morphology but at later time points than seen following Fsk treatment

LNCaP cells were seeded into 6-well plates coated with 0.1 mg/ml poly-D-lysine and transfected with 1 µg of either pCMV5 (panels A and B) or myc.Raf1:ΔER cDNA (panels C and D). Cells were then stimulated with either vehicle (0.1% (v/v) EtOH, panels A and C) or 100 nM of freshly prepared 4OHT for 0 – 18 h (panels B and D) with images captured at appropriate time points. Differentiation to a NE-like phenotype was determined by an increase in mean dendrite length (panel C) with results represented as mean values \pm SEM for $n = 3$ separate experiments. LNCaP cells expressing pCMV5 are shown as open or closed squares for vehicle and 100 nM 4OHT-stimulated cells respectively whilst results for cells expressing myc.Raf1:ΔER are shown as open (vehicle) or closed (100 nM 4OHT) circles (panel E). *** = $p < 0.001$ vs. 0 h, ### = $p < 0.001$ vs. pCMV5 at same time point, +++ = $p < 0.001$ vs. vehicle stimulated cells at same time point. In order to assess 4OHT efficacy, LNCaP cells were stimulated with 100 nM 4OHT for 15 min immediately prior to the end of the experiment and cell lysates immunoblotted for pThr²⁰²pTyr²⁰⁴ERK1/2 (panel F). Expression of myc.Raf1:ΔER was confirmed by immunoblotting for the myc epitope (panel F). Blot shown is representative of $n = 3$ separate experiments.

detectable change in cellular morphology until 8 h post-stimulation (Fig. 9.4, panels B and C), whilst it has previously been demonstrated that the majority of Fsk-induced morphological changes in LNCaP cells occur within the first 1 h post-stimulation.

These data suggest that activation of ERK1/2, which appears important for later stage dendrite extension, may not be a key pathway important in the early stages of dendrite outgrowth. It could be argued that this conclusion contradicts the earlier observation that pre-incubation with U0126 partially blocks the ability of Fsk to induce dendrite outgrowth in LNCaP cells (Fig. 9.2). However, this may not be the case when considering published data demonstrating that many inhibitors which were previously thought to selectively inhibit the MEK1/2-ERK1/2 pathway also have inhibitory effects on the MEK5-ERK5 pathway (Mody *et al.*, 2001). U0126 numbers amongst such inhibitors, thus it is possible that the inhibitory effect of U0126 on Fsk-induced dendrite extension arises not from blockade of ERK1/2 activation but from inhibitory effects on ERK5.

9.2.4 Expression of a dominant negative ERK5 inhibits Fsk-induced increases in mean dendrite length

In order to test the hypothesis that the ability of U0126 to inhibit early Fsk-induced morphological changes in LNCaP cells arose due to effects on the ERK5 pathway rather than blockade of MEK1/2-mediated ERK1/2 activation, a genetic approach was first adopted. LNCaP cells were transfected with 1µg either vector cDNA (pBabePuro), cDNA encoding wild-type ERK5 (ERK5) or cDNA encoding a dominant negative mutant of ERK5 (ERK5-AEF) as described previously. Vector cDNA was used as a control to demonstrate that any effects of expressing the ERK5 constructs on Fsk-induced changes in LNCaP morphology did not arise as a result of cDNA transfection. LNCaP cells were transfected with wild-type ERK5 to demonstrate that any effect of expressing a dominant negative ERK5 was not due to an effect of over-expressing ERK5. The dominant negative ERK5 used in this experiment represents ERK5 in which the Thr²¹⁸Glu²¹⁹Tyr²²⁰ (TEY) activation motif has been mutated to Ala²¹⁸Glu²¹⁹Phr²²⁰ (AEF) and is thus resistant to MEK5-mediated activation (Kato *et al.*, 1997).

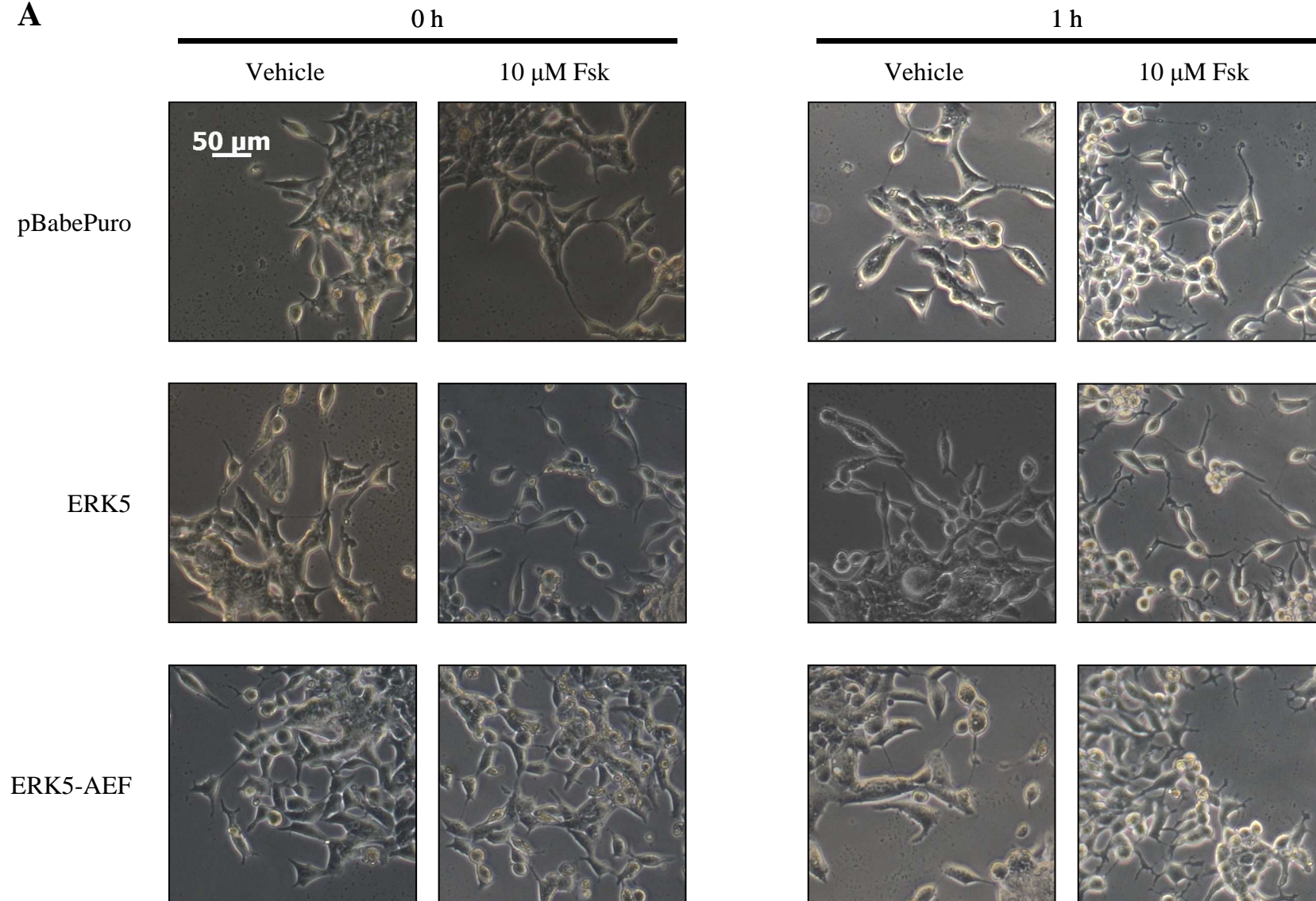
Prior to stimulation, culture medium on LNCaP cells was replaced with 1 ml of fresh culture medium and images of cells captured as described previously. Cells were then stimulated with either vehicle or 10 µM Fsk for 1 h and images captured at the end of this time period. Cells were harvested as described and activation of ERK5 confirmed *via*

immunoblotting for pThr²¹⁸pTyr²²⁰ERK5 (Fig. 9.5 panel C). Successful expression of the ERK5 constructs was confirmed by immunoblotting for total ERK5.

As seen previously, treatment of cells with vehicle failed to elicit any changes in LNCaP morphology whilst treatment of vector-transfected cells with 10 μ M Fsk promoted an increase in mean dendrite length from $15.90 \pm 0.4315 \mu\text{m}$ at 0 h post-stimulation to $28.09 \pm 0.5572 \mu\text{m}$ at 1 h post-stimulation (Fig. 9.5, panels A and B, *** = $p < 0.001$ vs. 0 h, ### = $p < 0.001$ vs. vehicle-stimulated cells at 1 h). Transfection of LNCaP cells with wild-type ERK5 did not enhance Fsk-induced increases in mean dendrite length with mean dendrite length increasing from $16.06 \pm 0.4003 \mu\text{m}$ at 0 h post-stimulation to $27.52 \pm 0.5757 \mu\text{m}$ at 1 h post-stimulation (Fig. 9.5, panels A and B, *** = $p < 0.001$ vs. 0 h, ### = $p < 0.001$ vs. vehicle-stimulated cells at 1 h). In contrast, expression of ERK5-AEF partially inhibited the ability of Fsk to induce increases in mean dendrite length with an increase in mean dendrite length from $18.21 \pm 0.5205 \mu\text{m}$ at 0 h to $22.93 \pm 0.4819 \mu\text{m}$ at 1 h post-stimulation (Fig. 9.5, panels A and B, *** = $p < 0.001$ vs. 0 h, ### = $p < 0.001$ vs. vehicle-stimulated cells at 1 h, +++ = $p < 0.001$ vs. vector and wild-type ERK5 at 1 h post-stimulation with Fsk). This corresponds to an almost 60 % decrease in the ability of Fsk to induce dendrite outgrowth in the presence of ERK5-AEF. The fact that expression of wild-type ERK5 had no effect on the ability of Fsk to induce morphological changes in LNCaP cells indicates that the inhibitory effect of ERK5-AEF on Fsk-induced changes in LNCaP morphology is due to the dominant negative effect of ERK5-AEF. When detected by immunoblotting, comparable levels of ERK5 were observed, indicating equal expression of the recombinant proteins. However, it must be noted that when for pThr²¹⁸pTyr²²⁰ERK5 was detected by immunoblotting, it appeared that treatment with Fsk promoted a decrease in dual-phosphorylated ERK5 whilst an increase in pThr²¹⁸pTyr²²⁰ERK5 was seen in LNCaP cells transfected with ERK5-AEF, suggestive of ERK5 activation. Whilst these results suggest that the ERK5-AEF is unsuitable for use as a dominant-negative construct, it is also possible that the results seen are an experimental artefact (see Discussion).

These results suggest that expression of a dominant negative ERK5 can impair the ability of Fsk to induce morphological changes in LNCaP cells, indicating that ERK5 activity is important for this phenomenon. It is therefore possible that the observed inhibitory effects of U0126 on Fsk-induced changes in LNCaP morphology arise due to impairment of ERK5 activation rather than ERK1/2 as was previously supposed.

A



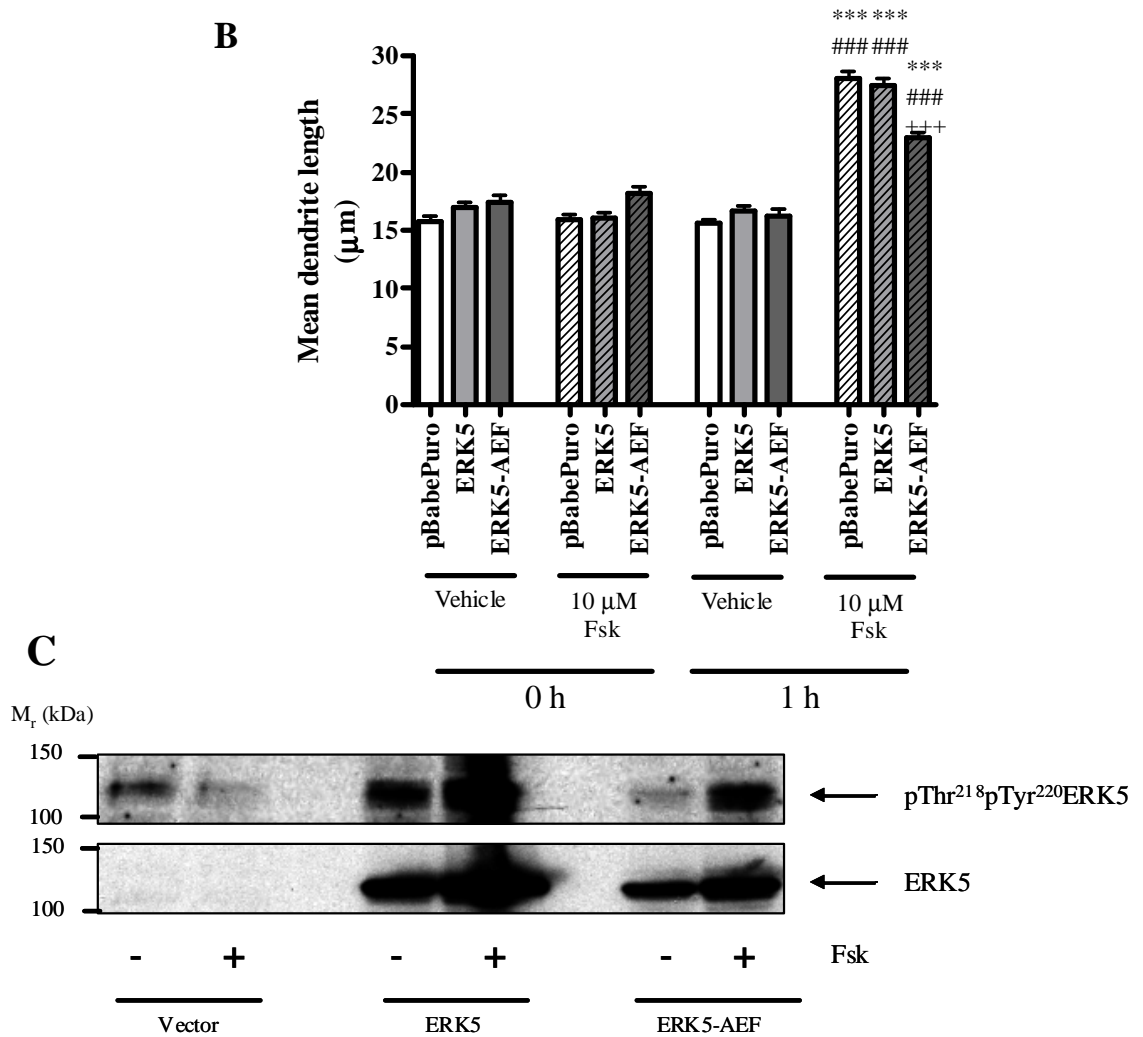


Fig. 9.5: Ectopic of dominant ERK5 impairs the ability of Fsk to induce morphological changes in LNCaP cells

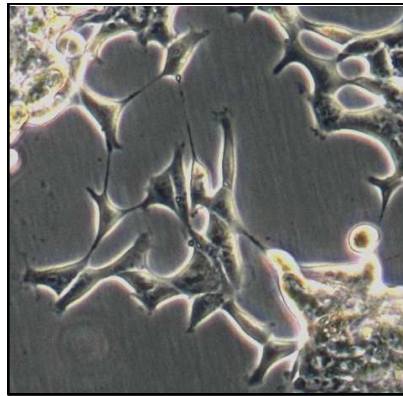
LNCaP cells were seeded into 6-well plates and transfected with 1 µg either vector cDNA (pBabePuro), cDNA encoding wild-type ERK5 (ERK5) or cDNA encoding a dominant negative mutant of ERK5 (ERK5-AEF) as described previously. Cells were then stimulated with either vehicle (0.1 % (v/v) EtOH) or 10 µM Fsk and images captured at 0 h and 1 h post-stimulation (panel A). Differentiation to a NE-like morphology was assessed *via* an increase in mean dendrite length (panel B) and values represent mean values \pm SEM for $n = 3$ separate experiments. *** = $p < 0.001$ vs. 0 h, ### = $p < 0.001$ vs. vehicle, +++ = $p < 0.001$ vs. vector and wild-type ERK5. Activation of ERK5 was determined *via* immunoblotting for pThr²¹⁸pTyr²²⁰ERK5 whilst successful construct expression was determined *via* immunoblotting for ERK5. Blot shown is representative for $n = 3$ separate experiments.

9.2.5 Selective inhibition of MEK5 blocks Fsk-mediated changes in mean dendrite length in LNCaP cells

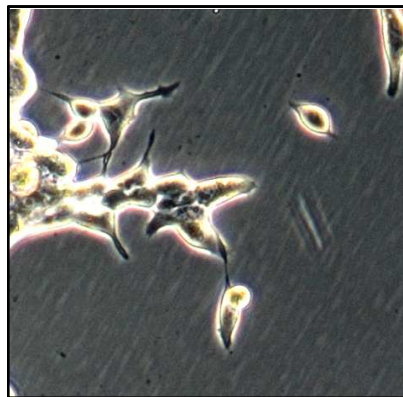
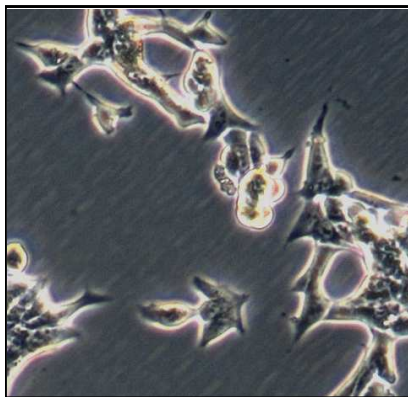
Whilst over-expression of dominant negative ERK5 effectively blocked the ability of Fsk to induce increases in mean dendrite length, the use of protein over-expression alone is not the ideal method by which to dissect the roles of intracellular signalling molecules. It is possible that temporal or spatial separation of signalling partners may be disrupted or that signalling pathways may be altered due to supraphysiological levels of a particular protein. In order to verify the role of ERK5 in Fsk-induced dendrite outgrowth in LNCaP cells, the MEK5-selective inhibitor BIX02188 was used. Until recently, no selective inhibitors of the MEK5-ERK5 pathway were available, with pharmacological inhibition of this pathway only achievable *via* inhibitors such as U0126 which were previously thought to act exclusively on the MEK1/2-ERK1/2 signalling pathway. To date, BIX02188 and its sister compound BIX02189 are the only published MEK5-selective inhibitors demonstrating high selectivity for MEK5 *in vitro* ($IC_{50} = 4.3$ nM and 1.5 nM for BIX02188 and BIX02189 respectively) (Tatake *et al.*, 2008). In comparison, the IC_{50} vs. MEK1 and MEK2 was in excess of 6000 nM, indicating the high degree of selectivity of BIX02188 and BIX02189 for the MEK5-ERK5 pathway in comparison to ERK1/2 (Tatake *et al.*, 2008). However, these studies determined the IC_{50} for BIX02188 against purified kinases and thus concentrations required for inhibition of MEK5 in intact cells are likely to be higher. It has recently been published that treatment with 30 μ M BIX02189 inhibited NGF-induced neurite outgrowth in PC12 cells (Obara *et al.*, 2009). To assess if this concentration of BIX02188 inhibited Fsk-mediated increases in mean dendrite length in LNCaP cells, cells were plated into 6-well tissue culture plates and incubated with either vehicle (0.3 % (v/v) DMSO) or 30 μ M BIX02188 for 1 h at 37°C , 5 % (v/v) CO_2 prior to incubation with either vehicle (0.1 % (v/v) EtOH) or 10 μ M Fsk for 1 h. Phase contrast images were captured at 0 h and immediately post-stimulation and analysed for changes in mean dendrite length as described previously.

As found previously, treatment with vehicle did not affect mean dendrite length (mean dendrite length = 17.43 ± 0.50 μ m and 15.80 ± 0.42 μ m at 0 h and post-stimulation respectively, Fig. 9.6, panels A and B). Similarly, treatment with BIX02188 alone had no effect on mean dendrite length with mean dendrite lengths measuring 17.78 ± 0.61 μ m at 0 h and 15.46 ± 0.41 μ m post-stimulation (Fig. 9.6, panels A and B). Treatment with Fsk resulted in an increase in mean dendrite length from 17.93 ± 0.42 μ m at 0 h to 33.80 ± 0.61

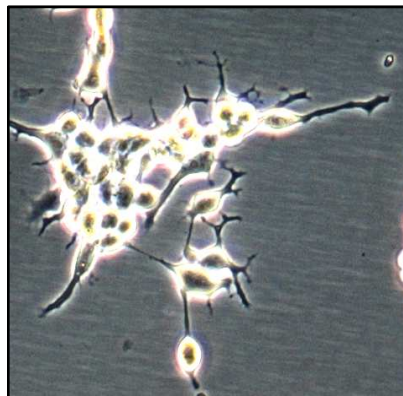
A



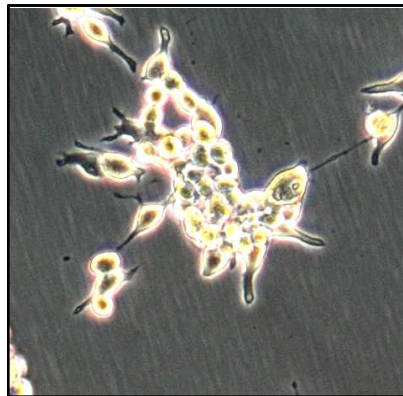
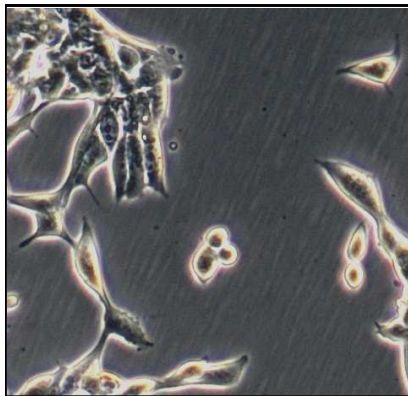
Vehicle



30 μ M BIX02188



10 μ M Fsk



30 μ M BIX02188
+ 10 μ M Fsk

0 h

post-stimulation

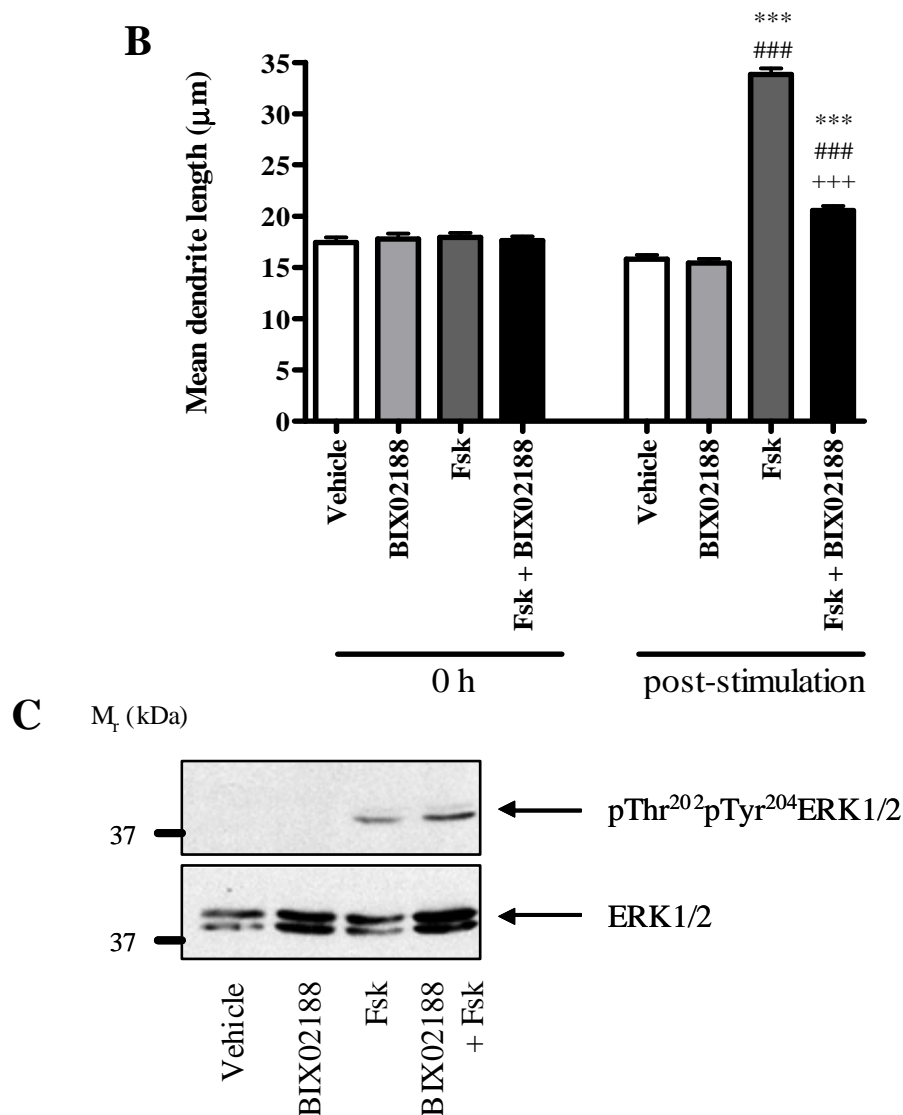


Fig. 9.6: The ability of Fsk to induce changes in LNCaP morphology requires MEK5 activity

LNCaP cells were seeded into 6-well plates and grown as described. In order to block activation of ERK5, cells were pre-incubated with vehicle (0.3 % (v/v) DMSO) or 0 µM of the MEK5-selective inhibitor BIX02188 for 60 min prior to stimulation with vehicle or 10 µM Fsk for 1 h. Cells were assessed for changes in mean dendrite length as an indicator of differentiation to a NE-like morphology (panels A and B). BIX02188 efficacy was established in parallel experiments in LNCaP cells seeded as described and transfected with 1 µg ERK5 cDNA prior to incubation with vehicle (0.3 % (v/v) DMSO) or 30 µM BIX02188 for 60 min and subsequent stimulation with vehicle (0.1% EtOH) or 10 µM Fsk for 15 min. Treatment with BIX02188 did not alter the ability of Fsk to activate ERK1/2 as detected *via* immunoblotting (panel C) Results are presented as mean values ± SEM for $n = 3$ experiments. *** = $p < 0.001$ vs. 0 h, ### = $p < 0.001$ vs. vehicle at same time point, +++ = $p < 0.001$ vs. Fsk at 1 h.

μm post-stimulation (Fig. 9.6, panels A and B, *** = $p < 0.001$ vs. 0 h, ### = $p < 0.001$ vs. vehicle). The ability of Fsk to induce an increase in mean dendrite length was attenuated following pre-incubation with 30 μM BIX02188, with mean dendrite length increasing from $17.63 \pm 0.41 \mu\text{m}$ at 0 h to just $20.54 \pm 0.45 \mu\text{m}$ post-stimulation (Fig. 9.6, panels A and B, *** = $p < 0.001$ vs. 0 h, ### = $p < 0.001$ vs. vehicle, +++ = $p < 0.001$ vs. Fsk). These results demonstrate that pre-incubation with BIX02188 blocks the ability of Fsk to induce changes in LNCaP cell morphology and support previous data in this study suggesting that activation of the ERK5 signalling pathway is an important effector in Fsk-mediated changes in LNCaP cell morphology.

Although BIX02188 is thought to be at least 3 orders of magnitude more selective for MEK5 in comparison to MEK1 or MEK2, it is possible that, at the higher concentrations used in intact cells, the inhibitor may be exerting non-selective effects on other signalling pathways. Of particular concern given the non-selective effects of MEK1/2-selective inhibitors such as U0126 on MEK5 is the possibility that ERK1/2 signalling may also be inhibited when using BIX02188 at a concentration of 30 μM . To assess whether this was indeed the case, LNCaP cells were seeded into 6-well tissue culture dishes as described previously and grown to 70 % confluency prior to serum starvation overnight to reduce basal activation of both ERK1/2 and ERK5. The following day, growth medium was replaced with fresh serum-free RPMI and LNCaP cells incubated for 1 h with either vehicle (0.3 % (v/v) DMSO) or 30 μM BIX02188 at 37°C, 5 % (v/v) CO₂. Cells were then stimulated with either vehicle (0.1 5 (v/v) EtOH) or 10 μM Fsk to induce ERK1/2 activation. Unfortunately, the amount of protein obtained from these experiments was insufficient to determine increases in pThr²¹⁸pTyr²²⁰ERK5, it was possible to determine that pre-incubation with BIX02188 had no discernible effect on Fsk-induced increases in pThr²⁰²pTyr²⁰⁴ERK1/2 (Fig. 9.6, panel C). These results indicate that the effects of BIX02188 on Fsk-induced changes in LNCaP cell morphology are due to selective inhibition of the MEK5-ERK5 signalling pathway and not due to effects on ERK1/2 signalling.

9.3 Discussion

Treatment with NGF, cAMP analogues and Fsk all result in neurite outgrowth in PC12 cells. All of these stimuli induce sustained activation of ERK1/2, a process which has been shown to be required for neurite outgrowth in PC12 cells. Activation of both PKA and EPAC has been implicated in this phenomenon with PKA activation being required for the

sustained activation of ERK1/2 (Yao *et al.*, 1998b). In the previous chapter, it was demonstrated that selective activation of PKA could mimic the effects of Fsk treatment on LNCaP cell morphology, suggesting that this phenomenon is PKA dependent. However, the effect of cAMP elevation on ERK1/2 activation in LNCaP cells has not been investigated. In this chapter, cAMP elevation promoted an increase in ERK1/2 activation as detected by an increase in pTyr²⁰²pThr²⁰⁴ERK1/2 and treatment with the MEK-selective inhibitor U0126 inhibited Fsk-induced changes in LNCaP cell morphology. However, whilst selective activation of ERK1/2 induced changes in LNCaP cell morphology, an increase in mean dendrite length was observed only at 8 h post-stimulation, suggesting that activation of ERK1/2 is not the primary pathway involved in Fsk-induced changes in LNCaP cell morphology.

In addition to MEK1/2, U0126 can also inhibit MEK5 at concentrations similar to those used in this study. In PC12 cells, it has recently been demonstrated that activation of ERK5 plays an important role in neurite outgrowth (Obara *et al.*, 2009), thus there may be a role for the MEK5/ERK5 signalling pathway in Fsk-induced changes in LNCaP cell morphology. To address this, ERK5-AEF, a dominant negative ERK5 was expressed in LNCaP cells. Treatment with Fsk promoted an increase in mean dendrite length in LNCaP cells transfected with vector or wild-type ERK5 but not in those expressing ERK5-AEF, indicating that ERK5 activation is important in this phenomenon. However, over-expression studies are not the ideal strategy by which to address the roles of signalling proteins as high levels of expression could induce protein interactions which would not happen physiologically. Thus, LNCaP cells were treated with the MEK5-selective inhibitor BIX02188 prior to stimulation with Fsk. Pharmacological blockade of MEK5 signalling prevented an increase in mean dendrite length following Fsk treatment, indicating that the MEK5/ERK5 signalling pathway is of importance in this phenomenon. At the concentration of BIX02188 used in this experiment, no effects on ERK1/2 activation were observed, indicating that the phenomenon is mediated by activation of ERK5.

In addition to MEK1/2, U0126 can also inhibit MEK5 at concentrations similar to those used in this study. In PC12 cells, it has recently been demonstrated that activation of ERK5 plays an important role in neurite outgrowth (Obara *et al.*, 2009), thus there may be a role for the MEK5/ERK5 signalling pathway in Fsk-induced changes in LNCaP cell morphology. To address this, ERK5-AEF, a dominant negative ERK5 was expressed in LNCaP cells. Treatment with Fsk promoted an increase in mean dendrite length in LNCaP cells transfected with vector or wild-type ERK5 but not in those expressing ERK5-AEF,

indicating that ERK5 activation is important in this phenomenon. However, over-expression studies are not the ideal strategy by which to address the roles of signalling proteins as high levels of expression could induce protein interactions which would not happen physiologically. Thus, LNCaP cells were treated with the MEK5-selective inhibitor BIX02188 prior to stimulation with Fsk. Pharmacological blockade of MEK5 signalling prevented an increase in mean dendrite length following Fsk treatment, indicating that the MEK5/ERK5 signalling pathway is of importance in this phenomenon. At the concentration of BIX02188 used in this experiment, no effects on ERK1/2 activation were observed, indicating that the phenomenon is mediated by activation of ERK5.

It cannot be ignored that in Fig. 9.5, determination of ERK5 phosphorylation demonstrated that treatment with Fsk resulted in an increase in pThr²¹⁸pTyr²²⁰ERK5 in LNCaP cells transfected with ERK5-AEF, suggestive that the construct is not functioning as a true dominant negative. Furthermore, treatment with Fsk promoted a decrease in endogenous pThr²¹⁸pTyr²²⁰ERK5 which suggests that Fsk is not able to activate ERK5 in these cells. However, whilst such observations dispute the conclusion above that ERK5 activation is an important mediator of Fsk-induced dendrite outgrowth in LNCaP cells, the immunoblotting results obtained may be experimental artefacts. Due to the poor quality of anti-pThr²¹⁸pTyr²²⁰ERK5 antibodies or low abundance of ERK5, cells were lysed directly into 12 % SDS sample buffer to maximise the amount of protein used for SDS-PAGE fractionation. Thus it was not possible to equalise samples for protein content prior to SDS-PAGE and subsequent immunoblotting. Due to the semi-quantitative nature of immunoblotting, it is possible that, particularly at the high levels of ERK5 expression seen in the transfected LNCaP cells, differences in protein loading would be masked by the high intensity of the protein signal. Therefore, the changes in ERK5 phosphorylation detected may be a simple result of changes in protein loading. Furthermore, it would be expected that only a fraction of the pool of cellular ERK5 would be activated in response to stimuli, thus the level of total ERK5 should be in excess to pThr²¹⁸pTyr²²⁰ERK5. This is particularly relevant when considering the observation that Fsk inhibits endogenous pThr²¹⁸pTyr²²⁰ERK5 (Fig. 9.5, panel C). The endogenous level of pThr²¹⁸pTyr²²⁰ERK5 detected appears comparable to that seen in lysates from LNCaP cells transfected with ERK5 or ERK5-AEF. However, in vector-transfected cells, endogenous ERK5 cannot be detected *via* immunoblotting. If there is insufficient endogenous ERK5 to detect by immunoblotting, these results question whether the anti- pThr²¹⁸pTyr²²⁰ERK5 antibody is reliably detecting dual phosphorylated ERK5.

These results suggest that ERK5 activation is required for cAMP-induced changes in cellular morphology. However, the ability of cAMP elevation to activate ERK5 in LNCaP cells has not been demonstrated due to problems detecting endogenous ERK5 and its activated form (data not shown and above) In HeLa cells, elevation of cAMP is associated with a decrease in EGF-induced activation of ERK5 due to PKA-mediated inhibition of MEKK2, an upstream kinase involved in ERK5 activation (Pearson *et al.*, 2006). In rat neonatal ventricular myocytes, it has been demonstrated that increases in cAMP can inhibit serum-induced activation of ERK5 *via* activation of EPAC rather than PKA, suggesting that the mechanisms by which cAMP elevation modulate ERK5 differs between cell type (Dodge-Kafka *et al.*, 2005). In DIV5 cortical neurones, treatment with Fsk induced activation of ERK1/2 but not ERK5 (Cavanaugh *et al.*, 2001). These results apparently contradict the observations in this chapter where it is suggested that treatment with Fsk can activate ERK5. However, an important difference between this study and previous data is that, in order to accurately measure mean dendrite length, LNCaP cells are stimulated at sub-maximal confluence. It has been demonstrated in NIH3T3 cells, that treatment with 8-Bromo-cAMP and the β_2 -adrenoceptor agonist isoproterenol can induce activation of ERK5 in 80 % confluent cells (Pearson & Cobb, 2002). In 50 % confluent NIH3T3 cell, treatment with a combination of Fsk and IBMX resulted in a transient activation of ERK5. However, in confluent NIH3T3 cells, cAMP attenuated EGF-induced activation of ERK5 and treatment with cAMP alone failed to induce ERK5 activation (Pearson & Cobb, 2002). Taken together, these results suggest that the ability of cAMP to induce ERK5 activation is dependent on cell conditions. Therefore, whilst cAMP elevation may be able to decrease ERK5 activation in response to cytokine stimulation, it is possible that, Fsk is able to activate ERK5 in sub-confluent LNCaP cells.

In PC12 cells, treatment with di-butryl-cAMP does not induce activation of ERK5 although robust activation of ERK5 can be induced by NGF. Treatment with NGF induces neurite outgrowth and is inhibited either by pre-incubation with BIX02189 or over-expression of dominant negative ERK5, indicating a crucial role for ERK5 in this process (Obara *et al.*, 2009). Although ERK5 activation appears to be critical in neurite outgrowth in PC12 cells and LNCaP cells, it is likely that the mechanism by which ERK5 activation is achieved varies between the cell types. This hypothesis is strengthened by observations in chapter 8 suggesting that the ability of Fsk to alter LNCaP cellular morphology is mostly mediated by activation of PKA and that EPAC activation may play a minor role in

this phenomenon, unlike the synergistic roles which PKA and EPAC are thought to play in PC12 cells.

It is hypothesised here that cAMP-mediated activation of ERK5 is important in NE-like differentiation of LNCaP cells; however, ERK5 activation has not been satisfactorily demonstrated. The ability of BIX02188 to inhibit Fsk-induced dendrite outgrowth in LNCaP cells corroborates data demonstrating that expression of ERK5-AEF can inhibit Fsk-induced changes in LNCaP cell morphology. However, although the concentration of BIX02188 used is consistent with previously published data (Obara *et al.*, 2009), it is possible that this compound is having non-selective effects on other pathways. Whilst an inhibitory effect of BIX02188 on MEK1/2 activation has been excluded it is possible that the compound may be acting on other kinases such as Src. BIX02188 shows far greater selectivity for Src in comparison to MEK1/2 at a test concentration of 3 μ M (Tatake *et al.*, 2008) and inhibition of Src could provide an alternative explanation for the BIX02188-mediated inhibition of Fsk-induced dendrite outgrowth observed in this study. In PC12 cells, NGF induces neurite outgrowth *via* a signalling pathway which involves Src-mediated activation of Ras and subsequent Raf activation (D'Arcangelo & Halegoua, 1993). Furthermore, as it has been proposed that activation of Rap1 is required for neuritogenesis, PKA-mediated activation of Src and subsequent activation of Rap1 has been demonstrated in PC12 cells in response to both NGF and cAMP elevation (Obara *et al.*, 2004). If such a pathway was present in LNCaP cells, it is possible that PKA-mediated activation of Src could provide a mechanism by which ERK1/2 is activated in response to Fsk and by which cAMP elevation induces dendrite outgrowth in these cells. To address whether BIX02188 is acting to inhibit Src activation, the phosphorylation status of Src substrates, such as Sin and Cas, which have been implicated in neurite outgrowth could be assessed (Yang *et al.*, 2002). Additionally, the role of Src activation in Fsk-induced changes in LNCaP cell morphology could be demonstrated *via* treatment with Src-selective inhibitors such as PP1. Whilst it is possible that BIX02188 is acting *via* inhibition of Src, it is still possible that ERK5 activation may play a role in Fsk-mediated changes in LNCaP cell morphology as ERK5 has been implicated in the activation of Src and subsequent limitation of RhoA in NIH3T3 cells (Schrapf *et al.*, 2008).

The observation that selective activation of ERK1/2 failed to induce early changes in LNCaP cell morphology was surprising as it was demonstrated that both Fsk and 4OHT treatment resulted in rapid activation of ERK1/2, indicating that it is important in the early stages of neurite outgrowth. It is possible that the signalling pathway which contributes to

ERK1/2 activation may play an important role in governing neuritogenesis. It has been proposed that sustained activation of B-Raf is important in neurite outgrowth as inhibition of p38 MAPK activity downstream of the EGFR results in sustained B-Raf and ERK1/2 activation. Of particular relevance is the observation that this sustained activation of B-Raf is associated with the conversion of EGF to a differentiation stimulus on PC12 cell, suggesting that activation of B-Raf, rather than Raf1 is important for neurite outgrowth (Yoon *et al.*, 2004). York *et al* (1998) demonstrated that sustained activation of ERK1/2 following NGF treatment required Rap1 activation and this was associated with downstream activation of B-Raf (York *et al.*, 1998). Indeed, treatment with NGF induces activation of B-Raf rather than Raf1 in PC12 cells (Jaiswal *et al.*, 1996) and supports the suggestion that B-Raf activation is key to neurite outgrowth. Thus, the role of ERK1/2 in this phenomenon cannot be excluded and use of a B-Raf: Δ ER chimera to selectively activate ERK1/2 may better delineate the role of this signalling pathway in neurite outgrowth. However, temporal differences in activation of the different ERK signalling cascades cannot be ignored and it may simply be the case that activation of ERK1/2 is necessary for later-stage processes necessary for NE-like differentiation in LNCaP cells.

It could be reasonably suggested that treatment with Fsk could induce sustained activation of ERK1/2 in LNCaP cells *via* EPAC2-mediated activation of Rap1 and subsequent activation B-Raf to promote neurite outgrowth. However, the previous chapter suggests that the effects of Fsk on changes in LNCaP cell morphology are mediated solely by the actions of PKA. Interestingly, PKA activation is required for Fsk-induced activation of Rap1 in PC12 cells through activation of the C3G Rap1-GEF (Wang *et al.*, 2006). Thus it is possible that a cAMP \rightarrow PKA \rightarrow C3G \rightarrow Rap1 \rightarrow B-Raf \rightarrow ERK1/2 signalling cascade exists in LNCaP cells which is important in Fsk-induced changes in LNCaP cell morphology.

It is currently unclear as to whether Raf proteins play a role in mediating activation of ERK5 following elevation of intracellular cAMP. It has been reported that activation of ERK5 downstream of Ras requires Raf1 and that ERK5 can bind full-length Raf1 *in vitro* and in cells (English *et al.*, 1999). However, in order to demonstrate this, cells were co-transfected with both the Raf1 and ERK5 constructs of interest (English *et al.*, 1999). Thus it is hard to ascertain whether the functional interaction of ERK5 and Raf1 is physiologically relevant as these results represent the interaction of over-expressed proteins.

It is possible that the predominant role of ERK5 in early changes in LNCaP cell morphology is mediated by the kinase exerting effects directly on the cytoskeleton. Given the critical role of the actin cytoskeleton in regulating cellular morphology, the ability of ERK5 to regulate actin polymerisation is of interest. ERK5 contains two proline-rich regions which are believed to target ERK5 to the actin cytoskeleton (Zhou *et al.*, 1995) and, importantly, are absent in ERK1/2 (Fig. 9.7). To date, there is no published data to demonstrate that ERK5 can interact with the actin cytoskeleton, although this could be readily determined by immunofluorescence to demonstrate colocalisation of ERK5 and actin. A Cdc24-like motif in MEK5 is associated with an increase in GTP → GDP exchange following interaction of CDC24 and CDC42 in *Saccharomyces cerevisiae* (Zhou *et al.*, 1995) and thus the MEK5/ERK5 pathway may dynamically regulate the actin cytoskeleton by acting to inhibit Cdc42 activity. Of particular interest to this study is the observation that ERK5 can directly limit RhoA activation *via* induction of RhoGAP7 expression (Schrapf *et al.*, 2008). It is therefore possible that activation of ERK5 as a result of cAMP elevation in LNCaP cells can inhibit RhoA activity in conjunction with PKA, although given the rapid changes in LNCaP cell morphology following Fsk stimulation, it is likely that induction of RhoGAP7 would play a minor role in changes in cellular morphology.

Whilst a role for PKA activation in the effects of ERK5 on changes in cellular morphology has not yet been determined, it is possible that PKA could directly activate MEKK3, MEK5 or ERK5. PKA phosphorylation sites for both proteins have been predicted in LNCaP cells (Table 9.1) although these need to be confirmed experimentally. Furthermore, as these sites are only predicted, it might be that they have no impact on ERK5 activity and thus *in vitro* and *in vivo* studies need to be performed to assess whether these sites exert regulatory roles on ERK5 activity. Interestingly, motifs for PKC-mediated phosphorylation were more frequently identified than PKA phosphorylation motifs and it might be that cAMP elevation can mediate activation of PKC in LNCaP cells as has been previously described in HUVECs (Borland *et al.*, 2009), neurones (Hucho *et al.*, 2005) and myocytes (Oestreich *et al.*, 2009). It is thought that cAMP-mediated activation of PKC occurs primarily through activation of EPAC (Borland *et al.*, 2009; Hucho *et al.*, 2005) but it is possible that the precise signalling networks responsible vary between cell types.

To summarise, data presented in this chapter suggest that the ability of cAMP elevation to induce early changes in LNCaP cell morphology may require activation of ERK5 and not ERK1/2 as was previously proposed. However, the precise nature of the signalling

pathways regulating ERK5 activity following cAMP elevation have not yet been defined and further work to delineate these may prove beneficial when investigating the emergence of NE cells in PCa.

```

ERK1 MAA-----AAAQGGGGEPRRTEGVGPGVPGVEVEMVKGQ---PFDVGPRYTQLQY 47
ERK2 MAA-----AAAAG-----AGP-----EMVRGQ---VFDVGPRYTINLSY 30
ERK5 MAEPLKEEDGEDGSAEPPGPVKAEPAPHTAASVAAKNLALLKARSFDTVFDVGDEYEI IET 60
**          .:*          ...          ::::          **** .*  :.

ERK1 IGEGAYGMVSSAYDHRKTRVAIKKIS-PFEHQTYCQRTLREIQILLRFRHENVIGIRDI 106
ERK2 IGEGAYGMVCSAYDNVNKVRVAIKKIS-PFEHQTYCQRTLREIKILLRFRHENIIGINDI 89
ERK5 IENGAYGVVSSARRRLTGQOVAIKKIPNAFDVVTNAKRTLRELKILKHFKHDNI IAIKDI 120
**:*:*:*:*.*.* .: .:*****. .:* * .:*****:*:* :*:*:*:*.*.***

ERK1 LRAST-LEAMRDVYIVQDLMETDLYKLLKS-QQLSNDHICYFLYQILRGLKYIHSANVLH 164
ERK2 IRAPT-IEQMKDVYIVQDLMETDLYKLLKT-QHLSNDHICYFLYQILRGLKYIHSANVLH 147
ERK5 LRPTVPYGEFKSVYVVLDLMESDLHQIIHSSQPLTLEHVRYFLYQLLRGLKYMHTSAQVIH 180
:*. . . . :.*:* *:*:*:*:*:*:* * * :* :* :* :* :* :* :* :* :* :*

ERK1 RDLKPSNLLINTTCDLKICDFGLAR-IADPEHDHTGFLTEYVATRWRAPAEIMLNSKGYT 223
ERK2 RDLKPSNLLLNTTCDLKICDFGLAR-VADPDHDHTGFLTEYVATRWRAPAEIMLNSKGYT 206
ERK5 RDLKPSNLLVNENCELKIGDFGMARGLCTSPAHEQYFMTEYVATRWRAPAEMLSLHEYT 240
*****:* .*:*** **:*:* . . . :* * :*****:*****:*.* : **

ERK1 KSIDIWSVGCILAEMLSNRPIFPKGHYLDQLNHILGILGSPSQEDLNCIINMKARNYLQS 283
ERK2 KSIDIWSVGCILAEMLSNRPIFPKGHYLDQLNHILGILGSPSQEDLNCIINLKARNYLLS 266
ERK5 QAIDLWSVGCIFGEMLARRQLFPKNYVHQLQLIMMVLGTPSPAVIQAVGAERVYRARIQS 300
:***:*****:.***:* :*****:*:*:* * :***:* :*: .* * :*

ERK1 LPSKTKVAWAKLFPKSDSKALDLLDRMLTFNPNKRITVEEALAHPPYLEQYYDPTDEPVAE 343
ERK2 LPHKNKVPWNR LFPNADSKALDLLDKMLTFNPHKRIEVEQALAHPPYLEQYYDPSDEPIAE 326
ERK5 LPPRQVPVWETVYPGADRQALSLLGRMLRFEP SARISAAAALRHPFLAKYHDPDDEPDCA 360
** : *.* :*: * :*.*.*:*:* * * . ** *:* :*:* * * .

ERK1 EPFTFAMELDDLPKERLKELI FQETA-----RFQPGVLEAP----- 379
ERK2 APFKFDMELDDLPKEKLELI FEETA-----RFQPGYRS----- 360
ERK5 PPFDFAFDREALTRERIKEAIVAEIEDFHARREGIROQIRFQPSLQPVASEPGCPDVEMP 420
* * * : : * .:*** * . * * * * .

ERK1 -----
ERK2 -----
ERK5 SPWAPSGDCAMESPPPAPPPCPGPAPDTIDLTLQPPPPVSEPAPKKDGAI SDNTKAALK 480

ERK1 -----
ERK2 -----
ERK5 AALLKSLRSRLRDGPSAPLEAPEPRKPVTAQERQREEREKRRRQERAKEREKRRQERER 540

ERK1 -----
ERK2 -----
ERK5 KERGAGASGGPSTDPLAGLVLSDNDRSLLERWTRMARPAAPALTSVPAPAPAPTPTPTPV 600

ERK1 -----
ERK2 -----
ERK5 QPTSPPPGPVAQPTGPPQPSAGSTSGPVQPACPPPGPAPHTGPPGPIVPAPPQIATS 660

ERK1 -----
ERK2 -----
ERK5 TSLLAQSLVPPPGLPGSSTPGVLPYFPPGLPPPDAGGAPQSSMSESPDVNLVTQQLSKS 720

ERK1 -----
ERK2 -----
ERK5 QVEDPLPPVFSGTPKSGAGYGVGFLEEF LNQSFDMGVADGPQDQADSASLSASLLAD 780

ERK1 -----
ERK2 -----
ERK5 WLEGHGMNPADIESLQREIQMDSPELLADLPDLQDP 816

```

Fig. 9.7: Sequence alignment of ERK1, ERK2 and ERK5 indicating proline-rich regions

MEKK3

Site	Kinase	Score	Site	Kinase	Score
S-9	PKA	0.54	S-243	PKG	0.57
T-30	PKC	0.78	S-246	PKC	0.61
S-39	PKC	0.63	S-246	PKA	0.54
S-43	PKC	0.53	S-246	PKG	0.51
S-61	PKC	0.76	S-250	RSK	0.56
T-74	cdc2	0.51	S-250	PKC	0.63
T-75	PKC	0.78	S-259	CKII	0.62
S-111	PKC	0.51	T-263	DNAPK	0.51
S-111	cdc2	0.52	T-263	PKC	0.53
S-112	RSK	0.57	Y-266	INSR	0.53
S-122	DNAPK	0.55	T-274	PKC	0.75
S-122	ATM	0.54	S-282	PKC	0.71
S-122	PKC	0.79	S-289	PKC	0.66
S-122	cdc2	0.55	T-307	cdc2	0.58
S-129	cdc2	0.52	S-312	PKA	0.57
S-130	cdc2	0.51	S-316	RSK	0.54
S-131	cdk5	0.56	T-317	PKC	0.70
S-145	DNAPK	0.59	S-337	RSK	0.56
S-145	PKA	0.58	S-337	PKB	0.69
T-153	PKC	0.54	S-337	PKA	0.57
Y-155	EGFR	0.58	S-337	PKG	0.56
S-162	GSK3	0.50	S-345	CKII	0.55
S-166	RSK	0.67	S-355	cdk5	0.58
S-166	PKB	0.72	T-384	CKII	0.53
S-166	PKC	0.54	S-399	CKI	0.60
S-166	PKA	0.62	S-399	p38MAPK	0.61
S-168	cdc2	0.55	S-399	GSK3	0.54
S-169	DNAPK	0.64	T-402	CKII	0.54
S-169	cdc2	0.60	S-407	CKII	0.64
S-175	PKG	0.51	S-450	PKC	0.65
S-176	cdk5	0.62	T-470	PKA	0.63
S-194	RSK	0.54	T-470	PKG	0.52
S-194	PKA	0.62	S-478	cdc2	0.51
Y-195	INSR	0.51	S-482	PKC	0.51
S-200	CKII	0.59	S-499	PKA	0.66
S-200	CKI	0.51	S-511	PKC	0.70
S-209	CKII	0.51	T-516	PKC	0.51
S-218	CKII	0.59	T-516	PKA	0.51
S-223	CKI	0.58	T-522	PKC	0.60
S-223	DNAPK	0.55	T-528	PKG	0.53
S-223	cdc2	0.51	T-530	GSK3	0.51
S-225	cdc2	0.55	T-530	cdk5	0.60
S-230	cdc2	0.55	S-535	cdk5	0.50
S-237	GSK3	0.51	S-552	PKA	0.64
S-239	PKC	0.74	Y-570	SRC	0.51
S-239	cdc2	0.53	T-581	DNAPK	0.63
S-243	PKA	0.68	S-590	PKC	0.69
			S-593	cdc2	0.52
			S-612	PKA	0.80

Highest score 0.80 PKA at position 612

MEK5

Site	Kinase	Score	Site	Kinase	Score
S-26	PKA	0.57	S-211	CKII	0.62
T-57	CKII	0.51	S-211	cdc2	0.51
T-58	CKII	0.58	Y-223	INSR	0.55
T-58	PKG	0.51	S-238	PKA	0.66
T-71	PKC	0.77	T-272	PKC	0.58
S-74	CKII	0.66	S-276	PKC	0.63
S-83	PKC	0.84	S-287	PKA	0.58
S-83	PKA	0.57	T-306	ATM	0.54
T-88	PKC	0.71	T-315	PKC	0.59
S-129	PKC	0.66	Y-322	EGFR	0.55
S-132	cdc2	0.58	S-329	PKA	0.51
S-133	p38MAPK	0.51	S-341	CKI	0.52
S-133	GSK3	0.54	S-345	CKII	0.51
S-133	cdk5	0.55	S-345	PKA	0.50
S-137	cdc2	0.58	S-365	PKA	0.74
S-142	PKC	0.56	S-380	p38MAPK	0.51
S-144	PKC	0.69	T-397	ATM	0.56
S-148	CKII	0.52	S-443	DNAPK	0.63
S-148	PKG	0.56	S-443	ATM	0.59
T-171	PKA	0.54			
T-179	PKC	0.63			

Highest score

0.84 PKC at position 83

ERK5

Site	Kinase	Score	Site	Kinase	Score
S-31	PKC	0.92	T-475	PKC	0.72
T-48	CKII	0.55	S-486	PKC	0.73
Y-55	SRC	0.53	S-489	PKC	0.58
Y-55	EGFR	0.51	S-489	cdc2	0.50
Y-55	INSR	0.54	S-496	cdc2	0.55
Y-66	SRC	0.53	S-548	PKC	0.63
S-70	PKC	0.51	S-585	PKC	0.68
S-71	PKC	0.79	T-594	p38MAPK	0.51
T-77	RSK	0.52	T-594	PKG	0.51
T-77	PKA	0.74	T-594	GSK3	0.52
T-94	PKC	0.78	T-594	cdk5	0.53
T-99	PKC	0.78	T-596	p38MAPK	0.51
S-142	CKII	0.52	T-596	cdk5	0.63
S-150	PKA	0.51	T-598	p38MAPK	0.52
S-151	DNAPK	0.62	T-598	GSK3	0.50
S-151	ATM	0.58	T-598	cdk5	0.67
S-151	PKA	0.56	S-604	p38MAPK	0.59
S-175	cdc2	0.50	S-604	GSK3	0.52
T-209	PKC	0.76	S-604	cdk5	0.55
S-210	p38MAPK	0.55	S-623	cdc2	0.57
T-240	DNAPK	0.55	T-624	PKC	0.57
S-247	PKC	0.71	S-625	cdc2	0.55
T-280	GSK3	0.50	T-643	PKG	0.59
Y-297	EGFR	0.56	T-661	cdc2	0.52
S-300	DNAPK	0.55	S-662	cdc2	0.52
S-300	PKC	0.62	S-668	cdc2	0.56
Y-313	SRC	0.51	S-679	cdc2	0.51
Y-313	EGFR	0.54	T-680	cdk5	0.56
S-322	PKC	0.63	S-703	CKII	0.53
S-333	cdc2	0.52	S-703	cdc2	0.51
S-337	PKA	0.66	S-720	CKII	0.53
S-337	PKG	0.56	S-720	ATM	0.60
T-373	PKC	0.64	T-733	p38MAPK	0.58
S-421	GSK3	0.51	T-733	GSK3	0.51
S-426	cdc2	0.54	T-733	cdk5	0.54
S-433	GSK3	0.50	S-737	PKG	0.53
S-433	cdk5	0.62	S-770	cdc2	0.51
S-472	CKII	0.51	S-794	DNAPK	0.55

Highest score

0.92 PKC at position 31

Table 9.1: Prediction of kinase phosphorylation sites within members of the ERK5 signalling cascade

The protein sequences for MEKK3, MEK5 and ERK5 were analysed for the presence of canonical phosphorylation sequences for a number of kinases using NetPhos 1.0 (Blom *et al.*, 2004). The presence of kinase phosphorylation sites were scored from 0 – 1 based on their identity to canonical sites with a score approaching 1 indicative of homology with known kinase phosphorylation sites. Key: ATM = ataxia telangiectasia mutated kinase, cdc2 = cell division cycle 2, cdk5 = cyclin dependent kinase 5, ckII = casein kinase II, DNAPK = DNA-activated protein kinase, EGFR = EGF receptor, GSK3 = glycogen synthase kinase 3, INSR = insulin receptor kinase, p38MAPK = p8 MAPK, PKA = protein kinase A, PKB = protein kinase B, PKC = protein kinase C, PKG = protein kinase G, RSK = ribosomal 6S kinase, SRC= Src kinase

10 Expression of the adenosine A_{2A} receptor alters LNCaP morphology

10.1 Introduction

Previously it was demonstrated that Fsk-mediated elevation of cAMP in LNCaP cells induced differentiation of this cell line to a NE-like phenotype through simultaneous inhibition of RhoA and activation of PKA and ERK5. Whilst a useful tool to investigate the effect of cAMP elevation on intracellular signalling pathways, treatment with Fsk globally activates membrane-associated adenylyl cyclase isoforms (Pinto et al., 2009). It is therefore possible that this strategy has limited physiological relevance due to the loss of temporal or spatial regulation of AC activation. It has previously been demonstrated that β -adrenergic receptor agonists such as isoproterenol can induce PKA-mediated NE differentiation of LNCaP cells (Cox et al., 2000), indicating that the effects of Fsk can be mimicked by endogenous $G\alpha_s$ -coupled GPCR activation.

GPCRs represent a diverse range of cell surface receptors involved in recognition of extracellular stimuli and subsequent activation of intracellular signal transduction pathways. GPCRs comprise an N-terminal extracellular domain, seven transmembrane domains connected by three intracellular and three extracellular loops and a C-terminal intracellular domain required for efficient signal transduction (Heilker et al., 2009). The intracellular regions of GPCRs are important for coupling to signalling modules within the cell, including the hetero-trimeric G-proteins from which this receptor superfamily get their name (Heilker *et al.*, 2009; Olah, 1997).

Intact G-proteins comprise of the $G\alpha$, $G\beta$ and $G\gamma$ subunits and cycle between the active, GTP-bound form and the inactive, GDP-bound complex. In the inactive conformation, the $G\alpha$ subunit is GDP-associated and is found in a complex with the $G\beta/G\gamma$ heterodimer. Receptor activation results in exchange of $G\alpha$ -associated GDP for GTP and subsequent dissociation of active $G\alpha$ -GTP from $G\beta/G\gamma$. $G\alpha$ proteins are directly able to regulate AC activity with four distinct families of $G\alpha$ proteins described. Of these, the $G\alpha_s$ and $G\alpha_i$ proteins are most relevant to this study as $G\alpha_i$ inhibits whilst $G\alpha_s$ promotes AC activation (Birnbaumer *et al.*, 1990; Oldham & Hamm, 2006).

As with all signal transduction pathways, it is necessary to negatively regulate GPCR-mediated signalling in order to maintain effective cellular homeostasis. This is partly intrinsic to the nature of G-protein signalling as $G\alpha$ subunits possess GTPase activity and

so act to attenuate their own activation. The return of GTP-associated $G\alpha$ to the GDP-bound conformation can be accelerated *via* interaction of $G\alpha$ with regulators of G-protein signalling (RGS) which enhance the GTPase activity of $G\alpha$ (Oldham & Hamm, 2006). GDP- $G\alpha$ subunits are then able to reassociate with $G\beta\gamma$, ready for further cycles of G-protein activation (Oldham & Hamm, 2006).

It is possible that tumour-specific expression or activation of $G\alpha_s$ -coupled GPCRs may be of therapeutic benefit in malignancies associated with chronic inflammation due to the ability of these receptors to activate AC and promote intracellular cAMP accumulation. In the case of PCa, it is possible that such an effect may be useful in impeding IL-6/STAT3 signalling in a similar fashion to that seen with cAMP elevation (see Chapter 7). Whilst it could be argued that activation of any G_s -protein coupled GPCR could be therapeutically beneficial, the coupling of these receptors to multiple signalling pathways guarantees that caution must be exercised in selecting appropriate GPCRs as potential therapeutic targets.

10.2 The A_{2A} adenosine receptor

One GPCR with potential for use in cancer-treatment strategies is the A_{2A} adenosine (Ado) receptor ($A_{2A}AR$). The Ado receptor (AR) family comprises the A_1 , A_{2A} , A_{2B} and A_3 ARs. A_1AR and A_3AR inhibit AC whilst $A_{2A}AR$ and $A_{2B}AR$ promote AC activation and subsequent accumulation of intracellular cAMP. Whilst tissue levels of Ado are typically low, with interstitial concentrations ranging between 1 and 50 nM, respiratory activity, inflammation or hypoxia can rapidly promote Ado accumulation of concentrations reaching 1000 nM (Rivkees et al., 2001). Accumulation of Ado is ubiquitous amongst tissues and thus activation of downstream signalling pathways is achieved by regulation at the receptor level with an affinity hierarchy of $A_1AR > A_{2A}AR > A_{2B}AR > A_3AR$ (Rivkees et al., 2001). Generation of extracellular Ado occurs under conditions of tissue hypoxia, inflammation and as a by-product of respiration *via* the conversion of released ATP to AMP by the CD39 ecto-pyrase and subsequently to Ado by the CD73 ecto-5' nucleotidase (Kaczmarek et al., 1996; Lennon et al., 1998)

10.2.1 $A_{2A}AR$ structure

The gene structure of the human $A_{2A}AR$ is similar to the other ARs comprising two exons with a single intron between the third and fourth transmembrane domains. The open reading frame (ORF) of Exon1 of $A_{2A}AR$ spans from +281 to +612 with the ORF of Exon 2 spanning from +7549 to +8362 (Fredholm et al., 2000). The $A_{2A}AR$ contains seven transmembrane helices characteristic of GPCRs and an eighth helix which does not span

the membrane and is stabilised *via* interaction with helix I (Jaakola et al., 2008). The transmembrane domains are separated by three intracellular loops spanning residues Leu33 - Val40, Ile108 - Gly118 and Leu208 – Ala221 and three extracellular loops extending from Thr68 to Cys74, Leu141 to Met174 and Cys259 to Trp268 (Jaakola et al., 2008).

The A_{2A}AR is a prototypical G_s-coupled GPCR and is able to activate adenylyl cyclase following receptor activation. Many GPCRs are thought to collide randomly with their cognate G-protein as they migrate through the lipid bilayer, a process known as collision coupling. However, A_{2A}AR displays restricted coupling with Gα_s with the two proteins displaying an extremely tight association which argues for precoupling of A_{2A}AR and Gα_s (Charalambous et al., 2008). Restricted movement of A_{2A}AR through the cell membrane is required for this precoupling effect and can be decreased following cholesterol sequestration. Cholesterol sequestration impairs the ability of A_{2A}AR to couple to Gα_s but has no impact on agonist/antagonist binding (Charalambous et al., 2008). In addition to activation of Gα_s and cAMP signalling, A_{2A}AR can activate signalling through the ERK1/2 pathway *via* a mechanism independent of Gα_s activation (Sexl et al., 1997), although the dependency on Gα_s signalling varies between cell type (Seidel et al., 1999).

Activation of the receptor promotes accumulation intracellular cAMP due to Gα_s activity which couples to A_{2A}AR through the amino-terminal region of intracellular loop three of the receptor (Olah, 1997). In comparison to the other AR family members, the A_{2A}AR possesses an unusually long C-terminal tail, approximately 80 amino acids greater in length than the other described AR, including the most closely related A_{2B}AR. This region appears not to be involved in governing the fidelity of Gα_s-A_{2A}AR coupling but may be involved in coupling of the receptor to other intracellular signalling pathways including the ERK1/2 pathway (Schulte & Fredhohn, 2003). Activation of the A_{2A}AR results in promotes AC activity and the subsequent increases in intracellular cAMP concentrations can exert a number of effects, many of which are immunomodulatory.

Of interest in this study are the anti-inflammatory properties of A_{2A}AR activation with the receptor displaying non-redundant anti-inflammatory roles both *in vitro* and *in vivo*. Ohta and Sitovsky (Ohta & Sitkovsky, 2001) demonstrated that mice deficient for A_{2A}AR (A_{2A}AR^{-/-}) were hypersensitive to endotoxin challenge. Sub-optimal dosing of A_{2A}AR^{-/-} mice resulted in 40% mortality, in comparison to 100% survival in wild-type littermate controls. These effects were shown to be independent of altered function of other G_s-protein coupled receptors indicating a crucial anti-inflammatory role for A_{2A}AR *in vivo*

(Ohta & Sitkovsky, 2001). Additionally, the A_{2A}AR has also been implicated in inhibiting pro-inflammatory leukocyte recruitment following tissue trauma. Selective stimulation of A_{2A}AR resulted in a 77% decrease in macrophage infiltration and decreased adhesion molecule expression inflammation in an *in vivo* model of carotid ligation (McPherson et al., 2001).

In a feline model of ischaemic/reperfusion injury, intravenous treatment with the A_{2A}AR agonist ATL313 inhibited apoptosis in the lung, an effect that was abolished following pre-treatment with the A_{2A}AR-selective inverse agonist ZM241385 (Rivo et al., 2007). The protective effects of A_{2A}AR activation in this model are thought to arise due a concurrent increase in Bcl-2 and decrease in Bax protein levels in ATL313-treated specimens (Rivo et al., 2007). A_{2A}AR activity can also prevent other responses associated with tissue damage and inflammation, including T-cell activation (Huang *et al.*, 1997), airway inflammation in murine models of allergy (Nadeem *et al.*, 2007) and inhibition of the NFκB signalling pathway (Sands et al., 2004). In human neutrophils, cAMP elevation resulting from A_{2A}AR occupancy reduced the ability of fMet-Leu-Phe to induce actin polymerisation. It was subsequently demonstrated that A_{2A}AR occupancy decreased the ability of fMLP to activate phospholipase D (PLD) and translocate Arf and RhoA to neutrophil membranes through a PKA-dependent pathway (Thibault et al., 2002). Given that RhoA translocation to membranes is indicative of RhoA activation, and that inhibition of actin polymerisation arises from A_{2A}AR occupation, it is possible that A_{2A}AR acts to inhibit RhoA. The similarities between the pathways involved in A_{2A}AR-mediated inhibition of fMLP effects (Thibault et al., 2002) and those seen in Fsk-mediated changes in LNCaP morphology, it is possible that A_{2A}AR expression and activation in LNCaP cells might induce a NE-like morphology in LNCaP cells.

To this end, we infected LNCaP cells with recombinant AdV expressing a Myc-tagged A_{2A}AR (AdV.A_{2A}AR) which contained a second open reading frame encoding GFP in order to monitor infection. Infection of LNCaP cells with AdV.A_{2A}AR, but not a control, GFP-expressing AdV (AdV.GFP) resulted in morphological changes in LNCaP cells consistent with those seen following Fsk treatment. These effects could be inhibited by treatment with the A_{2A}AR-selective inverse agonist ZM241385, indicating that receptor activation is required for the phenomenon.

10.3 Results

10.3.1 Titration of AdV.A_{2A}AR in LNCaP cells

In order to investigate the effects of AdV-mediated expression of the A_{2A}AR, it was first necessary to determine a suitable MOI at which to detect A_{2A}AR expression. The ideal MOI is the minimal value at which robust expression of the A_{2A}AR is detected but which is not associated with cytopathic effects (CPEs). LNCaP cells were seeded into 0.1 mg/ml poly-D-lysine coated 6-well tissue culture plates at a density of 3×10^5 cells/well and infected with AdV.A_{2A}AR at MOIs ranging from 0 – 20 ifu/cell. MOIs greater than 20 ifu/cell were not used as these were associated with CPEs in LNCaP cells as indicated by cellular detachment and membrane blebbing (data not shown). In order to maintain LNCaP cell survival, culture medium was replaced at 24 h post-infection and cells harvested for SDS-PAGE fractionation and subsequent immunoblotting at 48 h post-infection. The A_{2A}AR construct used to generate the recombinant AdV has a C-terminal Myc tag, thus, immunoblotting using an in-house anti-Myc antibody was used to detect AdV-mediated A_{2A}AR expression.

As expected, immunoblotting against Myc did not detect any appropriate bands in LNCaP cells which had not been infected with AdV.A_{2A}AR, thus verifying that all subsequent results are the result of genuine receptor expression and not due to non-specific antibody binding (Fig. 10.1). Infection of LNCaP cells with MOI > 2 ifu/cell resulted in increased A_{2A}AR expression, as detected by the C-terminal Myc epitope, with MOI = 6 ifu/cell resulting in consistently high A_{2A}AR expression (Fig. 10.1, ** = $p < 0.01$ vs. MOI = 0 ifu/cell). Further increases in MOI did not result in parallel increases in A_{2A}AR expression, indicating that MOI = 6 is optimal for AdV-mediated A_{2A}AR expression in LNCaP cells and this MOI was chosen for subsequent studies with AdV.A_{2A}AR expression. The changes in detected A_{2A}AR were independent from changes in GAPDH levels, indicating that the results do not arise from changes in protein loading. The detection of a double band at approximately 40 kDa following immunoblotting for the Myc epitope is likely due to differently glycosylated forms of the receptor as observed by others (Palmer & Stiles, 1999; Pierson *et al.*, 1994).

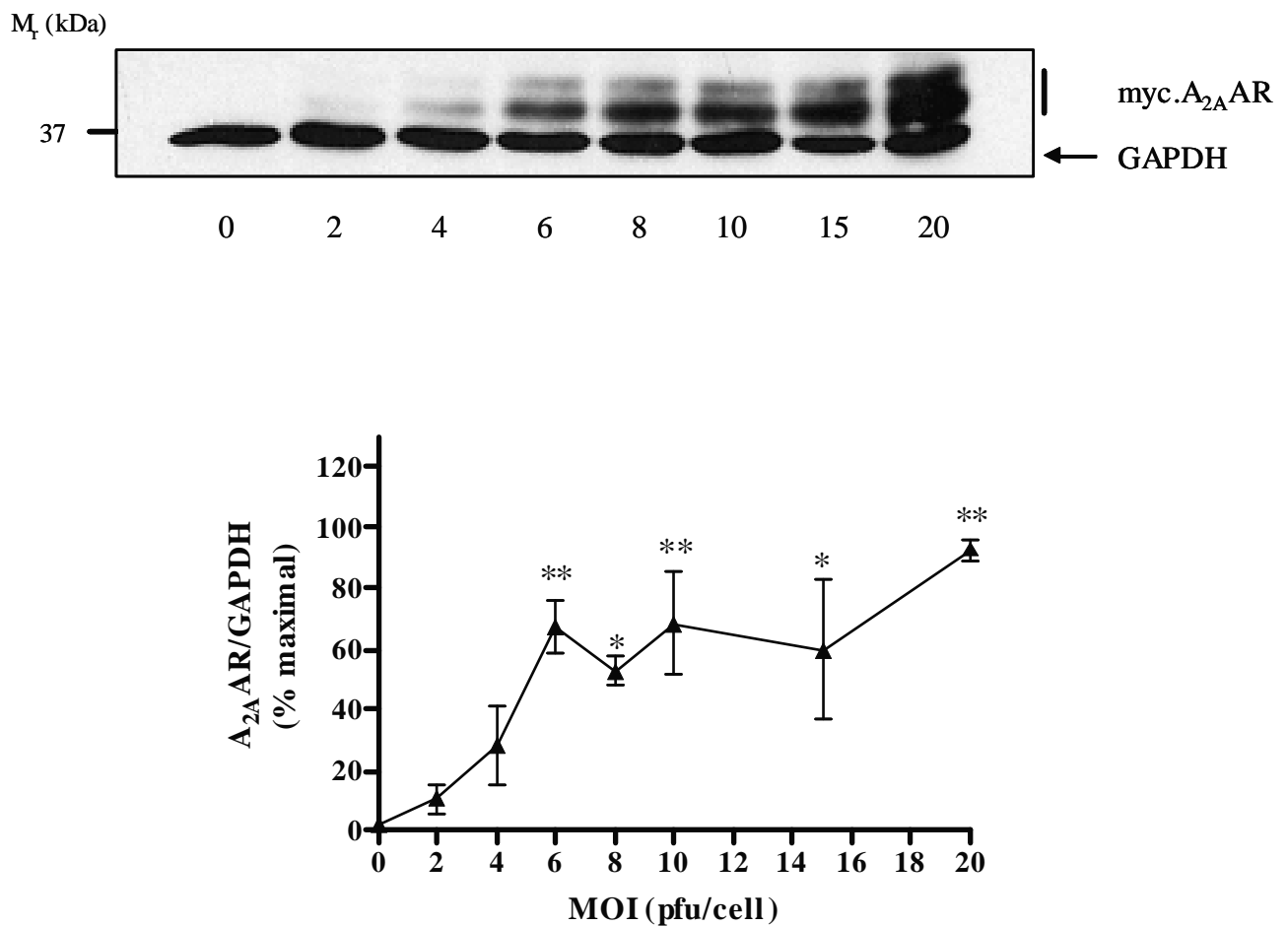


Fig. 10.1: Titration of the AdV.A_{2A}AR in LNCaP cells

3×10^5 LNCaP cells per well were seeded into poly-D-lysine-coated 6-well tissue culture dishes and infected with AdV.A_{2A}AR (panel A) (MOI = 0 - 20 ifu/cell). Medium was replenished at 24 h post-infection to promote cellular survival and infection was monitored by eGFP fluorescence. A_{2A}AR expression was detected *via* immunoblotting for the C-terminal Myc tag (panel C). Results are representative of $n = 3$ separate experiments with the A_{2A}AR/GAPDH ratio displayed as mean values \pm SEM. * = $p < 0.05$ vs. MOI = 0 ifu/cell, ** = $p < 0.01$ vs. MOI = 0 ifu/cell

10.3.2 Ligand binding assay

In order to determine subsequent effects of A_{2A}AR expression on cellular morphology, the levels of expression of the A_{2A}AR were assessed following infection with AdV.A_{2A}AR or the control AdV.GFP recombinant AdV. AdV.GFP encodes the second ORF encoding eGFP but not the Myc-tagged A_{2A}AR, thus allowing any effects of AdV.A_{2A}AR expression to be attributed to expression of the A_{2A}AR and not due effects of AdV infection. To determine comparative receptor numbers, 16.6 x 10⁶ LNCaP cells/flask were seeded into 0.1 mg/ml poly-D-lysine HBr coated 150 cm² tissue culture flasks prior to infection with either AdV.GFP or AdV.A_{2A}AR. At 48 h post-infection, cell membranes were prepared as described in Chapter 5 and incubated immediately with ³H-ZM241385 in the presence of either de-ionised water (dH₂O) or 50 μM of the non-specific agonist NECA to assess total and non-specific ³H-ZM241385 binding respectively. Following harvesting and liquid scintillation counting, the number of receptors per μg of protein was calculated as described in Chapter 5.

In LNCaP cells infected with AdV.GFP, no specific binding of ³H-ZM241385 could be detected, indicating that LNCaP cells do not basally express the A_{2A}AR. In cells infected with AdV.A_{2A}AR a concentration-dependent increase in ³H-ZM241385 was detected, indicative of an increase in A_{2A}AR expression. Using the B_{max} values for individual experiments, the number of bound ZM241385 molecules could be determined. Based on a 1:1 stoichiometric ratio of binding between ZM241385 and the A_{2A}AR the number of bound ZM241385 molecules could be directly equated to the number of receptors in each reaction. The protein content for each ligand binding assay was determined using the BCA assay described in chapter 5 and thus the number of receptors per μg of protein calculated. Infection of LNCaP cells with AdV.A_{2A}AR resulted expression of 7.615 ± 1.64 A_{2A}AR/μg protein.

10.3.3 A_{2A}AR expression induces changes in LNCaP morphology

LNCaP cells were seeded into poly-D-lysine coated 6-well plates and infected with recombinant AdV at MOI = 6 ifu/cell as described in section. To ensure that any changes in LNCaP morphology arising from infection with AdV.A_{2A}AR occur due to A_{2A}AR expression and not as a result of AdV infection, cells were infected in parallel with AdV expressing eGFP but not A_{2A}AR. Images were captured using phase contrast and fluorescence microscopy for each recombinant AdV at 0, 24 and 48 h post-infection.

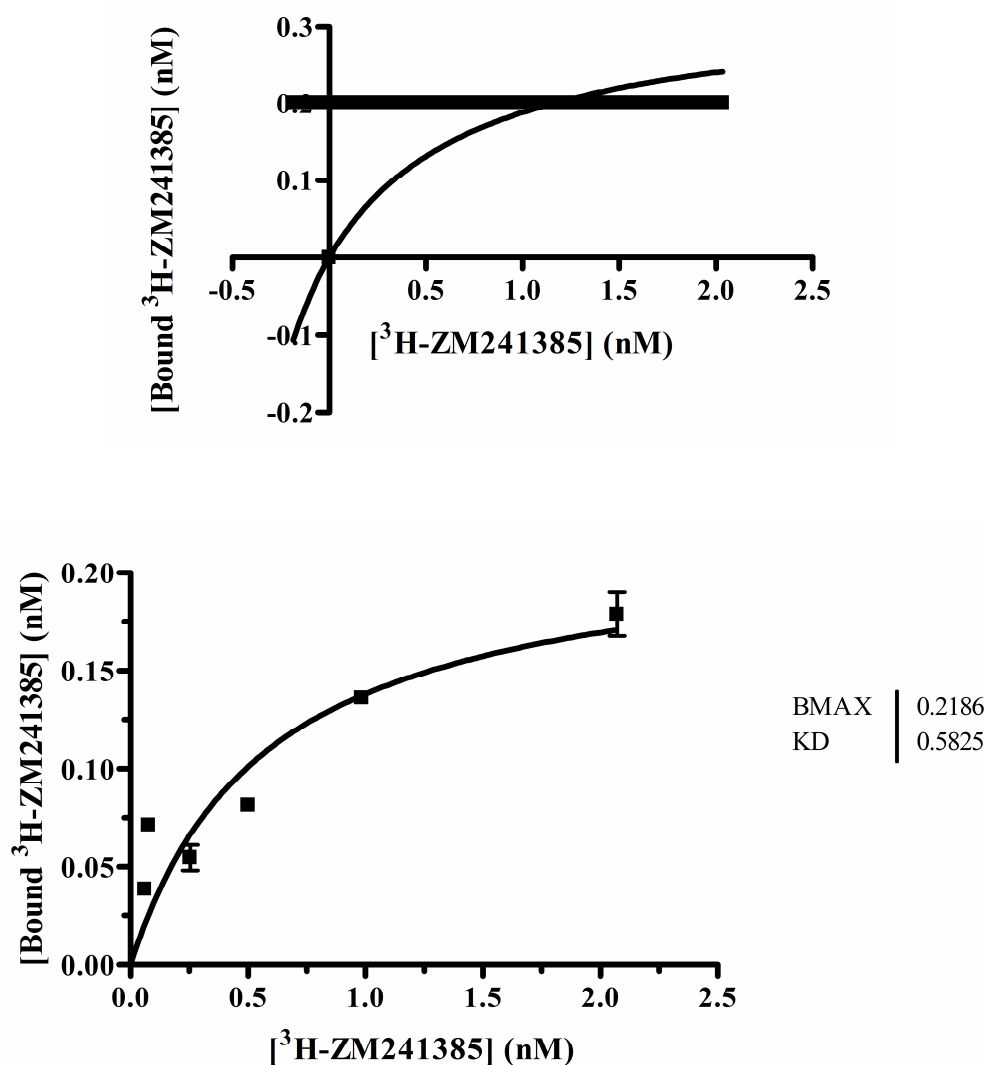


Fig. 10.2: Binding curve of ³H-ZM241385 in LNCaP cells infected with AdV.GFP or AdV.A_{2A}AR

LNCaP cells were seeded into a 75 cm² tissue culture flask at a density of 8.3 x 10⁵ cells/flask and infected with either AdV.GFP or AdV.A_{2A}AR at MOI = 6 ifu/ml. Cells were harvested at 48 h and membrane suspensions prepared *via* homogenisation. Membranes were incubated in duplicate with serial dilutions of ³H-ZM241385 for 1 h at 37°C in the presence of either dH₂O or 50 μM of the competing ligand NECA to determine total and non-specific binding respectively. Membranes were harvested using a Brandel harvester and subsequent radioligand incorporation determine *via* liquid scintillation counting. Subsequent determination of the binding curve and B_{max} values allowed the number of receptors per μg of protein to be determined following infection with either AdV.GFP (top) or AdV.A_{2A}AR (bottom).

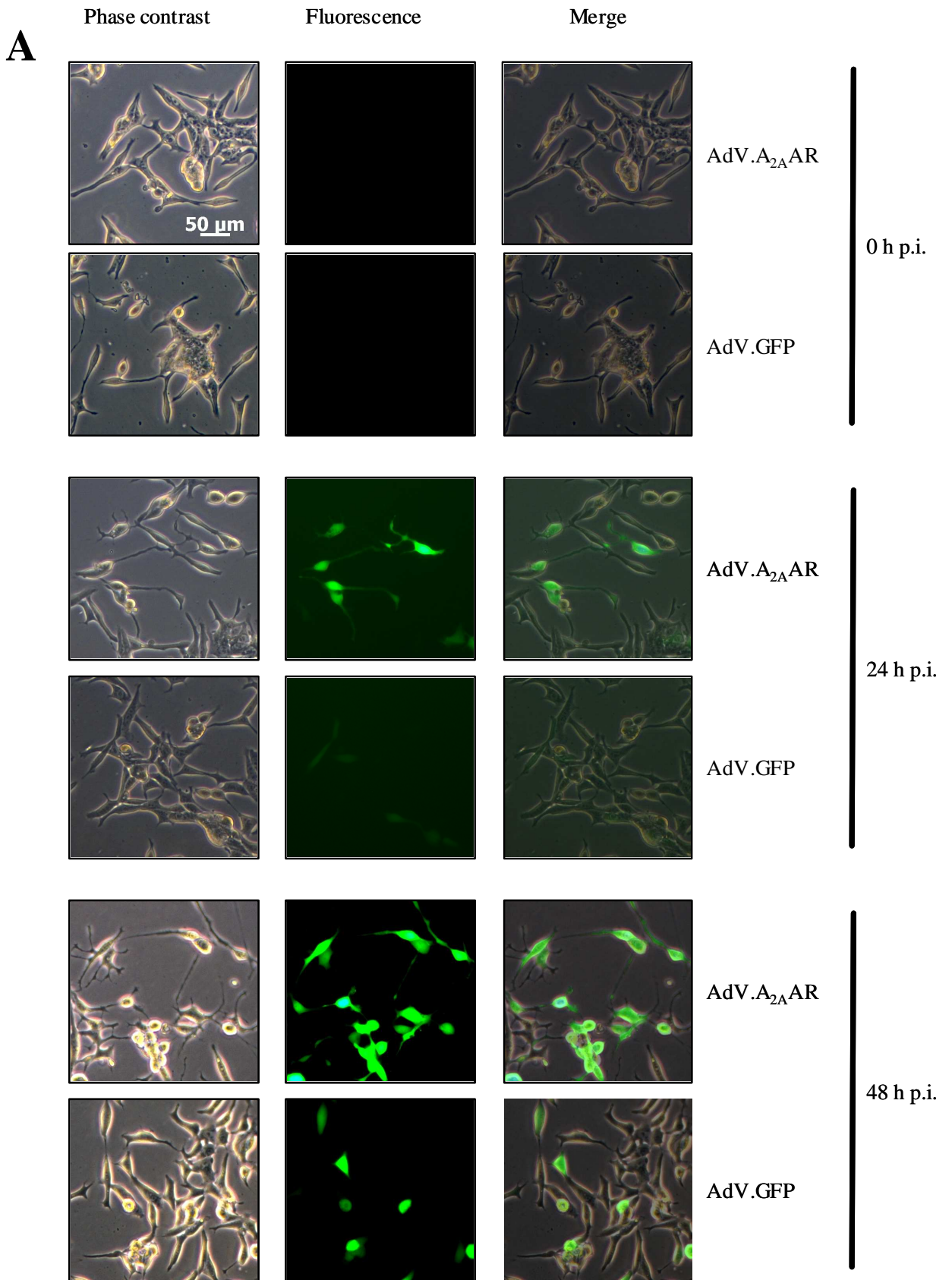
Prior to infection, AdV.GFP and AdV.A_{2A}AR-infected cells displayed no discernable difference in cell morphology (Fig. 10.3). Mean dendrite lengths for cells were $10.43 \pm 0.22 \mu\text{m}$ and $11.32 \pm 0.22 \mu\text{m}$ for AdV.GFP and AdV.A_{2A}AR infected cells respectively. Whilst LNCaP cells infected with AdV.GFP displayed no changes in morphology throughout the experiment with mean dendrite lengths of $14.08 \pm 0.26 \mu\text{m}$ and $12.95 \pm 0.24 \mu\text{m}$ at 24 h and 48 h post-infection respectively (Fig. 10.3). In contrast, AdV.A_{2A}AR-infected LNCaP cells displayed altered morphology with dendrite lengths increasing to $19.72 \pm 0.45 \mu\text{m}$ at 24 h post-infection and 26.20 ± 0.72 at 48 h post-infection (Fig. 10.3).

These results suggest that AdV-mediated A_{2A}AR expression is sufficient to induce changes in LNCaP cells to a NE-like morphology.

10.3.4 Expression of the A_{2A}AR is associated with NE-like morphological changes in LNCaP cells

It was demonstrated above that infection with AdV.A_{2A}AR and not AdV.GFP promoted changes in cell morphology consistent with NE-like differentiation. However, this result does not truly show that those cells expressing the A_{2A}AR are those that have undergone morphological changes, only that there is a tendency for A_{2A}AR expression to be associated with increases in mean dendrite length. To conclusively determine a correlation between A_{2A}AR expression and changes in cell morphology, the bright field and fluorescence images used above were merged and 50 random cells per field per experiment (750 cells in total) at the 48 h post-infection time point analysed. Cells were scored for both eGFP fluorescence, indicating successful AdV infection and recombinant protein expression, and also for changes in LNCaP cell morphology consistent with NE-like differentiation including rounding of the cell body, increase in dendrite length and presence of dendritic branching. The scoring of cells for eGFP fluorescence also enabled a comparison of the relative infection efficiencies of each recombinant AdV.

As expected, infection with AdV.GFP, was not associated with acquisition of a NE-like morphology with only 12 of the 312 eGFP-positive (eGFP⁺) cells displaying morphology resembling that of NE-like cells (Table 10.1, n.s. = $p > 0.05$ ($p = 0.76$)). In contrast, infection of LNCaP cells with AdV.A_{2A}AR resulted in a highly significant association between eGFP fluorescence and NE-like differentiation as determined by the χ^2 test (Table 10.1, *** = $p < 0.001$). 440 cells were found to be eGFP⁺ of which 251 displayed a NE-



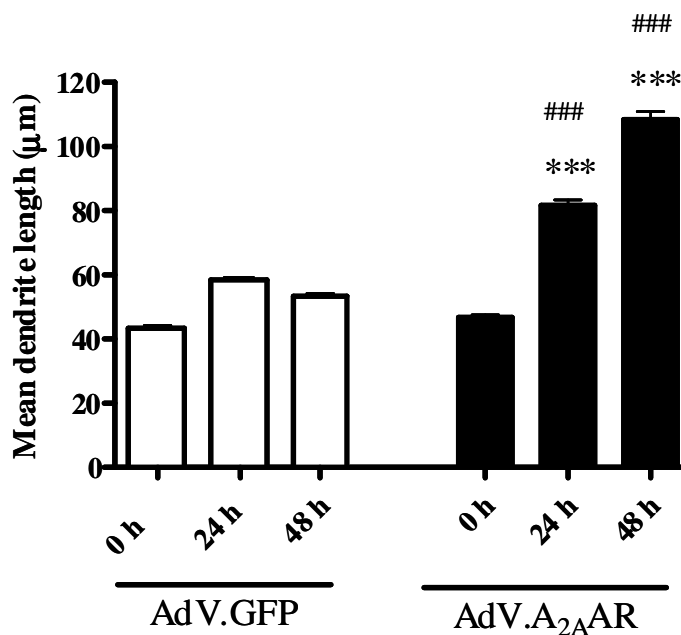
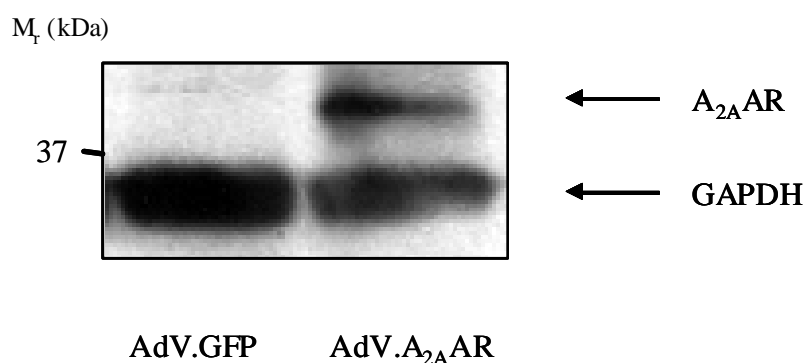
B**C**

Fig. 10.3: Expression of the A_{2A}AR in LNCaP cells mimics Fsk-induced morphological changes

6×10^5 LNCaP cells were seeded into poly-D-lysine-coated 6 cm tissue culture dishes and infected with AdV.GFP or AdV.A_{2A}AR (panel A) (MOI = 6 ifu/cell). Medium was replenished at 24 h post-infection to promote cellular survival and infection was monitored by eGFP fluorescence. Mean dendrite length was assessed at 0 h and 48 h post-infection as an indication of NE-like differentiation (panel B) whilst A_{2A}AR expression was detected *via* immunoblotting for the C-terminal Myc tag (panel C). Results are representative of $n = 3$ separate experiments with mean dendrite lengths shown as mean values \pm SEM. *** = $p < 0.001$ vs. 0 h, ### = $p < 0.001$ vs. AdV.GFP

	AdV.GFP			AdV.A _{2A} AR		
	NE ⁺	NE ⁻	Total	NE ⁺	NE ⁻	Total
eGFP⁺	12 ^{n.s.} (11.2)	300 (300.8)	312	251 ^{***} (211.2)	189 (228.8)	440
eGFP⁻	15 (15.8)	423 (422.2)	438	109 (148.8)	201 (161.2)	310
Total	27	723	750	360	390	750

Table 10.1: Association between eGFP fluorescence and NE-like morphology in LNCaP cells

LNCaP cells were infected with either AdV.GFP or AdV.A_{2A}AR (MOI = 6 ifu/cell) and maintained for 48 h post-infection. Five random fields per recombinant AdV were captured for $n = 3$ separate experiments and the fluorescence and phase-contrast images merged to allow simultaneous assessment of eGFP fluorescence (eGFP⁺) and NE-like differentiation (NE⁺) for 50 random cells per field. The results of the three experiments were pooled and the association between eGFP⁺ and NE⁺ determined *via* a χ^2 test for association. Results are represented as the observed and *expected* values for the pooled data. ^{n.s.} = $p > 0.05$, ^{***} = $p < 0.001$)

Fig. 10.4: Infection percentages for AdV.GFP and AdV.A_{2A}AR in LNCaP cells

LNCaP cells were infected with either AdV.GFP or AdV.A_{2A}AR (MOI = 6 ifu/cell) and maintained for 48 h post-infection. Five random fields per recombinant AdV were captured for $n = 3$ separate experiments and the fluorescence and phase-contrast images merged to allow assessment of eGFP fluorescence for 50 random cells per field. The number of eGFP⁺ cells was calculated as a percentage of the total number of cells analysed. Results are represented as mean values \pm SEM for $n = 3$ separate experiments, n.s. = $p > 0.05$

like morphology in comparison to 109 eGFP⁻ cells which displayed morphological changes consistent with NE-like differentiation. These results confirm that AdV-mediated expression of the A_{2A}AR in LNCaP cells is indeed associated with NE-like changes in morphology.

In order to determine relative abilities of the two recombinant AdV, the number of eGFP⁺ was calculated as a percentage of the total number of cells analysed. The mean percentage infection with AdV.GFP was 41.60 ± 5.00 % whilst for AdV.A_{2A}AR the mean percentage infection was 58.67 ± 3.42 %. Whilst there was a tendency for AdV.GFP to have lower percentage infection than AdV.A_{2A}AR this was not found to be statistically significant as determined by an unpaired t-test (Fig. 10.4, n.s. = $p > 0.05$ ($p = 0.639$)), indicating similar infection efficiencies between the two recombinant AdV.

10.3.5 The A_{2A}AR-selective inverse agonist ZM241385 blocks AdV.A_{2A}AR-mediated changes in LNCaP cell morphology

Although expression of A_{2A}AR alone in LNCaP cells induced differentiation of LNCaP cells to a NE-like phenotype, it was necessary to demonstrate that a functional receptor was required for this phenomenon and that the previous results were not simply an effect of receptor over-expression. To this end, LNCaP cells were seeded as described above and infected with either AdV.GFP or AdV.A_{2A}AR and grown for 48 h in the presence of vehicle or 1 μ M of the A_{2A}AR-selective antagonist ZM241385 (Poucher *et al.*, 1995). In order to retain ZM241385 activity over the course of the 48 h infection period, cell culture medium was replaced at 24 h post-infection with fresh culture medium containing either vehicle or 1 μ M ZM241385. In order to monitor morphological changes, LNCaP cells were photographed at 0 h and 48 h post-infection using both phase contrast microscopy and fluorescence microscopy to detect GFP fluorescence. At 48 h post-infection, LNCaP cells were harvested and immunoblotted to confirm A_{2A}AR expression.

At 0 h post-infection, the mean dendrite length was comparable across all experimental groups, indicating that any subsequent changes in mean dendrite length arise due to experimental procedures and not as a result of differing morphology prior to experimentation. At 48 h post-infection, LNCaP cells infected with AdV.GFP displayed no discernable difference in mean dendrite length whether cells were treated with vehicle or ZM241385. The mean dendrite length for AdV.GFP infected cells treated with vehicle for 48 h was 20.60 ± 0.58 μ m at 0 h and 17.97 ± 0.39 μ m at 48 h whilst for AdV.GFP-infected

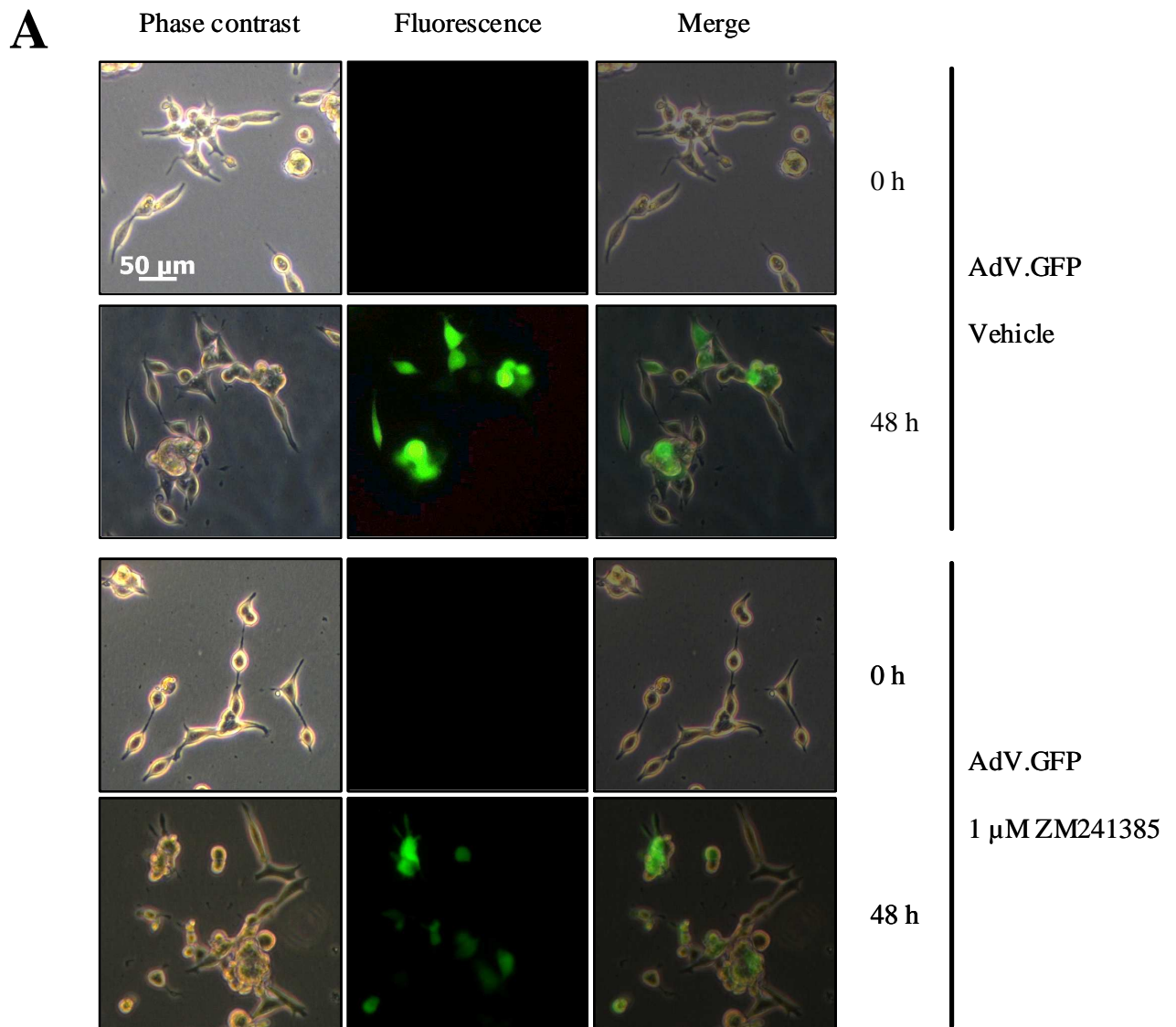
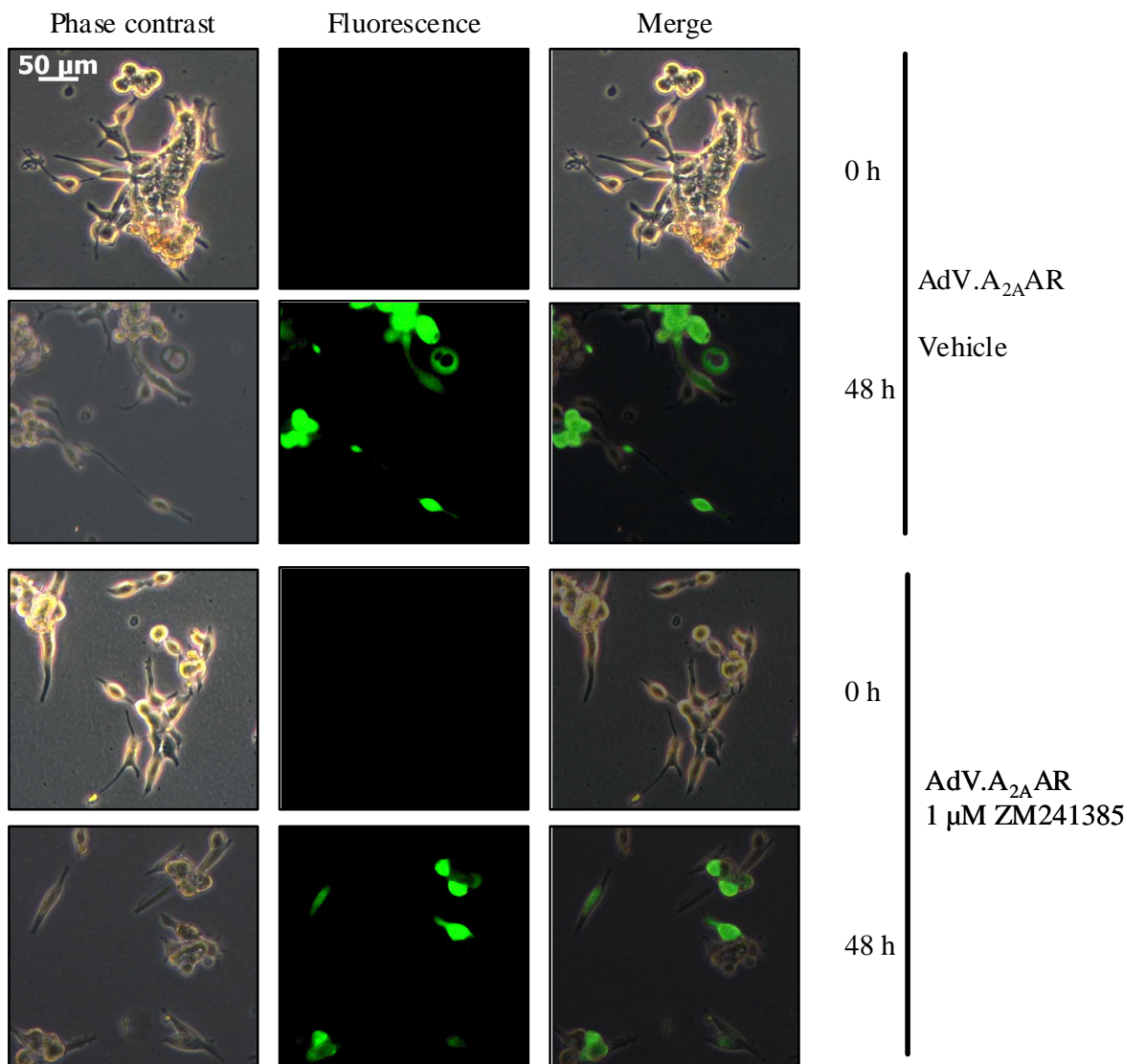
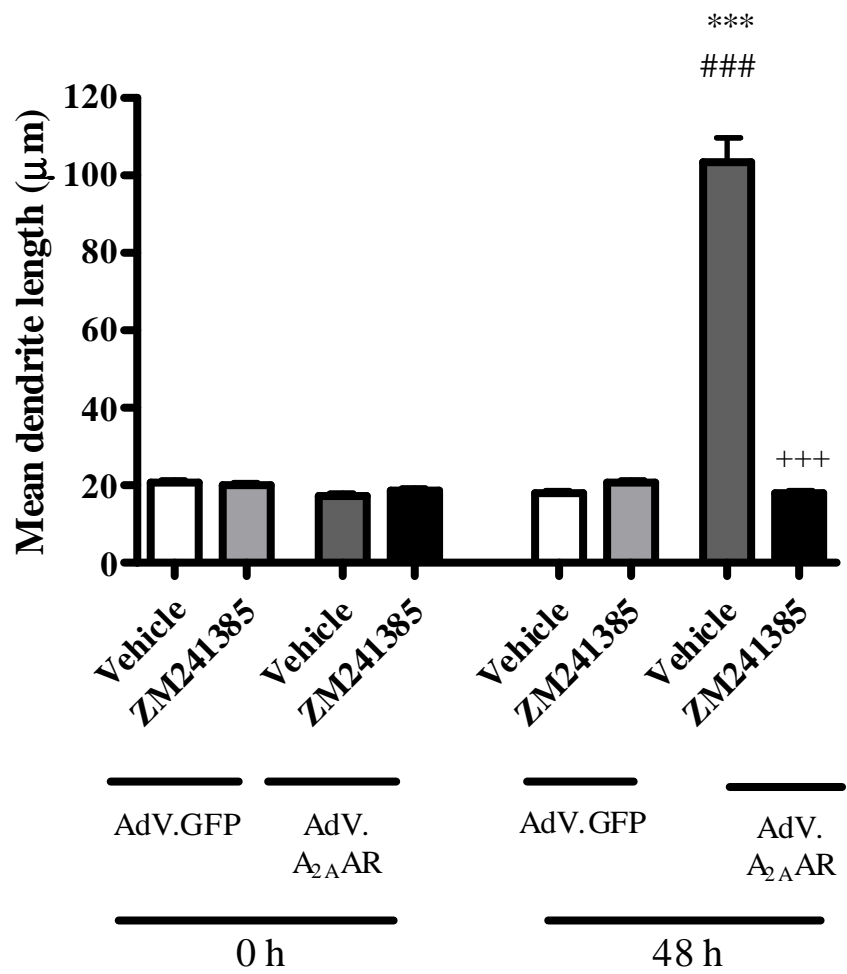
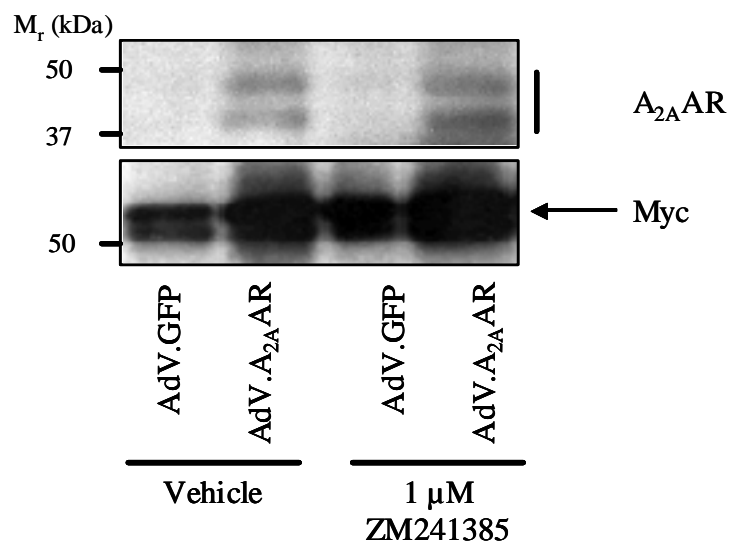


Fig. 10.5: Treatment with the A_{2A} AR-selective inverse agonist ZM241385 inhibits AdV. A_{2A} AR-mediated changes in LNCaP morphology

6×10^5 LNCaP cells were seeded into poly-D-lysine-coated tissue culture dishes and infected with AdV.GFP (panel A) or AdV. A_{2A} AR (panel B) (MOI = 6 ifu/cell) in the presence of either vehicle (0.1% DMSO) or 1 μ M ZM241385, an A_{2A} AR-selective inverse agonist. Medium was replenished at 24 h post-infection to ensure continued activity of ZM241385 and infection was monitored by eGFP fluorescence. Mean dendrite length was assessed at 0 h and 48 h post-infection as an indication of NE-like differentiation (panel C) whilst A_{2A} AR expression was detected *via* immunoblotting for the C-terminal Myc tag (panel D). Results are representative of $n = 3$ separate experiments with mean dendrite lengths shown as mean values \pm SEM. *** = $p < 0.001$ vs. 0 h, ### = $p < 0.001$ vs. AdV.GFP, +++ = $p < 0.001$ vs. vehicle

B



C**D**

LNCaP cells treated with ZM241385 for 48 h, mean dendrite length was found to be $19.91 \pm 0.54 \mu\text{m}$ at 0 h and 18.58 ± 0.46 at 48 h post-infection.

In contrast to LNCaP cells infected with AdV.GFP, vehicle-treated LNCaP cells infected with AdV.A_{2A}AR displayed an increase in mean dendrite length from $17.45 \pm 0.46 \mu\text{m}$ at 0 h post-infection to $103.40 \pm 5.80 \mu\text{m}$ at 48 h post-infection ($p < 0.001$ vs. 0 h and GFP-infected cells), supporting previous results that A_{2A}AR expression can induce morphological changes in LNCaP cells. However, treatment with $1 \mu\text{M}$ ZM241385 blocked the ability of A_{2A}AR expression to induce morphological changes in LNCaP cells. In these cells, initial dendrite length was 20.57 ± 0.63 at 0 h post-infection and 18.00 ± 0.45 at 48 h post-infection, indicating that selective antagonism of A_{2A}AR inhibits morphological changes in LNCaP cells. These results strengthen the hypothesis that A_{2A}AR expression induces differentiation to a NE-like phenotype in LNCaP cells.

10.4 Discussion

LNCaP cells have frequently been reported to undergo differentiation to NE-like cells following a number of treatments including androgen deprivation, chronic IL-6/gp130/STAT3 signalling and elevation of intracellular cAMP levels. Typically, intracellular accumulation of cAMP has been achieved by treatment with Fsk or with β -adrenergic receptor agonists, indicating that physiological stimuli can induce NE-like differentiation (Cox *et al.*, 2000;Deeble *et al.*, 2001). In order to further establish a role for cAMP elevation in LNCaP differentiation, the G α_s -coupled A_{2A}AR was expressed in these cells. It was found that AdV-mediated expression of A_{2A}AR could induce morphological changes in LNCaP cells consistent with differentiation to a NE-like phenotype and that this effect was blocked by the A_{2A}AR-selective inverse agonist ZM241385.

The ability of ZM241385 to block A_{2A}AR-mediated changes in LNCaP morphology indicates that this effect is mediated by activated A_{2A}AR due to the greater affinity of ZM241385 for the A_{2A}AR vs. the other adenosine receptor sub-types. ZM241385 is a non-xanthine A_{2A}AR-selective antagonist, displaying pA₂ values two orders of magnitude greater than at the closely related A_{2B}AR and approximately four orders of magnitude greater than at the A₁ and A₃ adenosine receptors (Poucher *et al.*, 1995). This conclusion is supported by the association of infection with AdV.A_{2A}AR but not AdV.GFP with an increase in mean dendrite length.

It is unclear why expression of A_{2A}AR induces changes in LNCaP morphology in the absence of an agonist. One possible explanation is that adenosine released into the culture medium as a result of normal cellular respiration (Sands & Palmer, 2005) causes activation of the receptor which is blocked by the binding of ZM241385. This matter could potentially be addressed by the addition of adenosine deaminase to the tissue culture medium during the infection period (Thibault *et al.*, 2002). However, it may also be the case that the apparent basal activation of AdV-expressed A_{2A}AR may arise from simple over-expression of the receptor. It has previously been demonstrated that over-expression of the A_{2A}AR can result in constitutive activity in dog thyrocytes with increased AC activity in the absence of agonist (Maenhaut *et al.*, 1990). Similar observations were made *in vivo* with thyroid-specific expression of the canine A_{2A}AR in mice resulting in severe hyperthyroidism (Ledent *et al.*, 1992). This phenomenon is not restricted to A_{2A}AR as other class A GPCRs also display constitutive activity as a result of receptor over-expression. For example, expression of the β_2 -adrenoceptor in the NG108-15 cell line resulted in an increase in basal AC activity only when high levels of receptor expression were achieved (Adie & Milligan, 1994). Treatment with the β_2 -adrenoceptor antagonist propranolol partially decreased the basal AC activity displayed in cells expressing high levels of β_2 -adrenoceptor (Adie & Milligan, 1994). Similarly, over-expression of splice variants of the metabotropic glutamate receptor 1 (mGluR1) in porcine kidney epithelial and HEK 293 cells demonstrated that over-expression of the mGluR1a isoform, but not the mGluR1b or mGluR1c, resulted in elevated basal activity of the receptor as determined by downstream generation of inositol phosphate generation by phospholipase C (Prezeau *et al.*, 1996). This observation is of particular interest to this study as mGluR1a has a far longer C-terminal domain in comparison to mGluR1b or mGluR1c, which may act to promote better coupling efficacy to either G-proteins or other modulatory protein families and so promote agonist-independent receptor activation (Ango *et al.*, 2001;Prezeau *et al.*, 1996). Given the unusually long C-terminal domain of A_{2A}AR, it is possible that a similar mechanism is employed by this receptor to promote activation in the absence of agonist.

Agonist-independent activation of G-protein signalling has been described for multiple GPCRs and is not necessarily dependent on supraphysiological expression of the receptor of interest but may arise due to mutations within the receptor (Seifert & Wenzel-Seifert, 2003). A two-state model of GPCR activity has been described which goes some way to explain the basis of constitutive GPCR activation in the absence of agonist and the increase in basal activation seen when GPCRs are over expressed. It has been proposed that GPCRs switch between an active (Rec*) or inactive (Rec) conformation, with the Rec* state being

stabilised by interaction with agonist and the Rec state stabilised by inverse agonists (Seifert & Wenzel-Seifert, 2003). Supraphysiological expression of a GPCR, whilst unlikely to alter the Rec/Rec* equilibrium, will simply increase the number of receptors in the Rec* state and thus increase the likelihood of agonist-independent effects. This effect may be more pronounced following expression of the A_{2A}AR or other GPCRs which display tight coupling between Gα_s and the receptor. In the traditional collision coupling mode, receptors in their active conformation are then reliant on random collision with their cognate G-protein in order to activate intracellular signalling, an event which may not occur before the receptor reverts to its inactive state. In the case of receptors, such as A_{2A}AR, where the GPCR is thought to be pre-coupled to its G-protein (Charalambous *et al.*, 2008), switching of the receptor to its active conformation has a far greater probability of activating downstream, signalling pathways and so result in the observed changes in LNCaP morphology.

It is also possible that receptor over-expression may enhance agonist-independent A_{2A}AR signalling through promoting dimerisation of the receptor *via* the fifth transmembrane domain (Thevenin & Lazarova, 2008). Dimerisation or oligomerisation of GPCRs has been associated with more efficient G-protein activation, greater agonist affinity and enhanced signal transduction (Baneres & Parello, 2003; Fotiadis *et al.*, 2006; Milligan, 2007). It is possible that the high level of A_{2A}AR expression arising from AdV-mediated gene transfer may promote high levels of receptor dimerisation or even oligomerisation. Such a response may potentiate basal activation of the receptor *via* more effective G-protein signalling and promote the activation of intracellular signalling pathways involved in changes in LNCaP morphology.

Previous studies using this recombinant AdV indicate that expression of the receptor is sufficient to induce anti-inflammatory effects in the absence of ligand stimulation (Sands *et al.*, 2004). It is possible that further enhancement of the morphological changes associated with AdV.A_{2A}AR expression might be seen with treatment with the A_{2A}AR-selective agonist CGS21680 as has been observed in other experimental systems. CGS21680 is a highly selective agonist for A₂ adenosine receptors, displaying minimal effects at A₁AR (Jarvis *et al.*, 1989) and no effects at either the A_{2B}AR (Yakel *et al.*, 1993) or A₃AR (Zhou *et al.*, 1992). In previous studies, the effect of A_{2A}AR expression could be enhanced by treatment with CGS21680 (Sands *et al.*, 2004). However, during preliminary studies in LNCaP cells expressing A_{2A}AR, treatment with 10 μM CGS21608, a concentration previously shown to be efficacious in numerous other cell lines in our laboratory, failed to

elicit an increase in ERK1/2 activation or to potentiate effects on LNCaP dendrite length (data not shown), suggesting that AdV-mediated expression of the receptor is sufficient to induce these effects.

Whilst expression of A_{2A}AR alone appears to mimic the effect of cAMP elevation on LNCaP morphology, the signalling pathways by which this is achieved are yet to be elucidated. As the A_{2A}AR is a G α_s -protein coupled GPCR, it is likely that activation of the receptor induces changes in LNCaP morphology through activation of G α_s and subsequent activation of AC leading to increased intracellular cAMP concentrations. It is to be anticipated that a similar pathway is activated in LNCaP cells following A_{2A}AR expression as that which follows Fsk treatment as both result in AC activation.

In addition to the hypothesised G α_s -mediated activation of AC downstream of A_{2A}AR in LNCaP cells, other pathways activated by A_{2A}AR may also play an important role in promoting differentiation to a NE-like phenotype. In addition to AC, A_{2A}AR can also promote activation of ERK1/2 in a manner independent of G α_s activation (Sexl *et al.*, 1997). In the previous chapter, it was found that selective activation of ERK1/2 could promote changes in LNCaP morphology but this pathway appeared to play a role later in the morphological changes associated with cAMP elevation. It is possible that the same holds true in the case of A_{2A}AR expression in these cells although it is more difficult to ascertain the contributing role of ERK1/2 in this instance as the separation of G α_s -dependent and -independent signalling pathways has not been achieved. Thus it is not possible to ascertain, at this stage, whether a role for ERK1/2 may arise due to activation directly downstream of A_{2A}AR (Sexl *et al.*, 1997) or as a later effect of G α_s -mediated cAMP elevation (Seidel *et al.*, 1999) as holds true in the previously described model. Future experiments involving the use of the MEK1/2-selective inhibitor U0126 and inhibitors of adenylyl cyclase activity such as t-Bu-SATE may help to delineate the roles of G α_s and ERK1/2 in this phenomenon.

In addition to impact on the ERK1/2 pathway, A_{2A}AR occupancy may also impact on the activation of RhoA, a process which appears to be central to the early changes in LNCaP morphology observed as a result of Fsk treatment in the previous chapter. It has been demonstrated in human neutrophils that treatment with the chemotactic reagent fMLP promoted activation of phospholipase D, a process which requires Rho activation and associated translocation of RhoA to the cell membrane (Fensome *et al.*, 1998). The PLD isoform PLD1 is believed to play an important role in neutrophil responses to agonists such

as fMLP due to its ability to generate the second messenger phosphatidic acid (Fensome et al., 1998). Adenosine deaminase-mediated inhibition of adenosine receptor signalling enhanced RhoA translocation to the cell membrane following fMLP treatment indicating that AR signalling inhibits RhoA membrane translocation. As might be anticipated, CGS21680-mediated activation of A_{2A}AR signalling promoted a decrease in fMLP-mediated activation of PLD which is indicative of an upstream decrease in RhoA activity and supported by the observation that treatment with CGS21680 impaired RhoA translocation to the cell membrane. These effects could be reversed following treatment with A_{2A}AR-selective antagonists, suggesting that A_{2A}AR signalling acts to negatively regulate RhoA membrane translocation (Thibault et al., 2000). In later experiments, it was determined that the ability of A_{2A}AR signalling to impair RhoA membrane translocation and subsequent PLD activation could be mimicked using the cAMP analogue Sp-cAMP, indicating a cAMP dependency of this phenomenon. The PKA-selective antagonists H89 and Rp-cAMP-S could reverse A_{2A}AR-mediated inhibition of RhoA membrane translocation (Thibault et al., 2002). Given that the activation of RhoA is associated with translocation of the protein to the cell membrane, these results suggest that A_{2A}AR activation inhibits RhoA activation *via* a PKA-dependent pathway, an effect comparable to the pathway elucidated in Chapter 8. It is therefore probable that the pathways important in Fsk-mediated changes in LNCaP morphology may play similar roles in A_{2A}AR-mediated morphological changes and represent a conserved pathway important in early NE-like differentiation in PCa.

11 Final discussion

Cancer is a universal condition resulting in abnormal cellular proliferation and survival. Whilst many factors can contribute to carcinogenesis, a large number of these potentiating factors unite in their ability to inappropriately regulate intracellular signalling pathways involved in key cellular process such as cell cycle progression and apoptosis (Hanahan & Weinberg, 2000). Of particular interest to this study was the role of chronic inflammatory responses in carcinogenesis, particularly the role of the IL-6/JAK/STAT3 signalling cascade in PCa. Elevation of serum IL-6 has been associated with every stage of PCa from initial diagnosis to terminal disease. (Barton *et al.*, 2004;Kuroda *et al.*, 2007;Michalaki *et al.*, 2004;Stark *et al.*, 2009). IL-6 mediates its intracellular effects through activation of the JAK/STAT pathway (Heinrich *et al.*, 2003) and hyperactivation of STAT3 has been described in a number of malignancies (Hodge *et al.*, 2005;Jing & Tweardy, 2005), concomitant with the oncogenic effects of this protein (Bromberg *et al.*, 1999). Inappropriate activation of STAT3 is associated with both an increase in cell cycle progression *via* induction of genes such as cyclin D1 and protection from apoptotic effects and Bcl-X_L (Barton *et al.*, 2004;Grandis *et al.*, 2000;Hodge *et al.*, 2005;Zhang *et al.*, 2007). Direct inhibition of STAT3 has been shown to induce apoptosis in PCa cell lines (Barton *et al.*, 2004), suggesting that targeting of this pathway would be of therapeutic benefit. Previously, it was demonstrated that elevation of intracellular cAMP can decrease STAT3 activation in vascular endothelial cells *via* induction of SOCS3 expression (Sands *et al.*, 2006). This is of therapeutic interest as chronic IL-6 signalling is associated with unstable atherosclerotic lesions and increased risk of thrombosis and stroke (Kes *et al.*, 2008).

In the current study, it was demonstrated that stimulation of cells with exogenous IL-6 resulted in increases in tyrosine phosphorylation of STAT3 in all cell lines tested but only induced activation of STAT1 in the control cell line used. The tumour-derived LNCaP and DU145 cell lines displayed no activation of STAT1 in response to IL-6 stimulation due to a lack of JAK1 expression and currently undefined signalling defects specific to IL-6 signalling respectively. Prolonged activation of STAT3 is an oncogenic event whilst STAT1 activation is generally ascribed a tumour suppressor function (Yu & Jove, 2004). Thus selective activation of STAT3 rather than STAT1 may act to promote tumour cell survival during initial carcinogenesis and subsequent suppression of anti-tumour immunosurveillance (Nefedova *et al.*, 2004;Yu & Jove, 2004). Given the association of

both elevated IL-6 levels and chronic STAT3 activation with numerous malignancies (Azare *et al.*, 2007;Hodge *et al.*, 2005;Jing & Tweardy, 2005;Lin *et al.*, 2007;Nefedova *et al.*, 2004;To *et al.*, 2004;Yu & Jove, 2004), preferential activation of STAT3 *versus* STAT1 in response to exogenous IL-6 may be a common feature of cancer cells. Expansion of this study to investigate other malignancies associated with hyperactivation of IL-6 or STAT3 signalling such as colorectal or gastric carcinoma (Esfandi *et al.*, 2006;To *et al.*, 2004) might indicate whether defective STAT1 activation in response to IL-6 is a general feature of inflammation-associated malignancies. Furthermore, it might be that modulating the balance between STAT1 and STAT3 activation following IL-6 stimulation in favour of STAT1 activation may represent a future avenue of research.

Currently however, strategies which inhibit IL-6-mediated STAT3 activation are being pursued as potential therapeutics (Jing & Tweardy, 2005). Previous work has demonstrated that elevation of intracellular cAMP can decrease STAT3 activation in vascular endothelial cells *via* induction of SOCS3 expression (Sands *et al.*, 2006). This is of therapeutic interest as chronic IL-6 signalling is associated with unstable atherosclerotic lesions and increased risk of thrombosis and stroke (Kes *et al.*, 2008). Furthermore, SOCS3 expression has been demonstrated to decrease inflammatory disease parameters in models of inflammatory RArt, suggesting that expression of this protein is a suitable anti-inflammatory therapy *in vivo* (Shouda *et al.*, 2001). In the current study, elevation of cAMP in prostate epithelial cell lines was able to decrease activation of STAT3 downstream of the IL-6R. However, whilst the data obtained strongly suggests that this effect is mediated by SOCS3 expression in DU145 and PZ-HPV-7 cells, in LNCaP cells no induction of SOCS3 expression was observed. The combination of previous observations that cAMP elevation can attenuate IL-6-induced STAT3 activation in HUVECs, MEFs (Sands *et al.*, 2006), COS1 (Yarwood *et al.*, 2008) and monocytic precursor cells (Mullen and Palmer, unpublished observations), the observations in this study that cAMP elevation can mediate similar effects in prostate epithelial cells suggest that this is a universal mechanism by which to attenuate inflammatory signalling. Whilst it has previously been demonstrated that cAMP elevation in HUVECs can attenuate IL-6 signalling *via* SOCS3 induction (Sands *et al.*, 2006), the results obtained in this study indicate that this may not be a universal pathway. The ability of cAMP elevation to inhibit STAT3 activation in DU145 and PZ-HPV-7 cells was correlated with increases in SOCS3 protein expression. However, in LNCaP cells, elevation of intracellular cAMP attenuated IL-6-induced STAT3 activation but did not alter SOCS3 protein levels, indicating the presence of other inhibitory pathways. It has been demonstrated in this study that elevation of cAMP acts to inhibit RhoA activity in

order to promote NE-like differentiation in LNCaP cells (Chapter 8). Published data have shown that RhoA activity can regulate tyrosine phosphorylation, and thus activation, of STAT3 (Aznar *et al.*, 2001;Debidda *et al.*, 2005) and thus it is possible that cAMP elevation inhibits STAT3 activation in LNCaP cells *via* inhibition of RhoA activation. In combination with previous data, the results obtained in this study strongly support the use of cAMP elevating agents as inhibitors of IL-6/STAT3 signalling.

However, the use of cAMP elevation to manipulate endogenous anti-inflammatory pathways may not represent a suitable strategy for all inflammatory conditions. This is of particular relevance in PCa as elevation of intracellular cAMP or over-expression of the A_{2A}AR, a G_{α_s}-coupled GPCR, promoted NE-like differentiation in LNCaP cells. Emergence of a NE cell population is associated with a poor patient prognosis and terminal disease (Shariff & Ather, 2006). Whilst tumours deriving solely from prostatic NE cells represent a rare and highly aggressive malignancy, these cells are frequently seen as foci of non-proliferating cells surrounded by a region of dividing epithelial cells due to the release of mitogenic factors such as bombesin (Noordzij *et al.*, 1996). Due to their senescent nature (Noordzij *et al.*, 1996), NE cells are often resistant to conventional chemotherapeutics which target actively dividing cells and, due to the androgen-independent nature of their growth, NE cells also resist the androgen ablation therapy conventionally used to treat PCa (Chen *et al.*, 1992). Thus whilst treatment of PCa patients with therapies which modulate intracellular cAMP concentrations may be therapeutically beneficial when considering one aspect of intracellular signalling or one disease it may not represent a universal strategy. This is particularly true when considering malignant disease as PKA is frequently over-expressed in cancer and thus, whilst elevation of cAMP may attenuate cell proliferation and survival mediated by STAT3 activation, the same therapy may also potentiate growth of cancer cells through PKA-mediated activation of CREB (James *et al.*, 2009;Naviglio *et al.*, 2009;Shankar *et al.*, 2005) and other key cellular pathways such as the ERK1/2 signalling pathway.

Indeed, this study has demonstrated that cAMP elevation can promote activation of ERK1/2 in LNCaP cells. This pathway is of particular importance in regulating cellular proliferation and survival and, whilst NE cells are non-proliferative, activation of ERK1/2 signalling by cAMP may play a role in promoting the survival of these cells. Activation of ERK1/2 plays an important role in neurite outgrowth in PC12 cells (Bouschet *et al.*, 2003;Kiermayer *et al.*, 2005;Monaghan *et al.*, 2008;Obara *et al.*, 2004;Robinson *et al.*, 1998) and was shown to be important for later stages of dendrite extension in LNCaP cells.

Interestingly, the more recently described ERK5 signalling pathway may play a role in mediating the early effects of cAMP elevation on LNCaP cell morphology. It is currently unclear as to the interplay between ERK1/2 and ERK5 in this system but the greater importance of ERK5 in the early stages of morphological change may arise due to direct interaction of this signalling protein with the actin cytoskeleton mediated by the proline rich domains in ERK5 (Zhou *et al.*, 1995). It is thus possible that the ERK5 signalling pathway may also regulate activation of Rho family GTPases in order to mediate the effects cAMP elevation on cellular morphology.

Treatment with Fsk was shown to induce inhibition of RhoA by a PKA-dependent pathway. Whilst this was correlated with an increase in pSer¹⁸⁸RhoA, the possibility that MEK5 could promote GTP → GDP exchange of Rho GTPase family members and so act to dynamically regulate cytoskeletal processes has not been excluded (Zhou *et al.*, 1995). If such a hypothesis was correct, it may provide an explanation for the role of the MEK5/ERK5 signalling pathway in early changes in LNCaP cell morphology. Indeed, further study of the ERK5 signalling pathway is likely to ascribe more functions which were thought to be ERK1/2-specific to this cascade as, until recently, it was not possible to pharmacologically inhibit the ERK5 signalling cascade without also inhibiting ERK1/2 activation (Mody *et al.*, 2001;Tatake *et al.*, 2008). Future research into the ERK5 signalling cascade may well demonstrate that this pathway is a key regulator of the actin cytoskeleton. As signalling pathways modulating actin polymerisation play a major role in many cellular processes such as neuronal differentiation (Nusser *et al.*, 2006) and tumour metastasis (Lin *et al.*, 2007;Zhao *et al.*, 2009a) it may be that compounds such as BIX02188 and BIX20189 may prove to be important tools for future therapeutic strategies.

Ultimately, whilst intracellular cAMP elevation results in attenuation of STAT3 activation in prostate epithelial cells, it is unlikely that therapeutic strategies which modulate cAMP signalling will be of future benefit in malignant disease due to potential side effects on cellular proliferation and differentiation. Other mechanisms by which to inhibit IL-6/STAT3 signalling such as JAK inhibitors or decoy oligonucleotides (Jing & Tweardy, 2005) are likely to be of far greater benefit in treating malignant disease. However, elevation of intracellular cAMP may prove beneficial in other diseases involving aberrant IL-6 signalling such as atherosclerosis or RA (Kallen, 2002). Thus, whilst apparently representing a universal strategy by which to attenuate IL-6 signalling, elevation of intracellular cAMP may not represent a universally suitable strategy and the interplay between signalling pathways must be carefully considered.

12 Future directions

12.1 Investigation of gp130-STAT1 interaction in response to IL-6 stimulation

In Chapter 6, both of the tumour-derived cell lines failed to activate STAT1 in response to exogenous IL-6. In the case of LNCaP cells, this was found to arise due to a lack of JAK1 expression whilst the mechanism by which this occurs in DU145 cells is currently unknown. DU145 cells activated STAT1 in response to exogenous IFN α , indicating that the lack of STAT1 phosphorylation in response to IL-6 is an effect specific to this signalling pathway. As IFN α stimulation is able to induce phosphorylation of Tyr⁷⁰¹ of STAT1, it is unlikely that there are alterations in STAT1 which render it unable to interact with cytokine receptors and to undergo JAK-mediated activation. It is thus more likely that the defects in IL-6-mediated activation of STAT1 arise due to alterations in the IL-6R/gp130 complex.

It is possible that STAT1 is unable to interact with gp130 in order to promote activation of STAT1 following stimulation with IL-6. Immunoprecipitation of gp130 and subsequent immunoblotting for STAT1 in IL-6-stimulated DU145 cells could be undertaken in order to address whether STAT1 does indeed interact with gp130. If it were found that STAT1 does not interact with gp130, there are several mechanisms which might prevent interaction of the two signalling molecules. Binding of SOCS proteins to cytokine receptor is able to sterically hinder STAT recruitment to the receptor/JAK complex (Ilangumaran *et al.*, 2004). In the case of SOCS3, this process requires phosphorylation of gp130 arising from cytokine stimulation (Ilangumaran *et al.*, 2004). As DU145 cells are the only cells in this study both to be described as displaying basal STAT3 activation arising from autocrine IL-6 production (Okamoto *et al.*, 1997) and also the only cells to display defects in STAT1 signalling specifically confined to the IL-6 pathway, SOCS3 could be basally associated with gp130 in these cells and so act to inhibit STAT1 activation following IL-6 stimulation. However, two lines of evidence argue against such a suggestion, firstly the lack of basal pTyr⁷⁰⁵STAT3 detected throughout this study and secondly, if SOCS3 were constitutively associated with gp130 in DU145 cells, it would be expected to impede activation of STAT3 following IL-6 stimulation which was not observed in this study. However, it is possible that constitutive interaction of another SOCS protein such as SOCS1 with gp130 is responsible for the loss in STAT1 activation observed. Interaction of SOCS1 with pTyr⁴⁴¹ of the IFN γ receptor blocks STAT1 activation (Qing *et al.*, 2005) and thus it may be that recruitment of SOCS1 to a site on gp130 may sterically hinder IL-6-

induced activation of STAT1. This could be tested by immunoprecipitation of gp130 and immunoblotting for SOCS1.

However, it may also be that the lack of STAT1 activation arising from IL-6 stimulation in DU145 cells is due to alterations in the STAT1 recruitment sites on the cytoplasmic chains of gp130. The receptor binding sites for STAT1, but not STAT3, require the presence of a proline residue two amino acids C-terminal to the phosphotyrosine (Gerhartz *et al.*, 1996; Hemmann *et al.*, 1996), thus mutation of the proline residue would be expected to inhibit STAT1/gp130 interaction but would not disrupt gp130/STAT3 interaction which does not require the Pro-Gln motif (Gerhartz *et al.*, 1996; Hemmann *et al.*, 1996). Furthermore, the presence of a leucine residue immediately C-terminal to the phosphotyrosine site is also required for STAT1 activation in response to gp130 activation (Gerhartz *et al.*, 1996). In the study, by Gerhartz *et al.* (1996) mutation of an IFN γ receptor sequence from YDKPH to YFKQH entirely altered subsequent STAT activation from predominantly increasing tyrosine phosphorylation of STAT1 to solely activating STAT3 (Gerhartz *et al.*, 1996). Given these observations, it is possible that the exclusive activation of STAT3 rather than STAT1 in DU145 cells following IL-6 stimulation demonstrated in this study may arise from mutations within the STAT1 recruitment sites on gp130, rendering STAT1 unresponsive to IL-6. The presence of point mutations altering STAT1/gp130 interaction could be determined *via* comparison of gp130 nucleotide sequences between DU145 and PZ-HPV-7 cells using RT-PCR.

STAT1 is thought to exert a tumour suppressor function whilst elevation of IL-6/STAT3 signalling is common in many malignancies (Hodge *et al.*, 2005). Thus it is possible that defective gp130/STAT1 coupling could be of importance in a spectrum of cancers. Whilst studies have investigated the role of gp130 point mutations in inflammatory diseases, these have either artificially introduced mutations in gp130 (Tsuji *et al.*, 2009) or have not correlated mutations in gp130 sequence to signalling defects (Rodriguez *et al.*, 1994). Screening of tumour cells for mutations in the cytoplasmic regions of gp130 which are associated with STAT1 recruitment and activation may identify a common mechanism by which oncogenesis can be achieved.

12.2 The role of SOCS proteins in cAMP-mediated attenuation of STAT3 activation

Previously, the ability of cAMP to attenuate cytokine-induced activation of STAT3 in HUVECs was demonstrated to be mediated *via* induction of SOCS3, an endogenous

inhibitor of IL-6 signalling (Sands *et al.*, 2006). However, whilst the decrease in STAT3 activation in DU145 and PZ-HPV-7 cells was associated with an increase in detected SOCS3 protein levels, this did not hold true in LNCaP cells. It is possible, given the lack of SOCS3 expression in the LNCaP cell line, that the promoter sequence for SOCS3 in these cells is methylated. Indeed, hypermethylation of the SOCS1 and SOCS3 promoters have been described in several cancers associated with aberrant IL-6 signalling (Komazaki *et al.*, 2004; Miyoshi *et al.*, 2004; Tischoff *et al.*, 2007; To *et al.*, 2004) and thus may represent a conserved mechanism by which malignant cells impede the tumour suppressor activities of SOCS proteins (Elliott *et al.*, 2008). Expression of SOCS3 following treatment with demethylating agents such as 5-aza-2-deoxycytidine (Wilson & Jones, 1983) would suggest that promoter methylation is indeed responsible for the lack of SOCS3 expression in LNCaP cells. It is possible that hypermethylation of the SOCS promoter is also important in the pathogenesis of other chronic inflammatory diseases associated with IL-6 elevation such as RA or atherosclerosis (Kallen, 2002).

Importantly, it has not been possible to conclusively demonstrate a role for SOCS3 in this phenomenon as selective knockdown of SOCS3 expression using siRNA has been unsuccessful. Further optimisation of siRNA protocols is required to demonstrate a role for SOCS3 in cAMP-mediated attenuation of STAT3 phosphorylation in DU145 and PZ-HPV-7 cells. If these continue to be unsuccessful, transient transfection of these cells with a plasmid encoding the relevant shRNA or establishment of stable SOCS3 knockdown prostate epithelial cell lines expressing the relevant shRNA may represent successful alternative strategies.

Importantly, this study has only addressed the role of SOCS3 in cAMP-mediated attenuation of STAT3 phosphorylation, and other SOCS proteins may be modulate IL-6 signalling. Whilst SOCS3 has been predominantly studied as an inhibitor of IL-6 signalling, SOCS1 has also been demonstrated to directly inhibit IL-6 signalling (Schmitz *et al.*, 2000). In order to address this issue, expression of other SOCS protein family members could be analysed by immunoblotting as performed in this study. Other than SOCS3, SOCS1 is the primary candidate for SOCS-mediated suppression of gp130-mediated signalling as both have been shown to inhibit IL-6-induced expression of STAT3-responsive genes (Schmitz *et al.*, 2000). Although the two SOCS proteins both inhibit STAT3 activity, they modulate IL-6/STAT3 signalling *via* different mechanisms as suggested by the observation that SOCS3 but not SOCS1 is recruited to Tyr⁷⁵⁹ of gp130. (Schmitz *et al.*, 2000) However, given the current poor quality of commercially available

antibodies to endogenous SOCS proteins, use of qRT-PCR to determine changes in SOCS family mRNA levels may prove an alternative experimental strategy. Caution must be exercised when interpreting such results as changes in mRNA levels may not necessarily correlate to changes in protein levels. Indeed, several proteins can be regulated *via* post-transcriptional mechanisms.

Whilst it has been demonstrated that *socs3* mRNA levels increase following stimulation with cAMP-elevating agents (Barclay *et al.*, 2007; Sands *et al.*, 2006), this effect may vary between cell types. In the PC3-AR PCa cell line, increased SOCS3 protein expression following stimulation of the AndR occurs due to increases in translation and not in transcription of *socs3* mRNA (Neuwirt *et al.*, 2007). Indeed, no significant changes in *socs3* mRNA were observed following androgen treatment, further indicating that transcriptional regulation plays a minor role in regulating SOCS3 expression in PCa cells (Neuwirt *et al.*, 2007). Furthermore, control of SOCS protein expression at the translational level has been demonstrated for SOCS1 expression in murine thymocytes with changes in SOCS1 protein expression occurring independently from changes in *socs1* transcript levels (Gregorieff *et al.*, 2000). In this case, inhibition of *socs1* translation was caused by the 5' untranslated region (UTR) which encodes an upstream ORF containing AUG initiation codons. The presence of upstream AUG codons can inhibit protein translation, possibly by interfering with ribosomal scanning for the genuine AUG required for protein translation (Gregorieff *et al.*, 2000). A similar, but non-identical sequence, is present in human *socs1* mRNA (Gregorieff *et al.*, 2000). Given that both SOCS1 and SOCS3 protein expression can be regulated at the translational as well as the transcriptional level, it is possible that 5'-UTR-mediated suppression of SOCS protein translation represents a conserved mechanism by which to regulate SOCS protein expression and thus qRT-PCR methods may not represent a suitable method to investigate the role of other SOCS proteins in cAMP-mediated suppression of STAT3 activation.

One potential method by which to assess whether other SOCS family members are involved in modulation of IL-6 signalling in prostate epithelial cells would be to exploit the interaction of these signalling proteins with gp130. Immunoprecipitation of gp130 and subsequent immunoblotting or mass-spectroscopic analysis of associated proteins following Fsk pre-treatment and subsequent IL-6-mediated activation of gp130 would identify proteins interacting with gp130. This might lead to the identification of other SOCS family members, or indeed other, novel proteins, involved in the attenuation of IL-6/STAT3 signalling following cAMP elevation in prostate epithelial cells. However, it

must be stressed that such a strategy only allows identification of inhibitory molecules which interact directly with gp130 and it may be that other proteins are involved in cAMP-mediated attenuation of STAT3 signalling in LNCaP cells. Investigation of protein tyrosine phosphatase (PTPase) expression and activity may highlight new pathways involved in IL-6 signalling regulation. Expression of the T-cell PTPase (TC-PTP) or the PTPeC PTPase can both promote STAT3 dephosphorylation (Tanuma *et al.*, 2001; Yamamoto *et al.*, 2002). It is possible that cAMP elevation may enhance PTPase activity in LNCaP cells in a manner similar to the ability of p-CPT-cAMP or Sp-cAMP to induce increases in osteotesticular-PTPase expression in rat osteoblasts (Mauro *et al.*, 1996). Thus microarray or RT-PCR analysis of PTPase expression could also be considered when investigating the mechanisms by which cAMP elevation inhibits IL-6 signalling in LNCaP cells.

12.3 The role of cAMP compartmentalisation in NE differentiation

The results obtained in this study demonstrate a key role for PKA activation in mediating changes in LNCaP cell morphology following cAMP elevation through inhibition of RhoA activation, the effects on Rac and Cdc42 activity are unknown. Further expansion of this project to investigate changes in GTP-associated Rac and Cdc42 following stimulation with Fsk or 6-Bnz-cAMP would help to determine their roles in this phenomenon. Furthermore, fluorescent imaging in real-time may determine whether particular subcellular pools of the Rho family GTPases are being mobilised to promote changes in LNCaP cell morphology following cAMP elevation. Recently, Fourier transform energy transfer- (FRET-) based techniques have been used to determine activation and localisation of specific Rho GTPase family members in response to extracellular stimuli in T-cell models of the immune synapse (Makrogianneli *et al.*, 2009). Recent advances in image analysis now enables direct quantification of Rho GTPase activity from fluorescence microscopy data (Tsukada *et al.*, 2008). It might thus be possible to investigate both the subcellular distribution and activation status of these signalling molecules in LNCaP cells following cAMP stimulation. The intracellular compartmentalisation of Rho GTPase signalling is of particular interest due to the emerging importance of subcellular compartmentalisation in regulating cAMP-mediated. Currently, the intracellular pools of cAMP elevation in LNCaP cells following Fsk treatment are unknown. However, FRET-based reporters to detect regions of cAMP elevation (Warrier *et al.*, 2005) could be used to identify whether LNCaP cells display compartmentalised increases in cAMP concentrations and how this relates to dendrite extension and branching. It has also been demonstrated that the genes induced in LNCaP cells during NE differentiation varies dependent on the stimulus used, although differences between cAMP-elevating agents

have not yet been analysed (Mori *et al.*, 2009). Furthermore, whilst Fsk, PACAP and di-Butyryl-cAMP all induce neurite outgrowth in PC12 cells as a result of cAMP elevation, each stimulus differentially regulates subsequent gene expression (Ravni *et al.*, 2008). It is possible that the distinct gene expression profiles arise from compartmentalisation of cAMP elevation and subsequent signalling pathway activation. As multiple β_2 -adrenergic receptor agonists and Fsk (Deeble *et al.*, 2001) induce NE differentiation in LNCaP cells, it would be interesting to see if differences in gene expression profiles arise and whether this can be correlated with changes in intracellular distribution of elevated cAMP. Furthermore, association of subcellular localisation of cAMP elevation and anchoring of particular PDE isoforms may identify novel therapeutic targets to impede NE differentiation during PCA progression. It appears that PDE activity is the primary factor governing intracellular compartmentalisation of cAMP elevation (Zaccolo & Pozzan, 2002) and thus family- or isoform-selective PDE inhibitors are likely to represent future directions in therapeutic strategies associated with cAMP signalling.

12.4 The interplay of the PKA/actin/ERK5 signalling pathways

Whilst it has been demonstrated that pharmacological or genetic inhibition of the ERK5 signalling pathway can inhibit the ability of Fsk to induce changes in LNCaP cell morphology, the ability of Fsk to activate ERK5 has not been determined. It is possible that immunoprecipitation of ERK5 and subsequent immunoblotting for pThr²¹⁸pTyr²²⁰ERK5 may enable identification of Fsk-induced activation of ERK5. Similarly, it has not been possible to identify endogenous ERK5 in LNCaP cells, an issue which may be resolved following improvements in the sensitivity of currently available antibodies. The observation that both PKA and ERK5 are important in Fsk-induced changes in LNCaP cell morphology begs the question as to whether the two proteins are acting *via* a common mechanism. In Chapter 9, PKA consensus sequences were identified on MEKK3, MEK5 and ERK5 using *in silico* prediction but their relevance has not been demonstrated *in vitro*. It is possible that PKA could activate ERK5, a question that could be addressed by treating cells with 6-Bnz-cAMP and observing whether a subsequent increase in ERK5 phosphorylation is observed. It would also be interesting to see if PKA can directly phosphorylate components of the ERK5 signalling pathway which could be implied following co-immunoprecipitation in order to determine whether PKA and components of the ERK5 signalling cascade can interact within LNCaP cells. However, this approach does not address whether PKA can directly activate components within the ERK5 signalling cascade. A yeast two-hybrid screen using recombinant isoforms of the PKA holoenzyme and the ERK5 signalling pathway components ERK5, MEK5 and

MEKK3 could be used to determine direct interaction between PKA and regulators of ERK5 activity. However, such an approach would need to be considered in conjunction with the aforementioned immunofluorescence and co-immunoprecipitation as yeast two-hybrid screens may not identify physiologically relevant interactions due to loss of temporal and spatial separation of proteins. Whilst such approaches would identify direct interaction of PKA with components of the ERK5 signalling pathway, they do not demonstrate that PKA can activate components of the ERK5 signalling pathway. This could be investigated using *in vitro* phosphorylation assays using purified components of the signalling cascade and the catalytic subunit of PKA in similar assays as described by Ellerbroek (2003).

Given the critical role of the actin cytoskeleton in regulating cellular morphology, the ability of ERK5 to regulate actin polymerisation is of interest. ERK5 contains two proline-rich regions which are believed to target ERK5 to the actin cytoskeleton (Zhou *et al.*, 1995) and, importantly, are absent in ERK1/2 (Fig. 9.x). Whilst ERK5 has been implicated in the inhibition of RhoA activity, there is currently no published data to demonstrate that ERK5 can directly interact with the actin cytoskeleton. Theoretically, demonstration of an ERK5/actin association could be readily achieved by a combination of co-immunoprecipitation or yeast 2-hybrid screening to determine protein-protein interaction and immunofluorescence to demonstrate colocalisation of ERK5 and actin. Given the importance of PKA in Fsk-induced changes in LNCaP cell morphology, it is not unreasonable to suppose that PKA may modulate ERK5 activity as suggested above. One mechanism by which to achieve specificity in cAMP signalling is to compartmentalise signalling proteins into complexes *via* interaction with scaffolding proteins such as AKAPs. ERK5 has already been shown to interact with mAKAP and modulate PDE4D3 activity (Dodge-Kafka *et al.*, 2005). Furthermore, WAVE1 has been shown to act as an AKAP linking PKA signalling and actin polymerisation. Thus, it is possible that a PKA-ERK5-AKAP-actin-RhoA or RhoGEF signalling complex exists which enables co-regulation of these pathways in order to facilitate changes in cellular morphology (Westphal *et al.*, 2000). Use of immunoprecipitation techniques could enable identification of proteins involved in such putative signalling complexes. The Cdc24-like motif in MEK5 is associated with an increase in GTP \rightarrow GDP exchange following interaction of CDC24 and CDC42 in *Saccharomyces cerevisiae* (Zhou *et al.*, 1995) and thus the MEK5-ERK5 signalling pathway may co-ordinate to dynamically regulate the actin cytoskeleton. It would be of interest to see whether either treatment with disrupting peptides or deletion/mutation of the proline-rich domains of ERK5 or the CDC24-like domain of

MEK5 alters the importance of this signalling cascade in Fsk-induced changes in LNCaP cell morphology.

Altered cytoskeletal dynamics are an important aspect of tumour metastasis as changes in actin polymerisation drive the cell motility required for cellular movement. Given that increased expression of MEK5 is correlated with PCa metastasis (Mehta *et al.*, 2003), it is also possible that dysregulation of MEK5/ERK5 signalling is of importance in the metastasis of other cancers. IHC, RT-PCR and immunoblotting analysis of metastatic lesions arising from multiple malignancies would indicate whether hyperactivation of the MEK5/ERK5 signalling pathway is a common factor to tumour metastases. If this is indeed the case, it is possible that use of pharmacological inhibitors of MEK5/ERK5 signalling such as BIX02188 and BIX02189 may have a novel application to complement or replace existing chemotherapeutic strategies.

13 References

- Aaronson, D. S. & Horvath, C. M. (2002). A road map for those who don't know JAK-STAT. *Science* **296**, 1653-1655.
- Adie, E. J. & Milligan, G. (1994). Regulation of Basal Adenylate-Cyclase Activity in Neuroblastoma X Glioma Hybrid, Ng108-15, Cells Transfected to Express the Human Beta-2-Adrenoceptor - Evidence for Empty Receptor Stimulation of the Adenylate-Cyclase Cascade. *Biochemical Journal* **303**, 803-808.
- Alberts, A. S., Montminy, M., Shenolikar, S., & Feramisco, J. R. (1994). Expression of A Peptide Inhibitor of Protein Phosphatase-1 Increases Phosphorylation and Activity of Creb in Nih 3T3 Fibroblasts. *Molecular and Cellular Biology* **14**, 4398-4407.
- Amsen, E. M., Pham, N., Pak, Y., & Rotin, D. (2006). The Guanine Nucleotide Exchange Factor CNrasGEF Regulates Melanogenesis and Cell Survival in Melanoma Cells. *Journal of Biological Chemistry* **281**, 121-128.
- Ango, F., Prezeau, L., Muller, T., Tu, J. C., Xiao, B., Worley, P. F., Pin, J. P., Bockaert, J., & Fagni, L. (2001). Agonist-independent activation of metabotropic glutamate receptors by the intracellular protein Homer. *Nature* **411**, 962-965.
- Azare, J., Leslie, K., Al Ahmadie, H., Gerald, W., Weinreb, P. H., Violette, S. M., & Bromberg, J. (2007). Constitutively activated Stat3 induces tumorigenesis and enhances cell motility of prostate epithelial cells through integrin beta 6. *Molecular and Cellular Biology* **27**, 4444-4453.
- Aznar, S., Valeron, P. F., del Rincon, S. V., Perez, L. F., Perona, R., & Lacal, J. C. (2001). Simultaneous tyrosine and serine phosphorylation of STAT3 transcription factor is involved in Rho A GTPase oncogenic transformation. *Molecular Biology of the Cell* **12**, 3282-3294.
- Baillie, G. S., Scott, J. D., & Houslay, M. D. (2005). Compartmentalisation of phosphodiesterases and protein kinase A: opposites attract. *FEBS Letters* **579**, 3264-3270.

- Bal, A., Unlu, E., Bahar, G., Aydog, E., Eksioglu, E., & Yorgancioglu, R. (2007). Comparison of serum IL-1 beta, sIL-2R, IL-6, and TNF-alpha levels with disease activity parameters in ankylosing spondylitis. *Clinical Rheumatology* **26**, 211-215.
- Balk, R. A. (2000). Pathogenesis and management of multiple organ dysfunction or failure in severe sepsis and septic shock. *Critical Care Clinics* **16**, 337-+.
- Balmano, K. & Cook, S. J. (2009). Tumour cell survival signalling by the ERK1/2 pathway. *Cell Death and Differentiation* **16**, 368-377.
- Baneres, J. L. & Parello, J. (2003). Structure-based Analysis of GPCR Function: Evidence for a Novel Pentameric Assembly between the Dimeric Leukotriene B4 Receptor BLT1 and the G-protein. *Journal of Molecular Biology* **329**, 815-829.
- Bang, Y. J., Pirnia, F., Fang, W. G., Kang, W. K., Sartor, O., Whitesell, L., Ha, M. J., Tsokos, M., Sheahan, M. D., Nguyen, P., Niklinski, W. T., Myers, C. E., & Trepel, J. B. (1994). Terminal Neuroendocrine Differentiation of Human Prostate Carcinoma-Cells in Response to Increased Intracellular Cyclic-Amp. *Proceedings of the National Academy of Sciences of the United States of America* **91**, 5330-5334.
- Baniyash, M. (2006). The inflammation-cancer linkage: A double-edged sword? *Seminars in Cancer Biology* **16**, 1-2.
- Barclay, J. L., Anderson, S. T., Waters, M. J., & Curlewis, J. D. (2007). Characterization of the SOCS3 promoter response to prostaglandin E-2 in T47D cells. *Molecular Endocrinology* **21**, 2516-2528.
- Barrow, A. J. & Wu, S. M. (2009). Low-Conductance HCN1 Ion Channels Augment the Frequency Response of Rod and Cone Photoreceptors. *Journal of Neuroscience* **29**, 5841-5853.
- Barton, B. E., Karras, J. G., Murphy, T. F., Barton, A., & Huang, H. F. S. (2004). Signal transducer and activator of transcription 3 (STAT3) activation in prostate cancer: Direct

STAT3 inhibition induces apoptosis in prostate cancer lines. *Molecular Cancer Therapeutics* **3**, 11-20.

Basoni, C., Nobles, M., Grimshaw, A., Desgranges, C., Davies, D., Perretti, M., Kramer, I. M., & Genot, E. (2005). Inhibitory control of TGF-beta 1 on the activation of Rap1, CD11b, and transendothelial migration of leukocytes. *Faseb Journal* **19**, 822-+.

Becker, S., Corthals, G. L., Aebersold, R., Groner, B., & Muller, C. W. (1998). Expression of a tyrosine phosphorylated, DNA binding Stat3 beta dimer in bacteria. *Febs Letters* **441**, 141-147.

Bellanger, J. M., Astier, C., Sardet, C., Ohta, Y., Stossel, T. P., & Debant, A. (2000). The Rac1-and RhoG-specific GEF domain of Trio targets filamin to remodel cytoskeletal actin. *Nature Cell Biology* **2**, 888-892.

Bellezza, I., Neuwirt, H., Nemes, C., Cavarretta, I. T., Puhr, M., Steiner, H., Minelli, A., Bartsch, G., Offner, F., Hobisch, A., Doppler, W., & Culig, Z. (2006). Suppressor of cytokine signaling-3 antagonizes cAMP effects on proliferation and apoptosis and is expressed in human prostate cancer. *American Journal of Pathology* **169**, 2199-2208.

Bergmann, C., Strauss, L., Zeidler, R., Lang, S., & Whiteside, T. (2007). Expansion and characteristics of human T regulatory type 1 cells in co-cultures simulating tumor microenvironment. *Cancer Immunology, Immunotherapy* **56**, 1429-1442.

Bhoj, V. G. & Chen, Z. J. (2009). Ubiquitylation in innate and adaptive immunity. *Nature* **458**, 430-437.

Biel, M. (2009). Cyclic Nucleotide-regulated Cation Channels. *Journal of Biological Chemistry* **284**, 9017-9021.

Birnbaumer, L., Abramowitz, J., & Brown, A. M. (1990). Receptor-effector coupling by G proteins. *Biochimica et Biophysica Acta (BBA) - Reviews on Biomembranes* **1031**, 163-224.

Bischoff, S. C., Deweck, A. L., & Dahinden, C. A. (1992). Peptide Analogs of Consensus Receptor Sequence Inhibit the Action of Cytokines on Human Basophils. *Lymphokine and Cytokine Research* **11**, 33-37.

Bittinger, M. A., McWhinnie, E., Meltzer, J., Iourgenko, V., Latario, B., Liu, X. L., Chen, C. H., Song, C. Z., Garza, D., & Labow, M. (2004). Activation of cAMP response element-mediated gene expression by regulated nuclear transport of TORC proteins. *Current Biology* **14**, 2156-2161.

Blom, N., Sicheritz-Ponten, T., Gupta, R., Gammeltoft, S., & Brunak, S. (2004). Prediction of post-translational glycosylation and phosphorylation of proteins from the amino acid sequence. *Proteomics* **4**, 1633-1649.

Boing, I., Stross, C., Radtke, S., Lippok, B. E., Heinrich, P. C., & Hermanns, H. M. (2006). Oncostatin M-induced activation of stress-activated MAP kinases depends on tyrosine 861 in the OSM receptor and requires Jak1 but not Src kinases. *Cellular Signalling* **18**, 50-61.

Borges, J., Pandiella, A., & Esparis-Ogando, A. (2007). Erk5 nuclear location is independent on dual phosphorylation, and favours resistance to TRAIL-induced apoptosis. *Cellular Signalling* **19**, 1473-1487.

Borland, G., Bird, R. J., Palmer, T. M., & Yarwood, S. J. (2009). Activation of Protein Kinase C alpha by EPAC1 Is Required for the ERK- and CCAAT/Enhancer-binding Protein beta-dependent Induction of the SOCS-3 Gene by Cyclic AMP in COS1 Cells. *Journal of Biological Chemistry* **284**, 17391-17403.

Boucher, M. J., Morisset, J., Vachon, P. H., Reed, J. C., Laine, J., & Rivard, N. (2000). MEK/ERK signaling pathway regulates the expression of Bcl-2, Bcl-X-L, and Mcl-1 and promotes survival of human pancreatic cancer cells. *Journal of Cellular Biochemistry* **79**, 355-369.

Boulton, T. G., Yancopoulos, G. D., Gregory, J. S., Slaughter, C., Moomaw, C., Hsu, J., & Cobb, M. H. (1990). An insulin-stimulated protein kinase similar to yeast kinases involved in cell cycle control. *Science* **249**, 64-67.

- Boulton, T. G., Nye, S. H., Robbins, D. J., Ip, N. Y., Radzlejewska, E., Morgenbesser, S. D., DePinho, R. A., Panayotatos, N., Cobb, M. H., & Yancopoulos, G. D. (1991). ERKs: A family of protein-serine/threonine kinases that are activated and tyrosine phosphorylated in response to insulin and NGF. *Cell* **65**, 663-675.
- Bouschet, T., Perez, V., Fernandez, C., Bockaert, J., Eychene, A., & Journot, L. (2003). Stimulation of the ERK pathway by GTP-loaded Rap1 requires the concomitant activation of ras, protein kinase C, and protein kinase A in neuronal cells. *Journal of Biological Chemistry* **278**, 4778-4785.
- Bousquet, C., Chesnokova, V., Kariagina, A., Ferrand, A., & Melmed, S. (2001). cAMP neuropeptide agonists induce pituitary suppressor of cytokine signaling-3: Novel negative feedback mechanism for corticotroph cytokine action. *Molecular Endocrinology* **15**, 1880-1890.
- Bravo, J. & Heath, J. K. (2000). Receptor recognition by gp130 cytokines. *Embo Journal* **19**, 2399-2411.
- Bromberg, J. F., Wrzeszczynska, M. H., Devgan, G., Zhao, Y., Pestell, R. G., Albanese, C., & Darnell, J. E. (1999). Stat3 as an Oncogene. *Cell* **98**, 295-303.
- Brown, W. M. (2007). Treating COPD with PDE4 inhibitors. *Int J Chron Obstruct Pulmon Dis* **2**, 517-533.
- Busca, R., Abbe, P., Mantoux, F., Aberdam, E., Peyssonnaud, C., Eychene, A., Ortonne, J. P., & Ballotti, R. (2000). Ras mediates the cAMP-dependent activation of extracellular signal-regulated kinases (ERKs) in melanocytes. *Embo Journal* **19**, 2900-2910.
- Calo, V., Migliavacca, M., Bazan, V., Macaluso, M., Buscemi, M., Gebbia, N., & Russo, A. (2003). STAT proteins: From normal control of cellular events to tumorigenesis. *Journal of Cellular Physiology* **197**, 157-168.
- Canalis, E., Mazziotti, G., Giustina, A., & Bilezikian, J. (2007). Glucocorticoid-induced osteoporosis: pathophysiology and therapy. *Osteoporosis International* **18**, 1319-1328.

- Carr, D. W., Stofkohahn, R. E., Fraser, I. D. C., Cone, R. D., & Scott, J. D. (1992). Localization of the Camp-Dependent Protein-Kinase to the Postsynaptic Densities by A-Kinase Anchoring Proteins - Characterization of Akap-79. *Journal of Biological Chemistry* **267**, 16816-16823.
- Cavanaugh, J. E., Ham, J., Hetman, M., Poser, S., Yan, C., & Xia, Z. (2001). Differential Regulation of Mitogen-Activated Protein Kinases ERK1/2 and ERK5 by Neurotrophins, Neuronal Activity, and cAMP in Neurons. *Journal of Neuroscience* **21**, 434-443.
- Chahdi, A. & Sorokin, A. (2007). PKA-dependent phosphorylation modulates β 1Pix-GEF activity through 14-3-3 β binding. *Molecular and Cellular Biology* MCB.
- Chang, F., Steelman, L. S., Lee, J. T., Shelton, J. G., Navolanic, P. M., Blalock, W. L., Franklin, R. A., & McCubrey, J. A. (2003). Signal transduction mediated by the Ras/Raf/MEK/ERK pathway from cytokine receptors to transcription factors: potential targeting for therapeutic intervention. *Leukemia* **17**, 1263-1293.
- Charalambous, C., Gsandtner, I., Keuerleber, S., Milan-Lobo, L., Kudlacek, O., Freissmuth, M., & Zezula, J. (2008). Restricted collision coupling of the A(2A) receptor revisited - Evidence for physical separation of two signaling cascades. *Journal of Biological Chemistry* **283**, 9276-9288.
- Chen, H. Z., Kirschenbaum, A., Mandeli, J., & Hollander, V. P. (1992). The Effect of Dihydrotestosterone and Culture Conditions on Proliferation of the Human Prostatic-Cancer Cell-Line Lncap. *Steroids* **57**, 269-275.
- Chen, W. G., Daines, M. O., & Hershey, G. K. K. (2004). Methylation of STAT6 modulates STAT6 phosphorylation, nuclear translocation, and DNA-binding activity. *Journal of Immunology* **172**, 6744-6750.
- Chen, Y. C., Wang, Y., Yu, H., Wang, F. W., & Xu, W. R. (2005). The cross talk between protein kinase A- and RhoA-mediated signaling in cancer cells. *Experimental Biology and Medicine* **230**, 731-741.

- Chen, Y. H., Dai, X. Z., Haas, A. L., Wen, R. R., & Wang, D. M. (2006). Proteasome-dependent down-regulation of activated Stat5A in the nucleus. *Blood* **108**, 566-574.
- Chijiwa, T., Mishima, A., Hagiwara, M., Sano, M., Hayashi, K., Inoue, T., Naito, K., Toshioka, T., & Hidaka, H. (1990). Inhibition of forskolin-induced neurite outgrowth and protein phosphorylation by a newly synthesized selective inhibitor of cyclic AMP-dependent protein kinase, N-[2-(p-bromocinnamylamino)ethyl]-5-isoquinolinesulfonamide (H-89), of PC12D pheochromocytoma cells. *Journal of Biological Chemistry* **265**, 5267-5272.
- Chow, D. C., Brevnova, L., He, X. L., Martick, M. M., Bankovich, A., & Garcia, K. C. (2002). A structural template for gp130-cytokine signaling assemblies. *Biochimica et Biophysica Acta-Molecular Cell Research* **1592**, 225-235.
- Chow, D. C., He, X. L., Snow, A. L., Rose-John, S., & Garcia, K. C. (2001a). Structure of an extracellular gp130 cytokine receptor signaling complex. *Science* **291**, 2150-2155.
- Chow, D. C., Ho, J., Pham, T. L. N., Rose-John, S., & Garcia, K. C. (2001b). In vitro reconstitution of recognition and activation complexes between interleukin-6 and gp130. *Biochemistry* **40**, 7593-7603.
- Christensen, A. E., Selheim, F., de Rooij, J., Dremier, S., Schwede, F., Dao, K. K., Martinez, A., Maenhaut, C., Bos, J. L., Genieser, H. G., & Doskeland, S. O. (2003). cAMP Analog Mapping of Epac1 and cAMP Kinase: DISCRIMINATING ANALOGS DEMONSTRATE THAT Epac AND cAMP KINASE ACT SYNERGISTICALLY TO PROMOTE PC-12 CELL NEURITE EXTENSION. *Journal of Biological Chemistry* **278**, 35394-35402.
- Chung, C. D., Liao, J. Y., Liu, B., Rao, X. P., Jay, P., Berta, P., & Shuai, K. (1997). Specific inhibition of Stat3 signal transduction by PIAS3. *Science* **278**, 1803-1805.
- Chung, S., Furihata, M., Tamura, K., Uemura, M., Daigo, Y., Nasu, Y., Miki, T., Shuin, T., Fujioka, T., Nakamura, Y., & Nakagawa, H. (2009). Overexpressing PKIB in prostate cancer promotes its aggressiveness by linking between PKA and Akt pathways. *Oncogene* **28**, 2849-2859.

- Clevers, H. (2004). At the crossroads of inflammation and cancer. *Cell* **118**, 671-674.
- Cochet, O., Frelin, C., Peyron, J. F., & Imbert, V. (2006). Constitutive activation of STAT proteins in the HDLM-2 and L540 Hodgkin lymphoma-derived cell lines supports cell survival. *Cellular Signalling* **18**, 449-455.
- Conklyn, M., Andresen, C., Changelian, P., & Kudlacz, E. (2004). The JAK3 inhibitor CP-690550 selectively reduces NK and CD8⁺ cell numbers in cynomolgus monkey blood following chronic oral dosing. *J Leukoc Biol* **76**, 1248-1255.
- Conkright, M. D., Canettieri, G., Sreaton, R., Guzman, E., Miraglia, L., Hogenesch, J. B., & Montminy, M. (2003). TORCs: Transducers of Regulated CREB Activity. *Molecular Cell* **12**, 413-423.
- Cook, S. J., Beltman, J., Cadwallader, K. A., McMahon, M., & McCormick, F. (1997). Regulation of mitogen-activated protein kinase phosphatase-1 expression by extracellular signal-related kinase-dependent and Ca²⁺-dependent signal pathways in rat-1 cells. *Journal of Biological Chemistry* **272**, 13309-13319.
- Costa-Pereira, A. P., Tininini, S., Strobl, B., Alonzi, T., Schlaak, J. F., Is'harc, H., Gesualdo, I., Newman, S. J., Kerr, I. M., & Poli, V. (2002). Mutational switch of an IL-6 response to an interferon-gamma-like response. *Proceedings of the National Academy of Sciences of the United States of America* **99**, 8043-8047.
- Coussens, L. M. & Werb, Z. (2002). Inflammation and cancer. *Nature* **420**, 860-867.
- Cowley, S., Paterson, H., Kemp, P., & Marshall, C. J. (1994). Activation of Map Kinase Kinase Is Necessary and Sufficient for Pc12 Differentiation and for Transformation of Nih 3T3 Cells. *Cell* **77**, 841-852.
- Cox, M. E., Deeble, P. D., Lakhani, S., & Parsons, S. J. (1999). Acquisition of neuroendocrine characteristics by prostate tumor cells is reversible: Implications for prostate cancer progression. *Cancer Research* **59**, 3821-3830.

Cox, M. E., Deeble, P. D., Bissonette, E. A., & Parsons, S. J. (2000). Activated 3',5'-Cyclic AMP-dependent Protein Kinase Is Sufficient to Induce Neuroendocrine-like Differentiation of the LNCaP Prostate Tumor Cell Line. *Journal of Biological Chemistry* **275**, 13812-13818.

Crawford, E. D., Rosenblum, M., Ziada, A. M., & Lange, P. H. (1999). Overview: hormone refractory prostate cancer. *Urology* **54**, 1-7.

Creedon, D. J., Johnson, E. M., & Lawrence, J. C. (1996). Mitogen-activated protein kinase-independent pathways mediate the effects of nerve growth factor and cAMP on neuronal survival. *Journal of Biological Chemistry* **271**, 20713-20718.

Crocker, B. A., Krebs, D. L., Zhang, J. G., Wormald, S., Willson, T. A., Stanley, E. G., Robb, L., Greenhalgh, C. J., Forster, I., Clausen, B. E., Nicola, N. A., Metcalf, D., Hilton, D. J., Roberts, A. W., & Alexander, W. S. (2003). SOCS3 negatively regulates IL-6 signaling in vivo. *Nat Immunol* **4**, 540-545.

Crowe, F. L., Key, T. J., Appleby, P. N., Travis, R. C., Overvad, K., Jakobsen, M. U., Johnsen, N. F., Tjonneland, A., Linseisen, J., Rohrmann, S., Boeing, H., Pischon, T., Trichopoulou, A., Lagiou, P., Trichopoulos, D., Sacerdote, C., Palli, D., Tumino, R., Krogh, V., Bueno-De-Mesquita, H. B., Kiemeny, L. A., Chirlaque, M. D., Ardanaz, E., Sanchez, M. J., Larranaga, N., Gonzalez, C. A., Quiros, J. R., Manjer, J., Wirfalt, E., Stattin, P., Hallmans, G., Khaw, K. T., Bingham, S., Ferrari, P., Slimani, N., Jenab, M., & Riboli, E. (2008). Dietary fat intake and risk of prostate cancer in the European Prospective Investigation into Cancer and Nutrition. *American Journal of Clinical Nutrition* **87**, 1405-1413.

Culig, Z., Steiner, H., Bartsch, G., & Hobisch, A. (2005). Interleukin-6 regulation of prostate cancer cell growth. *Journal of Cellular Biochemistry* **95**, 497-505.

Culig, Z., Bartsch, G., & Hobisch, A. (2002). Interleukin-6 regulates androgen receptor activity and prostate cancer cell growth. *Molecular and Cellular Endocrinology* **197**, 231-238.

D'Arcangelo, G. & Halegoua, S. (1993). A Branched Signalling Pathway for Nerve Growth Factor Is revealed By Src-, Ras-, and Raf-Mediated Gene Inductions. *Molecular and Cellular Biology* **13**, 3146-3155.

Daniel, P. B., Walker, W. H., & Habener, J. F. (1998). Cyclic AMP signaling and gene regulation. *Annual Review of Nutrition* **18**, 353-383.

Dankort, D., Curley, D. P., Cartlidge, R. A., Nelson, B., Karnezis, A. N., Damsky, W. E., You, M. J., DePinho, R. A., McMahon, M., & Bosenberg, M. (2009). Braf(V600E) cooperates with Pten loss to induce metastatic melanoma. *Nature Genetics* **41**, 544-552.

Dao, K. K., Teigen, K., Kopperud, R., Hodneland, E., Schwede, F., Christensen, A. E., Martinez, A., & Doskeland, S. O. (2006). Epac1 and cAMP-dependent Protein Kinase Holoenzyme Have Similar cAMP Affinity, but Their cAMP Domains Have Distinct Structural Features and Cyclic Nucleotide Recognition. *Journal of Biological Chemistry* **281**, 21500-21511.

Darnell, J. E. (1997). STATs and gene regulation. *Science* **277**, 1630-1635.

Das, K. P., Freudenrich, T. M., & Mundy, W. R. (2005). Assessment of PC12 cell differentiation and neurite growth: a comparison of morphological and neurochemical measures. *Neurotoxicology and Teratology* **26**, 397-406.

De Brabander, M. J., Van de Velre, R. M. L., Aerts, F. E. M., Borgers, M., & Janssen, P. A. J. (1976). The Effects of Methyl [5-(2-Thienylcarbonyl)-1H-benzimidazol-2-yl]carbamate, (R 17934; NSC 238159), a New Synthetic Antitumoral Drug Interfering with Microtubules, on Mammalian Cells Cultured in Vitro. *Cancer Research* **36**, 905-916.

De Miguel, F., Lee, S. O., Onate, S. A., & Gao, A. C. (2003). Stat3 enhances transactivation of steroid hormone receptors. *Nuclear Receptor* **1**.

de Rooij, J., Zwartkruis, F. J. T., Verheijen, M. H. G., Cool, R. H., Nijman, S. M. B., Wittinghofer, A., & Bos, J. L. (1998). Epac is a Rap1 guanine-nucleotide-exchange factor directly activated by cyclic AMP. *Nature* **396**, 474-477.

- de Visser, K. E., Korets, L. V., & Coussens, L. M. (2005). De novo carcinogenesis promoted by chronic inflammation is B lymphocyte dependent. *Cancer Cell* **7**, 411-423.
- Debidda, M., Wang, L., Zang, H., Poli, V., & Zheng, Y. (2005). A role of STAT3 in rho GTPase-regulated cell migration and proliferation. *Journal of Biological Chemistry* **280**, 17275-17285.
- Deeble, P. D., Murphy, D. J., Parsons, S. J., & Cox, M. E. (2001). Interleukin-6-and cyclic AMP-mediated signaling potentiates neuroendocrine differentiation of LNCaP prostate tumor cells. *Molecular and Cellular Biology* **21**, 8471-8482.
- Deepa, R., Vehnurugan, K., Arvind, K., Sivaram, P., Sientay, C., Uday, S., & Mohan, V. (2006). Serum levels of interleukin 6, C-reactive protein, vascular cell adhesion molecule 1, and monocyte chemotactic protein 1 in relation to insulin resistance and glucose intolerance - the Chennai Urban Rural Epidemiology Study (CURES). *Metabolism-Clinical and Experimental* **55**, 1232-1238.
- Dehmelt, L. & Halpain, S. (2004). Actin and microtubules in neurite initiation: Are MAPs the missing link? *Journal of Neurobiology* **58**, 18-33.
- Deutsch, P. J. & Sun, Y. (1992). The 38-Amino Acid Form of Pituitary Adenylate Cyclase-Activating Polypeptide Stimulates Dual Signaling Cascades in Pc12 Cells and Promotes Neurite Outgrowth. *Journal of Biological Chemistry* **267**, 5108-5113.
- Dhar, A., Young, M. R., & Colburn, N. H. (2002). The role of AP-1, NF-kappa B and ROS/NOS in skin carcinogenesis: The JB6 model is predictive. *Molecular and Cellular Biochemistry* **234**, 185-193.
- Dhir, R., Ni, Z., Lou, W., DeMiguel, F., Grandis, J. R., & Gao, A. C. (2002). Stat3 Activation in Prostatic Carcinomas. *The Prostate* **51**, 241-246.
- Dodge-Kafka, K. L., Soughayer, J., Pare, G. C., Michel, J. J. C., Langeberg, L. K., Kapiloff, M. S., & Scott, J. D. (2005). The protein kinase A anchoring protein mAKAP coordinates two integrated cAMP effector pathways. *Nature* **437**, 574-578.

- Dong, J. M., Leung, T., Manser, E., & Lim, L. (1998). cAMP-induced morphological changes are counteracted by the activated RhoA small GTPase and the Rho kinase ROK alpha. *Journal of Biological Chemistry* **273**, 22554-22562.
- Dony, E., Lai, Y. J., Dumitrascu, R., Pullamsetti, S. S., Savai, R., Ghofrani, H. A., Weissmann, N., Schudt, C., Fockerzi, D., Seeger, W., Grimminger, F., & Schermuly, R. T. (2008). Partial reversal of experimental pulmonary hypertension by phosphodiesterase-3/4 inhibition. *European Respiratory Journal* **31**, 599-610.
- Dostmann, W. R. G. (1995). (RP)-cAMPS inhibits the cAMP-dependent protein kinase by blocking the cAMP-induced conformational transition. *FEBS Letters* **375**, 231-234.
- Dunn, G. P., Sheehan, K. C. F., Old, L. J., & Schreiber, R. D. (2005). IFN unresponsiveness in LNCaP cells due to the lack of JAK1 gene expression. *Cancer Research* **65**, 3447-3453.
- Ellerbroek, S. M., Wennerberg, K., & Burridge, K. (2003). Serine Phosphorylation Negatively Regulates RhoA in Vivo. *Journal of Biological Chemistry* **278**, 19023-19031.
- Elliott, J., Hookham, M. B., & Johnston, J. A. (2008). The suppressors of cytokine signalling E3 ligases behave as tumour suppressors. *Biochemical Society Transactions* **36**, 464-468.
- Elliott, J. & Johnston, J. A. (2004). SOCS: role in inflammation, allergy and homeostasis. *Trends Immunol* **25**, 434-440.
- Endo, T. A., Masuhara, M., Yokouchi, M., Suzuki, R., Sakamoto, H., Mitsui, K., Matsumoto, A., Tanimura, S., Ohtsubo, M., Misawa, H., Miyazaki, T., Leonor, N., Taniguchi, T., Fujita, T., Kanakura, Y., Komiya, S., & Yoshimura, A. (1997). A new protein containing an SH2 domain that inhibits JAK kinases. *Nature* **387**, 921-924.
- English, J. M., Pearson, G., Hockenberry, T., Shivakumar, L., White, M. A., & Cobb, M. H. (1999). Contribution of the ERK5/MEK5 pathway to Ras/Raf signaling and growth control. *Journal of Biological Chemistry* **274**, 31588-31592.

- Esfandi, F., Ghobadloo, S. M., & Basati, G. (2006). Interleukin-6 level in patients with colorectal cancer. *Cancer Letters* **244**, 76-78.
- Fan, J., Zhang, B., Shu, H. F., Zhang, X. Y., Wang, X., Kuang, F., Liu, L., Peng, Z. W., Wu, R., Zhou, Z. A., & Wang, B. R. (2009). Interleukin-6 Increases Intracellular Ca²⁺ Concentration and Induces Catecholamine Secretion in Rat Carotid Body Glomus Cells. *Journal of Neuroscience Research* **87**, 2757-2762.
- Fasshauer, M., Klein, J., Lossner, U., & Paschke, R. (2002). Isoproterenol is a positive regulator of the suppressor of cytokine signaling-3 gene expression in 3T3-L1 adipocytes. *Journal of Endocrinology* **175**, 727-733.
- Favata, M. F., Horiuchi, K. Y., Manos, E. J., Daulerio, A. J., Stradley, D. A., Feeser, W. S., Van Dyk, D. E., Pitts, W. J., Earl, R. A., Hobbs, F., Copeland, R. A., Magolda, R. L., Scherle, P. A., & Trzaskos, J. M. (1998). Identification of a Novel Inhibitor of Mitogen-activated Protein Kinase Kinase. *Journal of Biological Chemistry* **273**, 18623-18632.
- Fensome, A., Whatmore, J., Morgan, C., Jones, D., & Cockcroft, S. (1998). ADP-ribosylation factor and Rho proteins mediate fMLP-dependent activation of phospholipase D in human neutrophils. *Journal of Biological Chemistry* **273**, 13157-13164.
- Finkel, T. & Holbrook, N. J. (2000). Oxidants, oxidative stress and the biology of ageing. *Nature* **408**, 239-247.
- Fischer, P., Lehmann, U., Sobota, R. M., Schmitz, J., Niemand, C., Linnemann, S., Haan, S., Behrmann, I., Yoshimura, A., Johnston, J. A., Muller-Newen, G., Heinrich, P. C., & Schaper, F. (2004). The role of the inhibitors of interleukin-6 signal transduction SHP2 and SOCS3 for desensitization of interleukin-6 signalling. *Biochemical Journal* **378**, 449-460.
- Fleming, Y. M., Ferguson, G. J., Spender, L. C., Larsson, J., Karlsson, S., Ozanne, B. W., Grosse, R., & Inman, G. J. (2008). TGF- β -mediated activation of RhoA signalling is required for efficient V12HaRas and V600EBRAF transformation. *Oncogene* **28**, 983-993.

- Forget, M. A., Desrosiers, R. R., Gingras, D., & Beliveau, R. (2002). Phosphorylation states of Cdc42 and RhoA regulate their interactions with Rho GDP dissociation inhibitor and their extraction from biological membranes. *Biochemical Journal* **361**, 243-254.
- Fotiadis, D., Jastrzebska, B., Philippsen, A., Müller, D. J., Palczewski, K., & Engel, A. (2006). Structure of the rhodopsin dimer: a working model for G-protein-coupled receptors. *Current Opinion in Structural Biology* **16**, 252-259.
- Fox, D. & Smulian, A. G. (1999). Mitogen-activated protein kinase Mkp1 of *Pneumocystis carinii* complements the slt2 Delta defect in the cell integrity pathway of *Saccharomyces cerevisiae*. *Molecular Microbiology* **34**, 451-462.
- Fredholm, B. B., Arslan, G., Halldner, L., Kull, B., Schulte, G., & Wasserman, W. (2000). Structure and function of adenosine receptors and their genes. *Naunyn-Schmiedeberg's Archives of Pharmacology* **362**, 364-374.
- Fukada, T., Hibi, M., Yamanaka, Y., Takahashi-Tezuka, M., Fujitani, Y., Yamaguchi, T., Nakajima, K., & Hirano, T. (1996). Two Signals Are Necessary for Cell Proliferation Induced by a Cytokine Receptor gp130: Involvement of STAT3 in Anti-Apoptosis. *Immunity* **5**, 449-460.
- Gao, C. J., Guo, H. T., Mi, Z. Y., Grusby, M. J., & Kuo, P. C. (2007). Osteopontin induces ubiquitin-dependent degradation of STAT1 in RAW264.7 murine macrophages. *Journal of Immunology* **178**, 1870-1881.
- Garaud, S., Le Dantec, C., Jousse-Joulin, S., Hanrotel-Saliou, C., Saraux, A., Mageed, R. A., Youinou, P., & Renaudineau, Y. (2009). IL-6 Modulates CD5 Expression in B Cells from Patients with Lupus by Regulating DNA Methylation. *The Journal of Immunology* **182**, 5623-5632.
- Gauzzi, M. C., Velazquez, L., McKendry, R., Mogensen, K. E., Fellous, M., & Pellegrini, S. (1996). Interferon-alpha-dependent activation of Tyk2 requires phosphorylation of positive regulatory tyrosines by another kinase. *Journal of Biological Chemistry* **271**, 20494-20500.

Gerard, N. P. & Gerard, C. (2002). Complement in allergy and asthma. *Current Opinion in Immunology* **14**, 705-708.

Gerhartz, C., Heesel, B., Sasse, J., Hemmann, U., Landgraf, C., SchneiderMergener, J., Horn, F., Heinrich, P. C., & Graeve, L. (1996). Differential activation of acute phase response factor/STAT3 and STAT1 via the cytoplasmic domain of the interleukin 6 signal transducer gp130 .1. Definition of a novel phosphotyrosine motif mediating STAT1 activation. *Journal of Biological Chemistry* **271**, 12991-12998.

Giembycz, M. A. (2006). An update and appraisal of the cilomilast Phase III clinical development programme for chronic obstructive pulmonary disease. *British Journal of Clinical Pharmacology* **62**, 138-152.

Giri, D., Ozen, M., & Ittmann, M. (2001). Interleukin-6 is an autocrine growth factor in human prostate cancer. *American Journal of Pathology* **159**, 2159-2165.

Goley, E. D. & Welch, M. D. (2006). The ARP2/3 complex: an actin nucleator comes of age. *Nature Reviews Molecular Cell Biology* **7**, 713-726.

Gomez, G. & Sitkovsky, M. V. (2003). Targeting G protein-coupled A2a adenosine receptors to engineer inflammation in vivo. *International Journal of Biochemistry & Cell Biology* **35**, 410-414.

Goto, M., Murakawa, M., Kadoshima-Yamaoka, K., Tanaka, Y., Inoue, H., Murafuji, H., Hayashi, Y., Miura, K., Nakatsuka, T., Nagahira, K., Chamoto, K., Fukuda, Y., & Nishimura, T. (2009). Phosphodiesterase 7A inhibitor ASB16165 suppresses proliferation and cytokine production of NKT cells. *Cellular Immunology* **258**, 147-151.

Grandis, J. R., Drenning, S. D., Zeng, Q., Watkins, S. C., Melhem, M. F., Endo, S., Johnson, D. E., Huang, L., He, Y. K., & Kim, J. D. (2000). Constitutive activation of Stat3 signaling abrogates apoptosis in squamous cell carcinogenesis in vivo. *Proceedings of the National Academy of Sciences of the United States of America* **97**, 4227-4232.

Greaves, M. (2000). The king of Naples and other silent witnesses. In *The King of Naples and other silent witnesses* Oxford University Press, Oxford.

Greco, C., Ameglio, F., Alvino, S., Cianciulli, A. M., Giovannelli, M., Mattei, F., Vitelli, G., Venturo, I., Lopez, M., & Gandolfo, G. M. (1994). Selection of Patients with Monoclonal Grammopathy of Undetermined Significance Is Mandatory for A Reliable Use of Interleukin-6 and Other Nonspecific Multiple-Myeloma Serum Markers. *Acta Haematologica* **92**, 1-7.

Greene, L. A. & Tischler, A. S. (1976). Establishment of A Noradrenergic Clonal Line of Rat Adrenal Pheochromocytoma Cells Which Respond to Nerve Growth-Factor. *Proceedings of the National Academy of Sciences of the United States of America* **73**, 2424-2428.

Greenlund, A. C., Morales, M. O., Viviano, B. L., Yan, H., Krolewski, J., & Schreiber, R. D. (1995). Stat recruitment by tyrosine-phosphorylated cytokine receptors: An ordered reversible affinity-driven process. *Immunity* **2**, 677-687.

Gregorieff, A., Pyronnet, S., Sonenberg, N., & Veillette, A. (2000). Regulation of SOCS-1 Expression by Translational Repression. *Journal of Biological Chemistry* **275**, 21596-21604.

Greten, F. R., Eckmann, L., Greten, T. F., Park, J. M., Li, Z. W., Egan, L. J., Kagnoff, M. F., & Karin, M. (2004). IKK beta links inflammation and tumorigenesis in a mouse model of colitis-associated cancer. *Cell* **118**, 285-296.

Grollman, A. P. (1968). Inhibitors of Protein Biosynthesis. V. EFFECTS OF EMETINE ON PROTEIN AND NUCLEIC ACID BIOSYNTHESIS IN HeLa CELLS. *Journal of Biological Chemistry* **243**, 4089-4094.

Grubb, R. L., Deng, J. H., Pinto, P. A., Mohler, J. L., Chinnaiyan, A., Rubin, M., Linehan, W. M., Liotta, L. A., Petricoin, E. F., & Wulfkühle, J. D. (2009). Pathway Biomarker Profiling of Localized and Metastatic Human Prostate Cancer Reveal Metastatic and Prognostic Signatures. *Journal of Proteome Research* **8**, 3044-3054.

Gryz, E. A. & Meakin, S. O. (2000). Acidic substitution of the activation loop tyrosines in TrkA supports nerve growth factor-independent cell survival and neuronal differentiation. *Oncogene* **19**, 417-430.

Gupta, M. & Yarwood, S. J. (2005). MAP1A Light Chain 2 Interacts with Exchange Protein Activated by Cyclic AMP 1 (EPAC1) to Enhance Rap1 GTPase Activity and Cell Adhesion. *Journal of Biological Chemistry* **280**, 8109-8116.

Haan, S., Keller, J. F., Behrmann, I., Heinrich, P. C., & Haan, C. (2005). Multiple reasons for an inefficient STAT1 response upon IL-6-type cytokine stimulation. *Cellular Signalling* **17**, 1542-1550.

Haan, S., Margue, C., Engrand, A., Rolvering, C., Schmitz-Van de Leur, H., Heinrich, P. C., Behrmann, I., & Haan, C. (2008). Dual Role of the Jak1 FERM and Kinase Domains in Cytokine Receptor Binding and in Stimulation-Dependent Jak Activation. *The Journal of Immunology* **180**, 998-1007.

Hacker, H. & Karin, M. (2006). Regulation and Function of IKK and IKK-Related Kinases. *Science Signaling* **2006**, re13.

Hakoshima, T., Shimizu, T., & Maesaki, R. (2003). Structural basis of the Rho GTPase signaling. *Journal of Biochemistry* **134**, 327-331.

Hanada, T., Kobayashi, T., Chinen, T., Saeki, K., Takaki, H., Koga, K., Minoda, Y., Sanada, T., Yoshioka, T., Mimata, H., Kato, S., & Yoshimura, A. (2006). IFN gamma-dependent, spontaneous development of colorectal carcinomas in SOCS1-deficient mice. *Journal of Experimental Medicine* **203**, 1391-1397.

Hanahan, D. & Weinberg, R. A. (2000). The hallmarks of cancer. *Cell* **100**, 57-70.

Hanson, E. M., Dickensheets, H., Qu, C. K., Donnelly, R. P., & Keegan, A. D. (2003). Regulation of the dephosphorylation of Stat6 - Participation of TYR-713 in the interleukin-4 receptor alpha, the tyrosine phosphatase SHP-1, and the proteasome. *J.Biol.Chem.* **278**, 3903-3911.

Hatakeyama, S., Kitagawa, M., Nakayama, K., Shirane, M., Matsumoto, M., Hattori, K., Higashi, H., Nakano, H., Okumura, K., Onoe, K., Good, R. A., & Nakayama, K. (1999). Ubiquitin-dependent degradation of I kappa B alpha is mediated by a ubiquitin ligase Skp1/Cul 1/F-box protein FWD1. *Proceedings of the National Academy of Sciences of the United States of America* **96**, 3859-3863.

He, D. L., Mu, Z. M., Le, X. F., Hsieh, J. T., Pong, R. C., Chung, L. W. K., & Chang, K. S. (1997). Adenovirus-mediated expression of PML suppresses growth and tumorigenicity of prostate cancer cells. *Cancer Research* **57**, 1868-1872.

Heilker, R., Wolff, M., Tautermann, C. S., & Bieler, M. (2009). G-protein-coupled receptor-focused drug discovery using a target class platform approach. *Drug Discovery Today* **14**, 231-240.

Heinrich, P. C., Behrmann, I., Haan, S., Hermanns, H. M., Muller-Newen, G., & Schaper, F. (2003). Principles of interleukin (IL)-6-type cytokine signalling and its regulation. *Biochemical Journal* **374**, 1-20.

Hemann, U., Gerhartz, C., Heesel, B., Sasse, J., Kurapkat, G., Grotzinger, J., Wollmer, A., Zhong, Z., Darnell, J. E., Jr., Graeve, L., Heinrich, P. C., & Horn, F. (1996). Differential Activation of Acute Phase Response Factor/Stat3 and Stat1 via the Cytoplasmic Domain of the Interleukin 6 Signal Transducer gp130. II. Src HOMOLOGY SH2 DOMAINS DEFINE THE SPECIFICITY OF STAT FACTOR ACTIVATION. *Journal of Biological Chemistry* **271**, 12999-13007.

Ho, P. L. & Raw, I. (1992). Cyclic-Amp Potentiates Bfgf-Induced Neurite Outgrowth in Pc12 Cells. *Journal of Cellular Physiology* **150**, 647-656.

Hobisch, A., Ramoner, R., Fuchs, D., Godoy-Tundidor, S., Bartsch, G., Klocker, H., & Culig, Z. (2001). Prostate cancer cells (LNCaP) generated after long-term interleukin 6 (IL-6) treatment express IL-6 and acquire an IL-6 partially resistant phenotype. *Clinical Cancer Research* **7**, 2941-2948.

Hodge, D. R., Hurt, E. M., & Farrar, W. L. (2005). The role of IL-6 and STAT3 in inflammation and cancer. *European Journal of Cancer* **41**, 2502-2512.

Hoey, T. & Schindler, U. (1998). STAT structure and function in signaling. *Current Opinion in Genetics & Development* **8**, 582-587.

Hoppmann, J., Baumer, W., Galetzka, C., Hofgen, N., Kietzmann, M., & Rundfeldt, C. (2005). The phosphodiesterase 4 inhibitor AWD 12-281 is active in a new guinea-pig model of allergic skin inflammation predictive of human skin penetration and suppresses both Th1 and Th2 cytokines in mice. *Journal of Pharmacy and Pharmacology* **57**, 1609-1617.

Horoszewicz, J. S., Leong, S. S., Kawinski, E., Karr, J. P., Rosenthal, H., Chu, T. M., Mirand, E. A., & Murphy, G. P. (1983). Lncap Model of Human Prostatic-Carcinoma. *Cancer Research* **43**, 1809-1818.

Hoshino, M., Li, M., Zheng, L. Q., Suzuki, M., Mochizuki, T., & Yanaihara, N. (1993). Pituitary Adenylate-Cyclase Activating Peptide and Vasoactive Intestinal Polypeptide - Differentiation Effects on Human Neuroblastoma Nb-Ok-1 Cells. *Neuroscience Letters* **159**, 35-38.

Huang, E. J. & Reichardt, L. F. (2003). Trk receptors: Roles in neuronal signal transduction. *Annual Review of Biochemistry* **72**, 609-642.

Huang, S., Apasov, S., Koshiba, M., & Sitkovsky, M. (1997). Role of A2a extracellular adenosine receptor-mediated signaling in adenosine-mediated inhibition of T-cell activation and expansion. *Blood* **90**, 1600-1610.

Hucho, T. B., Dina, O. A., & Levine, J. D. (2005). Epac Mediates a cAMP-to-PKC Signaling in Inflammatory Pain: An Isolectin B4(+) Neuron-Specific Mechanism. *Journal of Neuroscience* **25**, 6119-6126.

Humpolík, L., Kovář, J., Dusek, L., Lauerová, L., Boudník, V., Fait, V., Fojtová, M., Krejčí, E., & Kovář, A. (2009). Interferon-alpha treatment may negatively influence disease progression in melanoma patients by hyperactivation of STAT3 protein. *European Journal of Cancer* **45**, 1315-1323.

Hussain, S. P. & Harris, C. C. (2006). O49. p53 is a key molecular node in the inflammatory stress response network. *Nitric Oxide* **14**, 15.

Ilangumaran, S., Ramanathan, S., & Rottapel, R. (2004). Regulation of the immune system by SOCS family adaptor proteins. *Seminars in Immunology* **16**, 351-365.

Ingle, E. & Klinken, S. P. (2006). Cross-regulation of JAK and Src kinases. *Growth Factors* **24**, 89-95.

Ishizaki, T., Uehata, M., Tamechika, I., Keel, J., Nonomura, K., Maekawa, M., & Narumiya, S. (2000). Pharmacological Properties of Y-27632, a Specific Inhibitor of Rho-Associated Kinases. *Molecular Pharmacology* **57**, 976-983.

Jaakola, V. P., Griffith, M. T., Hanson, M. A., Cherezov, V., Chien, E. Y. T., Lane, J. R., IJzerman, A. P., & Stevens, R. C. (2008). The 2.6 Angstrom Crystal Structure of a Human A2A Adenosine Receptor Bound to an Antagonist. *Science* **322**, 1211-1217.

Jackson, M. J., Elliott, R. M., Lund, E., Papa, S., & Astley, S. B. (2002). Antioxidants, reactive oxygen and nitrogen species, gene induction and mitochondrial function. *Free Radical Research* **36**, 14.

Jacobson, B. S. & Branton, D. (1977). Plasma-Membrane - Rapid Isolation and Exposure of Cytoplasmic Surface by Use of Positively Charged Beads. *Science* **195**, 302-304.

Jaiswal, B. S. & Conti, M. (2001). Identification and Functional Analysis of Splice Variants of the Germ Cell Soluble Adenylyl Cyclase. *Journal of Biological Chemistry* **276**, 31698-31708.

Jaiswal, R. K., Weissinger, E., Kolch, W., & Landreth, G. E. (1996). Nerve Growth Factor-mediated Activation of the Mitogen-activated Protein (MAP) Kinase Cascade Involves a Signaling Complex Containing B-Raf and HSP90. *Journal of Biological Chemistry* **271**, 23626-23629.

- James, M. A., Lu, Y., Liu, Y., Vikis, H. G., & You, M. (2009). RGS17, an Overexpressed Gene in Human Lung and Prostate Cancer, Induces Tumor Cell Proliferation Through the Cyclic AMP-PKA-CREB Pathway. *Cancer Research* **69**, 2108-2116.
- Jarvis, M. F., Schulz, R., Hutchison, A. J., Do, U. H., Sills, M. A., & Williams, M. (1989). [3H]CGS 21680, a selective A2 adenosine receptor agonist directly labels A2 receptors in rat brain. *Journal of Pharmacology And Experimental Therapeutics* **251**, 888-893.
- Jay, P. Y., Pham, P. A., Wong, S. A., & Elson, E. L. (1995). A Mechanical Function of Myosin-Ii in Cell Motility. *Journal of Cell Science* **108**, 387-393.
- Jezeq, P. & Hlavata, L. (2005). Mitochondria in homeostasis of reactive oxygen species in cell, tissues, and organism. *International Journal of Biochemistry & Cell Biology* **37**, 2478-2503.
- Jimenez, A., Carrasco, L., & Vazquez, D. (2002). Enzymic and nonenzymic translocation by yeast polysomes. Site of action of a number of inhibitors. *Biochemistry* **16**, 4727-4730.
- Jing, N. & Tweardy, D. J. (2005). Targeting Stat3 in cancer therapy. *Anti-Cancer Drugs* **16**, 601-607.
- Johannessen, M., Delghandi, M. P., & Moens, U. (2004). What turns CREB on? *Cellular Signalling* **16**, 1211-1227.
- Johnston, J. A. (2004). Are SOCS suppressors, regulators, and degraders? *Journal of Leukocyte Biology* **75**, 743-748.
- Kaczmarek, E., Koziak, K., Sevigny, J., Siegel, J. B., Anrather, J., Beaudoin, A. R., Bach, F. H., & Robson, S. C. (1996). Identification and Characterization of CD39/Vascular ATP Diphosphohydrolase. *Journal of Biological Chemistry* **271**, 33116-33122.
- Kallen, K. J. (2002). The role of transsignalling via the agonistic soluble IL-6 receptor in human diseases. *Biochimica et Biophysica Acta-Molecular Cell Research* **1592**, 323-343.

Kamura, T., Sato, S., Haque, D., Liu, L., Kaelin, W. G. J., Conaway, R. C., & Conaway, J. W. (1998). The Elongin BC complex interacts with the conserved SOCS-box motif present in members of the SOCS, ras, WD-40 repeat, and ankyrin repeat families. *Genes Dev.* **12**, 3872-3881.

Kaptein, A., Paillard, V., & Saunders, M. (1996). Dominant negative stat3 mutant inhibits interleukin-6-induced Jak-STAT signal transduction. *Journal of Biological Chemistry* **271**, 5961-5964.

Karin, M. & Ben Neriah, Y. (2000). Phosphorylation meets ubiquitination: The control of NF-kappa B activity. *Annual Review of Immunology* **18**, 621-+.

Karin, M. (2006). Nuclear factor-[kappa]B in cancer development and progression. *Nature* **441**, 431-436.

Kasler, H. G., Victoria, J., Duramad, O., & Winoto, A. (2000). ERK5 Is a Novel Type of Mitogen-Activated Protein Kinase Containing a Transcriptional Activation Domain. *Molecular and Cellular Biology* **20**, 8382-8389.

Kato, Y., Kravchenko, V. V., Tapping, R. I., Han, J. H., Ulevitch, R. J., & Lee, J. D. (1997). BMK1/ERK5 regulates serum-induced early gene expression through transcription factor MEF2C. *Embo Journal* **16**, 7054-7066.

Kato, Y., Ozaki, N., Yamada, T., Miura, Y., & Oiso, Y. (2007). H-89 potentiates adipogenesis in 3T3-L1 cells by activating insulin signaling independently of protein kinase A. *Life Sciences* **80**, 476-483.

Kawasaki, H., Springett, G. M., Mochizuki, N., Toki, S., Nakaya, M., Matsuda, M., Housman, D. E., & Graybiel, A. M. (1998). A family of cAMP-binding proteins that directly activate Rap1. *Science* **282**, 2275-2279.

Kemp, B. E. & Pearson, R. B. (1990). Protein kinase recognition sequence motifs. *Trends in Biochemical Sciences* **15**, 342-346.

- Kes, V. B., Simundic, A. M., Nikolac, N., Topic, E., & Demarin, V. (2008). Pro-inflammatory and anti-inflammatory cytokines in acute ischemic stroke and their relation to early neurological deficit and stroke outcome. *Clinical Biochemistry* **41**, 1330-1334.
- Kiermayer, S., Biondi, R. M., Imig, J., Plotz, G., Haupenthal, J., Zeuzem, S., & Piiper, A. (2005). Epac Activation Converts cAMP from a Proliferative into a Differentiation Signal in PC12 Cells. *Molecular Biology of the Cell* **16**, 5639-5648.
- Kile, B. T. & Alexander, W. S. (2001). The suppressors of cytokine signalling (SOCS). *Cellular and Molecular Life Sciences* **58**, 1627-1635.
- Kim, H. Y., Pichavant, M., Matangkasombut, P., Koh, Y. I., Savage, P. B., DeKruyff, R. H., & Umetsu, D. T. (2009). The Development of Airway Hyperreactivity in T-bet-Deficient Mice Requires CD1d-Restricted NKT Cells. *The Journal of Immunology* **182**, 3252-3261.
- Kim, J., Adam, R. M., & Freeman, M. R. (2002). Activation of the Erk Mitogen-activated Protein Kinase Pathway Stimulates Neuroendocrine Differentiation in LNCaP Cells Independently of Cell Cycle Withdrawal and STAT3 Phosphorylation. *Cancer Research* **62**, 1549-1554.
- Kim, T. K. & Maniatis, T. (1996). Regulation of interferon-gamma-activated STAT1 by the ubiquitin-proteasome pathway. *Science* **273**, 1717-1719.
- Kimura, A., Kinjyo, I., Matsumura, Y., Mori, H., Mashima, R., Harada, M., Chien, K. R., Yasukawa, H., & Yoshimura, A. (2004). SOCS3 is a physiological negative regulator for granulopoiesis and granulocyte colony-stimulating factor receptor signaling. *Journal of Biological Chemistry* **279**, 6905-6910.
- Koenig, W., Khuseyinova, N., Baumert, J., Thorand, B., Loewel, H., Chambless, L., Meisinger, C., Schneider, A., Martin, S., Kolb, H., & Herder, C. (2006). Increased concentrations of C-reactive protein and IL-6 but not IL-18 are independently associated with incident coronary events in middle-aged men and women - Results from the MONICA/KORA Augsburg case-cohort study, 1984-2002. *Arteriosclerosis Thrombosis and Vascular Biology* **26**, 2745-2751.

Komazaki, T., Nagai, H., Emi, M., Terada, Y., Yabe, A., Jin, E., Kawanami, O., Konishi, N., Moriyama, Y., Naka, T., & Kishimoto, T. (2004). Hypermethylation-associated inactivation of the SOCS-1 gene, a JAK/STAT inhibitor, in human pancreatic cancers. *Japanese Journal of Clinical Oncology* **34**, 191-194.

Kotenko, S. V. & Pestka, S. (2000). Jak-Stat signal transduction pathway through the eyes of cytokine class II receptor complexes. *Oncogene* **19**, 2557-2565.

Krause, C. D. & Pestka, S. (2005). Evolution of the Class 2 cytokines and receptors, and discovery of new friends and relatives. *Pharmacology & Therapeutics* **106**, 299-346.

Krebs, D. L. & Hilton, D. J. (2001). SOCS proteins: Negative regulators of cytokine signaling. *Stem Cells* **19**, 378-387.

Kudlacz, E., Perry, B., Sawyer, P., Conklyn, M., McCurdy, S., Brisette, W., Flanagan, M., & Changelian, P. (2004). The novel JAK-3 inhibitor CP-690550 is a potent immunosuppressive agent in various murine models. *American Journal of Transplantation* **4**, 51-57.

Kuiperij, H. B., de Rooij, J., Rehmann, H., van Triest, M., Wittinghofer, A., Bos, J. L., & Zwartkruis, F. J. T. (2003). Characterisation of PDZ-GEFs, a family of guanine nucleotide exchange factors specific for Rap1 and Rap2. *Biochimica et Biophysica Acta (BBA) - Molecular Cell Research* **1593**, 141-149.

Kuroda, K., Nakashima, J., Kanao, K., Kikuchi, E., Miyajima, A., Horiguchi, Y., Nakagawa, K., Oya, M., Ohigashi, T., & Murai, M. (2007). Interleukin 6 is associated with cachexia in patients with prostate cancer. *Urology* **69**, 113-117.

Lang, S. H., Frame, F. M., & Collins, A. T. (2009). Prostate cancer stem cells. *Journal of Pathology* **217**, 299-306.

Laouar, Y., Sutterwala, F. S., Gorelik, L., & Flavell, R. A. (2005). Transforming growth factor-beta controls T helper type 1 cell development through regulation of natural killer cell interferon-gamma. *Nature Immunology* **6**, 600-607.

- Lebouille, G. & Muller, U. (2004). Synergistic activation of insect cAMP-dependent protein kinase A (type II) by cyclicAMP and cyclicGMP. *FEBS Letters* **576**, 216-220.
- Ledent, C., Dumont, J. E., Vassart, G., & Parmentier, M. (1992). Thyroid Expression of An A2 Adenosine Receptor Transgene Induces Thyroid Hyperplasia and Hyperthyroidism. *Embo Journal* **11**, 537-542.
- Lee, J. D., Ulevitch, R. J., & Han, J. H. (1995). Primary Structure of Bmk1 - A New Mammalian Map Kinase. *Biochemical and Biophysical Research Communications* **213**, 715-724.
- Leemhuis, J., Boutillier, S., Schmidt, G., & Meyer, D. K. (2002). The Protein Kinase A Inhibitor H89 Acts on Cell Morphology by Inhibiting Rho Kinase. *Journal of Pharmacology And Experimental Therapeutics* **300**, 1000-1007.
- Lennon, P. F., Taylor, C. T., Stahl, G. L., & Colgan, S. P. (1998). Neutrophil-derived 5'-Adenosine Monophosphate Promotes Endothelial Barrier Function via CD73-mediated Conversion to Adenosine and Endothelial A2B Receptor Activation. *The Journal of Experimental Medicine* **188**, 1433-1443.
- Leonard, W. J. & O'Shea, J. J. (1998). JAKS AND STATS: Biological implications. *Annual Review of Immunology* **16**, 293-322.
- Leslie, K., Lang, C., Devgan, G., Azare, J., Berishaj, M., Gerald, W., Kim, Y. B., Paz, K., Darnell, J. E., Albanese, C., Sakamaki, T., Pestell, R., & Bromberg, J. (2006). Cyclin D1 is transcriptionally regulated by and required for transformation by activated signal transducer and activator of transcription 3. *Cancer Research* **66**, 2544-2552.
- Li, M. O., Wan, Y. Y., Sanjabi, S., Robertson, A. K. L., & Flavell, R. A. (2006a). Transforming growth factor-beta regulation of immune responses. *Annual Review of Immunology* **24**, 99-146.

- Li, Y., Asuri, S., Rebhun, J. F., Castro, A. F., Parnavitana, N. C., & Quilliam, L. A. (2006b). The RAP1 guanine nucleotide exchange factor Epac2 couples cyclic AMP and Ras signals at the plasma membrane. *Journal of Biological Chemistry* **281**, 2506-2514.
- Liao, J. Y., Fu, Y. B., & Shuai, K. (2000). Distinct roles of the NH₂- and COOH-terminal domains of the protein inhibitor of activated signal transducer and activator of transcription (STAT) 1 (PIAS1) in cytokine-induced PIAS1-Stat1 interaction. *Proceedings of the National Academy of Sciences of the United States of America* **97**, 5267-5272.
- Lim, C. P. & Cao, X. M. (1999). Serine phosphorylation and negative regulation of Stat3 by JNK. *J.Biol.Chem.* **274**, 31055-31061.
- Lim, C. P. & Cao, X. M. (2006). Structure, function, and regulation of STAT proteins. *Molecular Biosystems* **2**, 536-550.
- Lin, M. T., Lin, B. R., Chang, C. C., Chu, C. Y., Su, H. J., Chen, S. T., Jeng, Y. M., & Kuo, M. L. (2007). IL-6 induces AGS gastric cancer cell invasion via activation of the c-Src/RhoA/ROCK signaling pathway. *International Journal of Cancer* **120**, 2600-2608.
- Ling, L., Cao, Z., & Goeddel, D. V. (1998). NF-kappaB-inducing kinase activates IKK-alpha by phosphorylation of Ser-176. *Proc.Natl.Acad.Sci.U.S.A* **95**, 3792-3797.
- Liu, B., Gross, M., ten Hoeve, J., & Shuai, K. (2001). A transcriptional corepressor of Stat1 with an essential LXXLL signature motif. *Proceedings of the National Academy of Sciences of the United States of America* **98**, 3203-3207.
- Liu, C., Takahashi, M., Li, Y., Song, S., Dillon, T. J., Shinde, U., & Stork, P. J. S. (2008). Ras Is Required for the Cyclic AMP-Dependent Activation of Rap1 via Epac2. *Molecular and Cellular Biology* **28**, 7109-7125.
- Liu, K. D., Gaffen, S. L., Goldsmith, M. A., & Greene, W. C. (1997). Janus kinases in interleukin-2-mediated signaling: JAK1 and JAK3 are differentially regulated by tyrosine phosphorylation. *Current Biology* **7**, 817-826.

Liu, L., McBride, K. M., & Reich, N. C. (2005). STAT3 nuclear import is independent of tyrosine phosphorylation and mediated by importin-alpha 3. *Proceedings of the National Academy of Sciences of the United States of America* **102**, 8150-8155.

Long, J. Y., Wang, G. N., Matsuura, I., He, D. M., & Liu, F. (2004). Activation of Smad transcriptional activity by protein inhibitor of activated STAT3 (PIAS3). *Proceedings of the National Academy of Sciences of the United States of America* **101**, 99-104.

LoRusso, P. M., Adjei, A. A., Varterasian, M., Gadgeel, S., Reid, J., Mitchell, D. Y., Hanson, L., DeLuca, P., Bruzek, L., Piens, J., Asbury, P., Van Becelaere, K., Herrera, R., Sebolt-Leopold, J., & Meyer, M. B. (2005). Phase I and Pharmacodynamic Study of the Oral MEK Inhibitor CI-1040 in Patients With Advanced Malignancies. *Journal of Clinical Oncology* **23**, 5281-5293.

Lutticken, C., Wegenka, U. M., Yuan, J., Buschmann, J., Schindler, C., Ziemiecki, A., Harpur, A. G., Wilks, A. F., Yasukawa, K., Taga, T., & et, a. (1994). Association of transcription factor APRF and protein kinase Jak1 with the interleukin-6 signal transducer gp130. *Science* **263**, 89-92.

Ma, J. & Cao, X. M. (2006). Regulation of Stat3 nuclear import by importin alpha 5 and importin alpha 7 via two different functional sequence elements. *Cellular Signalling* **18**, 1117-1126.

MacDonald, J. I. S., Gryz, E. A., Kubu, C. J., Verdi, J. M., & Meakin, S. O. (2000). Direct binding of the signaling adapter protein Grb2 to the activation loop tyrosines on the nerve growth factor receptor tyrosine kinase, TrkA. *Journal of Biological Chemistry* **275**, 18225-18233.

Maekawa, M., Ishizaki, T., Boku, S., Watanabe, N., Fujita, A., Iwamatsu, A., Obinata, T., Ohashi, K., Mizuno, K., & Narumiya, S. (1999). Signaling from rho to the actin cytoskeleton through protein kinases ROCK and LIM-kinase. *Science* **285**, 895-898.

Maenhaut, C., Van Sande, J., Libert, F., Abramowicz, M., Parmentier, M., Vanderhaegen, J. J., Dumont, J. E., Vassart, G., & Schiffmann, S. (1990). RDC8 codes for an adenosine

A2 receptor with physiological constitutive activity. *Biochemical and Biophysical Research Communications* **173**, 1169-1178.

Magiera, M. M., Gupta, M., Rundell, C. J., Satish, N., Ernens, I., & Yarwood, S. J. (2004). Exchange protein directly activated by cAMP (EPAC) interacts with the light chain (LC) 2 of MAP1A. *Biochemical Journal* **382**, 803-810.

Makrogianneli, K., Carlin, L. M., Keppler, M. D., Matthews, D. R., Ofo, E., Coolen, A., Ameer-Beg, S. M., Barber, P. R., Vojnovic, B., & Ng, T. (2009). Integrating Receptor Signal Inputs That Influence Small Rho GTPase Activation Dynamics at the Immunological Synapse. *Molecular and Cellular Biology* **29**, 2997-3006.

Matsumoto, K., Asano, T., & Endo, T. (1997). Novel small GTPase M-Ras participates in reorganization of actin cytoskeleton. *Oncogene* **15**, 2409-2417.

Mauro, L. J., Olmsted, E. A., Davis, A. R., & Dixon, J. E. (1996). Parathyroid hormone regulates the expression of the receptor protein tyrosine phosphatase, OST-PTP, in rat osteoblast-like cells. *Endocrinology* **137**, 925-933.

Mayr, B. & Montminy, M. (2001). Transcriptional regulation by the phosphorylation-dependent factor CREB. *Nature Reviews Molecular Cell Biology* **2**, 599-609.

McPherson, J. A., Barringhaus, K. G., Bishop, G. G., Sanders, J. M., Rieger, J. M., Hesselbacher, S. E., Gimple, L. W., Powers, E. R., Macdonald, T., Sullivan, G., Linden, J., & Sarembock, I. J. (2001). Adenosine A2A Receptor Stimulation Reduces Inflammation and Neointimal Growth in a Murine Carotid Ligation Model. *Arterioscler Thromb Vasc Biol* **21**, 791-796.

Mehta, P. B., Jenkins, B. L., McCarthy, L., Thilak, L., Robson, C. N., Neal, D. E., & Leung, H. Y. (2003). MEK5 overexpression is associated with metastatic prostate cancer, and stimulates proliferation, MMP-9 expression and invasion. *Oncogene* **22**, 1381-1389.

Meloche, S. & Pouyssegur, J. (2007). The ERK1//2 mitogen-activated protein kinase pathway as a master regulator of the G1- to S-phase transition. *Oncogene* **26**, 3227-3239.

Mezyk-Kopec, R., Bzowska, M., Stalinska, K., Chelmicki, T., Podkalicki, M., Jucha, J., Kowalczyk, K., Mak, P., & Bereta, J. (2009). Identification of ADAM10 as a major TNF sheddase in ADAM17-deficient fibroblasts. *Cytokine* **46**, 309-315.

Michalaki, V., Syrigos, K., Charles, P., & Waxman, J. (2004). Serum levels of IL-6 and TNF-alpha correlate with clinicopathological features and patient survival in patients with prostate cancer. *British Journal of Cancer* **90**, 2312-2316.

Michels, G., Brandt, M. C., Zagidullin, N., Khan, I. F., Larbig, R., van Aaken, S., Wippermann, J., & Hoppe, U. C. (2008). Direct evidence for calcium conductance of hyperpolarization-activated cyclic nucleotide-gated channels and human native If at physiological calcium concentrations. *Cardiovascular Research* **78**, 466-475.

Migone, T. S., Humbert, M., Rascole, A., Sanden, D., D'Andrea, A., & Johnston, J. A. (2001). The deubiquitinating enzyme DUB-2 prolongs cytokine-induced signal transducers and activators of transcription activation and suppresses apoptosis following cytokine withdrawal. *Blood* **98**, 1935-1941.

Milligan, G. (2007). G protein-coupled receptor dimerisation: Molecular basis and relevance to function. *Biochimica et Biophysica Acta (BBA) - Biomembranes* **1768**, 825-835.

Mima, T. & Nishimoto, N. (2009). Clinical value of blocking IL-6 receptor. *Current Opinion in Rheumatology* **21**, 224-230.

Mini, E., Nobili, S., Caciagli, B., Landini, I., & Mazzei, T. (2006). Cellular pharmacology of gemcitabine. *Annals of Oncology* **17**, v7-12.

Mitsuyama, K., Sata, M., & Rose-John, S. (2006). Interleukin-6 trans-signaling in inflammatory bowel disease. *Cytokine & Growth Factor Reviews* **17**, 451-461.

Miyoshi, H., Fujie, H., Moriya, K., Shintani, Y., Tsutsumi, T., Makuuchi, M., Kimura, S., & Koike, K. (2004). Methylation status of suppressor of cytokine signaling-1 gene in hepatocellular carcinoma. *Journal of Gastroenterology* **39**, 563-569.

Mody, N., Campbell, D. G., Morrice, N., Peggie, M., & Cohen, P. (2003). An analysis of the phosphorylation and activation of extracellular-signal-regulated protein kinase 5 (ERK5) by mitogen-activated protein kinase kinase 5 (MKK5) in vitro. *Biochemical Journal* **372**, 567-575.

Mody, N., Leitch, J., Armstrong, C., Dixon, J., & Cohen, P. (2001). Effects of MAP kinase cascade inhibitors on the MKK5/ERK5 pathway. *FEBS Letters* **502**, 21-24.

Moeller, S. & Sheaff, R. J. (2006). G1 Phase: Components, conundrums, context. In *Cell cycle regulation*, ed. Kaldis, P., Springer-Verlag.

Mohr, C., Koch, G., Just, I., & Aktories, K. (1992). ADP-ribosylation by Clostridium botulinum C3 exoenzyme increases steady-state GTPase activities of recombinant rhoA and rhoB proteins. *FEBS Letters* **297**, 95-99.

Molina, C. A., Foulkes, N. S., Lalli, E., & Sassonecorsi, P. (1993). Inducibility and Negative Autoregulation of Crem - An Alternative Promoter Directs the Expression of Icer, An Early Response Repressor. *Cell* **75**, 875-886.

Mollnes, T. E., Brekke, O. L., Fung, M., Fure, H., Christiansen, D., Bergseth, G., Videm, V., Lappégard, K. T., Kohl, J., & Lambris, J. D. (2002). Essential role of the C5a receptor in E-coli-induced oxidative burst and phagocytosis revealed by a novel lepirudin-based human whole blood model of inflammation. *Blood* **100**, 1869-1877.

Monaghan, T. K., MacKenzie, C. J., Plevin, R., & Lutz, E. M. (2008). PACAP-38 induces neuronal differentiation of human SH-SY5Y neuroblastoma cells via cAMP-mediated activation of ERK and p38 MAP kinases. *Journal of Neurochemistry* **104**, 74-88.

Mori, R., Xiong, S. G., Wang, Q. C., Tarabolous, C., Shimada, H., Panteris, E., Danenberg, K. D., Danenberg, P. V., & Pinski, J. K. (2009). Gene Profiling and Pathway Analysis of Neuroendocrine Transdifferentiated Prostate Cancer Cells. *Prostate* **69**, 12-23.

- Morimoto, H., Kondoh, K., Nishimoto, S., Terasawa, K., & Nishida, E. (2007). Activation of a C-terminal Transcriptional Activation Domain of ERK5 by Autophosphorylation. *Journal of Biological Chemistry* **282**, 35449-35456.
- Moss, S. F. & Blaser, M. J. (2005). Mechanisms of Disease: inflammation and the origins of cancer. *Nature Clinical Practice Oncology* **2**, 90-97.
- Mowen, K. A., Tang, J., Zhu, W., Schurter, B. T., Shuai, K., Herschman, H. R., & David, M. (2001). Arginine methylation of STAT1 modulates IFN alpha/beta-induced transcription. *Cell* **104**, 731-741.
- Murray, A. J. (2008). Pharmacological PKA Inhibition: All May Not Be What It Seems. *Science Signaling* **1**, re4.
- Muzio, M. & Mantovani, A. (2001). Toll-like receptors (TLRs) signalling and expression pattern. *Journal of Endotoxin Research* **7**, 297-300.
- Nadeem, A., Fan, M., Ansari, H. R., Ledent, C., & Jamal Mustafa, S. (2007). Enhanced airway reactivity and inflammation in A2A adenosine receptor-deficient allergic mice. *AJP - Lung Cellular and Molecular Physiology* **292**, L1335-L1344.
- Nadella, K. S., Saji, M., Jacob, N. K., Pavel, E., Ringel, M. D., & Kirschner, L. S. (2009). Regulation of actin function by protein kinase A-mediated phosphorylation of Limk1. *Embo Reports* **10**, 599-605.
- Nagata, S. & Glovsky, M. M. (1987). Activation of Human-Serum Complement with Allergens .1. Generation of C3A, C4A, and C5A and Induction of Human Neutrophil Aggregation. *Journal of Allergy and Clinical Immunology* **80**, 24-32.
- Naka, T., Narazaki, M., Hirata, M., Matsumoto, T., Minamoto, S., Aono, A., Nishimoto, N., Kajita, T., Taga, T., Yoshizaki, K., Akira, S., & Kishimoto, T. (1997). Structure and function of a new STAT-induced STAT inhibitor. *Nature* . **387**.

Nakaoka, Y., Nishida, K., Fujio, Y., Izumi, M., Terai, K., Oshima, Y., Sugiyama, S., Matsuda, S., Koyasu, S., Yamauchi-Takahara, K., Hirano, T., Kawase, I., & Hirota, H. (2003). Activation of gp130 transduces hypertrophic signal through interaction of scaffolding/docking protein Gab1 with tyrosine phosphatase SHP2 in cardiomyocytes. *Circulation Research* **93**, 221-229.

Nakashima, J., Tachibana, M., Horiguchi, Y., Oya, M., Ohigashi, T., Asakura, H., & Murai, M. (2000). Serum interleukin 6 as a prognostic factor in patients with prostate cancer. *Clinical Cancer Research* **6**, 2702-2706.

Naviglio, S., Caraglia, M., Abbruzzese, A., Chiosi, E., Di Gesto, D., Marra, M., Romano, M., Sorrentino, A., Sorvillo, L., Spina, A., & Illiano, G. (2009). Protein kinase A as a biological target in cancer therapy. *Expert Opinion on Therapeutic Targets* **13**, 83-92.

Nefedova, Y., Huang, M., Kusmartsev, S., Bhattacharya, R., Cheng, P. Y., Salup, R., Jove, R., & Gabrilovich, D. (2004). Hyperactivation of STAT3 is involved in abnormal differentiation of dendritic cells in cancer. *Journal of Immunology* **172**, 464-474.

Neuwirt, H., Puhr, M., Santer, F. R., Susani, M., Doppler, W., Marcias, G., Rauch, V., Brugger, M., Hobisch, A., Kenner, L., & Culig, Z. (2009). Suppressor of Cytokine Signaling (SOCS)-1 Is Expressed in Human Prostate Cancer and Exerts Growth-Inhibitory Function through Down-Regulation of Cyclins and Cyclin-Dependent Kinases. *American Journal of Pathology* **174**, 1921-1930.

Neuwirt, H., Puhr, M., Cavarretta, I. T., Mitterberger, M., Hobisch, A., & Culig, Z. (2007). Suppressor of cytokine signalling-3 is up-regulated by androgen in prostate cancer cell lines and inhibits androgen-mediated proliferation and secretion. *Endocrine-Related Cancer* **14**, 1007-1019.

Ng, Y. P., Wu, Z. G., Wise, H., Tsim, K. W. K., Wong, Y. H., & Ip, N. Y. (2009). Differential and Synergistic Effect of Nerve Growth Factor and cAMP on the Regulation of Early Response Genes during Neuronal Differentiation. *Neurosignals* **17**, 111-120.

Ni, C.-W. c. s. e. t. & Wang, D. L. l. s. e. t. (2003). IL-6-induced STAT3 activity is suppressing by shear flow via src-homology tyrosine phosphatase-2 in endothelial cells. *Faseb Journal* **17**.

Nishimoto, S., Kusakabe, M., & Nishida, E. (2005). Requirement of the MEK5-ERK5 pathway for neural differentiation in *Xenopus* embryonic development. *Embo Reports* **6**, 1064-1069.

Noordzij, M. A., vanWeerden, W. M., deRidder, C. M. A., vanderKwast, T. H., Schroder, F. H., & vanSteenbrugge, G. J. (1996). Neuroendocrine differentiation in human prostatic tumor models. *American Journal of Pathology* **149**, 859-871.

Nusser, N. r., Gosmanova, E., Makarova, N., Fujiwara, Y., Yang, L., Guo, F., Luo, Y., Zheng, Y., & Tigyi, G. (2006). Serine phosphorylation differentially affects RhoA binding to effectors: Implications to NGF-induced neurite outgrowth. *Cellular Signalling* **18**, 704-714.

Obara, Y., Labudda, K., Dillon, T. J., & Stork, P. J. S. (2004). PKA phosphorylation of Src mediates Rap1 activation in NGF and cAMP signaling in PC12 cells. *Journal of Cell Science* **117**, 6085-6094.

Obara, Y., Yamauchi, A., Takehara, S., Nemoto, W., Takahashi, M., Stork, P. J. S., & Nakahata, N. (2009). ERK5 activity is required for NGF-induced neurite outgrowth and stabilization of tyrosine hydroxylase in PC12 cells. *Journal of Biological Chemistry* **M109**.

Oestreich, E. A., Malik, S., Goonasekera, S. A., Blaxall, B. C., Kelley, G. G., Dirksen, R. T., & Smrcka, A. V. (2009). Epac and Phospholipase C{epsilon} Regulate Ca²⁺ Release in the Heart by Activation of Protein Kinase C{epsilon} and Calcium-Calmodulin Kinase II. *Journal of Biological Chemistry* **284**, 1514-1522.

Ohta, A. & Sitkovsky, M. (2001). Role of G-protein-coupled adenosine receptors in downregulation of inflammation and protection from tissue damage. *Nature* **414**, 916-920.

- Okamoto, M., Lee, C., & Oyasu, R. (1997). Interleukin-6 as a paracrine and autocrine growth factor in human prostatic carcinoma cells in vitro. *Cancer Research* **57**, 141-146.
- Olah, M. E. (1997). Identification of A(2a) adenosine receptor domains involved in selective coupling to G(s) - Analysis of chimeric A(1)/A(2a) adenosine receptors. *Journal of Biological Chemistry* **272**, 337-344.
- Oldham, W. M. & Hamm, E. (2006). Structural basis of function in heterotrimeric G proteins. *Quarterly Reviews of Biophysics* **39**, 117-166.
- Oppenheim, D. E., Roberts, S. J., Clarke, S. L., Filler, R., Lewis, J. M., Tigelaar, R. E., Girardi, M., & Hayday, A. C. (2005). Sustained localized expression of ligand for the activating NKG2D receptor impairs natural cytotoxicity in vivo and reduces tumor immunosurveillance. *Nature Immunology* **6**, 928-937.
- Orellana, S. A. & Mcknight, G. S. (1992). Mutations in the Catalytic Subunit of Camp-Dependent Protein-Kinase Result in Unregulated Biological-Activity. *Proceedings of the National Academy of Sciences of the United States of America* **89**, 4726-4730.
- Osborn, L., Kunkel, S., & Nabel, G. J. (1989). Tumor necrosis factor alpha and interleukin 1 stimulate the human immunodeficiency virus enhancer by activation of the nuclear factor kappa B. *Proc.Natl.Acad.Sci.U.S.A* **86**, 2336-2340.
- Pak, Y., Pham, N., & Rotin, D. (2002). Direct Binding of the β_1 Adrenergic Receptor to the Cyclic AMP-Dependent Guanine Nucleotide Exchange Factor CNrasGEF Leads to Ras Activation. *Molecular and Cellular Biology* **22**, 7942-7952.
- Palmer, J., Ernst, M., Hammacher, A., & Hertzog, P. J. (2005). Constitutive activation of gp130 leads to neuroendocrine differentiation in vitro and in vivo. *Prostate* **62**, 282-289.
- Palmer, J., Hertzog, P. J., & Hammacher, A. (2004). Differential expression and effects of gp130 cytokines and receptors in prostate cancer cells. *The International Journal of Biochemistry & Cell Biology* **36**, 2258-2269.

- Palmer, T. M. & Stiles, G. L. (1999). Stimulation of A(2A) adenosine receptor phosphorylation by protein kinase C activation: Evidence for regulation by-multiple protein kinase C isoforms. *Biochemistry* **38**, 14833-14842.
- Panchal, S. C., Kaiser, D. A., Torres, E., Pollard, T. D., & Rosen, M. K. (2003). A conserved amphipathic helix in WASP/Scar proteins is essential for activation of Arp2/3 complex. *Nature Structural Biology* **10**, 591-598.
- Papakonstanti, E. A. & Stournaras, C. (2008). Cell responses regulated by early reorganization of actin cytoskeleton. *FEBS Letters* **582**, 2120-2127.
- Park, B. H., Qiang, L., & Farmer, S. R. (2004). Phosphorylation of C/EBP beta at a consensus extracellular signal-regulated kinase/glycogen synthase kinase 3 site is required for the induction of adiponectin gene expression during the differentiation of mouse fibroblasts into adipocytes. *Molecular and Cellular Biology* **24**, 8671-8680.
- Park, J. I., Strock, C. J., Ball, D. W., & Nelkin, B. D. (2003). The Ras/Raf/MEK/extracellular signal-regulated kinase pathway induces autocrine-paracrine growth inhibition via the leukemia inhibitory factor/JAK/STAT pathway. *Molecular and Cellular Biology* **23**, 543-554.
- Payne, D. M., Rossomando, A. J., Martino, P., Erickson, A. K., Her, J. H., Shabanowitz, J., Hunt, D. F., Weber, M. J., & Sturgill, T. W. (1991). Identification of the Regulatory Phosphorylation Sites in Pp42/Mitogen-Activated Protein-Kinase (Map Kinase). *Embo Journal* **10**, 885-892.
- Pearson, G. W., Earnest, S., & Cobb, M. H. (2006). Cyclic AMP selectively uncouples mitogen-activated protein kinase cascades from activating signals. *Molecular and Cellular Biology* **26**, 3039-3047.
- Pearson, G. W. & Cobb, M. H. (2002). Cell Condition-dependent Regulation of ERK5 by cAMP. *Journal of Biological Chemistry* **277**, 48094-48098.

- Pernis, A. B. & Rothman, P. B. (2002). JAK-STAT signaling in asthma. *Journal of Clinical Investigation* **109**, 1279-1283.
- Peyssonaux, C. & Eychene, A. (2001). The Raf/MEK/ERK pathway: new concepts of activation. *Biology of the Cell* **93**, 53-62.
- Pflanz, S., Hibbert, L., Mattson, J., Rosales, R., Vaisberg, E., Bazan, J. F., Phillips, J. H., McClanahan, T. K., Malefyt, R. D., & Kastelein, R. A. (2004). WSX-1 and glycoprotein 130 constitute a signal-transducing receptor for IL-27. *Journal of Immunology* **172**, 2225-2231.
- Pham, N., Cheglakov, I., Koch, C. A., de Hoog, C. L., Moran, M. F., & Rotin, D. (2000). The guanine nucleotide exchange factor CNrasGEF activates Ras in response to cAMP and cGMP. *Current Biology* **10**, 555-558.
- Pierce, G. B. & Damjanov, I. (2006). The pathology of cancer. In *The biological basis of cancer*, eds. McKinnel, R. G., Parchment, R. E., Perantoni, A. O., Damjanov, I., & Pierce, G. B., Cambridge University Press, New York.
- Piersen, C. E., True, C. D., & Wells, J. N. (1994). A carboxyl-terminally truncated mutant and nonglycosylated A2a adenosine receptors retain ligand binding. *Molecular Pharmacology* **45**, 861-870.
- Pikarsky, E., Porat, R. M., Stein, I., Abramovitch, R., Amit, S., Kasem, S., Gulkovich-Pyest, E., Urieli-Shoval, S., Galun, E., & Ben Neriah, Y. (2004). NF-kappa B functions as a tumour promoter in inflammation-associated cancer. *Nature* **431**, 461-466.
- Pinto, C., Hubner, M., Gille, A., Richter, M., Mou, T. C., Sprang, S. R., & Seifert, R. (2009). Differential interactions of the catalytic subunits of adenylyl cyclase with forskolin analogs. *Biochemical Pharmacology* **78**, 62-69.
- Pollard, T. D. & Borisy, G. G. (2003). Cellular Motility Driven by Assembly and Disassembly of Actin Filaments. *Cell* **112**, 453-465.

Pollock, J. D., Krempin, M., & Rudy, B. (1990). Differential effects of NGF, FGF, EGF, cAMP, and dexamethasone on neurite outgrowth and sodium channel expression in PC12 cells. *Journal of Neuroscience* **10**, 2626-2637.

Poucher, S. M., Collis, M. G., Keddie, J. R., Stoggall, S. M., Singh, P., Caulkett, P. W. R., & Jones, G. (1995). The In-Vitro Pharmacology of Zm241385, A Novel, Nonxanthine, A2(A) Selective Adenosine Antagonist. *British Journal of Pharmacology* **114**, 100.

Pranada, A. L., Metz, S., Herrmann, A., Heinrich, P. C., & Muller-Newen, G. (2004). Real time analysis of STAT3 nucleocytoplasmic shuttling. *Journal of Biological Chemistry* **279**, 15114-15123.

Prezeau, L., Gomeza, J., Ahern, S., Mary, S., Galvez, T., Bockaert, J., & Pin, J. P. (1996). Changes in the carboxyl-terminal domain of metabotropic glutamate receptor 1 by alternative splicing generate receptors with differing agonist-independent activity. *Molecular Pharmacology* **49**, 422-429.

Prowse, C. N. & Lew, J. (2001). Mechanism of Activation of ERK2 by Dual Phosphorylation. *Journal of Biological Chemistry* **276**, 99-103.

Pullikuth, A. K. & Catling, A. D. (2007). Scaffold mediated regulation of MAPK signaling and cytoskeletal dynamics: A perspective. *Cellular Signalling* **19**, 1621-1632.

Qi, X. F., Kim, D. H., Yoon, Y. S., Li, J. H., Song, S. B., Jin, D., Huang, X. Z., Teng, Y. C., & Lee, K. J. (2009). The adenylyl cyclase-cAMP system suppresses TARC/CCL17 and MDC/CCL22 production through p38 MAPK and NF- κ B in HaCaT keratinocytes. *Molecular Immunology* **46**, 1925-1934.

Qiao, J., Huang, F., & Lum, H. (2003). PKA inhibits RhoA activation: a protection mechanism against endothelial barrier dysfunction. *AJP - Lung Cellular and Molecular Physiology* **284**, L972-L980.

- Qing, Y., Costa-Pereira, A. P., Watling, D., & Stark, G. (2005). Role of tyrosine 441 of interferon-gamma receptor subunit 1 in SOCS-1-mediated attenuation of STAT1 activation. *Journal of Biological Chemistry* **280**, 1849-1853.
- Qiu, M. S. & Green, S. H. (1992). Pc12 Cell Neuronal Differentiation Is Associated with Prolonged P21(Ras) Activity and Consequent Prolonged Erk Activity. *Neuron* **9**, 705-717.
- Raman, M., Chen, W., & Cobb, M. H. (2007). Differential regulation and properties of MAPKs. *Oncogene* **26**, 3100-3112.
- Ravni, A., Vaudry, D., Gerdin, M. J., Eiden, M. V., Falluel-Morel, A., Gonzalez, B. J., Vaudry, H., & Eiden, L. E. (2008). A cAMP-Dependent, Protein Kinase A-Independent Signaling Pathway Mediating Neuritogenesis through Egr1 in PC12 Cells. *Molecular Pharmacology* **73**, 1688-1708.
- Rehmann, H., Schwede, F., Doskeland, S. O., Wittinghofer, A., & Bos, J. L. (2003). Ligand-mediated activation of the cAMP-responsive guanine nucleotide exchange factor Epac. *Journal of Biological Chemistry* **278**, 38548-38556.
- Richter-Landsberg, C. & Jastorff, B. (1986). The role of cAMP in nerve growth factor-promoted neurite outgrowth in PC12 cells. *The Journal of Cell Biology* **102**, 821-829.
- Ridley, A. J. (2006). Rho GTPases and actin dynamics in membrane protrusions and vesicle trafficking. *Trends in Cell Biology* **16**, 522-529.
- Rivkees, S. A., Zhao, Z. Y., Porter, G., & Turner, C. (2001). Influences of adenosine on the fetus and newborn. *Molecular Genetics and Metabolism* **74**, 160-171.
- Rivo, J., Zeira, E., Galun, E., Einav, S., Linden, J., & Matot, I. (2007). Attenuation of reperfusion lung injury and apoptosis by A(2a) adenosine receptor activation is associated with modulation of Bcl-2 and bax expression and activation of extracellular signal-regulated kinases. *Shock* **27**, 266-273.

Roberts, P. J. & Der, C. J. (2007). Targeting the Raf-MEK-ERK mitogen-activated protein kinase cascade for the treatment of cancer. *Oncogene* **26**, 3291-3310.

Robinson, M. J., Stippec, S. A., Goldsmith, E., White, M. A., & Cobb, M. H. (1998). A constitutively active and nuclear form of the MAP kinase ERK2 is sufficient for neurite outgrowth and cell transformation. *Current Biology* **8**, 1141-1150.

Robinsonsteiner, A. M. & Corbin, J. D. (1983). Probable Involvement of Both Intrachain Camp Binding-Sites in Activation of Protein-Kinase. *Journal of Biological Chemistry* **258**, 1032-1040.

Rodriguez, C., Theillet, C., Portier, M., Bataille, R., & Klein, B. (1994). Molecular analysis of the IL-6 receptor in human multiple myeloma, an IL-6-related disease. *FEBS Letters* **341**, 156-161.

Rogers, R. S., Horvath, C. M., & Matunis, M. J. (2003). SUMO modification of STAT1 and its role in PIAS-mediated inhibition of gene activation. *J.Biol.Chem.* **278**, 30091-30097.

Rollins, B. J. (2006). Inflammatory chemokines in cancer growth and progression. *European Journal of Cancer* **42**, 760-767.

Roscioni, S. S., Elzinga, C. R. S., & Schmidt, M. (2008). Epac: effectors and biological functions. *Naunyn-Schmiedebergs Archives of Pharmacology* **377**, 345-357.

Rossomando, A. J., Payne, D. M., Weber, M. J., & Sturgill, T. W. (1989). Evidence That Pp42, A Major Tyrosine Kinase Target Protein, Is A Mitogen-Activated Serine Threonine Protein-Kinase. *Proceedings of the National Academy of Sciences of the United States of America* **86**, 6940-6943.

Rothwarf, D. M., Zandi, E., Natoli, G., & Karin, M. (1998). IKK- γ is an essential regulatory subunit of the I κ B kinase complex. *Nature* **395**, 297-300.

Saeed, B., Zhang, H. C., & Ng, S. C. (1997). Apoptotic program is initiated but not completed in LNCaP cells in response to growth in charcoal-stripped media. *Prostate* **31**, 145-152.

Saharinen, P., Vihinen, M., & Silvennoinen, I. (2003). Autoinhibition of Jak2 tyrosine kinase is dependent on specific regions in its pseudokinase domain. *Molecular Biology of the Cell* **14**, 1448-1459.

Sakhalkar, S. P., Patterson, E. B., & Khan, M. M. (2005). Involvement of histamine H1 and H2 receptors in the regulation of STAT-1 phosphorylation: Inverse agonism exhibited by the receptor antagonists. *International Immunopharmacology* **5**, 1299-1309.

Salgado, R., Junius, S., Benoy, I., Van Dam, P., Vermeulen, P., Van Marck, E., Huget, P., & Dirix, L. Y. (2003). Circulating interleukin-6 predicts survival in patients with metastatic breast cancer. *International Journal of Cancer* **103**, 642-646.

Samuels, M. L., Weber, M. J., Bishop, J. M., & McMahon, M. (1993). Conditional transformation of cells and rapid activation of the mitogen-activated protein kinase cascade by an estradiol-dependent human raf-1 protein kinase. *Molecular and Cellular Biology* **13**, 6241-6252.

Sands, W. A., Martin, A. F., Strong, E. W., & Palmer, T. M. (2004). Specific inhibition of nuclear factor-kappa B-dependent inflammatory responses by cell type-specific mechanisms upon A(2A) adenosine receptor gene transfer. *Molecular Pharmacology* **66**, 1147-1159.

Sands, W. A. & Palmer, T. M. (2005). Adenosine receptors and the control of endothelial cell function in inflammatory disease. *Immunology Letters* **101**, 1-11.

Sands, W. A., Woolson, H. D., Milne, G. R., Rutherford, C., & Palmer, T. M. (2006). Exchange Protein Activated by Cyclic AMP (Epac)-Mediated Induction of Suppressor of Cytokine Signaling 3 (SOCS-3) in Vascular Endothelial Cells. *Molecular and Cellular Biology* **26**, 6333-6346.

Sasaki, A., Inagaki-Ohara, K., Yoshida, T., Yamanaka, A., Sasaki, M., Yasukawa, H., Koromilas, A. E., & Yoshimura, A. (2003). The N-terminal truncated isoform of SOCS3 translated from an alternative initiation AUG codon under stress conditions is stable due to the lack of a major ubiquitination site, Lys-6. *Journal of Biological Chemistry* **278**, 2432-2436.

Sassone-Corsi, P. (1998). Coupling gene expression to cAMP signalling: role of CREB and CREM. *International Journal of Biochemistry & Cell Biology* **30**, 27-38.

Schaper, F., Gendo, C., Eck, M., Schmitz, J., Grimm, C., Anhuf, D., Kerr, I. M., & Heinrich, P. C. (1998). Activation of the protein tyrosine phosphatase SHP2 via the interleukin-6 signal transducing receptor protein gp130 requires tyrosine kinase Jak1 and limits acute-phase protein expression. *Biochemical Journal* **335**, 557-565.

Scheller, J., Ohnesorge, N., & Rose-John, S. (2006). Interleukin-6 trans-signalling in chronic inflammation and cancer. *Scandinavian Journal of Immunology* **63**, 321-329.

Schmandke, A., Schmandke, A., & Strittmatter, S. M. (2007). ROCK and Rho: Biochemistry and Neuronal Functions of Rho-Associated Protein Kinases. *The Neuroscientist* **13**, 454-469.

Schmitz, J., Weissenbach, M., Haan, S., Heinrich, P. C., & Schaper, F. (2000). SOCS3 exerts its inhibitory function on interleukin-6 signal transduction through the SHP2 recruitment site of gp130. *Journal of Biological Chemistry* **275**, 12848-12856.

Schottenfeld, D. & Beebe-Dimmer, J. (2006). Chronic inflammation: A common and important factor in the pathogenesis of neoplasia. *Ca-A Cancer Journal for Clinicians* **56**, 69-83.

Schrapf, M., Ying, O., Kim, T. Y., & Martin, G. S. (2008). ERK5 promotes Src-induced podosome formation by limiting Rho activation. *Journal of Cell Biology* **181**, 1195-1210.

- Schubert, D. & Whitlock, C. (1977). Alteration of Cellular Adhesion by Nerve Growth-Factor - (Sympathetic Nerve Cyclic Nucleotides Adhesion). *Proceedings of the National Academy of Sciences of the United States of America* **74**, 4055-4058.
- Schulte, G. & Fredhohn, B. B. (2003). Signalling from adenosine receptors to mitogen-activated protein kinases. *Cellular Signalling* **15**, 813-827.
- Schulze-Bahr, E., Neu, A., Friederich, P., Kaupp, U. B., Breithardt, G., Pongs, O., & Isbrandt, D. (2003). Pacemaker channel dysfunction in a patient with sinus node disease. *Journal of Clinical Investigation* **111**, 1537-1545.
- Scimeca, J. C., Ballotti, R., Nguyen, T. T., Filloux, C., & Vanobberghen, E. (1991). Tyrosine and Threonine Phosphorylation of An Immunoaffinity-Purified 44-Kda Map Kinase. *Biochemistry* **30**, 9313-9319.
- Seger, R., Ahn, N. G., Posada, J., Munar, E. S., Jensen, A. M., Cooper, J. A., Cobb, M. H., & Krebs, E. G. (1992). Purification and Characterization of Mitogen-Activated Protein-Kinase Activator(S) from Epidermal Growth Factor-Stimulated A431 Cells. *Journal of Biological Chemistry* **267**, 14373-14381.
- Sehrawat, S., Cullere, X., Patel, S., Italiano, J., Jr., & Mayadas, T. N. (2008). Role of Epac1, an Exchange Factor for Rap GTPases, in Endothelial Microtubule Dynamics and Barrier Function. *Molecular Biology of the Cell* **19**, 1261-1270.
- Seidel, M. G., Klinger, M., Freissmuth, M., & Holler, C. (1999). Activation of mitogen-activated protein kinase by the A(2A)-adenosine receptor via a rap1-dependent and via a p21(ras)-dependent pathway. *Journal of Biological Chemistry* **274**, 25833-25841.
- Seifert, R. & Wenzel-Seifert, K. (2003). The human formyl peptide receptor as model system for constitutively active G-protein-coupled receptors. *Life Sciences* **73**, 2263-2280.
- Semenza, G. L. (2000). Hypoxia, clonal selection, and the role of HIF-1 in tumor progression. *Critical Reviews in Biochemistry and Molecular Biology* **35**, 71-103.

Sen, M., Tosca, P. J., Zwyer, C., Ryan, M. J., Johnson, J. D., Knostman, K. A. B., Giclas, P. C., Peggins, J. O., Tomaszewski, J. E., McMurray, T. P., Li, C. Y., Leibowitz, M. S., Ferris, R. L., Gooding, W. E., Thomas, S. M., Johnson, D. E., & Grandis, J. R. (2009). Lack of toxicity of a STAT3 decoy oligonucleotide. *Cancer Chemotherapy and Pharmacology* **63**, 983-995.

Serezani, C. H., Ballinger, M. N., Aronoff, D. M., & Peters-Golden, M. (2008). Cyclic AMP: Master Regulator of Innate Immune Cell Function. *American Journal of Respiratory Cell and Molecular Biology* **39**, 127-132.

Sexl, V., Mancusi, G., Holler, C., GloriaMaercker, E., Schutz, W., & Freissmuth, M. (1997). Stimulation of the mitogen-activated protein kinase via the A(2A)-adenosine receptor in primary human endothelial cells. *Journal of Biological Chemistry* **272**, 5792-5799.

Shankar, D. B., Cheng, J. C., Kinjo, K., Federman, N., Moore, T. B., Gill, A., Rao, N. P., Landaw, E. M., & Sakamoto, K. M. (2005). The role of CREB as a proto-oncogene in hematopoiesis and in acute myeloid leukemia. *Cancer Cell* **7**, 351-362.

Shariat, S. F., Andrews, B., Kattan, M. W., Kim, J., Wheeler, T. M., & Slawin, K. M. (2001). Plasma levels of interleukin-6 and its soluble receptor are associated with prostate cancer progression and metastasis. *Urology* **58**, 1008-1015.

Shariff, A. H. & Ather, M. H. (2006). Neuroendocrine differentiation in prostate cancer. *Urology* **68**, 2-8.

Shouda, T., Yoshida, T., Hanada, T., Wakioka, T., Oishi, M., Miyoshi, K., Komiya, S., Kosai, K., Hanakawa, Y., Hashimoto, K., Nagata, K., & Yoshimura, A. (2001). Induction of the cytokine signal regulator SOCS3/CIS3 as a therapeutic strategy from treating inflammatory arthritis. *Journal of Clinical Investigation* **108**, 1781-1788.

Shuai, K. & Liu, B. (2005). Regulation of gene-activation pathways by pi3k proteins in the immune system. *Nature Reviews Immunology* **5**, 593-605.

Shuai, K., Schindler, C., Prezioso, V. R., & Darnell, J. E. (1992). Activation of Transcription by Ifn-Gamma - Tyrosine Phosphorylation of A 91-Kd Dna-Binding Protein. *Science* **258**, 1808-1812.

Shuai, K., Stark, G. R., Kerr, I. M., & Darnell, J. E. (1993). A Single Phosphotyrosine Residue of Stat91 Required for Gene Activation by Interferon-Gamma. *Science* **261**, 1744-1746.

Shuai, K., Horvath, C. M., Huang, L. H. T., Qureshi, S. A., Cowburn, D., & Darnell, J. (1994). Interferon activation of the transcription factor Stat91 involves dimerization through SH2-phosphotyrosyl peptide interactions. *Cell* **76**, 821-828.

Siewert, E., Muller-Esterl, W., Starr, R., Heinrich, P. C., & Schaper, F. (1999). Different protein turnover of interleukin-6-type cytokine signalling components. *European Journal of Biochemistry* **265**, 251-257.

Sirvent, A., Boureux, A., Simon, V., Leroy, C., & Roche, S. (2007). The tyrosine kinase Abl is required for Src-transforming activity in mouse fibroblasts and human breast cancer cells. *Oncogene* **26**, 7313-7323.

Sitkovsky, M. V. (2003). Use of the A(2A) adenosine receptor as a physiological immunosuppressor and to engineer inflammation in vivo. *Biochemical Pharmacology* **65**, 493-501.

Skiniotis, G., Boulanger, M. J., Garcia, K. C., & Walz, T. (2005). Signaling conformations of the tall cytokine receptor gp130 when in complex with IL-6 and IL-6 receptor. *Nature Structural & Molecular Biology* **12**, 545-551.

Skiniotis, G., Lupardus, P. J., Martick, M., Walz, T., & Garcia, K. C. (2008). Structural Organization of a Full-Length gp130/LIF-R Cytokine Receptor Transmembrane Complex. *Molecular Cell* **31**, 737-748.

Smith, P. D. & Crompton, M. R. (1998). Expression of v-src in mammary epithelial cells induces transcription via STAT3. *Biochemical Journal* **331**, 381-385.

Song, L., Bhattacharya, S., Yunus, A. A., Lima, C. D., & Schindler, C. (2006). Stat1 and SUMO modification. *Blood* **108**, 3237-3244.

Sousa, L. P., Carmo, A. F., Rezende, B. M., Lopes, F., Silva, D. M., Alessandri, A. L., Bonjardim, C. A., Rossi, A. G., Teixeira, M. M., & Pinho, V. (2009). Cyclic AMP enhances resolution of allergic pleurisy by promoting inflammatory cell apoptosis via inhibition of PI3K/Akt and NF-[kappa]B. *Biochemical Pharmacology* **78**, 396-405.

Srivastava, R. K., Srivastava, A. R., & Cho-Chung, Y. S. (1998). Synergistic effects of 8-chlorocyclic-AMP and retinoic acid on induction of apoptosis in Ewing's sarcoma CHP-100 cells. *Clinical Cancer Research* **4**, 755-761.

Stahl, N., Boulton, T. G., Farruggella, T., Ip, N. Y., Davis, S., Witthuhn, B. A., Quelle, F. W., Silvennoinen, O., Barbieri, G., Pellegrini, S., & et, a. (1994). Association and activation of Jak-Tyk kinases by CNTF-LIF-OSM-IL-6 beta receptor components. *Science* **263**, 92-95.

Stark, J. R., Li, H. J., Kraft, P., Kurth, T., Giovannucci, E. L., Stampfer, M. J., Ma, J., & Mucci, L. A. (2009). Circulating prediagnostic interleukin-6 and C-reactive protein and prostate cancer incidence and mortality. *International Journal of Cancer* **124**, 2683-2689.

Starr, R. & Hilton, D. J. (1999). Negative regulation of the JAK/STAT pathway. *Bioessays* **21**, 47-52.

Starr, R., Willson, T. A., Viney, E. M., Murray, L. J. L., Rayner, J. R., Jenkins, B. J., Gonda, T. J., Alexander, W. S., Metcalf, D., Nicola, N. A., & Hilton, D. J. (1997). A family of cytokine-inducible inhibitors of signalling. *Nature* **387**, 917-921.

Stehle, J. H., Foulkes, N. S., Molina, C. A., Simonneaux, V., Pevet, P., & Sassonecorsi, P. (1993). Adrenergic Signals Direct Rhythmic Expression of Transcriptional Repressor Crem in the Pineal-Gland. *Nature* **365**, 314-320.

Steinbrink, K., Wolfl, M., Jonuleit, H., Knop, J., & Enk, A. H. (1997). Induction of tolerance by IL-10-treated dendritic cells. *Journal of Immunology* **159**, 4772-4780.

- Stessin, A. M., Zipin, J. H., Kamenetsky, M., Hess, K. C., Buck, J., & Levin, L. R. (2006). Soluble adenylyl cyclase mediates NGF-induced activation of RAP1. *Journal of Biological Chemistry* **M603500200**.
- Sticht, C., Freier, K., Knopfle, K., Flechtenmacher, C., Pungs, S., Christof, H. M., Hahn, M., Joos, S., & Lichter, P. (2008). Activation of MAP kinase signaling through ERK5 but not ERK1 expression is associated with lymph node metastases in oral squamous cell carcinoma (OSCC). *Neoplasia* **10**, 462-U26.
- Stone, K. R., Mickey, D. D., Wunderli, H., Mickey, G. H., & Paulson, D. F. (1978). Isolation of A Human Prostate Carcinoma Cell Line (du 145). *International Journal of Cancer* **21**, 274-281.
- Stuhlmann-Laeisz, C., Lang, S., Chalaris, A., Paliga, K., Sudarman, E., Eichler, J., Klingmuller, U., Samuel, M., Ernst, M., Rose-John, S., & Scheller, J. (2006). Forced dimerization of gp130 leads to constitutive STAT3 activation, cytokine-independent growth, and blockade of differentiation of embryonic stem cells. *Molecular Biology of the Cell* **17**, 2986-2995.
- Suetsugu, S., Miki, H., & Takenawa, T. (1999). Identification of two human WAVE SCAR homologues as general actin regulatory molecules which associate with the Arp2/3 complex. *Biochemical and Biophysical Research Communications* **260**, 296-302.
- Sullivan, G. W. & Linden, J. (1998). Role of A(2A) adenosine receptors in inflammation. *Drug Development Research* **45**, 103-112.
- Sun, P., Watanabe, H., Takano, K., Yokoyama, T., Fujisawa, J., & Endo, T. (2006). Sustained activation of M-Ras induced by nerve growth factor is essential for neuronal differentiation of PC12 cells. *Genes to Cells* **11**, 1097-1113.
- Sunahara, R. K. & Taussig, R. (2002). Isoforms of Mammalian Adenylyl Cyclase: Multiplicities of Signaling. *Molecular Interventions* **2**, 168-184.

Takahashi-Tezuka, M., Yoshida, Y., Fukada, T., Ohtani, T., Yamanaka, Y., Nishida, K., Nakajima, K., Hibi, M., & Hirano, T. (1998). Gab1 acts as an adapter molecule linking the cytokine receptor gp130 to ERK mitogen-activated protein kinase. *Molecular and Cellular Biology* **18**, 4109-4117.

Takenawa, T. & Suetsugu, S. (2007). The WASP-WAVE protein network: connecting the membrane to the cytoskeleton. *Nature Reviews Molecular Cell Biology* **8**, 37-48.

Tanaka, T., Soriano, M. A., & Grusby, M. J. (2005). SLIM is a nuclear ubiquitin E3 ligase that negatively regulates STAT signaling. *Immunity* **22**, 729-736.

Tanuma, N., Shima, H., Nakamura, K., & Kikuchi, K. (2001). Protein tyrosine phosphatase epsilon C selectively inhibits interleukin-6- and interleukin- 10-induced JAK-STAT signaling. *Blood* **98**, 3030-3034.

Tatake, R. J., O'Neill, M. M., Kennedy, C. A., Wayne, A. L., Jakes, S., Wu, D., Kugler, J., Kashem, M. A., Kaplita, P., & Snow, R. J. (2008). Identification of pharmacological inhibitors of the MEK5/ERK5 pathway. *Biochemical and Biophysical Research Communications* **377**, 120-125.

Terstegen, L., Gatsios, P., Bode, J. G., Schaper, F., Heinrich, P. C., & Graeve, L. (2000). The inhibition of interleukin-6-dependent STAT activation by mitogen-activated protein kinases depends on tyrosine 759 in the cytoplasmic tail of glycoprotein 130. *J.Biol.Chem.* **275**, 18810-18817.

Tesmer, J. J., Sunahara, R. K., Gilman, A. G., & Sprang, S. R. (1997). Crystal Structure of the Catalytic Domains of Adenylyl Cyclase in a Complex with Gs{alpha}?GTPS. *Science* **278**, 1907-1916.

Thevenin, D. & Lazarova, T. (2008). Stable interactions between the transmembrane domains of the adenosine A(2A) receptor. *Protein Science* **17**, 1188-1199.

Thibault, N., Burelout, C., Harbour, D., Borgeat, P., Naccache, P. H., & Bourgoin, S. G. (2002). Occupancy of adenosine A2a receptors promotes fMLP-induced cyclic AMP

accumulation in human neutrophils: impact on phospholipase D activity and recruitment of small GTPases to membranes. *Journal of Leukocyte Biology* **71**, 367-377.

Thibault, N., Harbour, D., Borgeat, P., Naccache, P. H., & Bourgoin, S. G. (2000). Adenosine receptor occupancy suppresses chemoattractant-induced phospholipase D activity by diminishing membrane recruitment of small GTPases. *Blood* **95**, 519-527.

Thoennissen, N. H., Iwanski, G. B., Doan, N. B., Okamoto, R., Lin, P., Abbassi, S., Song, J. H., Yin, D., Toh, M., Xie, W. D., Said, J. W., & Koeffler, H. P. (2009). Cucurbitacin B Induces Apoptosis by Inhibition of the JAK/STAT Pathway and Potentiates Antiproliferative Effects of Gemcitabine on Pancreatic Cancer Cells. *Cancer Research* **69**, 5876-5884.

Thompson, J. D., Higgins, D. G., & Gibson, T. J. (1994). Clustal-W - Improving the Sensitivity of Progressive Multiple Sequence Alignment Through Sequence Weighting, Position-Specific Gap Penalties and Weight Matrix Choice. *Nucleic Acids Research* **22**, 4673-4680.

Thun, M. J., Henley, S. J., & Patrono, C. (2002). Nonsteroidal anti-inflammatory drugs as anticancer agents: Mechanistic, pharmacologic, and clinical issues. *Journal of the National Cancer Institute* **94**, 252-266.

Tischoff, I., Hengge, U. R., Vieth, M., Ell, C., Stolte, M., Weber, A., Schmidt, W. E., & Tannapfel, A. (2007). Methylation of SOCS-3 and SOCS-1 in the carcinogenesis of Barrett's adenocarcinoma. *Gut* **56**, 1047-1053.

To, K. F., Chan, M. W. Y., Leung, W. K., Ng, E. K. W., Yu, J., Bai, A. H. C., Lo, A. W. I., Chu, S. H., Tong, J. H. M., Lo, K. W., Sung, J. J. Y., & Chan, F. K. L. (2004). Constitutional activation of IL-6-mediated JAK/STAT pathway through hypermethylation of SOCS-1 in human gastric cancer cell line. *British Journal of Cancer* **91**, 1335-1341.

Traverse, S., Gomez, N., Paterson, H., Marshall, C., & Cohen, P. (1992). Sustained Activation of the Mitogen-Activated Protein (Map) Kinase Cascade May be Required for Differentiation of Pc12 Cells - Comparison of the Effects of Nerve Growth-Factor and Epidermal Growth-Factor. *Biochemical Journal* **288**, 351-355.

- Troppmair, J., Bruder, J. T., Munoz, H., Lloyd, P. A., Kyriakis, J., Banerjee, P., Avruch, J., & Rapp, U. R. (1994). Mitogen-activated protein kinase/extracellular signal-regulated protein kinase activation by oncogenes, serum, and 12-O-tetradecanoylphorbol-13-acetate requires Raf and is necessary for transformation. *Journal of Biological Chemistry* **269**, 7030-7035.
- Tsao, S. W., Tramoutanis, G., Dawson, C. W., Lo, A. K. F., & Huang, D. P. (2002). The significance of LMP1 expression in nasopharyngeal carcinoma. *Seminars in Cancer Biology* **12**, 473-487.
- Tscherne, J. S. & Pestka, S. (1975). Inhibition of Protein-Synthesis in Intact Hela-Cells. *Antimicrobial Agents and Chemotherapy* **8**, 479-487.
- Tsuji, F., Yoshimi, M., Katsuta, O., Takai, M., Ishihara, K., & Aono, H. (2009). Point mutation of tyrosine 759 of the IL-6 family cytokine receptor, gp130, augments collagen-induced arthritis in DBA/1J mice. *Bmc Musculoskeletal Disorders* **10**.
- Tsukada, Y., Aoki, K., Nakamura, T., Sakumura, Y., Matsuda, M., & Ishii, S. (2008). Quantification of Local Morphodynamics and Local GTPase Activity by Edge Evolution Tracking. *Plos Computational Biology* **4**.
- Tsygankova, O. M., Kupperman, E., Wen, W., & Meinkoth, J. L. (2000). Cyclic AMP activates Ras. *Oncogene* **19**, 3609-3615.
- Turjanski, A. G., Vaque, J. P., & Gutkind, J. S. (2007). MAP kinases and the control of nuclear events. *Oncogene* **26**, 3240-3253.
- Ueda, T., Bruchofsky, N., & Sadar, M. D. (2002). Activation of the Androgen Receptor N-terminal Domain by Interleukin-6 via MAPK and STAT3 Signal Transduction Pathways. *Journal of Biological Chemistry* **277**, 7076-7085.
- Ungureanu, D., Vanhatupa, S., Gronholm, J., Palvimo, J. J., & Silvennoinen, O. (2005). SUMO-1 conjugation selectively modulates STAT1-mediated gene responses. *Blood* **106**, 224-226.

van de Geijn, G.-J., Gits, J., & Touw, I. P. (2004). Distinct activities of suppressor of cytokine signaling (SOCS) proteins and involvement of the SOCS box in controlling G-CSF signaling. *J Leukoc Biol* **76**, 237-244.

van Gurp, E. A. F. J., Schoordijk-Verschoor, W., Klepper, M., Korevaar, S. S., Chan, G., Weimar, W., & Baan, C. C. (2009). The Effect of the JAK Inhibitor CP-690,550 on Peripheral Immune Parameters in Stable Kidney Allograft Patients. *Transplantation* **87**.

van Kempen, L. C. L., de Visser, K. E., & Coussens, L. M. (2006). Inflammation, proteases and cancer. *European Journal of Cancer* **42**, 728-734.

Verkhovskiy, A. B., Svitkina, T. M., & Borisy, G. G. (1999). Self-polarization and directional motility of cytoplasm. *Current Biology* **9**, 11-20.

Waetzig, V. & Herdegen, T. (2003). The concerted signaling of ERK1/2 and JNKs is essential for PC12 cell neuriteogenesis and converges at the level of target proteins. *Molecular and Cellular Neuroscience* **24**, 238-249.

Wang, J., Rao, Q., Wang, M., Wei, H., Xing, H., Liu, H., Wang, Y., Tang, K., Peng, L., Tian, Z., & Wang, J. (2009). Overexpression of Rac1 in leukemia patients and its role in leukemia cell migration and growth. *Biochemical and Biophysical Research Communications* **386**, 769-774.

Wang, R., Cherukuri, P., & Luo, J. Y. (2005). Activation of Stat3 sequence-specific DNA binding and transcription by p300/CREB-binding protein-mediated acetylation. *J.Biol.Chem.* **280**, 11528-11534.

Wang, R., Griffin, P. R., Small, E. C., & Thompson, J. E. (2003). Mechanism of Janus kinase 3-catalyzed phosphorylation of a Janus kinase 1 activation loop peptide. *Archives of Biochemistry and Biophysics* **410**, 7-15.

Wang, X. & Tournier, C. (2006). Regulation of cellular functions by the ERK5 signalling pathway. *Cellular Signalling* **18**, 753-760.

- Wang, Z., Dillon, T. J., Pokala, V., Mishra, S., Labudda, K., Hunter, B., & Stork, P. J. S. (2006). Rap1-Mediated Activation of Extracellular Signal-Regulated Kinases by Cyclic AMP Is Dependent on the Mode of Rap1 Activation. *Molecular and Cellular Biology* **26**, 2130-2145.
- Ward, A. C., Csar, X. F., Hoffmann, B. W., & Hamilton, J. A. (1996). Cyclic AMP Inhibits Expression of D-Type Cyclins and cdk4 and Induces p27Kip1 in G-CSF-Treated NFS-60 Cells. *Biochemical and Biophysical Research Communications* **224**, 10-16.
- Warrier, S., Belevych, A. E., Ruse, M., Eckert, R. L., Zaccolo, M., Pozzan, T., & Harvey, R. D. (2005). beta-adrenergic- and muscarinic receptor-induced changes in cAMP activity in adult cardiac myocytes detected with FRET-based biosensor. *American Journal of Physiology-Cell Physiology* **289**, C455-C461.
- Watanabe, N., Madaule, P., Reid, T., Ishizaki, T., Watanabe, G., Kakizuka, A., Saito, Y., Nakao, K., Jockusch, B. M., & Narumiya, S. (1997). p140mDia, a mammalian homolog of *Drosophila diaphanous*, is a target protein for Rho small GTPase and is a ligand for profilin. *Embo Journal* **16**, 3044-3056.
- Waterman-Storer, C., Duey, D. Y., Weber, K. L., Keech, J., Cheney, R. E., Salmon, E. D., & Bement, W. M. (2000). Microtubules remodel actomyosin networks in *Xenopus* egg extracts via two mechanisms of F-actin transport. *Journal of Cell Biology* **150**, 361-376.
- Webb, C. P., Van Aelst, L., Wigler, M. H., & Vande Woude, G. F. (1998). Signaling pathways in Ras-mediated tumorigenicity and metastasis. *Proceedings of the National Academy of Sciences of the United States of America* **95**, 8773-8778.
- Weber, A., Hengge, U. R., Bardenheuer, W., Tischhoff, I., Sommerer, F., Markwarth, A., Dietz, A., Wittekind, C., & Tannapfel, A. (2005). SOCS-3 is frequently methylated in head and neck squamous cell carcinoma and its precursor lesions and causes growth inhibition. *Oncogene* **24**, 6699-6708.
- Wegner, A. M., Nebhan, C. A., Hu, L., Majumdar, D., Meier, K. M., Weaver, A. M., & Webb, D. J. (2008). N-WASP and the Arp2/3 Complex Are Critical Regulators of Actin in

the Development of Dendritic Spines and Synapses. *Journal of Biological Chemistry* **283**, 15912-15920.

Wehbe, H., Henson, R., Meng, F. Y., Mize-Berge, J., & Patel, T. (2006). Interleukin-6 contributes to growth in cholangiocarcinoma cells by aberrant promoter methylation and gene expression. *Cancer Research* **66**, 10517-10524.

Weigert, C., Dufer, M., Simon, P., Debre, E., Runge, H., Brodbeck, K., Haring, H. U., & Schleicher, E. D. (2007). Upregulation of IL-6 mRNA by IL-6 in skeletal muscle cells: role of IL-6 mRNA stabilization and Ca²⁺-dependent mechanisms. *AJP - Cell Physiology* **293**, C1139-C1147.

Weijerman, P. C., Konig, J. J., Wong, S. T., Niesters, H. G. M., & Peehl, D. M. (1994). Lipofection-Mediated Immortalization of Human Prostatic Epithelial-Cells of Normal and Malignant Origin Using Human Papillomavirus Type-18 Dna. *Cancer Research* **54**, 5579-5583.

Weston, C. R., Balmanno, K., Chalmers, C., Hadfield, K., Molton, S. A., Ley, R., Wagner, E. F., & Cook, S. J. (2003). Activation of ERK1//2 by [Delta]Raf-1[thinsp]:[thinsp]ER[ast] represses Bim expression independently of the JNK or PI3K pathways. *Oncogene* **22**, 1281-1293.

Westphal, R. S., Soderling, S. H., Alto, N. M., Langeberg, L. K., & Scott, J. D. (2000). Scar/WAVE-1, a Wiskott-Aldrich syndrome protein, assembles an actin-associated multi-kinase scaffold. *EMBO J* **19**, 4589-4600.

Wetsel, R. A., Kilsgaard, J., & Haviland, D. L. (2000). Complement anaphylatoxins (C3a, C4a, C5a) and their receptors (C3aR, C5aR/CD88) as therapeutic targets in inflammation. In *Contemporary Immunology: Therapeutic interventions in the complement system*, eds. Lambris, J. D. & Holers, V. M., Humana Press Inc., Totowa.

Wilde, C., Genth, H., Aktories, K., & Just, I. (2000). Recognition of RhoA by Clostridium botulinum C3 exoenzyme. *Journal of Biological Chemistry* **275**, 16478-16483.

- Wilson, V. L. & Jones, P. A. (1983). Inhibition of DNA methylation by chemical carcinogens in vitro. *Cell* **32**, 239-246.
- Wittmann, T. & Waterman-Storer, C. M. (2001). Cell motility: can Rho GTPases and microtubules point the way? *Journal of Cell Science* **114**, 3795-3803.
- Wojtowicz-Praga, S. (2003). Reversal of tumor-induced immunosuppression by TGF-beta inhibitors. *Investigational New Drugs* **21**, 21-32.
- Woolson, H. D., Thomson, V. S., Rutherford, C., Yarwood, S. J., & Palmer, T. M. (2009). Selective inhibition of cytokine-activated extracellular signal-regulated kinase by cyclic AMP via Epac1-dependent induction of suppressor of cytokine signalling-3. *Cellular Signalling* **21**, 1706-1715.
- Wu, C. Y., Guan, Q., Wang, Y. J., Zhao, Z. J., & Zhou, G. W. (2003). SHP-1 suppresses cancer cell growth by promoting degradation of JAK kinases. *Journal of Cellular Biochemistry* **90**, 1026-1037.
- Wu, L. T., Bijian, K., & Shen, S. S. (2009). CD45 recruits adapter protein DOK-1 and negatively regulates JAK-STAT signaling in hematopoietic cells. *Molecular Immunology* **46**, 2167-2177.
- Xi, S. C., Gooding, W. E., & Grandis, J. R. (2005). In vivo antitumor efficacy of STAT3 blockade using a transcription factor decoy approach: implications for cancer therapy. *Oncogene* **24**, 970-979.
- Xu, Q., Briggs, J., Park, S., Niu, G. L., Kortylewski, M., Zhang, S. M., Gritsko, T., Turkson, J., Kay, H., Semenza, G. L., Cheng, J. Q., Jove, R., & Yu, H. (2005). Targeting Stat3 blocks both HIF-1 and VEGF expression induced by multiple oncogenic growth signaling pathways. *Oncogene* **24**, 5552-5560.
- Yakel, J. L., Warren, R. A., Reppert, S. M., & North, R. A. (1993). Functional expression of adenosine A2b receptor in *Xenopus* oocytes. *Molecular Pharmacology* **43**, 277-280.

Yamagami, H., Kitagawa, K., Nagai, Y., Hougaku, H., Sakaguchi, M., Kuwabara, K., Kondo, K., Masuyama, T., Matsumoto, M., & Hori, M. (2004). Higher levels of interleukin-6 are associated with lower echogenicity of carotid artery plaques. *Stroke* **35**, 677-681.

Yamamoto, T., Sekine, Y., Kashima, K., Kubota, A., Sato, N., Aoki, N., & Matsuda, T. (2002). The nuclear isoform of protein-tyrosine phosphatase TC-PTP regulates interleukin-6-mediated signaling pathway through STAT3 dephosphorylation. *Biochemical and Biophysical Research Communications* **297**, 811-817.

Yamaoka, K., Saharinen, P., Pesu, M., Holt, V. E. T., Silvennoinen, O., & O'Shea, J. J. (2004). The Janus kinases (Jaks). *Genome Biology* **5**.

Yang, L.-T., Alexandropoulos, K., & Sap, J. (2002). c-SRC Mediates Neurite Outgrowth through Recruitment of Crk to the Scaffolding Protein Sin/Efs without Altering the Kinetics of ERK Activation. *Journal of Biological Chemistry* **277**, 17406-17414.

Yang, Y. N., Pan, X. C., Lei, W. W., Wang, J., Shi, J., Li, F. Q., & Song, J. G. (2006). Regulation of transforming growth factor-beta 1-induced apoptosis and epithelial-to-mesenchymal transition by protein kinase A and signal transducers and activators of transcription 3. *Cancer Research* **66**, 8617-8624.

Yao, H., York, R. D., Misra-Press, A., Carr, D. W., & Stork, P. J. S. (1998a). The cyclic adenosine monophosphate-dependent protein kinase (PKA) is required for the sustained activation of mitogen-activated kinases and gene expression by nerve growth factor. *Journal of Biological Chemistry* **273**, 8240-8247.

Yao, H., York, R. D., Misra-Press, A., Carr, D. W., & Stork, P. J. (1998b). The Cyclic Adenosine Monophosphate-dependent Protein Kinase (PKA) Is Required for the Sustained Activation of Mitogen-activated Kinases and Gene Expression by Nerve Growth Factor. *J.Biol.Chem.* **273**, 8240-8247.

Yarwood, S. J., Borland, G., Sands, W. A., & Palmer, T. M. (2008). Identification of CCAAT/Enhancer-binding Proteins as Exchange Protein Activated by cAMP-activated

Transcription Factors That Mediate the Induction of the SOCS-3 Gene. *Journal of Biological Chemistry* **283**, 6843-6853.

Yasukawa, H., Misawa, H., Sakamoto, H., Masuhara, M., Sasaki, A., Wakioka, T., Ohtsuka, S., Imaizumi, T., Matsuda, T., Ihle, J. N., & Yoshimura, A. (1999). The JAK-binding protein JAB inhibits Janus tyrosine kinase activity through binding in the activation loop. *Embo Journal* **18**, 1309-1320.

Yeh, J. J., Routh, E. D., Rubinas, T., Peacock, J., Martin, T. D., Shen, X. J., Sandler, R. S., Kim, H. J., Keku, T. O., & Der, C. J. (2009). KRAS/BRAF mutation status and ERK1/2 activation as biomarkers for MEK1/2 inhibitor therapy in colorectal cancer. *Molecular Cancer Therapeutics* **8**, 834-843.

Yoon, S., Seger, R., Choi, E. J., & Yoo, Y. S. (2004). SB203580 Induces Prolonged B-Raf Activation and Promotes Neuronal Differentiation upon EGF Treatment of PC12 Cells. *Biochemistry (Moscow)* **69**, 799-805.

York, R. D., Yao, H., Dillon, T., Ellig, C. L., Eckert, S. P., McCleskey, E. W., & Stork, P. J. S. (1998). Rap1 mediates sustained MAP kinase activation induced by nerve growth factor. *Nature* **392**, 622-626.

Yu, C. L., Jin, Y. J., & Burakoff, S. J. (2000). Cytosolic Tyrosine Dephosphorylation of STAT5. POTENTIAL ROLE OF SHP-2 IN STAT5 REGULATION. *J.Biol.Chem.* **275**, 599-604.

Yu, H. & Jove, R. (2004). The stats of cancer - New molecular targets come of age. *Nature Reviews Cancer* **4**, 97-105.

Yuan, T. C., Veeramani, S., & Lin, M. F. (2007). Neuroendocrine-like prostate cancer cells: Neuroendocrine transdifferentiation of prostate adenocarcinoma cells. *Endocrine-Related Cancer* **14**, 531-547.

Zaccolo, M. & Pozzan, T. (2002). Discrete microdomains with high concentration of cAMP in stimulated rat neonatal cardiac myocytes. *Science* **295**, 1711-1715.

Zelada, A., Passeron, S., Gomes, S. L., & Cantore, M. L. (1998). Isolation and characterisation of cAMP-dependent protein kinase from *Candida albicans* - Purification of the regulatory and catalytic subunits. *European Journal of Biochemistry* **252**, 245-252.

Zen, K., Yasui, K., Nakajima, T., Zen, Y., Zen, K., Gen, Y., Mitsuyoshi, H., Minami, M., Mitsufuji, S., Tanaka, S., Itoh, Y., Nakanuma, Y., Taniwaki, M., Arii, S., Okanoue, T., & Yoshikawa, T. (2009). ERK5 is a Target for Gene Amplification at 17p11 and Promotes Cell Growth in Hepatocellular Carcinoma by Regulating Mitotic Entry. *Genes Chromosomes & Cancer* **48**, 109-120.

Zhang, X. L., Zhang, J., Wei, H. M., & Tian, Z. G. (2007). STAT3-decoy oligodeoxynucleotide inhibits the growth of human lung cancer via down-regulating its target genes. *Oncology Reports* **17**, 1377-1382.

Zhao, S. Y., Sun, Y., Lai, Z. S., Nan, Q. Z., Li, K., & Zhang, Z. S. (2009a). Inhibition of migration and invasion of colorectal cancer cells via deletion of Rac1 with RNA interference. *Molecular and Cellular Biochemistry* **322**, 179-184.

Zhao, X. S., Lu, L., Pokhriyal, N., Ma, H., Duan, L., Lin, S., Jafari, N., Band, H., & Band, V. (2009b). Overexpression of RhoA Induces Preneoplastic Transformation of Primary Mammary Epithelial Cells. *Cancer Research* **69**, 483-491.

Zhao, Z. S. & Manser, E. (2005). PAK and other Rho-associated kinases - effectors with surprisingly diverse mechanisms of regulation. *Biochemical Journal* **386**, 201-214.

Zheng, X. G., Diraviyam, K., & Sept, D. (2007). Nucleotide effects on the structure and dynamics of actin. *Biophysical Journal* **93**, 1277-1283.

Zhou, G. C., Bao, Z. Q., & Dixon, J. E. (1995). Components of A New Human Protein-Kinase Signal-Transduction Pathway. *Journal of Biological Chemistry* **270**, 12665-12669.

Zhou, Q. Y., Li, C. Y., Olah, M. E., Johnson, R. A., Stiles, G. L., & Civelli, O. (1992). Molecular-Cloning and Characterization of An Adenosine Receptor - the A3 Adenosine

Receptor. *Proceedings of the National Academy of Sciences of the United States of America* **89**, 7432-7436.

Zhou, Y. J., Hanson, E. P., Chen, Y. Q., Magnuson, K., Chen, M., Swann, P. G., Wange, R. L., Changelian, P. S., & O Shea, J. J. (1997). Distinct tyrosine phosphorylation sites in JAK3 kinase domain positively and negatively regulate its enzymatic activity. *Proceedings of the National Academy of Sciences of the United States of America* **94**, 13850-13855.